Geology of the Blue Mountains Region of Oregon, Idaho, and Washington:

The Idaho Batholith and Its Border Zone

U.S. GEOLOGICAL SURVEY PROFESSIONAL PAPER 1436

Geology of the Blue Mountains Region of Oregon, Idaho, and Washington:

The Idaho Batholith and Its Border Zone

TRACY L. VALLIER *and* HOWARD C. BROOKS, *editors*

U.S. GEOLOGICAL SURVEY PROFESSIONAL PAPER 1436

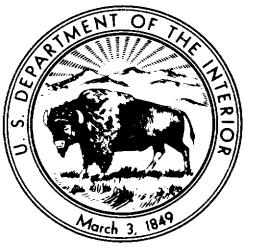

UNITED STATES GOVERNMENT PRINTING OFFICE, WASHINGTON : 1987

DEPARTMENT OF THE INTERIOR

DONALD PAUL HODEL, *Secretary*

U.S. GEOLOGICAL SURVEY

Dallas L. Peck, *Director*

Library of Congress Cataloging-in-Publication Data

The Idaho batholith and its border zone.

(U.S. Geological Survey Professional Paper 1436. Geology of the Blue Mountains region of Oregon, Idaho, and Washington)
Includes bibliographies.
Supt. of Docs. No.: I 19.16:1436
1. Idaho batholith (Idaho and Mont.) I. Vallier, T. L. (Tracy L.) II. Brooks, Howard C. III. Series: U.S. Geological Survey Professional Paper 1436. IV. Series: Geology of the Blue Mountains region of Oregon, Idaho, and Washington.
QE611.5.U6133 1987 552'.3'09796 86-600206

**For sale by the Books and Open-File Reports Section,
U.S. Geological Survey, Federal Center, Box 25425, Denver, CO 80225**

PREFACE

This U.S. Geological Survey Professional Paper is one volume of a series that focuses on the geology, paleontology, and mineral resources of eastern Oregon, western Idaho, and southeastern Washington. The purpose of this series is to familiarize readers with the work that has been completed in the Blue Mountains region and to emphasize the region's importance for understanding island arc processes and the accretion of an allochthonous terrane. These professional papers provide current interpretations of a complex island arc terrane that was accreted to ancient North America in the late Mesozoic Era, of a large batholith that was intruded after accretion had occurred, and of overlying Cenozoic volcanic rocks that were subsequently uplifted and partly stripped off the older rocks by erosion.

Modern island arcs are not well understood, and even less so are ancient arcs that have been deformed, metamorphosed, and subsequently accreted to continents. We have learned that characteristics of modern arcs change significantly both along and across the arcs' axes, and that studies of arc fragments are less than satisfactory because they generally do not characterize an entire arc. For example, the landward trench slopes of arcs can differ greatly, depending on whether materials from the descending slab are being accreted or the slope is being tectonically eroded; which process dominates apparently is related to the volume of sediment in the adjacent trench and the vector of plate convergence. In addition, some arcs (Aleutian) have broad, long, and sediment-filled forearc basins, whereas in others (Tonga-Kermadec) the forearc insular slopes descend precipitously to trench depths and are only interrupted in places by narrow fault-bounded terraces. Moreover, some arcs have erupted primarily tholeiitic igneous products throughout their histories (Tonga-Kermadec) and others (Aleutian) have a long history of both calc-alkaline and tholeiitic eruptive activity. Ridge axes of the arcs may be narrow or broad, and in some arcs (Solomons and Vanuatu) the axial regions have extended to form deep bathymetric and sedimentary basins. Even back-arc basins may have different origins and histories of development. Some (Mariana Trough and Lau Basin) have active spreading ridges whereas others (Aleutian basin of the Bering Sea) are floored by ancient oceanic crust that was trapped behind the arc.

Because our knowledge of the diverse processes within modern arcs is limited, it becomes even more important to study ancient analogues. Just by the nature of their on-land exposures, ancient arcs can provide insights into sedimentary facies, magmatic evolution, and deep crustal processes that can only be studied in modern arcs by geophysical methods, dredging, and drilling. Few ancient island arcs have exposures as well developed and as extensive as those in the Blue Mountains province. Particularly spectacular and helpful are outcrops provided by intensive stream erosion, which has left some canyon walls more than 2 km deep (Snake River canyon west of the Seven Devils Mountains).

Most earth scientists who have worked in the Blue Mountains region agree that the pre-Tertiary rocks there form one or more allochthonous terranes. The importance of such terranes in the evolution of circum-Pacific continental margins has been recognized for about a decade, but many complex questions remain. For example, how, when, and where did most of the circum-Pacific allochthonous terranes form? How did they accrete to continents? What are the mechanisms of amalgamation processes during terrane formation and transport? And, perhaps most importantly, what are the effects of these processes on mineral and hydrocarbon resources? While these volumes provide some answers, the data and interpretations contained in them will no doubt raise new and equally intriguing questions for future generations of earth scientists.

CONTENTS

[Numbers designate the chapters]

1. THE IDAHO BATHOLITH AND ITS BORDER ZONE: A REGIONAL PERSPECTIVE

By TRACY L. VALLIER and HOWARD C. BROOKS[1]

ABSTRACT

The geology of the Idaho batholith and its border zone is interpreted by papers in this volume. The geology of the northern (Bitterroot) lobe of the batholith is well described in chapters by Toth, Reid, Wiswall and Hyndman, and Bittner, who discuss aspects of the petrology, structural geology, emplacement history, and zones of migmatization, respectively. Criss and Fleck concentrate on chemical and isotopic evidence for the origin of the batholith and some of its hydrothermal systems. Onasch discusses the structural geology of the western border zone near Riggins; Bonnichsen describes the geology of the border zone farther south near New Meadows. Lewis and others concentrate their attention on ages, chemical compositions, emplacement history, and source regions of plutons in the southern (Atlanta) lobe of the batholith. Ages of intrusions in the batholith are well constrained by radiometric dating; excluding the complex western border zone, where some plutons from the accreted Blue Mountains island arc terrane may be structurally involved, most plutons composing the batholith crystallized between 95 and 45 Ma. Calc-alkaline volcanism began in central Oregon about 55 Ma, at approximately the same time that the last phase of plutonism began in the Idaho batholith. Major phases of Late Cretaceous and early Tertiary magmatism can be correlated with directions and rates of Farallon and Pacific plate motions.

INTRODUCTION

In this paper we briefly summarize the major findings presented in eight other chapters of this volume and subsequently propose a speculative Late Cretaceous and early Tertiary geologic history of the Oregon-Idaho region that places the Idaho batholith into a time and space setting and that relates its formation in part to movements of oceanic plates in the Pacific basin. These speculations are not new (for example, Coney, 1978), but on the basis of recently published papers of Pacific plate movements and the new radiometric ages and interpretations presented by authors of chapters in this volume, we can offer a more precise correlation scheme.

[1]Oregon Department of Geology and Mineral Industries, Baker, Oregon 97814.

A review of the literature on the Idaho batholith region is beyond the scope of this paper. Important early papers on the batholith and its border zone are by Lindgren (1904), Ross (1928, 1934, 1952, 1965), Langton (1935), Anderson (1942, 1952), Larson and Schmidt (1958), Reid (1959), Hamilton (1963), and Hietanen (1963). Significant later papers, among many others, are by Chase (1973), Greenwood and Morrison (1973), Swanberg and Blackwell (1973), Armstrong and others (1977), Chase and Johnson (1977), Scholten and Onasch (1977), Hyndman (1980, 1983, 1984), Criss and others (1982), and Criss and Taylor (1983). Reid (chapter 3) reviews several important papers in the context of describing the geology of the northern part of the batholith. Our major interpretations of the geology of the Blue Mountains region west of the Idaho batholith can be found in Vallier (1977), Vallier and others (1977), and Brooks and Vallier (1978).

We appreciate the critical reviews of this paper by R.E. Criss, R.J. Fleck, R.R. Reid, Bill Bonnichsen, C.G. Wiswall, D.W. Hyndman, C.M. Onasch, and D.C. Engebretson. Their comments greatly improved both the content and style.

MAJOR CONCLUSIONS OF PAPERS IN THIS VOLUME

This section outlines the major conclusions from papers in the volume. The approximate area of study for each chapter is shown in figure 1.1, and the presentation order follows the table of contents.

Toth (Chapter 2: Petrology and origin of the Bitterroot lobe) presents mineralogic, chemical, and field data on the Bitterroot lobe of the batholith. The Bitterroot lobe consists of foliated tonalite and quartz diorite I-type plutons of Late Cretaceous age that were intruded by voluminous Paleocene monzogranite and granodiorite S-type plutons that form the bulk of the lobe. Subsequently, Eocene

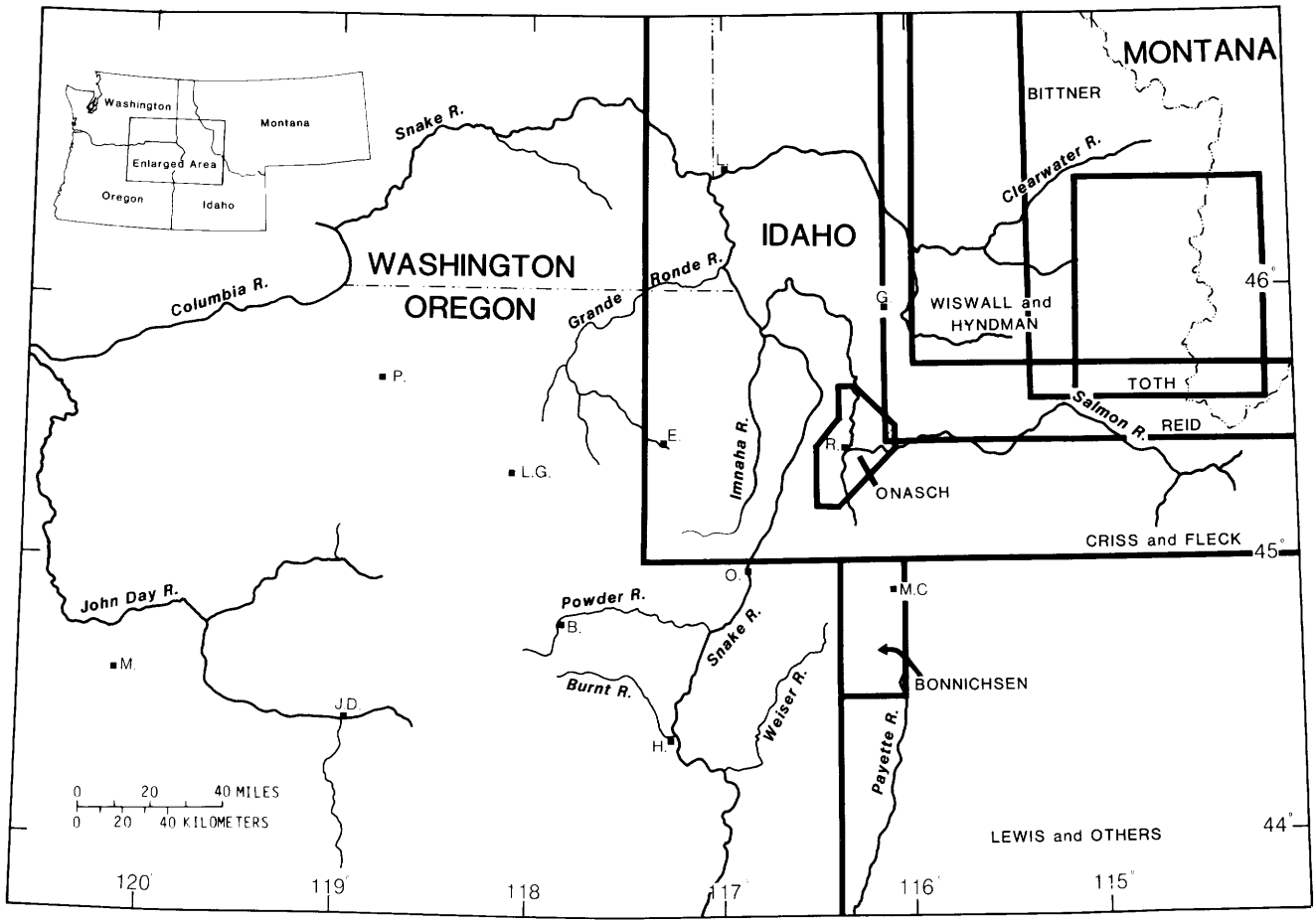

FIGURE 1.1.—Index map showing areas discussed by authors in this volume. Each area is outlined and authors are identified by name within outlined areas. Area discussed by Lewis and others extends below figure a few miles to about latitude 43° N. Abbreviations, approximately from left to right, are M., Mitchell; J.D., John Day; P., Pendelton; L.G., La Grande; B., Baker; H., Huntington; O., Oxbow; E., Enterprise; L., Lewiston; G., Grangeville; R., Riggins; and M.C., McCall.

syenodiorite and quartz syenite A-type high-level plutons intruded the older rocks. The rocks were further injected by several sets of dikes. The oldest I-type plutons show some chemical variations in the western bodies which apparently reflect the assimilation of some Precambrian metasedimentary material. The S-type granitic rocks that form the bulk of the lobe were probably derived from partial melting of metasedimentary material. The A-type syenitic rocks may have been generated as a consequence of regional metamorphism and anatexsis of continental crust. Toth further concludes that most of the oldest plutons were emplaced between 100 and 80 Ma, the voluminous, middle-stage plutons cooled at about 66 to 57 Ma, and the youngest plutons formed 51 to 46 Ma.

Reid (Chapter 3: Structural geology and petrology of a part of the Bitterroot lobe) discusses the influence of structure on the emplacement of the north-central part of the Bitterroot lobe. The granitic massif, which consists of tonalite and younger granite and granodiorite, is zoned vertically from calcic granodiorite at the base to granite at the top. The emplacement of the pluton was synkinematic into an active thrust zone that resulted in a metamorphic core complex. Three phases of deformation were followed by arching. Uplift of as much as 30 km is implied by the data.

Wiswall and Hyndman (Chapter 4: Emplacement of the main plutons of the Bitterroot lobe) compare mineralogic, chemical, and field relations to show that the magmas may have been emplaced mostly by lateral spreading, rather than diapiric rise, which formed a mushroom-shaped body at mesozonal to catazonal depths. Evidence suggests that the northern part of the Bitterroot lobe had a somewhat shallower level of emplacement than the southern part. Different styles of emplacement also are indicated; for example, in the north forcible injection apparently occurred along foliation near the batholith's margins,

whereas in the south the more ductile country rock flowed around the laterally spreading magmas. In spite of these differences in style of deformation, the country rocks and sequence of deformation are similar throughout the Bitterroot lobe of the batholith.

Bittner (Chapter 5: Migmatite zones in the Bitterroot lobe) describes selected migmatite screens within the Bitterroot lobe. She reports that they are oriented largely east-west and presents evidence that the migmatites were derived from the wall and (or) roof rocks. Magma flow from west to east apparently caused the east-west orientation. The migmatite protolith was injected by magmas of several types and, in places, was intricately folded. Five deformational events are recorded.

Criss and Fleck (Chapter 6: Petrogenesis, geochronology, and hydrothermal systems of the northern Idaho batholith area) describe the geochemical character of the northern Idaho batholith and adjacent areas to the west using strontium and oxygen isotopic data, K-Ar ages, Rb/Sr and D/H ratios, and major-element chemical data. In addition, they discuss Late Cretaceous and early Tertiary hydrothermal systems that created many of the region's ore deposits. Older plutons in the western accreted island arc terrane have some chemical characteristics that are compatible with derivation from mantle materials, whereas the main mass of the batholith formed from magmas that probably were derived primarily from Precambrian lower crust rocks and modified somewhat by assimilation of Precambrian wall rocks. The Eocene plutons also have Sr-isotopic values that suggest the presence of a Precambrian rock component in the melts. K-Ar ages of hornblende and biotite range from >125 Ma for typical plutons in the accreted terrane to about 45 Ma for the Eocene granitic rocks. Apparent ages decrease, in general, from west to east across central Idaho. The oldest plutons, discounting those associated with the accreted terrane, yield K-Ar ages of 87 to 75 Ma and are concentrated along the boundary between the island arc rocks of the accreted terrane and the western margin of the Precambrian sialic crust. The younger zone of concordant ages of plutons (51 to 44 Ma) is along the Idaho-Montana border within the Bitterroot lobe. The age pattern in, and adjacent to, the suture zone between the accreted terrane and the sialic crust to the east restricts the age of accretion to the period between about 135 and 75 Ma. Several lines of evidence indicate strong uplift of the batholith during the Late Cretaceous and early Tertiary.

Onasch (Chapter 7: Temporal and spatial relations between folding, intrusion, metamorphism, and thrust faulting in the Riggins area, west-central Idaho) studied the western border zone that includes the suture between the western accreted terrane of ensimatic rocks and the ensialic North American continent. It is an extremely complex region, not only because of multiple stages of metamorphism and thrusting, but also because of the original complicated stratigraphy of the ensimatic rocks of the accreted terrane. Several fold phases were mapped which change along strike of the contact. The time of thrust faulting, however, seems to be nearly synchronous along the contact region. Intrusions of a probable early trondhjemitic phase of the Idaho batholith accompanied the peak of metamorphism. Relative to folding and thrust faulting, the locus of trondhjemitic activity and metamorphism shifted progressively northward through the succession of fold phases. He agrees with Hamilton (1963) that the Rapid River thrust may mark the overlap of two orogens. Faulting apparently took place in the Late Cretaceous.

Bonnichsen (Chapter 8: Pre-Cenozoic geology of the West Mountain-Council Mountain-New Meadows area, west-central Idaho) takes the reader farther south along the contact zone to where parts of the Atlanta lobe of the batholith and the western accreted terrane are juxtaposed. He discusses the area in light of current ideas on both the Blue Mountains region (accreted western terrane) and the Idaho batholith. Ultramafic rocks and quartz-rich sedimentary rocks (chert protolith?) of the western sequence are in contact with metamorphosed rocks of the complicated border zone along a major tectonic boundary. Plutons in the border zone have K-Ar apparent ages of 86 to 80 Ma (biotite) and 120 to 92 Ma (hornblende). One of the plutons (No Business Mountain pluton) is unique to the region because of its alkalic composition; Bonnichsen speculates that it may be part of the continental-margin group of early alkalic plutons that have been described from exposures farther south in California. The metamorphosed rocks of the western terrane probably are part of the ancestral Pacific basin rather than the Precambrian North American continent. The plutons, then, represent early intrusive phases of the Idaho batholith.

Lewis and others (Chapter 9: Lithologic and chemical characteristics of the central and southeastern part of the southern lobe) identify several plutonic phases in the southern (Atlanta) lobe, determine their ages and chemical compositions, and speculate about the depths of emplacement and source regions. In addition, they compare the Bitterroot and Atlanta lobes of the Idaho batholith and the Idaho and Sierra Nevada batholiths. The Atlanta lobe is predominantly biotite granodiorite and muscovite-biotite granite with subordinate amounts of tonalite, hornblende-biotite granodiorite, K-feldspar megacryst granodiorite, and leucocratic granite. The oldest plutons, lying along the western side of the Atlanta lobe, are tonalite with emplacement ages of 95 to 85 Ma. The youngest plutons are the 75- to 70-Ma leucocratic granite plutons. The tonalite plutons yield low radiogenic Sr ratios

and probably formed above a subducting slab, whereas younger plutons have high ratios, probably reflecting partial melting of the lower continental crust with only a minor mantle contribution. The Atlanta and Bitterroot lobes are very similar chemically and mineralogically, although the Atlanta lobe contains no significant foliation and lineation and has no metamorphosed basaltic dikes. The Idaho batholith differs from the Sierra Nevada batholith by having a lower mafic mineral content and by lacking the numerous zoned plutons in sharp contact with one another that is characteristic of the Sierra Nevada batholith. Most differences between the two batholiths can be accounted for by ascribing to differences in water contents of the magmas and in the nature of the source regions.

LATE CRETACEOUS AND EARLY TERTIARY HISTORY

Using mostly the data and interpretations of Engebretson (1982), Vallier and Engebretson (1984), Engebretson and others (1984), Robinson and others (1984), Walker and Robinson (in press), Criss and Fleck (chapter 6), and Lewis and others (chapter 9), we can speculate on major motions of plates in the Pacific and their effects on plutonism and volcanism in the Oregon-Idaho region during the Cretaceous and early Tertiary. A thorough discussion is beyond the scope of this paper, but the correlation of events is surprisingly good and some obvious relations can be pointed out. Several attempts have been made to correlate plate movements with the Laramide orogeny and with magmatism in the Pacific Northwest (for example, Coney, 1978; Ewing, 1980; Engebretson and others, 1984; Henderson and others, 1984; Jurdy, 1984; among many others), and it is apparent that there are close correlations. No attempt has been made, however, to speculate on the relations in the narrow Oregon-Idaho-Montana belt that is described in part by the papers in this volume.

Vallier and Engebretson (1984) stated that the upper Paleozoic through Lower Cretaceous rocks of the Blue Mountains probably were parts of a single allochthonous intra-oceanic island arc composed of several "terranes" and that these rocks have been coherent since at least the Middle Triassic and perhaps since the Early Permian. The island arc may have migrated either from the southwestern Pacific (if it had been part of the Farallon plate) or from the equatorial zone of the eastern Pacific (if attached to the Kula plate). Accretion probably occurred throughout the Early Cretaceous and culminated before 80 Ma. The early part of the arc's history has been discussed by many authors, but in the present paper we discuss only the period between about 135 and 21 Ma. Engebretson (1982) and Engebretson and others (1984) dealt with all known plates in the ancestral Pacific (for example, Farallon, Kula, Izanage, and Phoenix plates) during that time frame, but we emphasize the interactions of the Farallon, Kula, and Pacific plates as they may relate to plutonism and volcanism in the Oregon-Idaho region during the Late Cretaceous and early Tertiary.

The primary ages of plate reorganization are about 135, 85, 56, and 43 Ma (table 1.1). At these times, there were not only changes in directions but also changes in velocities (half-rates) of plate movements. The correlation between plate movements (table 1.1) and plutonic-volcanic sequences in the Idaho-Oregon region (table 1.2) is surprisingly good (table 1.3).

Engebretson's (1982) conclusions include the following major points. (1) Changes in relative plate motion in the ancestral Pacific basin occurred at about 135, 85, and 56 Ma. (2) Spreading rates along the Pacific-Kula ridge uniformly decreased between 72 and 56 Ma. (3) Soon after 56 Ma, a major reorganization in the Pacific-Farallon and Pacific-Kula ridge systems occurred, accompanied by an abrupt increase in Pacific-Kula ridge spreading. The reorganization apparently happened during 56 to 48 Ma. (4) At about 43 Ma, Pacific-Kula ridge spreading ceased and the Kula-Farallon ridge evolved into alignment with the Pacific-Farallon ridge, which increased in spreading rate. (5) The Pacific-Farallon ridge relative motion, however, remained nearly fixed from 48 to 28 Ma.

TABLE 1.1.—*Changes in plate motions within the Pacific basin*

[Data are from Engebretson (1982) and Engebretson and others (1984)]

Time of major plate change (m.y.B.P.)	Pacific-Farallon spreading rate (half-rate, in degrees per million years)	Growth or demise of plates and other changes in plate motion
135------	Increase from 0.31 to 0.45.	Pacific-Izanagi ridge also increases in half-rate spreading, but from 0.43°/m.y. to 1.17°/m.y.
85------	Decrease from 0.43 to 0.36.	Pacific-Kula ridge half-rate spreading decreases from 0.49°/m.y. to 0.16°/m.y.
56------	Increase from 0.36 to 0.67.	Pacific-Kula ridge increases in half-rate spreading from 0.16°/m.y. to 0.65°/m.y. Major reorganization in Pacific, Kula, and Farallon plates.
43------	Increase from 0.74 to 0.99.	Demise of the Pacific-Kula ridge.
48-28------		Pacific-Farallon ridge relative motion fixed.

TABLE 1.2.—*Major plutonic and volcanic events in Oregon and Idaho*

Age (Ma)	Event
135-125-----	Demise of plutonism in the Blue Mountains island arc.
120-85------	Early phase of Idaho batholith intruded along the present western border zone of the batholith (and old North American continent).
85-70-------	Intrusion of most plutons of the Idaho batholith not associated with the western border zone.
65-62-------	Possible pulse of Idaho batholith plutonism (Criss and Fleck, chapter 6) that is not reported in the Atlanta lobe (Lewis and others, chapter 9).
55-40-------	Eruption of calc-alkaline volcanic rocks of the Clarno Formation.
51-46-------	Emplacement of granitic plutons in the Idaho batholith; emplacement of some shallow-level alkalic plutons; eruption of Challis Volcanics.
37-21-------	Eruption of rhyolitic tuffs of the John Day Formation in Oregon, marking early eruptions of Cascade Range volcanoes.

TABLE 1.3.—*Possible correlation of plate movements, uplift, and magmatic events during the period 135 to 21 Ma*

Age (Ma)	Event
135-85----	Accretion of Blue Mountains island arc to the North American continent during increase in spreading rates. Most accretion probably occurred in the late Early and early Late Cretaceous (120-95 Ma). Small plutons emplaced along the present western border zone of the Idaho batholith during 120-85 Ma (Bonnichsen, chapter 8; Toth, chapter 2; Lewis and others, chapter 9). Early thrusting in Idaho probably associated with accretion of the Blue Mountains island arc terrane.
85-56-----	Decrease in spreading rates along both the Pacific-Farallon and Pacific-Kula ridges; a possible low-angle subduction zone beneath the continent may have created the major plutonic phases of the Idaho batholith between 85 and 70 Ma with a possible pulse at 65 to 62 Ma (Criss and Fleck, chapter 6). Emplacement of the Boulder batholith between 78 and 68 Ma (D.W. Hyndman, written commun., 1984). Successively younger parts of the Farallon plate were subducted beneath North America. Gradual uplift of the southern Idaho batholith. Two-mica granites (~72 Ma) cut major overthrusts in eastern Idaho (E.H. Bennett, oral commun, 1986).
56-43-----	Intrusion of the youngest plutons of the batholith (51-46 Ma). Volcanic eruptions responsible for the Clarno Formation and Challis Volcanics. Major volcanism occurred throughout the Pacific Northwest (Ewing, 1980). Increase in spreading rates along both the Pacific-Kula and Pacific-Farallon ridges; major reorganization of plates leading to chaotic distribution of eruptive products during probable changes of subduction angles and directions. Continued and greatly accelerated uplift of the Idaho batholith; some faulting in the overthrust belt of Idaho, Wyoming, and Montana.
43-37-----	Reorganization of plates. Increase in spreading rates and the probable demise of the Pacific-Kula spreading ridge. Change in Pacific plate motion. Decrease in volcanic eruptions and the end of batholith plutonism.
37-21-----	Calc-alkaline volcanism responsible for the John Day Formation from eruptive centers near the present axis of the Cascade Range; unnamed calc-alkaline rocks widespread in central and western parts of the Blue Mountains. Probable westward jump of subduction zone and (or) steepening of the subduction angle; fixed Pacific-Farallon relative motion.

Criss and Fleck (chapter 6) report three major ages of plutonism in the Idaho batholith: 82–75, 65–62, and 51–46 Ma, with averages (K-Ar apparent ages on hornblende) of about 80, 65, and 50 Ma. Lewis and others (chapter 9) provide data on pluton ages of 95 to 70 Ma. Bonnichsen (chapter 8) suggests that there may be an earlier phase (120–92 Ma) of Idaho batholith plutonism along the southern border. Robinson and others (1984) and Walker and Robinson (in press) discuss the Tertiary volcanism in Oregon and extreme western Idaho. Periods of major volcanic eruptions occurred between 55 and 40 Ma, when calc-alkaline volcanic rocks of the Clarno Formation and correlative strata were deposited from local vents within the Blue Mountains, and between 37 and 21 Ma, when the John Day Formation was deposited from vents near the present axis of the Cascade Range. Ewing (1980, p. 622) compiled data that indicate a robust pulse of volcanism during 53 to 42 Ma in the Pacific Northwest.

The K-Ar apparent ages from the western transition (border) zone of the batholith show a broad range, probably because of multiple heating events associated with the Idaho batholith intrusions and because older plutons were structurally involved in the border zone before intrusion of a large part of the batholith. For example, U-Pb dating of separated zircons from a tonalite pluton within the border zone north of Riggins yielded an Early Permian age (N.W. Walker, written commun., 1983), which is the same age as several metamorphosed plutons within the Blue Mountains (Walker, 1983). In addition, Jurassic and Cretaceous (about 165–130 Ma based on K-Ar ages) plutons also have been identified within the border zone (for example, Armstrong and others, 1977). These ages suggest that the older plutons probably were structurally involved during formation of the border—or transitional—zone; thus, the K-Ar ages from this area, which previously had been related to the Idaho batholith per se, should be suspect. We believe that very few, if any, plutons of the Idaho batholith crystallized before 100 Ma.

It is tempting to relate not only the ages of major changes in plate motions to ages of magmatism, but also to faulting events in the overthrust belt of eastern Idaho. On the basis of our limited data base, it would be somewhat presumptuous to conclude that the overthrusting in eastern Idaho was related directly to plate movements and the intrusion and uplift of the Idaho batholith, but the correlation—at least locally—cannot be disregarded. In fact, as pointed out by Hyndman (1980) there may be some cause and effect relations in the Montana-Idaho-Wyoming region of the overthrust belt. The dating of overthrusting, however, is difficult. Hoffman and others (1976) dated K-bentonites from western Montana that they believed had been metamorphosed by the additional load of the overthrust sheets and reported ages of 72 to 56 Ma for the metamorphism. This area was small, and no doubt the ages of thrusting vary along the trend of the overthrust belt. Most thrusting along the eastern edge of the batholith had been completed prior to the intrusion of the 80- to 70-Ma plutons (E.H. Bennett, oral commun., 1986). This means that the thrusting may be related to compressive forces that were exerted during the final accretion of the Blue Mountains island arc terrane to North America. We suspect that the accelerated uplift of the batholith (table 1.3), particularly during the period 56 to 43 Ma, may have been responsible for some late-stage overthrusting in the region.

REFERENCES CITED

Anderson, A.L., 1942, Endomorphism of the Idaho batholith: Geological Society of America Bulletin, v. 53, p. 1099-1126.

_____ 1952, Multiple emplacement of the Idaho batholith: Journal of Geology, v. 60, p. 255-265.

Armstrong, R.L., Taubeneck, W.H., and Hales, P.O., 1977, Rb-Sr and K-Ar geochronometry of Mesozoic granitic rocks and Sr isotopic composition, Oregon, Washington, and Idaho: Geological Society of America Bulletin, v. 88, p. 397-411.

Brooks, H.C., and Vallier, T.L., 1978, Mesozoic rocks and tectonic evolution of eastern Oregon and western Idaho, *in* Howell, D.G., and MacDougall, K.A., eds., Mesozoic paleogeography of the Western United States: Pacific Coast Paleogeography Symposium, 2d, Society of Economic Paleontologists and Mineralogists, p. 133-146.

Chase, R.B., 1973, Petrology of the northeastern border zone of the Idaho batholith, Bitterroot Range, Montana: Montana Bureau of Mines and Geology Memoir 43, 28 p.

Chase, R.B., and Johnson, B.R., 1977, Border-zone relationships of the northern Idaho batholith: Northwest Geology, v. 6-1, p. 38-50.

Coney, P.J., 1978, Mesozoic-Cenozoic cordilleran plate tectonics: Geological Society of America Memoir 152, p. 33-50.

Criss, R.E., Lanphere, M.A., and Taylor, H.P., Jr., 1982, Effects of regional uplift, deformation, and meteoric-hydrothermal metamorphism on K-Ar ages of biotites in the southern half of the Idaho batholith: Journal of Geophysical Research, v. 87, p. 7029-7046.

Criss, R.E., and Taylor, H.P., Jr., 1983, An $^{18}O/^{16}O$ and D/H study of Tertiary hydrothermal systems in the southern half of the Idaho batholith: Geological Society of America Bulletin, v. 94, p. 640-663.

Engebretson, D.C., 1982, Relative motions between oceanic and continental plates in the Pacific basin: Stanford, Calif., Stanford University, Ph.D. dissertation, 211 p.

Engebretson, D.C., Cox, Allan, and Thompson, G.A., 1984, Correlation of plate motions with continental tectonics: Laramide to Basin and Range: Tectonics, v. 3, p. 115-119.

Ewing, T.E., 1980, Paleogene tectonic evolution of the Pacific Northwest: Journal of Geology, v. 88, p. 619-638.

Greenwood, W.R., and Morrison, D.A., 1973, Reconnaissance geology of the Selway-Bitterroot Wilderness Area: Idaho Bureau of Mines and Geology Pamphlet 1543, 30 p.

Hamilton, Warren, 1963, Metamorphism in the Riggins quadrangle, western Idaho: U.S. Geological Survey Professional Paper 436, 95 p.

Henderson, L.J., Gordon, R.G., and Engebretson, D.C., 1984, Mesozoic aseismic ridges on the Farallon plate and southward migration of shallow subduction during the Laramide orogeny: Tectonics, v. 3, p. 121-132.

Hietanen, Anna, 1963, Idaho batholith near Pierce and Bungalow, Clearwater County, Idaho: U.S. Geological Survey Professional Paper 344-D, 42 p.

Hoffman, Janet, Hower, John, and Aronson, J.L., 1976, Radiometric dating of time of thrusting in the disturbed belt of Montana: Geology, v. 4, p. 16-20.

Hyndman, D.W., 1980, Bitterroot dome-Sapphire tectonic block, an example of a plutonic-core gneiss-dome complex with its detached suprastructure, *in* Coney, P.J., Crittenden, M.D., Jr., and Davis, G.H., eds., Cordilleran metamorphic core complexes: Geological Society of America Memoir 153, p. 427-443.

_____ 1983, The Idaho batholith and associated plutons, Idaho and western Montana, *in* Roddick, J., ed., Circum-Pacific plutonic terranes: Geological Society of America Memoir 159, p. 213-240.

_____ 1984, A petrographic and chemical section through the northern Idaho batholith: Journal of Geology, v. 92, p. 83-102.

Jurdy, D.M., 1984, The subduction of the Farallon plate beneath North America as derived from relative motions: Tectonics, v. 3, p. 107-113.

Langton, C.M., 1935, Geology of the northeast part of the Idaho batholith and adjacent region in Montana: Journal of Geology, v. 43, p. 27-60.

Larsen, E.S., and Schmidt, R.G., 1958, A reconnaissance of the Idaho batholith and comparison with the southern California batholith: U.S. Geological Survey Bulletin 1070-A, p. 1-33.

Lindgren, W., 1904, A geologic reconnaissance across the Bitterroot Range and adjacent region in Montana: Journal of Geology, v. 43, p. 27-60.

Reid, R.R., 1959, Reconnaissance geology of the Elk City region, Idaho: Idaho Bureau of Mines and Geology Pamphlet 120, 74 p.

Robinson, P.T., Brem, G.F., and McKee, E.H., 1984, John Day Formation of Oregon: a distal record of early Cascade volcanism: Geology, v. 12, p. 229-232.

Ross, C.P., 1928, Mesozoic and Tertiary granitic rocks in Idaho: Journal of Geology, v. 36, p. 673-693.

_____ 1934, Geology and ore deposits of the Casto quadrangle, Idaho: U.S. Geological Survey Bulletin 854, 135 p.

_____ 1952, The eastern front of the Bitterroot Range, Montana: U.S. Geological Survey Bulletin 974-E, p. 135-175.

_____ 1965, The Idaho batholith: Geological Society of America Special Paper 82, 343 p.

Scholten, R., and Onasch, C.M., 1977, Genetic relations between the Idaho batholith and its deformed eastern and western margins: Northwest Geology, v. 6-1, p. 25-37.

Swanberg, C.A., and Blackwell, D.D., 1973, Areal distribution and geophysical significance of heat generation in the Idaho batholith and adjacent intrusions in eastern Oregon and western Montana: Geological Society of America Bulletin, v. 84, p. 1261-1282.

Vallier, T.L., 1977, The Permian and Triassic Seven Devils Group, western Idaho and northeastern Oregon: U.S. Geological Survey Bulletin 1437, 58 p.

Vallier, T.L., Brooks, H.C., and Thayer, T.P., 1977, Paleozoic rocks in eastern Oregon and western Idaho, *in* Stewart, J., and others, eds., Paleozoic paleogeography of the Western United States: Pacific Coast Paleogeography Symposium, 1st, Society of Economic Paleontologists and Mineralogists, p. 455-466.

Vallier, T.L., and Engebretson, D.C., 1984, The Blue Mountains island arc of Oregon, Idaho, and Washington: an allocthonous terrane from the ancestral Pacific Ocean?, *in* Howell, D.G., and others, eds., Proceedings of the Circum-Pacific Terrane Conference: Stanford University Publications in the Geological Sciences, v. 18, p. 197-199.

Walker, G.W., and Robinson, P.T., in press, Paleocene (?), Eocene, and early Oligocene rocks of the Blue Mountains and adjacent areas, *in* Walker, G.W., ed., Geology of the Blue Mountains region of Oregon, Idaho, and Washington: Cenozoic geology of the Blue Mountains region: U.S. Geological Survey Professional Paper 1437.

Walker, N.W., 1983, Pre-Tertiary tectonic evolution of northeastern Oregon and west-central Idaho: constraints based on U/Pb ages of zircons [abs.]: Geological Society of America Abstracts with Programs, v. 15, p. 371.

2. PETROLOGY AND ORIGIN OF THE BITTERROOT LOBE OF THE IDAHO BATHOLITH

By MARGO I. TOTH

ABSTRACT

The Bitterroot lobe of the Idaho batholith was emplaced in Cretaceous and Paleocene time into highly deformed Proterozoic metasedimentary rocks east of a subduction zone that was active until at least Triassic(?) time. The lobe consists of foliated tonalite and quartz diorite plutons intruded by voluminous foliated monzogranite and granodiorite plutons. Younger epizonal syenogranite and quartz syenite plutons partially encircle the northern, western, and southern sides of the lobe.

Hornblende-biotite tonalite and quartz diorite were emplaced in Cretaceous time into lower mesozonal levels as small isolated plutons that now mark the western and northeastern margins of the lobe. They are most similar to I-type granite and were probably derived by partial melting of metaigneous source rocks involving an upper-mantle component. However, chemical variation is large in some of these plutons, reflecting varying degrees of assimilation of Precambrian metasedimentary material.

Foliated muscovite-biotite granodiorite and monzogranite plutons, intruded into mesozonal or upper mesozonal levels during Paleocene time, form the bulk of the Bitterroot lobe. They are chemically homogeneous, suggesting that they belong to a single comagmatic suite, but they can be distinguished on the basis of mineralogical and textural differences. The plutons show characteristics of S-type granites and were most likely derived by partial melting of relatively homogeneous metasedimentary rocks of the Middle Proterozoic Belt Supergroup or pre-Belt material. Rare-earth-element patterns indicate strong fractionation, possibly reflecting residual hornblende in the source rock, and Eu anomalies are generally very small.

The youngest mesozonal pluton is chemically and mineralogically zoned, from a hornblende-biotite granodiorite rim to a hornblende-biotite monzogranite core. Biotite, hornblende, and minor plagioclase crystallized early and accreted along the outer margins of the pluton with some trapped magma to form the granodiorite. The remaining magma was displaced inward to form the monzogranite. This pluton is an I-type granite, and its intrusion marked a radical change in the petrology and the source region for the mesozonal granitic rocks of the lobe.

Nonfoliated Eocene syenogranite and quartz syenite plutons, partially encircling the lobe, were intruded into epizonal levels as shallow as 1.5 km and in at least one place intrude their own volcanic ejecta. The plutons are characterized chemically by high SiO_2, high $K_2O + Na_2O$, high K_2O/Na_2O, and low CaO. They show strong enrichment of incompatible elements such as La, Nb, Sn, and Y and large negative Eu anomalies (Eu/Eu^* as low as 0.3). These plutons are most similar to A-type granite, and the magmas were probably derived by partial melting of relatively felsic granulite in previously depleted lower crust.

Large dike complexes and isolated dikes of diorite, quartz diorite, and tonalite are abundant in the granitic rocks in the central and southern parts of the lobe. Some of these intrusive bodies show synplutonic relations with the host granitic rocks. However, chemical characteristics indicate they are mantle derived and have ingested various amounts of crustal material during emplacement. Original emplacement of these magmas into the crust may have provided some of the heat necessary for partial melting and formation of the granitic magmas. The occurrence of similar dikes in other batholithic terranes may imply a similar causal relation to the generation of granitic magmas.

INTRODUCTION

In 1978 the U.S. Geological Survey undertook a five-year study to assess the mineral resources of the Selway-Bitterroot Wilderness, which comprises 1.25 million acres in Idaho and western Montana (fig. 2.1) and encompasses much of the central and southern parts of the Bitterroot lobe of the Idaho batholith. This paper describes the field relations and petrology of the granitic rocks of the lobe within and adjacent to the wilderness, studied in conjunction with the mineral-resource appraisal. These observations, combined with geochemical and isotopic data and with considerations of regional geology, provide a framework for interpreting the origin and evolution of the granitic rocks in the Bitterroot lobe.

The wilderness program utilized extensive helicopter support and consisted of geologic mapping at 1:24,000 scale, sampling of stream sediments and rocks for trace-element and major-element analyses, and a geophysical study. Geological and geochemical maps were produced at 1:125,000 scale (Coxe and Toth, 1983a; Toth, 1983a; Toth and others, 1983) along with geophysical reports (Brickey and others, 1980; Bankey and others, 1982) and detailed reports on the geology of certain areas within the wilderness (Lund, 1980; Bradley, 1981; Motzer, 1981; Bittner, chapter 5; Bittner-Gaber, 1983; Garmezy, 1983; Toth, 1983b; Reid, chapter 3). Major-element and trace-element analyses of stream sediments and rock samples

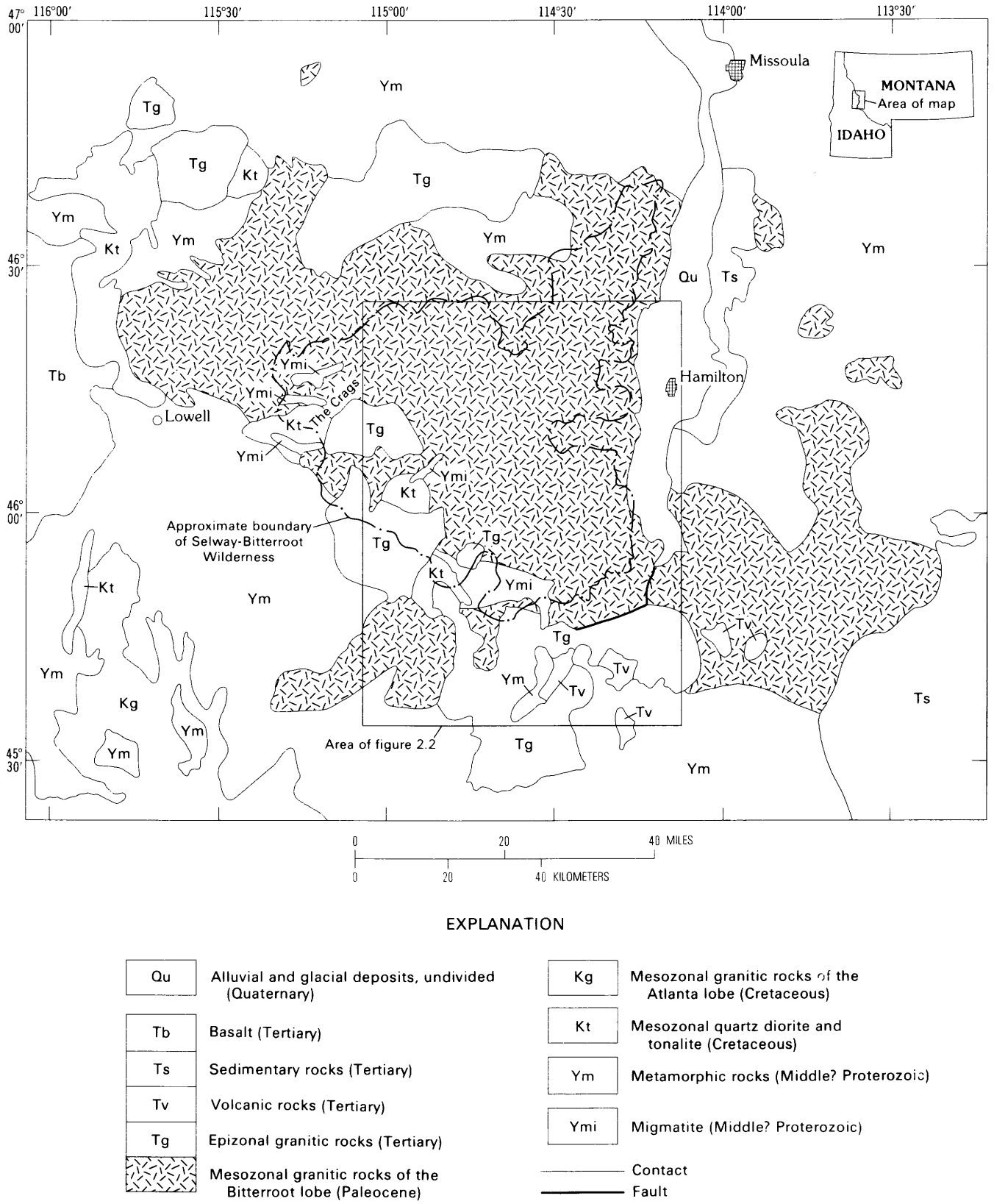

FIGURE 2.1.—Simplified geologic map of the Bitterroot lobe of the Idaho batholith and adjacent areas. Modified from Bond (1978), Lund and others (1983), and Toth (1983a).

were done by U.S. Geological Survey laboratories in Denver, Colorado, and the geochemical data and methods of analyses are presented in Coxe and others (1982), Koesterer and others (1982), Coxe and Toth (1983a, 1983b), and Toth (1983b). Some of the major-oxide data were recalculated into mesonorms (Kosinowski, 1982) assuming an $FeO:Fe_2O_3$ ratio of 2:1 and are presented in Toth (1983b). Microprobe analyses and methods of study are also presented in Toth (1983b).

Granitic rocks in this paper are classified according to Streckeisen and others (1973). I have also classified them according to their probable source rocks (Chappell and White, 1974; Loiselle and Wones, 1981; Collins and others, 1982) in an attempt to understand the generation of the magmas of a batholith and their evolution through time. The granites are designated as "I-type" (igneous), "S-type" (sedimentary), or "A-type" (restite), referring to their origin by partial melting of igneous source rock, pelitic material, or restite material, respectively. The different source rocks are reflected in the mineralogy, chemistry, and field occurrence of the resultant plutons (table 2.1). Although this classification is a useful tool, some granites do not fit within these guidelines, especially those with complex histories involving fractionation or contamination; many granites also show characteristics of both S- and I-type (Lee and Christiansen, 1983). The depths of emplacement for the various plutons of the lobe were estimated on the basis of structural criteria as outlined by Buddington (1959) and of mineralogical criteria.

In this report FeO* refers to total iron as FeO. Rare-earth-element concentrations were normalized to the chondritic abundances of Hanson (1980).

TABLE 2.1.—*Characteristics of S-, I-, and A-type granites*
[Modified from Chappell and White (1974), Collins and others (1982), and Loiselle and Wones (1981)]

S-type granite
1. Contains muscovite ± garnet, cordierite, sillimanite, and andalusite.
2. Contains ilmenite as an accessory mineral.
3. Molecular proportion $Al_2O_3/Na_2O + K_2O + CaO > 1.1$.
4. Relatively low sodium: $Na_2O < 3.2$ percent in rocks with 5 percent K_2O; $Na_2O < 2.2$ percent in rocks with 2 percent K_2O.
5. Relatively restricted in composition to high-silica types with 66-77 percent SiO_2.
6. Irregular variation diagrams.
7. Initial Sr ratios >0.708, isochrons show scatter of points, possible homogenization of strontium or heterogeneous source.
8. Associated with regional metamorphism up to amphibolite grade; migmatites and xenoliths of metasedimentary rocks common.
9. Normative corundum >1 percent in CIPW norm.
I-type granite
1. No peraluminous minerals; contains hornblende, sphene.
2. Contains magnetite as an accessory mineral.
3. Molecular proportion of $Al_2O_3/Na_2O + K_2O + CaO < 1.1$.
4. High sodium, commonly higher than 3.2 percent in felsic varieties, decreasing to <2.2 percent in more mafic types.
5. Broad spectrum of compositions.
6. Linear variation diagrams.
7. Low initial Sr ratios, 0.704-0.706.
8. Rarely associated with regional metamorphism or migmatites.
9. Normative corundum <1 percent in CIPW norm.
A-type granite
1. Contains Fe-rich minerals such as annite; feldspar is mostly alkali feldspar.
2. Mildly alkaline with low CaO and Al_2O_3.
3. High K_2O and high K_2O/Na_2O.
4. Enriched in incompatible trace elements but showing strong negative Eu anomalies.
5. Variable initial Sr ratios from 0.703 to 0.712.
6. F and Cl contents in the magmas are high.
7. Intruded late in the magmatic cycle; commonly associated with tensional tectonic regimes.

ACKNOWLEDGMENTS

Many geologists have made contributions to this work, and I would like to acknowledge particularly the assistance and collaboration of Rolland R. Reid, William R. Greenwood, Enid Bittner-Gaber, Lawrence Garmezy, Dirk S. Hovorka, Mary E. Koesterer, Karen I. Lund, Warren M. Rehn, and William E. Motzer. Although this paper is partly based on their mapping and petrologic work, the interpretations presented here are my sole responsibility. This paper benefited from reviews by Don E. Lee and Alan R. Wallace of the U.S. Geological Survey.

PREVIOUS WORK

The earliest descriptions of the granitic rocks of the Bitterroot lobe were based on large-scale reconnaissance projects by Lindgren (1900, 1904) and Anderson (1930). Williams (1977, p. 8-12) presents a comprehensive review of studies done since those early geologists. Because of the inaccessibility of the interior of the Bitterroot lobe, most earlier work was concentrated along the more accessible northeastern and eastern margins of the lobe. Prior to the present study, a reconnaissance investigation by the Idaho Bureau of Mines from 1965 to 1968 (Greenwood and Morrison, 1973) was the only study made of the central and southern parts of the Bitterroot lobe.

GENERAL GEOLOGY

The Idaho batholith is 390 km long and 80 to 160 km wide and extends from north-central Idaho and western Montana to southern Idaho, where it is covered by basalt of the Snake River Plain. A probable arch of Proterozoic metasedimentary rocks divides the batholith into two parts (Armstrong, 1975): the Atlanta lobe in the south and

the smaller and younger Bitterroot lobe, the subject of this paper, in the north (fig. 2.1). Forming a northwest-trending tabular body, the Bitterroot lobe underlies approximately 14,000 km^2 and intrudes Proterozoic metasedimentary rocks that are correlated with the Belt Supergroup-correlative Yellowjacket Formation and Lemhi Group to the south and southwest. The western margin of the lobe is in contact with allochthonous metavolcanic and metasedimentary rocks of probable Mesozoic age that were emplaced along a suture between a western Paleozoic and Mesozoic volcanic arc terrane and an eastern continental terrane (Hamilton, 1976). Metamorphic grade in the country rocks surrounding the batholith increases from greenschist facies to upper amphibolite facies close to the contact, but this zoning is locally truncated by granodiorite and monzogranite plutons near the northern end of the batholith (Nold, 1968). The northeastern contact with the country rock is relatively sharp and mostly concordant in outcrop. However, the northeast border of the batholith consists of a zone as much as 15 to 20 km wide of numerous screens of metasedimentary rock hundreds of meters thick and showing varying degrees of assimilation and injection by the granitic rocks (Bradley, 1981).

Cretaceous plutons of foliated hornblende-biotite tonalite and quartz diorite form the western border of the Bitterroot lobe, and similar rocks also are present along the northeastern border as isolated plutons (not shown in figure 2.1). Paleocene mesozonal plutons of foliated muscovite-biotite granodiorite and monzogranite form the major part of the lobe and intrude the tonalite and quartz diorite on the west, southwest, and north. Complex migmatite terranes sometimes separate different plutons (figs. 2.1, 2.2) and involve septa of Middle(?) Proterozoic and possibly older metasedimentary rocks. The appearance, chemistry, and mineralogy of the granitic rocks are fairly homogeneous, but the recent work of Williams (1977), Toth (1983b), and Hyndman (1984) has outlined at least ten plutons with different textural and (or) chemical variations; more plutons may be present but as yet unidentified.

Large Eocene epizonal plutons of subalkalic syenogranite and quartz syenite intrude the Proterozoic metasedimentary rocks and all the earlier igneous phases of the Bitterroot lobe along the northern, southwestern, and southern sides (fig. 2.1). Granophyric textures and fluorite-filled miarolitic cavities are common in these plutons. An extensive network of northeast-trending rhyodacite and rhyolite dikes extends outward from all of the plutons and crosscuts all older lithologic units. Rhyolitic to andesitic tuff and lava flows are preserved in two places in down-dropped fault blocks and locally overlie parts of the epizonal plutons on the south side of the Bitterroot lobe (Lund and others, 1983).

A 200- to 500-m-thick mylonite zone, which has a shallow eastward dip, borders the eastern and southeastern sides of the Bitterroot lobe, adjacent to the Bitterroot River valley, Montana (fig. 2.2). The mylonite zone is younger than all other rock units except the epizonal plutons. Its formation has been attributed to gravity sliding of an overlying block (Hyndman, 1977), to emplacement-related phenomena (Garmezy and Greenwood, 1981), and to extensional tectonism or crustal thinning (Garmezy, 1983). Mylonitic textures in the granodiorite and monzogranite plutons extend into the center of the lobe.

Two types of faults are widely distributed throughout the Bitterroot lobe and are most evident in the higher elevations, where vegetation is sparse. The more common type consists of normal faults with a consistent trend of azimuth 020° that dip dominantly to the southeast and crosscut all lithologic units. Offsets average 4 to 10 m but are as much as 1.5 km along a few of the more extensive faults (Lund, 1980). A steep normal fault along the eastern and southeastern margins of the Bitterroot lobe separates the mesozonal mylonitic rocks of the batholith to the west from younger and shallower, upper mesozonal to epizonal rocks to the east and southeast. The absence of mesozonal granitic rocks south and east of the fault suggests that major postbatholithic uplift along this fault exposed the more deeply emplaced plutons of the Bitterroot lobe (Garmezy, 1983). The second type of faults trends northwestward and consists of thrust faults that have shallow dips to the southwest and are pre-Eocene in age. Offsets of as much as 10 m were measured, and they may be greater because the faults crosscut relatively homogeneous rock units in which offset is difficult to determine.

TECTONIC SETTING

The Idaho batholith is one in a chain of probably subduction-related granitic batholiths extending from Alaska to Mexico along the western cordillera of North America and emplaced during the Mesozoic. In age and petrology the Idaho batholith is similar to the other granitic batholiths, but it is anomalous in its position at the eastern border of the Columbia arc and in its emplacement into mostly Proterozoic continental and miogeoclinal metasedimentary rocks instead of Phanerozoic eugeoclinal rocks. Small Cretaceous tonalite, diorite, and quartz diorite plutons along the western margin of the Bitterroot lobe intrude eugeoclinal accretional complexes formed in Triassic(?) time (Hamilton, 1963), or possibly

FIGURE 2.2.—Geologic map of the central part of the Bitterroot lobe of the Idaho batholith showing different plutonic units.

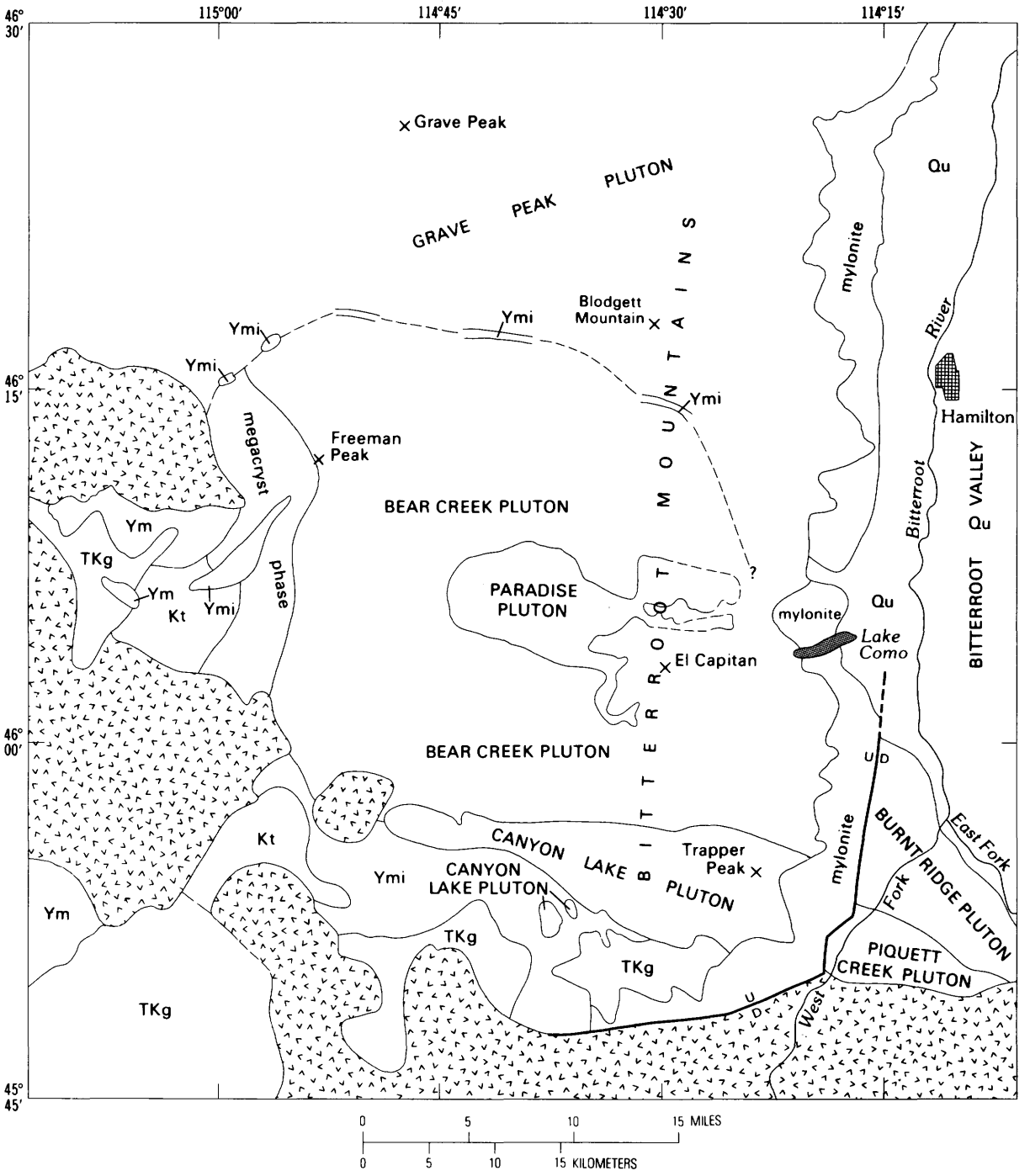

EXPLANATION

- Qu — Alluvial and glacial deposits (Quaternary)
- Epizonal granitic rocks (Tertiary)
- TKg — Mesozonal granitic rocks of the Bitterroot lobe, undifferentiated (Paleocene)
- Kt — Mesozonal quartz diorite and tonalite (Cretaceous)
- Ym — Metamorphic rocks (Middle? Proterozoic)
- Ymi — Migmatite (Middle? Proterozoic)
- Contact — Dashed where inferred
- Fault — Dashed where inferred; U, upthrown side; D, downthrown side

as late as Late Jurassic into Cretaceous time (T.L. Vallier, written commun., 1984). According to Hamilton (1978), these accretional complexes are the youngest direct evidence of subduction along the northwest margin of the continent. Farther east, the younger and more abundant tonalite and quartz diorite plutons of the Bitterroot lobe were intruded into Precambrian metasedimentary rocks in latest Cretaceous time, probably long after subduction had ceased along the western margin. Furthermore, the more voluminous granitic rocks were not intruded until the Paleocene. Thus, in contrast to many other batholiths in the western cordillera, a direct time relationship cannot be established between subduction and plutonism for most of the Idaho batholith.

Extensional tectonism in the Bitterroot lobe as early as 51 Ma is documented by the emplacement of the structureless epizonal Whistling Pig pluton (Lund, 1980; K-Ar age on hornblende, R.J. Fleck, written commun., 1981), but it may have begun as early as 54 Ma (Toth, 1983b) with the intrusion of the Paradise pluton. This tectonism involved widespread normal faulting and crustal thinning (Garmezy, 1983) and continued during emplacement of the other epizonal plutons surrounding the lobe.

AGE OF THE BITTERROOT LOBE

The study of the geochronology of the Bitterroot lobe, as described by Garmezy (1983), has been hampered by the effects of several major penecontemporaneous events including mylonitization, rapid uplift of the lobe, and the thermal effects from the intrusion of Eocene epizonal plutons. Nevertheless, U-Pb study of different zircon size-fractions, combined with K-Ar, Ar-Ar, and some Rb-Sr work has outlined the major intrusive episodes (fig. 2.3).

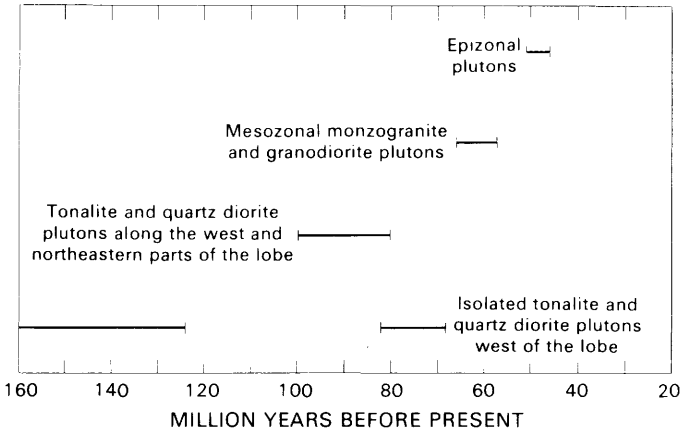

FIGURE 2.3.—Summary of geochronology of the Bitterroot lobe of the Idaho batholith. Data from Armstrong and others (1977), Chase and others (1978, 1983), Bickford and others (1981), and J.S. Stacey (written commun., 1982).

The tonalite and quartz diorite plutons along the western and northeastern margins of the Bitterroot lobe were emplaced between 100 Ma and 80 Ma (Ferguson, 1972, 1975; Chase and others, 1978; R.J. Fleck, written commun., 1981; J.S. Stacey, written commun., 1982). A few satellite quartz diorite, diorite, and tonalite plutons to the west of the main body of the lobe are the only rocks that give ages greater than 100 Ma (Armstrong and others, 1977; J.S. Stacey, written commun., 1982). Chase and others (1978, 1983), Bickford and others (1981), and J.S. Stacey (written commun., 1982) have identified a Proterozoic zircon component in the volumetrically more important granodiorite and monzogranite plutons of the Bitterroot lobe and have derived a latest Cretaceous and Paleocene emplacement age of 66 to 57 Ma for the bulk of the rocks. This major emplacement episode was closely followed by the intrusion of the epizonal plutons between 51 and 46 Ma.

ISOTOPIC DATA

Work by Armstrong and others (1977) and Criss and Fleck (1983) has shown that all the plutonic rocks west of the boundary between Phanerozoic eugeoclinal rocks and Precambrian crust in Idaho have initial Sr ratios less than 0.7043, and all those east of it have initial ratios greater than 0.7055; there are no known exceptions to this observation. The Bitterroot lobe lies to the east of that boundary and is surrounded on three sides by Middle Proterozoic Belt Supergroup or pre-Belt metasedimentary rocks. Chase and others (1978) studied granodiorite and monzogranite plutons along the northeastern border of the Bitterroot lobe and obtained high initial Sr ratios ranging from 0.7103 to 0.7128. R.J. Fleck (written commun., 1978–1982) and Criss and Fleck (1983) found that the rocks in the rest of the lobe have more scattered and also high initial Sr ratios (0.7070–0.7190) and that points on Rb-Sr diagrams generally failed to define isochrons, results similar to those of Armstrong and others (1977) and Chase and others (1978). They also found that initial Sr ratios in the tonalite and quartz diorite plutons increase in proximity to the screens of Precambrian migmatites.

TONALITE AND QUARTZ DIORITE PLUTONS

Minor amounts of tonalite and quartz diorite are present along the western and southwestern border of the Bitterroot lobe (fig. 2.1) and along the northeastern margin as small isolated plutons (not shown in fig. 2.1). Field evidence for individual plutons along the western border of the lobe is absent, and it is possible that the tonalite and quartz diorite magmas were emplaced simultaneously as a single intrusion. The structure of these rocks and their relationship to the Precambrian

country rock are described in detail elsewhere in this volume (Reid, chapter 3). Large migmatite screens commonly separate the quartz diorite and tonalite plutons from younger monzogranite and granodiorite plutons.

In hand specimen the tonalite and quartz diorite are gneissic to well foliated, gray, equigranular, and medium to more rarely fine grained, and contain accessory biotite and euhedral hornblende. Tonalite composition is more common than quartz diorite (fig. 2.4). In thin section, oligoclase (average An_{27}, optical determination) forms subhedral to euhedral unzoned grains, which generally have sutured boundaries and are bent or fractured. Quartz showing undulatory extinction forms granoblastic grains, the larger of which are elongate parallel to biotite and have developed tails of annealed subgrains. Some of the samples contain anhedral microcline (1–5 percent). Brown biotite shows minor alteration to pennine and rutile, and green hornblende makes up from 0 to 26 percent of the rock, increasing in abundance westward. Accessory minerals in the tonalite and quartz diorite include sphene, epidote, apatite, prismatic zircon, allanite, magnetite, and thorite.

Four analyzed samples of tonalite and quartz diorite from the western part of the Bitterroot lobe (table 2.2) have compositions ranging from 60 to 69 percent SiO_2 and from 2.8 to 3.7 percent Na_2O. The fairly wide range in $Na_2O + K_2O$ (fig. 2.5) possibly reflects varying amounts of assimilated Precambrian rock. One sample high in $Na_2O + K_2O$ was taken adjacent to a screen of pelitic migmatite, indicating local assimilation of Na + K-rich Precambrian material. The ratio of molecular $Al_2O_3/CaO + K_2O + Na_2O$, generally an index of alumina

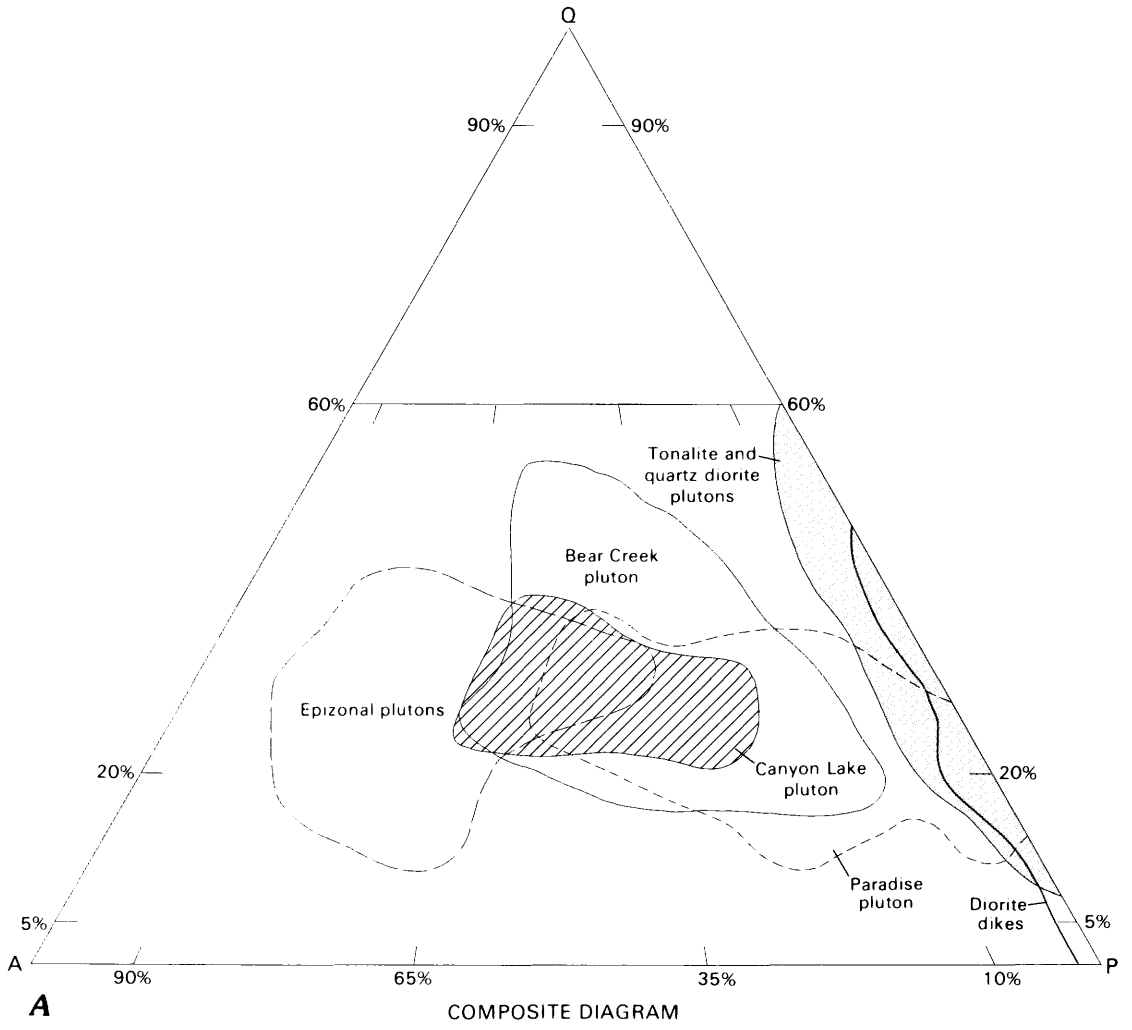

FIGURE 2.4.—Composite triangular diagram and triangular modal plots for some plutonic phases of the Bitterroot lobe of the Idaho batholith. A, alkali feldspar; P, plagioclase; Q, quartz. Boundaries from Streckeisen and others (1973). Total number of samples, n. Data for tonalite and quartz diorite plutons from R.R. Reid (written commun., 1982) and for epizonal plutons from W.E. Motzer (written commun., 1982). *A*, Composite diagram. *B*, *C*, Modal plots.

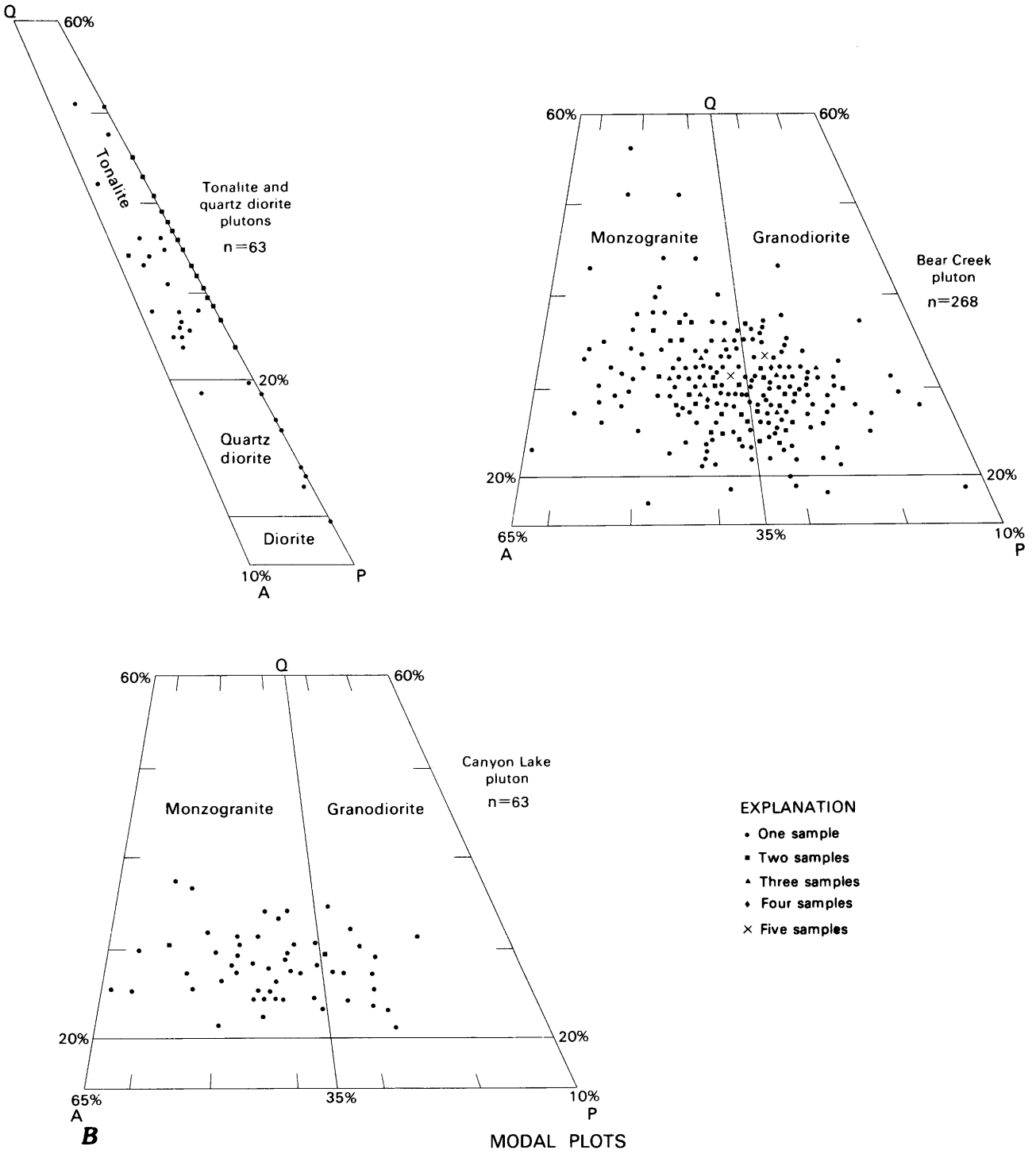

FIGURE 2.4.—Continued.

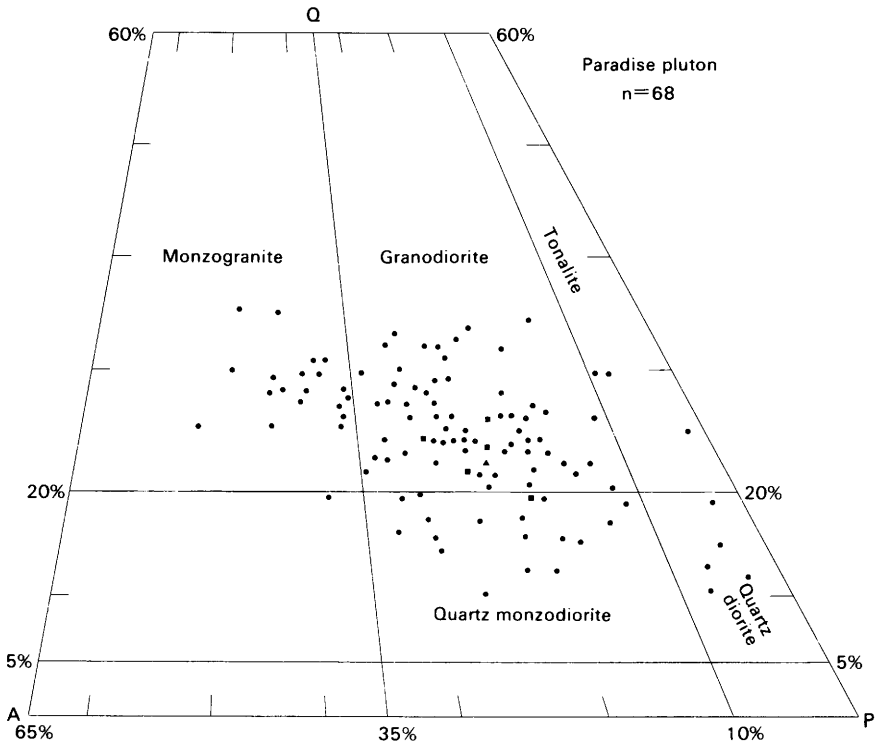

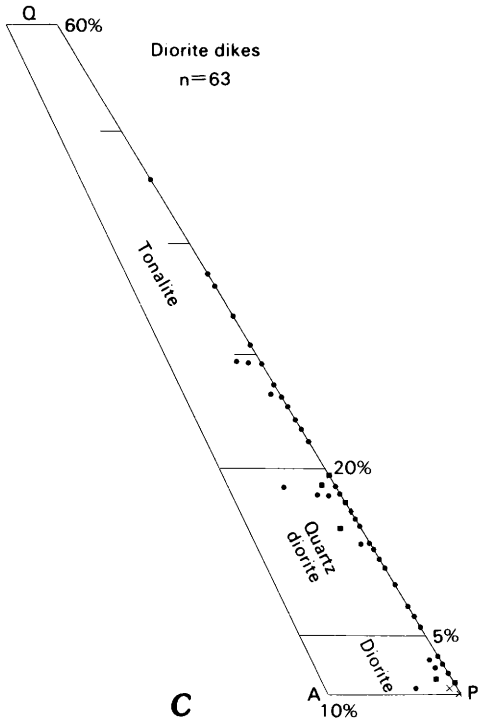

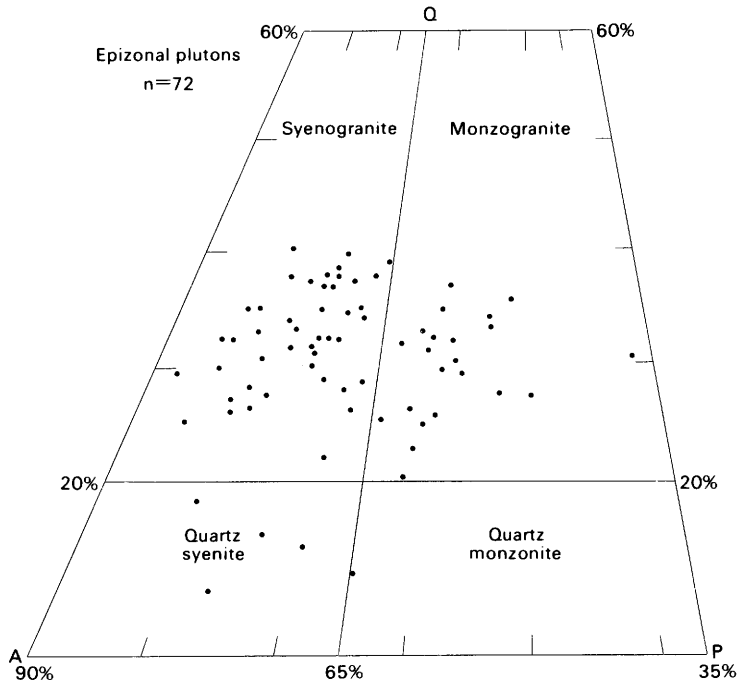

FIGURE 2.4.—Continued.

TABLE 2.2.—*Representative major-element analyses, normative mineral calculations,*

[A value followed by L indicates that the element was not detected at the indicated lower detection limit; n.d., not determined; LOI, loss of water upon ignition; Fe_2O_3 is total iron. DI, epizonal syenogranite and quartz syenite plutons from R.R. Reid

Pluton	Quartz diorite and tonalite pluton(s)				Bear Creek pluton				
Sample	78RR078	78RR095	78RR138	78RR132	80MT185	80MT220	80MT080	80MT142	80MT254
Lithology	Tonalite	Tonalite	Tonalite	Quartz diorite	Monzo-granite (core)	Monzo-granite (core)	Grano-diorite (rim)	Grano-diorite (rim)	Quartz diorite (zone I)
Major oxide analyses									
SiO_2	64.11	60.19	69.34	65.49	72.5	72.8	71.4	70.5	63.0
Al_2O_3	16.49	16.99	15.87	15.97	15.4	15.7	14.7	15.5	16.6
Fe_2O_3	5.15	7.78	2.29	4.68	1.33	1.22	1.75	2.11	4.55
MgO	2.19	2.98	.67	1.58	.30	.40	.74	.76	2.90
CaO	3.92	4.42	1.96	3.49	1.66	2.46	1.65	1.80	4.12
Na_2O	3.74	3.48	3.41	2.77	4.00	4.80	3.70	3.80	4.30
K_2O	2.07	2.47	4.04	1.78	4.00	2.16	4.41	4.13	2.87
TiO_2	.66	.92	.30	.59	.15	.14	.28	.29	.68
P_2O_5	.27	.29	.07	.13	.01L	.01L	.10	.20	.20
MnO	.05	.10	.03	.05	.02L	.02L	.02L	.03	.07
ZrO_2	.03	.04	.02	.05	n.d.	n.d.	n.d.	n.d.	n.d.
LOI	n.d.	n.d.	n.d.	n.d.	.52	.34	.59	.41	.55
Total	98.83	99.82	98.22	96.83	99.86	100.02	99.3	99.53	99.84
Molecular $Al_2O_3/CaO+K_2O+Na_2O$	1.07	1.04	1.17	1.25	1.11	1.11	1.06	1.10	.94
Mesonorms									
Q	26.7	21.7	29.9	35.4	30.4	31.3	29.6	29.2	17.6
Ab	31.7	29.5	28.9	23.5	33.9	40.7	31.3	32.2	36.4
Or	3.4	2.0	20.6	3.4	22.0	10.9	23.0	21.0	9.0
An	17.7	20.0	9.3	16.5	7.9	11.9	7.5	7.6	16.0
Bi	14.3	20.5	5.3	11.6	2.8	3.3	4.9	5.5	12.6
Hb	0.0	0	0.0	0	0	0	0	0	4.8
Mt	2.5	3.8	1.1	2.3	.6	.6	.8	1.0	2.2
Il	0.6	0.9	0.3	0.6	.1	.1	.3	.3	0.6
R	-0.6	-0.8	-0.2	-0.5	.4	.2	.4	0	-0.4
Ap	0.6	1.2	0.2	0.3	.1	.1	.2	.5	0.5
C	1.6	0.7	2.5	3.4	1.6	1.1	1.1	2.0	0
D.I.	61.8	73.2	79.4	62.3	86.2	82.9	84.0	82.4	63.0
Modal analyses									
Quartz	25	28	3	16	28	29	30.5	30.5	9.0
Plagioclase	57	59	51	45	42	42	42	43.5	63.5
K-spar	0	3	0	0	27	25	20	20.5	5
Biotite	18	9	42	35	3	4	7.5	5.5	12
Hornblende	0	0	0	3	0	0	0	0	9.5
Accessories	0	1	4	0	0	0	0	0	1

and modal compositions of rocks from the Bitterroot lobe of the Idaho batholith

differentiation index Q+Ab+Or. Major oxide analyses and mesonorms in weight percent; modal analyses in volume percent. Modal analyses of tonalite and quartz diorite plutons and and W.E. Motzer, respectively (written commun., 1982)]

Paradise pluton				Epizonal syenogranite and quartz syenite plutons			
81MT134 Granodiorite (zone II)	80MT258 Granodiorite (zone III)	80MT017 Monzogranite (zone IV)	80MT138 Tonalite (upper contact)	78WM010 Syenogranite	78WM018 Syenogranite	78WM060 Syenogranite	78WM020 Syenogranite
			Major oxide analyses				
66.4	70.0	72.5	62.6	77.3	72.0	73.7	76.6
16.0	15.4	15.2	16.5	12.4	13.9	13.4	12.7
2.95	2.24	1.28	5.03	1.37	2.58	2.15	1.18
1.71	.78	.60	3.25	.10L	.20	.20	.10
3.06	2.08	1.77	4.50	.20	.61	.62	.34
4.10	4.25	3.79	3.91	3.40	3.30	3.50	3.20
3.40	3.27	4.35	1.93	4.86	5.91	5.34	5.19
.49	.41	.32	.71	.12	.25	.20	.09
.14	.15	.01L	.16	.010L	.10L	.10L	.10L.
.03	.06	.01L	.09	.02L	.02	.02	.02L
n.d.	n.d.	n.d.	n.d.	n.d.	n.d.	n.d.	n.d.
.25	.48	.32	.59	.66	.87	.42	.34
98.53	99.12	100.13	99.28	99.0	99.7	99.6	99.8
1.00	1.07	1.05	.99	1.36	1.01	1.08	1.11
			Mesonorms				
23.2	26.2	29.4	23.2	38.4	28.8	31.4	38.4
34.7	36.0	33.0	33.1	28.8	28.0	29.6	28.8
13.9	14.2	23.2	0.1	27.5	32.6	29.5	27.5
14.3	11.0	8.5	21.3	1.0	3.0	3.1	1.0
9.9	8.2	4.0	18.1	2.1	4.1	3.5	2.1
0	0	0.0	0.0	0.0	0.0	0.0	0.0
1.4	0	0.7	2.4	0.7	1.2	1.0	0.7
.5	0.4	0.2	0.7	0.1	0.2	0.2	0.1
-0.2	0.1	0.2	-0.1	0.6	0.7	0.3	0.6
.3	0.4	0.1	0.4	0.0	0.0	0.0	0.0
.3	0.4	0.9	0.2	1.2	1.0	0.7	1.2
71.8	76.4	85.6	56.3	84.7	89.4	90.5	94.7
			Modal analyses				
19	25.5	29	26	33	24	32.5	40
51	54	39	46.5	52	59	48	46
16	11.5	27	2.5	13	11	15	12
8	6	3.5	15	2	1	2.5	2
6	3	1	10	.3	5	1.5	0
0	0	0	0	.2	.7	.4	.2

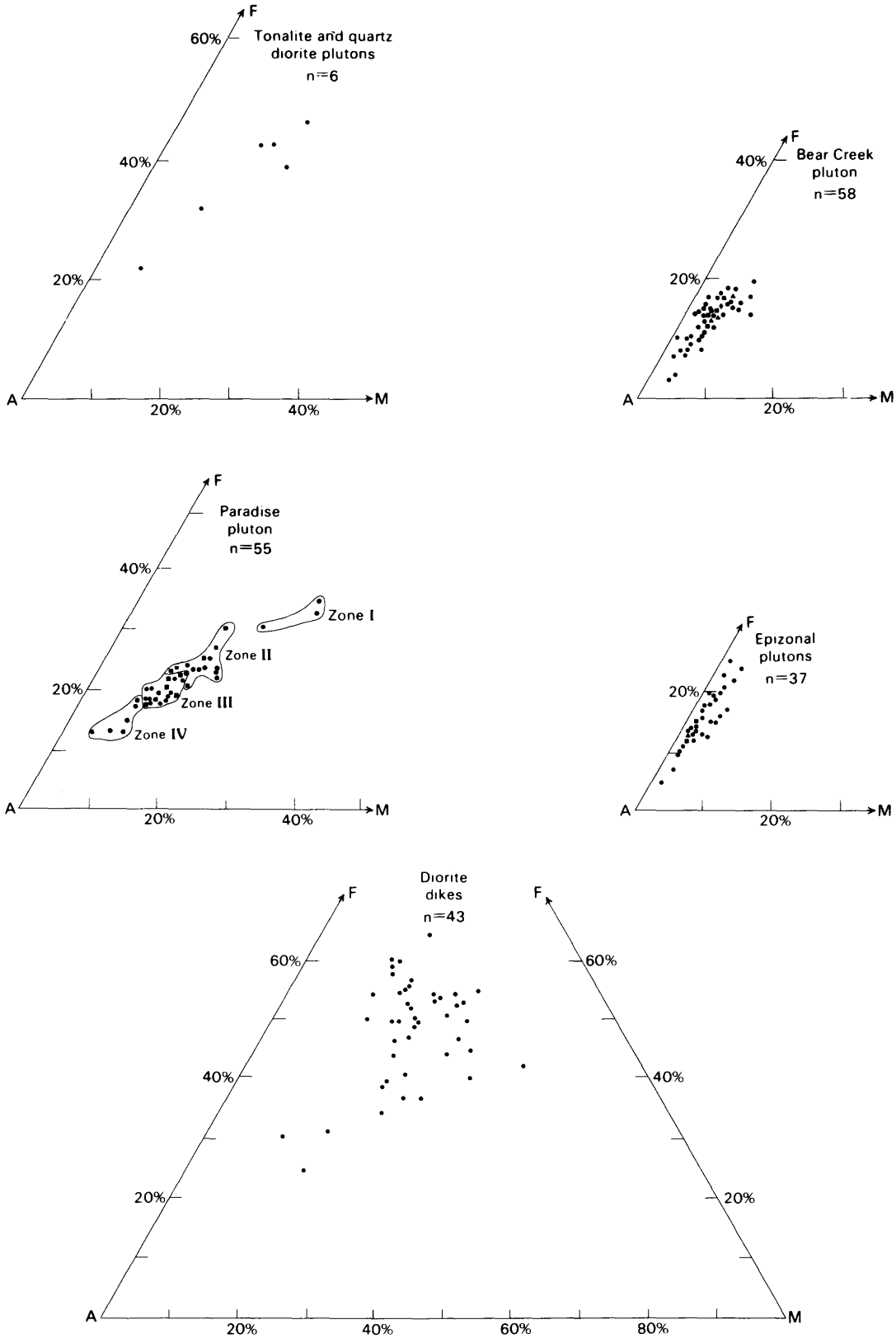

FIGURE 2.5.—AFM diagrams for some plutonic phases of the Bitterroot lobe of the Idaho batholith. A, $Na_2O + K_2O$; F, FeO*; M, MgO. Dot, one sample; square, two samples; triangle, three samples; diamond, four samples; n, total number of samples.

saturation, ranges from 1.04 to 1.25 (table 2.2, fig. 2.6) and indicates that some of the rocks are peraluminous. Three samples with ratios higher than 1.1 were taken adjacent to or at least near migmatite bodies, and their high ratios may reflect local assimilation of metasedimentary material; samples taken far from the migmatite bodies have ratios less than 1.1. Mesonorms indicate a range in the differentiation index (D.I. = Q + Ab + Or) from 62.3 to 79.5 and an average value of 72.1. Normative corundum ranges from 1.2 to 3.4 percent, consistent with a peraluminous composition.

The characteristics of the tonalite and quartz diorite plutons along the northern, western, and southwestern sides of the Bitterroot lobe are most similar to those of I-type granites (table 2.1). They contain no peraluminous minerals, have hornblende, sphene, and magnetite, show a broad spectrum of compositions, and have very high Na_2O contents. However, they also show some characteristics typical of S-type granite: they are associated with regional metamorphism and migmatites and have more than 1 percent normative corundum, molecular $Al_2O_3/CaO+K_2O+Na_2O$ ratios from 1.04 to 1.25, and initial Sr ratios greater than 0.7070 (Criss and Fleck, 1983). The initial Sr ratios, molecular $Al_2O_3/CaO+K_2O+Na_2O$ ratios, and normative corundum values all increase toward migmatite units, and the high values that give these rocks some S-type characteristics most likely resulted from the assimilation of Precambrian metasedimentary material.

Primary tonalite and andesite magmas are generated at temperatures that are probably too high (about 1,100 °C) for crustal conditions (Wyllie and others, 1976), and therefore they probably do not form within the continental crust. The tonalite and quartz diorite plutons of the Bitterroot lobe were most likely derived by partial melting of material at upper mantle depths, and this may have involved metavolcanic eugeoclinal rocks or sub-

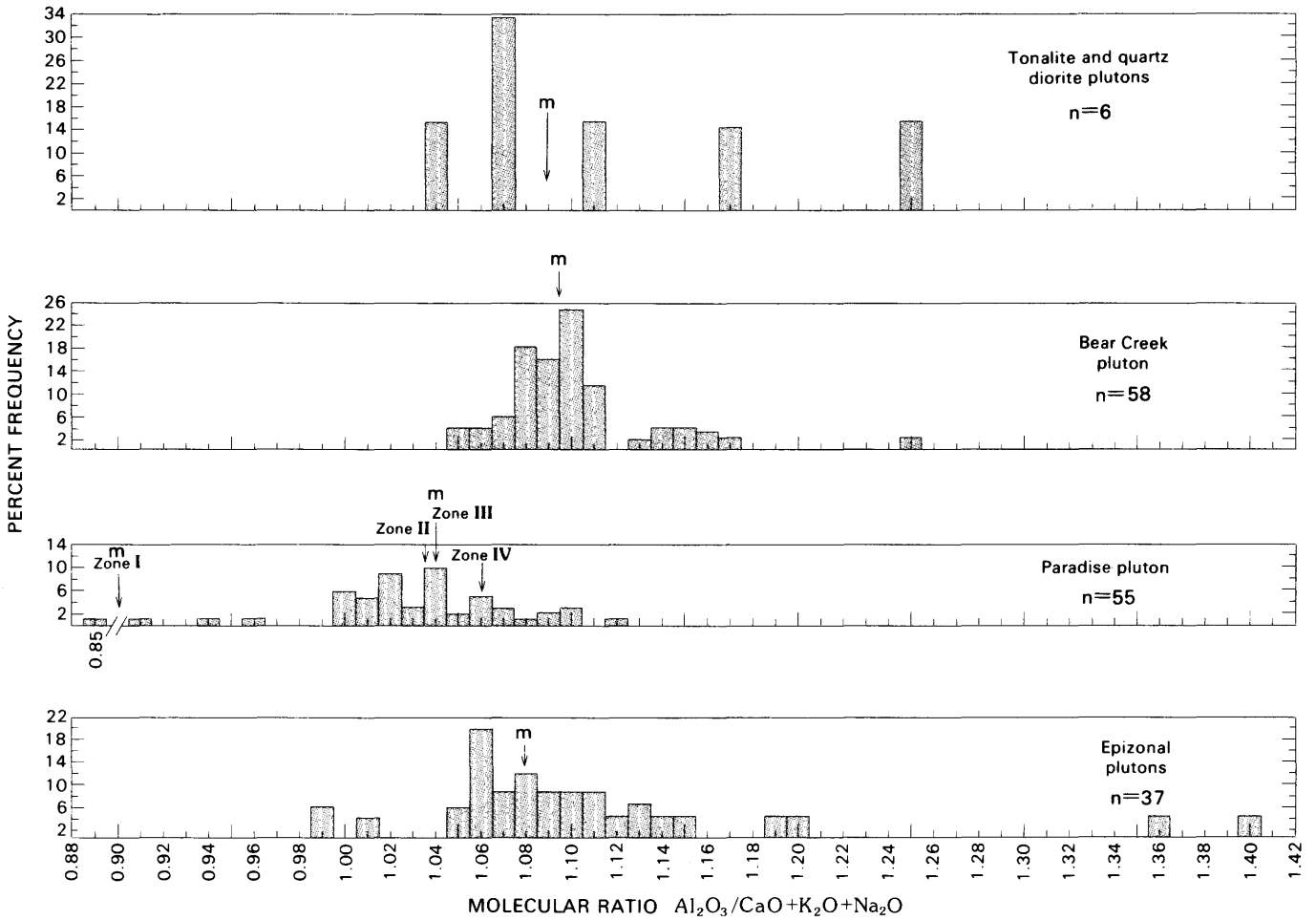

FIGURE 2.6.—Percent frequency of the ratio of molecular $Al_2O_3/CaO+K_2O+Na_2O$ for various plutonic phases of the Bitterroot lobe of the Idaho batholith. Median value, m; number of samples, n.

ducted oceanic lithosphere. Ingestion and assimilation of Precambrian rock occurred as the magmas moved through and were emplaced in the crust.

MONZOGRANITE AND GRANODIORITE PLUTONS

Monzogranite and granodiorite plutons constitute the major part of the Bitterroot lobe and are generally well exposed in its central and southern parts. Outcrops range in elevation from about 900 m in the lower creek bottoms to over 3,050 m at Trapper Peak, thereby exposing a substantial vertical section through the batholith. Most of this part of the batholith was previously thought to be chemically and mineralogically homogeneous, but Williams (1977) delineated five separate plutons in the north-central part of the lobe, and our mapping has outlined at least six mesozonal or lower epizonal plutons in the southern and central parts of the lobe (fig. 2.2). These plutons are strikingly similar in their major- and trace-element chemistry and have been distinguished and mapped on the basis of texture, mineralogy, and crosscutting relationships. Further detailed mapping may show that the Bitterroot lobe consists of a composite of possibly 20 or more different plutons, distinguishable by slight textural, mineralogical, or chemical differences. Geochronologic studies (R.J. Fleck, written commun., 1982; J.S. Stacey, written commun., 1982) suggest that the times of intrusion of these plutons were fairly close to one another.

BEAR CREEK PLUTON

The northern boundary of the Bear Creek pluton is defined by a string of elongate, mostly east-west-trending migmatite units (fig. 2.2) of Proterozoic metasedimentary rocks that the pluton intruded in both lit-par-lit and strongly disharmonic fashions. Large feldspar phenocrysts (average 3–5 cm long) are common in the western parts of the pluton, suggesting the pluton grades into a border phase or possibly another separate pluton. The eastern boundary of the pluton has not been located, but the rocks east of the Bitterroot Mountains crest contain substantially more accessory muscovite and may be a part of another pluton. The location of the southern boundary is also unknown, but may lie as far south as the Canyon Lake pluton (fig. 2.2). Primary flow foliation in rocks of the pluton is weakly to moderately well defined by aligned feldspar and biotite grains, compositional layering, and rare biotite schlieren. Xenoliths are generally rare and consist dominantly of calc-silicate gneiss, with less common quartzofeldspathic schist and quartzite, all correlative with Belt or pre-Belt metasedimentary rocks.

The rocks of the Bear Creek pluton are typically white to light gray and slightly porphyritic and contain subhedral to euhedral feldspar phenocrysts 6 to 8 mm long in a groundmass of medium-grained feldspar, quartz, and biotite, and rare fine-grained muscovite. Medium-grained equigranular rocks are less abundant. Modal compositions range from granodiorite to monzogranite; the average composition of the pluton lies on the granodiorite-monzogranite boundary at about 30 percent quartz (fig. 2.4). Variations from the average composition may reflect the varying amount of phenocrysts.

In thin section, the texture of the granitic rocks from the Bear Creek pluton is medium-grained hypidiomorphic granular to slightly porphyritic. Compositions of oligoclase (average $Ab_{76}An_{21}Or_3$, microprobe determination) show very little variation throughout the pluton. Poikilitic orthoclase also shows very little compositional variation (average $Ab_{17}An_0Or_{83}$, microprobe determination), although some very slight normal and reverse zoning was detected. Biotite (1–4 percent) is characteristically altered to a combination of chlorite and subhedral to needle-like opaque minerals. All of the main mineral phases show varying degrees of deformation and (or) recrystallization related to mylonitization.

Muscovite is present in trace amounts in epitaxial intergrowths with biotite, as an alteration of plagioclase and more rarely potassium feldspar, and as small primary interstitial grains. Larger primary grains are present only in the northernmost part of the pluton adjacent to the migmatite unit, where they increase in abundance to 3 percent of the rock. Using the criteria of Miller and others (1981) for distinguishing primary and secondary muscovite, unequivocal primary grains were identified only in rocks from the northernmost part of the pluton. The compositions of primary and secondary grains from one sample (table 2.3) show that the muscovite in the Bear Creek pluton is far from ideal muscovite ($KAl_{13}Si_3O_{10}(OH)_2$) and contains substantial celadonite, ferrimuscovite, and Ti-muscovite components. TiO_2 ranges from 3.2 to 3.5 percent, MgO from 0.6 to 0.7 percent, and FeO* from 1.1 to 1.8 percent. Secondary muscovite is richer in SiO_2, Al_2O_3, and K_2O, poorer in MgO, and contains similar amounts of TiO_2 and FeO* (table 2.3).

Accessory minerals in the Bear Creek pluton consist of magnetite and minor ilmenite, zircon (with cloudy, anhedral cores), monazite, apatite, and rare euhedral pale-green epidote. Sillimanite is absent, although Williams (1977) identified fibrolitic sillimanite in similar granite of the Tom Beal Park granite in the central part of the Bitterroot lobe.

MAJOR- AND TRACE-ELEMENT CHEMISTRY

The SiO_2 content of rocks from the Bear Creek pluton ranges from 68 to 75 percent, but more than half of the samples contain from 71 to 73 percent SiO_2. The pluton

is slightly zoned with respect to SiO_2 content (table 2.2), which increases from less than 72 percent on the margins to 72 to 74.5 percent in the center. The zonation is not strictly concentric, however, and the distribution of other major oxides mimics this variation only erratically. No regular variation in mineralogy has been observed. The relative homogeneity in the chemistry of the pluton is demonstrated by the slight variation on an AFM diagram (fig. 2.5) and the slight variation in the mesonorm geochemistry. The D.I. of samples from the pluton ranges from 90 to 96 and averages 93.3. Apart from those that contribute to the D.I., the normative constituents are anorthite (4.0–11.9 percent), biotite (1.2–5.4 percent), corundum (0.8–3.4 percent), and minor magnetite, ilmenite, and rutile. The molecular ratio of $Al_2O_3/CaO + K_2O + Na_2O$, which ranges from 1.05 to 1.25 (fig. 2.6) and has a median value of 1.1, indicates the rocks are dominantly peraluminous.

Rare-earth-element (REE) concentrations in rocks from the Bear Creek pluton (fig. 2.7) are also markedly similar, showing little variation from sample to sample. They are characterized by strong fractionation of light REE (LREE) relative to the heavy REE (HREE); Ce/Yb ratios range from 44.0 to 171.4 and average 95.2. Strongly fractionated REE patterns such as these have commonly been interpreted as a reflection of garnet in the source region (Arth and Hanson, 1972, 1975), but Arth and Barker (1976) have demonstrated that hornblende as a residual phase can also cause HREE depletion in a coexisting felsic liquid. The depleted HREE patterns of the Bear Creek pluton may therefore represent residual hornblende and (or) garnet in the source rock. The unusually high abundance of LREE in the pluton is presently unknown, but it may reflect a LREE-enriched source.

All but two of the samples from the pluton show almost no europium anomaly, having Eu/Eu* very close to 1 (Eu* is the expected Eu concentration obtained by simply interpolating between Sm and Gd; the ratio Eu/Eu* is therefore a measure of the Eu anomaly). The absence of an Eu anomaly is usually an indication that plagioclase fractionation did not occur in the evolution of the magma or that plagioclase was not an equilibrated residual phase in the source rock. The absence of such an anomaly might also reflect oxidation of Eu^{+2} to Eu^{+3}. One sample near the eastern edge of the pluton has an Eu anomaly of 0.5, possibly indicating that plagioclase fractionation was operative along the margin of the pluton.

The Bear Creek pluton is an S-type granite body and was probably derived by partial melting of metasedimentary crustal material. I infer this because the pluton contains primary muscovite; has a mean molecular ratio of $Al_2O_3/CaO + K_2O + Na_2O$ of about 1.1, more than 1 percent normative corundum, high SiO_2 content of 68 to 75 percent, somewhat irregular variation diagrams, and initial Sr ratios of more than 0.708 with irregular isochrons; is associated with regional metamorphism; and has migmatites and xenoliths of metasedimentary origin. The only ways in which the pluton does not meet S-type criteria are in having some accessory magnetite instead of ilmenite (which may reflect the oxygen fugacity), and in having relatively high Na_2O contents. In rocks with 5 percent K_2O, Na_2O is about 3.5 percent or greater (versus 3.2 percent for typical S-type granite), and in rocks with 2 percent K_2O, Na_2O is about 4.5 percent (versus 2.2 percent).

Granitic magma such as that which formed the Bear Creek pluton is generated as a consequence of regional metamorphism and anatexis of continental crust (Wyllie and others, 1976). It can be generated in the presence of excess H_2O (Piwinskii, 1968; Winkler, 1979) or in dry rock containing hydrous minerals such as muscovite, biotite, or hornblende (Brown and Fyfe, 1970; Robertson and Wyllie, 1971). The presence of H_2O substantially lowers the solidus, so dry systems need significantly higher temperatures to initiate melting. When breakdown curves of biotite, muscovite, or hornblende are reached, the release of excess H_2O lowers the solidus and allows melting to begin. As pointed out by both Hyndman (1981a, b) and Miller (1981), however, water supplied by the breakdown of hydrous minerals in the source rocks is probably insufficient for the formation of a large mass of granite. Hyndman (1981a, b) suggests that additional water released in dehydration reactions in subduction zones may rise into the overlying continental crust and so contribute to the partial melting of the rocks.

Anatectically derived magmas commonly contain suspended restite material (Winkler, 1979). In the Bear Creek pluton, however, there is no evidence of restite material other than cores of Precambrian age in zircon grains and possibly some rare schlieren layers. Except where some assimilation of country rock is observed, the composition of the pluton therefore represents the composition of the magma from which it crystallized. If restite material did exist, it was removed sometime in the evolution of the pluton before emplacement.

The major source of the magma for the Bear Creek pluton was probably metamorphosed Belt or pre-Belt metasedimentary rocks. Melting may have been related to subduction, but the timing and mechanics are still unclear; subduction may have caused melting by providing necessary heat, by supplying necessary water from dehydration reactions in the upper mantle, or both. Armstrong and others (1977) indicate that initial Sr ratios in Idaho batholith rocks are generally too low to permit simple anatectic intracrustal genesis, and as a result they suggest some upper mantle contribution.

Our geochemical studies (Koesterer and others, 1982; Coxe and Toth 1983a, b; Toth, 1983b) show that in major-

TABLE 2.3.—*Microprobe analyses and structural formulas*

[Al(iv) is alumina in the tetrahedral site and Al(vi) is alumina in the octahedral site. n.d., not detected; ---, not determined. Oxides in weight

	Bear Creek pluton MUSCOVITE				Paradise pluton BIOTITE				
	Primary			Secondary	Zone II		Zone IV		Upper contact
SiO_2----	44.3	44.8	44.5	46.3	38.45	38.78	40.55	39.74	38.15
TiO_2----	3.5	3.2	3.4	3.5	2.57	2.53	2.54	3.11	2.59
Al_2O_3---	32.1	32.0	33.1	33.9	15.55	14.06	14.05	14.52	14.18
MgO-----	.6	.7	.7	.2	12.10	12.63	12.55	12.29	14.27
FeO*----	1.6	1.1	1.8	1.7	14.56	15.04	16.50	16.94	13.57
MnO-----	---	---	---	---	.22	.23	.36	.30	.27
CaO-----	---	---	---	---	.04	.03	.03	.03	.03
Na_2O----	n.d.	n.d.	n.d.	.1	.06	.08	.05	.17	.14
K_2O-----	10.3	10.1	10.3	11.1	9.63	9.05	9.76	9.77	9.44
La_2O_3---	---	---	---	---	---	-----	---	---	---
Ce_2O_3---	---	---	---	---	---	-----	---	---	---
Total	92.4	91.9	93.8	96.8	93.27	92.43	96.39	96.87	93.64
Si------	6.18	6.24	6.08	6.14	5.85	5.93	5.99	5.87	5.76
Ti------	.40	.38	.38	.40	.27	.29	.28	.35	.29
Al(iv)--	1.82	1.76	1.93	1.86	2.15	2.06	2.01	2.13	2.24
Al(vi)--	3.48	3.48	3.42	3.46	.57	.46	.44	.40	.46
Mg------	.12	.14	.14	.04	2.80	2.80	2.04	2.09	3.06
Fe------	.18	.10	.16	.16	1.80	2.00	1.76	1.70	1.80
Mn------	---	---	---	---	.03	.03	.04	.04	.03
Ca------	---	---	---	---	.01	.01	0	.01	.01
Na------	n.d.	n.d.	n.d.	.02	.01	.02	.01	.05	.04
K-------	1.84	1.78	1.78	1.88	1.76	1.81	1.84	1.84	1.81
La------	---	---	---	---	---	-----	---	---	---
Ce------	---	---	---	---	---	-----	---	---	---
Fe/Fe+Mg	.60	.42	.53	.80	.39	.41	.43	.44	.37

and trace-element geochemistry the Bear Creek pluton is strikingly similar to other granodiorite and monzogranite plutons in the central and southern parts of the Bitterroot lobe. Much of the lobe may consequently belong to a single comagmatic suite, as suggested by the work of Hyndman (1984) and Wiswall and Hyndman (chapter 4). The plutons of the central and southern parts of the lobe were therefore probably derived from a homogeneous source rock and underwent very little differentiation or assimilation before emplacement. The homogeneous chemistry also suggests that the plutons did not travel very far from their source rock before they finished crystallizing. However, the notable absence of restite material does suggest the plutons are at least somewhat removed from their source regions.

GRAVE PEAK PLUTON

The Grave Peak pluton crops out north of the Bear Creek pluton, from which it is separated by a string of elongate migmatite units (fig. 2.2); its other contacts have not been mapped. It is similar in all respects to the Bear Creek pluton, except that it everywhere contains 3 percent or more of primary muscovite and also contains substantially more accessory epidote. This pluton may be a part of the Tom Beal Park granite as mapped by Williams (1977). It has characteristics most similar to an S-type granite, and its origin is presumably closely related to that of the Bear Creek pluton.

CANYON LAKE PLUTON

The Canyon Lake pluton crops out as an elongate east-west body underlying approximately 190 km^2 along the southern border of the Bitterroot lobe (fig. 2.2). It intrudes the Bear Creek pluton to the north and is bounded on its west and south margins by migmatite units and granitic rocks similar in appearance and chemistry to those of the Bear Creek pluton. The pluton grades eastward into mylonite, which is truncated by the border fault. The

of minerals from the Bear Creek and Paradise plutons

percent. Structural formulas of muscovite, biotite, and hornblende based on 22 oxygens; structural formulas of allanite based on 12 oxygens]

Paradise pluton HORNBLENDE					Paradise pluton ALLANITE				
Zone II		Zone IV		Upper contact	Zone II		Zone IV		Upper contact
45.96	45.37	46.55	46.86	47.34	31.31	32.33	30.79	30.83	34.00
.93	.93	1.12	.94	.83	.84	.69	1.07	.86	.42
10.40	8.89	10.13	9.02	8.69	16.00	16.72	14.07	14.59	18.46
10.90	11.15	9.98	10.63	12.86	1.01	.81	1.12	.82	.89
14.27	14.01	16.42	16.27	12.95	13.82	13.08	14.73	15.09	12.56
.30	.48	.56	.42	.40	.26	.28	.36	.38	.28
11.46	11.44	11.60	12.00	12.03	11.41	13.02	11.53	10.85	13.41
1.50	1.57	1.78	1.60	1.19	---	---	---	---	---
1.28	1.06	1.40	1.21	.82	---	---	---	---	---
---	---	---	---	5.35	6.08	7.53	5.84	5.63	
---	---	---	---	9.77	10.03	11.83	11.02	8.49	
97.00	94.90	99.54	99.84	96.63	89.77	93.04	93.03	90.28	94.14
6.54	6.60	6.53	6.52	6.67	2.98	2.97	2.95	2.99	3.01
.10	.10	.12	.10	.09	.06	.05	.08	.06	.03
1.46	1.40	1.47	1.48	1.33	.02	.03	.05	.01	0
.28	.13	.20	.12	.11	1.78	1.78	1.54	1.66	1.92
2.32	2.42	2.09	2.36	2.70	.14	.11	.16	.12	.12
1.69	1.71	1.93	1.82	1.53	1.10	1.01	1.18	1.22	.93
.04	.06	.07	.05	.05	.02	.02	.03	.03	.02
1.74	1.79	1.74	1.79	1.82	1.16	1.28	1.18	1.13	1.27
.43	.44	.50	.42	.32	---	---	---	---	---
.23	.20	.30	.21	.15	---	---	---	---	---
---	---	---	---	.19	.21	.27	.21	.18	
---	---	---	---	.34	.34	.41	.39	.27	
.42	.43	.48	.43	.36	.89	.94	.91	.93	.88

Canyon Lake pluton has four synplutonic phases: extremely porphyritic rocks in the west; equigranular rocks in the central part; highly deformed, heterolithologic rocks in the east; and orbicular rocks along the southern border, in contact with Precambrian migmatite. Primary flow foliation is generally weak or absent, but a strong phenocryst lineation is commonly present in the porphyritic rocks.

Monzogranite and lesser granodiorite dominate the Canyon Lake pluton (fig. 2.4), but minor components range from syenogranite to diorite (not shown in fig. 2.4). The major phases of the pluton mentioned above are not distinguishable chemically and have been mapped on the basis of distinctive textures and the relative abundances of certain trace minerals.

Dominating the western part of the pluton is a monzogranite and granodiorite main phase characterized by large (as much as 5 cm by 9 cm), euhedral, poikilitic orthoclase megacrysts, which constitute 15 to 25 percent of the rock, and by 1 to 3 percent granular (as large as 1 mm across) magnetite. The matrix consists of medium-grained equigranular plagioclase, quartz, and biotite, along with minor orthoclase.

In the central part of the pluton, a fine- to medium-grained equigranular monzogranite is commonly associated with the main phase. Contacts, though sharp in hand specimen, are irregular and deformed on a large scale and suggest simultaneous emplacement of these phases. Fine-grained magnetite constitutes a trace amount to 3 percent of the rock and is generally concentrated along joint surfaces. This phase of the Canyon Lake pluton is most abundant along its northern contact and commonly contains highly folded and deformed biotite schlieren.

In the eastern part of the pluton, large outcrops show crosscutting, deformed, and swirled bodies of quartz diorite, granodiorite, syenogranite, quartz monzodiorite, and diorite, all of which are commonly crosscut by dioritic dikes. A few outcrops show as many as twelve texturally or mineralogically distinct subphases which were

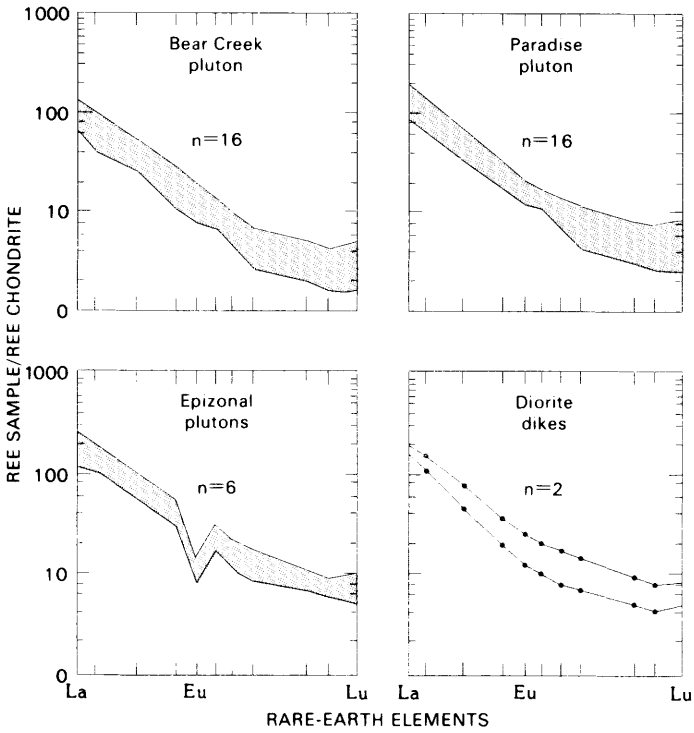

FIGURE 2.7.—Chondrite-normalized rare-earth-element (REE) concentrations in some plutonic phases of the Bitterroot lobe of the Idaho batholith. Number of samples, n; stippled pattern shows range of data.

apparently emplaced nearly simultaneously. Most of the subphases are fine to medium grained, but porphyritic granodiorite is locally present. Early intrusive subphases also contain minor diorite xenoliths, which are elongate and lie parallel to the borders of the enclosing subphase. Primary flow foliation defined by biotite is highly variable but generally parallels contacts between subphases. Magnetite concentrations as much as 4 cm thick and 0.5 m^2 in area are present along joint surfaces and foliation planes in the main subphase. No genetic relations between subphases were observed in the outcrops where intrusive relationships could be determined, and it is not known whether these subphases were derived from several different sources or resulted from remobilization, mixing, or assimilation of earlier intrusions.

Orbicular rocks are present at six localities along and near the southern contact of the Canyon Lake pluton. They are present as small (0.5–4 m^2), mostly undeformed pods of orbicular monzogranite and granodiorite along single structural horizons in the main phase of the pluton and as individual orbicules in a matrix of medium-grained granite. Five types of orbicules are present, ranging from 2 to 12 cm in diameter; some contain hornblende-biotite-plagioclase cores and single or multiple concentric shells of plagioclase, biotite, and magnetite oriented in a radial or tangential manner.

In thin section, orthoclase phenocrysts of the main phase display Carlsbad twinning and are strongly poikilitic. The groundmass is hypidiomorphic, and matrix orthoclase shows well-developed flame perthite. Small primary(?) grains of muscovite are present in minor amounts. Magnetite is present both as small inclusions in feldspar and as large poikilitic interstitial grains. Zircon is a common accessory mineral, and monazite, sphene, and secondary calcite are present in trace amounts.

The major- and trace-element chemistry of the Canyon Lake pluton is generally indistinguishable from that of the Bear Creek pluton, suggesting a similar origin and source rock for both. However, the Bear Creek pluton is clearly S-type, whereas the Canyon Lake pluton shows some characteristics of I-type granite in that it does contain magnetite and may lack primary muscovite. Because it is bordered on the south by a large body of migmatite, the Canyon Lake pluton may have assimilated some metasedimentary material.

PARADISE PLUTON

The Paradise pluton intrudes the middle of the Bear Creek pluton in the south-central part of the Bitterroot lobe (fig. 2.2), and its intrusion marked major changes in structural style of intrusion, mineralogy, and chemistry of the mesozonal granitic rocks. The lobe-shaped main phase of the pluton underlies about 105 km^2 in the west and has vertical walls on its northern and western sides. Toward the south and east the pluton becomes sheetlike and nearly horizontal and has a thickness of approximately 1,450 m (fig. 2.8). This sheet phase extends at least 5 km south to El Capitan, and possibly as far as 16 km south, and it becomes increasingly interlayered with the Bear Creek pluton southward, away from the main phase. A petrologically distinct, finer grained, equigranular contact rock of varying thickness forms a third phase along the vertical walls of the main phase and at the top of the sheet phase (contact phase on figure 2.8).

The lower contact of the Paradise pluton's sheet phase and the contacts along the vertical walls of the main phase are sharp and locally mylonitized. The upper contact of the sheet phase generally has a zone 2 to 100 m thick showing degrees of intermixing with the Bear Creek pluton and contains abundant xenoliths of calc-silicate rock and quartzite along foliation planes; some large xenoliths of igneous rock from the Bear Creek pluton are also present. This mixed zone is extremely deformed, as shown by folding, shearing, and crenulation of the rocks. In two places the upper contact is sharp and flat beneath large coherent blocks of metasedimentary rock that could be remnants of wall or roof material.

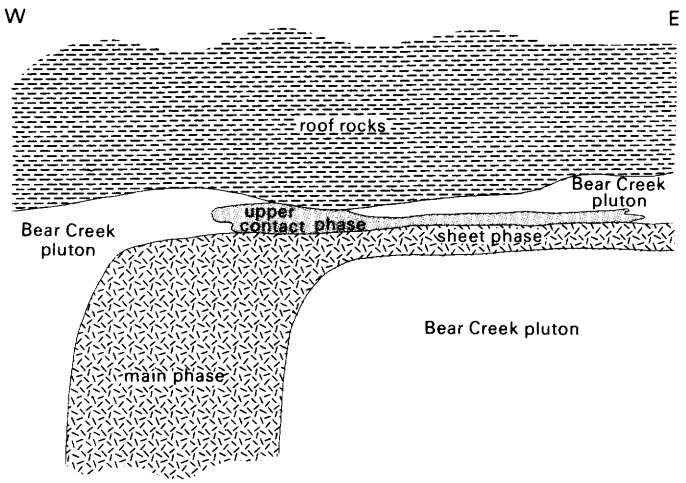

FIGURE 2.8.—Schematic cross section showing structure and main, sheet, and upper contact phases of Paradise pluton (stippled).

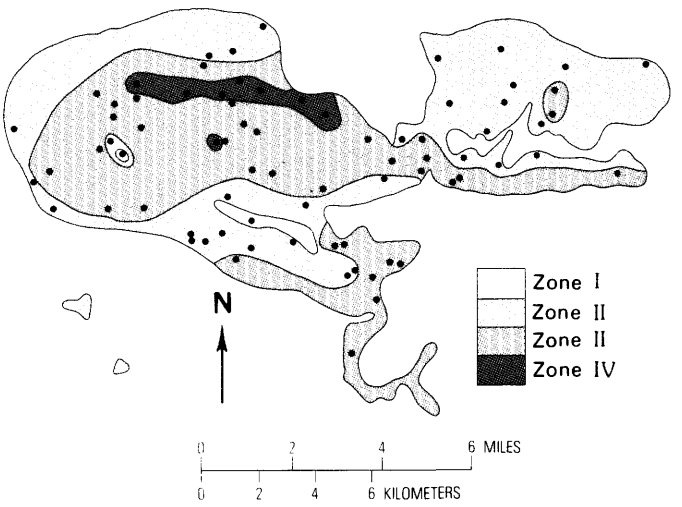

FIGURE 2.9.—Simplified lithologic zonation of Paradise pluton as determined from point counts and major-element chemical data. Zone I, tonalite and quartz diorite; zone II, granodiorite and quartz monzodiorite; zone III, granodiorite and quartz monzodiorite; zone IV, monzogranite. See text for differentiation between zones II and III. Dots are sample locations for major-element chemistry.

Rocks from the main and sheet phases of the Paradise pluton are foliated, light to dark gray, and slightly porphyritic. They contain 10 to 30 percent potassium feldspar phenocrysts, which are very poikilitic, subhedral to euhedral, and 6 to 10 mm long, in a groundmass of medium-grained euhedral plagioclase, subhedral biotite and hornblende, and anhedral quartz. The rocks are less porphyritic toward the core of the main phase. Euhedral prisms of sphene are common as grains that average 1 to 2 mm but are as large as 5 mm across.

The composition of the main phase of the Paradise pluton varies extremely widely (fig. 2.4), and the spatial relationships (fig. 2.9) indicate the pluton is compositionally zoned. The main phase ranges from plagioclase-rich granodiorite and monzogranite in a rim 0.25 to 3 km wide (zone II), through more potassium feldspar-rich granodiorite and monzogranite that forms the bulk of the pluton (zone III), to monzogranite in an elongate zone 0.25 to 0.5 km wide in the core (zone IV). Hornblende and biotite decrease from approximately 7 to 10 percent (combined) on the outer margins to 3 to 5 percent in the inner core. This compositional zonation is rough and only approximately concentric, and compositions vary somewhat erratically within each zone. A small, elongate tonalite to quartz diorite body (zone I) in the southern part of the main phase also complicates the zonal pattern. Rocks in the sheet phase have a range in composition similar to that in the main phase, but the variation is much less systematic. Petrography also suggests that the sheet phase has a slight vertical zonation marked by upward increase in plagioclase and decrease in potassium feldspar.

Rocks from the upper contact phase are dark gray and equigranular; they have average grain sizes of about 4 mm and porphyritic varieties are absent. Compositions vary widely and include diorite, quartz diorite, tonalite, and minor granodiorite. The rocks are characterized by very low potassium feldspar content (less than 5 percent) and highly varied amounts of quartz (1–45 percent). Biotite ranges from 6 to 56 percent and averages 17 percent, and hornblende is locally present.

Thin sections show that the granitic rocks in the sheet and main phases are slightly porphyritic; medium-grained equigranular varieties are less common. Albite-twinned oligoclase (zone I, $Ab_{70}An_{27}Or_3$; zone IV, $Ab_{77}An_{20}Or_3$, microprobe determinations) is zoned normally and occurs in slightly poikilitic subhedral to euhedral laths. Orthoclase (zone I, $Ab_{16}An_1Or_{83}$; zone IV, $Ab_{13.5}An_{0.5}Or_{86}$, microprobe determinations) forms subhedral oikocrysts containing 10 to 80 percent (mostly less than 40 percent) inclusions and more rarely occurs as an interstitial phase. Green poikilitic hornblende is present in highly varied amounts (trace to 7 percent) but rarely exceeds biotite in abundance. From zone II to zone IV hornblende composition shows increases in SiO_2, FeO*, K_2O, Na_2O, and TiO_2 (table 2.3); the Fe/Fe+Mg ratio also increases from 0.42 to 0.48. The changes in the chemistry of subhedral brown biotite are similar to those for hornblende, and the Fe/Fe+Mg ratio increases from 0.39 to 0.44 (table 2.3). Zoned allanite (trace to 1 percent) increases in abundance, size, and euhedral form from zone I to zone IV, where it reaches an abundance of 0.5 percent and sizes as large as 2 mm. The chemistry of the allanite also changes

systematically from zone II to zone IV: La_2O_3, Ce_2O_3, FeO*, and MgO increase, whereas Al_2O_3, CaO, and SiO_2 decrease (table 2.3). Accessory minerals consist of sphene, apatite, zircon (some with cloudy, anhedral cores), monazite, magnetite, and rare pyrite; ilmenite and muscovite are notably absent. All of the main minerals have been deformed and (or) recrystallized to varying degrees during mylonitization.

Thin sections show that the equigranular upper-contact rocks have a hypidiomorphic granular texture and average grain sizes of 3 to 4 mm. Plagioclase occurs as euhedral, rarely poikilitic grains, and sparse orthoclase forms small anhedral grains. Olive-green biotite is extremely fresh, and hornblende is present in euhedral poikilitic grains that contain 10 percent inclusions of round quartz. Strongly zoned light-brown allanite is present in very small amounts in all samples. Apatite, sphene, magnetite, and rare thorite make up the accessory minerals.

MAJOR- AND TRACE-ELEMENT CHEMISTRY

The chemistry of the main phase of the pluton (table 2.2) reflects the mineralogical variation observed in the point-count data: an outer, mafic margin grades concentrically inward and upward into more felsic rocks, as shown by variations in the weight percent of the major oxides. SiO_2 increases inward from 63 to 72.5 percent, Al_2O_3 decreases inward from >17 percent to <15.3 percent, FeO* decreases inward from 3.6 percent to <2.1 percent, CaO decreases inward from 4.1 to 1.8 percent, and MgO decreases inward from 2.9 to <1 percent. Na_2O and K_2O show highly varied concentrations in the pluton; K_2O is zoned only on the largest scale, increasing slightly inward. From zone I to zone IV, the main phase shows an increase in $Na_2O + K_2O$ and a corresponding decrease in FeO* and MgO (fig. 2.5). The variation is continuous from zones II through IV, but there is a compositional gap between zones I and II, suggesting that these rocks may not be directly related. The sheet phase of the Paradise pluton may also be zoned, because the major-element chemistry shows a general vertical trend of increasing SiO_2 downward and correspondingly decreasing Al_2O_3, FeO*, MgO, CaO, and Na_2O (Toth, 1983b).

In the main phase of the pluton, the mesonorm chemistry shows the following trends from zone I to zone IV: normative hornblende, biotite, anorthite, and albite decrease, and normative orthoclase increases; normative corundum increases from 0 to 1.2 percent, although most of the samples contain less than 1 percent. The D.I. ranges from 54 in zone I (reflecting high quantities of normative hornblende and biotite) to 85.6 in zone IV. Molecular $Al_2O_3/CaO + K_2O + Na_2O$ ratios vary from 0.85 to 1.12 (fig. 2.6), indicating that much of the pluton is metaluminous.

The rocks of the Paradise pluton, like those of the Bear Creek pluton, typically exhibit an extreme fractionation of LREE over HREE (fig. 2.7); Ce/Yb ratios range from 38.4 to 120 and average 77.5. As indicated previously, these strongly fractionated patterns may indicate residual hornblende or garnet in the source rocks, although the high abundance of LREE is still unknown. REE concentrations increase from zone IV to zone I in the main phase; this reflects the increase in the amount of hornblende, the major site for the REE. The Eu anomalies, which vary within each zone and range from 0.64 to 0.93, suggest some plagioclase fractionation.

Concentric zonation of the main phase of the Paradise pluton is demonstrated in silica variation diagrams, AFM variation, mesonorm chemistry, REE chemistry, and mineral chemistry. Speculations regarding the origin of the zonation must take into account the apparent absence of any intrusive contacts within the pluton and the absence of any xenoliths of country or basement rock. The field evidence favors a continuous process rather than multiple intrusions of magma, and it seems to preclude assimilation as a possible mechanism. Three mechanisms for the origin of the zonation should be considered: thermogravitative diffusion, fractional crystallization by crystal settling, and fractional crystallization by inward crystallization and (or) filter pressing. These mechanisms are discussed in detail in Toth (1983b), where I utilize data for major, trace, and rare-earth elements and modeling of Rb-Sr-Ba fractionation to conclude that the origin of the zonation involved fractional crystallization of the latter type. Biotite, hornblende, and minor plagioclase crystallized early and were accreted along the outer margins of the pluton together with some trapped magma. The remaining magma was in this way displaced inward to form the inner zones.

The intrusion of the Paradise pluton marked a major change in the evolution of the Bitterroot lobe, from intrusion of massive amounts of S-type granite to intrusion of a single I-type granite. The pluton lacks any peraluminous minerals, contains hornblende, sphene, and magnetite, has a molecular ratio of $Al_2O_3/CaO + K_2O + Na_2O$ of less than 1.1, and has less than 1 percent normative corundum. The Na_2O content is greater than 4 percent in most of the rocks, and the SiO_2 content covers a broad range from 60 to 74 percent. Variation diagrams are typically linear (Toth, 1983b).

The main deviation of the Paradise pluton from I-type granite in the classification of Chappell and White (1974) is that the initial Sr ratios are greater than 0.708 (R.J. Fleck, personal commun., 1981; Criss and Fleck, chapter 6). Most I-type granite has low initial Sr ratios (0.704–0.706). The relatively higher ratios for the Paradise pluton may indicate that either (1) the source rock for the Paradise pluton was chemically more primitive and much

lower in the crust than the source for the Bear Creek pluton; ingestion of Precambrian crustal material as the magma ascended increased its initial Sr ratios; or (2) the source rock for the Paradise pluton was closely related to that of the Bear Creek pluton but was of a markedly contrasting composition (such as metabasalt or metaandesite) that required higher melting temperatures. The younger age of the Paradise pluton would allow time for temperature to increase and for melt to be produced from the amphibolite. Until more detailed Rb-Sr work is done on the Paradise pluton, it is not possible to determine which of these origins is more likely. However, all of the chemical data appear to require a source rock markedly different from that of the Bear Creek pluton. Furthermore, the Paradise pluton was intruded at the start of major regional extension, and therefore a different depth of origin for the melt might be expected.

BURNT RIDGE PLUTON

The Burnt Ridge pluton crops out in the southeastern part of the Bitterroot lobe on the east side of the bordering normal fault (fig. 2.2). It is in sharp contact to the south with the Piquett Creek pluton and is covered by alluvium to the north; its eastern margin has not been mapped. Along the western border of the pluton, brecciation of the rocks increases in proximity to the fault, and a quartz-flooded, sillimanite-bearing marginal phase is intermittently present adjacent to the fault. The western border also contains various-size inclusions of the Bear Creek pluton, which are evidence that the Burnt Ridge pluton is younger.

The pluton consists of medium-grained equigranular granodiorite containing 35 to 40 percent quartz. Foliation is very weakly defined by aligned mica grains and elongate, cigar-shaped quartz crystals. Quartz crystals are subhedral to euhedral and rarely terminated, and may have been derived from a liquidus phase. Microcline poikilitically includes all the other minerals. Euhedral oligoclase (An_{28-30}, optical determination) is albite-twinned and normally zoned, and the more calcic cores are preferentially altered to saussurite. Biotite dominates over primary muscovite, and the two constitute 3 to 5 percent of the rock; epitaxial intergrowths between them are common. Accessory minerals include anhedral to subhedral opaque minerals, zircon, xenotime, apatite, and rare sphene.

Mineralogically the Burnt Ridge pluton is a slightly peraluminous S-type granite, but without chemical data it is difficult to classify its origin. The presence of possible liquidus quartz suggests that the pluton intruded at a relatively shallow level (Tuttle and Bowen, 1958). These attributes may indicate a change in the depth of origin and possibly in the source rock for the younger plutons of the Bitterroot lobe.

PIQUETT CREEK PLUTON

The Piquett Creek pluton crops out in an elongate east-west area in the southeast part of the Bitterroot lobe, east of the bordering normal fault (fig. 2.2). It is bounded on the north and east by the Burnt Ridge pluton, on the west by the border fault, and on the south by Eocene epizonal granite. Age relations with the Burnt Ridge pluton are unknown, but the two plutons are in mutually sharp contact.

The composition of rocks in the Piquett Creek pluton ranges from granodiorite to syenogranite. The pluton contains distinctive euhedral Carlsbad-twinned orthoclase phenocrysts 5 to 6 cm long (a few are as much as 10 cm long) in a medium-grained groundmass generally devoid of potassium feldspar. Phenocrysts constitute 15 to 20 percent of the rock and contain zonally arranged inclusions of biotite; many phenocrysts were aligned by flow, but others show random orientations. Quartz in these rocks is subhedral to euhedral and has circular cross sections 5 to 6 mm in diameter; terminated ends on some crystals in a few samples suggest that quartz was possibly a liquidus phase. The quartz is strongly aligned and is commonly the only mineral defining the primary flow foliation.

In thin section, quartz is seen to be strained and almost totally recrystallized into mosaics of subgrains averaging 0.5 mm across. Orthoclase phenocrysts poikilitically include all the other minerals, and euhedral plagioclase (An_{23-25}, optical determination) is complexly twinned and normally zoned. Biotite is the only mafic mineral and makes up 5 to 9 percent of the rock. Primary(?) muscovite is present, and secondary muscovite is abundant in altered plagioclase. Accessory minerals include euhedral iron-titanium oxide minerals, allanite, zircon, thorite, and rare apatite.

Like the Burnt Ridge pluton, the Piquett Creek pluton contains possible liquidus quartz, suggesting a shallower depth of intrusion than the other monzogranite and granodiorite plutons of the lobe. It has mineralogical characteristics similar to S-type granite, but definite classification is not possible without chemical data.

SYENOGRANITE AND QUARTZ SYENITE PLUTONS

Eocene epizonal plutons surround the Bitterroot lobe on the south, southwest, and north sides and have been studied in some detail by Hall (1980), Holloway (1980), Lund (1980), Motzer (1981), Pawlowski (1981), Rehn and Lund (1981), Lund and others (1983), Toth (1983a, b), and Rehn (1984). Outcrops of these plutons are generally

deeply weathered and extremely friable. The plutons were intruded to very shallow levels (1.5 km; Rehn and Lund, 1981) during Eocene time, and they locally intrude their own volcanic ejecta. The nonfoliated textures of these plutons suggest post-tectonic emplacement; for some of the plutons, normal faults apparently controlled the emplacement. Miarolitic cavities are abundant and contain crystals of fluorite, smoky quartz, and microcline. The cavities average 4 cm across but are as large as 15 cm by 25 cm by 30 cm. Contacts of the plutons with the country rock are extremely sharp, and hydrothermal alteration effects from the plutons extend as far as 2 km into the country rock. A network of northeast-trending rhyodacite and rhyolite dikes extends outward from most of the plutons, the density of dikes decreasing rapidly away from each pluton.

The plutons consist of medium- to coarse-grained syenogranite, quartz syenite, and monzogranite (fig. 2.4), with lesser amounts of alkali feldspar granite and quartz monzonite (not shown in figure 2.4) (Hall, 1980; Lund, 1980; Pawlowski, 1981). Thin sections show the texture of the rocks to be hypidiomorphic granular to seriate and, in places, porphyritic. Orthoclase perthite is the dominant mineral and contains as much as 50 percent plagioclase in the form of elongate stringers, patches, and irregular blebs. Plagioclase also forms subhedral tabular grains that are commonly zoned from about An_{16} in the core to An_4 at the rim (optical determination, W.E. Motzer, written commun., 1983). Biotite is present in all of the samples (average 8 percent), and hornblende occurs sporadically (average 3 percent). Accessory minerals include allanite, apatite, baddeleyite, cassiterite, fluorite, monazite, sphene, thorite, zircon (both primary and possibly inherited), and iron-titanium oxide minerals (Motzer, 1981).

The epizonal plutons are characterized by high SiO_2, high $K_2O + Na_2O$ and K_2O/Na_2O, and low CaO (table 2.2). The SiO_2 contents in 37 samples from the Whistling Pig, Running Creek, Bad Luck, and Painted Rocks plutons range from 70 to 81 percent, and three-quarters of the samples contain between 74 and 78 percent SiO_2. The sum of $Na_2O + K_2O$ ranges from 7.38 to 9.43 percent, K_2O/Na_2O ranges from 1.06 to 2.03, and CaO ranges from 0.20 to 0.92 percent. The rocks have abnormally low MgO and high but variable amounts of $Na_2O + K_2O$ (fig. 2.5). Molecular ratios of $Al_2O_3/CaO + K_2O + Na_2O$ (fig. 2.6) range from 0.99 to 1.40 and have a median value of 1.08. The mesonorm data show a wide D.I. range, from 85.4 to 95.6 in the more highly differentiated rocks. Normative corundum ranges from 0.5 to 2.0 percent.

The plutons are also very enriched in incompatible elements such as Be, La, Nb, Sn, and Y (Rehn, 1984); the magmas that formed them were saturated with H_2O and had high F contents. The REE patterns for the plutons (fig. 2.7) show a strong fractionation of LREE over HREE, although not as strong as that in the Bear Creek and Paradise plutons; Ce/Yb ratios range from 64.2 to 102.1 and average 79.6. The epizonal granites also have substantial Eu anomalies (Eu/Eu* as low as 0.3), suggesting plagioclase fractionation or a strongly depleted source rock.

With the exception of their high H_2O content, the Eocene epizonal granites have chemical and mineralogical signatures typical of A-type granite. They have low MgO and CaO, high $Na_2O + K_2O$, and high F, are enriched in the incompatible elements, and have strongly negative Eu anomalies. Collins and others (1982) conclude that A-type granite is derived in the lower crust by partial melting of relatively felsic granulite that had previously been melted to produce granite. Vapor-absent melting of the granitic source rock at high temperatures generates a relatively anhydrous melt containing F. The fluorine forms complexes with large highly charged cations, including the REE, thereby producing the high abundances of these elements. A depleted source rock would also explain the Eu anomalies, caused by the earlier depletion of plagioclase. It is unlikely that the epizonal granitic plutons were derived from partial melting of the mesozonal granitoids or Precambrian metasedimentary material. However, relatively high initial Sr ratios in the younger plutons do suggest some assimilation of crustal material.

DIKE ROCKS

Four types of dike rocks (not shown on figures 2.1 and 2.2) are present in the central and southern parts of the Bitterroot lobe: leucocratic pegmatite; fine-grained biotite and hornblende-biotite granite; hornblende-biotite diorite, quartz diorite, and tonalite; and hypabyssal rhyolite and rhyodacite. Aplite dikes are notably absent.

PEGMATITE DIKES

Scattered and minor pegmatite dikes intrude the mesozonal granitic rocks and are locally more abundant along contacts and near the roofs of the plutons. They generally have shallow dips and are randomly discordant to the flow foliations of the host rock, but in places they lie within the foliation. The dikes are commonly massive, but in some places strong foliation is present and is concordant to that in the host rock. Contacts are very sharp, and widths of the dikes average 20 to 30 cm.

The pegmatite dikes range compositionally from monzogranite to syenogranite and consist of orthoclase, quartz, and lesser amounts of sodic plagioclase. The dikes are generally homogeneous in composition, but a few are zoned, with feldspars on the margin and gray quartz in the core. Grain size averages 3 to 4 cm but in a few places

is as much as 8 cm. Mafic minerals are very rare and consist mostly of trace amounts of biotite. Minor amounts of muscovite and hornblende are present in one location near the northeastern contact of the Bear Creek pluton. Garnet-bearing layers are abundant in a pegmatite on the northern contact of the Bear Creek pluton, adjacent to a pelitic migmatite unit.

FINE-GRAINED GRANITIC DIKES

Fine-grained granitic dikes are widely distributed in mesozonal rocks throughout the central and southern parts of the Bitterroot lobe and constitute 1 to 3 percent of the mesozonal plutons. They are locally present in greater abundance near the northern and northeastern margins of the Bear Creek pluton, near the margins of the main phase of the Paradise pluton, and along the upper contact of the sheet phase of the Paradise pluton. They range in thickness from 0.2 to 4 m but are typically 0.5 to 1 m. The dikes generally have a limited lateral extent and feather out within 8 to 10 m along strike, although a few of the thicker dikes extend at least 30 m. Contacts are straight-sided to less commonly crenulate and are generally sharp, although in a few places they are diffuse over an interval of 2 to 3 cm. Chilled borders are absent, and biotite selvages occur along the margins of a few of the dikes. Many of the granitic dikes lie within the plane of flow foliation of the host rock, and weak foliation in the dikes is concordant with that of the host rock. Angular inclusions of the coarser grained granitic country rock are common in the dikes; these are 6 to 10 cm long, commonly aligned with the foliation, and show varying degrees of assimilation.

The granitic dike rocks have a sucrosic texture, are light to medium gray, fine grained, and equigranular, and contain varying amounts of accessory biotite. They range in composition from granodiorite to monzogranite and contain 20 to 35 percent quartz; this quartz content is similar to that of the coarse-grained compositional equivalents in their respective plutons. In thin section, the texture of the dike rocks is seen to be fine-grained xenomorphic granular with an average grain size of about 0.5 mm. Biotite and minor muscovite are the accessory minerals in most of the dikes, but dikes crosscutting the Paradise pluton also contain sphene, allanite, and rare hornblende. Foliation is weakly to strongly defined by aligned biotite grains and, more rarely, by aligned feldspar grains. Few deformational features are present.

The fine-grained granitic dikes intrude the plutons generally along foliation planes or at low angles to the foliation planes; the dikes also have the same mineralogy as their host plutons. They most likely originated late in the crystallization history of each pluton and represent some of the last compositions of each melt. Dikes that crosscut all structures, however, may have originated from another pluton at depth.

DIORITE DIKES

Diorite, quartz diorite, and tonalite dikes are moderately abundant in the central and southern parts of the lobe and are collectively referred to herein as diorite dikes. They have been described in detail by Toth (1983b) and are present in two modes: large, multiphase complexes and small, solitary dikes.

Several large, multiphase complexes of diorite dikes crop out in the Bear Creek, Paradise, and Canyon Lake plutons, generally close to the pluton boundaries. The complexes extend at an azimuth of 290° as far as 8 km and are as thick as 500 m. In each complex, several textural and chemical phases of diorite intruded the host plutons concordantly to slightly discordantly. Granitic material is commonly present within the complexes as partially ingested xenoliths and averages 10 to 15 volume percent. Intrusive relationships among the various phases of the diorite, and between the granitic rocks and the diorite, are complex; they indicate the sequential intrusion of medium- to coarse-grained diorite, fine-grained diorite, and porphyritic diorite into the granitic plutons. The ages of the various diorite phases overlap, indicating that the diorite units are partly contemporaneous. Field relationships indicate that, although the granitic rocks are mostly older than the diorite, in places they reintrude the diorite; this relationship further indicates a general contemporaneity.

Most of the isolated diorite dikes are related to the larger diorite dike complexes, and the density of dikes decreases rapidly away from the complexes. Fine-grained and porphyritic diorite dikes range in thickness from 0.4 to 10 m and have a lateral extent commonly greater than 10 m. Contacts are generally sharp and well defined, but in a few places they are slightly ragged and crenulate. Most of the dikes parallel the foliation in the country rock, but some crosscut the foliation at low angles (10°–25°). Foliation is moderately to well defined by biotite and hornblende, is developed parallel to the contact, and is most likely flow related. The isolated diorite dikes generally lack inclusions of their host plutons. Partially assimilated small inclusions were noted, however, in a few samples, and feldspar xenocrysts from the Bear Creek pluton were also observed. The dikes commonly crosscut the rocks of the pluton in sharp contact, but at one locality the diorite shows synplutonic relationships typical of those found in the multiphase complexes.

Fine-grained diorite is equigranular, light gray, and rarely aphanitic. The rocks commonly have a porphyritic texture containing 5 to 20 percent plagioclase phenocrysts that are 1 to 2 mm long and sometimes show flow align-

ment. The porphyritic samples contain rare glomerophyric clots of hornblende and biotite 4 to 5 mm across. Large plagioclase xenocrysts, presumably from the granitic plutons that the dikes intrude, are intensely corroded and altered. Medium-grained diorite is equigranular and is either light gray or has a salt-and-pepper appearance. Prismatic hornblende dominates over biotite, and together they constitute 10 to 15 percent of the rock. Potassium feldspar is generally absent, and anhedral quartz is present in highly variable amounts. In three localities, medium-grained rocks grade into rocks of similar composition that have average grain sizes greater than 1 cm. Euhedral sphene is present in many of the samples.

The dike rocks range from diorite to tonalite and quartz content varies from virtually zero to almost as much as total feldspar (fig. 2.4). Biotite (1 to 46 percent) and hornblende (2 to 52 percent) make up the varietal minerals. Major-element chemistry of the diorite dikes demonstrates the widely varying composition of the rocks (fig. 2.5), which reflects large amounts of assimilation of granitic material. Silica variation diagrams also show a relatively high degree of scatter in major-oxide concentrations (Toth, 1983b). The REE concentrations in two dikes are similar to those in the Bear Creek and Paradise plutons (fig. 2.7), but the dikes have slightly lower Ce/Yb ratios (81.9 and 107.1). The two samples also have small Eu anomalies of 0.83 and 0.95. The similarity between the dikes and their host plutons in REE concentrations and Eu anomalies probably reflects the ingestion of some crustal material by both groups of rocks.

The diorite dikes in the central and southern parts of the Bitterroot lobe are mostly younger than the host granitic plutons. Because dioritic magma cannot be produced by the differentiation of a granitic magma, the diorite dikes must have an origin different from that of the granitic plutons. Comparable initial Sr ratios (R.J. Fleck, written commun., 1982), however, suggest a similar source. Synplutonic diorite dikes like these in the Bitterroot lobe have been noted and described in granitic batholiths worldwide (see, for example, Grout and Balk, 1934; Roddick and Armstrong, 1959; Pitcher and Read, 1960; Gastil, 1975; Pitcher, 1978). The dikes are generally small, have consistent orientation within a pluton, and, most important, are intruded over the entire emplacement history of a plutonic complex.

Primary tonalite and andesite magmas are believed to be mantle derived (Wyllie and others, 1976). Initial Sr ratios of diorite dikes in the Bitterroot lobe indicate that the dikes have ingested crustal material with relatively high initial Sr ratios, supporting field observations that the diorite dikes commonly contain partially assimilated inclusions of granitic material. Probably, therefore, the diorite dikes in the Bitterroot lobe are mantle derived and during their emplacement ingested crustal material. Their original emplacement into the crust may have provided much of the heat necessary for the partial melting that formed the granitic magmas, and their occurrence in other granitic batholithic terranes might also indicate a close link to the generation of the granitic magmas. The dikes may have been emplaced at depth throughout the entire formation and crystallization of the granitic plutons, but only penetrated into higher levels late in each pluton's consolidation.

RHYOLITE AND RHYODACITE DIKES

Rhyolite and rhyodacite dikes are associated with Eocene epizonal plutons and are most common within and in close proximity to these plutons. They are buff, gray, or light purple and typically about 1 m thick, and they form conspicuous topographic ribs and walls. Commonly porphyritic, they contain 15 to 20 percent phenocrysts in a matrix that is microcrystalline to cryptocrystalline and displays plumose and spherulitic devitrification textures. The phenocrysts consist of plagioclase, embayed bipyramidal quartz, and subhedral biotite and hornblende. Flow banding and miarolitic cavities are common. Major- and trace-element chemistry is similar to that of the epizonal plutons.

DEPTH OF EMPLACEMENT OF THE BITTERROOT LOBE

Metamorphic grade of the Belt Supergroup surrounding the Bitterroot lobe increases toward the lobe from greenschist to upper amphibolite facies (Reid and Greenwood, 1968). Sillimanite-zone rocks crudely encircle the lobe, although the lobe truncates the isograds along its northern border (Johnson, 1975). Because the metamorphism was probably coincident with or very close in time to batholith emplacement (Wehrenberg, 1972; Williams, 1977; Hyndman, 1980), the metamorphic grade constrains the emplacement level of at least part of the batholith to mesozonal or possibly upper catazonal levels. Wehrenberg (1972) indicates that kyanite is locally present in sillimanite-bearing gneiss, and the coexistence of these two aluminum silicates constrains depth and pressure estimates. The pressure for the kyanite-sillimanite-andalusite invariant point is controversial, but a minimum pressure is probably about 3.75 kbars, equivalent to a depth of about 13 km (Holdaway, 1971). This is supported by estimates that the thickness of overburden during emplacement of the Bitterroot lobe was 13 to 21 km (Hyndman, 1983). It is quite likely, however, that the metamorphism was directly related to the emplacement of only the quartz diorite and tonalite plutons on the north-

ern, western, and southern sides of the Bitterroot lobe. Because the more felsic granitic rocks of the Bitterroot lobe were intruded 30 to 40 m.y. later, their level of emplacement may have been substantially shallower.

The presence of primary muscovite in granitic rocks has been used in the past as a petrogenetic indicator, allowing estimation of a lower limit for the pressure or depth of intrusion of a granitic body. The intersection of the muscovite stability curve with the water-saturated granite solidus was used as an upper limit of intrusion; it has been experimentally determined to be at 3 to 4 kbars (11 to 15 km), depending on which muscovite breakdown reaction is used. Recent work by Anderson and Rowley (1981), however, has shown that adding a celadonite component (phengitic muscovite) to muscovite allows it to coexist with liquids at much lower pressures. Their calculations indicate that muscovite can coexist with H_2O-saturated adamellite-granite melts at 2.6 to 3.1 kbars, corresponding to depths of 9.6 to 11.5 km. However, as they also point out, granitic rocks formed at depths as shallow as 5 km contain primary celadonite (see Benoit, 1971; Nelson and Sylvester, 1971; Sylvester and others, 1978; Bradfish, 1979), so their estimates may be further decreased as better thermodynamic data become available. Because the granite solidus is at slightly higher temperatures for nonsaturated systems, its intersection with the muscovite stability curve will be at slightly higher pressure and temperature in such systems.

The presence of primary celadonite in the Bear Creek pluton should put some constraints on the depth of crystallization for the granitic rocks of the central part of the Bitterroot lobe. According to thermodynamic data, minimum depths of crystallization are about 10 km for saturated systems and somewhat greater for nonsaturated systems. However, because there are several documented cases of celadonite-bearing epizonal granitic plutons, depth of crystallization for the granitic rocks of the lobe could have been substantially shallower.

The plutons southeast of the bordering fault (Piquett Creek and Burnt Ridge plutons) represent magmas that were intruded at depths between mesozonal and epizonal. They contain inclusions of mesozonal granite that crop out west of the fault, and they are therefore younger than the other granitic rocks of the lobe. They show a very weak flow foliation, suggesting shallower depths of intrusion, and have no mylonitic textures. Possible liquidus quartz in the plutons also suggests relatively shallow depths of intrusion (Tuttle and Bowen, 1958).

The Eocene plutons on the northern, southwestern, and southern sides of the Bitterroot lobe were clearly intruded into epizonal levels, possibly as shallow as 1.5 km (Rehn and Lund, 1981). They are generally structureless, contain abundant miarolitic cavities, and in places intrude their own volcanic ejecta.

CONCLUSIONS

The history of the Bitterroot lobe is characterized by the intrusion of compositionally very variable plutons over a relatively short period of time in a changing tectonic regime. Early intrusion of minor amounts of tonalite and quartz diorite into Mesozoic eugeoclinal rocks was related to subduction off the west coast of North America. This was followed by the intrusion, farther eastward, of Late Cretaceous tonalite and quartz diorite plutons, which had probable mantle components but assimilated large amounts of Precambrian crustal material as they moved upward and were emplaced in the crust. Voluminous monzogranite and granodiorite plutons were intruded about 30 to 40 m.y. later at mesozonal to upper mesozonal levels. These plutons are compositionally homogeneous, had a relatively homogeneous source rock, and underwent little differentiation before emplacement. They were almost immediately uplifted to epizonal levels, concurrently with a change in the tectonic environment to one of extension. Large, highly differentiated syenogranite and quartz syenite plutons of lower crustal origin were then intruded. The granitic rocks of the lobe changed during its history from I-type (with a mantle source and the generation of tonalite and quartz diorite magmas) to S-type (with a crustal source and the emplacement of the large monzogranite and granodiorite plutons that constitute most of the lobe), and finally to A-type (with a depleted crustal source and the emplacement of epizonal syenogranite and quartz syenite plutons). The transition from S-type to A-type was marked by the intrusion of a small, compositionally zoned I-type granitic pluton.

REFERENCES CITED

Anderson, A.L., 1930, Geology and mineral resources of the region about Orofino, Idaho: Idaho Bureau of Mines and Geology Pamphlet 34, p. 8-12.

Anderson, J.L., and Rowley, M.C., 1981, Synkinematic intrusion of peraluminous and associated metaluminous granitic magmas, Whipple Mountains, California: Canadian Mineralogist, v. 19, p. 83-101.

Armstrong, R.L., 1975, Precambrian (1500 m.y. old) rocks of central Idaho—the Salmon River arch and its role in cordilleran sedimentation and tectonics: American Journal of Science, v. 275-A, p. 437-467.

Armstrong, R.L., Taubeneck, W.H., and Hales, P.O., 1977, Rb-Sr and K-Ar geochronometry of Mesozoic granitic rocks and their Sr isotopic composition, Oregon, Washington, and Idaho: Geological Society of America Bulletin, v. 88, p. 397-411.

Arth, J.G., and Barker, F., 1976, Rare-earth partitioning between hornblende and dacitic liquid and implications for genesis of trondhjemitic-tonalitic magmas: Geology, v. 4, p. 534-536.

Arth, J.G., and Hanson, G.N., 1972, Quartz diorites derived by partial melting of eclogite or amphibolite at mantle depths: Contributions to Mineralogy and Petrology, v. 3, p. 161-174.

_____ 1975, Geochemistry and origin of the early Precambrian crust of northeastern Minnesota: Geochimica et Cosmochimica Acta, v. 39, p. 325-362.

Bankey, Viki, Brickey, Michael, and Kleinkopf, D.M., 1982, Principal facts for gravity stations in the Selway-Bitterroot Wilderness: U.S. Geological Survey Open-File Report 82-708, 17 p.

Benoit, W.R., 1971, Vertical zoning and differentiation in granitic rocks, central Flint Creek Range, Montana: Missoula, Mont., University of Montana, M.S. thesis, 53 p.

Bickford, M.E., Chase, R.B., Nelson, B.K., Shuster, R.D., and Arruda, E.C., 1981, U-Pb studies of zircon cores and overgrowths, and monazite: implications for age and petrogenesis of the northeastern Idaho batholith: Journal of Geology, v. 89, no. 4, p. 433-457.

Bittner-Gaber, Enid, 1983, Geology of selected migmatite zones within the Bitterroot lobe of the Idaho batholith, Idaho and Montana: Moscow, Idaho, University of Idaho, Ph.D. thesis, 173 p.

Bond, J.G., compiler, 1978, Geologic map of Idaho: Idaho Department of Lands, Bureau of Mines and Geology, with contributions from the U.S. Geological Survey, scale 1:500,000, 1 sheet.

Bradfish, L.J., 1979, Petrogenesis of the Tea Cup granodiorite, Pinal County, Arizona: Tucson, Ariz., University of Arizona, M.S. thesis, 160 p.

Bradley, M.D., 1981, Geology of the northeastern Selway-Bitterroot Wilderness area, Idaho and Montana: Moscow, Idaho, University of Idaho, M.S. thesis, 51 p.

Brickey, Michael, Bankey, Viki, and Kleinkopf, D.M., 1980, Principal facts for gravity stations of part of the Selway-Bitterroot Wilderness, Idaho and Montana: U.S. Geological Survey Open-File Report 80-1241, 14 p.

Brown, G.S., and Fyfe, W.S., 1970, The production of granitic melts during ultrametamorphism: Contributions to Mineralogy and Petrology, v. 28, p. 310-318.

Buddington, A.F., 1959, Granite emplacement with special reference to North America: Geological Society of America Bulletin, v. 70, p. 671-747.

Chappell, B.W., and White, A.J.R., 1974, Two contrasting granite types: Pacific Geology, v. 8, p. 173-174.

Chase, R.B., Bickford, M.E., and Arruda, C.E., 1983, Tectonic implications of Tertiary intrusion and shearing within the Bitterroot dome, northeastern Idaho batholith: Journal of Geology, v. 91, p. 462-470.

Chase, R.B., Bickford, M.E., and Tripp, S.E., 1978, Rb-Sr and U-Pb isotopic studies of the northeastern Idaho batholith and border zone: Geological Society of America Bulletin, v. 89, p. 1325-1334.

Collins, W.J., Beams, S.D., White, A.J.R., and Chappell, B.W., 1982, Nature and origin of A-type granites with particular reference to southeastern Australia: Contributions to Mineralogy and Petrology, v. 80, p. 189-200.

Coxe, B.W., Mosier, E.L., and McDougal, C.M., 1982, Magnetic tape containing analyses of rocks and stream sediments from the Selway-Bitterroot Wilderness, Idaho County, Idaho, and Ravalli and Missoula Counties, Montana: U.S. Geological Survey Report USGS-GD-82-011 (text) and USGS-GD-012 (magnetic tape); available only from U.S. Department of Commerce, National Technical Information Service, Springfield, VA 22161, as report PB-82 253 386.

Coxe, B.W., and Toth, M.I., 1983a, Geochemical maps of the Selway-Bitterroot Wilderness, Idaho County, Idaho, and Missoula and Ravalli Counties, Montana: U.S. Geological Survey Miscellaneous Field Studies Map MF-1495-C, scale 1:125,000.

_____ 1983b, Statistical tables, sample locality maps, and an explanation of data sets for samples from the Selway-Bitterroot Wilderness, Idaho County, Idaho, and Missoula and Ravalli Counties, Montana: U.S. Geological Survey Open-File Report 83-54, 94 p.

Criss, R.E., and Fleck, R.J., 1983, Isotopic characteristics of granitic rocks from the north half of the Idaho batholith [abs.]: Geological Society of America Abstracts with Programs, v. 15, no. 6, p. 550.

Ferguson, J.A., 1972, Fission track and K-Ar dates on the northeastern border zone of the Idaho batholith: Missoula, Mont., University of Montana, M.S. thesis, 32 p.

_____ 1975, Tectonic implications of some geochronometric data from the northeastern border zone of the Idaho batholith: Northwest Geology, v. 4, p. 53-58.

Frey, F.A., Chappell, B.W., and Roy, S.D., 1978, Fractionation of rare-earth elements in the Tuolumne Intrusive Series, Sierra Nevada batholith, California: Geology, v. 6, p. 239-242.

Garmezy, Larry, 1983, Geology and geochronology of the southeast border of the Bitterroot dome: implications for structural evolution of the mylonite carapace: University Park, Pa., Pennsylvania State University, Ph.D. thesis, 269 p.

Garmezy, L.G., and Greenwood, W.R., 1981, Mylonitization coincident with batholith emplacement: Bitterroot lobe, Idaho batholith [abs.]: Geological Society of America Abstracts with Programs, v. 13, p. 1981.

Gastil, R. G., 1975, Plutonic zones in the Peninsular Ranges of southern California and northern Baja California: Geology, v. 3, p. 361-363.

Greenwood, W.R., and Morrison, D.A., 1973, Reconnaissance geology of the Selway-Bitterroot Wilderness area: Idaho Bureau of Mines and Geology Pamphlet 154, 30 p.

Grout, F.F., and Balk, R., 1934, Internal structures in the Boulder batholith: Geological Society of America Bulletin, v. 45, p. 877-896.

Hall, B. S., 1980, Petrography and geochemistry of a part of the Painted Rocks pluton, Idaho County, Idaho: Cheney, Wash., Eastern Washington University, M.S. thesis, 94 p.

Hamilton, Warren, 1963, Metamorphism in the Riggins region, western Idaho: U.S. Geological Survey Professional Paper 436, 95 p.

_____ 1976, Tectonic history of west-central Idaho [abs.]: Geological Society of America Abstracts with Programs, v. 8, p. 378-379.

_____ 1978, Mesozoic tectonics of the Western United States, *in* Howell, D.G., and McDougall, K.A., eds., Mesozoic paleogeography of the Western United States: Society of Economic Paleontologists and Mineralogists, Pacific Section, Pacific Coast Paleogeography Symposium, v. 2, p. 33-70.

Hanson, G.N., 1980, Rare earth elements in petrogenetic studies of igneous systems: Annual Review of Earth and Planetary Sciences, v. 8, p. 371-406.

Holdaway, M.J., 1971, Stability of andalusite and the aluminum silicate phase diagram: American Journal of Science, v. 271, p. 97-131.

Holloway, C.D., 1980, Petrology of the Eocene volcanic sequence, Nez Perce and Blue Joint Creeks, Southern Bitterroot Mountains, Montana: Missoula, Mont., University of Montana, M.S. thesis, 129 p.

Hyndman, D.W., 1977, Mylonitic detachment zone and the Sapphire tectonic block, *in* Geological Society of America Field Guide no. 1: Rocky Mountain Section meeting, University of Montana, Missoula, Montana, p. 25-31.

_____ 1980, Bitterroot dome-Sapphire tectonic block, an example of a plutonic-core gneiss-dome complex with its detached suprastructure, *in* Crittenden, M.D., Jr., Coney, P.J., and Davis, G.H., eds., Cordilleran Metamorphic Core Complexes: Geological Society of America Memoir 153, p. 427-433.

_____ 1981a, Controls on source and depth of emplacement of granitic magmas: Geology, v. 9, p. 244-249.

_____ 1981b, Reply to comment on controls on source and depth of emplacement of granitic magma: Geology, v. 9, p. 503-504.

_____ 1983, The Idaho batholith and associated plutons, Idaho and western Montana, *in* Roddick, J.A., ed., Circum-Pacific plutonic terranes: Geological Society of America Memoir 159, p. 213-240.

_____ 1984, A petrographic and chemical section through the northern Idaho batholith: Journal of Geology, v. 92, p. 83-102.

Johnson, B.R., 1975, Migmatites along the northern border of the Idaho batholith: Missoula, Mont., University of Montana, Ph.D. thesis,

120 p.
Koesterer, M.E., Bartel, A.J., Elsheimer, H.N., Baker, J.W., King, B.S., and Espos, L.F., 1982, Major-element XRF spectroscopy analyses from the Selway-Bitterroot Wilderness, Idaho County, Idaho, and Missoula and Ravalli Counties, Montana: U.S. Geological Survey Open-File Report 82-1094, 36 p.
Kosinowski, M.H.F., 1982, MSONRM, a fortran program for the improved version of mesonorm calculation: Computers and Geosciences, v. 8, no. 1, p. 11-26.
Lee, D.E., and Christiansen, E.H., 1983, The granite problem as exposed in the southern Snake Range, Nevada: Contributions to Mineralogy and Petrology, v. 83, p. 99-116.
Lindgren, W., 1900, The gold and silver veins of Silver City, De Lamar and other mining districts in Idaho: U.S. Geological Survey 20th Annual Report, part 3, p. 65-256.
_____ 1904, Geological reconnaissance of Bitterroot Range and Clearwater Mountains: U.S. Geological Survey Professional Paper 27, 123 p.
Loiselle, M.C., and Wones, D. R., 1981, Characteristics and origin of anorogenic granites [abs.]: Geological Society of America Abstracts with Programs, v. 11, no. 7, p. 468.
Lund, K.I., 1980, Geology of the Whistling Pig pluton, Selway-Bitterroot Wilderness, Idaho: Boulder, Colo., University of Colorado, M.S. thesis, 115 p.
Lund, K.I., Rehn, W.M., and Holloway, C.D., 1983, Geologic map of the Blue Joint Wilderness Study Area, Ravalli County, Montana, and the Blue Joint Roadless Area, Lemhi County, Idaho: U.S. Geological Survey Miscellaneous Field Studies Map MF-1557-B, scale 1:50,000.
Miller, C.F., 1981, Comment on controls on source and depth of emplacement of granitic magma: Geology, v. 9, p. 503.
Miller, C.F., Stoddard, E.F., Bradfish, L.J., and Dollase, W.A., 1981, Composition of plutonic muscovite: genetic implications: Canadian Mineralogist, v. 19, p. 25-34.
Motzer, W.E., 1981, Tertiary epizonal plutonic rocks of the Selway-Bitterroot Wilderness, Idaho [abs.]: Geological Society of America Abstracts with Programs, v. 13, p. 210.
Nelson, C.A., and Sylvester, A.G., 1971, Wall rock decarbonation and forcible emplacement of the Birch Creek pluton, southern White Mountains, California: Geological Society of America Bulletin, v. 82, p. 2891-2904.
Nold, J.L., 1968, Geology of the northeastern border zone of the Idaho batholith, Montana and Idaho: Missoula, Mont., University of Montana, Ph.D. thesis, 159 p.
Pawlowski, M.R., 1981, Geology and exploration geochemistry of the Magruder Corridor, Idaho County, Idaho: Moscow, Idaho, University of Idaho, M.S. thesis, 128 p.
Pitcher, W.S., 1978, The anatomy of a batholith: Journal of the Geological Society of London, v. 135, p. 157-182.
Pitcher, W.S., and Read, H.H., 1960, Early transverse dykes in the Main Donegal granite: Geological Magazine, v. 97, p. 53-61.
Piwinskii, A.J., 1968, Experimental studies of igneous rock series: central Sierra Nevada batholith, California: Journal of Geology, v. 76, p. 548-570.
Rehn, W.M., 1984, Petrology and geochemistry of the Blue Joint Area, Idaho and Montana: Golden, Colo., Colorado School of Mines, M.S. thesis, 202 p.
Rehn, W.M., and Lund, K.I., 1981, Eocene extensional plutonism in the Idaho batholith region [abs.]: Geological Society of America Abstracts with Programs, v. 13, p. 536.
Reid, R.R., and Greenwood, W.R., 1968, Multiple deformation and associated progressive polymetamorphism in the Beltian rocks north of the Idaho batholith, Idaho, U.S.A.: Geology of Precambrian, International Geological Congress, 23rd, Prague, Czechoslovakia, 1968, Proceedings, v. 4, p. 75-87.
Robertson, J.K., and Wyllie, P.J., 1971, Rock-water systems with special reference to the water-deficient region: American Journal of Science, v. 271, p. 252-277.
Roddick, J.A., and Armstrong, J.E., 1959, Relict dikes in the Coast Mountains near Vancouver, British Columbia: Journal of Geology, v. 67, p. 603-613.
Streckeisen, A.L., chairman, and others, 1973, Plutonic rocks—classification and nomenclature recommended by the IUGS subcommission on the systematics of igneous rocks: Geotimes, v. 18, no. 10, p. 26-30.
Sylvester, A.G., Oertel, G., Nelson, C.A., and Christie, J.M., 1978, Papoose Flat pluton: a granitic blister in the Inyo Mountains, California: Geological Society of America Bulletin, v. 89, p. 1205-1219.
Toth, M.I., 1983a, Reconnaissance geologic map of the Selway-Bitterroot Wilderness, Idaho County, Idaho, and Missoula and Ravalli Counties, Montana: U.S. Geological Survey Miscellaneous Field Studies Map MF-1495-B, scale 1:125,000.
_____ 1983b, Structure, petrochemistry, and origin of the Bear Creek and Paradise plutons, Bitterroot lobe of the Idaho batholith: Boulder, Colo., University of Colorado, Ph.D. thesis, 337 p.
Toth, M.I., Coxe, B.W., Zilka, N.T., and Hamilton, M.M., 1983, Mineral resource potential of the Selway-Bitterroot Wilderness, Idaho County, Idaho, and Missoula and Ravalli Counties, Montana: U.S. Geological Survey Miscellaneous Field Studies Map MF-1495-A, scale 1:125,000.
Tuttle, O.F., and Bowen, N.L., 1958, Origin of granite in light of experimental studies in the system $NaAlSi_3O_8$-$KAlSi_3O_8$-SiO_2-H_2O: Geological Society of America Memoir 74, 153 p.
Wehrenberg, J.P., 1972, Geology of the Lolo Peak area, northern Bitterroot Range, Montana: Northwest Geology, v. 7, p. 25-32.
Williams, L.D., 1977, Petrology and petrography of a section across the Bitterroot lobe of the Idaho batholith: Missoula, Mont., University of Montana, Ph.D. thesis, 212 p.
Winkler, H.G.F., 1979, Petrogenesis of metamorphic rocks, 5th edition: New York, Springer-Verlag, 348 p.
Wyllie, P.J., Huang, W.-L., Stern, C.R., and Maaloe, Sven, 1976, Granitic magmas: possible and impossible sources, water contents, and crystallization sequences: Canadian Journal of Earth Sciences, v. 13, no. 8, p. 1007-1019.

3. STRUCTURAL GEOLOGY AND PETROLOGY OF A PART OF THE BITTERROOT LOBE OF THE IDAHO BATHOLITH

By ROLLAND R. REID[1]

ABSTRACT

Mapping of an area about 15 km north-south by 85 km east-west across the north-central part of the Bitterroot lobe of the Idaho batholith shows that the structure of the lobe is asymmetrical. Flow foliation along the western margin strikes northwesterly and dips steeply. Within the lobe, migmatite screens dip varying amounts and strike at predominantly az 090°, near the primary flow lineation trend. Foliation becomes progressively more intense to the east and drapes over a north-south arch near the Bitterroot mylonite front. Primary flow foliation is strongly overprinted to destroyed by a secondary flow foliation and lineation trending near az 290° in a wedge-shaped area that widens to the east. The disposition of secondary lineation suggests an original batholith thickness in excess of 30 km. Features of gneissic foliation, nonpenetrative blastomylonite, and mylonite are consistent in their indication of cover-rock movement toward az 110° throughout three structural phases.

The asymmetric structure began to develop with the rise of tonalite magma along a north- to northwest-trending fracture set near the western margin of the lobe. This was followed by voluminous mixed granite-granodiorite magma, with minor anorthosite and tonalite in deeper parts, which spread to the east in a sheet perhaps controlled by a low-angle thrust near its base. The granitic part of the massif is vertically zoned, from calcic granodiorite near its base to granite at the top. During emplacement, primary flow foliation formed, and migmatite screens were rotated into an east-west trend. After consolidation, shearing of still-hot rock created secondary foliation, later blastomylonite, and still later mylonite in episodes that continued during arching and rise to higher crustal levels. Some east-west extension occurred in conjunction with thrusting during the later stages of cooling.

INTRODUCTION

The rocks discussed in this paper form part of the Bitterroot lobe of the Idaho batholith (fig. 3.1). They occur in north-central Idaho and extend into southwestern Montana, in a region with local relief up to 2,000 m (6,000 ft). Quartzite and calc-silicate gneiss provisionally correlated with units of the Belt Supergroup (its Ravalli Group and Wallace Formation, respectively) are the country rocks into which the batholith was intruded. The rocks in the western part of the Bitterroot lobe broadly comprise tonalite cut by later granitic rocks, which become major to the east. The igneous rock nomenclature used herein is that of Streckeisen and others (1973).

This paper stems from work done on the U.S. Geological Survey project (1978–1981) to assess the mineral potential of the Selway-Bitterroot Wilderness Area. I mapped the structure in the field and made structural geometric analyses and petrographic studies. Terry Hayden mapped in my stead during one summer after I broke a leg. I studied a total of 1,064 thin sections and did 619 modal analyses. Modes were measured in thin section for rocks of grain size 2 mm or smaller. For medium-grained rocks coarser than 2 mm, modes were measured both in thin section and on stained slabs and the results combined. For coarsely porphyritic rocks, the percentage of phenocrysts was measured at the outcrop using a knotted string devised by Bill Greenwood and the results combined with thin-section and stained-slab analyses of the matrix. Anywhere from 200 to 1,600 points per specimen were counted, depending on grain size and inhomogeneity of the rocks. Plagioclase composition was determined in thin section using the standard a-normal method.

Detailed data from this work are given in an open-file report available from the U.S. Geological Survey (Reid, 1984). This paper is a shortened version.

PREVIOUS WORK

Reconnaissance investigations constituted the early work in the Bitterroot lobe of the Idaho batholith and its environs. Lindgren (1904) was the earliest worker in the area; he wrote of a Mesozoic quartz monzonite mass with an eastern schistose slope probably due to a great fault.

[1]Department of Geology, University of Idaho, Moscow, Idaho.

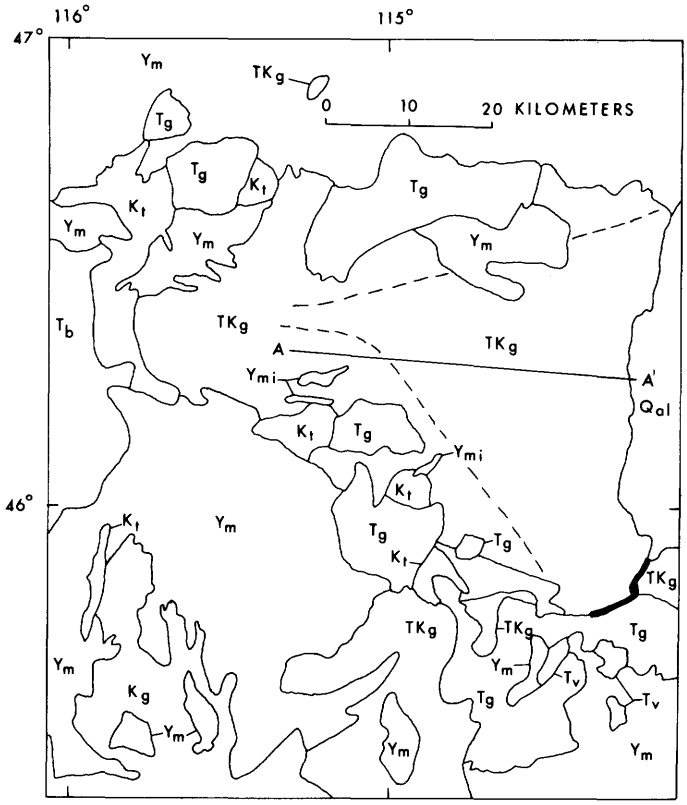

EXPLANATION

Qal	Alluvium (Quaternary)
Tb	Basalt (Miocene)
Tv	Volcanic rocks (Eocene)
Tg	Epizonal granite (Eocene)
TKg	Mesozonal granitic rocks of the Bitterroot lobe (Paleocene and Cretaceous)
Kt	Mesozonal tonalite, diorite and quartz diorite (Cretaceous)
Kg	Granitic rocks of the Atlanta lobe of the Idaho batholith (Cretaceous)
Ymi	Migmatite (Middle Proterozoic?)
Ym	Metamorphic rocks (Middle Proterozoic?)
	Major fault

FIGURE 3.1.—Generalized geologic map of the Bitterroot lobe of the Idaho batholith. Dashed lines show approximate boundaries of the field of secondary strain, which is the area affected by metamorphic core complex phenomena. A-A′, line of section of figure 3.2, and the approximate line of quadrangles mapped, shown in figure 3.2. Other geologic features after Toth (1983).

Ross (1928) showed that the Idaho batholith is post-Triassic and pre-Tertiary and is cut by younger granitic masses. Langton (1935) studied the northeastern Idaho batholith, showing two deformations in the country rock and thrusts related to the emplacement of the batholith.

Later studies became more detailed. Anderson (1952) did further work on the concept of multiple emplacement of the batholith, a theme developed in the earlier reconnaissance of Ross (1928). Ross (1952) developed a granitization hypothesis to explain the eastern frontal gneiss of the Bitterroot Mountains, inferring that emanations from the batholith converted sedimentary rock to gneiss. Reconnaissance modal and chemical compositional studies by Larsen and Schmidt (1958) showed a considerable variety of rock types (eleven) in the Idaho batholith. Reid (1959) discovered three sets of synmetamorphic folds, predating emplacement of the batholith, in wall rocks on its west side. Leischner (1959) studied the batholith in the vicinity of Lolo Hot Springs, Montana, and found an intrusive sequence from early diorite through quartz diorite to quartz monzonite. Ross (1965) found that the main interior mass of the Idaho batholith is largely granodiorite and quartz monzonite and is surrounded by a narrow discontinuous roof and border zone of quartz diorite and quartz diorite gneiss. Thrusting occurred away from the batholith interior on the eastern and western margins, in part preceding and in part following batholith emplacement. Chase (1968) studied country rock in the northeast contact zone of the Idaho batholith and found metasedimentary units regionally metamorphosed in three phases of synmetamorphic penetrative deformation before emplacement of the Idaho batholith, the deformation phases perhaps comparable to those discovered by Reid (1959). Morrison (1968) also found three prebatholithic metamorphic episodes in the Lochsa area northwest of the batholith, plus a fourth episode synchronous with batholith emplacement. Further study in the country rock northeast of the batholith (Berg, 1969) disclosed 20 concordant anorthosite bodies, dominantly labradorite, within the gneiss.

Beginning broader work, the Idaho Bureau of Mines and Geology studied the reconnaissance geology and mineral potential of the Selway-Bitterroot Wilderness Area, which includes much of the Bitterroot lobe of the Idaho batholith (Greenwood and Morrison, 1973). In a regional study, Ryder and Scholten (1973) showed that the thick accumulations of syntectonic conglomerate of the Beaverhead Formation in Montana were derived from the northeast margin of the Idaho batholith in Early Cretaceous to middle Paleocene time. Armstrong (1974) discussed relations between tectonic activity and magmatism in the cordillera; this work delineates the broad temporal and structural framework within which the batholith was emplaced. Nold (1974) showed that the Belt Supergroup

and associated orthoamphibolite and orthogneiss units were deformed at least four times before they were injected by the quartz diorite to granite of the Idaho batholith. This interpretation corresponds well with earlier results obtained northwest of the batholith by Morrison (1968) and west of the batholith by Reid (1959). In a detailed structural analysis, Cheney (1975) showed that anorthosite bodies in the country rock near the northeast margin of the batholith have experienced three structural events. They are thus closer in age to the country rock than to the batholith. Armstrong (1975a) suggested the name "Bitterroot lobe" for the northern part of the Idaho batholith. Williams (1977) showed that the northern Bitterroot lobe consists largely of foliated, medium- to coarse-grained, megacrystic, two-mica granite, intruded by granodiorite. Wiswall (1979) suggested that the base of the Bitterroot lobe was exposed south of my map area, where gneiss and migmatite are overlain by granitic rock of the batholith. Bradley (1981) studied a gneissic tonalitic phase of the Bitterroot lobe along its northeastern border. This is a part of Ross' (1965) roof and border zone of quartz diorite gneiss. Bradley showed the gneissic tonalite to be earlier than the granitic phase of the Bitterroot lobe. Toth (1981) defined two major plutons, the Bear Creek pluton and the younger Cub Creek pluton, within the main Bitterroot lobe. The Bear Creek pluton is a medium-grained granite having varied amounts of poorly defined potassium feldspar phenocrysts and 3 to 5 percent biotite, 3 to 5 percent hornblende, and as much as 3 percent sphene. These units may correspond to those described by Williams (1977). The relevant geologic mapping was published by Toth in 1983.

As a part of the continuing more detailed study of the Bitterroot lobe, work has been done on the extensive migmatite within and peripheral to the lobe. Johnson (1975) inferred that the migmatite formed by injection, metamorphic differentiation, and anatexis. Bittner-Gaber (1983) showed that the migmatite screens within the lobe are oriented largely east-west (p. 22) and were derived from the wall rocks and (or) roof rocks (p. 114). Their east-west orientation is due to magma flow, postulated to be from west to east. The migmatite protolith has been strongly injected by magma of several types, and the resulting migmatite has in many places been intricately folded.

The continuing detailed studies have resulted in the interpretation of a part of the Bitterroot lobe as a metamorphic core complex (Chase and Hyndman, 1977; Hyndman, 1980). Many workers, too numerous to list here, have concentrated on the eastern mylonitic detachment zone (hearkening back to Lindgren's idea of a major fault zone). Core-complex effects extend some distance west within the lobe. Toth (1981), for example, showed that both the Bear Creek and Cub Creek plutons have moderately to well-developed flow foliation that decreases in dip upward, suggesting increasing proximity to the roof of the batholith. Primary mineral lineations, defined by igneous fabric elements, and small fold axes trend at az 290° (down-plunge direction) and plunge at shallow angles. Secondary mineral lineations, defined by crystalloblastic fabric elements, trend at az 290° and az 110° and also plunge at shallow angles, with the az 110° element increasing in abundance toward the eastern bordering mylonite front. Garmezy and Sutter (1983) have done the most detailed work on the mylonite zone. Mylonitization began at about 45.5 Ma at a depth probably greater than 10 km and continued for about 2 m.y. during a period of rapid uplift. Mylonitic fabric indicates eastward tectonic transport of the hanging wall throughout the 500- to 1,000-m-thick mylonite zone. The presence of ductile normal faults in this zone, which have a sense of displacement parallel to the mylonitic lineation, suggests that mylonitization occurred in an extensional environment in which a principal extension direction was aligned at az 110°.

The inferred movement direction of the cover rock above the detachment zone has been controversial, but increasing evidence is coming to support eastward transport. This view was presented early by Hyndman (1980) and has lately been presented with convincing evidence for the Okanogan dome of north-central Washington (Goodge, 1983).

Much radiometric dating has been done on the Bitterroot lobe and its country rock. Armstrong (1975b) compiled voluminous data and noted (p. 32) that the ages for the Bitterroot lobe are all less than 70 Ma. Chase and others (1978) arrived at an age of 66 Ma for the main-stage batholithic emplacement and an age of 46 to 39 Ma for a late thermal-plutonic event. Bickford and others (1981), in a very detailed study, showed the following intrusive history, based on lower intercept ages (p. 453): quartz diorite gneiss at about 73 Ma, medium-grained granite at about 55 Ma, and cataclastic granite at 49 to 46 Ma. The age for cataclastic granite is close to the time of beginning of mylonitization, given by Garmezy and Sutter (1983) at 45.5 Ma. Upper intercept ages are given by Bickford and others (1981, p. 454) in the range 1,700 to 2,300 Ma. These ages are interpreted as due to country-rock contributions either in partial melting or in contamination.

WALL ROCK SOUTHWEST OF THE BITTERROOT LOBE

STRUCTURE

The southwestern contact of the Bitterroot lobe of the Idaho batholith consists of metasedimentary and

metaigneous rock marginal to quartz diorite and tonalite of the batholith. The northern part of this area contains granite and granodiorite injected into the tonalite (figs. 3.1, 3.2).

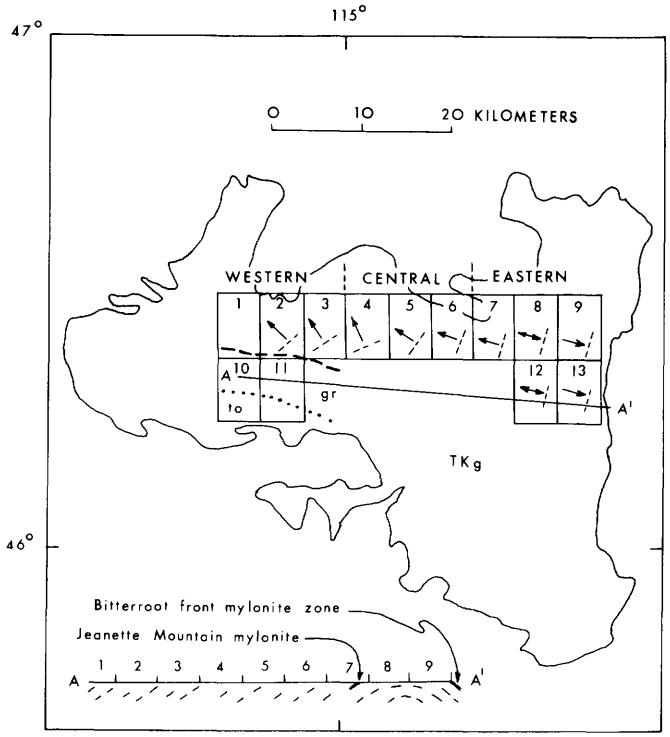

EXPLANATION

TKg Mesozonal granitic rocks of the Bitterroot lobe (Paleocene and Cretaceous)

gr Granitic rocks, part of TKg

to Older tonalite, part of TKg

····· Generalized contact between granitic rocks and older tonalite

-- Southern limit of secondary strain

Direction of generally 30°-plunging flow lineation, averaged for each quadrangle

Horizontal flow lineation at the Bitterroot arch

--- Extension joint trends; the joints average to be near perpendicular to flow lineation

METASEDIMENTARY ROCKS

Calc-silicate gneiss is the principal country rock exposed at the southwestern margin of the lobe, whereas biotite quartzite is abundant in migmatite screens inside the batholith. The calc-silicate gneiss is deformed in folds of steep but varied plunge. Schistosity lies parallel or subparallel to the igneous contact and to original bedding in the calc-silicate gneiss; this schistosity has been deformed in small passive-flow folds showing both clockwise and counterclockwise rotation somewhat randomly through the outcrops. The axial planes of these small folds are everywhere parallel to the foliation of the enclosing rocks, regardless of the orientation of the major foliation. Mineral lineation parallels the minor fold axes and consists of elongate biotite clots, diopside and hornblende prisms, and quartz rods.

Pegmatite, alaskite, and aplite have been injected along the foliation and are folded with it; in places, the igneous material cuts both foliation and minor folds and is itself folded. The pegmatite is partly in lozenge boudins, which show separations of as much as 1.5 m along the layering.

The small folds mentioned above are all conical. A set of small isoclinal folds, seen in a few places, predates the conical folds, as the conical folds deform the foliation formed by their axial-plane schistosity. The isoclinal-fold foliation stands vertical, and the fold axes plunge 90°. The isoclinal folds, the oldest folds recognized in the rock, are assigned to a deformation phase D_1, and the conical folds are assigned to D_2. Sequential measurement of the orientation of small conical-fold axes downward along their plunge shows that the bearing and plunge change. Thus, the folds may be characterized as helical or screwlike.

The axial planes of the conical folds are deformed in a larger synform. The concentric style and low-angle plunge of this fold suggest that it is distinctly younger and should be assigned a D_3 age. Low-angle crinkle lineation in the rock is probably related to this fold set.

In addition to calc-silicate gneiss, three other wall rock types occur: biotite quartzite (predominant), biotite gneiss, and biotite-muscovite schist (minor). Rare calc-silicate

FIGURE 3.2.—Outline map showing the thirteen 7.5-minute quadrangles entirely or partly mapped across the Bitterroot lobe of the Idaho batholith, and along section line A-A′ of figure 3.1. Quadrangle names: 1, Huckleberry Butte; 2, Greenside Butte; 3, Fish Lake; 4, McConnell Mountain; 5, Hungry Rock; 6, Cedar Ridge; 7, Jeanette Mountain; 8, Blodgett Mountain; 9, Printz Ridge; 10, Chimney Peak; 11, Fenn Mountain; 12, Tenmile Lake; 13, Ward Mountain. These quadrangle names are used for geographic reference throughout the report. Flow directions in granitic rocks, shown as average for each quadrangle by solid arrows, form a fan-shaped array. The chlorite-coated, microbrecciated shear joints in the several quadrangles are believed to be tension fractures initially perpendicular to flow lines and reactivated in younger movements.

layers are generally thin but locally reach 65 m in thickness. The rock structure was analyzed in a profile section perpendicular to the 30°-southeast plunge. The overall structure is a nearly recumbent, somewhat refolded isoclinal fold. The D_1 minor folds are isoclinal and have axial-plane schistosity. Amphibolite and tonalite sheets occur along the schistosity and are deformed by the D_1 isoclinal folds. The rocks were injected synkinematically by concordant and discordant pegmatites, which are folded and schistose parallel to the external schistosity. Orbicules are flattened in the plane of the schistosity.

The D_2 folds developed a secondary axial-plane schistosity (S_2) largely restricted to their hinges. Lineated biotite and muscovite parallel the fold axes. Boudins produced by stretching in D_1 are locally folded in D_2; crenulation folds (late D_2 or D_3) kink the earlier schistosity and the igneous-rock sheets along it. Biotite and muscovite are further lineated parallel to kink-fold axes. Late shears of diverse orientation contain sheared-out, streaked muscovite and annealed slickensides, all trending nearly due east.

Poles to foliation/bedding locally show a diffuse girdle indicative of folding about an axis oriented to the southeast; early fold axes are of scattered orientation, as are crenulation fold axes. Mineral lineation trends are also widely scattered.

METAIGNEOUS ROCKS

Tonalitic gneiss occurs as concordant sheets as much as 1 or 2 km thick in the country rock southwest of the Bitterroot lobe. Attitudes on foliation in the gneiss indicate steep dips and a considerable range of strikes forming conical folds. Axes of minor folds in the gneiss plunge vertically or nearly so, but the axial planes display widely varied trends. Mineral lineation consisting of elongate biotite streaks and clots commonly parallels the axes of the minor folds. The folds show both clockwise and counterclockwise rotation more or less randomly through the outcrops. Concordant veins of trondhjemite were injected along the foliation and are folded with the gneiss.

PETROGRAPHY

The wall rocks comprise (1) pelitic quartzite and schist, from quartz sand and shale, and (2) calc-silicate quartzite and gneiss, from dolomitic quartzite and shale-dolomite mixtures.

In the pelitic schist, quartz is present in two populations. The first consists of platy grains 2 to 4 mm across that are oriented parallel to the schistosity and elongate parallel to mineral lineations within it. These grains enclose oriented biotite, muscovite, and fibrolite, and are cut by *a-c* extension fractures spaced at intervals of 0.3 to 0.7 mm. The second population consists of irregular grains 0.3 to 0.5 mm across. Most grains in both populations show undulatory extinction.

Plagioclase occurs as unzoned granoblastic grains 0.5 to 1 mm in diameter and has compositions ranging from An_{20} to An_{30}. Clay alteration is minor but ubiquitous.

Biotite is lepidoblastic as grains 0.3 to 2 mm in diameter, most of them stretched and elongate or forming clusters streaked out in a lineation. Pennine alteration varies from weak to strong. Some biotite is in vermiform intergrowths with quartz. Muscovite occurs as flakes 0.1 to 0.3 mm across, replacing biotite and mostly of random orientation. Some muscovite is also in vermiform intergrowths with quartz. Sillimanite is in only a few of the rocks sampled. Representative prisms are 0.03 mm by 0.15 mm and oriented parallel to other mineral lineations in the rock. Prisms are commonly broken and stretched parallel to their length.

Microcline grains are platy and oriented parallel to the foliation; within the foliation, they are elongate (for example, 1.5 mm by 4 mm as seen in an *a-b* section) parallel to other mineral lineations. Microcline encloses small, oriented biotite flakes. Sillimanite is mostly absent in microcline grains, even where it is found elsewhere in the same rock, and the few grains that are found in microcline are mere shreds that appear to be undergoing replacement. The microcline is cut by *a-c* extension fractures spaced at 0.1- to 0.2-mm intervals. Stained slabs show microcline to be concentrated in certain folia.

Accessory minerals include magnetite (elongate grains parallel to other mineral lineations), zircon, baddeleyite, thorite, apatite, epidote, and schorlite.

In calc-silicate quartzite and gneiss, quartz is present as granoblastic grains 0.5 mm across and as elongate flattened blebs parallel to other mineral lineation. Plagioclase is present as unzoned, granoblastic, 1-mm grains, some of which are as elongate plates parallel to other mineral lineation. Their composition ranges from An_{25} to An_{43}. Hornblende and diopside form lineated prisms lying in the foliation. Scapolite is in one specimen as granoblastic grains 0.5 mm across.

TONALITE OF THE SOUTHWESTERN BITTERROOT LOBE

STRUCTURE

A quartz diorite to tonalite intrusive unit invades the country rock of the southwestern batholith margin (fig. 3.2). The intrusive unit shows a strong flow foliation, rather swirled and of varied attitudes, that generally has a northerly trend and a westerly dip of about 70°. Flow lineation consisting of oriented hornblende prisms or

biotite grains and clusters plunges down the dip of the flow foliation. Rare, dark inclusions are drawn out into elongate spindles parallel to the hornblende lineation and flattened in the plane of the flow foliation.

Pegmatite, alaskite, and aplite dikes of shallow to steep dip cut the intrusion. The shallow-dipping sheets, mostly trondhjemitic, have a northerly trend and easterly dip of about 20°, but the steep dikes show no preferred orientation.

At some places, the flow foliation is complexly swirled in small folds showing both clockwise and counterclockwise rotation randomly through the outcrop.

Tonalitic rocks, including pegmatite and alaskite, are locally cut by cataclastic shear surfaces on which slickensides are "frozen" or recrystallized, resulting in microrodding and grooving. These features are best shown in the pegmatitic rocks, on both near-horizontal and steeply dipping surfaces.

Migmatite is abundant both here and in the granitic rocks described below. It has been discussed by Bittner-Gaber (1983).

PETROGRAPHY

Tonalite occurs in major amounts in the western Bitterroot lobe of the Idaho batholith (fig. 3.1). It is coarsely foliated and medium grained, and has a varied flow lineation that is strongest near the margin of the intrusion. The flow lineation consists mostly of hornblende prisms plunging steeply down the dip of the foliation.

Hornblende is relatively abundant in the western part of the intrusion, but less abundant to absent toward the eastern part. It occurs in 2-mm prisms, partly altered to biotite.

Biotite occurs in 0.5- to 2-mm flakes in crude lepidoblastic array in the flow foliation. Grains display olive-brown to strong reddish-brown pleochroism and minor pennine-epidote-sericite alteration. Some grains are bent cataclastically.

Plagioclase (An_{27-37}) is euhedral to subhedral in 2- to 3-mm grains, which have albite twinning and are mostly unzoned. Anorthite content of the plagioclase shows no systematic areal variation. A few plagioclase grains show normal zoning from cores of An_{28} to rims of An_{25}. Alteration products are minor sericite and epidote, and a few grains have bent albite-twin lamellae.

Quartz occurs in 0.5- to 2-mm grains, most showing undulatory extinction and many having sutured quartz-quartz grain boundaries. A trace to 5 percent microcline is in a few specimens. Accessory minerals include allanite, baddeleyite, magnetite, sphene, thorite, and zircon.

Rare, dark, spindled and lineated xenoliths of diorite in the tonalite perhaps represent cognate inclusions. They have a fairly uniform grain size of 0.5 mm and consist of hornblende, biotite, and unzoned granoblastic plagioclase having a composition of An_{37}. Accessory minerals are apatite, baddeleyite, magnetite, and zircon.

Tonalitic gneiss has intruded the country rock near the batholith in concordant sheets at least several hundred meters thick. Its mineralogy is like that of the batholithic tonalite, from which the rock differs only in its gneissic structure.

Quartz occurs partly as small, equant grains and partly as large, flattened, elongate platelets, typically 1 mm by 3 mm by 6 mm, oriented with their long direction parallel to the other lineation in the rock. Prisms of hornblende and plagioclase (An_{37}) 4 to 6 mm long also lie parallel to the lineation. Biotite in 3- to 4-mm flakes is partly stretched into elongate grains and grain clusters that parallel the lineation as well. In quartz-rich varieties of the tonalite, minor sillimanite occurs in fibers parallel to the lineation, and plagioclase is more sodic (An_{27}) than in quartz-poor varieties. Muscovite also occurs in some specimens. Accessory minerals include apatite, baddeleyite, magnetite, sphene, thorite, and zircon.

Trondhjemite in the form of lit-par-lit veinlets has intruded the tonalitic gneiss parallel to its foliation. Quartz in these veinlets has mild undulatory extinction and forms elongate platelets 4-6 mm long that are arranged in a crude linear array. Elongate grains and grain aggregates of biotite also form a linear array parallel to that of the quartz platelets. Plagioclase in 2- to 3-mm grains is more sodic (An_{25}) than plagioclase in the enclosing tonalitic gneiss. Plagioclase grains are mostly granoblastic and unzoned, but some patchy, irregular relict(?) zoning is seen. A trace of muscovite occurs, together with chlorite, magnetite, thorite, and zircon.

The tonalite and neighboring rocks are cut by dikes and sheets of pegmatite, alaskite, and aplite. Alaskite sheets are most common and are representative of the mineralogy of the pegmatite suite; they are mostly trondhjemitic, although three sheets of granitic alaskite were found. Trondhjemite plagioclase (An_{31}) occurs in 2-mm prisms and is mostly unzoned, but a few grains show some oscillatory normal zoning. Quartz and biotite are as 1- to 2-mm grains, and accessories include apatite, epidote, muscovite, pennine, and thorite.

In the granitic alaskite, microcline occurs in grains more than 8 mm in diameter. Plagioclase (An_{20}) is in grains as much as 6 mm in diameter, which are unzoned and partly myrmekitic where in contact with microcline grains. Plagioclase is partly altered to muscovite. Quartz shows some undulatory extinction and sutured grain boundaries.

In both the trondhjemite and the granitic alaskite, some shear reduction of quartz and feldspar occurs in cataclastic zones with partial strain recovery. Grain size in the cataclastic zones averages 0.3 mm. Many cataclastically

reduced grains are free of undulatory extinction, and the sutured grain boundaries are annealed.

GRANITE, GRANODIORITE, AND RELATED ROCKS OF THE WESTERN, CENTRAL, AND EASTERN SECTORS

Granite, granodiorite, and smaller amounts of quartz monzonite, quartz monzodiorite, tonalite, diorite, and anorthosite crop out in a row of nine 7.5-minute quadrangles approximately along latitude 46°15′ N., representing a continuous east-west transect across the Bitterroot lobe of the Idaho batholith (figs. 3.1, 3.2). No significant modal variations in the main rock types occur over this transect, and granite and granodiorite are present in about equal amounts. For convenience and because of structural variations, however, the rocks are divided for discussion into western, central, and eastern sectors. All of these rocks in the three sectors belong to the Bear Creek pluton as defined by Toth (1981).

STRUCTURE

The western sector covers all or parts of the following 7.5-minute quadrangles: Fenn Mountain, Chimney Peak, Huckleberry Butte, Greenside Butte, and Fish Lake (fig. 3.2). The sector is discussed in terms of two zones, northern and southern, whose structures are different.

In this area granite and granodiorite cut the previously discussed tonalite unit of the southwestern batholth (fig. 3.1). Xenoliths of tonalite occur in the granite.

The granitic rock of the southern zone has a strong primary flow foliation parallel to the tonalite contact. The near-vertical orientation of flow lineation is comparable to that of the lineation in the tonalite. Thus, a degree of flow coupling may have existed between the granitic magma and its wall rock during the emplacement of the granite. Orientations of pegmatite dikes and sheets in the granitic rock are different from those in the tonalite, indicating a different system of flow and stretching.

Farther into the granitic pluton and across a subtle but major zone of structural transition, the Greenside Butte area is representative of the northern zone of the western sector. The rocks here are principally granite and granodiorite, which show local flow foliation formed mostly by biotite or microcline bands and less commonly by biotite-rich schlieren. The orientation of the flow foliation, shown in figure 3.3, is characteristic of both the western and central sectors; to a lesser extent, it is also characteristic of the eastern sector. Poles to the flow foliation, including some blastomylonite discussed below, lie in a diffuse girdle whose axis is oriented west-northwest.

Reconnaissance mapping suggests that the various igneous rocks are rather thoroughly intermixed. In a representative traverse for 11 km along a ridge in well-exposed rocks, different rock types were encountered in the following order: granite; granite; granodiorite and foliated tonalite at the same outcrop; granite; migmatite; granite; migmatite; granite and granodiorite at the same outcrop; granodiorite; porphyritic granodiorite; tonalite; foliated, porphyritic granodiorite, granite, migmatite; granodiorite; granodiorite. The rocks, all medium grained and gray, look much alike and are not recognized as separate varieties in the field; no unit contacts were discerned other than those of the migmatite zones. This traverse is judged to be indicative of the degree of variation of granitic rock types in the entire mapped area of the Bitterroot lobe, because samples from less well exposed parts of the area show similar variation.

Flow foliation is sporadically present in the rocks of the northern zone; about one-third of the specimens collected there are coarsely foliated and the rest massive. The two types are irregularly mixed over the area among all the rock types present. Mostly, the flow foliation is primary, expressed not only by rather coarse banding but also by aligned schlieren and platy xenoliths.

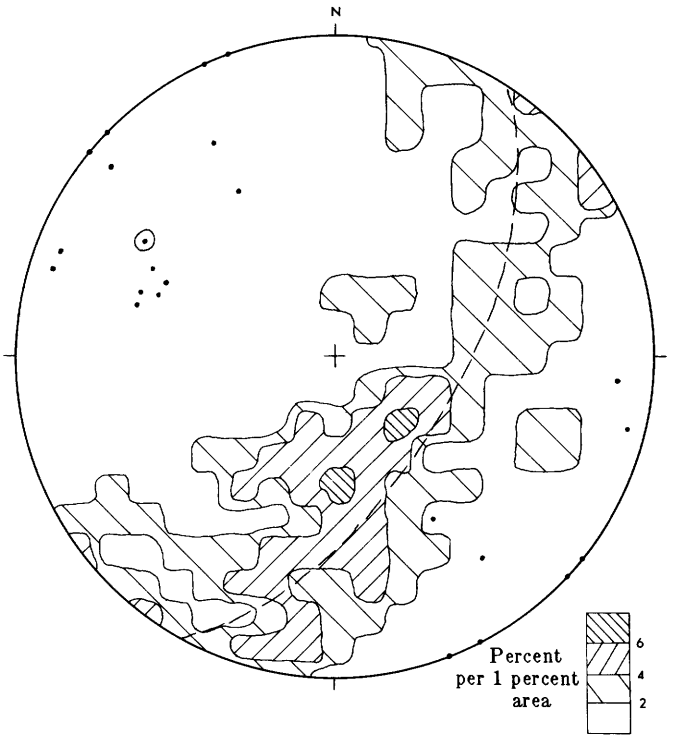

FIGURE 3.3.—Poles to 125 foliation planes from the area mapped in the Bitterroot lobe of the Idaho batholith. The data define a diffuse girdle centering on the dashed great circle. Lineation data (.). The circled point is the pole to the girdle; it lies reasonably close to the average plunge of the lineation. Data are plotted on the lower hemisphere of the Schmidt equal area stereonet.

Some of the plutonic rocks of the northern zone show subtle foliation expressed principally by flattened quartz and feldspar grains. This style of foliation is herein termed "secondary foliation"; generally too weakly developed in the northern zone to be recognized in weathered outcrops, it has been seen principally in stained slabs. The secondary foliation is present in several specimens of granitic rock and pegmatite for which a primary foliation was measured at the outcrop; therefore, the secondary foliation is at least partly parallel to primary foliation inasmuch as it is parallel to it in the hand specimens. This is also indicated by figure 3.3, which shows the orientations of both foliation sets and which suggests that they formed in response to a common stress field. Poles to pegmatite dikes and to the foliation in them lie generally in the girdle of figure 3.3, and rodding in them plunges at a small angle to the west-northwest, parallel to lineation in the granitic rock.

The central sector covers all or parts of the following 7.5-minute quadrangle sheets: McConnell Mountain, Hungry Rock, and Cedar Ridge (fig. 3.2). This area is underlain almost entirely by intermixed granite and granodiorite in roughly equal amounts and lies entirely within the zone of secondary fabric defined by the wedge-shaped area in figure 3.1. In the western part of this area (McConnell Mountain quadrangle), the plutonic rock is about two-thirds massive and one-third foliated and lineated. In the central part (Hungry Rock quadrangle), only about half the rock is massive, and in the eastern part (Cedar Ridge quadrangle) massive rock makes up only about one-third, the remaining two-thirds being foliated and lineated. Foliated granite and granodiorite are distributed more or less randomly through the massive granite and granodiorite. Both massive and foliated rocks are locally porphyritic, with K-feldspar phenocrysts making up from 1 to 20 percent of the rock.

Foliation is expressed in various ways: zones as much as half a meter thick of oriented biotite, which may be the sole expression of foliation in otherwise massive rock; parallel biotite grains; biotite streaks; schlieren; platy xenoliths oriented parallel in flow; or parallel K-feldspar phenocrysts, the resultant foliation plane of which dips more steeply than foliation due to biotite in the same outcrops. The feldspar and biotite planes strongly resemble the C and S surfaces defined by Berthé and others (1979, p. 33). In many places, a northwest-trending secondary foliation expressed principally by flattened quartz and feldspar grains crosses and even destroys the primary foliation, along whose former trace may remain only some schlieren. Secondary lineation is expressed in schlieren by linear biotite streaks and in xenoliths of biotite quartzite and schist by minor fold axes and linear biotite arrays. Both primary and secondary flow foliation and lineation are plotted in figure 3.3.

In the Cedar Ridge quadrangle, a concordant sheet of biotite-hornblende quartz diorite as much as several hundred meters thick has been injected more or less along the gneissic foliation and extends for several kilometers along the strike. Its outer parts are foliated and metamorphosed to about the same degree as the enclosing gneissic granite; its central parts are more massive, although the fabric is still predominantly metamorphic.

Injected sheets and dikes of fine-grained biotite granite, granodiorite, and tonalite 10 to 70 cm thick, both parallel and crosscut the foliation in gneissic granitic rocks. These sheets and dikes are cut in turn by pegmatite, and the secondary foliation cuts all the rocks.

The eastern sector, which is entirely within the field of secondary strain (fig. 3.1), is underlain by commingled granite, granodiorite, and minor tonalite and anorthosite. Parts of the following 7.5-minute quadrangles were mapped: Jeanette Mountain, Blodgett Mountain, Tenmile Lake, Printz Ridge, and Ward Mountain (fig. 3.2). Few contacts were found, because the various rock types look much alike in the field. As in other parts of the pluton mapped, granite and granodiorite occur in roughly equal amounts and are more or less intermixed. About 20 percent of the rock is porphyritic, more than in the areas to the west. The various textural types are commingled in random fashion.

Most of the rock in the eastern sector is foliated. Foliation is expressed by biotite-rich bands, parallel biotite grains, flattened or rodded quartz and feldspar grains, parallel schlieren, feldspar prisms partly parallel to flow planes, and parallel slabby xenoliths of biotite quartzite and fine-grained schist derived from biotite diorite, amphibolite, or fine-grained biotite tonalite.

The relations of foliation and lineation are more complex in the eastern sector than in the two sectors to the west, and they require description in three subareas, A, B, and C (fig. 3.4). The structure in subarea A displays markedly axial symmetry. Much of the foliation appears to be secondary and expressed in the texture of medium-grained rocks. In places it cuts across folded schlieren of various trends that appear to reflect an early, primary flow foliation; locally it also cuts and distorts pegmatite. In other places it parallels primary foliation defined by slabby xenoliths and schlieren. The plunge of lineation is low to horizontal through this subarea, in contrast to the average of about 30° west-northwestward plunge seen in the central and western sectors. This reflects a broad arch in the lineation (and foliation) across the area (cross section in figure 3.2), from westerly plunges on the west to easterly plunges on the east. Lineation includes axes of passive flow folds in schlieren, streaked-out biotite, long axes of oriented feldspar phenocrysts, and long axes of flattened quartz and feldspar grains. In a few places the rocks are strongly lineated but not foliated in zones no

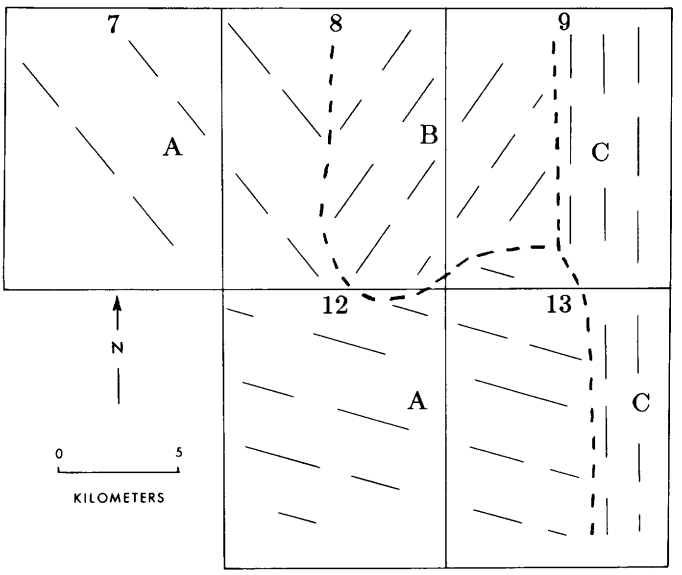

FIGURE 3.4.—Structural sketch map of subareas A, B, and C of the eastern sector, Bitterroot lobe of the Idaho batholith. The long dashes show foliation trends. Trend differences in subarea A are due to different folia in the axial flow system, all developed in flow along the az 290° axis; the lineation trend is the same throughout the subarea. Quadrangle numbers as in figure 3.2.

more than a few meters thick. Furthermore, quartzite-sheet xenoliths and related migmatites, with thicknesses measured at meter to kilometer scales in screens, have orthogonal crossing relations. One sheet stands vertical in the foliation and another is perpendicular to it and dips at low angles; they intersect in the lineation, and the symmetry is axial.

In the Tenmile Lake quadrangle, sheets of tonalite as much as 20 cm thick occur as discontinuous layers along the primary flow foliation in the gneissic granitic rock and are themselves gneissic. They pass laterally into biotite schlieren having a popcorn texture imparted by the idiomorphic habit of the remaining small amounts of feldspar. Some of the layers are folded with the flow foliation. The tonalite layers show gradual transition to granite through zones about 5 mm thick. Tonalite also forms 5- to 10-cm laminae of lit-par-lit character in biotite quartzite sheet xenoliths.

The eastward transition to the foliation orientation in subarea B involves crossing relations. A biotite quartzite stringer, oriented in the primary flow foliation and having the form of an isoclinal fold extending more than 30 m at az 020° along its axial plane, is cut across by a secondary foliation trending az 300° and is refolded in it. This has caused the development of crossing, secondary foliation in the fold limbs parallel to the az 300° trend. A related feature is shown by a slabby, 10-cm-thick, biotite quartzite xenolith that extends more than 25 m at az 020° along the relict primary flow direction. Streaky biotite lineation in the xenolith plunges 20° at az 290°, in the general direction of the secondary foliation.

Foliation in subarea B trends north-northeast and dips steeply (fig. 3.4). Angular relations between primary and secondary foliations are comparable to those in subarea A, except for the absence of extensive flattening and mineral rodding. Lineation is rare and is expressed mostly by small, northeast-trending fold axes in the gneiss. The small folds are part of a conical fold set perhaps caused by secondary deformation of the primary flow foliation.

The rocks in the northern part of subarea B are more complex than those in adjoining areas. Both granite and granodiorite occur as early phases, apparently emplaced at the same time and recrystallized equally in the secondary strain field. A younger granite injected along the foliation remains unaffected by the secondary strain; it may equate to or postdate the sheets of fine-grained granitic rocks in neighboring areas, no other equivalent of which is seen in subarea B. Major migmatite occurs, with granodiorite as the principal paleosome.

The northeast trends die out quickly to the south, in areas that were sparsely mapped or bypassed in reconnaissance mapping. If small structures recapitulate the large ones, then a major, steep-plunging fold hinge on the primary flow foliation should exist near the southern margins of Blodgett Mountain and Printz Ridge quadrangles, overprinted and perhaps destroyed by strong development of secondary foliation to the south.

Foliation subarea C is part of the Bitterroot frontal-gneiss zone. Foliation dips at shallow angles to the east, and its orientations yield an inclined axial symmetry suggesting a tilted dome. Foliation is expressed by oriented biotite flakes and by flattened quartz and feldspar grains. In the transitions, not studied in detail, from subareas A and B, the foliation becomes stronger, feldspar grains are generally flattened in the foliation, and the rocks in places become strongly lineated in the same general trend as the rocks to the west. The lineation is expressed by elongate biotite grains, trains of small biotite flakes, rodded quartz and feldspar grains, and minor fold axes in biotite quartzite xenoliths. Some zones several hundred meters thick are lineated but not foliated.

The remaining structural features to be discussed are common to subareas A and C, but are largely or completely absent in subarea B. Feldspar prisms, some of them coarse grained to porphyritic in the medium-grained matrix, lie with their prism faces mostly parallel to low-angle foliation. This is seen in the rock faces exposing the *a-c* section (inferring the *a* and *c* kinematic axes on the assumption that rodded quartz and feldspar grains represent along their length the direction of extension and therefore the slip line). Viewed along the *a*-direction

(normal to the *b-c* section), the feldspar-prism cross sections show an axial symmetry, being oriented in all possible directions relative to the foliation. But not all the feldspars seen in the *a-c* section of the outcrop face have their *c*-axes parallel to the foliation. At a particularly favorable and representative exposure, all the large feldspar grains, whose *c*-axes are roughly aligned east-southeast, were counted in a 37 cm by 39 cm area on a near-vertical face in that direction. Viewed looking north-northeast, seven of the 23 large grains present show counterclockwise rotation from the foliation plane, one shows clockwise rotation, and 15 are not rotated. None of these rotations is large and most of them are less than 25°. Here, as in the central sector, the resemblance of the defined feldspar plane to the S-plane of Berthé and others (1979) is remarkable.

Late-stage secondary shears, developed after the pegmatite stage, reduce feldspar phenocrysts to flaser structures fairly penetratively, but with intensity varying through gradational zones. The reduced phenocrysts are distorted into flattened, somewhat lenticular rods, which are parallel to streaky biotite and rodded quartz grains and generally also to other lineation. At one representative locality, 30 grains were measured, ten in each of three orthogonal faces: *a-c*, *b-c*, and *a-b* (kinematic axes). The average dimensions of the flattened rods are: *c*, 6.7 mm; *b*, 8.6 mm; and *a*, 13.6 mm; these give an axial ratio of 1:1.3:2. Most of the undeformed phenocrysts are stubby prisms and are not in linear array, so that stretching seems clearly indicated in rod formation. Thin, quartz-filled extension fractures normal to their length taken as kinematic *a* in the rodded feldspar grains bear out this inference.

A few blocks of anorthositic orbiculite were seen in granite talus; sparse orbicules occur strung out and rotated along primary flow foliation planes in the granite. Anorthosite was found in place at two localities; because of its physical resemblance to neighboring granodiorite, it was not recognized as anorthosite during field work but only when stained slabs were made.

Xenoliths include biotite quartzite, andesine quartzite, calc-silicate gneiss, biotite granodiorite, biotite granodiorite gneiss, tonalite gneiss and schist, quartz diorite, quartz diorite gneiss, biotite diorite schist, and amphibolite. They are considerably more plentiful in the eastern sector than in the central sector.

Numerous dikes and sheets of fine-grained granite, granodiorite, and tonalite occur in subareas A and C. They are injected as sheets along the primary foliation and as dikes in fractures containing the secondary lineation or perpendicular to it. All are cut by the secondary foliation and are intruded by aplite and pegmatite, which are themselves partly gneissic because of the secondary foliation.

PETROGRAPHY

Granitic rocks across the mapped part of the Bitterroot lobe are principally an intricate mixture of granite and granodiorite, with smaller amounts of quartz monzonite, quartz monzodiorite, tonalite, and anorthosite. Modes are summarized in figure 3.5*A*. All these rocks share the same pattern of petrographic variation, in which the rocks on the west are mildly metamorphosed and weakly foliated, if at all, and these grade to rocks on the east that are strongly metamorphosed and foliated on three successive *s* planes: gneissic, blastomylonitic, and mylonitic. Because of this, the petrography is generalized to cover all rock types present and is described mineral by mineral.

Plagioclase occurs as 0.5- to 4-mm grains. Here and in the following descriptions such measures refer to the range of average grain sizes determined in the several thin sections studied. Plagioclase composition ranges from An_{15} to An_{33}. Both modal amount and composition of plagioclase vary more or less randomly over the area, and this applies indeed to all mineral modes over the entire map area. Virtually all the plagioclase is unzoned; only in a few rocks were zoned grains (cores An_{26-28}, rims An_{20-23}) seen, and even there they are mostly relics. Grains are equant to prismatic, euhedral to subhedral; some of the subhedral grains may be crystalloblastic. Some plagioclase is myrmekitic against K-feldspar, interpreted as due to strain effects. In three specimens, much of the plagioclase is in clusters of 0.5- to 0.7-mm grains of irregular granoblastic form with interfacial angles approaching 120° and with some microcline inclusions. These clusters are in part enclosed within K-feldspar. In several specimens, plagioclase grains are cut by filled,

FIGURE 3.5.—Plot of plutonic rock modes from the Bitterroot lobe of the Idaho batholith, Idaho-Montana, on a quartz-plagioclase-K-feldspar ternary diagram. Rock names are from Streckeisen and others (1973). Modes recalculated to 100 percent. *A*, Summary plot of 509 plutonic rock modes; number of modes for each rock type given in parentheses: 1a, quartzolite (0); 1b, quartz-rich granitoids (7); 2, alkali-feldspar granite (2); 3, granite (211); 4, granodiorite (194); 5, tonalite (68); 6, alkali-feldspar quartz syenite (0); 7, quartz syenite to syenite (1); 8, quartz monzonite to monzonite (4); 9, quartz monzodiorite/quartz monzogabbro to monzodiorite/ monzogabbro (2); 10, quartz diorite/quartz gabbro/quartz anorthosite to diorite/gabbro/ anorthosite (20). *B*, Plot of 46 plutonic rock modes from the southwestern Bitterroot lobe; numbers of modes: 1b, (4); 2, (1); 3, (6); 4, (2); 5, (28); 10, (5). *C*, Plot of 155 plutonic rock modes from the western sector (see figure 3.2) of the Bitterroot lobe; numbers of modes: 1b, (3); 2, (1); 3, (78); 4, (51); 5, (15); 7, (1); 8, (3); 9, (1); 10, (2). *D*, Plot of 171 plutonic rock modes from the central sector (see figure 3.2) of the Bitterroot lobe; numbers of modes: 3, (77); 4, (78); 5, (11); 8, (1); 9, (1); 10, (3). *E*, Plot of 137 plutonic rock modes from the eastern sector (see figure 3.2) of the Bitterroot lobe; numbers of modes: 3, (50); 4, (63); 5, (14); 10, (10).

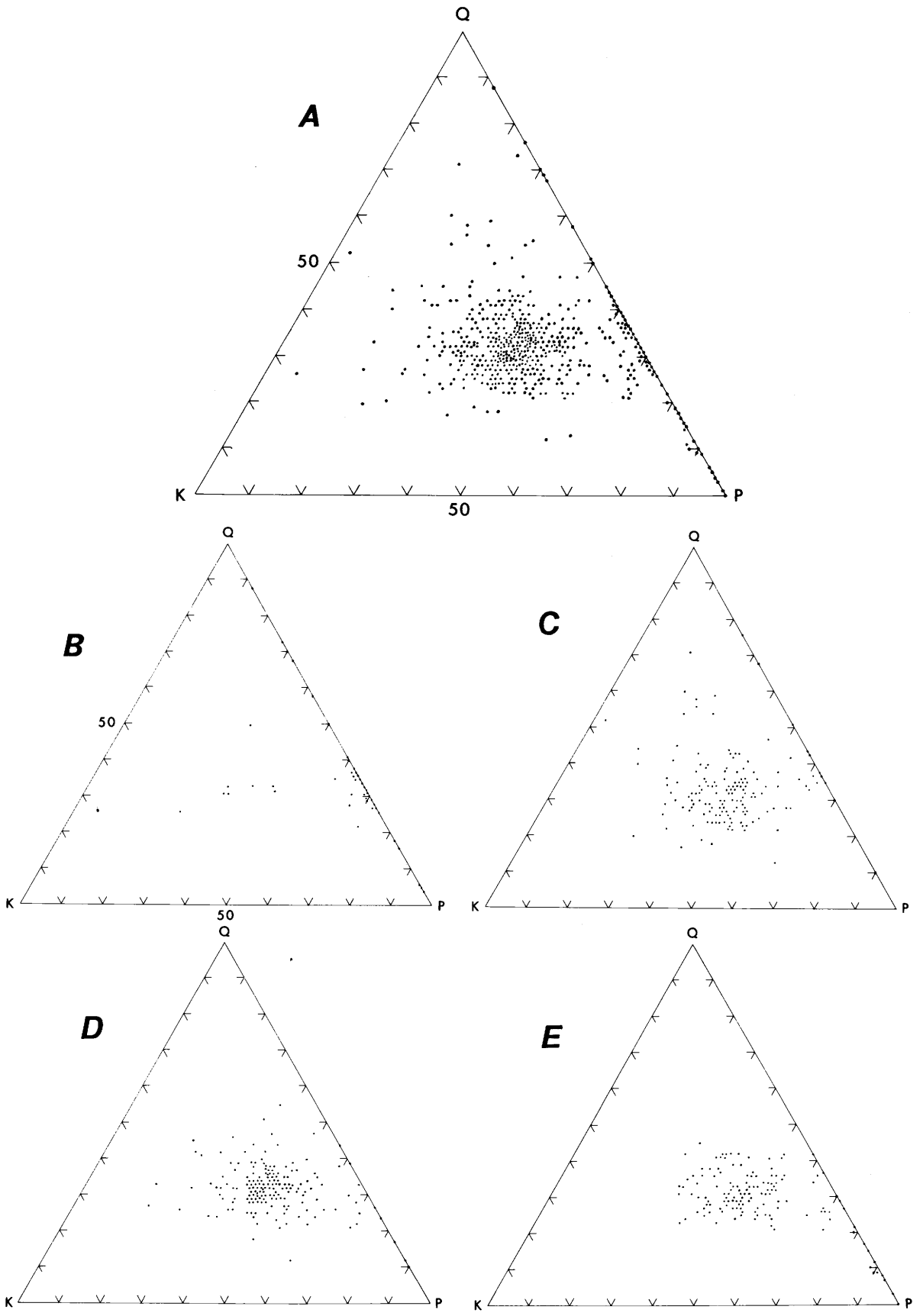
A
Q
50
K
50
P
B
Q
50
K
50
P
C
Q
K
P
D
Q
K
P
E
Q
K
P

0.1-mm-thick, extension fractures that are perpendicular to lineation; filling minerals include K-feldspar, quartz, and pennine. Plagioclase in some rocks is in flattened grains which in stained slabs impart a distinctly foliated aspect to the rock; some of these flattened grains are broken into 0.5-mm, strain-free subgrains. These rocks contain the strongest development of secondary fabric seen in the area. In the plagioclase of one granite, rodding is developed on grains 3 mm by 8 mm or longer, segmented into several parts by extension fractures 0.2 to 0.3 mm thick, which are filled with pennine-muscovite-microcline-allanite-quartz. Considering the mobility of microcline and quartz, the rodding may have developed before the granite was completely crystallized. In places, plagioclase is broken and recrystallized in 0.3-mm, strain-free, granoblastic subgrains together with quartz and microcline of comparable size, in zones as much as 0.5 mm across. This is a blastomylonitic texture, and it is overprinted in places by subparallel mylonite. Cataclastic effects of microbrecciation along crossing, narrow shears include bending of plagioclase twin lamellae, undulatory extinction, and breaking of quartz and feldspar grains.

Quartz occurs as 1.5- to 4-mm grains. The habit of quartz in the western sector differs between the northern zone and the southern zone. A subtle but major zone of structural transition trends approximately east-west through the southern half of the Huckleberry Butte and Greenside Butte quadrangles and continues east near the southern boundary of the Fish Lake quadrangle, well within the area of granitic rocks. Beyond the Fish Lake quadrangle, this zone continues southeastward (fig. 3.1). Quartz of the northern zone, typical also of the central and eastern sectors, is altogether broken into 0.5- to 0.7-mm subgrains, free of strain effects where not affected by younger cataclasis. Some rocks contain flattened grains 2 mm by 4 to 6 mm that are also broken into strain-free subgrains. Four northern zone specimens show blastomylonitic shear zones less than 1 mm thick along which 0.2-mm, granoblastic, strain-free grains of quartz occur. Quartz of the southern zone is largely as single, optically continuous grains free of subgrains, the development of which dies out to the north over a zone approximately one kilometer wide.

In the central and eastern sectors, the quartz grains are flattened (from 0.7 mm by 1.5 mm to 1 mm by 7 mm) parallel to foliation, and all have strain-free subgrains. Quartz in some rocks is cut by blastomylonitic shear zones less than 0.5 mm thick, within which the quartz occurs as 0.2-mm, strain-free subgrains. Along restricted shear zones less than 0.3 mm wide in the western part of the eastern sector, many small grains show undulatory extinction. This may be a result of blastomylonite development in which strain outlasted recrystallization, or it may involve late mylonitic overprint. In some of the gneiss in the central and eastern parts of the eastern sector, blastomylonite zones pass laterally into curved, single-grain quartz ribbons as large as 0.5 mm by 2 mm. Blastomylonite zones and large, platy quartz grains nearly wrap some of the feldspar grains, and in part quartz masses formed by segregation effects from quartz formerly reduced to fine grain size in blastomylonitic shear. The latter view is reinforced by the presence of inclusions of blastomylonitic mica within the quartz.

Many rocks show effects ranging from mild to severe of cataclastic deformation in quartz. The milder effects include undulatory extinction and subgrain boundary suturing in strain-induced boundary migration. Stronger effects include breaking into 0.03- to 0.3-mm cataclastic subgrains, which show undulatory extinction and more or less intricate microsuturing of subgrain boundaries. Some of these stronger effects can be related to shear zones mapped at the outcrop.

K-feldspar occurs as 1- to 8-mm grains, and also as 1- to 4-cm phenocrysts in the porphyritic rocks. Over much of the area, the K-feldspar mineral varies: about one-third of the rocks contain microcline, another one-third contain submicroscopically twinned microcline, and the remaining one-third contain orthoclase. In a few rocks, both orthoclase and submicroscopically twinned microcline are present. In the eastern sector, only microcline occurs, the larger grains of which contain many inclusions of plagioclase, biotite, and quartz. Extension fractures filled by quartz and muscovite cut the K-feldspar in several specimens. In foliated rocks, the K-feldspar occurs as lenticular grains from 1 mm by 3 mm to 3 mm by 8 mm in size and oriented parallel to the foliation. The variety of K-feldspar is independent of the degree of flattening. Flattened grains are generally broken into strain-free, 0.5-mm subgrains. Part of the K-feldspar in zones of blastomylonite also occurs as 0.5-mm subgrains.

Biotite occurs as 0.3- to 1-mm grains, crudely lepidoblastic in part of the rock and randomly oriented in the rest. Minor pennine alteration is ubiquitous. Fibrolite inclusions occur in some biotite. In blastomylonite zones, biotite grain size is near 0.2 mm, and in later mylonite zones, 0.02 mm. Muscovite, where present, occurs as 0.5- to 1-mm grains, but it is absent in many rocks; its occurrence is otherwise much like that of biotite. Accessory minerals seen, in approximate order of decreasing abundance, include magnetite, zircon, apatite, thorite, monazite, baddeleyite, allanite, and sphene. Magnetite is more abundant in the western sector than all other accessories together. Averages of all the modes for granitic rocks show 0.6 percent accessories in the western sector, 0.1 percent in the central sector, and 0.4 percent in the eastern sector.

A concordant sheet of biotite-hornblende quartz diorite occurs in the Cedar Ridge quadrangle and is the source

of abundant black sands in several creeks in its vicinity. It was injected along the secondary foliation in the gneissic granitic rocks and then metamorphosed. Plagioclase (An_{45}) as 2.5-mm grains is unzoned, prismatic, and subhedral. Quartz as 0.5-mm grains is interstitial and largely broken into 0.2-mm, strain-free subgrains. Biotite is as 2-mm flakes which partly include and replace 1.5-mm grains of green hornblende. Accessories include magnetite and apatite.

One or more small bodies of primary flow-foliated quartz diorite, free of secondary foliation, are exposed in the Printz Ridge quadrangle. Plagioclase (An_{35}) occurs as 2-mm, mostly unzoned, prismatic grains; a few relics of normal zoning persist. Biotite and hornblende are important constituents and occur as 1-mm grains. Quartz is minor and forms 0.5-mm grains free of any subgrains. Accessories include magnetite, apatite, and sphene.

Anorthosite was found at three locations in the Blodgett Mountain quadrangle; the rock closely resembles granodiorite in physical appearance and was not recognized as anorthosite until analyzed in the laboratory. I suspect it to be synplutonic with the granitic rocks. Plagioclase occurs as 4- to 8-mm unzoned grains of composition An_{27-29}. These grains are partly converted to granoblastic, pavement-textured grains 0.5 to 1 mm in diameter. Quartz occurs as irregular 2-mm grains and contains a few strain-free subgrains 0.5 mm in diameter. Microcline is minor and occurs as 1-mm aggregates of 0.5-mm subgrains with approximately 120° triple junctions. Biotite and muscovite occur in trace amounts.

Dikes of fine-grained granitic rocks ranging in composition from tonalite to granite intrude the granitic rocks in the central and eastern sectors, except in subarea B. The dikes lie both along and across the secondary foliation and are themselves cut by it. Plagioclase (An_{25-35}) occurs as 0.3- to 0.5-mm, mostly unzoned, equant to prismatic grains. Quartz occurs as irregular, 0.5-mm grains to platy grains 0.3 mm by 0.5 mm in size, flattened parallel to the foliation; some have subgrains and some do not. Microcline, submicroscopically twinned, occurs in much the same way as quartz. Biotite and muscovite (which is absent in some rocks) are lepidoblastic as 0.3- to 0.5-mm grains. Accessory minerals seen include zircon, apatite, allanite, and sphene.

A 16-m-diameter pipe in the Blodgett Mountain quadrangle contains miarolitic intrusive rock identified as a younger anorthosite. The plagioclase (An_{37}) is as stubby, prismatic, unzoned 3-mm grains, which show mild alteration to sericite and clay. Biotite occurs as 0.5-mm grains, and a few 0.3-mm grains of quartz occur. A little sanidine, intimately intergrown with plagioclase in 0.3-mm grains, occurs around miarolitic cavities. The pipe is cut by a fine-grained, low-angle blastomylonite shear zone 10 cm thick. The shear zone is filled with pavement-textured, unzoned, strain-free plagioclase grains (An_{37}) of 0.5-mm size, showing clay and sericite alteration. A comparable anorthosite occurs in the Tenmile Lake quadrangle as a 1-m-thick dike oriented at a high angle to the extension lineation.

The western, central, and eastern sectors show somewhat different average compositions. A total of 463 modes of plutonic rocks were determined: 155 in the western sector, 171 in the central sector, and 137 in the eastern sector. These modes when recalculated to total 100 percent for light minerals and then averaged should give a reasonable estimate of the bulk composition of the Bitterroot lobe in each sector. For the western sector, the resulting average composition is 43 percent plagioclase, 33 percent quartz, and 24 percent K-feldspar. For the central sector, the average composition is 46 percent plagioclase, 32 percent quartz, and 22 percent K-feldspar; and for the eastern sector it is 51 percent plagioclase, 30 percent quartz, and 19 percent K-feldspar. Thus, from east to west, the pluton decreases in plagioclase and increases in quartz and K-feldspar. The rocks of the western sector are generally granite, those of the central sector granodiorite, and those of the eastern sector more calcic granodiorite. The dark minerals, principally micas and accessory minerals, average 9 volume percent in each of the three sectors. Modal distribution is summarized in figure 3.5*A*, *C*, *D*, and *E*, and listed in table 3.1. Modes of the southwestern Bitterroot lobe (46, given in fig. 3.5*B*) are not considered here.

BLASTOMYLONITE

The granitic rocks, together with their associated dikes and mineral-lined or filled primary fractures, are cut in places by fine-grained blastomylonitic schistosity or by zones of blastomylonite as much as 35 cm thick; these features are strongest on the east and grade to virtual absence on the west. Bell and Etheridge (1973) suggested that mylonite is generally the result of ductile rather than brittle strain. Their suggestion seems applicable to the mylonitic rocks of the Bitterroot lobe. However, their definition of mylonite seems too general for discrimination of rocks encountered in this study. For instance, both the rocks termed blastomylonite and those termed mylonite in this study would qualify as mylonite under their definition. Therefore, the definitions in the Glossary of Geology (Bates and Jackson, 1980) are used in this paper. According to those, blastomylonite is a mylonitic rock in which some recrystallization and (or) neomineralization has taken place. In the blastomylonite described here, a large amount of recrystallization has occurred, so that the small pavement-like grains of the fabric are entirely free of strain effects; that is, no undulatory extinction is seen.

TABLE 3.1.—*Distribution of plutonic rock modes from the western, central, and eastern sectors of the Bitterroot lobe of the Idaho batholith*

Plutonic rock field from Streckeisen and others (1973)	Western sector (fig. 3.5C)		Central sector (fig. 3.5D)		Eastern sector (fig. 3.5E)	
	Number present	Percent of total	Number present	Percent of total	Number present	Percent of total
1a. Quartzolite	0	0	0	0	0	0
1b. Quartz-rich granitoids	3	1.9	0	0	0	0
2. Alkali-feldspar granite	1	.6	0	0	0	0
3. Granite	78	50.3	77	45.0	50	36.5
4. Granodiorite	51	32.9	78	45.6	63	46.0
5. Tonalite	15	9.7	11	6.4	14	10.2
6. Alkali-feldspar quartz syenite to alkali feldspar syenite	0	0	0	0	0	0
7. Quartz syenite to syenite	1	.6	0	0	0	0
8. Quartz monzonite to monzonite	3	1.9	1	.6	0	0
9. Quartz monzodiorite/ quartz monzogabbro to monzodiorite/monzogabbro	1	.6	1	.6	0	0
10. Quartz diorite/quartz gabbro to diorite/gabbro	2	1.3	3	1.7	10	7.3

The blastomylonitic schistosity partly parallels and partly crosscuts flow foliation and is developed independently in massive granitic rock. The blastomylonite contains streaky fine-grained biotite lineation, and most of it is foliated. Blastomylonite is also developed in pegmatite-suite, and other earlier, dikes, either parallel to their walls or crossing at various angles. The blastomylonitic shears vary widely in their orientation, but their poles lie near an inclined girdle whose axis plunges west-northwest (fig. 3.3). One gently dipping pegmatite sheet 2 cm thick is split by a blastomylonitic shear parallel to its walls. Two large phenocrysts were split by this shear and their top halves transported 5 cm to the southeast. Steps on exposed parts of the shear surface suggest the same sense of displacement as that shown by the offset phenocrysts.

Blastomylonite shear zones cut the gneiss of the Bitterroot frontal-gneiss zone along dips somewhat shallower than those of the gneiss; thus, arching of the secondary foliation and therefore doming had already begun when the blastomylonite shear zones formed. Stretching produced quartz-filled fractures, whose geometry also indicates that tops moved to the southeast.

MYLONITE

Late-stage mylonitic shears that cut earlier structures, including blastomylonite, were found in several places. Mylonite (Bates and Jackson, 1980) "may * * * be described as a microbreccia with flow texture." Implicit in this definition is the presence of deformation features, such as strong undulatory extinction in the mineral particles, and the absence of recrystallization, at least as viewed on the microscopic scale. Mylonitic shears are all relatively thin, mostly less than 0.5 mm thick, although one 8-cm-thick shear was found. They are strongly lineated owing to fine grooving and streaky sericite. The shears are all shallow dipping, and their lineations plunge near either az 120° or az 300°, depending on the dip direction. Shear steps suggest that the tops moved to the east. The mylonitic shears are more numerous in and near the gneissic Bitterroot front, where they occur in sheeted zones 2 to 5 cm thick and spaced 8 to 100 cm apart. Some mylonite zones are crossed at angles of 15° to 30° to the bounding shear surfaces, by shears internal to the zones. These are taken to be Riedel shears; the sense of shear transport derived from the Riedel shears is the same as that shown independently by shear steps.

STRUCTURAL EVOLUTION OF THE WALL ROCKS

The calc-silicate gneiss has a flow-foliation fabric containing steeply plunging mineral lineation of diopside, hornblende, biotite clots and streaks, and quartz rods. Although the order of growth of the minerals in the fabric is not entirely clear, the single lineation direction of all

the minerals present appears to require a single recrystallization event. Any preexisting metamorphic fabric has therefore been completely destroyed in the latest event.

Deformation associated with the metamorphism formed minor passive flow folds. Their axes plunge steeply and the axial planes parallel foliation in the enclosing gneiss. These small folds show both clockwise and counterclockwise sense of shear, distributed more or less randomly through the outcrops. This suggests an orthorhombic symmetry with flattening perpendicular to the x-y plane.

The parallelism of the mineral lineation and the minor fold axes suggests a common origin. One possibility is that all the linear elements were generated in a horizontal attitude in the plane parallel to the near-vertical flow direction, taken as imposed on the wall rock of the batholith by upward-moving magma. In that case, the linear elements were rotated toward kinematic a during continuing flow. A second possibility is that the linear elements were generated in the direction of kinematic a during flow. Available evidence does not permit a choice between these two possibilities.

The structure in the tonalitic gneiss strongly resembles that in the calc-silicate gneiss; the two rocks must have been subjected to the same structural history. This requires that the tonalitic gneiss be injected before or during the metamorphism that produced the steeply plunging minor folds and mineral lineation in the rocks. The fabric of the tonalitic gneiss does not look metamorphic; rather, it has the appearance of an intense primary flow foliation, in which the plagioclase retains much of its igneous form. Therefore, the tonalitic gneiss is inferred to be a synkinematic intrusion.

Lit-par-lit stringers of trondhjemite formed by injection of late-stage alaskitic material lie along the foliation in the tonalitic gneiss and the calc-silicate gneiss. The total fabric suggests a single-stage event involving metamorphic recrystallization and igneous injection during near-vertical flow.

Quartzite is exposed in the southwestern wall rocks. The D_1 fold set in the quartzite is sharply isoclinal, as shown by small outcrops in which minor folds assigned to D_1 have axial-plane foliation. The varied plunges of the fold axes, from near the strike line to the dip line, suggest, following Hansen (1971), that younger shear in the plane of the foliation has rotated D_1 folds toward the slip line of a younger or continuing deformation. Pegmatite was injected into the D_1 structures at some time during that later event, here taken as D_2.

Folds assigned to D_3 appear to be the youngest in the section; they are concentric and have varied but relatively shallow plunges. They clearly deform lineations assigned to D_2: the axes of the conical folds and the mineral lineations parallel to them. To analyze the D_2 structures, it is best to remove the D_3 overprint. When the D_3 folding has been removed, the sequence of metaquartzite is nearly vertical. Conical folds with mineral lineation parallel to their axes plunge down the dip of the near-vertical sequence.

In the Elk City area (Reid, 1959), the isoclinal D_1 folds, which have axial-plane foliation, were recumbent before later deformation. Perhaps the D_1 fold set of that region extended into the southwestern wall rocks, only about 30 miles to the northeast. Near the batholith, the isoclinally folded rocks, which were initially recumbent, steeply tilted as the batholith rose diapirically into and through superjacent rocks. This resulted in a D_2 strain axis not parallel to the layering, the general requirement for the generation of conical folds (Stauffer, 1964). Because the slip line is nearly vertical, the axes of the conical folds generated will also be nearly vertical, plunging down the dip of the vertical foliation. The active folding of some injected pegmatite in conical folds supports the proposed contemporaneity of batholith intrusion and D_2 folding, although pegmatite continued to be injected after some conical folds had already developed. The helical or screwlike character of the axes of the conical folds is attributable to unstable, vertical viscous flow during D_2, in which a rotational component was imparted to the vertically flowing rocks. Reid and others (1979) discussed evidence showing that the wall rocks flowed vertically downward (in the absolute sense) along the wall of the rising batholith.

The D_3 folds are viewed as a major drag-fold set imposed by the batholith on its wall rocks late in its rise. The D_2 conical folds are draped over the hinges of the concentric D_3 folds, roughly at right angles to their axes. The complex geometry implicit in this structural array is no doubt responsible for the wide scatter of poles to foliation in the wall rocks of the southwestern batholith.

It is important to note that lineation of biotite and muscovite parallels the axes of all three fold sets. Apparently the three fold sets developed during a single phase of metamorphism in the hornblende hornfels facies. Given the abundant igneous injection into the rocks and the metamorphism of much of that igneous material, it seems clear that the thermal and mechanical energy for the metamorphism was from the emplacement of the Idaho batholith.

STRUCTURE OF THE TONALITE

Flow foliation in the tonalite intrusive unit of the southwestern lobe dips about 70° southwest. Flow lineation plunges about 70° in the plane of the foliation and is believed to represent the direction of flow parallel to the contact. Steep flow within the intrusion has no doubt generated the steep flow structures in the wall rock through a mechanism of frictional drag on the walls and

resulting passive flow in the strongly heated walls of the intrusion. Metamorphic rock in the migmatite screens in the batholith behaved similarly. The axial symmetry shown by flow elements in these several units supports the idea of diapiric intrusion.

Sheets of trondhjemite and granite alaskite with gentle dips are nearly perpendicular to the inferred batholith contact and to the direction of flow lineation. The lineation is thus a stretching lineation, and the sheets represent primary tensional joints perpendicular to the direction of stretching (see Balk, 1937). Similar sheets are found in the wall rock, which was stretched in the same way. The alaskitic material invaded the primary joints as they formed. The varied dike composition, trondhjemite and granite, suggests more than one intrusive episode; simultaneous emplacement would require synmagmatic emplacement of different magmas. Granite synplutonic with the dikes was not found, but it may be represented by granite xenoliths found in the younger granite discussed below.

In most thin sections of the biotite tonalite, the plagioclase is euhedral and unzoned, and there is no systematic variation in its anorthite content. Plagioclase, the predominant constituent, is free of any strain phenomena that might indicate protoclasis has occurred. Therefore, it seems that the magma crystallized slowly at approximately equilibrium conditions.

The foregoing general formulation does not explain a number of details. Consider the complex folds in the flow foliation: they are arrayed about a steeply plunging axis and are not clearly either cylindrical or conical, although both kinds are seen. The pattern is one of axial symmetry like that within salt stocks, and flow mechanics comparable to those within salt stocks may be postulated. Moreover, a twisting or torsional component was present in the vertically directed flow in the intrusion, as in the wall rock, leading to the complexly twisted or curved axes of some of the steeply plunging folds. Associated minor folds show both clockwise and counterclockwise rotation randomly distributed through individual small outcrops, suggesting that the folding was not systematic.

Dikes of leucocratic biotite tonalite cut the tonalite intrusion. These were sheared while still hot, and they recrystallized as fine-grained biotite-plagioclase schist or blastomylonite with strong field resemblance to mylonite. The shearing, which predated intrusion of the pegmatite, suggests faulting along trends parallel to the trans-Idaho discontinuity (Yates, 1968). That discontinuity may therefore have been active during or shortly after tonalite emplacement.

The age of the tonalitic rocks presents a problem. Reid and others (1973) inferred, on the basis of $^{207}Pb/^{206}Pb$ zircon ages, that the tonalitic gneiss and related augen gneiss in the country rock of the batholith were Precambrian. Field work on this project has led to an alternative idea that the tonalite gneiss was derived from the intrusive rock emplaced in the Cretaceous as an early precursor of the batholith. The zircon ages might then reflect the age of the parent rock from which this earlier tonalite magma was derived. Hornblende K-Ar work by R.J. Fleck (oral commun., 1979) has shown the age of both the tonalite gneiss and the tonalite to be about 65 Ma. The tonalite gneiss and the tonalite were apparently intruded nearly simultaneously, though the tonalite cuts the tonalite gneiss and is thus at least slightly younger. An age of about 73 Ma was determined by Bickford and others (1981, p. 453) for a quartz diorite gneiss that is found at the northeast contact of the batholith and is both structurally and petrographically similar to the tonalite gneiss of this study.

PETROLOGY AND STRUCTURE OF THE GRANITIC ROCKS

MAGMATIC FEATURES

The granitic rocks of the Bitterroot lobe are clearly younger than the tonalite of the southwestern area, inasmuch as there are xenoliths of tonalite in them near the contact. The granitic rocks are predominantly granite and granodiorite, apparently more or less randomly commingled with each other and with smaller amounts of quartz monzonite, quartz monzodiorite, tonalite, and anorthosite. These rocks share many petrographic similarities and may have been emplaced synplutonically.

As shown earlier, the average composition of plutonic rocks in the Bitterroot lobe is granite in the western sector and changes to calcic granodiorite in the eastern sector. Structural analysis shows that the surface rocks of the western sector represent the upper part of the batholith, grading to the lower batholith in the eastern sector (fig. 3.2). The batholith is therefore vertically zoned, from granite at the top to calcic granodiorite near the base. This would appear to require a differentiation process, but examination of the kind of differentiation is beyond the scope of this paper.

Tabular tonalite bodies along the primary flow foliation in the Tenmile Lake quadrangle appear to have been still liquid at the time of granite intrusion; this suggests synplutonic emplacement, accompanied perhaps by some mixing with granite and granodiorite magma.

The anorthosite bodies in the eastern Bitterroot lobe, herein referred to as anorthosite I, require special comment. Anorthosite is generally held to be exclusively of Precambrian age; if that were so, the anorthosite here would have to be in rafted hypoxenoliths. Because no evidence for rafted hypoxenoliths was seen, however, it is believed that the conditions for generation of anor-

thositic magma were met in this area, which is near the base of the batholith and hence near the base of the crust at the time of emplacement. The anorthosite I bodies are therefore inferred to be magmatic.

The K-feldspar varies across the pluton: microcline is the sole K-feldspar near the eastern margin, whereas elsewhere orthoclase is present in addition to microcline. Because the batholith cooled more slowly near its base, conditions there allowed orthoclase to invert completely to microcline.

The granitic rock of the western sector (upper batholith) contains some relict crystalloblastic plagioclase, possibly incompletely melted material that has partially retained its metamorphic aspect. The source for the granitic rock may therefore include older granitic material partly melted at depth.

Steep flow lineation in the granitic rock near its contact with the older tonalite in the southwestern area indicates near-vertical flow along a locally east-trending contact. Near-horizontal pegmatite sheets are consistent with vertical stretching along this contact. The features seen along this contact are taken to represent the magma tectonics of the granitic rocks; these features have been extensively modified or obliterated in areas to the north and east.

Schistosity/foliation in the northern zone of the western sector is highly discordant to that of the granitic rock in the southern zone, near the contact. The average lineation suggests a dip direction near 30°, az 320°. Orientations of pegmatite and aplite dikes, combined with other data, portray an ill-defined girdle (fig. 3.3). The pole to this girdle is oriented near 10°, az 300°, not far from the slip line for flow in the granitic rock, based on stretching lineation. Based on regional structural history, an alternative explanation for the girdle involving northeast-southwest compression and folding is not viable. Solid-state flow evidently continued on about the same axis as the liquid-state flow after the granitic rock had consolidated sufficiently to sustain shear. Fractures generated in the solid-state flow were injected by pegmatitic magma.

Blastomylonite schistosity has an average orientation of az 320°, 40° SW., and the associated lineation, taken as the slip line, averages 30°, az 290°, similar to the orientations of the slip lines postulated above, but rotated counterclockwise with respect to them. Therefore, it appears that continuing movement along the az 290° trend after pegmatite intrusion led to blastomylonite development.

SECONDARY FOLIATION

Unzoned plagioclase occurs in rocks throughout the area. It is possible that cooling under near-equilibrium conditions allowed originally zoned plagioclase to equilibrate. Secondary strain may have aided this process, but unzoned plagioclase seems to have developed about as well outside the area affected by secondary strain as within it. This idea needs to be tested farther away from the field of secondary strain.

Plagioclase composition is roughly the same in granite and in granodiorite, ranging from about An_{18} to An_{33} randomly over the whole area. Cores in relict zoned grains in granodiorite are somewhat more calcic than those in granite, suggesting that the granodiorite magma had the potential to form more calcic plagioclase. However, the secondary strain has affected both rocks in the same pressure-temperature interval during solid-state strain, and the plagioclase in both was reequilibrated to lie in the same compositional range.

Evidence of movement in the igneous rock in the late-liquid stage, when the crystal meshwork was sufficiently established to undergo strain, is found in quartz-microcline-filled extension fractures in plagioclase. Quartz-filled extension fractures in microcline indicate continued movement near the end of the magmatic stage. Extension fractures that developed later during continuing solid-state strain are filled with muscovite, quartz, and pennine. These fractures all stand more or less perpendicular to the mineral lineation and are due to stretching along that lineation.

The fabric elements produced in secondary strain are identical in the granite and the granodiorite as well as in the less common varieties of granitic rocks. This suggests that the several rocks are about the same age (synplutonic), inasmuch as they experienced the same post-consolidation, high-temperature strain event. This strain event was severe enough that the granitic rock of the entire area can be considered as essentially a metamorphic unit.

The shallow plunge of secondary elements in granitic rocks of northern areas (northern zone of the western sector and areas to the east), compared to the steep plunge of linear elements in the older tonalite and younger granitic rocks in the southern zone, shows that the rocks experienced dramatically different tectonic environments. Granite of the southern zone rose vertically along its contact, crystallized, and experienced no further activity. In rocks of the northern areas, on the other hand, secondary foliation began to form before they were entirely solid, as shown by extension fractures in the feldspar that are filled with late-stage magmatic material. Strain that continued after consolidation formed gneissic foliation, flattened feldspar and quartz, and deformed the later, fine-grained dikes and the still later pegmatite and aplite. The strain is principally axial on the west, but becomes more orthorhombic to the east.

The diffuse boundaries of the secondary strain field in the granitic rocks are interpreted as bounding a broad

zone of distributed shear. Primary flow foliation formed independently of these boundaries. Axial solid-state flow in the secondary strain field overprinted and largely destroyed the primary foliation within its boundaries. The axis of this flow generally plunges at shallow angles to the west-northwest, but changes to an east-southeast plunge over an arch near the eastern margin of the pluton, indicating axial flow symmetry that was later arched.

The principal petrographic criteria for secondary strain include anhedral to flattened quartz grains with strong development of annealed subgrains; filled extension fractures in the feldspar perpendicular to the stretching lineation; flattened feldspar grains; and subgrain development in the feldspar.

The eastward-increasing proportion of foliated rocks in the area reflects the approach to a zone of more intense strain near the base of the pluton. Strain-free subgrains in the plagioclase become more common to the east, deeper in the pluton, because of higher deformation temperatures and greater concomitant annealing in that direction. Mica generally becomes oriented in the rock only under more intense strain than that in which quartz and feldspar first become flattened. This may be due to the type of strain farther to the east: considerably more strain may be required to reorient a mica grain in a field of flattening strain than in one of rotational strain.

In many places in the eastern sector, feldspar grains are out of parallelism with the main foliation, forming a feldspar foliation that dips more steeply than the biotite foliation. Thin-section analysis suggests that biotite grains lie on shear surfaces; therefore, as suggested above, the C and S surfaces of Berthé and others (1979) may be present. Analysis based on this assumption and on data from three exposures indicates that the upper rocks sheared southeast relative to the lower rocks during the generation of gneiss early in the tectonic sequence.

A root zone for thrusting may therefore have cut through the pluton near the base during its intrusion; alternatively, perhaps the pluton spread laterally along a thrust zone and was subsequently cut by continuing movement of the thrust. The thickness of the pluton would require that this happened deep in or even near its base.

The flow lines in the Bitterroot lobe have been important in the generation of structures in the late-liquid and postconsolidation stages of the batholith (fig. 3.2). The granitic rock apparently rose into or crossed a structural discontinuity, subsequent movement on which deformed it during igneous flow and similarly during solid-state flow. The flow is inferred to have been extensional, a conclusion supported by the presence of curving extension fractures perpendicular to the flow lines (fig. 3.2). This flow pattern implies thinning during deformation. The fact that the gneissic foliation in the granitic rock dies out quickly to the north is consistent with the 30° northwesterly plunge of the flow lineation and with the concept of its relation to thrusting. Thrusting would appear to be inconsistent with the evidence for extension, but this may be only apparent. The work of Williams and Chapman (1983) has shown that thrust sheets are subject to extension behind the advancing ductile bead associated with the thrust tip. Extension is therefore an integral part of the thrusting process.

FLOW TRENDS AND ARCHING

A compilation of average flow directions in the granitic rocks of the project area is given in figure 3.2. These average directions are based on both primary and secondary flow features, as well as blastomylonite where it has developed. The flow trends form a fan-shaped array opening out to the southeast, within the field of secondary strain, and stand more or less perpendicular to fractures interpreted to have originated as tensional openings. Flow lines plunge northwestward at about 30° over most of the area, but to the east they become horizontal near the Bitterroot arch (cross section in fig. 3.2), and then plunge about 30° southeast in the Bitterroot gneissic front, to the east of the arch.

The structure section given in figure 3.2 is based on the disposition of flow lineation across the mapped interval. As noted above, the intensity of the strain fabric becomes less to the west, in areas that the section shows are structurally higher in the pluton. The mylonite zone at the eastern margin of the pluton (cross section in fig. 3.2) is cut off by erosion and is not certainly seen again farther west. If it continued westward as a low-angle zone, it must have become highly discordant both to the secondary flow lineation and to the blastomylonite.

As the arch shown in the section appears to be due wholly to upward arching of the secondary flow lineation and allied features, the batholith must have been 30 km or more thick prior to arching. Therefore, the former situation of the mylonite zone to the west becomes a major question.

A mylonite zone about 30 m thick trends north-south and dips shallowly to the west in the Jeanette Mountain quadrangle. More detailed mapping should investigate the possibility that this mylonite is the westward continuation of the frontal mylonite. The structural position seems about right (fig. 3.2). If this is the continuation, then the mylonite zone appears to be dying out westward within the igneous mass.

Evaluating other work in terms of the cross section given in figure 3.2, it is notable that Wiswall's (1979) proposed base of the batholith south of the cross section lies along the trend of the arch. That proposed base appears to be consistent with the regional structure inferred in this paper. On the other hand, Toth (1981) proposed that the Bear Creek and Cub Creek plutons south of the cross

section occupy a position near the roof of the batholith. This now seems unlikely, as those plutons lie just west of the axis of the arch and therefore deep within the batholith, possibly near its base.

The area affected by secondary strain is part of the Bitterroot gneiss dome described by Hyndman (1980) as a metamorphic core complex. The boundaries of the wedge-shaped area defined in this project (fig. 3.1) outline the complex; but that is very approximate, as the boundaries are based on extrapolation of a few known points on the north and south sides.

DEVELOPMENT OF SUBAREA B OF THE EASTERN SECTOR

Flattened mineral grains are scarce and much less strongly developed in the rocks of subarea B than in those of adjoining areas. At a late stage in consolidation, when magma could still move as a partly solidified mush, the continuing flow became of secondary character, but strain was along directions at only small angles to the earlier flow, so that the two flow foliations have much the same geometry. Tangential compression seems to have predominated, and flattening was much subdued; what little flattening was produced parallels the steep axial planes of the folds and is not related to the low-angle flattening of adjacent strain fields.

The primary and secondary flow foliation were deformed in a gigantic fold during early flow, perhaps because of impingement of an eastward-moving sheet of granitic rock against an eastern buttress or wall—the eastern batholith contact.

THE BITTERROOT GNEISSIC FRONT

Near the eastern margin of the eastern sector, the foliation dips become shallow and the trends change (fig. 3.4) to nearly north-south, cutting abruptly across the trends of subareas A and B. Structural analysis yields a near-domical symmetry, which may be of only local significance but which raises the possibility of a series of coalescing marginal domes concealed in the tilted foliation along the eastern side of the Bitterroot lobe. This domical symmetry and the easterly trending lineation are features common to the metamorphic core complexes of the western cordillera (see, for example, Davis and Coney, 1979). Hyndman (1980) applied a metamorphic-core-complex interpretation to the Bitterroot lobe, and his discussion is particularly germane to the rocks of the gneissic front. The possibility of thrusting in this area, mentioned above, suggests another way for the lineation to form besides the extensional mechanism envisioned by Davis and Coney; during the preparation of this paper, Mattauer and others (1983) proposed a thrusting model for metamorphic core complexes.

Foliation is stronger in the gneiss of the Bitterroot frontal zone than in the gneissic granite to the west, raising the possibility that they are of different ages. This possibility is supported by Bickford and others (1981, p. 453), who show "cataclastic granite" to have an age in the range 49 to 46 Ma. This contrasts with their age of 55 Ma, mentioned above, for medium-grained granitic rocks of the Bitterroot lobe interior. Petrographic data, on the other hand, suggest that the rocks are all the same age. Both rock types formed earlier than the pegmatite, which intruded along their foliation, and the fabric in both types is virtually identical. The problem remains unsolved.

To the west, the dips change with the lineation (fig. 3.2) from eastward to westward over an arch and in a narrow transition zone (fig. 3.4) give way either to the steep northeast trends of the giant fold or to the northwest trends of axial symmetry. This geometry may mirror the dual constraints of deep shear zone and eastern contact.

FINE-GRAINED DIKES

Dikes and sheets of fine-grained granite, granodiorite, and tonalite are present in the central and eastern sectors, but were not seen in the western sector. Except for subarea B, where none was seen, they are most abundant in the eastern sector, which is deep in the intrusion. Their distribution is thus asymmetrical and appears to correlate with depth in the intrusion and perhaps with strain intensity. The fine-grained sheets were emplaced into planes of secondary shear during secondary strain and were metamorphosed during continuing movement. Fine-grained dikes were emplaced at the same time and were also metamorphosed. These fine-grained igneous rocks may have come from the same sources as the main-stage batholithic rocks; an alternative possible source was still-unconsolidated batholithic material deep in the magma chamber. Some fine-grained dikes were injected into extensional fractures perpendicular to the stretching lineation of the secondary strain field, showing in yet another way the extensional character of the secondary strain.

ANORTHOSITE II

The miarolitic andesine anorthosite pipe in the Blodgett Mountain quadrangle and the miarolitic andesine anorthosite dike in the Tenmile Lake quadrangle are products of the late-stage emplacement of anorthosite magma. These features may bear the same relation to anorthosite I as the fine-grained granitic dikes do to the granitic rocks of the Bitterroot lobe. Because the anorthosite is medium grained, it must have been emplaced either (1) as a crystal mush largely crystallized at a deeper level before emplacement or (2) at a deep level in rocks of high temperature, in which crystallization occurred slowly. Like the fine-

grained granitic dikes, the andesine anorthosite is cut by blastomylonitic shears, themselves developed while the country rock was hot. The anorthosite bears a strong resemblance to the anorthosite I rock of the Blodgett Mountain quadrangle and may well be a late product of the same magma chamber(s).

BLASTOMYLONITE

Blastomylonite is rare in the western sector, becomes more common in the central sector, and is abundant in the eastern sector. Its abundance thus reflects the intensity of the secondary strain foliation. Petrographic features of the blastomylonite suggest simultaneous shear and recrystallization along restricted zones of shear. Where crystallization outlasted deformation, the fabric is strongly annealed. In a few places, deformation outlasted crystallization, and polygonal arcs are only imperfectly developed. Some blastomylonitic shears in the western sector parallel secondary foliation and thus mirror the axial symmetry of the secondary strain event. Therefore, they represent renewed strain late in that event. In some places, blastomylonite plagioclase is slightly more sodic than plagioclase equilibrated in the secondary strain event, indicating slightly lower temperature. In most places, however, both kinds of plagioclase have the same composition, reflecting little or no change in temperature between the two events. Biotite also formed in blastomylonite, although its grain size is reduced because of shear.

In the central sector, blastomylonite shears have axial symmetry about an axis that plunges toward the northwest, parallel to the strain axis of the secondary strain event (fig. 3.3). The two sets of structural features formed sequentially in response to the same stress field; they evidently shared a common slip line defined by the secondary strain axis, which is also the girdle pole. Rodding developed in some blastomylonite because of more intense axial strain. Low-angle blastomylonite shears in arrays that strike more or less perpendicular to the trend of the girdle axis are small, ductile thrust faults. At one of these the upper halves of two phenocrysts were thrust 5 cm to the southeast; therefore, the strain has an element of monoclinic symmetry. Steeper shears that strike more or less parallel to the trend of the girdle axis function as small, ductile tear faults.

Blastomylonite zones are more abundant in the eastern sector than in the other sectors, although they were not found in subarea B. They are present throughout the other subareas, and they resemble those of the other sectors in all but two respects. First, in thin section they are seen to terminate at large, lenticular grains of quartz or quartz ribbons, although fine-grained mica of the blastomylonite continues as inclusion trains in the large quartz grains. Large quartz grains transected by blastomylonite have evidently recrystallized during or after blastomylonite formation in a "quartz-ribbon event," possibly related to somewhat higher temperature. Second, the blastomylonite shears are mostly low-angle; blastomylonite appears to have formed in low-angle, ductile thrust faults more abundantly than to the west, and only a few associated ductile tear faults are present. Though the ductile shear zones of these thrusts average only 8 cm in thickness, they can be traced along their strike for kilometers. Their generally westward dip, except where arched, is consistent with a thrust mechanism, though the original dips may have been substantially changed by the younger arching.

MYLONITE

Mylonite is rare in the western and central sectors but more important in the eastern sector, where it occupies low-angle shears. Streaky lineation trends west-northwest, like lineation in blastomylonite and secondary gneiss. Tops moved east for the most part, as indicated by shear steps on the shear surfaces. Local conjugate shears in the eastern sector show the opposite direction of movement. All of these shears have developed mylonite that is similar both petrographically and in outcrop. The change in stress response, from thrusting farther west to conjugate, high-angle reverse shears in the east is ascribed to late-stage arching of gneiss in the Bitterroot frontal zone. Arching associated with active uplift changed the orientation of effective stress across the top of the arch.

CONCLUSIONS

1. Tonalite and a later granite/granodiorite massif, together making up the Bitterroot lobe of the Idaho batholith, were emplaced into metasedimentary country rock (possibly of Beltian age) as a sheetlike body that spread to the east.
2. The granitic massif, originally more than 30 km thick, is vertically zoned, from average calcic granodiorite at the base to average granite at the top.
3. Classic magma tectonics occurred in the southwestern part of the lobe; the resulting steep primary flow structures were cut and strongly modified by low-angle secondary foliation and lineation within the pluton.
4. The emplacement of the pluton was synkinematic into an active thrust zone, resulting in the formation of a metamorphic core complex.
5. Three phases of deformation yielded gneiss (high pressure and temperature), blastomylonite (intermediate pressure, high temperature), and mylonite (lower pressure, intermediate temperature).

6. Arching occurred during and following deformation, and the base of the massif now lies at and near the surface on the east side.

7. More than 30 km of relative vertical movement (east side up) is implied on the north-south lineament along the eastern margin of the Bitterroot lobe. This movement may reflect the combined effects of diapirism and arching.

REFERENCES CITED

Anderson, A.L., 1952, Multiple emplacement of the Idaho batholith: Journal of Geology, v. 60, p. 255-259.

Armstrong, R.L., 1974, Magmatism, orogenic timing, and orogenic diachronism in the cordillera from Mexico to Canada: Nature, v. 247, p. 348-351.

_____ 1975a, Precambrian (1500 m.y. old) rocks of central Idaho—the Salmon River arch and its role in cordilleran sedimentation and tectonics: American Journal of Science, v. 275-A, p. 437-467.

_____ 1975b, The geochronometry of Idaho: Isochron West, no. 14, p. 1-288.

Balk, Robert, 1937, Structural behavior of igneous rocks: Geological Society of America Memoir 5, 177 p.

Bates, R.L., and Jackson, J.A., eds., 1980, Glossary of geology (2nd ed.): Falls Church, Virginia, American Geological Institute, 751 p.

Bell, T.H., and Etheridge, M.A., 1973, Microstructure of mylonites and their descriptive terminology: Lithos, v. 6, p. 337-348.

Berg, R.B., 1969, Petrology of anorthosite of the Bitterroot Range, Montana, *in* Origin of anorthosite and related rocks: New York State Museum and Science Service Memoir 18, p. 387-398.

Berthé, D., Choukroune, P., and Jegouzo, P., 1979, Orthogneiss, mylonite and non coaxial deformation of granites: the example of the South Armorican shear zone: Journal of Structural Geology, v. 1, p. 31-42.

Bickford, M.E., Chase, R.B., Nelson, B.K., Shuster, R.D., and Arruda, E.C., 1981, U-Pb studies of zircon cores and overgrowths, and monazite: Implications for age and petrogenesis of the northeastern Idaho batholith: The Journal of Geology, v. 89, p. 433-457.

Bittner-Gaber, Enid, 1983, Geology of selected migmatite zones within the Bitterroot lobe of the Idaho batholith, Idaho and Montana: Moscow, Idaho, University of Idaho, Ph.D. dissertation, 173 p.

Bradley, M.D., 1981, Geology of northeastern Selway-Bitterroot Wilderness Area, Idaho and Montana: Moscow, Idaho, University of Idaho, M.S. thesis, 51 p.

Chase, R.B., 1968, Petrology of the northeast contact zone of the Idaho batholith, northern Bitterroot Range, Montana: Missoula, Montana, University of Montana, Ph.D. dissertation, 158 p.

Chase, R.B., Bickford, M.E., and Tripp, S.E., 1978, Rb-Sr and U-Pb isotope studies of the northeastern Idaho batholith and border zone: Geological Society of America Bulletin, v. 89, 1325-1334.

Chase, R.B., and Hyndman, D.W., 1977, Mylonite detachment zone, eastern flank of the Idaho batholith: Missoula, Montana, Department of Geology, University of Montana, Rocky Mountain Section, Geological Society of America Field Guide no. 1, 31 p.

Cheney, J.T., 1975, Kyanite, sillimanite, phlogopite, cordierite layers in the Bass Creek anorthosite, Bitterroot Range, Montana: Northwest Geology, v. 4, p. 77-82.

Davis, G.H., and Coney, P.J., 1979, Geological development of the cordilleran metamorphic core complexes: Geology, v. 7, p. 120-124.

Garmezy, Lawrence, and Sutter, J.F., 1983, Mylonitization coincident with uplift in an extensional setting, Bitterroot Range, Montana-Idaho [abs.]: Geological Society of America Abstracts with Programs, v. 15, no. 6, p. 578.

Goodge, J.W., 1983, Fold reorientation and quartz microfabric in the Okanogan dome mylonite zone, Washington: Kinematic and tectonic implications: Missoula, Montana, University of Montana, M.S. thesis, 65 p.

Greenwood, W.R., and Morrison, D.A., 1973, Reconnaissance geology of the Selway-Bitterroot Wilderness Area: Idaho Bureau of Mines and Geology Pamphlet 154, 30 p.

Hansen, Edward, 1971, Strain facies: New York, Springer-Verlag, 207 p.

Hyndman, D.W., 1980, Bitterroot dome-Sapphire tectonic block, an example of a plutonic-core gneiss-dome complex with its detached suprastructure, *in* Crittenden, M.D., Jr., Coney, P.J., and Davis, G.H., eds., Cordilleran metamorphic core complexes: Geological Society of America Memoir 153, p. 427-443.

Johnson, B.R., 1975, Migmatites along the northern border of the Idaho batholith: Missoula, Montana, University of Montana, Ph.D. dissertation, 120 p.

Langton, C.M., 1935, Geology of the northeast part of the Idaho batholith and adjacent region in Montana: Journal of Geology, v. 43, p. 27-60.

Larsen, E.S., and Schmidt, R.G., 1958, A reconnaissance of the Idaho batholith and comparison with the southern California batholith: U.S. Geological Survey Bulletin 1070-A, 33 p.

Leischner, L.M., 1959, Border-zone petrology of the Idaho batholith in vicinity of Lolo Hot Springs, Montana [abs.]: Geological Society of America Bulletin, v. 70, p. 1782.

Lindgren, Waldemar, 1904, A geological reconnaissance across the Bitterroot Range and Clearwater Mountains in Montana and Idaho: U.S. Geological Survey Professional Paper 27, 123 p.

Mattauer, Maurice, Collot, Bernard, and Van den Driessche, Jean, 1983, Alpine model for the internal metamorphic zones of the North American cordillera: Geology, v. 11, p. 11-15.

Morrison, D.A., 1968, Reconnaissance geology of the Lochsa area, Idaho County, Idaho: Moscow, Idaho, University of Idaho, Ph.D. dissertation, 126 p.

Nold, J.L., 1974, Geology of the northeastern border zone of the Idaho batholith, Montana and Idaho: Northwest Geology, v. 3, p. 47-52.

Reid, R.R., 1959, Reconnaissance geology of the Elk City region, Idaho: Idaho Bureau of Mines and Geology Pamphlet 120, 74 p.

_____ 1984, Structural geology and petrology of a part of the Bitterroot lobe of the Idaho batholith, Idaho County, Idaho, and Missoula and Ravalli Counties, Montana: U.S. Geological Survey Open-File Report 84-517, 117 p.

Reid, R.R., Bittner, Enid, Greenwood, W.R., Ludington, Steve, Lund, Karen, Motzer, W.E., and Toth, Margo, 1979, Geologic section and road log across the Idaho batholith: Idaho Bureau of Mines and Geology Information Circular 34, 20 p.

Reid, R.R., Morrison, D.A., and Greenwood, W.R., 1973, The Clearwater orogenic zone: a relict of Proterozoic orogeny in central and northern Idaho, *in* Belt Symposium 1973: Department of Geology, University of Idaho, Moscow, Idaho, v. 1, p. 10-56.

Ross, C.P., 1928, Mesozoic and Tertiary granitic rocks in Idaho: Journal of Geology, v. 36, p. 673-693.

_____ 1952, The eastern front of the Bitterroot Range, Montana: U.S. Geological Survey Bulletin 974-E, p. 135-175.

_____ 1965, Idaho batholith [abs.]: Geological Society of America Special Paper 82, p. 343.

Ryder, R.T., and Scholten, Robert, 1973, Syntectonic conglomerates in southwestern Montana: their nature, origin, and tectonic significance: Geological Society of America Bulletin, v. 84, p. 773-796.

Stauffer, M.R., 1964, The geometry of conical folds: New Zealand Journal of Geology and Geophysics, v. 7, p. 340-347.

Streckeisen, A.L., and others, 1973, Plutonic rocks: Classification and nomenclature recommended by the IUGS Subcommission on the Systematics of Igneous Rocks: Geotimes, v. 18, no. 10, p. 26-30.

Toth, M.I., 1981, Petrology and structure of the east-central Bitterroot

lobe of the Idaho batholith [abs.]: Geological Society of America Abstracts with Programs, v. 13, no. 4, p. 228.

_____ 1983, Reconnaissance geologic map of the Selway-Bitterroot Wilderness, Idaho County, Idaho, and Missoula and Ravalli Counties, Montana: U.S. Geological Survey Miscellaneous Field Studies Map MF-1495-B, scale 1:125,000.

Williams, Graham, and Chapman, Timothy, 1983, Strains developed in the hangingwalls of thrusts due to their slip/propagation rate: a dislocation model: Journal of Structural Geology, v. 5, no. 6, p. 563-571.

Williams, L.D., 1977, Petrology and petrography of a section across the Bitterroot lobe of the Idaho batholith: Missoula, Montana, University of Montana, Ph.D. dissertation, 251 p.

Wiswall, C.G., 1979, The base of the Idaho batholith [abs.]: Geological Society of America Abstracts with Programs, v. 11, p. 305.

Yates, R.G., 1968, The trans-Idaho discontinuity: International Geological Congress, 23d, Prague, Czechoslovakia, Proceedings, v. 1, p. 117-123.

4. EMPLACEMENT OF THE MAIN PLUTONS OF THE BITTERROOT LOBE OF THE IDAHO BATHOLITH

By C. GIL WISWALL[1] and DONALD W. HYNDMAN[2]

ABSTRACT

Mineralogic, chemical, and field relationships indicate that the Bitterroot lobe of the Idaho batholith was formed by magmas that underwent limited diapiric rise and may have been emplaced by lateral spreading to form one or more mushroom-shaped bodies at mesozonal to catazonal levels. The main-phase granitoid intrusion exhibits a high degree of mineralogic, textural, and chemical homogeneity and so may comprise a single comagmatic suite of rocks. Although the country rocks and the sequence of deformation are similar throughout the Bitterroot lobe, contact relationships and styles of deformation on the northern and southern margins of the batholith show different levels and modes of emplacement. The northern exposures exhibit somewhat shallower levels of emplacement near the top of the intrusion. The base of the batholith crops out in the south as granitoid cappings on ridge crests underlain by migmatites across a near-horizontal contact. Several lines of evidence indicate limited rise of the magmas and their emplacement near the source area, but conditions evidently varied sufficiently to produce different styles of emplacement. In the north, the country rock was competent enough to cause either lateral or upward forcible injection along foliation near the batholith margins, whereas in the south the more ductile country rock flowed around the laterally spreading magmas. The different levels of exposure appear to be in sharp structural contact, possibly as a result of postemplacement tectonic modification associated with the formation of the Bitterroot dome.

INTRODUCTION

The Late Cretaceous Idaho batholith occupies much of northern Idaho and part of western Montana. The 39,000-km^2 area is divided into a northern (Bitterroot) lobe and a southern (Atlanta) lobe by the northwest-trending Salmon River arch (Armstrong, 1975). The larger (25,000 km^2) Atlanta lobe trends north-south, whereas the smaller (14,000 km^2) Bitterroot lobe trends northwest-southeast.

The Idaho batholith lies approximately 600 km from the present Pacific coastline, in contrast to the more typical distance of 150 to 200 km observed for the Coast Range Plutonic Complex of British Columbia, the Sierra Nevada batholith of California, and the Andean plutonic arc. The batholith lies northeast of the Blue Mountains island arc, one of the numerous Mesozoic allochthonous terranes that make up the western margin of North America (Coney and others, 1980). Although the timing and process of accretion are poorly understood, eastward thrusting of the arc sequence against the North American craton was complete prior to the emplacement of the oldest plutons of the Idaho batholith (Vallier and Engebretson, 1984). The resultant boundary is exceedingly sharp both geologically and isotopically, suggesting the removal of the intervening crust, either by subduction or by lateral transport. From the timing of accretion and the spatial relations between the Blue Mountains island arc and North America, it can be inferred that a subduction zone existed to the west of the allochthonous terrane before intrusion of the Idaho batholith began in the Late Cretaceous (Vallier and Engebretson, 1984). Therefore, although the clearly related pair of accretionary prism and magmatic arc recognized in other batholithic terranes (for example, Sierra Nevada) has not been established, it seems probable that the Idaho batholith resulted from Mesozoic subduction.

Detailed studies of other major batholiths reveal composite bodies consisting of numerous individual plutons belonging to several comagmatic suites. Magmatic suites and individual plutons commonly show concentric zoning, both compositional and textural, to varying degrees of complexity (see, for example Bateman and Chappel, 1979). Both modeling experiments (Ramberg, 1970) and field studies (Pitcher and Berger, 1972; Green and Kridoharto, 1975; Sweeny, 1975, 1976; Koller, 1978; Sylvester and others, 1978; Wiswall, 1979a) indicate that plutons deeper than the brittle/ductile transition rise diapirically and may undergo lateral spreading at the level of emplacement to form mushroom-shaped bodies. Our studies suggest that

[1]Department of Geology and Astronomy, West Chester University, West Chester, Pennsylvania 19383.
[2]Department of Geology, University of Montana, Missoula, Montana 59812.

most of these general observations apply to the Idaho batholith.

Comparison of the northern Idaho batholith with tectonically similar terranes has been hampered by a lack of data. Prior to 1976, detailed work was limited to the margins of the batholith. More recently, several detailed studies (fig. 4.1) concentrated on the interior of the Bitterroot lobe (Williams, 1977; Wiswall, 1979a, b; Hyndman, 1984). We summarize these studies here in order to present an overview of the tectonics of emplacement and to provide a framework for further study. Perhaps the most surprising conclusion from this detailed work is that individual plutons are difficult to identify. In fact, petrographic and chemical evidence suggest that approximately

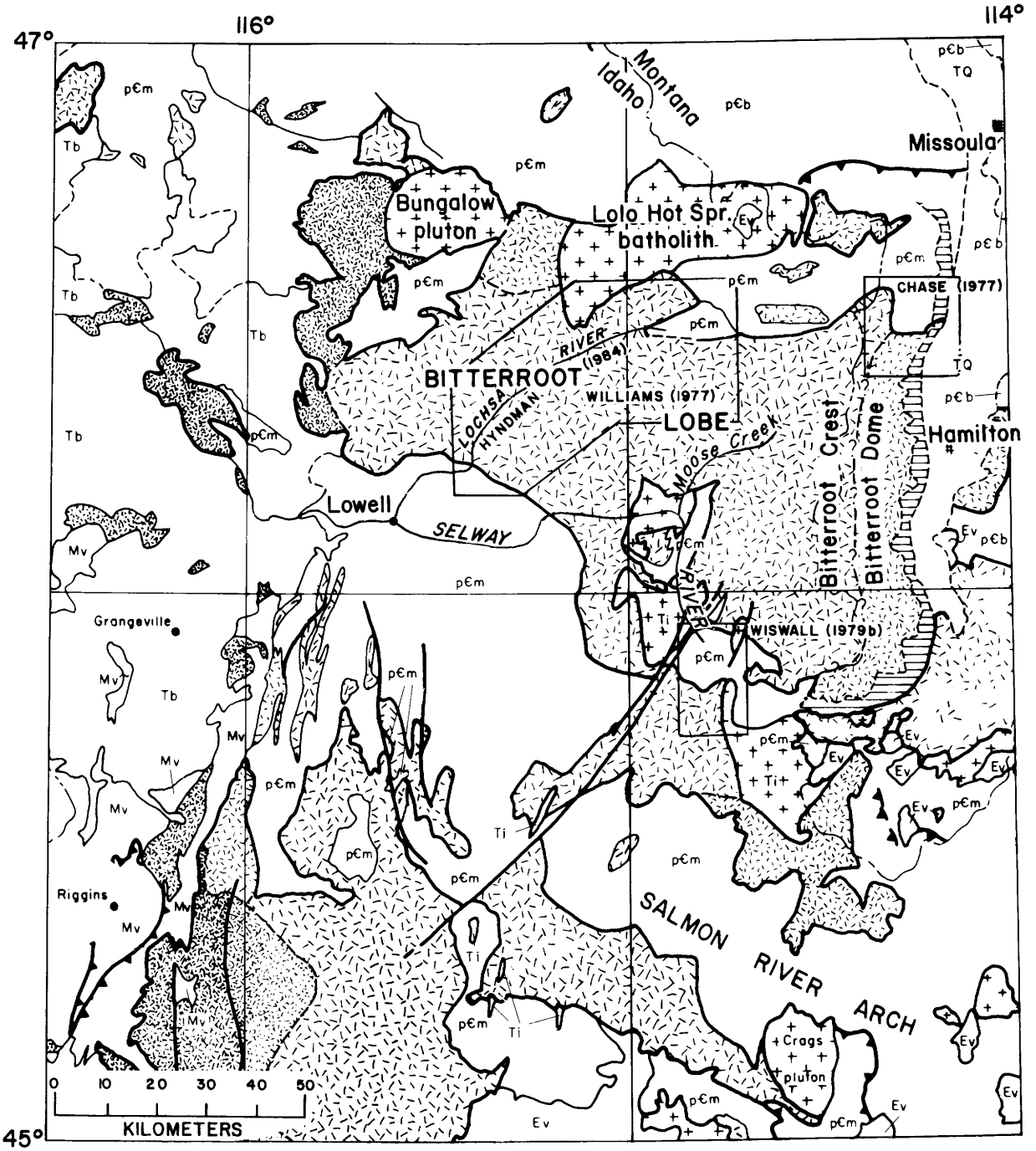

FIGURE 4.1.—Geologic map of the Bitterroot lobe of the Idaho batholith showing locations of studies referred to in text. Area designated Wiswall (1979b) is shown in figure 4.2; section along Lochsa River designated Hyndman (1984) appears in figure 4.5.

40 percent of the volume of Cretaceous rocks in the Bitterroot lobe may belong to one comagmatic suite. Border-zone relationships, structural analyses, and the form of the batholith contact indicate that diapiric rise followed by lateral spreading at the level of emplacement produced one or more mushroom-shaped bodies. However, apparent differences in the level of exposure along the margin suggest that the batholith underwent postemplacement modification.

The data presented here are primarily from five detailed studies distributed around the lobe (fig. 4.1): Williams (1977) and Hyndman (1984) reported on exposures in the Lochsa River canyon (herein referred to as the northern Bitterroot lobe, northwestern and northeastern border zones); Wiswall (1979a, b) studied metamorphic and associated granitoid rocks in the upper Selway River canyon (southern Bitterroot lobe, southwestern border zone); and Chase (1973) described relationships in the northern Bitterroot Range (eastern Bitterroot lobe and border zone).

ACKNOWLEDGMENTS

Financial support for this work was provided by a Penrose grant from the Geological Society of America and by National Science Foundation grant 76-84399. We thank P.C. Bateman, R.B. Chase, and R.R. Reid for reviews of the manuscript.

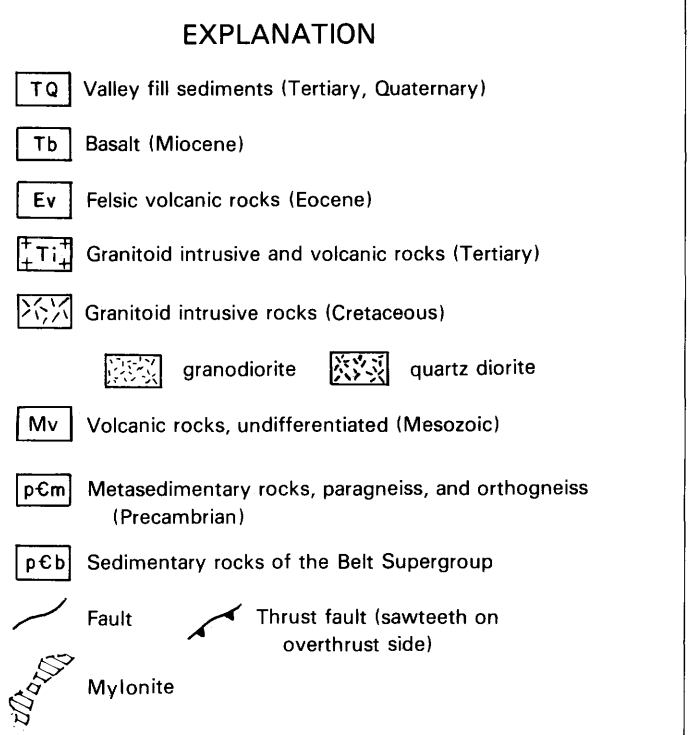

FIGURE 4.1.—Continued.

COUNTRY ROCKS

Country rocks of the Bitterroot lobe include both metasedimentary rocks, generally correlated with the Proterozoic Belt Supergroup, and orthogneisses interpreted as pre-Belt basement (Greenwood and Morrison, 1973; Armstrong, 1975; Hyndman, 1983a). The Belt metasedimentary rocks consist of abundant muscovite-biotite quartzofeldspathic schists and gneisses, which locally contain kyanite and almandine, and subordinate quartzite, micaceous quartzite, and diopside-hornblende-plagioclase gneiss. Pods or boudins of amphibolite are present in some places. The lithologic succession suggests correlation with the Prichard and Wallace Formations and the Ravalli Group (see, for example, Greenwood and Morrison, 1973). Belt metasedimentary rocks in the area mapped by Wiswall (1979a) are largely anatectic migmatites. Composition of the pre-Belt basement varies widely, from felsic to ultramafic. Rock types include hornblende quartz monzonite augen gneiss, quartz diorite to diorite orthogneiss, meta-anorthosite, and small bodies of amphibolite, metagabbro, and hornblende pyroxenite. The distributions of these pre-Belt rocks is poorly known, but they appear to form a discontinuous band adjacent to the southern and western margins of the Bitterroot lobe (Hyndman and Williams, 1977). Layered meta-anorthosites found along the northern and eastern margins (Berg, 1964; Cheney, 1972; Chase, 1973; Jens, 1974) suggest basement exposures there as well.

Before the formation of the batholith, a regional dynamothermal metamorphic event affected the country rocks over an area extending several kilometers beyond the present batholith contacts. The rocks adjacent to the batholith are in the upper amphibolite facies (sillimanite zone), but the degree of metamorphism decreases away from the batholith margins in a broadly concentric fashion. Intense deformation accompanying the metamorphism produced a penetrative schistosity subparallel to compositional layering; this schistosity controlled subsequent deformation and, in some areas, emplacement of the intrusive phases. Although complexly deformed, the schistosity maintains a consistent northwesterly strike and steep easterly dip.

The country rocks around the Bitterroot lobe exhibit several generations of mesoscopic structures. Correlation between areas, however, is difficult because detailed structural analyses are widely scattered. The sequences of structural development in the north and southwest are similar, but they differ in style. In general, four generations of folds are recognized (Greenwood and Morrison, 1973; Chase and Johnson, 1977; Wiswall, 1979a). The earliest event (F_1), which accompanied sillimanite-muscovite to sillimanite-orthoclase regional metamorphism, produced rare, tight to isoclinal, sharp-crested, similar-style

folds in compositional layering and a penetrative axial-plane schistosity (S_1). Because many F_1 structures are rootless intrafolial folds, strong transposition is inferred to have accompanied deformation (Wiswall, 1979a). The second deformation (F_2) occurred after the peak of metamorphism but resulted from movements similar to those during F_1. The structures of F_2 are tight shear folds that deform S_1 and show characteristics of both similar and parallel styles. The extremely ductile behavior exhibited by the less competent units indicates fairly high temperatures during deformation; however, a new penetrative *s* surface was not produced. Concentric features are confined to more competent units where ductility contrasts were low. Where F_1 and F_2 folds are present in the same outcrop, they are roughly coaxial. Although there is no orientation pattern of the fold axes due to subsequent deformation, axial-plane orientations are generally reflected in the northwesterly trending structural grain as a result of the control exerted by S_1 during deformation. Thus, F_1 and F_2 appear to represent a progressive deformation accompanying metamorphism, in which the end of F_1 marks the peak of metamorphism.

The age of this tectonic cycle is uncertain because of the complex thermal history of the area. Norwick (1972) documented a nondeformational burial metamorphism which raised the lower part of the Belt section in Precambrian time to the lower amphibolite facies. The metamorphism associated with F_1 and F_2 deformation is superimposed on this earlier event. Geochronometric data from early tonalite and quartz diorite bodies on the northern margin of the batholith indicate an age of 85 to 70 Ma (Grauert and Hofmann, 1973; Ferguson, 1975; Chase and others, 1978). Many of these intrusive bodies exhibit a strong foliation parallel to that in the country rocks, and their emplacement must have occurred either before or synchronous with metamorphism. Reid (chapter 3) has concluded that the tonalite bodies on the southern and western margins of the Bitterroot lobe are synkinematic. Furthermore, the control exerted by S_1 on the emplacement of the main-phase granite/granodiorite demonstrates the completion of F_1/F_2 deformation before the onset of major intrusion. Thus, although the timing of metamorphism is as yet uncertain, inferred relationship between metamorphism and generation of the Idaho batholith favors a Cretaceous age.

In the southwest, Wiswall (1979a) reported a third set of structures (F_3), which range in scale from microscopic to macroscopic and exhibit a variety of forms including both similar and parallel styles. The macroscopic structure is revealed by the outcrop pattern of the country rock units (fig. 4.2) and the regional foliaton orientation (fig. 4.3). A large northwesterly plunging antiform straddles the Selway River in this area. Mesoscopic structures fall into two major categories: (1) earlier, tight, symmetric to asymmetric, similar-style fold sets accompanied by reorientation of S_1 in fold crests and minor recrystallization to form a weak axial-plane schistosity (S_3); and (2) parallel-style, asymmetric, drag-type folds that consistently show a northeast-over-southwest sense of movement away from the batholith and local transposition at the crests forming fracture surfaces with fairly consistent northeasterly dips of 35° to 60°. These groupings are not mutually exclusive, and individual folds may show characteristics of both groups. Fold orientation data from the southwestern mesoscopic F_3 structures are shown in figure 4.4. Fold axis orientations of F_3 form a cluster that is nearly coincident with the pole to the great circle defined by poles to foliation (see figs. 4.3, 4.4*A*), but the distribution of poles to F_3 axial planes indicates subsequent deformation. Domainal analysis of F_3 axial-plane orientations demonstrates that deformation was progressive and continued through the cooling of the rocks. The earlier similar-style folds, which exhibit ductile behavior, were continually reoriented about the axis of folding. The drag-type folds fall into domains (based on constant axial-plane orientation) that reflect the macroscopic antiform. Thus the F_3 deformation in this area began at elevated temperature, proceeded through cooling and increasing competence of the country rocks, and culminated in the formation of the macroscopic antiform. Data presented below suggest that this deformation is related to emplacement of the batholith.

To the north, along the lower Selway and Lochsa Rivers, F_3 structures are parallel-style tight to open folds and fold sets which deform F_2 structures (Greenwood and Morrison, 1973; Wiswall, 1979a; Hyndman, unpublished data). These folds do not exhibit the same diversity of form observed to the southwest. In particular, the earlier similar-style structures are missing. Granitoid sills are commonly concordant with F_3 structures; however, no causal relationship has been established for this concordance. Data from other areas suggest that F_3 is related to batholith emplacement.

The fourth deformation (F_4) was similar in the north and southwest and produced open, broad-crested, parallel-style folds and warps. Recognition of F_4 folds is based on warping of F_3 fold axes. The F_4 folds are upright, horizontal or gently plunging structures that trend north-south in the north (Greenwood and Morrison, 1973) to west-northwest in the southwest (Wiswall, 1979b). The orientations and textural evidence indicate that these folds formed by vertical movements and cataclasis at low temperature and therefore presumably postdate batholith emplacement.

The structural evolution of the northeastern margin, as described by Chase (1973, 1977) and Chase and others (1978), bears a superficial similarity to that of the southwestern and northern borders, but they are not

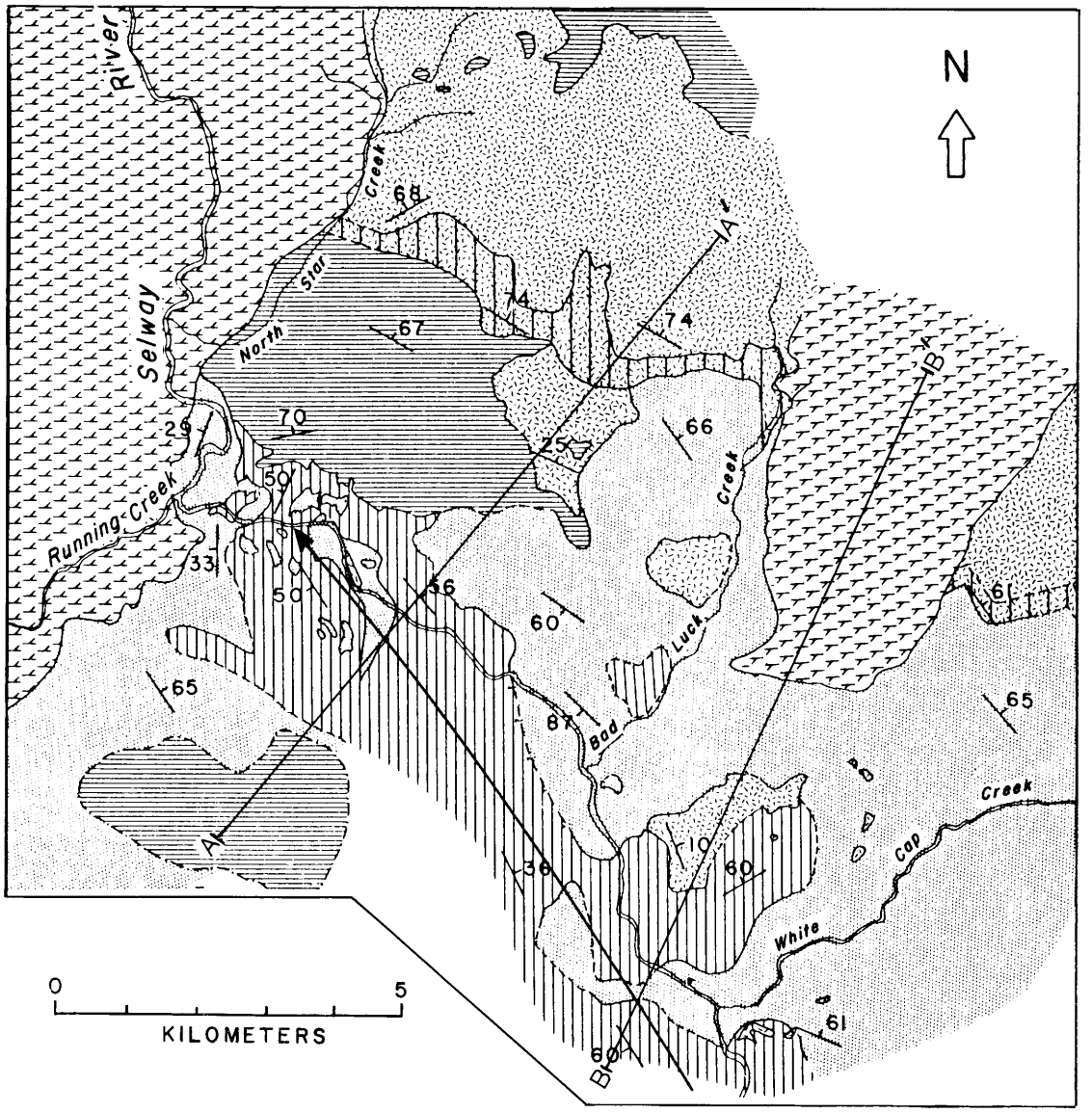

FIGURE 4.2.—Geologic map of the upper Selway River (from Wiswall, 1979a). See figure 4.1 for location. Structure sections A-A′ and B-B′ appear in figure 4.6.

readily correlatable. Chase noted five generations of deformation, the youngest of which has been recognized only along the eastern margin of the Bitterroot lobe. The oldest deformation (F_1) seems to be the same as recognized elsewhere: similar-style isoclines accompanied by high pressure (kyanite-sillimanite) prograde metamorphism and transposition. Second-generation (F_2) folding deformed the schistosity and produced a variety of structures by flexural-slip, which resulted in crenulation and a localized axial-plane schistosity. The F_3 event produced an incipient axial-plane schistosity in some areas and was accompanied by transposition, which was strongest adjacent to the batholith and in mechanically weak pelitic schists. Chase and others (1978) attributed F_1 and F_2 to preemplacement deformation and F_3 to deformation either slightly preceding or accompanying intrusion. Recognition of F_4 is based on domainal analysis of F_3 structures, although Chase (1973) noted that the variation in orientation of F_3 fabric elements may be the result of inhomogeneous folding. The youngest deformation (F_5) is a pronounced mylonitic event primarily affecting the easternmost section of the batholith and the adjacent country rocks. This deformation is attributed to east-southeast movement of the suprastructure (Hyndman and others, 1975; Hyndman, 1980) or to mylonitization associated with the formation of the Bitterroot dome (Chase and others, 1983). Chloritic breccia that overlies and is superimposed on the lower, eastern exposures of the mylonite may have formed during isostatic rise and doming of the mylonite (Hyndman, 1983b).

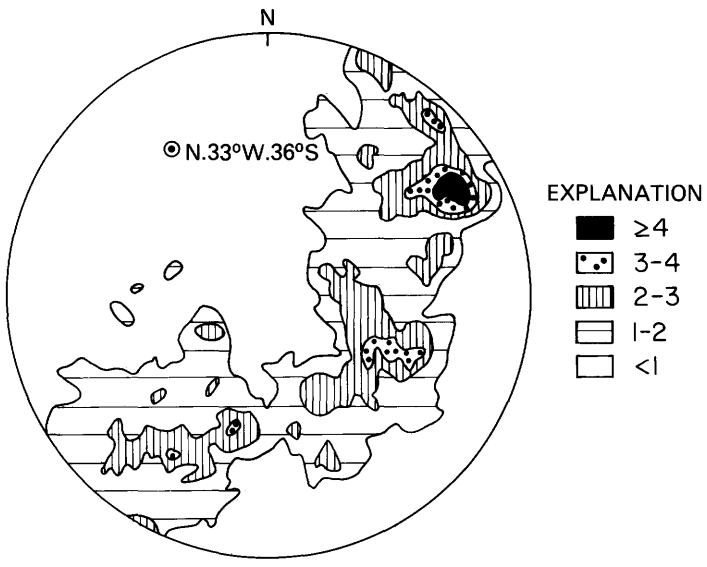

FIGURE 4.3.—Lower hemisphere projection of 267 poles to foliation in country rocks in the upper Selway River area shown in figure 4.2. Contours at 1, 2, 3, and 4 percent per 1 percent area (from Wiswall, 1979a). Bull's-eye marks the pole to the great circle defined by the foliation orientations.

GRANITOID ROCKS

The mineralogic and chemical variations within granitoid rocks of the Bitterroot lobe, especially in the interior parts of the batholith, are only now coming to light. Most workers identify a more mafic granodioritic border phase, which encloses the main-phase granodiorite to granite of the batholith interior. However, complex intrusive relationships, gradational contacts, and subtle mineralogic and textural variations, coupled with poor exposures, deep weathering and poor access have until recently hampered the delineation of individual intrusive

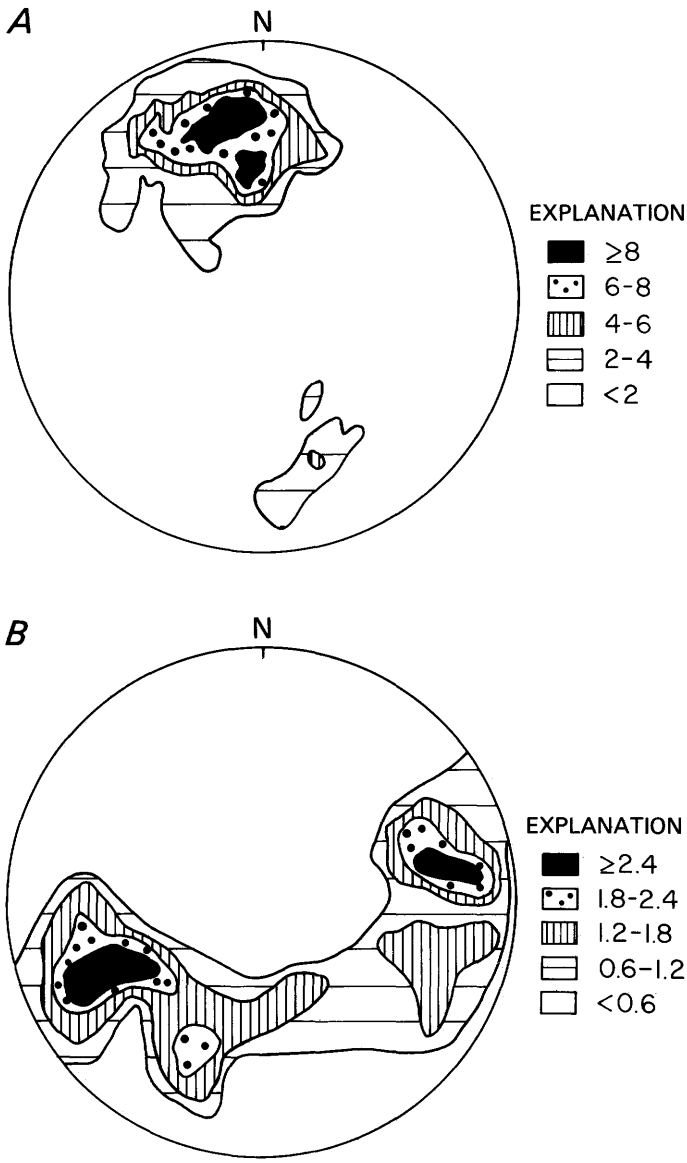

FIGURE 4.4.—Lower hemisphere plots of F_3 structural features from the upper Selway River area shown in figure 4.2. *A*, Total of 95 F_3 fold axes; contours at 2, 4, 6, and 8 percent per 1 percent area. *B*, Total of 60 poles to F_3 axial planes; contours at 0.6, 1.2, 1.8, and 2.4 percent per 1 percent area.

bodies. Williams (1977) and Hyndman (1984) recognized subunits within both the border phase and the main phase of the Bitterroot lobe along the Lochsa River. Toth (chapter 2) identified six separate plutons within the batholith interior. Available data suggest that the Bitterroot lobe may indeed be a composite body such as is seen in other batholithic terranes, but that the plutons are much larger and fewer than observed elsewhere.

Comparison of the available petrographic data from the interior of the Bitterroot lobe leads to the conclusion that the main-phase granitoid intrusive is fairly homogeneous on a regional scale. In hand specimen, the rock is a massive to weakly foliated, white to light gray, medium-grained equigranular hypidiomorphic biotite granodiorite to biotite granite. Mineralogically, it averages about 50 percent plagioclase, 25 percent quartz, 20 percent K-feldspar, 5 percent biotite, and a trace of muscovite (see table 4.1). Hornblende is absent. All workers report similar textural and compositional variations of an irregular and gradational nature: (1) variable grain size, commonly finer near the margins; (2) variable abundance (0 to 5 percent or more) of late, anhedral to subhedral, pale pink to white K-feldspar megacrysts, which are more abundant near the margins in some areas (Wiswall, 1979b); (3) localized irregular lenses of biotite granodiorite in otherwise homogeneous biotite granite (Williams, 1977); (4) local predominance of muscovite over biotite (Williams, 1977); (5) moderate to strong foliation, defined by subparallel biotite, schlieren, and streaks of biotite, feldspar, and megacrysts near the margins, fading to massive rock toward the interior; (6) rare isoclinal folds defined by schlieren, not necessarily confined to the margin; and (7) broad distribution of streaky schlieren, which are somewhat more mafic than the enclosing rock and are especially common near xenoliths or remnants of country rock.

The origin of the foliation and schlieren is unclear. The foliation generally is parallel to and more strongly developed adjacent to contacts, and it may therefore have a magmatic origin. The diffuse, streaky, and discontinuous schlieren suggest incorporation of metasedimentary restite from the source area, digested xenoliths, or both. From the eastern border of the batholith toward its interior, xenoliths of quartzofeldspathic gneiss and pelitic schist become increasingly diffuse and finally are represented only by wispy concentrations of mafic minerals (Bickford and others, 1981). Old xenocrystic zircon in the granitoid rocks, noted in the same study (Bickford and others, 1981), suggests either preservation of refractory components from the source or contamination by crustal material. Hyndman (1984) concluded on the basis of chemical and trace-element studies that assimilation had not played a major role in the evolution of the batholith as a whole. This conclusion favors the restite origin for the schlieren and zircon, and it further suggests a source composition close to that of the pelitic schist and quartzofeldspathic gneiss that border the batholith. However, both the granodiorite of the border zone and the main-phase granites show microscopic evidence of late-magmatic or postconsolidation alteration, metamorphism, and deformation (Williams, 1977; Hyndman, 1984). For example, quartz commonly shows strong undulose extinction, subgrain development, and sutured grain boundaries. Plagioclase is only weakly twinned, and twin planes are commonly bent or broken. Primary biotite grains are bent or shredded, and a significant proportion of the biotite in the main phase is recrystallized or secondary. Reid (chapter 3) distinguished two generations of foliation: a primary flow foliation defined by parallel biotite flakes, schlieren, and platy xenoliths; and a secondary foliation defined by flattened quartz and feldspar grains. The two are commonly parallel. Therefore, the apparently conflicting characteristics may be explained by different mechanisms operating during and after crystallization of the magma.

Granitoid rocks from the Bitterroot lobe that are inferred on other grounds to be Cretaceous consistently yield K-Ar ages ranging from about 56 to 37 Ma. These ages are commonly interpreted to indicate a widespread Eocene thermal event (Armstrong, 1974; Criss and Taylor, 1983) possibly associated with igneous activity that resulted in the formation of the Paleocene (?) and Eocene Challis Volcanics. Because Tertiary granite plutons and volcanic rocks are widespread throughout the Idaho batholith, this thermal event is a possible cause of the alteration observed in the Cretaceous intrusive suite. However, the distribution and timing of development of the secondary foliation (Reid, chapter 3) suggest that it is more likely a result of late-magmatic or postconsolidation vertical tectonism associated with formation of the Bitterroot dome, as discussed below.

Subdivision of the main phase is generally based on the predominance of one or more of the textural or compositional variations cited above. For example, Hyndman (1984) distinguished four subunits of the main phase (M_1 through M_4) on the basis of textural and compositional variation (fig. 4.5). Subunits M_1 to M_3 are associated with complexities near the northwest border zone and are volumetrically small compared with M_4, which constitutes approximately 60 percent of the main phase along the line of Hyndman's section (see fig. 4.5). Toth (chapter 2), noting the similar major- and trace-element chemistry throughout the lobe, mapped individual plutons on the basis of texture, mineralogy, and crosscutting relationships. The most striking feature of her map (fig. 2.2) is the immense size of the Bear Creek and Grave Peak plutons. The large areal extent and general lack of mineralogic and textural variation in the Bitterroot lobe suggests that the bulk of it is formed by a few enormous plutons.

TABLE 4.1.—*Comparison of modes of major minerals for main-phase granitic rocks from the Bitterroot lobe of the Idaho batholith*

[Modes given in weight percent; anorthite (An) content of plagioclase in cation percent. tr., trace; n.d., no data]

Area or unit	Unit M_4		SE. border		Tom Beal Park pluton		NE. border		Bear Creek pluton	
Reference	Hyndman (1984)		Wiswall (1979b)		Williams (1977)		Chase (1973)		Toth (this volume)	
Number of analyses	12		14		44		33		4	
	Range	Avg	Range	Avg	Range	Avg	Range	Avg	Range	Avg
Quartz	16.2 -36.5	26.2	21-31	26.1	25-44	32.4	15-42	28	28-30.5	29.5
Plagioclase	34.9 -59.2	48.5	32-63	49.8	10-45	32.1	27-69	42	42-43.5	42.4
An content	n.d.	n.d.	(22)-(46)	(33)	(19)-(30)	(23)	(20)-(36)	(27)	n.d.	n.d.
K-feldspar	10.8 -29.7	20.0	1-35	16.3	21-40	31.4	tr.-49	22	20-27	23.1
Biotite	1.9 - 6.8	4.4	3-11	6.1	tr.-7	3.0	1-16	5	3- 7.5	5.0
Muscovite	.03- 1.7	.5	0-1	.4	tr.-3	1	0-7	1	----	----

This conclusion is supported by a striking lack of chemical variation. Hyndman (1984) found no clear chemical distinctions in either major or trace elements between units nor any discontinuities at the contacts between units that were defined on the basis of textural and mineralogic variation. Analyses of 12 representative samples showed only minimal variation in SiO_2, Al_2O_3, Na_2O, K_2O, and Fe oxides across the whole batholith. Toth (chapter 2) arrived at a similar conclusion. Available major-element analyses reported by other workers for rocks from the main body of the Bitterroot lobe exhibit average compositions generally similar to that reported by Hyndman (1984). From these sets of analyses (table 4.2), it may be noted that (1) average values of SiO_2 and Al_2O_3 vary less than 5 percent; (2) average Na_2O and K_2O values vary less than 10 percent; (3) if two analyses of unusually mafic rocks are excluded, then the average values of CaO and K_2O also vary less than 5 percent; and (4) Fe oxides and MgO show significant variation. On the basis of available data, the chemical uniformity noted by Hyndman (1984) appears to extend over a significant part of the Bitterroot lobe.

The internal form of the northern Bitterroot lobe is revealed by a weak to moderate foliation (fig. 4.5). Orientations of biotite, plagioclase, diffuse schlieren, and some K-feldspar megacrysts define a broad arch plunging 30° to 50° northward. The arch is flat-topped through the central part of the batholith but has near-vertical limbs at its margins. Granodiorite in the western limb of the arch (unit M_1 of Hyndman, 1984) contains 3 to 4 percent K-feldspar megacrysts along with irregular pegmatitic pods having rare, large miarolitic cavities. The crest of the arch (unit M_2 and M_3) contains as much as 5 percent K-feldspar megacrysts. The eastern limb of the arch consists of the biotite granodiorite to quartz monzodiorite (unit M_4) that constitutes the bulk of the intrusive rocks in this area. Xenoliths and schlieren are less prevalent here than farther west. An intrusion breccia 250 m thick cuts this unit near the center of its outcrop width.

Reid (chapter 2) has identified a foliation/lineation arch similar to that described above and concluded that it formed late in the crystallization history of the batholith in response to the formation of the Bitterroot dome. We do not believe that the arch along the Lochsa River and

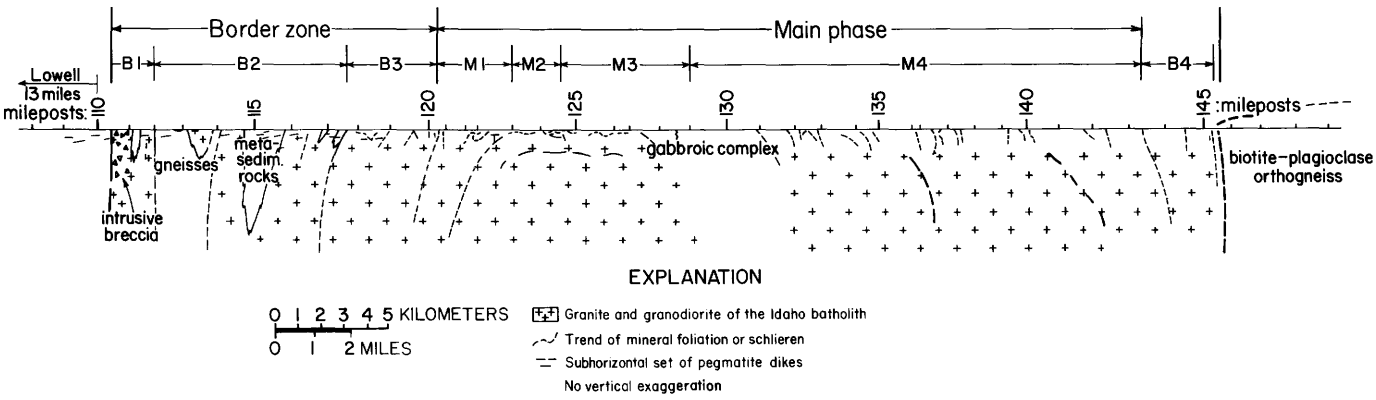

FIGURE 4.5.—Geologic cross section through the main-phase granitoid intrusive rocks and border zone of the northern Bitterroot lobe along the Lochsa River canyon (from Hyndman, 1984). See figure 4.1 for location.

TABLE 4.2—*Comparison of major-mineral analyses of main-phase granitic rocks from the Bitterroot lobe of the Idaho batholith*
[Values given in weight percent. n.d., no data]

Area or Unit	Unit M_4		Tom Beal Park pluton		NE. border		Idaho batholith	Bear Creek pluton	
Reference	Hyndman (1984)		Williams (1977)		Chase (1973)		Larsen and Schmidt (1958)	Toth (this volume)	
Number of analyses	9		5		9		1	4	
	Range	Avg	Range	Avg	Range	Avg	Avg	Range	Avg
SiO_2	69.96-72.21	71.13	66.5 -73.7	70.23	63.3-73.5	67.8	71.66	70.5 -72.8	71.8
TiO_2	.18- .25	.22	.17- .22	.20	.2- .6	.28	.22	.14- .29	.22
Al_2O_3	15.23-16.11	15.73	15.2 -17.15	16.01	14.4-16.7	15.41	15.48	14.7 -15.7	15.33
Fe_2O_3	.38- .76	.61	(as FeO)		1.3- 5.3	2.7	.56	(as FeO)	
FeO	.58- 1.04	.74	1.67- 2.12	1.95	(as Fe_2O_3)		1.45	1.22- 2.11	1.60
MnO	.02- .05	.025	.03- .05	.04	n.d.	n.d.	.04	.02- .03	.02
MgO	.12- .47	.40	.34- .43	.38	.6- 1.5	1.0	.47	.30- .76	.55
CaO	1.46- 2.72	1.92	1.90- 2.29	2.0	1.5- 3.5	2.24	1.97	1.65- 2.46	1.89
Na_2O	4.03- 4.76	4.46	3.82- 4.57	4.38	3.9- 5.4	4.60	4.34	3.70- 4.80	4.08
K_2O	2.55- 4.16	3.69	3.05- 3.93	3.45	1.6- 5.1	3.6	3.24	2.16- 4.41	3.68

the one identified by Reid are related. Firstly, although the trends of the plunges of the two arches are similar, the crest of Reid's arch lies approximately 70 km to the east of the Lochsa arch. The arches could not, therefore, be connected by a continuous crest. More importantly, we believe that the arch along the Lochsa River is at least partly of primary origin; it is defined by primary flow features (primary mineral grains and schlieren). Furthermore, the arch structure is concordant with structure in the country rock. Therefore, the Lochsa arch appears to be a primary magmatic feature and reflects the original gross internal structure of the batholith in this region. However, the occurrence of late K-feldspar megacrysts oriented parallel to the arch (Hyndman, 1984) may indicate accentuation of the arch throughout the crystallization history.

BORDER ZONE AND CONTACT RELATIONSHIPS

The contact between the Bitterroot lobe and its country rocks varies significantly at different locations. In the north the margin is a generally steeply dipping zone of interdigitated intrusive and metamorphic rocks that contains numerous dikes, whereas in the south the contact lacks dikes and is gently dipping and sharp. Complex interaction between the earlier granitoid phases and the country rock make the northern margin of the batholith difficult to place and necessitates the subdivision of the batholith into the main-phase intrusions and a border-zone complex.

The 10-km-thick northwestern border zone of the batholith is characterized by concordant sheets of granodiorite (older than the main phase of the batholith) separated by remnants of country rock; the granodiorite sheets constitute about 70 percent of the border zone (see Hyndman, 1984, for a more detailed description of the border zone). The metamorphic rocks within the border zone show more strongly developed gneissic layering than those farther west beyond the batholith contact. The granodioritic magmas were forcibly injected along foliation planes, and in many places they produced intrusion breccias. Xenoliths and schlieren are common within the border-zone intrusions, becoming more abundant northeastward toward the contact between the border-zone and main-phase granites (Wiswall, 1979b). Dikes are present throughout the border complex and range in composition from basalt through granite pegmatite or aplite. Hyndman (1984) distinguished four periods of dike emplacement that produced: (1) early, synmetamorphic, deformed, anatectic pegmatites; (2) tabular pegmatites occurring parallel to planar structural features; (3) tabular, subhorizontal pegmatites or aplites that intrude without regard for structural grain; and (4) contemporaneous or younger dikes, basalt to andesite, intruded along fractures and exhibiting chilled margins. Other significant features of the northwestern batholith margin include a general increase in grain size of granitoid rock within the border zone from west to east and a concentration of K-feldspar megacrysts near the contact between the border complex and the main mass of the batholith. Concordance between granitoid phases and the country-rock foliation suggests that the northwestern contact dips steeply eastward.

To the southeast, near the confluence of Moose Creek with the Selway River (fig. 4.1), the northwestern border zone includes a block of country rock that is underlain by commingled Cretaceous and Tertiary granitoid intrusions (Wiswall, 1979b). The quartzites, pelitic schists, and gneisses of the block are heavily invaded by Cretaceous granitic sills injected along steep foliation planes, showing a relationship similar to that farther north along the Lochsa River. Angular xenoliths of country rock in the sills and apophyses of granite in the country rock imply brittle behavior during intrusion. Overprinting relationships indicate that the country rocks underwent three

periods of deformation having the same sequence and style as F_1 through F_3 noted in the Lochsa area to the northwest. The gross structure of the block along the Selway River is an arch or dome underlain by granitoid rock. On their reconnaissance map, Greenwood and Morrison (1973) showed this block enclosed by Cretaceous igneous phases and partly concentric to the Tertiary Moose Creek pluton. These relationships suggest a roof pendant in the batholith that was deformed into an arch during the intrusion of the Tertiary pluton.

The southwestern margin of the batholith exposed in the upper Selway River canyon is distinctly different from the northern margin. The intrusive rocks are divisible into two mappable units: a main intrusive phase and a marginal intrusive phase. The main phase is fairly homogeneous granite to granodiorite. Textures vary from weakly or moderately foliated at the contact with the marginal phase to massive within the main mass. Xenoliths, schlieren, pegmatite dikes, and K-feldspar megacrysts are rare to absent. The marginal phase is a medium-grained, moderately foliated granodiorite to quartz monzodiorite that contains K-feldspar megacrysts. It forms a shell of rather constant thickness along the main batholith contact, contains numerous schlieren, and has distinct layering defined by mafic concentrations parallel to foliation near the contact with the country rock. The contact between marginal phase and country rock here is sharp and lacks the country-rock remnants that are common to the north. Adjacent to the batholith, the contact dips steeply to the east and is concordant with the country rock, but it flattens outward perpendicular to the strike of the margin. There it becomes discordant to the regional foliation, and the granitic rocks, found only on ridge crests, overlie the migmatitic rocks exposed in the valley bottoms (fig. 4.6). Hamilton (1978) noted similar relationships in the Salmon River area within the Atlanta lobe. Therefore, the entire southwestern flank of the batholith may be in the form of a mushroom: a broad, steep feeder stem capped by a tabular mass of granitic rock. The floor of this tabular body is subhorizontal but not planar. Alternate interpretations include the ideas that (1) the southwestern flank may not be part of the main-phase plutons but may represent a large granitic sill or laccolithic intrusion (P.C. Bateman, written communication, 1984) and that (2) the country rocks may have intruded the batholith as a diapir. The consistent northeast-over-southwest sense of movement recorded in the F_3 mesoscopic structures argues against the diapiric model. The form of the intrusive contact and the enveloping surface of the F_3 antiform described above are concordant, indicating a syngenetic relationship. Furthermore, the sense of movement, the progressive nature of folding about an axis parallel to the batholith contact, and cooling during F_3 folding all suggest participation of the country rocks during granite emplacement. Although sufficient information is not available to distinguish between the remaining two possibilities, we favor the interpretation of the planar body as a subhorizontal extension of the main-phase plutons.

The northeastern border zone described by Chase (1973), like that in the Lochsa area, consists of numerous interdigitated granitic sills generally concordant with the country rock. Xenoliths are common near the contact, especially in regions where calcsilicate rocks are the host, but become rarer toward the interior of the batholith. However, the form of the contact here resembles the mushroom shape of that to the southwest. In the easternmost exposure, country rocks dipping 20° to 30° to the west concordantly underlie granitic rocks that cap the ridges. The contact steepens westward to approximately 60° adjacent to the main batholith (Chase, 1973). Just to the north of the area mapped by Chase, the northeastern margin of the main body of the Bitterroot lobe shows a major reentrant along the Lochsa River (fig. 4.1). Reconnaissance mapping there shows the same topographic distribution noted to the south: intrusive rocks on ridge crests overlie country rocks, a relation suggesting a low-angle, west-dipping contact (Williams, 1977; Hyndman, unpublished data).

FORM OF THE BITTERROOT LOBE

The field relationships at various localities within the Bitterroot lobe indicate, as noted above, that it or some of its component bodies have the form of a mushroom. This shape apparently formed during more-or-less continuous intrusion that emplaced large bodies of magma of uniform composition. These interpretations are based on (1) the lack of variation in mineralogy and texture within the main granitic phase, (2) the lack of significant chemical variation across the batholith, (3) recognition of a foliation arch in the northern part of the Bitterroot lobe (Hyndman, 1984), and (4) exposure of a subhorizontal basal contact on the southwestern and northeastern borders. Mineralogic and textural relationships within the main-phase granitoid rocks indicate that the bulk of the magma was emplaced over a limited period of time, perhaps in a single protracted intrusive event (see Toth, chapter 2; Reid, chapter 3).

Differences in the contact relationships from place to place may be due to the level of exposure. The northern Bitterroot lobe forms a central diapiric or mushroomlike body which is complexly interdigitated with the country rocks near its margins. Border-zone relationships suggest intrusion either laterally or from below under conditions conducive to parallel-style folding, brecciation, and at least in later stages, fracturing. The preexisting structural grain (S_1) exerted significant control on the emplacement

of the magmas. Intrusion began with smaller granodiorite plutons (Hyndman, 1984) emplaced as sheets throughout the area now occupied by the batholith and border zone. This was followed by a major intrusive event that emplaced the main-phase granodiorite to granite pluton(s) into the center of the previous intrusive activity. The shape of the northwest-plunging foliation arch, numerous xenoliths near the crest of the arch, abundant injection migmatites, and the possible roof pendant along the Selway River suggest that the level of exposure in the north is near the top of the mushroom cap. Miarolitic cavities in late, crosscutting granite pegmatite dikes indicate that crystallization was not complete when the magmas attained relatively shallow levels in the crust (see Toth, chapter 2). The presence of late-magmatic or postconsolidation deformation and alteration suggest accentuation of the foliation arch during diapiric rise or uplift late in the crystallization history of the magmas. Miarolitic cavities in late pegmatites also support this conclusion. Although the presence of numerous schlieren in the granitoid rocks of the main mass suggest deep exposure near the source area, these can also be interpreted either as restite carried up with the magma from the source or as digested xenoliths derived from the overlying country rock and stretched out during rise and emplacement of the magma. Thus, exposures in the northwestern Bitterroot lobe seem to represent sites near the top of the intrusion, which attained shallow levels prior to complete crystallization.

In contrast, the southwestern margin of the Bitterroot lobe along the Selway River exhibits (1) a more ductile style of folding characterized by relatively small domains of homogeneous deformation and a lack of significant brecciation; (2) a sharp boundary between the batholith and country rock; and (3) the presence of abundant anatectic migmatites. In addition, the intrusive rocks here clearly overlie the country rocks. These characteristics suggest a deeper level of exposure, near the bottom of the intrusive mass. The eastern border shows characteristics of both northwestern and southwestern borders; data from it suggest that the change in style may be gradational over the length of the batholith and that the batholith floor has a northerly dip.

If the interpretations concerning the level of exposure

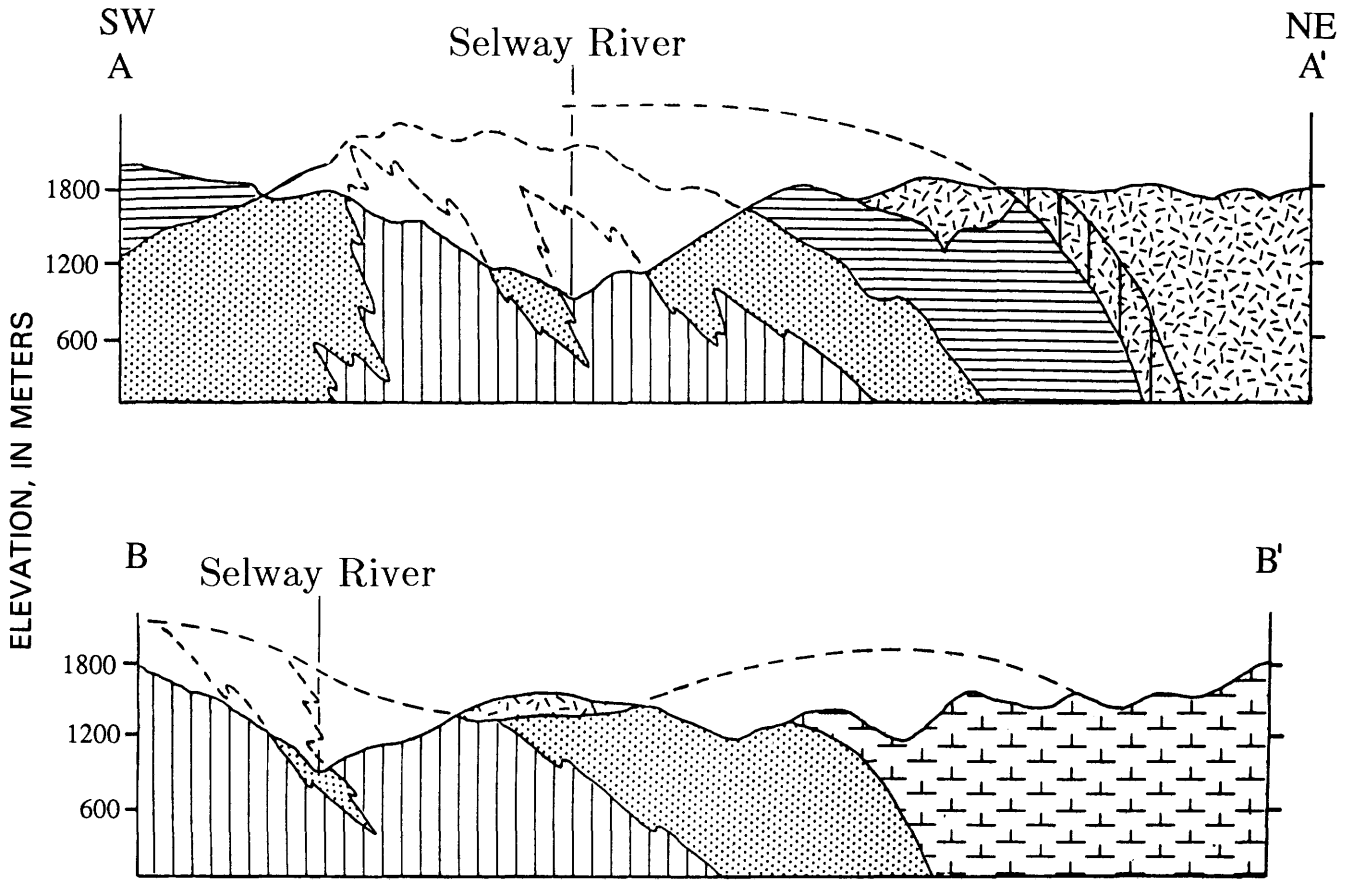

FIGURE 4.6.—Geologic structure sections across the upper Selway River. See figure 4.2 for location and explanation of symbols. No vertical exaggeration.

are correct, we may broadly sketch the three-dimensional structure of the batholith, at least for the primary level of emplacement. The floor marks a distinct break between the underlying anatectic migmatites and early igneous phases and the overlying main-phase or flanking units. The exposed southwest and east edges of the floor are subhorizontal and gently undulating. The underlying country rocks are in structural concordance with the floor and form an antiform that nestles into the concavity between the mushroom cap and stem. At higher levels the form is more strongly controlled by the preexisting structural grain. Along the sides and roof, the magma injected forcibly either laterally or vertically, following planes of weakness in the somewhat brittle country rocks and producing the characteristics observed in the border zone to the north.

If the batholith is a northerly plunging, mushroom-shaped body having its basal part exposed in the south and its roof in the north, a section from the southwestern basal exposure northward along the Selway River should show the same gradational change in the level of exposure as is suggested by the intermediate characteristics noted on the eastern side. However, reconnaissance mapping by Wiswall (1979b) did not show the expected relationship; instead, the change in characteristics appears to be abrupt. The batholith floor is exposed for 12 km along the Selway River from White Cap Creek, north to North Star Creek where it is truncated by a Tertiary pluton (fig. 4.2). North of this Tertiary pluton, a Cretaceous quartz monzodiorite crops out for 10 km along the river and is in contact along its northern margin with the possible roof pendant described above. The quartz monzodiorite is mineralogically and texturally distinct from the intrusive phases to the south, and therefore a sharp structural discontinuity is apparently masked by the younger intrusive phase. Possible interpretations of this relationship are discussed below.

TECTONICS OF EMPLACEMENT

Field relationships of the intrusive rocks and the known shape of the batholith allow speculation about the tectonics of emplacement. Although the present data are still rather sketchy, they show significant similarities in areas throughout the Bitterroot lobe.

Diapirs are classically pictured as teardrop-shaped bodies that rise by forcing the overlying rocks laterally, causing them to flow down along the margins of the diapir and fill in behind as the diapir passes. In a magmatic diapir the rising magma thus makes room for itself by displacing the overlying rocks, which move by viscous flow around the intrusion. The shape of the Bitterroot lobe and the structural events recorded in the country rocks support such a view of its rise in the crust. Although the lobe is presently in the form of a mushroom, this is probably the result of its final emplacement rather than its rise. The top of a teardrop-shaped pluton will reach its solidus temperature before the bottom and hence stop rising. Continued rise of the lower parts of the diapir will then cause lateral spreading at the level of emplacement, thereby altering the shape of the body to that of a mushroom. The movement pattern for F_3 deformation in the southwest is consistent with this mechanism, for F_3 was a progressive deformation that continually reoriented earlier formed structures about an axis parallel to the batholith margin and that proceeded through cooling of the rocks. The consistent northeast-over-southwest sense of movement recorded in the mesocopic F_3 structures in the southwest is coincident with the direction of spreading there of the magmas at the level of emplacement. On the basis of these relationships, Wiswall (1979a) concluded that the F_3 event records the rise and emplacement of the magma. Furthermore, the association of anatectic migmatites, which underwent F_3 deformation, with the floor of the batholith suggests that some of the source rocks rose together with the magma.

Several lines of evidence suggest that the magmas did not rise far and were emplaced at depths close to the source area in the lower continental crust. Contact relationships indicate mesozonal to catazonal levels of emplacement. In addition, Hyndman (1981) presented independent mineralogic and stratigraphic evidence for the northeastern border zone that suggested emplacement at 0.5 to 0.6 MPa (5–6 kilobars) or a corresponding depth of 17 to 20 km. Phase considerations, assuming a muscovite-bearing parent, would permit only limited rise before intersection of the solidus. Finally, the batholith margin is generally parallel to regional metamorphic isograds in the horizontal plane and occurs within the sillimanite zone (Chase and Johnson, 1977). However, the batholith contact cuts across the isograds in the third dimension (Nold, 1968, 1974), a situation that could reflect limited rise of the magma out of the central thermal high into the overlying, somewhat lower grade rocks.

Field relationships suggest that the mechanism of batholith emplacement varied from north to south, though this change may be a function of the vertical position within the intrusion. The main phase(s) throughout the lobe generally followed a similar path, rising as a limited number (three or four?) of very large diapirs. The path was centered in the highest temperature regions and controlled to some extent by the regional northwest-trending foliation. However, the differences in the nature of the batholith margin and the structural relationships noted above suggest a range in physical conditions at the site of emplacement. In the north, where structural control was strongest, early magmas were constrained to inject forcibly along foliation planes, thereby incorporating numerous remnants of country rock into the border zone. The country rocks were not ductile enough to flow early

in the emplacement history, a conclusion supported by the presence of intrusion breccias in the northwestern border zone. The main phase was emplaced as a diapir, but the steep sides of the foliation arch indicate that the country rocks were competent enough to prevent lateral spreading. The change in style of emplacement with time may be a function of larger volumes of magma resulting from a higher degree of partial melting and more complete coalescence, coupled with a higher ductility in the country rocks because of continued intrusion. The numerous xenoliths present near the margins suggest at least minor stoping, but the absence of large roof pendants (with the possible exception cited along the lower Selway River) shows that stoping did not play a major role in batholith emplacement.

In the south, on the other hand, the magmas were emplaced by lateral spreading. The country rocks were ductile enough throughout emplacement to flow passively in response to movement of the magma, producing the concordance of the macroscopic country-rock structure with the margin of the batholith and preventing forcible injection or brecciation. We propose that these observed differences in style of emplacement reflect the level of exposure within the batholith and deserve further study as indicators of relative depth.

POSTEMPLACEMENT HISTORY

Any tectonic interpretation of the northern Idaho batholith must consider the postemplacement history. Throughout this discussion we have emphasized the difference between the apparent levels of exposure in the Lochsa Canyon and in the upper Selway Canyon. We have noted that the eastern border seems to occupy an intermediate level and thus to suggest a gradational change, but an apparently sharp change occurs north along the Selway River from the exposed batholith floor. Reconnaissance work shows an equally abrupt change where granitic rocks reappear in creek bottoms westward from the exposed base (Wiswall, 1979b). The contact between the two levels of emplacement is not exposed, but outcrop patterns suggest it has an easterly dip. Thus both to the north and west, outcroppings of the batholith floor appear to be in sharp contact with batholith exposures that were originally emplaced at shallower levels. All of these rocks must, however, already have been at shallow levels by the Eocene, as shown by the clearly shallow Teritiary plutons.

Chase and Talbot (1973) proposed a domal structure, the Bitterroot dome, to explain the eastern exposure of the batholith floor, maintaining that this dome is ringed by Tertiary plutons. Hyndman (1980) presented additional evidence on the extent and timing of dome formation and noted that placing the western margin is difficult because of the asymmetry in structural fabric. Many workers have observed cataclastic deformation that is late, vertically directed, and distinct from the mylonite exposed around the eastern half of the Bitterroot lobe (Chase, 1973; Greenwood and Morrison, 1973; Hyndman, 1980). Such deformation features are also present in the southwestern exposure of the batholith floor.

Assuming that the Bitterroot dome is symmetrical and that the Bitterroot divide marks its crest, projection westward from the crest a distance equal to that of the eastern margin (approximately 20 km) would place the western margin in the vicinity of the Selway River (fig. 4.1). The area of abrupt change in level of exposure along the Selway River may mark the zone of dislocation formed during isostatic rise of the dome following eastward movement of the suprastructure (Hyndman and others, 1975; Hyndman, 1980). If this is so, it can explain (1) the apparently abrupt changes in the level of exposure; (2) the presence and distribution of the exposures of the batholith floor; (3) the F_4 structural event; (4) the position of Tertiary plutons; (5) numerous steep fractures with down-dip lineations in the eastern half of the lobe (Hyndman, 1980); and (6) the course of the Selway River. It should be noted that the Tertiary ages obtained by Chase and others (1983) from main-phase (?) plutons suggest that the formation of the Bitterroot dome is not due to unroofing of the eastern Bitterroot lobe but rather may be the result of diapiric rise associated with emplacement of those plutons. This suggestion underscores the need for continued study and reflects the rapid evolution of geologic thought in this tectonically complex area.

Beyond the scope of this paper, but worth consideration on a broader scale, is the possibility of a major prebatholith tectonic suture in the western border zone, perhaps in the area of the Selway River. Differences in lithology, depth of exposure, and structural style across this boundary could mark the edge of a microcontinental fragment that impinged on the west. The main-phase Idaho batholith might have been emplaced along this suture. In such a model, mylonites in the eastern Bitterroot lobe could be related to continued continental collision, in the style outlined by Brown and Read (1983), Mattauer and others (1983), and Rhodes and Hyndman (1984) for areas farther to the northwest.

REFERENCES CITED

Armstrong, R.L., 1974, Geochronometry of the Eocene volcanic-plutonic episode in Idaho: Northwest Geology, v. 3, p. 1-15.

——— 1975, Precambrian (1500 m.y. old) rocks of central Idaho: the Salmon River arch and its role in cordilleran sedimentation and tectonics: American Journal of Science, v. 275-A, p. 437-467.

Bateman, P.C., and Chappell, B.W., 1979, Crystallization, fractionation, and solidification of the Tuolumne Intrusive Series, Yosemite National Park, California: Geological Society of America Bulletin, v. 90, p. 465-482.

Berg, R.B., 1964, Petrology of anorthosite bodies, Bitterroot Range, Ravalli County, Montana: Missoula, Montana, University of Montana, Ph.D. dissertation, 158 p.

Bickford, M.E., Chase, R.B., Nelson, B.K., Shuster, R.D., and Arruda, E.C., 1981, U-Pb studies of zircon cores and overgrowths, and monazite: implications for age and petrogenesis of the northeastern Idaho batholith: Journal of Geology, v. 89, p. 433-457.

Brown, R.L., and Read, P.B., 1983, Shuswap terrane of British Columbia: a Mesozoic "core complex": Geology, v. 11, p. 164-168.

Chase, R.B., 1973, Petrology of the northeastern border zone of the Idaho batholith, Bitterroot Range, Montana: Montana Bureau of Mines and Geology Memoir 43, 28 p.

_____ 1977, Structural evolution of the Bitterroot dome and zone of cataclasis, *in* Geological Society of America Field Guide No. 1: Rocky Mountain Section Meeting, Missoula, Montana, University of Montana, p. 1-24.

Chase, R.B., Bickford, M.E., and Arruda, E.C., 1983, Tectonic implications of Tertiary intrusion and shearing within the Bitterroot dome, northeastern Idaho batholith: Journal of Geology, v. 91, p. 462-470.

Chase, R.B., Bickford , M.E., and Tripp, S.E., 1978, Rb-Sr and U-Pb isotopic studies of the northeastern Idaho batholith and border zone: Geological Society of America Bulletin, v. 89, no. 9, p. 1325-1334.

Chase, R.B., and Johnson, B.R., 1977, Border-zone relationships of the northern Idaho batholith: Northwest Geology, v. 6-1, p. 38-50.

Chase, R.B., and Talbot, J.L., 1973, Structural evolution of the northeastern border zone of the Idaho batholith, western Montana [abs.]: Geological Society of America Abstracts with Programs, v. 5, no. 6, p. 470-471.

Cheney, J.T., 1972, Petrologic relationships of layered meta-anorthosites and associated rocks, Bass Creek, western Montana: Missoula, Montana, University of Montana, M.A. thesis, 112 p.

Coney, P.J., Jones, D.L., and Monger, J.W.H., 1980, Cordilleran suspect terranes: Nature, v. 288, p. 329-333.

Criss, R.E. and Taylor, H.P., Jr., 1983, An $^{18}O/^{16}O$ and D/H study of Tertiary hydrothermal systems in the southern half of the Idaho batholith: Geological Society of America Bulletin, v. 94, no. 5, p. 640-663.

Ferguson, J.A., 1975, Tectonic implications of some geochronometric data from the northeastern border zone of the Idaho batholith: Northwest Geology, v. 4, p. 53-58.

Grauert, B., and Hofmann, A., 1973, Old radiogenic lead components in zircons from the Idaho batholith and its metasedimentary aureole: Carnegie Institution of Washington Yearbook, no. 72, p. 297-299.

Green, Ronald, and Kridoharto, P., 1975, New evidence on the form of the granitic instrusions in New England, N.S.W.: Journal of the Geological Society of Australia, v. 22, p. 51-59.

Greenwood, W.R., and Morrison, D.A., 1973, Reconnaissance geology of the Selway-Bitterroot Wilderness Area: Idaho Bureau of Mines and Geology Pamphlet 154, 30 p.

Hamilton, Warren, 1978, Mesozoic tectonics of the Western United States, *in* Howell, D.G., and McDougall, K.A., eds., Mesozoic paleogeography of the Western United States: Society of Economic Paleontologists and Mineralogists, Pacific Section, Pacific Coast Paleogeography Symposium, no. 2, p. 33-70.

Hyndman, D.W., 1980, Bitterroot dome-Sapphire tectonic block, an example of a plutonic-core gneiss-dome complex with its detached suprastructure, *in* Crittenden, M.D., Jr., Coney, P.J., and Davis, G.H., eds., Cordilleran metamorphic core complexes: Geological Society of America Memoir 153, p. 427-443.

_____ 1981, Controls on source and depth of emplacement of granitic magma: Geology, v. 9, p. 244-249.

_____ 1983a, The Idaho batholith and associated pluton, Idaho and western Montana, *in* Roddick, J.A., ed., Circum-Pacific plutonic terranes: Geological Society of America Memoir 159, p. 213-240.

_____ 1983b, Structure along the Bitterroot front, western Montana, *in* Hobbs, S.W., ed., Guide to Field Trips, Belt Symposium II: Missoula, Montana, University of Montana, p. 115-124.

_____ 1984, A petrographic and chemical section through the northern Idaho batholith: Journal of Geology, v. 92, 83-102.

Hyndman, D.W., and Talbot, J.L., 1976, The Idaho batholith and related subduction complex: Geological Society of America Cordilleran Section Field Guide No. 4, 15 p.

Hyndman, D.W., Talbot, J.T., and Chase, R.B., 1975, Boulder batholith: a result of emplacement of a block detached from the Idaho batholith infrastructure?: Geology, v. 3, p. 401-405.

Hyndman, D.W., and Williams, L.D., 1977, The Bitterroot lobe of the Idaho batholith: Northwest Geology, v. 6-1, p. 1-16.

Jens, J.C., 1974, A layered ultramafic intrusion near Lolo Pass, Idaho: Northwest Geology, v. 3, p. 38-46.

Koller, G.R., 1978, Geophysical investigation of the Lexington batholith of west-central Maine: a subhorizontal, tabular, composite intrusion [abs.]: Geological Society of America Abstracts with Programs, v. 10, no. 2, p. 71.

Larsen, E.S., and Schmidt, R.G., 1958, A reconnaissance of the Idaho batholith and comparison with the southern California batholith: U.S. Geological Survey Bulletin 1070-A, p. 1-33.

Mattauer, Maurice, Collot, Bernard, and Van den Driessche, Jean, 1983, Alpine model for the internal metamorphic zones of the North American cordillera: Geology, v. 11, p. 11-15.

Nold, J.L., 1968, Geology of the northeastern border zone of the Idaho batholith, Montana and Idaho: Missoula, Montana, University of Montana, Ph.D. dissertation, 159 p.

_____ 1974, Geology of the northeastern border zone of the Idaho batholith: Northwest Geology, v. 3, p. 47-52.

Norwick, S.A., 1972, The regional Precambrian metamorphic facies of the Prichard Formation of western Montana and northern Idaho: Missoula, Montana, University of Montana, Ph.D. dissertation, 129 p.

Pitcher, W.S., and Berger, A.R., 1972, The geology of Donegal: a study of granite emplacement and unroofing: New York, Wiley Interscience, 435 p.

Ramberg, Hans, 1970, Model studies in relation to intrusion of plutonic bodies, *in* Newall, Geoffrey, and Rast, Nicholas, eds., Mechanism of igneous intrusion: Geological Journal (Liverpool) Special Issue, no. 2, p. 261-286.

Rhodes, B.P., and Hyndman, D.W., 1984, Kinematics of mylonites in the Priest River "metamorphic core complex," northern Idaho and northeastern Washington: Canadian Journal of Earth Sciences, v. 21, no. 10, p. 1161-1170.

Sweeny, J.F., 1975, Diapiric granite batholith in south-central Maine: American Journal of Science, v. 275, p. 1183-1191.

_____ 1976, Subsurface distribution of granitic rocks, south-central Maine: Geological Society of America Bulletin, v. 87, p. 241-249.

Sylvester, A.G., Oertel, Gerhard, Nelson, C.A., and Christie, J.M., 1978, Papoose Flat pluton: a granitic blister in the Inyo Mountains, California: Geological Society of America Bulletin, v. 89, p. 1205-1219.

Vallier, T.L., and Engebretson, D.C., 1984, The Blue Mountains island arc of Oregon, Idaho, and Washington: an allochthonous coherent terrane from the ancestral western Pacific Ocean?, *in* Howell, D.G., Jones, D.L., Cox, Allan, and Nur, Amos, eds., Proceedings of the Circum-Pacific Terrane Conference: Stanford University Publications, Geological Sciences, v. 18, p. 197-199.

Williams, L.D., 1977, Petrology and petrography of a section across the Bitterroot lobe of the Idaho batholith: Missoula, Montana, University of Montana, Ph.D. dissertation, 221 p.

Wiswall, C.G., 1979a, Field and structural relationships below the Idaho batholith: Northwest Geology, v. 8, 18-28.

_____ 1979b, Structure and petrography below the Bitterroot dome, Idaho batholith near Paradise, Idaho: Missoula, Montana, University of Montana, Ph.D. dissertation, 129 p.

5. MIGMATITE ZONES IN THE BITTERROOT LOBE OF THE IDAHO BATHOLITH

By Enid Bittner[1]

ABSTRACT

The Bitterroot lobe of the Idaho batholith is a complex of migmatite zones, plutons, and crosscutting mafic dikes. The migmatite zones are concentrated in the inner border of the batholith, where they make up about 70 percent of the rock; within the lobe itself they make up 10 to 20 percent of the rock. Selected migmatite zones were studied on the western and southern borders of the lobe and in the central and eastern parts of the lobe interior.

The migmatite formed by the intrusion, metasomatism, and partial assimilation of the country rock by tonalite, granodiorite, and granite of the batholith. The country rocks included in the migmatite zones consist of tonalite gneiss, quartzite, calc-silicate rocks, schist, quartzofeldspathic gneiss, and amphibolite. They show petrologic and chemical affinities to the Belt Supergroup and to other country rocks older than the batholith.

The migmatite zones reflect a sequence of five deformational events: D_1, Jurassic and Early Cretaceous isoclinal and recumbent folding accompanied by igneous intrusions and kyanite-zone metamorphism; D_2, emplacement of the Bitterroot lobe beginning at about 90 Ma and resulting in noncylindrical folding, hornblende hornfels contact metamorphism, and the alignment of migmatite screens east-west, parallel to the primary flow direction; D_3, Late Cretaceous and Early Tertiary northwest-southeast extension that produced a secondary axial-symmetric annealing strain fabric, metamorphism of sillimanite-muscovite facies, and cylindrical folding; D_4, postcrystallization axial-symmetric deformation resulting in blastomylonitization and mylonitization; and D_5, late faulting and arching of the eastern part of the batholith.

The migmatite units have retained their original east-west flow alignment and thus form good strain indicators.

INTRODUCTION

The Selway-Bitterroot Wilderness Area is located in north-central Idaho and western Montana and contains most of the Bitterroot lobe of the Idaho batholith (fig. 5.1). Migmatitic screens and remnants have been mapped around the border of the lobe and to a lesser extent in its interior. The screens predominantly consist of metasedimentary rocks that resemble the country rock, and they define specific structural trends.

The main objectives of this study were: (1) to map the major migmatite zones within the Selway-Bitterroot Wilderness Area on a reconnaissance basis; (2) to describe the petrography, chemistry, and structure of the migmatite zones and their associated igneous rocks; (3) to determine the relationship of the migmatite to the country rock; and (4) to propose a model to explain frequency of migmatite occurrence and the consistent east-west trend.

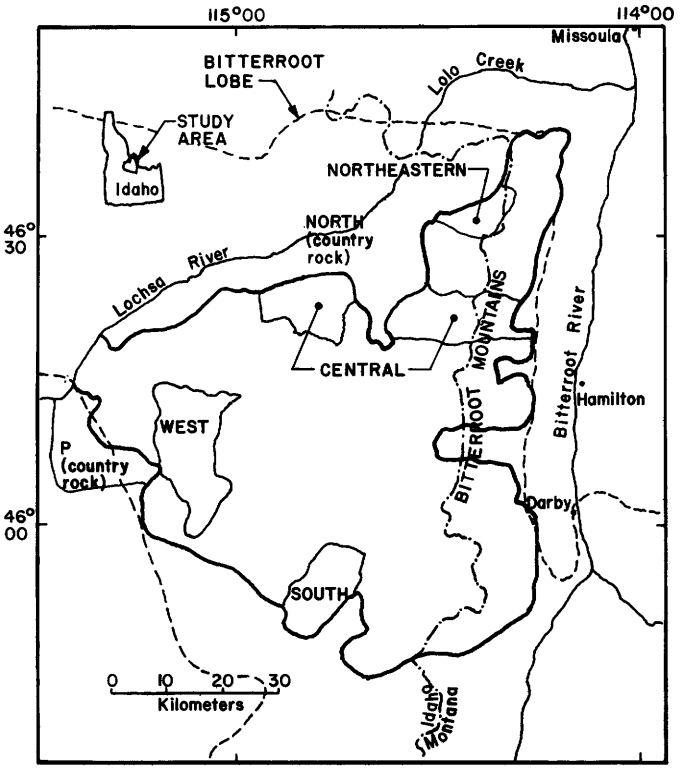

FIGURE 5.1.—Location map, simplified from Toth (1982), for the Selway-Bitterroot Wilderness (outlined by the heavy black line). Areas of reconnaissance mapping are designated P (perimeter country rock), North (country rock parallel to the Lochsa River), West, South and Central.

[1]Auburn University, Auburn, Alabama 36849.

The Bitterroot lobe of the Idaho batholith extends 100 km east-west and 50 km north-south. The Selway-Bitterroot Wilderness Area lies within the Bitterroot lobe and covers an area of approximately 5,000 km^2 (1.24 million acres) in Idaho County, Idaho, and Missoula and Ravalli Counties, Montana.

ACKNOWLEDGMENTS

This study was condensed and revised from my doctoral dissertation done at the University of Idaho. Financial support for the dissertation was provided by Health Education and Welfare Fellowship, a Sigma Xi grant, and an Idaho Bureau of Mines grant. I thank R.R. Reid for review of the manuscript.

PREVIOUS WORK

Reconnaissance mapping of the Bitterroot and Clearwater Mountains was first done by Lindgren (1904), who identified metasedimentary rocks intruded by plutonic rocks. Anderson (1952) and Toth (1982) recognized the plutonic event as one of multiple intrusions. More complete mapping of the wilderness area by Greenwood and Morrison (1973) and more recently by the U.S. Geological Survey Wilderness Evaluation study (Toth, 1983) has delimited the eastern and western borders of the Bitterroot lobe and established major structural elements.

Ross (1928) first suggested that the igneous complex of the Bitterroot lobe was of Mesozoic age. Subsequently, Tripp and Chase (1976), Chase and others (1978), and J.S. Stacey (oral commun., 1979) narrowed the age of the main stage of batholith intrusion to between 75 and 55 Ma by U-Pb dating methods. A later (Eocene) thermal event, identified by Armstrong (1974, 1976), Ferguson (1975), and Armstrong and others (1977), has reset many of the K-Ar, fission tract, and Rb-Sr isotope ages, and so accurate dating of the rock by these methods is problematical.

Reid and Greenwood (1968) and Reid and others (1973) defined the Clearwater orogenic zone as a zone of metasedimentary and metaigneous rocks enclosing the Bitterroot lobe. This zone extends north to the St. Joe River and east to the Bitterroot River valley but has undefined western and southern borders. Studies of the metasedimentary rocks by Reid (1959), Hietanen (1961b, 1963b, 1968), Chase (1968), Nold (1968), and Harrison (1972) show regional low-grade metamorphism, accompanied by multiple preintrusion deformations, which increases through greenschist to amphibolite and hornblende hornfels facies nearer the contact zone of the batholith.

Hietanen (1963a), Morrison (1968), and Bradley (1981) identified rocks of the border contact zone of the intrusion as diorite to quartz diorite. The initial diorite-quartz diorite phase was intruded by a later two-mica granite mapped by Williams (1977) and a granodiorite-quartz monzonite phase described by Leischner (1959), Ross (1963a, 1965), Wehrenberg (1968), and Toth (1982). Hamilton and Meyers (1967), Hamilton (1969), and Hyndman and Williams (1977) related the granodiorite-quartz monzonite phase of the Bitterroot lobe to Late Cretaceous subduction of the Pacific plate, which induced melting in the lower crust and subsequent plutonism. More recent works by Coney (1980) and Hyndman (1980) have related the formation of the eastern zone of the Bitterroot lobe to the 55- to 15-Ma event that produced the core complexes (Davis, 1975) along the western cordillera of the United States. Coney (1980) suggested that the two major belts along which these core complexes lie diverge at the Idaho batholith.

Migmatite zones were mapped around the northern, northwestern, and southern contact zones of the Bitterroot lobe by Johnson (1975), Reid and others (1979), Wiswall (1979), and Allen (1980). Kell and Chase (1976) noted migmatite screens extending 8 to 10 km outward from the batholith. Johnson (1975) interpreted the migmatite zones as open systems of metasomatism and injection and inferred that only minor amounts of metamorphic differentiation and anatexis took place.

METHODS OF INVESTIGATION

This investigation was part of the United States Geological Survey Mineral Evaluation study of the Selway-Bitterroot Wilderness Area. Three field seasons, from 1978 to 1980, were spent in reconnaissance mapping on 19 U.S. Geological Survey 7½-minute (1:24,000) topographic sheets. Special attention was paid to migmatitic terrain within designated study areas. Information on areas not mapped by the author was gathered from coworkers.

Field work included chip and hand-specimen sampling, stream-sediment sampling and reconnaissance mapping. Modal analyses were done by point counting both thin sections, where grain size allowed, and slabs. Because of the remarkable heterogeneity of grain size and mineral content, thin-section modal analyses are considered to have little statistical viability. The modal analyses were plotted on a ternary quartz-potassium feldspar-plagioclase diagram, and the rocks were named according to Streckeisen and others' (1973) plutonic rock classification. Structural data were plotted on the lower hemisphere of the Wulff stereonet.

Chemical analyses were done on 119 selected samples, including migmatite and Cretaceous and Tertiary intrusive rocks. Whole-rock analyses were run on 108 samples and trace-element analyses on 33.

The whole-rock analyses were done at Washington State University on a PW 1410-70 Phillips X-ray spectrometer and at the U.S. Geological Survey, Denver. The samples were analyzed for 9 elements: Si, Al, Fe (total), Mn, Ca, Mg, K, Na, and P. The standard deviations for error in the whole-rock analyses range from 0 to 0.61 and average 0.13 for 8 samples and replicates. Silica yields the greatest deviations (between 0.13 and 0.61) and Fe_2O_3, MgO, CaO, TiO_2, P_2O_5, and MnO yield the lowest deviations (between 0 and 0.6).

Trace elements were determined by neutron activation analysis at the Washington State University's nuclear reactor. The samples were run for 35 elements.

GEOLOGIC AND TECTONIC SETTING

In the Northwestern United States, sediments of the Middle Proterozoic Belt Supergroup were deposited on an older crystalline basement in a marine trough between 1,500 and 1,100 Ma. After the deposition of the Belt Supergroup, orogenic events produced multiple episodes of metamorphism, deformation, and magmatic intrusion.

A major period of deformation and plutonism in the Western United States began in the Mesozoic at about 180 Ma, and recurring episodes of deformation and plutonism continued into the Cenozoic (Coney, 1972, 1981; Roberts, 1972; Drewes, 1978). The Idaho batholith was intruded during the mid-Sevier orogeny of the Late Cretaceous. Local plutonism continued, producing the "Tertiary pink granites," which intruded the Idaho batholith. A regional metamorphism (55 to 15 Ma), recognized in northwest Washington and Idaho (Coney, 1980; Hyndman, 1980), formed metamorphic core complexes during post-Cretaceous extensional tectonics. Two core-complex belts formed, one developed on oceanic crust adjacent to the cordilleran batholiths, the other closer to the eastern cordillera on the original North American craton. These belts merge in the region of the Idaho batholith (Coney, 1980). The period of extension was overlapped and followed by volcanism, which formed the basalts of the Columbia and Snake River regions during the Pliocene (Hietanen, 1960).

The Idaho batholith is separated into two lobes, the northern (Bitterroot) lobe and the southern (Atlanta) lobe (Armstrong, 1975). The Bitterroot lobe extends from the North Fork of the Clearwater River south to the crystalline Salmon River arch, which divides the batholith into the two lobes.

The Bitterroot lobe is bounded on the north, east, and west by Precambrian crystalline basement rocks, Belt rocks, and the Early Mesozoic Riggins and Seven Devils Groups. The eastern part of the lobe was uplifted along the north-south-trending Bitterroot front fault zone. On the south the lobe is bordered by metasedimentary rocks and Eocene plutons across northwest-trending fault zones.

The first phase of batholith intrusion induced an amphibolite grade of metamorphism in the adjacent Belt Supergroup. This first intrusive phase consisted of tonalite-quartz diorite, which now crops out on the northeastern, western, and southern borders of the lobe. Most of the lobe, however, is made up of gray granodiorite to monzogranite, which has been subdivided into separate plutons (table 5.1). Late Cretaceous and the Paleocene plutons are considered to be mesozonal in origin, and depths of emplacement from 11 to 19 km have been calculated by Williams (1977), W.E. Motzer (unpub. data, 1979), and J.E. Selverstone (oral commun., 1979). Migmatite zones make up 20 to 70 percent of the border phase and inner boundary of the lobe but decrease to 0 to 15 percent in the inner granodiorite. The major phase of the batholith emplacement was followed by intrusion of granodiorite and monzogranite, in the Paleocene and Eocene, and epizonal syenogranite to monzogranite in the Eocene (table 5.1).

The long axis of the Bitterroot lobe lies along a northwest trend, concordant to the foliation of the surrounding country rocks. Steeply dipping structures were formed on the western border of the lobe during the emplacement of the batholith. Farther east, a secondary strain field of penetrative shearing has overprinted the primary fabric and developed axial symmetry about a shallowly plunging west-northwest axis. Late-stage uplift has formed a north-south-trending domal structure through the eastern section of the lobe (Reid, chapter 3; Wiswall and Hyndman, chapter 4). The eastern front is characterized by a zone of mylonitizaton, trending north-northeast, in which zones of ultramylonite to pseudotachylyte are interlaminated with mylonite. Faults that also trend north-northeast cut both the Cretaceous and Eocene granitic rocks.

METAMORPHIC ROCKS AND MIGMATITE COMPLEXES

GENERAL STATEMENT

The wall rock of the Idaho batholith has been tentatively correlated by numerous workers (for example, Nold 1968; Greenwood and Morrison, 1973; Allen, 1980) as units of the Belt Supergroup. Wall rock on the northeastern and northern borders of the Bitterroot lobe are correlated with the Wallace Formation, the Ravalli Group, and the Belt's basal unit, the Prichard Formation (table 5.2). The Wallace Formation consists primarily of diopside gneiss intercalated with pelitic schist and gneiss, the Ravalli Group is noted for thick sequences of quartzite and pelite,

TABLE 5.1.—*Mapped individual plutons within the Bitterroot lobe of the Idaho batholith and their sequence of intrusion*

[Informal names and descriptions of plutons from Bradley (1981) and Toth (1983) except where otherwise noted. Sr rations (analysed by R.J. Fleck) from Reid and others (1978); radiometric ages from Ferguson (1975), Chase and others (1978), R.J. Fleck (written commun., 1982), and J.S. Stacey (oral commun., 1982). Order of emplacement mainly from intrusive contacts]

Geologic age	Radiometric age (Ma)	$^{87}Sr/^{86}Sr$	Rock description	Plutons mapped	Elongation of pluton
Eocene	51.3±10 (K-Ar, Fleck)	--	syenogranite-monzogranite	Running Creek Whistling Pig Fire Mountain Painted Rocks Lolo Springs[1]	
Paleocene and Eocene	--	--	granodiorite biotite, microcline An_{28-30}	Burnt Ridge	
			granodiorite-monzogranite biotite, orthoclase An_{23-25}	Piquett Creek	
			diorite-gabbro biotite, augite An_{57}	White Sand Creek[1]	east-west
			quartz diorite-granodiorite biotite, orthoclase An_{24-38}	Bushy Fork[1]	east-west
Late Cretaceous and Paleocene			tonalite-monzodiorite biotite+hornblende porphyritic	Paradise	northeast
	57±10 (U-Pb, Stacey) 66±10 (U-Pb, Chase)	0.7094 .7089	granodiorite-monzogranite biotite, muscovite megacrysts aplite, pegmatite dikes	Canyon Creek Bear Creek	northeast
			monzogranite-granodiorite biotite+muscovite magnetite	Canyon Lake	east-west
			granite-granodiorite biotite, muscovite megacrysts (orthoclase)	Tom Beal Park [2]	
			granite biotite, muscovite megacrysts aplite, pegmatite	Boulder Creek[2]	
	81 (Ferguson)		granite-granodiorite diorite biotite, hornblende An_{20-45}	Skookum Butte[1]	northeast?
		.715	migmatites, quartzofeldspathic gneiss, schist, amphibolite, quartzite, calc-silicate rocks, tonalite-monzogranite	Black Canyon complex[2]	east-west
Cretaceous	94±10 Lowell, Id. (U-Pb, Stacey)	0.7130, 0.7196	tonalite-quartz diorite biotite, hornblende		
	82±10 NE. border (U-Pb, Chase)				
Precambrian		0.7147	metasedimentary rocks metaigneous rocks		

[1]Informal name and description of pluton from Nold (1968).
[2]Informal name and description of pluton from Williams (1977, 1979).

TABLE 5.2.—*Lithology of Belt Supergroup and Belt-correlative rocks from Coeur d'Alene to Clearwater and Idaho Counties, Idaho*
[Lithologies from Hietanen (1962), Harrison and Campbell (1963), Harrison (1972), Greenwood and Morrison (1973), Allen (1980), and Reid and others (1981)]

Stratigraphic unit	Lithology, relict structures, metamorphic grade		
	Coeur d'Alene area	St. Joe area	Clearwater and Idaho Counties
Wallace Formation (carbonaceous, shallow-water marine, and littoral sediments)	Interlayered clastic rocks, black limestone, and dolomite	Argillite with interlayered dolomitic quartzite; minor scapolite	Diopside-plagioclase gneiss interbedded with pelitic schist; biotite-garnet-sillimanite schist
	Oolites, stromatolites	Ripples, mudcracks, slumps, graded beds	
	Chlorite-sericite zone greenschist facies	Greenschist to amphibolite facies; Na increases with grade	Sillimanite facies, hornblende-hornfels facies
Ravalli Group (guartzitic and pelitic, shallow-water marine sediments)			
Revett Formation	Quartzite (60-90 percent)	Thick beds of quartzite	Quartzite and pelite
St. Regis and Burke Formations	Interlayered siltite, argillite, and sericitic quartzite; Na=K	Thin siliceous beds, dark argillite, sericitic quartzite and schist	Quartzite interbedded with pelitic schist and gneiss, biotite-feldspar-garnet-kyanite schist
	Crossbeds		
	Biotite zone greenschist facies	Greenschist to amphibolite facies	Amphibolite facies
Prichard Formation (argillaceous, thinly interbedded, turbidite sediments)	Argillaceous upper unit, black pyritic lower unit, interbedded argillite and quartzite	Argillite, quartzite, and garnet schist, muscovite quartzite	Pelitic quartzite, biotite-muscovite schist, white quartzite with kyanite, garnet-mica schist, aluminosilicate schist
	Biotite zone greenschist facies	Amphibolite facies	Amphibolite facies

and the Prichard Formation is characterized by massive white quartzite intercalated with pelitic schist and gneiss.

Remnants of older rocks included within the batholith closely resemble the wall rock. They are concentrated in migmatitic terrains near the margins of the plutons and occur as swarms of dismembered rafts and concordant slabs ranging from one meter to more than two kilometers in extent. Different degrees of assimilation have resulted in indistinct xenolith contacts, diffuse lamination, and mafic schlieren. Inclusions of tonalite and orthoamphibolite, as well as strongly sheared and recrystallized gneiss, also constitute part of the migmatitic terrain.

PERIMETER OF THE BATHOLITH

The northern, western, and southern borders of the Bitterroot lobe contain the highest concentrations of included material, ranging from 20 to 70 percent. Screens of metamorphic rock are intruded by both concordant and discordant sheets of diorite, tonalite, and granite. The migmatite consists of these intrusive rocks and included screens and megabreccia blocks of quartzite, pelitic gneiss, calc-silicate rock, and amphibolite. The inclusions generally display sharp to partially diffuse contacts, but these are more disseminated and diffuse where assimilation has been more complete.

In the northeastern corner of the lobe, the inclusions of country rock consist of calc-silicate, biotite quartzite, and minor amphibolite. Inclusions make up more than 20 percent of the total rock and are predominantly mixed with tonalite gneiss (M.D. Bradley, oral commun., 1981). At lower elevations in this northeastern area, the percentage of inclusions is less, declining to less than 10 percent in massive gray tonalite gneiss.

The migmatite screens of the western margin are made up mainly of two-mica schist, white quartzite, biotite gneiss, and minor calc-silicate inclusions, which occur as blocks or stretched xenoliths that have diffuse borders and show complex migmatitic folding. The screens are flat lying, as much as several kilometers long, and one-half to one kilometer wide. Extensive veining has broken up the sheets of metasedimentary rocks. The blocks of the brecciated rocks display sharp contacts and are typically separated by a few meters of igneous material.

Migmatite screens near the southern margin of the Bitterroot lobe have been truncated on the south-southwest by the Running Creek pluton and by other Eocene granite.

Overall, igneous rocks constitute a slightly greater percentage of the volume of the migmatite. Medium-grained granitic rock makes up as much as 35 percent of the total rock, pegmatite as much as 20 percent, and aplite as much as 10 percent. The biotite quartzite and gneiss range from 20 to 50 percent of the total rock, and schist forms 15 to 20 percent.

CENTRAL AREA AND EASTERN FRONT

From the central part of the lobe to the eastern front of the Bitterroot Mountains, xenolith concentrations are low. The xenoliths are generally large blocks or disseminated rafts, which lie on an east-west trend and are as long as four kilometers.

Along the eastern front, blocks and elongate xenoliths of quartz diorite and tonalite gneiss, biotite gneiss, biotite quartzite, amphibolite, and calc-silicate rocks occur in granodiorite and granite. The xenoliths make up 5 to 40 percent of the total rock volume.

QUARTZITE

Massive white quartzite to finely laminated biotite quartzite contain relict sedimentary features which have withstood metamorphism; these features include crossbeds, pebbles, and graded bedding. The relict crossbeds are in a finer grained sugary-textured quartzite. The grain size generally ranges from less than 1 mm to 5 mm, but pebble conglomerates are interbedded with the white quartzite in the western border zone. These conglomerates contain quartzite pebbles, which have been orthogonally stretched and average 5 cm in length, in a matrix of medium-grained quartz and mica.

In the northeastern corner of the Bitterroot lobe, biotite quartzite in layers 0.5 to 1 cm thick are interlayered with granodiorite to quartz monzonite layers as much as 1 m wide. The competent, fine-grained (1 to 2 mm) quartzite remnants have sharp contacts and show only minor assimilation. Where assimilation has been more complete, the igneous rock shows an increase in the concentrations of quartz and sillimanite (M.D. Bradley, oral commun., 1980).

QUARTZOFELDSPATHIC GNEISS

The quartzofeldspathic gneiss units are granodioritic to tonalitic in composition. They were formed either by lit-par-lit injection of biotite quartzite and schist or by shearing-induced metamorphic differentiation and equilibration.

The alternating leucosome amd melanosome layers in the gneiss range in width from 1 to 10 cm. The layers consist of the following ranges of minerals (in volume percent):

	Quartz	Plagioclase	K-feldspar	Biotite	Muscovite
Leucosome	29–30	17–50	0–47	0–20	0–6
Melanosome	41–60	10–31	0–11	17–26	1–10

The tonalite gneiss, like the enveloping granitic rock, has high percentages of quartz and feldspar (An_{30-34}). The gneiss is finely laminated. The neosome contains lepidoblastic biotite, muscovite, and sillimanite, minor amounts of sericite, and granoblastic quartz and feldspar. Biotite forms a mafic selvage parallel to the leucosome. The leucosome contains quartz, feldspar, and minor amounts of muscovite and biotite.

SCHIST

Biotite-muscovite-sillimanite schist containing varying amounts of garnet are interbedded with quartzite, injected lit-par-lit by granodiorite, and crosscut by aplite and pegmatite dikes. The schist units occur as blocks within the igneous host. Partial assimilation has affected the margins of the blocks, and in some cases near-total assimilation has left only remnant schlieren.

A complex sequence of events is evident in the schist. The original schistose rock, composed of biotite, muscovite, and minor feldspar and garnet, was intruded by granodiorite parallel to schistosity. This rock was subjected to a second metamorphic event which concentrated sillimanite along shear zones and within muscovite and feldspar. Metamorphism was followed by cataclasis and the formation of sericite. During or after the sillimanite-grade metamorphism, feldspar was introduced or remobilized along and into fractures. The leucocratic layers of the schist generally consist of quartz, plagioclase, and pennine. The garnet, which is relict from the earlier metamorphic event, is rounded, fractured, and partly altered to biotite.

CALC-SILICATE ROCKS

The calc-silicate rocks occur as blocky inclusions, 1 to 10 m in length, interlayered with biotite quartzite and with granodiorite, tonalite, or quartz monzonite. Large screens commonly are broken and brecciated.

Layers of plagioclase and quartz generally alternate with layers of amphibole or pyroxene in the calc-silicate rocks. Individual bands range from 1 to 10 cm in width and are defined by composition, color, textural changes, and sills parallel to the layering. Two metamorphic events are indicated by the occurrence of diopside and younger amphibole and epidote.

HORNBLENDE GNEISS AND AMPHIBOLITE

Amphibolite occurs as rounded or teardrop-shaped xenoliths along the western border zone and in the northeast corner of the Bitterroot lobe. The inclusions range from 0.5 to 15 m in length and from 0.25 to 10 m in width. Smaller inclusons in the form of lenticular pods or boudins locally parallel the gneissic foliation. The rocks are garnet-rich orthoamphibolite that developed reaction rims as much as 6 cm wide adjacent to the host.

Plagioclase ranges from An_{24} to An_{65} depending upon locality. Amphibole occurs as hornblende or tremolite or as hornblende cores with rims of actinolite. The zoned hornblende may indicate a second, weaker metamorphism, which induced the growth of actinolite.

CHEMICAL TRENDS IN COUNTRY ROCKS AND INCLUSIONS

The metamorphic mineral assemblages and major-oxide chemical data for the country rock are summarized in table 5.3. The mineral assemblages indicate metamorphism in the sillimanite-muscovite zone of the amphibolite facies (fig. 5.2*A*). R.R. Reid (oral commun., 1980) noted in the western country rock the presence of minor cordierite and andalusite, which may represent a contact metamorphic zone of hornblende hornfels facies (fig. 5.2*B*). Kyanite occurs in the metamorphic rocks to the west and north of the batholith, as observed by Hietanen (1961, 1962) and by R.R. Reid (unpub. data, 1979), who described kyanite altered to muscovite in the rocks closest to the western contact. The relict kyanite indicates an earlier metamorphic event, possibly before emplacement of the batholith, under pressures greater than 400 MPa (Turner, 1981). Sillimanite and muscovite are found in all of the country rock, and their formation represents the last event in the amphibolite-facies metamorphism.

The major-oxide chemical data and metamorphic mineral assemblages for the country-rock inclusions are given in table 5.4. The mineral assemblages represent a recrystallization event in the sillimanite-muscovite zone of the amphibolite facies (fig. 5.3). A previous metamorphic event is indicated by partly altered garnet in a matrix of recrystallized plagioclase, biotite, and quartz.

Slight variations are present in the K_2O and Na_2O contents of the migmatite units. Near the southern border there is a slight decrease in Na_2O and an increase in K_2O. The variation in Na_2O in the metasedimentary rocks is similar to that in the granodiorite where the inclusions are found.

Chondrite-normalized rare-earth-element (REE) data for the country rock and migmatite units are plotted in figure 5.4. The country-rock data show a linear trend with a substantial negative Eu anomaly (fig. 5.4*A*). The migmatite units show a similar linear trend (fig. 5.4*B*). The REE trends for the granite and tonalite gneisses in the migmatite correspond closely to the trends for the country rock. They differ, however, from those in the tonalite and granite units of the batholith, and two separate intrusive events are thus indicated.

IGNEOUS ROCKS

The rocks of the batholith fall mostly within the granite, granodiorite, and tonalite-trondhjemite fields of the Streckeisen and others (1973) classification (fig. 5.5). They are not distinguishable in the field.

WESTERN BORDER

Near the western border of the Bitterroot lobe, the granite, granodiorite, and tonalite of the batholith are partly intermixed and laterally gradational. Concordant sheets of country-rock tonalite gneiss were intruded by younger quartz diorite and tonalite. The older tonalite gneiss and other country rock occur in migmatite screens and as xenoliths.

Granite and granodiorite vary from massive, weakly foliated rock which contain sparse but large plagioclase and potassium feldspar phenocrysts to sheared gneissic rocks. Biotite, feldspar, and a later generation of muscovite and sericite lie parallel to the shear planes. Most of the younger muscovite is an alteration product of biotite and plagioclase. Muscovite also fills fractures cutting across lepidoblastic biotite at right angles. Sericite is the predominant mica in highly sheared zones. Extension fractures are commonly filled with epidote and remobilized quartz.

Included in the granite are xenoliths of granodiorite gneiss. These range from well-defined blocky inclusions to more intensely assimilated stretched lenses. The coherent nature of the xenoliths suggests at least partial consolidation prior to granite intrusion. In other areas the granodiorite-granite contacts are gradational.

TABLE 5.3.—*Chemical analyses for country rock of the Bitterroot lobe of the Idaho batholith and corresponding metamorphic mineral assemblages*

[Analyses given in weight percent. N (north), from Hietanen (1962); P (perimeter), from Reid (1980); LS, from Ross (1963b); H, from Hobbs and others (1965). Each analysis represents one sample unless other number (n) given, in which case the average is given]

Rock type	Calc-silicate				Schist	Quartzite		Gneiss		Amphibolite
Sample area	N	P	LS	HH	N (n=2)	N	P	N	P	P
	Weight percent									
SiO_2	63.2	64.7	58.8	47.9	67.3	90.6	78.9	75.5	70.3	50.4
Al_2O_3	11.2	10.9	9.0	7.0	15.6	5.6	8.6	11.7	11.5	14.2
Fe_2O_3	.24	3.4	.28	.5	.9	.04	3.1	.21	6.7	13.9
FeO	3.4		1.9	3.9	6.8	.13		1.7		
MgO	5.3	4.9	4.5	15.7	1.7	.15	1.8	2.4	2.7	6.1
CaO	14.8	8.5	21.1	21.6	.41	.5	.55	1.4	.89	9.1
Na_2O	.76	2.7	1.3	1.0	.85	2.5	1.4	3.6	1.2	2.6
K_2O	.12	2.0	2.3	1.6	3.2	.26	2.4	1.7	3.5	1.1
TiO_2	.44	.43	.4	.19	2.0	.19	.47	.57	.91	1.8
P_2O_5	.09	.11	.08	.09	.81	.05	.06	.05	.15	.21
MnO	.01	.11	.04	.22	.04	.05	.04	.02	.07	.17
Total	99.56	97.75	99.70	99.70	99.61	100.07	97.32	98.86	97.92	99.58
	Metamorphic mineral assemblages									
	Plagioclase-microcline-biotite-hornblende-diopside	Plagioclase-diopside-scapolite	Plagioclase±albite-orthoclase-diopside-actinolite±calcite	Plagioclase-orthoclase-diopside-calcite-albite	Plagioclase-biotite-muscovite-sillimanite-garnet	Plagioclase-biotite-muscovite-microcline-chlorite	Plagioclase-biotite-muscovite-sillimanite	Biotite-muscovite-sillimanite-chlorite	Plagioclase-biotite-potassium feldspar±muscovite-sillimanite±garnet	Plagioclase-potassium feldspar-biotite-muscovite-sillimanite-garnet	Plagioclase±potassium feldspar-biotite-amphibole

CENTRAL REGION TO EASTERN BORDER

In the central regions of the Bitterroot lobe and east to its eastern border, the granitic rock is both intruded by and synkinematic with tonalite, quartz diorite, diorite, and pegmatitic and aplitic dikes. The granitic rock is porphyritic and has tabular to augen-shaped phenocrysts of potassium feldspar and plagioclase, which range in size from 1.5 to 7 cm and total 10 to 40 percent of the rock mode.The granitic rocks are massive to medium grained, gray, and lineated and have an average color index of 15. The fabric changes from the central regions, where the

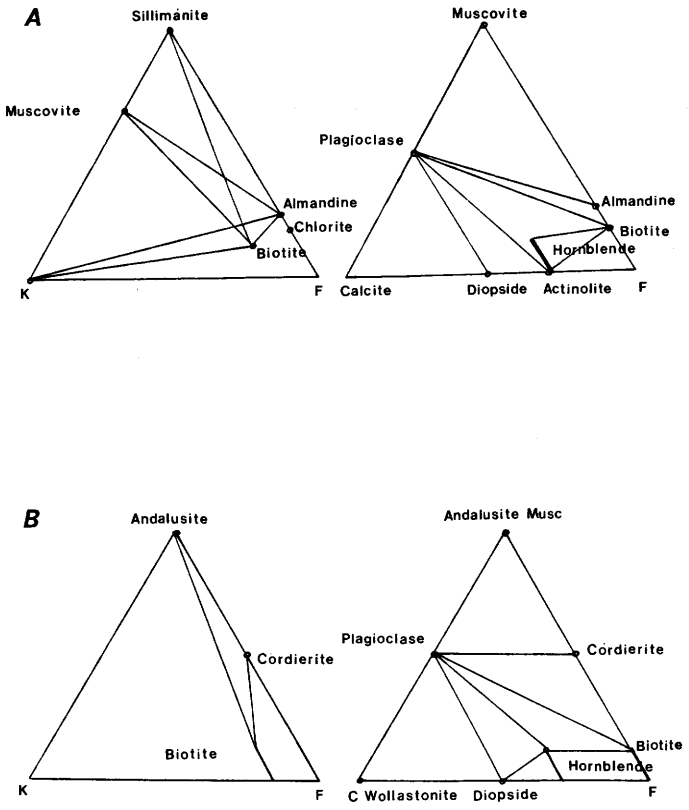

FIGURE 5.2.—AKF and ACF diagrams applicable to the country rock of the Bitterroot lobe of the Idaho batholith (from Turner, 1981). *A*, Diagrams representing the sillimanite-muscovite zone of metamorphism. *B*, Diagrams representing the hornblende hornfels facies of metamorphism.

rocks are generally massive and lineated, eastward toward the eastern border, where they are locally foliated.

At higher elevations the rocks are layered and consist of pegmatite interfingered with medium-grained granitic rock and finely ground cataclastic rock. Layers vary from 1 cm to 2 m in thickness. At lower elevations the rocks are more massive and lineated, and pegmatite dikes are absent. The metamorphic inclusions are in varying stages of assimilation from undeformed blocks to very stretched and folded incompetent bodies, and they become more abundant eastward and toward higher elevations.

East from the Bitterroot crest the intensity of cataclasis increases. The medium-grained, massive granitic rocks become more equigranular and have alternating concentrations of quartz, feldspar, and biotite. The grain size is generally 3 to 5 mm; phenocrysts are as large as 5 cm but are mostly smaller. Foliation is better defined and coarser than it is to the west. Layers are rich in lepidoblastic and microschlieren biotite, which makes up as much as 10 to 20 percent of the finer grained granulated rock. Locally the shearing was so intense that sheets of mylonite and ultramylonite were formed. The ultramylonite occurs as zones 7 to 14 cm wide and contains porphyroblasts as long as 1 cm. The shears average 1 cm in width. Chlorite and epidote are concentrated along fractures.

Compositionally, the granitic rocks differ in plagioclase composition and percentage, in mafic content and minerals, and in potassium feldspar percentage. Plagioclase in the granodiorite ranges from An_{21} to An_{34}, but is mostly around An_{25-27}. The mafic minerals are biotite and minor actinolite, which has altered to biotite and chlorite and includes some apatite and zircon. Plagioclase in the tonalite has a higher An range, from An_{32} to An_{36}. The mafic mineral of the tonalite is biotite. Quartz monzonite and quartz monzodiorite have plagioclase that is slightly more sodic, from An_{23} to An_{27}. Mafic minerals here are biotite and hornblende. The hornblende is subhedral and averages 1.25 mm in size, is partly altered to biotite, and includes apatite and zircon.

CHEMISTRY OF IGNEOUS ROCKS

Oxide and normative mineral percentages for the igneous rocks are shown in table 5.5. The uneven distribution of data among the various areas representing the major batholithic rocks makes interpretation difficult. In spite of the probably insufficient data, however, trend analyses and interpretations have been attempted.

The diagrams of oxides versus SiO_2 (fig. 5.6) clearly demonstrate the absence of a linear fractionation trend between the tonalites and the granites and granodiorites, the absence of chemical distinctions between the granites and granodiorites, and an irregular distribution of composition within the several rock types.

Concentrations of Na_2O do not noticeably vary between areas or between rock types. This uniformity may indicate a redistribution of Na during shearing or an original irregular distribution of Na among the different magma types. The K_2O/Na_2O ratios fall between 0.45 and 2.11 (average of 0.99) for the granites, between 0.39 and 1.54 (average of 0.88) for the granodiorites, and between 0.29 and 0.97 (average of 0.51) for the tonalites. When compared to the data of Cox and others (1979), these ratios are within the range for granites (0.7) and tonalites (0.3 to 0.5) but are high for the granodiorite range (0.5 to 0.7). The high ratios for granodiorite indicate a higher K_2O concentration from biotite or feldspar. As a result, there is little or no difference between the granites and granodiorites.

From the composition of the rocks it should be possible to infer the chemistry and origin of the magma from which they were derived. Table 5.6 gives data for those oxides and minerals which are used to determine the source of the igneous rocks in Chappell and White's (1974) classifi-

TABLE 5.4.—*Chemical analyses of metamorphic rocks in migmatite of the Bitterroot lobe of the Idaho batholith and corresponding metamorphic mineral assemblages*

[Analyses given in weight percent. Areas: C, central; S, southern; W, western. Each analysis represents one sample unless other number (n) given, in which case the average is given]

Rock type	Calc-silicate		Schist		Quartzite		Gneiss		Amphibolite
Sample area	C	S (n=3)	S	W (n=3)	S (n=5)	W (n=5)	S	W (n=5)	C
SiO_2	64.3	69.3	46.6	66.1	87.5	86.4	67.8	73.8	66.2
Al_2O_3	10.2	12.0	25.4	18.2	5.2	6.7	16.3	12.7	17.3
Fe_2O_3	1.4	1.3	11.8	3.3	1.4	.95	4.2	1.5	1.6
FeO	1.6	1.5		3.8	1.2	1.1		1.5	1.8
MgO	5.6	4.9	2.8	1.7	.88	1.1	.95	1.9	1.7
CaO	10.8	3.9	.26	.06	.07	.73	.07	2.3	3.9
Na_2O	3.1	2.4	.24	.78	.74	.88	.83	2.2	4.3
K_2O	2.4	4.2	4.3	4.8	2.0	1.6	6.0	2.8	2.3
TiO_2	.4	.23	2.0	1.0	.46	.33	.59	.49	.63
P_2O_5	.13	.04	.05	.05	.03	.04	.05	.11	.17
MnO	.09	.05	.14	.06	.03	.04	.02	.07	.05
Total	100.02	99.72	93.95	99.85	99.51	99.87	96.81	99.37	99.95

Metamorphic mineral assemblages
Plagioclase-orthoclase-diopside-hornblende
Plagioclase-diopside-garnet-epidote
Plagioclase-orthoclase-diopside-actinolite±calcite
Plagioclase-biotite-muscovite-sillimanite±garnet
Plagioclase±biotite-sillimanite
Plagioclase±biotite±muscovite±garnet
Plagioclase-microcline-biotite-muscovite
Plagioclase-microcline-biotite-muscovite-sillimanite±epidote±garnet
Plagioclase±microcline-biotite±garnet
Plagioclase-tremolite
Plagioclase-hornblende-actinolite-epidote

cation, as well as for those minerals which may contribute to REE fractionation trends.

The high Al_2O_3/K_2O+Na_2O+CaO ratio and the high normative corundum values for the granites and granodiorites support an interpretation as S-type rocks. However, the values of these parameters are also high for the tonalites.

The southern granites, granodiorites, and tonalites differ from the central and western rocks mainly in their higher values of normative enstatite, forsterite, magnetite, and ilmenite, which are characteristic of I-type rocks.

S-type granite contains metasedimentary restite material (White and Chappell, 1977). Where xenoliths are present in the granitic rocks of the Bitterroot lobe the in-

clusions are predominantly metasedimentary rocks, although some are orthogneiss. The xenolith material could be restite in granitic rocks that represent minimum melts, or the xenoliths could be stoped and brecciated blocks of the country rock. The presence of these metasedimentary inclusions supports an interpretation of the rocks as S-type granite.

The southern granites, like the others, include a high percentage of metasedimentary and tonalitic xenoliths. Their I-type characteristics, therefore, may be the result of assimilating more igneous material.

Data on REE in rocks from the western and southern areas show two curves on the chondrite-normalized diagrams (fig. 5.7): (1) a general linear trend of LREE (light rare-earth-element) enrichment and a negative Eu anomaly and, (2) a saddle-shaped pattern of HREE (heavy rare-earth-element) abundances accompanied by a small positive Eu anomaly and LREE enrichment. Minimum melting of a metasedimentary source, which would involve a high degree of fractionation of amphiboles, garnet, and feldspars (Albuquerque, 1977; Hanson, 1978), would produce a linear trend like that seen in the granites.

Compositional data for the tonalites and granodiorites are varied and complex. Tonalites can be derived from graywacke (Albuquerque, 1977) or from an igneous source (Arth and Hanson, 1972; Wyllie and others, 1976). The high Al_2O_3 and Na_2O values in the tonalites here support a graywacke source, but they could also be the result of contamination or assimilation of metasedimentary material. The tonalites are rich in apatite and contain hornblende; as a result they have high abundances of both LREE and HREE.

The close association between the granites and granodiorites in the field and their chemical similarity suggest they are synplutonic. The characteristic REE patterns for the granodiorites indicate partial fractionation of plagioclase, hornblende, and pyroxene (Albuquerque, 1977; Hanson, 1978); possibly a higher content of garnet in the melt is indicated by the trough-shaped HREE pattern.

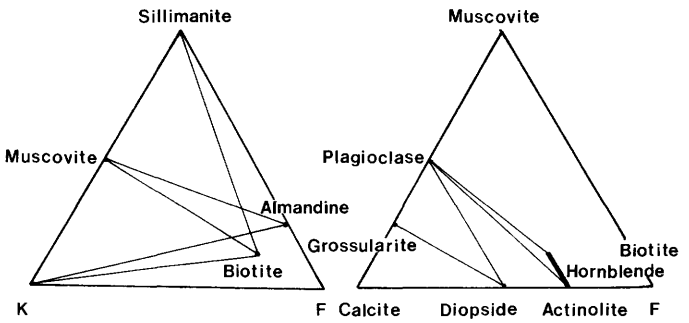

FIGURE 5.3.—AKF and ACF diagrams applicable to the prebatholithic rocks in the migmatite of the Bitterroot lobe of the Idaho batholith. The diagrams represent the sillimanite-muscovite zone of the amphibolite facies of metamorphism (from Turner, 1981).

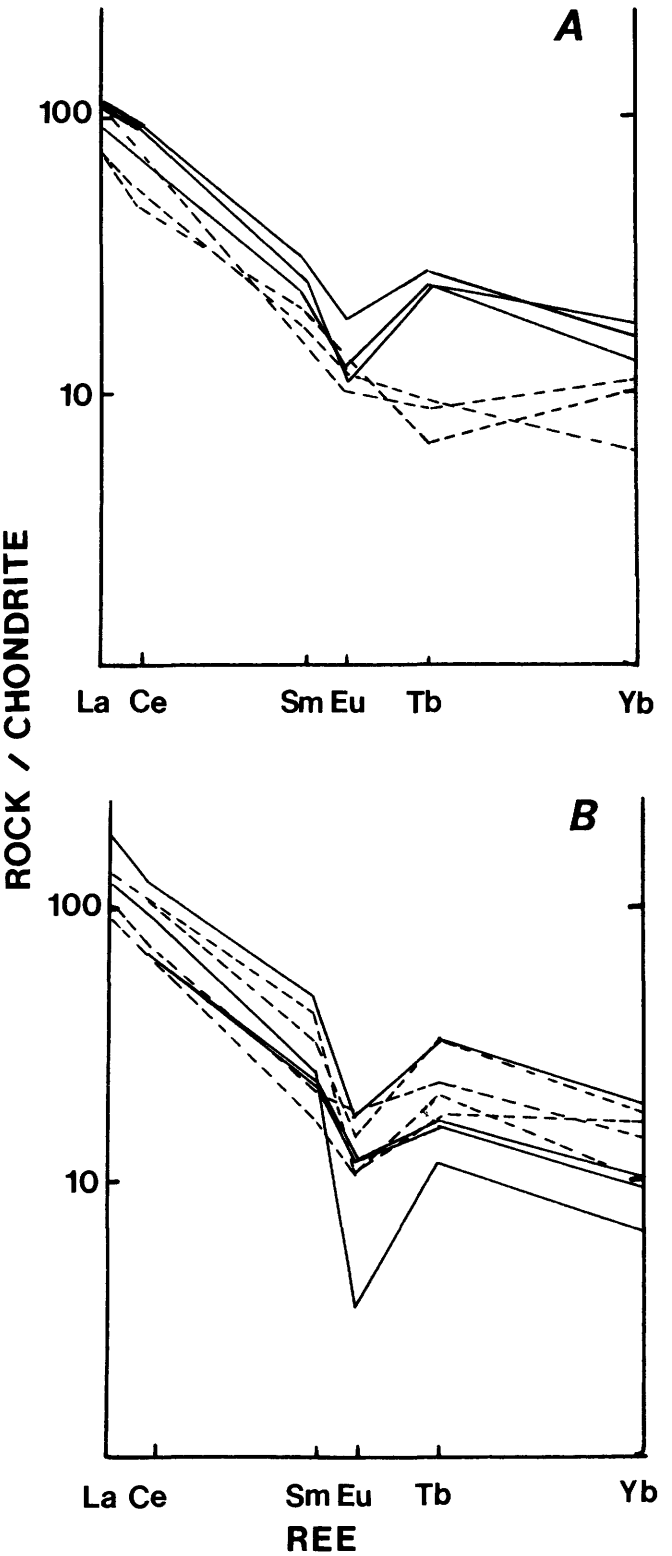

FIGURE 5.4.—Chondrite-normalized rare-earth-element abundances in metamorphic rocks associated with the Bitterroot lobe of the Idaho batholith. Chondrite data from Masuda and others (1973). *A*, Country-rock gneiss (solid lines) and schist (dashed lines). *B*, Prebatholithic migmatite rocks: quartzite and calc-silicate quartzite (solid lines); gneiss (dashed lines).

INFERRED INTRUSIVE AND METAMORPHIC HISTORY

Several deformational and metamorphic episodes prior to batholith emplacement are indicated by the chemical trends, mineralogy, and field relationships of the rocks. The following sequence of intrusion is represented by the field relationships: (1) Tonalite gneiss including plagioclase quartzite; (2) granite gneiss including tonalite gneiss; (3) pegmatite including granite gneiss; and (4) the batholith rocks. A prebatholithic event is indicated by the tonalite and granite gneiss and by evidence for earlier kyanite-grade metamorphism (500 °C and 10–30 km depth) in other rocks. The negative anomalies for Eu in the gneisses indicate derivation from melts depleted in Eu, either from the basement (Albuquerque, 1977; Haskin, 1977) or by anatexis from the enclosing metasedimentary rocks. Original metamorphism of the tonalite and granite gneisses in the migmatite was prior to batholith emplacement, as indicated by crosscutting relationships, and these rocks are distinctly different from the batholithic rocks in their REE trends.

The emplacement of the batholithic tonalites along the northern, western, and southern borders, as early as approximately 90 Ma (table 5.1), caused lit-par-lit intrusion, assimilation, rafting, and contact metamorphism of the country rock to hornblende hornfels facies.

Intrusion of the magma amd metasomatism were the major contributors to migmatization. Partial melting and assimilation of the older metamorphosed units did, however, play some role, producing variable oxide data, high alkali and Al values, and the high $^{87}Sr/^{86}Sr$ values of 0.7196 (table 5.1).

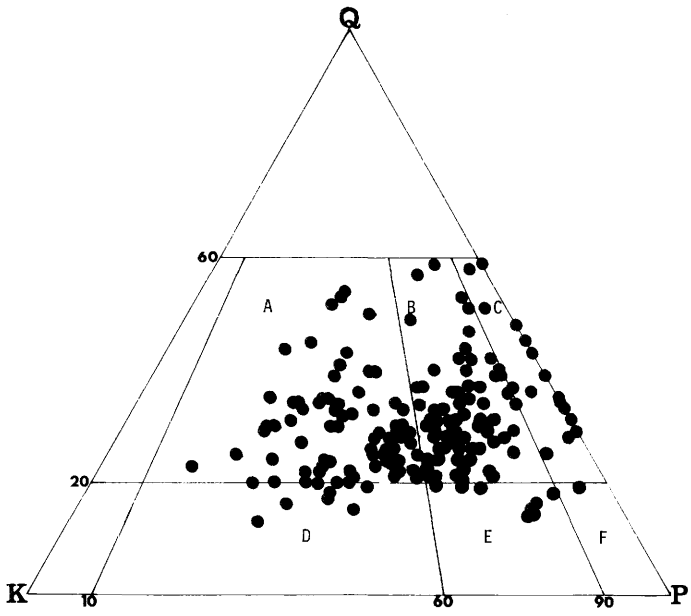

FIGURE 5.5.—Classification of the batholithic rocks of the Bitterroot lobe of the Idaho batholith using Streckeisen and others' (1973) plutonic rock classification. Data from modal analyses. Fields are: A, granite; B, granodiorite; C, tonalite; D, quartz monzonite; E, quartz monzodiorite; F, quartz diorite.

Later intrusions of the batholithic granites and granodiorites included xenoliths of tonalite and migmatized rock as well as the country rock. The rafts and xenoliths became aligned during the upward and eastward flow of the granitic crystalline mush.

Blastomylonitic shearing and annealing strain resulted in sillimanite-muscovite zone recrystallization and a strong axial symmetry within the plutonic, migmatitic, and adjacent country rocks. After solidification and the major metamorphic event, the rocks underwent sericitization and low-temperature alteration and shearing.

STRUCTURE

The western, central, and southern areas can be divided into a western and an eastern structural domain. Lineation in the western domain, which is defined by fold axes and oriented minerals, has a southerly trend and plunges steeply. Foliation mostly strikes northwest to west and dips northward from 10° to 90°, but some strike northeast to east and dip steeply (fig. 5.8).

The eastern structural domain includes most of the Bitterroot lobe and extends southward and westward to the inner western margin of the batholith (fig. 5.8). It is characterized by axial symmetry about a shallowly plunging northwest axis. The rocks generally have a linear fabric, which parallels fold axes, or locally a linear-planar fabric. Lineation trends predominantly west-northwest and has a relatively shallow plunge. Foliation strikes roughly northwest and varies in dip from vertical to horizontal. Eastward toward the Bitterroot front mylonite zone (fig. 5.8), which extends along the east border of the lobe, the fabric of the rock develops into a linear-planar fabric with a strong east to northeast trend. The mylonite zone is bordered on the west by the Bitterroot Mountain front and on the east by the Bitterroot River valley. Lineation in the mylonite zone plunges gently to the southeast and a pervasive, gently dipping planar fabric is present.

The southern border of the lobe lies within the eastern domain and has a strong linear-planar fabric with a suggestion of axial symmetry about a northwest axis (fig. 5.8).

Four separate fold events (F_1 to F_4) are in the western and eastern domains.

The earliest folding (F_1) was prior to intrusion and produced rootless isoclinal and recumbent folds in country rock xenoliths and migmatite. These folds occur locally along the margins of plutons along the western and southern borders and in the northeast corner of the lobe. Dikes intruded along existing axial-plane foliation (S_1).

TABLE 5.5.—*Average chemical and normative-mineral compositions for granitic rocks of the Bitterroot lobe of the Idaho batholith*

[Analyses and norms in weight percent. Areas: C, central; S, southern; W, western; N, northern]

Rock type	Granite			Granodiorite			Quartz diorite		Tonalite		
Sampling area	C	S	W	C	S	W	N	W	N	S	W
Number of samples	12	4	5	11	6	5	2	1	3	7	11
Weight percent											
SiO_2	72.1	69.9	72.6	70.2	70.9	72.8	59.7	65.4	68.8	65.4	65.5
Al_2O_3	15.5	16.2	15.8	15.9	14.9	14.8	18.2	16.1	16.7	16.4	16.5
Fe_2O_3	1.32	1.27	.46	1.43	1.44	.98	1.42	2.27	.36	2.45	2.33
FeO	.16	.62	.53	.15	1.4	1.12	3.85	3.30	2.13	1.09	2.44
MgO	.55	.96	.46	.62	.95	.73	2.98	1.83	1.06	2.55	1.74
CaO	1.98	2.27	1.46	2.19	2.05	1.91	6.21	4.1	4.1	5.0	4.15
Na_2O	4.16	4.34	3.77	4.43	3.60	3.57	3.90	3.75	4.06	3.83	3.77
K_2O	3.38	3.82	4.6	2.95	3.67	3.30	1.37	2.29	1.37	1.97	2.18
TiO_2	.18	.28	.15	.19	.50	.11	.79	.59	.44	.50	.71
P_2O_5	.06	.11	.06	.06	.14	.32	.28	.21	.11	.14	.20
MnO	.02	.02	.02	.02	.03	.02	.10	.06	.02	.05	.06
Total	98.41	99.49	99.91	98.14	99.58	99.66	98.71	99.90	99.15	99.38	98.58
CIPW norms											
Q	28.2	23.7	28.1	26.1	30.2	29.5	12.8	--	28.6	22	24.6
C	1.24	1.11	2.6	.68	1.33						
or	23.1	22.6	28.8	11.3	21.7	20.3	8.12	--	8.1	11.7	11.9
ab	29.7	36.8	31.4	24.8	30.5	26.5	33.0	--	34.3	32.6	33.8
an	7.76	10.4	6.6	8.4	9.29	6.34	28.0	--	19.6	20.2	17.4
en	1.28	2.4	1.2	1.6	2.38	1.71	7.43	--	2.64	6.39	3.58
fs	--	.43	.45	--	.84	.72	4.76	--	2.93	.72	1.6
mt	--	.79	.77	--	1.78	1.39	2.06	--	.52	1.39	2.4
il	.03	.36	.32	.05	.92	.61	1.5	--	.84	.33	.46
ap	.14	.26	.13	.18	.33	.08	.67	--	.27	.33	.46

The second folding (F_2) formed steep concordant structures within plutonic rocks and prebatholithic screens during continued deformation and batholith emplacement. Along the western, southern, and northeastern borders of the lobe, the F_1 folds are refolded by conical and cylindrical folds. These folds developed axial-plane schistosity (S_2) having axes and lineations plunging steeply to the south-southwest, structures characteristic for the western structural domain. Primary folia are steep and concordant with the country-rock contact. Structures of F_2 along the southern border include reclined isoclinal folds and tight folds that plunge more gently to the south-southwest. Granitic plutonism that progressed eastward from the steep western border aligned the country rock parallel to its flow and formed a primary flow foliation. Pegmatites and aplites intruding along F_2 axial planes were synkinematically folded.

A third folding (F_3) was caused by continued flow and deformation. The F_2 structures were folded and the primary east-west foliation was overprinted by a secondary annealing strain fabric, which defines the eastern structural domain. The secondary strain sheared the rocks, thus flattening and annealing feldspar and quartz, and developing lepidoblastic mica and quartz-filled tension fractures. The secondary strain field does not extend north of the Lochsa River nor into the northeast corner of the lobe. The northern border and the southeast extension of the secondary strain outlines the wedge-shaped eastern structural domain (R.R. Reid, oral commun., 1980). North of the western domain, eastward to the Bitterroot River valley and southeast to the southern border, F_3 is the predominant event. The F_2 folds are refolded by open to gentle folds having axes plunging shallowly to the northwest.

Protoclasis accompanied F_3 folding and formed a penetrative foliation that obliterated the primary foliation. Migmatite zones and prebatholithic inclusions also developed a secondary strain fabric, although they retained their primary east-west alignment. Mineral lineations produced by the secondary strain have a shallow plunge to the northwest; the foliation is axially symmetric about this trend. Deformation continued after intrusion

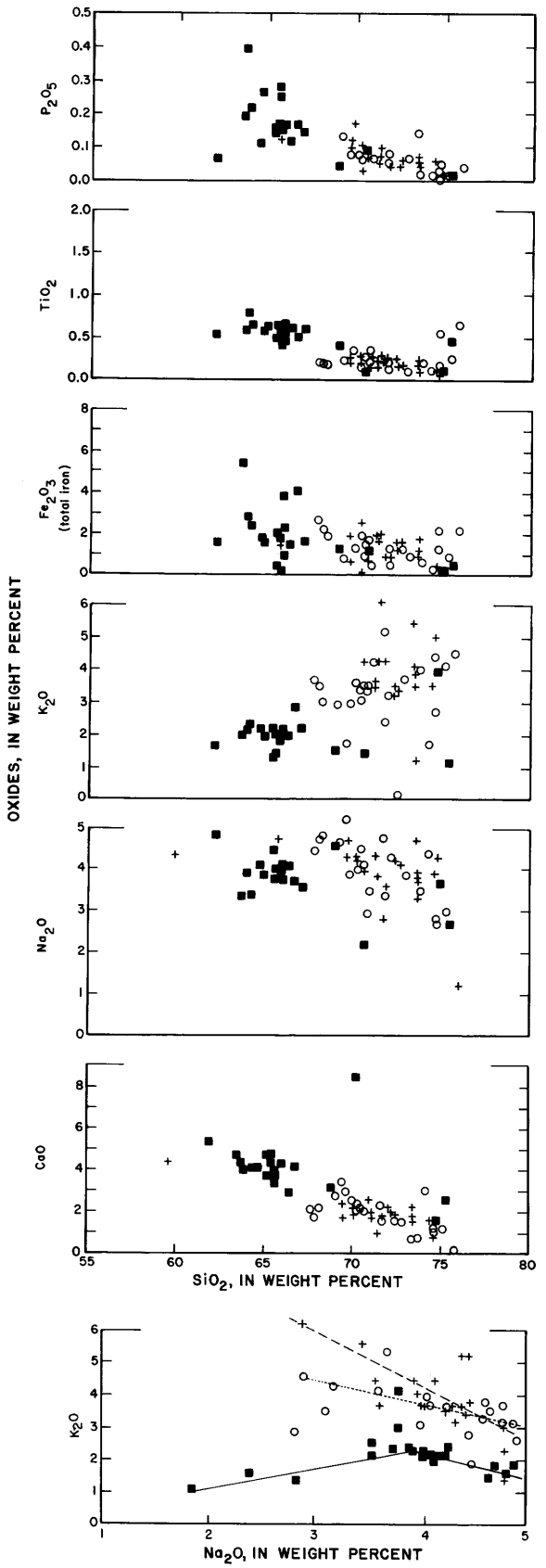

FIGURE 5.6.—Variation diagrams of major oxides in the batholithic granitic rocks of the Bitterroot lobe of the Idaho batholith based on whole-rock chemical data. Filled squares, tonalite; open circles, granodiorite; crosses, granite.

and solidification, as indicated by discordant relationships with plutonic contacts, and resulted in coaxial blastomylonitization and later mylonitization.

The latest folding (F_4) is represented by the gentle warping of the northwest axis about a northeast axis, resulting in linear trends plunging both northwest and southeast.

PREBATHOLITHIC STRUCTURES IN THE WESTERN DOMAIN

RELICT STRUCTURES

The prebatholithic rocks in the western domain are included in the granitic rock as xenoliths and large remnants and have formed large migmatitic screens having westerly trends. The structures in the metasedimentary rocks reflect multiple folding but also include relict sedimentary structures. Among relict structures in the metasedimentary units are orthogonally stretched pebbles, relict bedding defined by differences in grain size and mineral composition, and heavy-mineral concentrations that define crossbed sets. Locally, bedding trends are discordant to the foliation, either because of rotation of blocks or from overprinting of the more stable bedding planes by foliation and schistosity planes.

FOLIATION

The prebatholithic rocks have developed a fabric concordant with the local trend, which strikes variously from northeast through west to northwest and dips steeply (fig. 5.8).

The northeast corner of the Bitterroot lobe structurally resembles the western border zone and therefore reflects the western domain (fig. 5.8). Country-rock inclusions make up more than 30 percent of the total rock. The layering and foliation strike east to northeast and have moderate dips.

LINEATIONS

Rodded quartz grains, stretched biotite, and sillimanite are all aligned with their long dimensions parallel to the F_2 fold axes and define a lineation. This lineation generally plunges steeply to the south (fig. 5.8).

The fold axes in the northeastern corner of the lobe plunge steeply to the southwest; they show evidence of

TABLE 5.6.—*Selected compositional data for granitic rocks of the Bitterroot lobe of the Idaho batholith compared with characteristics of I- and S-type granites*

[Criteria for granite types from Chappell and White (1974). Areas: C, central; S, southern; W, western. HREE, heavy rare earth elements. Sr-isotope ratios from table 5.2. M, muscovite; B, biotite; H, hornblende; A, amphibole; Px, pyroxene; Sp, sphene; Ep, epidote; Gr, garnet; S, sillimanite; Ap, apatite; An, anorthite; Cd, cordierite; Ep, epidote; metased., metasedimentary]

Rock type	Granite			Granodiorite			Tonalite			I-type granite	S-type granite
Sample area	C	S	W	C	S	W	N	S	W		
					Weight percent						
Na_2O	4.2	4.3	3.7	4.4	3.6	3.6	4.1	3.8	3.7	3.2	3.2
K_2O	3.4	3.8	4.6	2.9	3.7	3.3	1.4	1.9	2.2		5 or 2
Al_2O_3/K_2O+Na_2+CaO	1.6	1.6	1.6	1.7	1.6	1.7	1.8	1.5	1.6	1.1	1.1
SiO_2	72	70	73	70	71	73	69	65	66		high
					Norms						
C	1.3	1.1	2.6	1.2	1.7	3.0	1.4	0.7	1.3	1.0	1.0
il	.04	.4	.3	.05	.9	.6	.8	.7	1.0		il
mt	.0	.8	.8	.0	1.8	1.4	.5	1.4	2.4	mt	
en	1.3	2.4	1.2	1.6	2.4	1.7	2.6	6.4	3.6	di	
fs	.0	.4	.4	.0	.8	.7	2.9	.7	1.6		
					Minerals present for HREE concentration						
	M+B Gr	H+B+M	B+M S	B+M+Px Gr+S	B+M+An	B+M	H+B	H+B	B+M	H	B+M Gr+Cd
Accessory minerals	Ap	Ap	Ap Sp	Ap	Ap Ep	Ap Ep	Ap Sp	Ap Sp+Ep	Ap Sp+Ep	Ap Sp	Ap Ep
$^{87}Sr/^{86}Sr$ ratios							0.7103,		0.7196	0.704 .706	0.708
Xenolith types	metased.			metased. H-bearing			metased. H-bearing			H-bearing	metased.

a later folding about a northeast-trending axis. Biotite lineation is not parallel to the prevailing fold-axis direction but plunges steeply to the northwest. This northwest trend may be a reflection of the eastern structural domain.

FOLDS

Three distinct fold sets are well displayed in the migmatite in the western domain and reflect the first three of the fold events discussed earlier. The F_1 folds consist of overturned to recumbent folds, from 0.5 to 5 m wide, and rootless folds showing axial-plane schistosity (S_1).

The F_1 folds were refolded about a south-southwest axis by conical and cylindrical upright to overturned folds (F_2), which have developed axial-plane schistosity. The axial planes, defined by lepidoblastic biotite, muscovite, and sillimanite, have random strike and dips ranging from 50° to vertical; they are commonly invaded by dikes.

The third fold event (F_3), weakly developed on the western margin, is a reflection of the eastern domain overprinting the western. It is indicated by open to gentle parallel and asymmetrical folds which refold F_2 about a northwest-trending axis. The F_3 folds are as wide as 3 m from crest to trough.

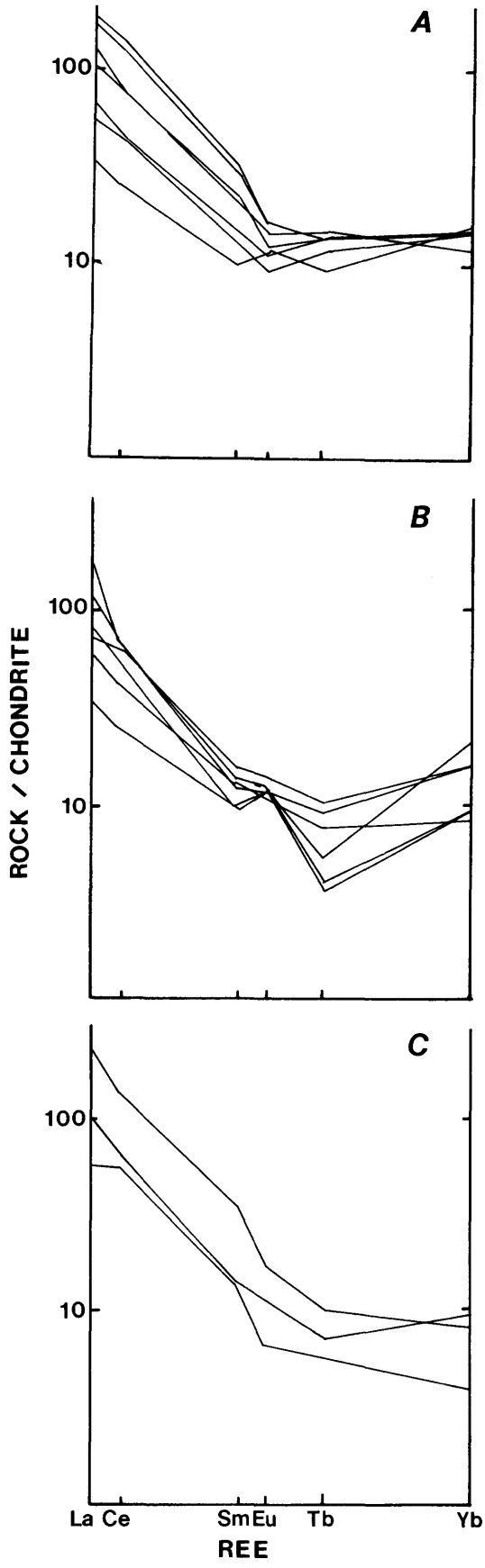

FIGURE 5.7.—Chondrite-normalized rare-earth-element abundances in batholithic rocks of the Bitterroot lobe of the Idaho batholith. Chondrite data from Masuda and others (1973). *A*, Tonalitic rocks. *B*, Granodioritic rocks. *C*, Granitic rocks.

BATHOLITHIC STRUCTURES IN THE WESTERN DOMAIN

Along the western contact zone, the rocks of the batholith show the same northwesterly structural trends as the prebatholithic rocks.

FOLIATION

The igneous rocks range from flow foliated to gneissic. Biotite aligned in the plane of flow defines the foliation, which strikes from northwest through north to northeast and dips moderately (fig. 5.8).

LINEATION

The lineation trends southwesterly, has a shallow to steep plunge (fig. 5.8), and cuts across the foliation. Stretched biotite, elongate feldspar phenocrysts, and sillimanite needles define the lineation; they lie in the plane of maximum extension and are aligned parallel to F_2 fold axes.

PROTOCLASIS

Protoclastic recrystallization and shearing are common throughout the western area. Sillimanite, which is an indicator of the intensity of these effects, lies in the plane of shear and defines a lineation for the protoclastic event. Quartz grains are extended parallel to the lineated sillimanite. Lepidoblastic biotite and muscovite are concentrated along the shear planes.

Subsequent shearing possibly linked to overprinting by the eastern domain has truncated the primary schistosity in the batholithic rocks and has reoriented fold axes and rodded grains to the northwest (az 300°–330°) in the migmatitic terrain.

The principal ductile shear planes were later crosscut by northeast-trending shears, which granulated the batholithic rocks. These shears are only 1 cm wide and cut the protoclastic fabric and the pegmatites. Subgrains of feldspar and strained quartz and semialigned secondary sericite and muscovite have developed along these narrow shears.

FOLDS

Large, open, cylindrical F_2 folds affect both the prebatholithic and batholithic rocks. The folds plunge to the southwest (az 250°) and southeast (az 150°).

DIKES

Pegmatite and aplite have intruded primary joints, foliation surfaces, and shear surfaces. Poles to the pegmatite dikes have a crude axial symmetry like that of the poles to the foliations (S_2).

PREBATHOLITHIC STRUCTURES IN THE EASTERN DOMAIN

Prebatholithic rocks in the eastern domain have not retained relict sedimentary structures nor depositional fabric. The rocks are present as xenoliths and remnants and in rare migmatite zones. The inclusions trend predominantly eastward through the central part of the domain, but are at various orientations along the southern border. The fabric of the included rock is axially symmetric about a shallow northwest-trending axis (az 297°, plunge 36°).

Along the southern border of the Bitterroot lobe is a migmatitic contact zone formed by screens of metasedimentary rock and tonalite gneiss separated by concordant sheets of granodiorite and granite. The migmatite screens have been truncated on the south-southwest by Eocene granitic intrusions.

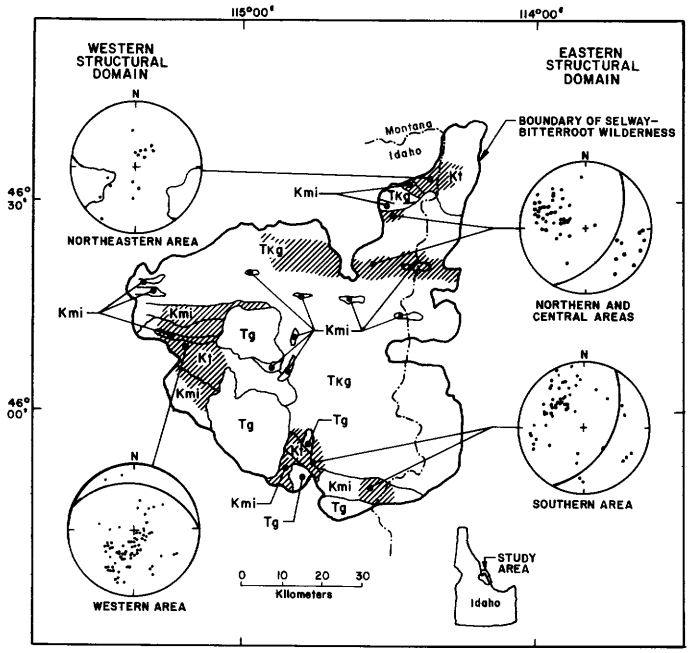

FIGURE 5.8.—Stereonet plots of structural data from areas assigned to the western and eastern structural domains of the Bitterroot lobe of the Idaho batholith. Plots are on the lower hemispheres of the Wulff stereonet. Dots are lineations and fold axes; great circles are derived from poles to foliation (girdle from scattered poles in northeastern area). Rock units: Tg; Tertiary granite; TKg, Late Cretaceous and early Tertiary granite and granodiorite; Kt, Cretaceous tonalite; Kmi, Cretaceous migmatite.

Xenoliths and remnants of prebatholithic rock in the central area trend east-west. They range from 1 m to 3 km in length, and rotated blocks are locally present.

FOLIATION

Rotation of xenoliths during emplacement has resulted in foliation and schistosity that are not everywhere concordant with the prevailing trend of the inclusions. The initial flow and rotation were followed by protoclasis, which developed a penetrative foliation that strikes from northwest through north to northeast and dips shallowly to steeply (fig. 5.8).

LINEATION

Biotite lineation along the foliation planes plunges gently to the northwest (az 270° to 305°; fig. 5.8). Elongate feldspar grains commonly are spindled and have been rotated clockwise or counterclockwise to become perpendicular to the lineation.

FOLDING

In the migmatitic rocks of the eastern domain the predominant folds represent the F_2, F_3, and F_4 events.

The F_2 folds are identified by fold axes plunging variously to the southwest and northeast. Near the southern border a quartzite schistosity has been recumbently folded about a shallow southwest-trending axis. An axial-plane schistosity formed by lepidoblastic biotite and muscovite (S_2) has developed. In the central area, F_2 folds are symmetric to isoclinal and have axes plunging moderately to the southwest.

The F_3 folds are generally open cylindrical and conical folds with axes plunging shallowly to the northwest and southeast. Small symmetric and ptygmatic parasitic and flow folds have formed in the inclusions and in the granitic rocks. These folds were formed during the same refolding event and have axes which also plunge shallowly to the northwest and southeast. The varying directions of rotation and symmetry shown by the folds indicate formation in an environment of flattening or pure shear.

Uplift and doming during F_4 have refolded F_2 and F_3 about a northeast-trending axis.

BATHOLITHIC STRUCTURES IN THE EASTERN DOMAIN

A single structural pattern of axial symmetry about a lineation plunging shallowly to the northwest characterizes the batholithic rocks in the eastern domain.

FOLIATION

Shearing that represents the F_3 event has produced a nonplanar foliation, which overprints a weak primary foliation at a small angle. The primary foliation is defined by aligned biotite and undeformed feldspar crystals having normal zonation. An alignment of xenoliths and migmatitic zones in the east-west direction suggests that that was the primary flow direction.

The flow structure of the secondary strain event is characterized by protoclastic texture resulting from solid-state flow and recrystallization. The flow structure becomes better developed and more pervasive eastward to the mylonite zone. Poles to the shear planes are concentrated in a broad girdle that strikes northeast and dips moderately to the southeast (fig. 5.8).

LINEATION

Preferred orientations of stretched lepidoblastic biotite and rodded quartz grains, both parallel to the direction of shear, define a linear fabric trending northwest (fig. 5.8). Phenocrysts of feldspar form elongate clumps along the strike of the foliations; in the plane of shear they have been rotated clockwise and counterclockwise to positions perpendicular to the lineation. Crenulation and fold axes parallel the predominant linear trend.

FOLDS

Folds in the gneiss and migmatite correspond to the F_3 and F_4 events. The F_3 folds are large, similar, reclined isoclinal to tight folds and have axes plunging shallowly to the southwest. Parasitic and shear folds that formed during the F_3 event developed an axial-plane schistosity, which cuts the F_2 schistosity. Later doming (F_4) refolded the lineations and fold axes about a northeast-trending axis. The refolding has produced a second concentration of lineations trending southeast at az 110°.

BLASTOMYLONITIZATION

Axial deformation continued beyond protoclasis to produce blastomylonitic shears. The shears are nonpenetrative and have biotite covering the shear planes. These biotite-coated shears, which cut the secondary penetrative schistosity, strike predominantly east-west and have moderate dips. The preferred orientation of biotite on the shear surfaces defines a lineation plunging to the northwest or southeast. The shear planes decrease in dip and become more concentrated in the mylonite front eastward from the Bitterroot crest.

MYLONITIZATION

The mylonite zone trends north-south along the Bitterroot front (fig. 5.8). The rock grades from a mylonite gneiss to a protomylonite-mylonite interlayered with sheets of ultramylonite that contain pseudotachylyte. The ultramylonite sheets are 12 to 14 cm wide and have porphyroclasts as much as 1 cm long. As the intensity of shearing increased, prominent planes of relative movement formed. Smeared-out grains of chlorite and mica are parallel to striations on the shear surface.

DIKE INTRUSION

Pegmatite and aplite dikes invaded fractures during the late stages of cooling before the imposition of secondary strain. The dikes have been cut and offset by the penetrative secondary shear event. Secondary shear folds (F_3) also formed during rotation of the dikes into parallelism with the foliation. Dikes synkinematic with the penetrative deformation intruded along the schistosity as veins and sheets and were subsequently deformed.

SUMMARY OF DEFORMATIONAL EVENTS

The events in the structural history of the Bitterroot lobe can be grouped into five stages of deformation.

(1) Kyanite-zone metamorphism and folding of the country rock before intrusion of the batholith.

(2) Injection of the batholithic tonalite to granodiorite, followed by pulses of the main-phase granite and granodiorite; steep concordant flow foliations and lineations along the western border and shallow flow foliations and lineations in the central, eastern, and southern areas of the lobe; migmatite screens and xenoliths oriented in east-west alignment and conical and cylindrical folding that refolded F_1 around a southwest-trending axis; hornblende hornfels contact metamorphism.

(3) Development of a secondary annealing strain fabric at the sillimanite-muscovite facies of metamorphism; overprinting by the secondary fabric of the primary foliation of stage 2; formation of shallow axial-symmetric fabrics and refolding of F_2 about a shallow northwest axis by open gentle cylindrical folds.

(4) Blastomylonitic shearing and intense mylonitization after crystallization of the batholith; formation of the eastern-front mylonite zone defined by bands of mylonite, ultramylonite, and pseudotachylyte that have varied strikes and lineations plunging shallowly to the southeast.

(5) Refolding of F_3 and of the lineations of stages 3 and 4 by faulting and arching of the eastern batholith.

CONCLUSIONS

Significant deformation and metamorphism occurred in the area before the batholith was intruded. The structural setting at the time included thrust blocks that were east directed and strike-slip faults and lineaments that trended northwest. Plutonism occurring at about 90 Ma invaded the country rocks and thrust blocks in a lit-par-lit manner. The plutonism was accompanied by deformation and migmatization, and it resulted in high-grade metamorphism of the kyanite zone. Assimilation of the country rock or an anatectic origin for the magma may account for the high $^{87}Sr/^{86}Sr$ ratios (0.7103 to 0.7196) in the tonalite gneisses and their similarity to those of the country rock. The similar REE patterns in country rock and tonalite gneiss may support an anatectic origin for the migmatitic rocks.

Major structural amd metamorphic events accompanied batholithic intrusion of the Bitterroot lobe. Emplacement of the lobe was by lower crustal melting and thrusting. The shape of the lobe, elongate in a west-northwest direction, suggests emplacement along a major lineament of that trend. Yates (1968) and Taubeneck and Armstrong (1974) have inferred the existence of a northwest-trending transform, the trans-Idaho discontinuity, in the vicinity of the lobe. Such a preexisting transform would have provided a pathway in the crustal rocks for the ascending melt.

The major plutonism that produced the lobe occurred during the mid-Sevier orogenic period. The magma intruded the country rock lit-par-lit and in the cores of folds, and locally intrusion was forceful enough to break up the wall rock. Blocks and screens of country rock were incorporated and aligned parallel to the flow direction of the intruding material. The west to northwest alignment of the migmatized country rock could represent the primary flow direction of the intruding magma. Some of the screens may represent dividers between separate plutonic intrusions. Plutonism continued through the Late Cretaceous into early Tertiary. Chemical analyses suggest a lower crustal "S-type" paragenesis which would support melting in the lower crust.

Migmatite zones formed around the periphery of the lobe and sparsely within its interior. The last plutonic phases of the batholith incorporated early batholithic phases and migmatized material. Complex zones were formed by intrusion and assimilation of prebatholithic metasedimentary rocks and orthogneiss by the final phases of batholithic plutonism. The screens and blocks are concentrated mostly at higher elevations, capping ridges and peaks. In the western and southern areas, zones of migmatization are at lower elevations and have a more assimilated appearance. The high concentration of migmatized rock at lower elevations in the western and southern areas may represent exposures at greater depth within the batholith, near the basal contact. The sparsely concentrated migmatite zones in the batholith interior may have resulted from breaking up, stoping, or rafting of the roof rocks into ascending magma. Wall-rock and plutonic fabrics indicate an initially steep flow and a folding about a southwest-trending axis during the intrusion of the batholith.

Deformation continued through the late stages of batholith emplacement and afterward. During the final stages of plutonism a penetrative axial-symmetric annealing strain fabric overprinted the plutonic primary foliations and migmatite schistosities. Continued plutonism and protoclasis of the cooling magma against an unyielding roof may have caused development of strain. Other possible causes are crustal extension, perhaps the driving force in the Cenozoic development of the west coast metamorphic core complexes (Coney, 1980), and renewed low-angle faulting and movement along the proposed trans-Idaho transform.

Axial-symmetric deformation developed blastomylonitic shear zones after crystallization of the batholith. The strain regime remained in effect after protoclasis and produced nonpenetrative biotite-covered shears subparallel to the secondary foliation. The blastomylonitic shearing granulated and recrystallized the rock. On the eastern front of the Bitterroot Range the protoclastic fabric and blastomylonitic shears are cut by a third zone of cataclasis, the eastern front mylonite zone, which is characterized by bands of mylonite, ultramylonite, and pseudotachylyte. Shear lineations in the zone plunge shallowly to the southeast. Recent work by Garmezy (1983) and by Chase and others (1983) has suggested that the cause of mylonitization was an Eocene (45.5 Ma) episode of extension and domal uplift along a fault parallel to the Bitterroot River valley. The principal direction of extension was in a southeast (az 110°) direction (Garmezy, 1983). The episode of doming refolded the F_3 structures and the lineations of deformation stages 3 and 4.

REFERENCES CITED

Albuquerque, C.A.R. de, 1977, Geochemistry of the tonalitic and granitic rocks of the Nova Scotia southern plutons: Geochimica et Cosmochimica Acta, v. 41, p. 1-13.

Allen, C.C., 1980, Petrologic and chemical study of a portion of the northeastern border zone of the Idaho batholith, east-central Idaho: Williamstown, Mass., Williams College, independent study, 43 p.

Anderson, A.L., 1952, Multiple emplacement of the Idaho batholith: Journal of Geology, v. 60, p. 255-265.

Armstrong, R.L., 1974, Magmatism, orogenic timing, and orogenic diachronism in the cordillera from Mexico to Canada: Nature, v. 247, p. 348-351.

——— 1975, Precambrian (1500 m.y. old) rocks of central Idaho—the Salmon River arch and its role in cordilleran sedimentation and tec-

tronics: American Journal of Science, v. 275A, p. 437-467.
_____ 1976, Geochronometry of the Idaho batholith and nearby rocks [abs.]: Geological Society of America Abstracts with Programs, v. 8, no. 3, p. 350-351.
Armstrong, R.L., Taubeneck, W.H., and Hales, P.O., 1977, Rb-Sr and K-Ar geochronometry of Mesozoic granite rocks and their Sr isotopic composition, Oregon, Washington and Idaho: Geological Society of America Bulletin, v. 88, p. 397-411.
Arth, J.G., and Hanson, G.N., 1972, Quartz diorites derived by partial melting of eclogite or amphibolite at mantle depths: Contributions to Mineralogy and Petrology, v. 37, p. 161-174.
Bence, A.E., and Albee, A.L., 1968, Empirical correction factors for the electron microanalysis of silicates and oxides: Journal of Geology, v. 76, p. 382-403.
Bradley, M.D., 1981, Geology of northeastern Selway-Bitterroot Wilderness Area, Idaho and Montana: Moscow, Idaho, University of Idaho, Masters thesis, 51 p.
Chappell, B.W., and White, A.J.R., 1974, Two contrasting granite types: Pacific Geology, v. 8, p. 173-174.
Chase, R.B., 1968, Petrology of the northeast contact zone of the Idaho batholith, northern Bitterroot Range, Montana: Missoula, Montana, University of Montana, Ph.D. dissertation, 158 p.
Chase, R.B., Bickford, M.E., and Arruda, E.C., 1983, Tectonic implications of Tertiary intrusion and shearing within the Bitterroot dome, northeastern Idaho batholith: Journal of Geology, v. 91, p. 462-470.
Chase, R.B., Bickford, M.E., and Tripp, S.E., 1978, Rb-Sr and Pb-Pb isotopic studies of the northeastern Idaho batholith and border zone: Geological Society of America Bulletin, v. 89, p. 1325-1334.
Coney, P.J., 1972, Cordilleran tectonics and North America plate motion: American Journal of Science, v. 272, p. 603-628.
_____ 1980, Cordilleran metamorphic core complexes: an overview: Geological Society of America Memoir 153, p. 7-31.
_____ 1981, Accretionary tectonics in western North America, *in* Dickinson, W.R., and Payne, W.D., eds., Relations of tectonics to ore deposits in the southern cordillera: Arizona Geological Society Digest, v. 14, p. 23-39.
Cox, K.G., Bell, J.D., and Pankhurst, R.J., 1979, The interpretation of igneous rocks: London, George Allen and Unwin, 445 p.
Davis, G.H., 1975, Gravity-induced folding of a gneiss dome complex, Rincon Mountains, Arizona: Geological Society of America Bulletin, v. 86, p. 979-990.
Drewes, Harald, 1978, The cordilleran orogenic belt between Nevada and Chihuahua: Geological Society of America Bulletin, v. 89, p. 641-657.
Ferguson, J.A., 1975, Tectonic implications of some geochronometric data from the northeastern border zone of the Idaho batholith: Northwest Geology, v. 4, p. 53-58.
Garmezy, Lawrence, 1983, Mylonitization coincident with uplift in an extensional setting, Bitterroot Range, Montana-Idaho [abs.]: Geological Society of America Abstracts with Programs, v. 15, no. 6, p. 578.
Greenwood, W.R., and Morrison, D.A., 1973, Reconnaissance geology of the Selway-Bitterroot Wilderness Area: Idaho Bureau of Mines and Geology Pamphlet 154, 30 p.
Hamilton, Warren, 1969, The volcanic central Andes—a modern model for the Cretaceous batholiths and tectonics of western North America, *in* Proceedings of the Andesite Conference: Oregon Department of Geology and Mineral Industries Bulletin, 65, p. 175-184.
Hamilton, Warren, and Meyers, W.B., 1967, The nature of batholiths: U. S. Geological Survey Professional Paper 554-C, p. C1-C30.
Hanson, G.N., 1978, The application of trace elements to the petrogenesis of igneous rocks of granitic composition: Earth and Planetary Science Letters, v. 38, p. 26-43.
Harrison, J.E., 1972, Precambrian Belt basin of Northwestern United States: its geometry, sedimentation, and copper occurrences: Geological Society of America Bulletin, v. 83, p. 1215-1240.
Harrison, J.E., and Campbell, A.B., 1963, Correlations and problems in Belt Series stratigraphy, northern Idaho and western Montana: Geological Society of America Bulletin, v. 74, p. 1413-P1427.
Haskin, L.A., 1977, On rare-earth element behavior in igneous rocks, *in* Ahrens, L.H., ed., Origin and distribution of the elements: New York, Pergamon Press, p. 175-189.
Hietanen, Anna, 1960, Superposed deformations northwest of the Idaho batholith: International Geological Congress, 21st, Copenhagen, Proceedings, v. 26, p. 87-102.
_____ 1961, Relation between deformation, metamorphism, metasomatism, and intrusion along the northwest border zone of the Idaho batholith, Idaho: U.S. Geological Survey Professional Paper 424-D, p. D161-D164.
_____ 1962, Metasomatic metamorphism in western Clearwater County, Idaho: U.S. Geological Survey Professional Paper 344-A, p. A1-A116.
_____ 1963a, Idaho batholith near Pierce and Bungalow, Clearwater County, Idaho: U.S. Geological Survey Professional Paper 344-D, p. D1-D42.
_____ 1963b, Metamorphism of the Belt Series in the Elk River-Clarkia area, Idaho: U.S. Geological Survey Professional Paper 344-C, p. C1-C49.
_____ 1968, Belt Series in the region around Snow Peak and Mallard Peak, Idaho: U.S. Geological Survey Professional Paper 344-E, p. E1-E34.
Hobbs, S.W., Griggs, A.B., Wallace, R.E., and Campbell, A.B., 1965, Geology of the Coeur d'Alene district, Shoshone County, Idaho: U.S. Geological Survey Professional Paper 478, 139 p.
Hyndman, D.W., 1980, Bitterroot dome-Sapphire tectonic block, *in* Cordilleran metamorphic core complexes: Geological Society of America Memoir 153, p. 427-444.
Hyndman, D.W., and Williams, L.D., 1977, The Bitterroot lobe of the Idaho batholith: Northwest Geology, V. 6, p. 1-16.
Johnson, B.R., 1975, Migmatites along the northern border of the Idaho batholith: Missoula, Montana, University of Montana, Ph.D. dissertation, 120 p.
Kell, R.E., and Chase, R.B., 1976, Multiphase deformation and polymetamorphism along the north-central border zone of the Idaho batholith, Kelly Fork district, Clearwater County, Idaho [abs.]: Geological Society of America Abstracts with Programs, v. 8, no. 4, p. 485-486.
Leischner, L.M., 1959, Border-zone petrology of the Idaho batholith in vicinity of Lolo Hot Springs, Montana [abs.]: Geological Society of America Bulletin, v. 70, p. 1782.
Lindgren, Waldemar, 1904, A geological reconnaissance across the Bitterroot Range and Clearwater Mountains in Montana and Idaho: U.S. Geological Survey Professional Paper 27, 123 p.
Masuda, Akimasa, Nakamura, Noboru, and Tanaka, Tsuyoshi, 1973, Fine structures of mutually normalized rare-earth patterns of chondrites: Geochimica et Cosmochimica Acta, v. 37, p. 239-248.
Morrison, D.A., 1968, Reconnaissance geology of the Lochsa area, Idaho County, Idaho: Moscow, Idaho, University of Idaho, Ph.D. dissertation, 126 p.
Nold, J.L., 1968, Geology of the northeastern border zone of the Idaho batholith, Montana and Idaho: Missoula, Montana, University of Montana, Ph.D. dissertation, 159 p.
Reid, R.R., 1959, Reconnaissance geology of the Elk City region, Idaho: Idaho Bureau of Mines and Geology Pamphlet 120, 74 p.
Reid, R.R., Bittner, Enid, Greenwood, W.R., Ludington, Steve, Lund, Karen, Motzer, W.E., and Toth, Margo, 1979, Geologic section and road log across the Idaho batholith: Idaho Bureau of Mines and Geology, Information Circular 34, 20 p.
_____ 1980, U.S. Geological Survey Selway-Bitterroot Mineral Evaluation Study: U.S. Geological Survey Open-File Report.

Reid, R.R., and Greenwood, W.R., 1968, Multiple deformation and associated progressive polymetamorphism in the Beltian rocks north of the Idaho batholith, Idaho, U.S.A.: International Geological Congress, 23rd, Prague, Proceedings, v. 4, p. 75-87.

Reid, R.R., Morrison, D.A., and Greenwood, W.R., 1973, The Clearwater orogenic zone: a relict of Proterozoic orogeny in central and northern Idaho: Idaho Bureau of Mines Belt Symposium 1973, v. 1, p. 10-56.

Reid, R.R., Greenwood, W.R., Nord, G.L., 1981, Metamorphic petrology and structure of the St. Joe area, Idaho: Geological Society of America Bulletin, pt. II, v. 92, p. 94-205.

Roberts, R.J., 1972, Evolution of the cordilleran fold belt: Geological Society of America Bulletin, v. 83 p. 1989-2003.

Ross, C.P., 1928, Mesozoic and Tertiary granitic rocks in Idaho: Journal of Geology, v. 36, p. 673-693.

_____ 1963a, Modal composition of the Idaho batholith: U.S. Geological Survey Professional Paper 475-C, p. C86-C90.

_____ 1963b, The Belt series in Montana: U.S. Geological Survey Professional Paper 346, 122 p.

_____ 1965, Idaho batholith [abs.]: Geological Society of America Special Paper 82, p. 343.

Streckeisen, A.L., and others, 1973, Plutonic rocks: classification and nomenclature recommended by the IUGS Subcommission on the Systematics of Igneous Rocks: Geotimes, v. 18, no. 10, p. 26-30.

Taubeneck, W.H., and Armstrong, R.L., 1974, The trans-Idaho discontinuity viewed as a transform fault [abs.]: Geological Society of America Abstracts with Programs, v. 6, no. 5, p. 478.

Toth, M.I., 1982, Reconnaissance geologic map of the Selway-Bitterroot Wilderness, Idaho County, Idaho, and Missoula and Ravalli Counties, Montana: U. S. Geological Survey Miscellaneous Field Studies Map MF-1495-B, scale 1:125,000.

Tripp, S.E., and Chase, R.B., 1976, Rb/Sr and U/Pb geochronology of the northeastern border of the Idaho batholith, Bitterroot Range, Montana [abs.]: Geological Society of America Abstracts with Programs, v. 8, no. 4, p. 514-515.

Turner, F.J., 1981, Metamorphic petrology; mineralogical, field, and tectonic aspects (2nd ed.): New York, McGraw-Hill, 524 p.

Wehrenberg, J.P., 1968, Structural development of the northern Bitterroot Range, western Montana [abs.]: Geological Society of America Special Paper 115, 456 p.

White, A.J.R., and Chappell, B.W., 1977, Ultrametamorphism and granitoid genesis: Tectonophysics, v. 43, p. 7-22.

Williams, L.D., 1977, Petrology and petrography of a section across the Bitterroot lobe of the Idaho batholith: Missoula, Montana, University of Montana, Ph.D. dissertation, 189 p.

_____ 1979, General geology of a section across the Bitterroot lobe of the Idaho batholith: Northwest Geology, v. 8, p. 29-39.

Wiswall, C.G., 1979, The structure and petrography below the Bitterroot dome, Idaho batholith, near Paradise, Idaho: Missoula, Montana, University of Montana, Ph.D. dissertation, 129 p.

Wyllie, P.J., Huang, W.L., Stern, C. R., and Maaloe, Sven, 1976, Granitic magmas: possible and impossible sources, water contents, and crystallization sequences: Canadian Journal of Earth Sciences, v. 13, p. 1007-1019.

Yates, R.G., 1968, The trans-Idaho discontinuity: International Geological Congress, 23rd, Prague, Proceedings, v. 1, p. 117-123.

6. PETROGENESIS, GEOCHRONOLOGY, AND HYDROTHERMAL SYSTEMS OF THE NORTHERN IDAHO BATHOLITH AND ADJACENT AREAS BASED ON $^{18}O/^{16}O$, D/H, $^{87}Sr/^{86}Sr$, K-Ar, AND $^{40}Ar/^{39}Ar$ STUDIES

By Robert E. Criss and Robert J. Fleck

ABSTRACT

Geochemical, geological, and geochronological variations among the granitoid rocks of north-central Idaho and adjacent areas indicate that the region is composed of two essentially different terranes. Jurassic and Cretaceous plutons intrude Permian to Jurassic volcanic and sedimentary rocks of the Wallowa-Seven Devils terrane, a province devoid of Precambrian rocks that probably represents an accreted island-arc complex. These Jurassic and Cretaceous plutons are distinguished by low initial $^{87}Sr/^{86}Sr$ ratios (r_i) of 0.7030 to 0.7042, Rb/Sr ratios less than 0.08, $\delta^{18}O$ values of +5.5 to +10.5 per mil, and δD values of −41 to −82 per mil, all of which are compatible with derivation, at least in part, from mantle materials. These rocks are separated from the main mass of the Idaho batholith by a 5- to 25-km-wide suture zone containing deformed, Late Cretaceous transition zone plutons. Steep gradients in r_i, $\delta^{18}O$, δD, and major element concentrations of the plutons occur across this zone and reflect the contrasting characteristics of the bordering source regions. The main mass or Bitterroot lobe of the northern Idaho batholith intrudes the Belt-Yellowjacket terrane, which contains abundant Precambrian rocks. These granitic plutons can be divided into a Cretaceous-early Tertiary main-phase suite and an Eocene epizonal suite. The main-phase plutons have high r_i values of $\geq$0.708, Rb/Sr ratios of 0.04 to 0.24, and high primary $\delta^{18}O$ values of +8.0 to +12.4 per mil. These magmas apparently were derived primarily from Precambrian lower crust, but they also display evidence of substantial assimilation of Precambrian wall rock. The Eocene epizonal plutons all have r_i values $\geq$0.704 (mean value of 0.7088), suggesting the presence of an ancient component, but several values between 0.704 and 0.708 indicate minimal wall-rock involvement. The Rb/Sr ratios of these plutons are very large (as much as 49.0), probably due to differentiation.

Extensive hydrothermal circulation systems developed during the emplacement of both the Cretaceous-early Tertiary plutons and the Eocene plutons. Belt Supergroup (Wallace Formation) metasedimentary rocks around the northern Idaho batholith show a progressive decrease from $\delta^{18}O \cong +15 \pm 1$ per mil in low-grade metamorphic zones more than 60 km from mapped pluton contacts to $\delta^{18}O \cong +11.5 \pm 1$ per mil in the highest grade metamorphic zones (sillimanite ± kyanite) adjacent to the batholith. These data reflect large-scale and deep circulation of high-$\delta^{18}O$ metamorphic-hydrothermal fluids during Cretaceous-early Tertiary time. In contrast, meteoric-hydrothermal interactions involving heated, low-δD, low-$\delta^{18}O$ fluids occurred around the Eocene epizonal plutons and caused large reductions in δD values (−120 to −148 per mil) over an approximately 7,000-km^2 area of the Bitterroot lobe. Major $\delta^{18}O$ depletions (as low as −0.3 per mil) of the rocks occur only in restricted areas, however, indicating that the overall water/rock ratios were not very large. Most ore deposits occur near the perimeter of the Bitterroot lobe and therefore are probably related to the hydrothermal systems established during emplacement of the main batholith mass rather than to the Eocene meteoric-hydrothermal systems, in marked contrast to relations in the southern Idaho batholith. Although the whole-rock Rb-Sr isochron systematics of the Cretaceous-early Tertiary plutons and particularly the Eocene plutons were relatively unaffected by the hydrothermal systems, the metamorphic-hydrothermal activity appears to have significantly altered the isochrons of Precambrian Belt metasedimentary rocks.

K-Ar ages of hornblende range from $\geq$160 Ma for some Jurassic plutons in the Wallowa-Seven Devils terrane to less than 51 Ma for Eocene granitic rocks in the Bitteroot lobe. Some low-r_i plutons in the Wallowa-Seven Devils terrane have concordant hornblende and biotite K-Ar ages of 135 Ma and show no geochemical indication of proximity to the Precambrian craton. These data, together with K-Ar ages of 87 to 75 Ma for transition zone plutons, indicate that the tectonic suture between the Wallowa-Seven Devils terrane and the Belt-Yellowjacket terrane formed between 135 and 75 Ma, and probably between 95 and 80 Ma. Most of the Bitterroot lobe was emplaced after this probable accretionary event. However, the K-Ar apparent ages of biotite and hornblende become systematically younger toward the east-central part of the Bitterroot lobe, where biotite data define a 10,000-km^2 area where apparent ages range from 51 to 44 Ma. The relations are thought to reflect temporal migration of magmatism as well as rapid uplift and cooling of the region.

INTRODUCTION

Stable- and radiogenic-isotope studies have contributed much new knowledge to the geology of the Idaho batholith. K-Ar studies by McDowell and Kulp (1969), Armstrong (1974), Armstrong and others (1977), and Criss and others (1982) helped establish the regional importance of Tertiary plutonism and placed constraints on the emplacement age and uplift history of the batholith. Sr-isotope data of Armstrong and others (1977), Chase and others (1978), and Fleck and Criss (1985) also constrained age relations, helped identify the source materials from which the batholith was made, and were used to map a fundamental terrane boundary that coincides with the edge of

the Precambrian continental crust in the Pacific Northwest. U-Pb studies by Reid and others (1970, 1973), Grauert and Hofmann (1973), and Bickford and others (1981) provided some information on the emplacement ages of the plutons and presented unequivocal evidence that a significant Precambrian component is present in most of them. The hydrogen- and oxygen-isotope data of Taylor and Magaritz (1978) and Criss and Taylor (1983) demonstrated the importance of Tertiary hydrothermal metamorphism in the batholith and were used to map individual hydrothermal systems and to relate those systems to ore deposits.

This paper presents considerable new $\delta^{18}O$, δD, $^{87}Sr/^{86}Sr$, K-Ar, $^{40}Ar/^{39}Ar$, and chemical data from northern Idaho and adjacent areas. We attempt to summarize the salient results of pertinent previous investigations, provide more detailed maps of isotopic variations in the batholith, and augment present understanding of regional geologic relations. Data tabulated in this paper include results presented graphically in a companion study by Fleck and Criss (1985).

ACKNOWLEDGMENTS

We thank J.F. Sutter, M.A. Lanphere, H.P. Taylor, T.L. Vallier, and J.R. O'Neil for discussion and criticism, and W.R. Greenwood for providing assistance and invaluable information in the field. Elliot Kollman and Anne Tapay assisted in Rb-Sr analyses. Jarel Von Essen, James Saburomaru, Suzanne Makita, and Elliot Kollman performed argon analyses and assisted in sample preparation. Potassium analyses were made by Paul Klock, Sarah Neil, and David Vivit.

GEOLOGIC SETTING

The Idaho batholith includes granitic plutons intruded into Precambrian crystalline and metasedimentary rocks. However, a contiguous but geologically distinct group of plutons west of the main batholithic mass is in a region entirely devoid of Precambrian rocks. In this report we will use the terms "plutons of the Bitterroot lobe" to refer to the northern part of the Idaho batholith where Precambrian-hosted plutons occur, the "Jurassic and Cretaceous plutons in the Wallowa-Seven Devils terrane" (WSD) to refer to the distinct group of plutons in the accreted terrane west of the Bitterroot lobe, and "plutons of north-central Idaho" to refer to both groups of plutons in a general sense. The term "transition zone plutons" is used to refer to a distinct group of geochemically variable, Late Cretaceous granitoids that occur only within and near the boundary between the WSD and Belt-Yellowjacket terranes.

The Bitterroot lobe underlies a nearly 15,000-km^2 area of north-central Idaho and adjacent parts of Montana (fig. 6.1). The plutons of the Bitterroot lobe can be divided into a Cretaceous-early Tertiary main-phase group and an Eocene epizonal group (Greenwood and Morrison, 1973; Hyndman and Williams, 1977). The main-phase plutons generally comprise leucocratic granodiorite and granite, are metaluminous to weakly peraluminous, and define a calcic to calc-alkaline trend (Criss, 1981; Hyndman, 1984). Hyndman (1983) has likened the main-phase plutons to the sodic series of the Boulder batholith, Montana, described by Tilling (1973). The main-phase plutons were emplaced at relatively deep crustal levels of generally $\geq$10 km (Swanberg and Blackwell, 1973; Hyndman, 1981, 1983). No definitely comagmatic volcanic rocks are known, although volcanic detritus occurs in several Cretaceous formations in eastern Idaho, Montana, and Wyoming. The emplacement of the main-phase plutons was attended by high-grade regional metamorphism of sedimentary rocks of the Belt Supergroup of Middle Proterozoic age (Hietanen, 1962, 1963, 1984). However, a regional discordance between some of the metamorphic isograds and the margin of the batholith (Chase and Johnson, 1977; Lang and Rice, 1985) suggests that this metamorphism in part predated batholith emplacement or that large areas of high-grade metamorphic rocks may be underlain by part of the batholith. Numerous inliers and screens of metamorphic rock occur within the Bitterroot lobe (Larsen and Schmidt, 1958; see fig. 6.1).

A significant part of the east-central Bitterroot lobe includes Eocene epizonal plutons (fig. 6.1). These calc-alkaline plutons consist predominantly of pink granite, although granodiorite and quartz diorite are also present, and tend to be metaluminous to weakly peraluminous. Distinctive characteristics of many of these Eocene plutons include high heat-generation values (Swanberg and Blackwell, 1973), smoky quartz, and common miarolitic cavities (Bennett, 1980); additional properties are described by Ross (1934), Williams (1979), Criss (1981), Criss and Champion (1984), and Motzer (1985). Although some deep-seated plutons are Eocene in age (Bickford and others, 1981; Chase and others, 1983) most plutons of Eocene age had an epizonal emplacement, and some intrude approximately coeval rocks of the Challis Volcanics (Ross, 1934; Cater and others, 1973; Swanberg and Blackwell, 1973; Armstrong, 1974).

The Bitterroot lobe is bounded on the east by a 100-km-long mylonite zone (fig. 6.1) that dips approximately 25° east along the prominent front of the Bitterroot Mountains (Lindgren, 1904; Langton, 1935; Chase, 1973). Various models have been advanced to explain this major structure, which may be related in some way to a domelike uplift—termed the "Bitterroot dome"— of the batholith interior (Chase and Talbot, 1973; Hyndman and others,

1975; Chase and others, 1983). Major Cretaceous and early Tertiary uplift of the greater Idaho batholith region is required to explain (1) tectonic features (Chase and Talbot, 1973; Scholten and Onash, 1977), (2) the juxtaposition of Cretaceous-early Tertiary and Eocene plutons having markedly different inferred emplacement depths (Swanberg and Blackwell, 1973; Chase and others, 1983), (3) fission-track and K-Ar apparent ages (Ferguson, 1975; Criss and others, 1982; Garmezy and Sutter, 1983; Sutter and others, 1984), and (4) the record of clastic sedimentation (Ryder and Ames, 1970; Ryder and Scholten, 1973). However, the uplift documented by Criss and others (1982) for the southern Idaho batholith may have started earlier and was much more gradual than that inferred by Garmezy and Sutter (1983) for the Bitterroot lobe.

In western Idaho, the Bitterroot lobe is bounded by another zone of intense deformation. This 5- to 25-km-wide zone coincides with an important tectonostratigraphic boundary between the cratonal Belt-Yellowjacket terrane on the east and the Wallowa-Seven Devils terrane on the west; the latter may be an accreted microplate (Hamilton, 1976; Jones and others, 1977). Stratified rocks in the Wallowa-Seven Devils terrane are predominantly Permian and Triassic volcanic and volcaniclastic rocks, in places overlain by Jurassic flyschlike sedimentary rocks (Vallier, 1977; Walker, 1983). These rocks were affected by low-grade metamorphism and west-directed thrusting, followed by and in places associated with intrusion of Jurassic and Cretaceous quartz diorite gneiss, tonalite, and trondhjemite (Hamilton, 1963). These plutons are generally calcic and metaluminous (see Hietanen, 1963), and in many places were also emplaced at deep levels (Swanberg and Blackwell, 1973; Zen and Hammarstrom, 1984). All the above rocks are thought to represent an island arc (Hamilton, 1976; Vallier, 1977).

Juxtaposition of the Wallowa-Seven Devils terrane and the Belt-Yellowjacket terrane apparently occurred during the Late Cretaceous (Fleck and Criss, 1985), insofar as their suture zone is intruded by deformed transition zone plutons having K-Ar ages of 87 to 75 Ma and characteristics intermediate between those of the WSD and the Bitterroot lobe. Most plutons in the Bitterroot lobe were emplaced after this period of accretion. Initial intrusion of the main phase of the Idaho batholith apparently coincided with submergence and renewed marine sedimentation in the epicontinental Cretaceous seaway to the east, which extended from the Gulf Coast to the Arctic Ocean (McGookey and others, 1972).

METHODS

The $^{87}Sr/^{86}Sr$ ratios, Rb and Sr concentrations, and $\delta^{18}O$ and δD values were made on crushed (−200 mesh) whole-rock powders of samples. Standard techniques were used in all cases; details pertinent to the Sr-isotope study are given by Fleck and Criss (1985). Rb and Sr concentrations were measured by isotope dilution or by X-ray fluorescence, and strontium-isotope ratios were measured on a thermal-ionization mass spectrometer. Calculations of initial $^{87}Sr/^{86}Sr$ ratios (r_i) utilized the measured isotopic ratios of Sr, the Rb/Sr ratios, and assumed ages as discussed by Fleck and Criss (1985). However, in cases where independent age data were available, these ages were used in the calculations. Because Rb/Sr ratios are low in all but the Eocene epizonal plutons, the calculated r_i values are generally insensitive to large uncertainties in age.

Determinations of $\delta^{18}O$ values on the whole-rock samples were made by techniques similar to those described by Clayton and Mayeda (1963) and by Borthwick and Harmon (1982); the techniques used for δD determination are similar to those described by Friedman (1953) and by Godfrey (1962). All δD and $\delta^{18}O$ determinations are reported in the ordinary notation as per mil deviations from the SMOW standard (Craig, 1961); precision is generally better than ± 0.2 per mil for $\delta^{18}O$ and ± 1.0 per mil for δD. K-Ar ages reported here were determined utilizing conventional isotope-dilution techniques (Dalrymple and Lanphere, 1969), with selected samples studied by $^{40}Ar/^{39}Ar$ methods (Dalrymple and Lanphere, 1971). All data are reported in tables 6.1–6.5; refer to table 6.1 for sample locations.

GEOCHEMICAL CHARACTER OF THE PLUTONIC ROCKS

REGIONAL VARIATIONS OF R_i, Rb/Sr, AND MAJOR-ELEMENT CHEMISTRY

Kistler and Peterman (1973) discovered that the r_i values of Sierra Nevada plutons vary with geographic position relative to the Paleozoic miogeosyncline and eugeosyncline of the cordillera. Armstrong and others (1977) extended this concept to the Idaho batholith region and demonstrated that the r_i values changed abruptly (from $\leqslant 0.704$ to $\geqslant 0.706$) across the geologic transition between the Phanerozoic eugeosyncline to the west and Precambrian crust to the east. They attributed these variations to contamination of mantle-derived magmas by assimilation of enclosing crustal rocks having different chemical and isotopic characteristics. These mechanisms, together with large-scale anatexis, were confirmed by the results of Fleck and Criss (1985).

New determinations of r_i in the Idaho batholith region (table 6.1; fig. 6.2) are in large part consistent with the observations of Armstrong and others (1977). Whereas the WSD plutons in the accreted terranes all have r_i values less than 0.7042, most Bitterroot lobe plutons in

the Belt-Yellowjacket terrane have r_i values greater than 0.7080. The highest r_i values (as high as 0.732) occur in plutons adjacent to screens and pendants of Precambrian rocks (compare figs. 6.1 and 6.2), indicating significant incorporation of such material in the magmas (Fleck and Criss, 1985). Away from such zones, the r_i values of plutons in the Bitterroot lobe generally range from 0.7080 to 0.7100.

Deformed plutons having r_i values between 0.704 and 0.708 generally occur within the 5- to 25-km-wide tectonic zone along the boundary between the Wallowa-Seven Devils terrane and the Belt-Yellowjacket terrane. These transition zone plutons contain materials derived from both the accreted and Precambrian terranes, and therefore provide important clues regarding the significance of r_i variations in Idaho as well as on the geochronology of the tectonic suture zone they intrude. Fleck and Criss (1985) provide a detailed discussion of the r_i, $\delta^{18}O$, and Rb and Sr relations of these rocks and of the neighboring Bitterroot lobe and WSD plutons.

The Rb and Sr concentration data also distinguish the plutonic series that comprises the northern Idaho batholith region (fig. 6.3). The low Rb concentrations and low Rb/Sr ratios of the WSD plutons contrast markedly with the high Rb contents and high Rb/Sr ratios of the Eocene epizonal plutons, whereas the Rb contents and Rb/Sr ratios of the main-phase granitoids of the Bitterroot lobe are intermediate. This variation is clearly paralleled by

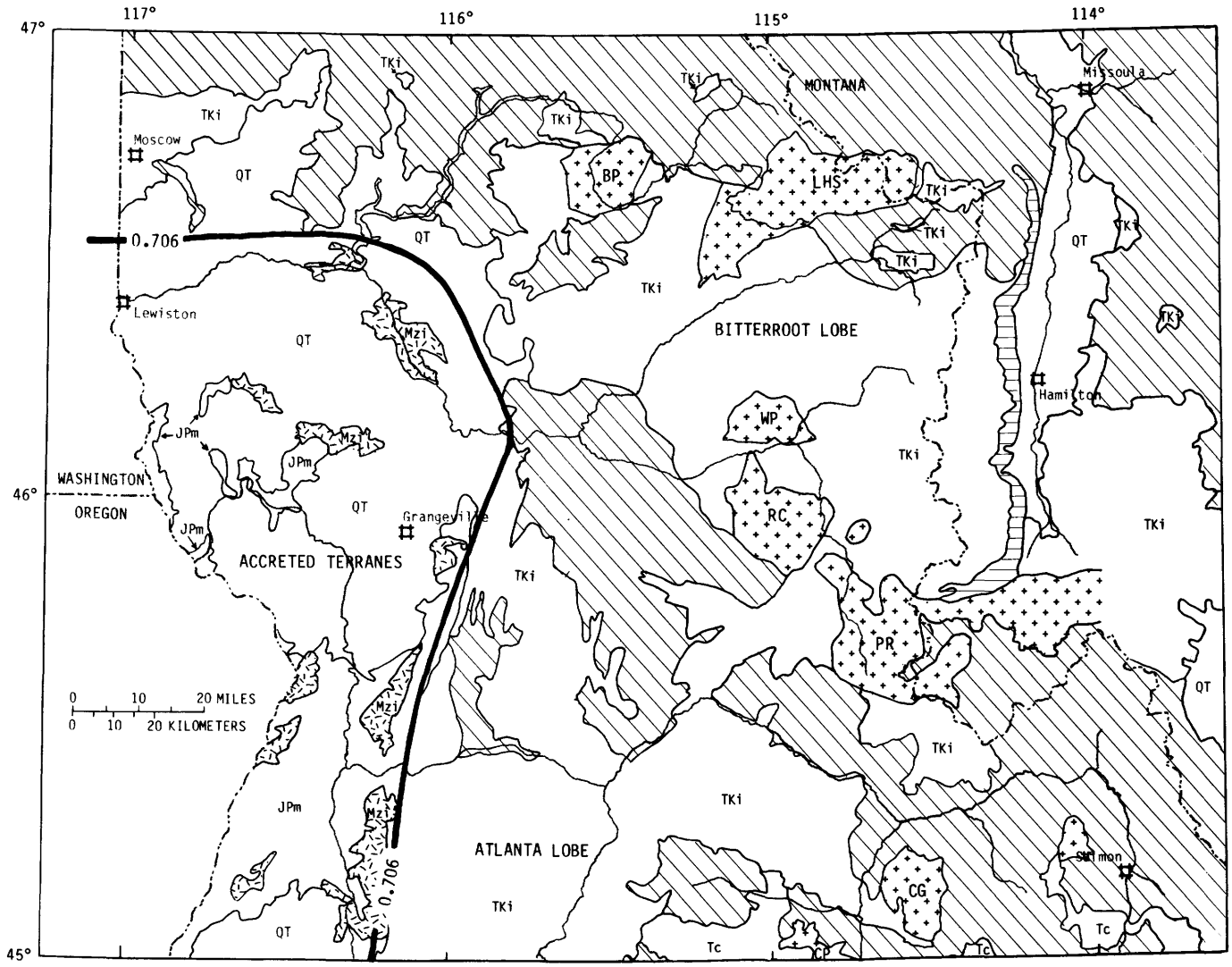

FIGURE 6.1.—Generalized geologic map of north-central Idaho and adjacent areas, modified from Ross and others (1955), Bond (1978), Chase and others (1978), and Toth and others (1983). Heavy line is the 0.706 initial-Sr contour (see figure 6.2), which approximately delineates a major suture zone between the Precambrian craton to the east and the accreted Wallowa-Seven Devils terrane. Abbreviations of Eocene epizonal plutons are BP (Bungalow pluton), LHS (Lolo Hot Springs pluton), WP (Whistling Pig pluton), RC (Running Creek pluton), PR (Painted Rocks pluton), CG (Crags pluton), and CP (Casto pluton).

variations in K, with the alkalis generally increasing transverse to orogenic structures, as has been documented in the Sierra Nevada batholith by Bateman and Dodge (1970). As pointed out by Hyndman (1984), however, no clearcut eastward trend appears if the main-phase plutons are considered alone.

Consistent differences between the various plutonic groups are also revealed by bulk chemical analyses (table 6.2). A variation diagram (fig. 6.4) illustrates that plutons in the Wallowa-Seven Devils terrane are significantly more calcic than the calcic to calc-alkaline plutons in the Bitterroot lobe. Figure 6.5 shows that the Eocene epizonal plutons lie along the calc-alkaline trend defined by the Challis Volcanics.

Temporal trends also appear in the chemical data (see tables 6.1 and 6.2). Aside from being more calcalkaline, younger plutons tend to have higher SiO_2 concentrations and higher degrees of aluminum saturation than older plutons. Exceptions are common, however, probably indicating that shorter differentiation cycles or other effects are superimposed on these overall chemical trends.

$\delta^{18}O$ AND δD DATA

The $\delta^{18}O$ and δD values for the Mesozoic and Tertiary granitoids of north-central Idaho exhibit great variations. Whole-rock $\delta^{18}O$ values range from -0.3 to $+12.4$ per mil, and the δD values range from -148 to -41 per mil (table 6.1). As discussed below, the large $\delta^{18}O$ variations can be partly attributed to variable source characteristics of the plutons. However, the lowest $\delta^{18}O$ and δD values result from hydrothermal alteration processes, and these secondary effects must be quantified before discussion of the primary isotopic variations is possible.

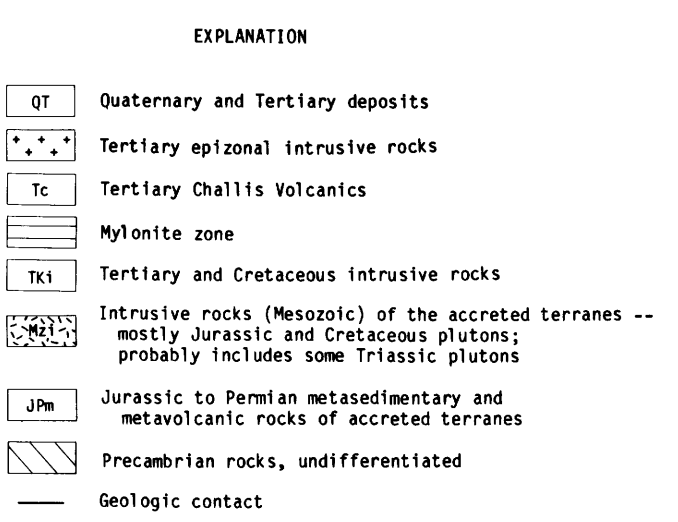

FIGURE 6.1.—Continued.

Taylor and Magaritz (1978) proposed that hydrothermal circulation systems involving fluids derived from low $\delta^{18}O$, low δD meteoric waters developed in the Idaho batholith during the intrusion of the Eocene epizonal plutons. Isotopic exchange between this meteoric-hydrothermal fluid and the rocks produced the major $\delta^{18}O$ and δD depletions in the rocks within and peripheral to the Eocene plutons. Criss and Taylor (1983) estimated that the Eocene meteoric waters in the southern Idaho batholith had $\delta^{18}O$ and δD values of -16 and -120 per mil, respectively; the Bitterroot lobe hydrothermal fluids were apparently derived from waters with similarly low values.

A graph of $\delta^{18}O$ versus δD values (fig. 6.6) shows that most Bitterroot lobe samples with $\delta^{18}O \leqslant +8.0$ per mil have extremely low δD values (-120 per mil or less). As discussed by Taylor (1977), the coupled isotopic depletions in such rocks are inferred to have been produced by meteoric-hydrothermal alteration at high water/rock ratios. On the other hand, the great range in δD observed in rocks with $\delta^{18}O \geqslant +8.0$ per mil is attributed to weak (low water/rock ratios) hydrothermal interactions that, for material balance reasons described by Taylor (1977), can markedly lower the δD values without significantly modifying the $\delta^{18}O$ values.

According to the above interpretation, the primary (igneous) whole-rock $\delta^{18}O$ values of the plutons in the Bitterroot lobe and the northern Atlanta lobe range from $+8.0$ to $+12.4$ per mil. This result is similar to the range of $+8$ to $+11$ per mil obtained by Criss and Taylor (1983) for the bulk of the southern (Atlanta) lobe of the batholith. On the other hand, the low $\delta^{18}O$ values of some of the WSD plutons cannot be attributed to these meteoric-hydrothermal interactions because they are far from the Eocene epizonal plutons and because their δD values are invariably $\geqslant -82$ per mil. Although it is possible that the WSD plutons underwent interactions with hydrothermal fluids having different isotopic characteristics (for example, sea water), the $\delta^{18}O$ and δD values of the rocks are not correlated in a systematic way that would be expected if this were the case. We prefer the interpretation that the $\delta^{18}O$ range of $+5.5$ to $+10.5$ per mil observed in WSD plutons is primary.

Because of the sensitivity of δD values to alteration processes, the primary δD range of the plutons of north-central Idaho is more difficult to establish. Taylor and Magaritz (1978) suggested that primary δD values of major cordilleran batholiths range from about -50 to -85 per mil, which is similar to the range observed in most deep-seated, isotopically normal igneous rocks throughout the world. Similar δD values (> -85 per mil) occur within the WSD plutons and in parts of the Bitterroot lobe that are remote from mapped Eocene epizonal plutons. Thus, the δD values in these zones are probably primary, an interpretation supported by δD measurements of biotite-

TABLE 6.1.—*Results of Rb-Sr, $\delta^{18}O$, and δD analyses*

Sample	North Latitude	West Longitude	Rb (ppm)	Sr (ppm)	$^{87}Rb/^{86}Sr$	$^{87}Sr/^{86}Sr$	$(^{87}Sr/^{86}Sr)_o$	Age (Ma)	$\delta^{18}O$	δD
787-18A	46°14.0'	115°24.6'	87.8	986	0.25766	0.70940	0.7092	60	8.2	-88
18B	46°15.1'	115°24.0'	115.5	647	.51661	.71077	.7104	60	9.6	-86
18C	46°17.1'	115°23.1'	80	488	.47453	.71471	.7143	60	10.3	-95
18D	46°21.5'	115°17.2'	95.6	535	.51743	.71221	.7118	60	10.8	-107
18E	46°24.3'	115°10.2'	75.5	864	.25272	.70940	.7092	60	9.2	-113
18F	46°27.1'	115°05.3'	82.5	944	.25291	.70892	.7087	60	9.7	-98
18G	46°28.5'	114°53.1'	93.9	500	.54378	.71045	.7100	60	10.7	-111
18H	46°34.9'	114°36.5'	89.2	695	.37143	.70923	.7089	60	6.0	-145
18I	46°34.9'	114°36.5'	83.6	822	.29419	.70943	.7092	60	9.3	-127
18J	46°40.6'	114°34.3'	184.4	55.9	9.548	.71361	.7072	45	7.2	-126
19A	46°09.5'	115°21.7'	53.1	542	.2835	.71169	.7114	70	8.8	-98
19B	46°09.1'	115°21.7'	42.2	594	.2056	.71103	.7108	70	8.5	--
19C	46°08.9'	115°21.6'	59.4	510	.3374	.71108	.7107	70	8.5	-73
19E	46°10.6'	115°13.8'	52.5	567	.2682	.71183	.7116	70	7.5	-127
19F	46°14.9'	115°12.6'	131	469	.8102	.71332	.7126	60	9.3	-59
19G	46°14.9'	115°12.6'	157	437	1.0361	.71213	.7114	60	10.0	-76
20A	46°10.3'	115°11.6'	59.4	524	.32775	.71219	.7119	60	8.3	-109
20C	46°12.8'	115°09.6'	106	492	.62453	.71965	.7191	60	10.3	-103
20D	46°04.9'	115°08.5'	44.7	599	.21604	.71404	.7138	70	8.8	-73
20E	46°04.9'	115°08.5'	42.0	607	.20000	.71475	.7146	70	8.0	-78
21A	46°03.3'	114°57.2'	157	364	1.158	.70818	.7073	45	9.3	-145
21B	45°59.0'	114°57.9'	237	8.2	84.063	.76360	.7065	48	9.0	--
21C	45°58.9'	114°57.9'	220	26.5	24.043	.72294	.7075	48	8.2	-128
21D	45°58.4'	115°00.1'	224	148	4.3786	.71149	.7085	48	9.0	-126
21E	46°01.1'	114°50.7'	50.3	1033	.14098	.70937	.7092	60	9.1	--
21F	46°01.1'	114°50.7'	59.6	1055	.16340	.70967	.7095	60	8.8	-131
24A	46°10.2'	114°38.5'	71.6	1014	.20429	.70901	.7088	60	9.2	-100
24B	46°10.2'	114°38.6'	74	1039	.20624	70904	.7089	60	8.8	--
24C	46°10.2'	114°38.6'	70	1224	.16555	.70829	.7081	60	9.0	-81
24D	46°08.1'	114°36.9'	68	864	.22751	.70987	.7097	60	9.0	--
24E	46°08.1'	114°36.8'	<1	806	<.00124	.71032	.7103	60	8.8	-117
24F	46°08.2'	114°36.9'	78.2	759	.29805	.71000	.7097	60	8.8	--
24G	46°08.2'	114°36.9'	57.8	561	.29805	.70648	.7063	50	8.5	-108
24H	46°05.3'	114°32.6'	97.7	432	.65442	.70944	.7090	50	8.8	-85
24I	46°05.3'	114°32.7'	105	542	.56022	.70942	.7090	50	9.5	-80
25A	46°07.5'	114°56.0'	139	90.7	4.4226	.71206	.7089	50	1.2	-141
25B	46°04.8'	114°58.4'	177	206	2.4898	.71068	.7089	50	2.3	-141
25C	46°04.8'	114°25.5'	102	746	.39433	.70926	.7090	50	10.8	-91
26A	46°13.2'	115°31.9'	87.6	883	.28726	.70888	.7086	70	9.3	-72
26B	46°13.2'	115°31.9'	59.2	898	.19073	.70937	.7092	70	7.2	-136
26C	46°13.2'	115°31.9'	54.2	814	.19273	.70924	.7090	70	8.7	-129
26D	46°12.0'	115°32.5'	43.6	889	.14186	.71360	.7135	70	9.9	-109
26E	46°12.0'	115°32.5'	32.9	682	.13963	.71492	.7148	70	9.1	-85
26F	46°12.0'	115°32.5'	56.7	435	.37747	.71388	.7135	70	8.4	-141

797-18A	45°33.3'	114°32.9'	223.6	210.2	3.0782	0.70745	0.7053	50	6.9	-131
18B	45°33.4'	114°32.8'	221.2	83.63	7.6638	.72402	.7153	80	--	--
18C	45°38.4'	114°25.1'	288.4	46.86	17.826	.71850	.7058	50	8.4	-118
18D	45°39.6'	114°30.1'	205.6	117.9	5.04708	.71089	.7073	50	--	--
18E	45°33.8'	114°34.1'	206	219.7	2.7132	.70859	.7067	50	--	--
19A	45°43.1'	114°28.0'	215.4	68.17	9.1496	.71530	.7088	50	--	--
19B	45°43.1'	114°28.0'	232.7	61.51	10.953	.71574	.7087	45	8.1	--
19C	45°41.5'	114°28.9'	221.4	226.5	2.8288	.70978	.7079	45	--	--
19D	45°32.7'	114°24.4'	36.63	142.5	.74731	.70752	.7067	80	3.4	-157
19E	45°32.5'	114°24.8'	31.27	135.9	.66627	.72124	.7205	80	6.3	-145
19F	45°32.5'	114°24.8'	31.9	138.2	.66906	.72452	.7238	80	4.4	--
19G	45°32.6'	114°26.6'	251.1	59.91	12.137	.71800	.7094	50	9.8	-126
20A	45°44.8'	114°26.8'	272.9	19.90	39.804	.74003	.7080	50	--	--
20B	45°42.4'	114°36.0'	335.9	6.728	145.88	.80904	.7054	50	5.8	-133
20C	45°42.1'	114°38.3'	174.1	257.9	1.9539	.71260	.7112	50	--	--
20D	45°41.6'	114°39.3'	220.1	214.2	2.9744	.71193	.7098	50	--	--
20E	45°44.0'	114°44.8'	106.1	318.1	.96552	.71076	.7101	50	--	--
20F	45°44.1'	114°45.0'	151.6	82.40	5.3263	.71140	.7076	50	--	-152
20G	45°39.0'	114°35.7'	214.2	54.18	11.452	.71797	.7098	50	-0.3	-133
21A	45°43.2'	114°16.6'	325.8	14.46	65.469	.75402	.7074	50	7.8	-140
22A	46°09.7'	114°47.2'	82.40	845.6	.28196	.70882	.7086	60	10.2	-95
22B	46°13.2'	114°27.1'	61.88	904.9	.19788	.70923	.7091	60	9.4	-90
22C	46°13.3'	114°27.0'	60.35	1003	.17584	.70882	.7087	60	9.2	-89
23A	46°08.4'	115°36.1'	29.61	704.3	.12164	.70866	.7085	93	--	--
23B	46°20.4'	115°06.7'	115.4	808.7	.41286	.71144	.7111	60	9.9	-123
23C	46°18.1'	115°01.4'	92.15	816.6	.32655	.70950	.7092	60	3.4	-131
24A	45°56.2'	115°03.0'	203.9	32.44	18.211	.72093	.7080	50	--	--
24B	45°54.6'	114°43.9'	124.6	122.6	2.9410	.71090	.7088	50	--	-131
24C	45°57.4'	114°37.4'	79.26	1013	.22647	.70855	.7083	60	--	-141
25A	46°08.2'	115°37.3'	51.29	946.1	.15688	.70948	.7093	90	--	--
25B	46°08.2'	115°37.3'	44.16	902.7	.14155	.70941	.7092	90	10.1	--
25C	46°08.3'	115°39.4'	-8.31	111.7	.21756	.81459	.8144	75	--	--
25D	46°08.2'	115°45.1'	76.70	483.2	.45923	.70798	.7075	75	--	--
25E	46°08.2'	115°45.1'	48.28	653.9	.21361	.70753	.7073	80	9.4	-71
25F	46°08.5'	115°51.8'	23.05	615.3	.10837	.70349	.7034	80	6.7	-78
25G	46°01.8'	115°58.4'	.533	304.9	.00505	.70408	.7041	80	--	--
25H	46°01.5'	115°58.2'	16.46	261.7	.18191	.70424	.7046	80	--	-71
25I	46°00.4'	115°57.5'	9.48	333.9	.08210	.70398	.7039	80	6.6	-58
26A	46°15.3'	116°03.8'	7.142	269.2	.07673	.70378	.7037	80	5.5	-64
26B	45°57.0'	115°58.7'	15.35	635	.06988	.70325	.7032	80	7.8	-51
26C	45°57.0'	115°58.7'	5.52	379	.04214	.70391	.7039	80	5.9	-46
26D	45°53.3'	116°02.1'	26.19	524.6	.14439	.70386	.7037	80	9.0	-82
26E	45°50.5'	115°59.9'	26.25	805.5	.09425	.70387	.7038	80	8.5	-66
26F	45°49.7'	115°33.3'	96.89	88.18	3.2032	.78462	.7810	80	11.3	--
26G	45°47.6'	115°45.1'	69.95	368.4	.54996	.71751	.7170	60	11.2	-79
26H	45°49.2"	115°49.7'	114	562.3	.58696	.71654	.7159	80	10.2	-83
26I	45°49.6'	115°54.1'	64.46	900.5	.20718	.70808	.7078	80	9.6	--

TABLE 6.1.—*Results of Rb-Sr, $\delta^{18}O$, and δD analyses*—Continued

Sample	North Latitude	West Longitude	Rb (ppm)	Sr (ppm)	$^{87}Rb/^{86}Sr$	$^{87}Sr/^{86}Sr$	$(^{87}Sr/^{86}Sr)_o$	Age (Ma)	$\delta^{18}O$	δD
807-27A	45°50.1'	115°58.9'	23.2	832	0.08065	0.70375	0.7037	86	10.4	--
27B	45°49.8'	115°58.4'	68.6	189	1.05002	.70624	.7050	86	--	--
27C	45°49.8'	115°55.9'	38.2	852	.12969	.70493	.7048	86	9.1	--
28A	45°50.1'	115°57.9'	51.9	513	.29261	.70420	.7038	86	--	--
28B	45°50.2'	115°56.0'	33.3	1228	.07844	.70476	.7047	86	8.5	--
28C	45°48.2'	115°58.6'	9.71	303	.09269	.70488	.7048	80	--	--
28D	45°48.2'	115°58.6'	17.2	357	.13936	.70497	.7048	80	--	--
28E	45°48.2'	115°58.6'	34	107	.91930	.70695	.7059	80	--	--
28F	45°49.8'	115°55.8'	54.8	988	.16045	.70588	.7057	86	9.8	--
28G	45°49.7'	115°55.5'	45.6	842	.15666	.70577	.7056	86	10.2	--
28H	45°49.6'	115°55.5'	29.9	1406	.06152	.70657	.7065	86	10.4	--
28I	45°49.4'	115°55.0'	41.7	709	.01702	.70748	.7073	86	9.2	--
29A	45°49.4'	115°51.6'	110	461	.69079	.71377	.7130	80	11.2	--
29B	45°49.4'	115°51.5'	104	529	.56905	.71180	.7112	80	10.2	--
29C	45°49.3'	115°51.3'	96.8	599	.46774	.71142	.7109	80	11.6	--
29D	45°49.3'	115°50.7'	65.5	726	.26110	.71017	.7099	80	9.9	--
29E	45°49.0'	115°48.9'	184	14.2	37.5833	.73292	.7089	45	--	--
29F	45°52.0'	115°48.5'	98.5	449	.63268	.71645	.7157	80	12.1	--
29G	45°48.5'	115°48.0'	89.1	513	.50290	.71529	.7147	80	11.4	--
29H	45°48.0'	115°47.0'	62.9	672	.27123	.72338	.7231	80	11.5	--
29I	45°47.8'	115°46.2'	108.4	407	.77148	.71929	.7184	80	10.9	--
29J	45°47.7'	115°45.5'	97.8	710	.39869	.71142	.7110	80	10.4	--
30A	45°47.8'	115°44.7'	72.7	570	.36924	.71376	.7133	80	10.9	--
30B	45°47.7'	115°43.5'	66.0	517	.36927	.71512	.7147	80	10.0	--
30C	45°47.7'	115°43.5'	88.3	479	.53373	.71483	.7142	80	10.9	--
30D	45°47.9'	115°42.7'	59.2	610	.28101	.71556	.7152	80	11.5	--
30E	45°48.7'	115°39.5'	117	163	2.08641	.75502	.7526	80	10.8	--
30F	45°48.7'	115°39.7'	113.7	167	1.97866	.75328	.7510	80	10.9	--
30G	45°48.7'	115°39.7'	67.3	189	1.03416	.75248	.7513	80	12.0	--
30H	45°48.7'	115°39.5'	106.1	192	1.60481	.74575	.7439	80	9.5	--
30I	45°48.4'	115°38.4'	113.1	326	1.00628	.73313	.7320	80	9.1	--
30J	45°48.8'	115°37.8'	83.7	433	.55998	.72046	.7198	80	10.4	--
30K	45°48.7'	115°37.8'	284.5	94.3	8.93133	.94462	.9345	80	8.9	--
31A	45°49.7'	115°37.3'	167.9	277.1	1.75735	.73241	.7304	82	11.0	--
31B	45°49.7'	115°37.3'	92.9	356.4	.75520	.72151	.7206	82	10.7	--
31C	45°49.7'	115°36.7'	60.1	426.9	.40863	.74081	.7404	65	10.6	--
31D	45°49.5'	115°35.7'	57.9	397	.42239	.71787	.7175	65	11.1	--
31E	45°49.4'	115°35.0'	49.7	805	.17881	.71820	.7180	65	10.1	--
31F	45°49.8'	115°34.9'	50.9	1262	.11680	.71683	.7167	65	10.4	--
31G	45°49.4'	115°34.1'	59.8	651	.26612	.72092	.7207	65	10.9	--
31H	45°49.4'	115°34.1'	35.6	620	.16635	.72137	.7212	65	10.9	--
31I	45°49.9'	115°33.4'	42.5	490	.25130	.72207	.7218	65	10.6	--
31J	45°49.8'	115°33.4'	84.1	298	.81862	.73385	.7329	80	10.3	--
31K	45°49.8'	115°33.4'	66.6	91.2	2.11955	.73995	.7374	85	8.7	--

808-01A	45°49.5'	115°31.6'	77.8	898	0.25107	0.72425	0.7240	80	12.4	--
01B	45°49.5'	115°30.4'	125.6	415	.88122	.77252	.7717	65	9.5	--
01C	45°49.7'	115°30.1'	62.8	60.6	3.01601	.76790	.7645	80	9.4	--
01D	45°49.2'	115°29.5'	123	203	1.76165	.75762	.7556	80	9.8	--
01E	45°48.4'	115°28.6'	196	124	4.61352	.79761	.7924	80	10.0	--
01F	45°48.2'	115°24.7'	194	93.7	6.06141	.82884	.8220	80	9.9	--
01G	45°47.7'	115°24.0'	178	88.3	5.89950	.82513	.8184	80	9.3	--
01H	45°48.4'	115°28.3'	143	176	2.36352	.76295	.7603	80	9.7	--
01I	45°48.2'	115°28.3'	35	144	.70411	.72045	.7196	80	7.7	--
01J	45°47.8'	115°27.9'	154	130	3.45392	.78662	.7827	80	9.2	--
01K	45°47.8'	115°26.4'	117	194	1.75157	.74658	.7446	80	10.3	--
01L	45°47.7'	115°26.3'	158	247	1.85547	.73357	.7315	80	--	--
04A	45°58.4'	114°08.2'	68.2	523	.37748	.71286	.7125	65	7.8	-111
04B	45°58.1'	114°08.4'	74.5	538	.40087	.71342	.7130	65	8.4	--
04C	45°56.8'	114°12.3'	76.6	114	1.94976	.73747	.7361	50	--	--
04D	45°55.8'	114°13.4'	75	563	.38535	.70562	.7053	65	--	--
04E	45°55.1'	114°09.9'	70.5	594	.34361	.71401	.7137	55	--	-141
04F	45°55.2'	114°09.7'	77.4	536	.41803	.71325	.7129	55	--	--
04G	45°55.3'	114°09.6'	224	87.1	7.44514	.71353	.7093	40	--	--
05A	46°17.6'	114°16.1'	102	700	.42175	.71137	.7110	55	10.5	-76
05B	46°17.4'	114°20.4'	128	574	.64546	.71191	.7114	55	10.4	--
05C	46°17.4'	114°24.6'	118	585	.58382	.71147	.7110	55	10.6	-72
05D	46°17.0'	114°28.2'	34	1381	.07127	.71243	.7124	55	10.3	--
05E	46°17.8'	114°36.3'	92	638	.41736	.71107	.7107	55	10.6	-60
05F	46°08.7'	114°26.2'	62.3	861	.20941	.71023	.7101	55	9.3	--
06A	46°08.6'	114°28.3'	73.4	727	.29220	.71070	.7105	55	9.3	--
06B	46°07.1'	114°29.6'	77.6	870	.25814	.71034	.7101	55	8.9	--
06C	46°08.5'	114°30.1'	78.4	834	.27207	.71090	.7107	55	9.5	--
06D	46°08.8'	114°30.1'	62	872	.20576	.71002	.7099	55	--	--
06E	46°08.8'	114°30.1'	67.6	901	.21713	.71008	.7099	55	--	--
06F	46°08.9'	114°30.0'	85.6	751	.32988	.71066	.7104	55	--	--
06G	46°08.4'	114°25.9'	65.8	1062	.17931	.71013	.7100	55	9.3	--
06H	46°08.3'	114°25.2'	51.7	1006	.14873	.71005	.7099	55	--	--
06I	46°08.3'	114°24.2'	61.2	853	.20763	.70981	.7096	55	8.8	-61
818-09A	46°48.6'	117°00.4'	72	494	.42195	.71379	.7134	65	9.8	-93
09B	46°41.4'	116°58.3'	177	724	.70742	.70887	.7082	65	--	--
09C	46°41.5'	116°58.6'	220	662	.96169	.70943	.7085	65	--	--
09D	46°57.6'	116°19.2'	70.2	1070	.18990	.71167	.7115	80	--	--
09E	46°46.2'	116°14.3'	94.9	371	.74033	.71090	.7101	80	--	--
09F	46°46.2'	116°14.3'	55.7	949	.16985	.70982	.7096	80	11.7	-71
09G	46°50.7'	116°10.8'	89.1	344.7	.74780	.70660	.7059	65	--	--
09H	46°53.5'	116°08.5	65.8	599	.31452	.70989	.7095	80	--	--
09I	46°53.3'	116°08.5'	69.8	588	.34353	.70975	.7094	80	--	-116
09J	46°51.9'	116°11.0'	110.1	260	1.22370	.70688	.7058	65	--	--
10A	46°29.7'	116°27.7'	<1	229	<.00437	.70297	.7030	160	--	--
10B	46°28.2'	116°25.2'	33.5	461	.21017	.70383	.7034	160	--	--
10C	46°30.0'	116°23.2	23.4	577	.11729	.70357	.7033	160	--	--
10D	46°30.1'	116°21.1'	2.5	896	.00807	.70345	.7034	160	--	--
10E	46°29.7'	116°16.4'	17.23	905	.05506	.70379	.7037	160	--	--

TABLE 6.1.—*Results of Rb-Sr, $\delta^{18}O$, and δD analyses*—Continued

Sample	North Latitude	West Longitude	Rb (ppm)	Sr (ppm)	$^{87}Rb/^{86}Sr$	$^{87}Sr/^{86}Sr$	$(^{87}Sr/^{86}Sr)_o$	Age (Ma)	$\delta^{18}O$	δD
818-10F	46°30.8'	116°17.9'	23.7	756	0.09067	0.70411	0.7039	160	--	--
10G	46°30.5'	116°18.8'	46.6	587	.22961	.70400	.7035	160	--	--
11A	46°36.5'	116°10.8'	44.4	811	.15839	.70723	.7071	65	--	--
11B	46°36.0'	116°10.4'	53.8	795	.19588	.71199	.7118	65	11.1	--
11C	46°26.1'	116°12.8'	3.683	661	.01611	.70342	.7034	160	6.2	-41
11D	46°24.7'	116°11.7'	12.8	682	.05428	.70344	.7033	160	--	--
11E	46°22.6'	116°10.6'	8.3	864	.02778	.70349	.7034	160	--	--
11F	46°19.4'	116°08.4'	25.7	629	.11817	.70357	.7033	160	--	-56
11G	46°17.4'	115°58.5'	21.1	773	.07894	.70355	.7034	160	--	--
12A	46°19.9'	115°49.4'	38.8	623	.18023	.70987	.7095	130	--	--
12B	46°19.4'	115°49.2'	56	624	.25974	.71091	.7104	130	--	--
12C	46°20.6'	115°43.8'	76.6	833	.26613	.71039	.7099	65	--	--
12D	46°14.7'	115°46.6'	57.2	610	.27150	.71501	.7145	130	9.5	-52
12E	46°08.6'	115°50.7'	1.1	347	.00917	.70912	.7091	130	7.0	-63
12F	46°08.3'	115°47.8'	30.9	616	.14508	.70389	.7037	85	--	--
13A	45°35.1'	115°40.8'	61.7	859	.20836	.71067	.7104	80	10.0	-72
13B	45°35.1'	115°40.8'	178	150	3.43631	.71638	.7125	80	--	--
13C	45°31.1'	115°40.1'	107	451	.68682	.71330	.7125	80	10.8	-52
13D	45°37.3'	115°46.4'	124	278	1.29138	.71434	.7129	80	--	--
13E	45°20.6'	115°52.5'	122	437	.80805	.71158	.7107	80	10.7	-62
13F	45°32.4'	115°27.8'	76.8	435	.51133	.71785	.7173	80	10.0	-62
14A	45°30.7'	115°02.0'	307	7.602	117.62028	.77563	.7043	43	9.7	-105
14B	45°30.5'	115°00.9'	231	216	3.09502	.71030	.7083	45	--	--
14C	45°38.7'	115°11.3'	204	49.3	11.98380	.71749	.7090	45	--	--
15A	45°47.9'	115°57.2'	44.2	1093	.11697	.70506	.7049	80	--	--
15B	45°38.9'	115°59.0'	71.1	826	.24906	.70830	.7080	80	--	-71
15C	45°38.7'	115°59.3'	66.4	949	.20246	.70852	.7083	80	--	--
15D	45°37.8'	116°04.5'	3.055	1556	.00568	.70402	.7040	80	--	--
15E	45°37.9'	116°04.5'	19.7	986	.05779	.70387	.7038	80	8.9	-67
15F	45°38.2'	116°06.3'	28.1	144	.56444	.70488	.7042	80	--	--
16A	45°24.0'	116°13.4'	.3	610	.00142	.70401	.7040	160	--	--
16B	45°24.0'	116°12.6'	11.5	546	.06092	.70391	.7038	160	--	--
16C	45°24.0'	116°12.6'	39.9	85.4	1.35187	.70826	.7033	260	--	--
16D	45°25.1'	116°10.2'	2	254	.02277	.70389	.7039	80	6.4	-63
16E	45°25.6'	116°08.1'	21.2	857	.07155	.70411	.7040	80	--	--
16F	45°24.6'	116°07.5'	48.6	693	.20290	.70750	.7073	80	--	--
16G	45°24.4'	116°07.5'	84	486	.50007	.70745	.7069	80	--	--
16H	45°24.2'	116°05.5'	142	52.1	7.90246	.72929	.7203	80	--	--
16I	45°25.4'	116°02.5'	65	644	.29203	.70782	.7075	80	9.1	-62
16J	45°27.2'	115°59.2'	103	537	.55498	.70805	.7074	80	--	--
16K	45°25.8'	115°56.5'	87.1	450	.56014	.70986	.7092	80	11.4	-70

827-26A	46°15.7'	117°36.8'	9.466	752.9	0.03636	0.70324	0.7032	160	--	--
26B	46°15.7'	117°36.8'	6.948	709.9	.03636	.70317	.7032	160	--	--
26C	46°35.4'	116°43.4'	39.78	394.4	.29216	.71939	.7191	80	--	-54
26D	46°35.2'	116°43.0'	59.68	206.3	.84321	.78356	.7826	80	--	--
27A	46°27.8'	116°07.2'	33.65	569.7	.17083	.70392	.7035	160	8.3	--
27B	46°28.7'	116°06.0'	17.39	662.8	.07588	.70381	.7036	160	--	-63
27C	46°29.2'	116°05.1'	55.47	657.1	.24425	.70794	.7077	80	9.1	--
27D	46°29.1'	116°05.5'	6.198	356.6	.05028	.70534	.7052	160	--	--
27E	46°29.1'	116°05.5'	5.828	1653	.01020	.70560	.7056	160	--	--
27F	46°28.9'	116°06.0'	2.735	1111	.00712	.70398	.7040	160	--	--
28A	46°29.4'	116°11.7'	3.732	542.3	.01991	.70486	.7048	160	--	--
28B	46°29.2'	116°03.0'	42.50	420.8	.29214	.70503	.7047	80	--	--
28C	46°29.2'	116°14.7'	35.12	635.9	.15974	.70431	.7039	160	--	--
28D	46°28.3'	116°14.8'	.6681	280.1	.00690	.70316	.7031	160	--	--
28E	46°23.2'	116°10.4'	2.755	763.7	.01043	.70337	.7033	160	6.4	--
28F	46°17.2'	116°06.8'	32.26	467.2	.19971	.70376	.7033	160	--	--
28G	46°11.5'	116°00.5'	42.76	535.4	.23099	.70390	.7034	160	--	--
29A	45°38.1'	116°14.2'	15.91	504.5	.09121	.70390	.7037	160	--	--
29B	45°38.0'	116°13.8'	.188	104.7	.00519	.70391	.7039	160	--	--
29C	45°38.2'	116°08.6'	16.88	691.6	.07059	.70387	.7037	160	--	--
29D	45°38.4'	116°07.3'	20.27	459.?	.12768	.70455	.7044	80	--	--
29E	45°38.0'	116°00.7'	52.60	1013	.15024	.70829	.7081	80	--	--
29F	45°37.7'	116°00.9'	59.72	916.1	.18863	.70864	.7084	80	--	--
29G	45°26.9'	116°10.6'	9.618	127.4	.21836	.70457	.7043	80	--	--
29H	45°25.4'	116°09.4'	46.65	950.4	.14199	.70567	.7055	80	--	--
29I	45°25.7'	116°08.6'	14.25	682.4	.06040	.70417	.7041	80	--	--
29J	45°25.7'	116°08.6'	25.96	379.9	.19766	.70530	.7051	80	--	--
29K	45°25.4'	116°07.8'	42.31	919.7	.13310	.70726	.7071	80	--	--
29L	45°25.5'	116°07.8'	51.66	932.5	.16024	.70477	.7046	80	--	--
30A	45°10.0'	116°18.0'	6.905	1078	.01853	.70393	.7039	80	--	--
30B	45°07.8'	116°17.1'	20.94	911.1	.06647	.70372	.7036	80	--	--
30C	44°57.5'	116°12.5'	11.32	475.2	.06890	.70403	.7040	80	--	--
30D	44°57.5'	116°12.5'	34.08	705.5	.13972	.70417	.7040	80	--	--
30E	44°57.5'	116°12.5'	9.448	688.2	.03971	.70395	.7039	80	--	--
30F	44°58.0'	116°11.1'	63.56	764.8	.24038	.70461	.7043	80	--	--
30G	44°58.0'	116°10.9'	37.49	984.9	.11011	.70587	.7057	80	--	--
30H	44°57.8'	116°10.4'	33.88	890.5	.1100[illegible]	.70545	.7053	80	--	--
30I	44°55.0'	116°00.2'	168.7	310.9	1.57048	.71108	.7093	80	--	--
30J	44°55.6'	116°01.2'	187.2	139.2	3.89342	.71404	.7096	80	--	--
30K	44°58.1'	116°03.2'	65.52	727.3	.26069	.70923	.7089	80	--	--
30L	44°57.7'	116°05.5'	114.5	473.4	.69991	.70927	.7085	80	--	--
837-23A	46°35.2'	116°48.5'	287.5	690.7	1.20498	.71337	.7123	80	--	--
23B	46°35.5'	116°46.4'	25.46	923.6	.07976	.70772	.7076	80	--	--
23C	46°35.3'	116°18.3'	92	621.2	.42853	.70835	.7079	80	--	--
24A	46°30.7'	116°17.4'	30.46	698.1	.12619	.70363	.7035	80	--	--
24B	46°30.6'	116°16.7'	45.22	433.8	.30149	.70380	.7035	80	--	--

TABLE 6.1.—*Results of Rb-Sr, $\delta^{18}O$, and δD analyses*—Continued

Sample	North Latitude	West Longitude	Rb (ppm)	Sr (ppm)	$^{87}Rb/^{86}Sr$	$^{87}Sr/^{86}Sr$	$(^{87}Sr/^{86}Sr)_o$	Age (Ma)	$\delta^{18}O$	δD
837-24C	46°31.7'	116°18.4'	93.6	663.9	0.40796	0.70888	0.7084	80	--	--
24D	46°30.6'	116°16.0'	3.04	743.2	.01183	.70487	.7049	80	--	--
24E	46°33.3'	116°15.1'	37.68	966.9	.11274	.70654	.7064	80	--	--
24F	46°29.8'	116°15.4'	32.73	113.2	.83640	.70578	.7048	80	--	--
25A	46°21.9'	116°05.6'	3.638	1284	.00819	.70356	.7035	80	--	--
25B	46°21.9'	116°04.7'	11.19	867.1	.03733	.70407	.7040	80	7.4	--
25C	46°17.8'	115°58.5'	14.39	903.7	.04606	.70423	.7042	80	--	--
25D	46°18.5'	116°02.8'	20.65	557	.10723	.70467	.7046	80	--	--
25E	46°16.3'	115°58.9'	15.05	803.5	.05417	.70345	.7034	80	--	--
25F	46°14.5'	115°59.9'	12.42	453.5	.07921	.70335	.7033	80	--	--
25G	46°15.1'	115°57.6'	2.537	610.2	.01202	.70356	.7035	80	--	--
26A	46°30.7'	116°19.0'	36.49	584.1	.18068	.70378	.7036	80	--	--
26B	46°33.0'	116°17.7'	.5	248.7	.00582	.70546	.7054	80	--	--
26C	46°32.9'	116°18.4'	31.77	580.9	.15819	.70484	.7047	80	10.3	--
26D	46°32.8'	116°18.4'	44.48	638.2	.20160	.70504	.7048	80	--	--
27A	46°34.9'	115°45.3'	30.59	728.3	.12155	.70952	.7094	65	--	-79
27B	46°34.9'	115°45.3'	20.77	741.7	.08104	.70940	.7093	65	--	--
27C	46°34.5'	115°39.1'	59.55	832.2	.20707	.70911	.7089	65	--	--
27D	46°35.4'	115°35.3'	58.32	744.4	.22671	.70930	.7091	65	--	-148
27E	46°36.9'	115°30.3'	272.9	64.53	12.24150	.71235	.7045	45	--	-131
27F	46°42.9'	115°33.6'	222.8	22.45	28.75622	.72272	.7043	45	-	-111
27G	46°32.3'	115°37.9'	60.85	595.8	.29563	.71225	.7120	65	--	-79
27H	46°27.2'	115°36.3'	64.05	1091	.16994	.71268	.7125	60	--	-66
27I	46°25.2'	115°24.9'	64.29	866.6	.21468	.70961	.7094	60	--	-124
27J	46°27.1'	115°14.7'	100.6	64.91	4.48600	.71187	.7087	50	--	-102
27K	46°29.6'	115°09.1'	170	202.3	2.43158	.70866	.7069	50	--	--
27L	46°30.5'	115°05.7'	175.1	172.8	2.93218	.70896	.7069	50	--	-132
27M	46°28.4'	115°05.3'	123.1	397.9	.89503	.70669	.7060	50	--	--
28A	45°57.2'	115°55.8'	148.4	271.3	1.58308	.71063	.7088	80	--	--
28B	45°58.8'	115°53.0'	94.47	574.5	.47578	.70796	.7074	80	--	--
28C	45°58.8'	115°52.4'	72.36	778.7	.26887	.70832	.7080	80	--	--
28D	45°58.7'	115°51.5'	139.3	343.7	1.17351	.71527	.7139	80	--	--
28E	45°58.5'	115°52.0'	115.3	498.9	.66886	.71056	.7098	80	--	--
28F	45°57.8'	115°54.6'	79.88	702.3	.32906	.70694	.7066	80	--	--
28G	45°49.5'	115°53.2'	181.5	547.8	.96020	.72467	.7236	80	--	--
28H	45°49.5'	115°53.4'	96.95	723.8	.38760	.70904	.7086	80	--	--
29A	45°24.1'	116°06.8'	103.2	365.7	.81662	.70937	.7084	80	--	--
29B	45°24.6'	116°04.7'	16.68	50.37	.95831	.70976	.7097	80	--	--
29C	45°25.6'	116°00.4'	179.4	225.3	2.30614	.71779	.7152	80	--	--
29D	45°25.5'	116°01.5'	145.6	544.8	.77337	.70935	.7085	80	--	--
29E	45°24.1'	116°08.6'	27.26	1056	.07466	.70398	.7039	80	--	--
29F	45°24.1'	116°09.1'	37.89	890.8	.12302	.70408	.7039	80	--	--
29G	45°17.5'	116°14.6'	26.15	603.4	.12534	.70395	.7038	80	--	--
29H	45°17.5'	116°14.6'	33.24	633.9	.15166	.70401	.7038	80	--	--

muscovite pairs from the Atlanta lobe (Criss and Taylor, 1983). However, Masi and others (1981) discovered a relation between δD values and water contents in the Sierra Nevada batholith and proposed that this trend is primary. If the latter is true, granitic rocks having low water contents may have primary δD values as low as -110 per mil. Such low primary values can be excluded in most of the Idaho batholith, but may apply in certain cases, such as in the Eocene epizonal plutons. Unfortunately, the intimate association of these epizonal plutons with the meteoric-hydrothermal systems will complicate resolution of this possibility.

RELATION OF R_i AND $\delta^{18}O$

Values of r_i and $\delta^{18}O$ are governed by fundamentally different processes, and graphs of these two parameters have provided much insight into the petrogenesis of igneous rocks (for example, Magaritz and others, 1978; Taylor, 1981). Taylor and Silver (1978) constructed a graph of r_i versus $\delta^{18}O$ for the Peninsular Ranges batholith (PRB) and discovered that most data points comprise a linear band extending from mantlelike igneous rocks (fig. 6.7). They suggested that the source materials for the PRB were dominated by two end members, one derived from upper mantle materials and the other from high-^{18}O, high $^{87}Sr/^{86}Sr$ materials probably related to sedimentary or metasedimentary rocks. Evidence for a third end member was found in the rocks of the San Jacinto block, which have high r_i values relative to the PRB trend (fig. 6.7); Taylor and Silver (1978) suggested that involvement of ancient cratonal rocks may be implicated. In contrast, Masi and others (1981) found that

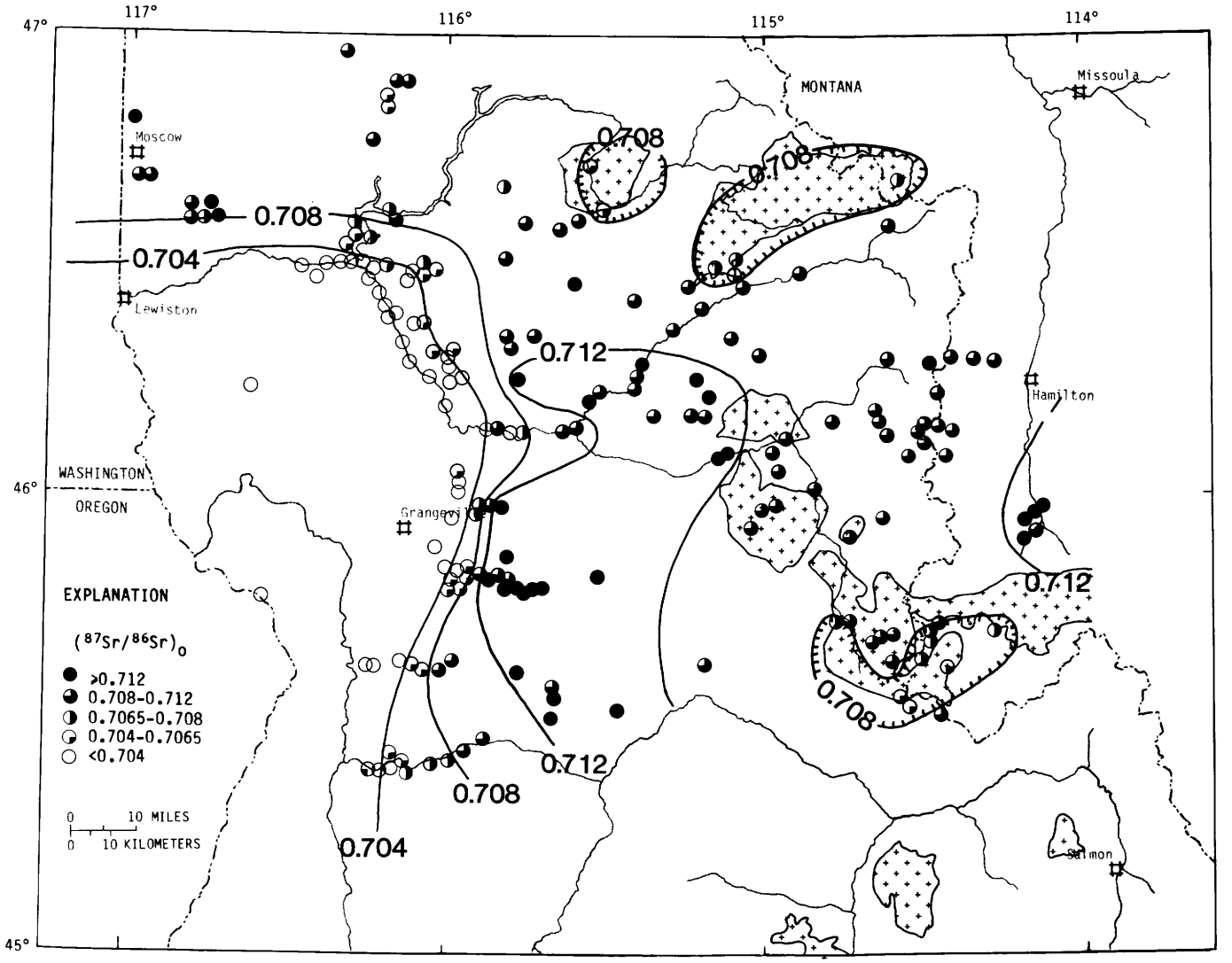

FIGURE 6.2.—Contour map showing the distribution of initial $^{87}Sr/^{86}Sr$ (r_i) for the Jurassic to Eocene plutons of north-central Idaho. Note the well-defined 0.704 and 0.708 contours that separate the high-r_i, Precambrian-hosted plutons of the Belt-Yellowjacket terrane on the east from the low-r_i plutons of the accreted Wallowa-Seven Devils terrane (compare with figure 6.1). Patterned areas same as in figure 6.1.

only about half the data points for Sierra Nevada plutons conform to the PRB trend. The remaining analyses also have high r_i values relative to the PRB trend, similar to the San Jacinto block as well as to most Mojave Desert granitoids (fig. 6.7). Masi and others (1981) also showed that Klamath Mountains plutons are distinguished by r_i values that are uniform and low ($\leq$0.705), independent of the $\delta^{18}O$ values.

The Idaho batholith is unique among the major cordilleran batholiths in that very few plutons have r_i and $\delta^{18}O$ values that conform to the trend of PRB granitoids (fig. 6.8). Practically all Bitterroot lobe samples, including both the Cretaceous-early Tertiary main-phase plutons and the Eocene epizonal plutons, have high r_i values relative to the PRB trend. These plutons are most similar to granitoids of the San Jacinto block, the Mojave Desert, and other areas that are known or inferred to contain Precambrian rocks. This observation could possibly indicate that mantle-derived plutons have assimilated a great deal of ancient crystalline rocks in all these areas; such a model was proposed by Armstrong and others (1977) for the radiogenic rocks of the Idaho batholith. Although Fleck and Criss (1985) demonstrated that assimilation of upper crustal Precambrian wall rock was important in the Bitterroot lobe magmas, the mixing trends for the main-phase granitoids indicate that the magmatic end member has r_i values (about 0.708) and Rb/Sr ratios that are much too high to characterize materials derived from depleted mantle. Fleck and Criss (1985) proposed that the main-phase magmas primarily

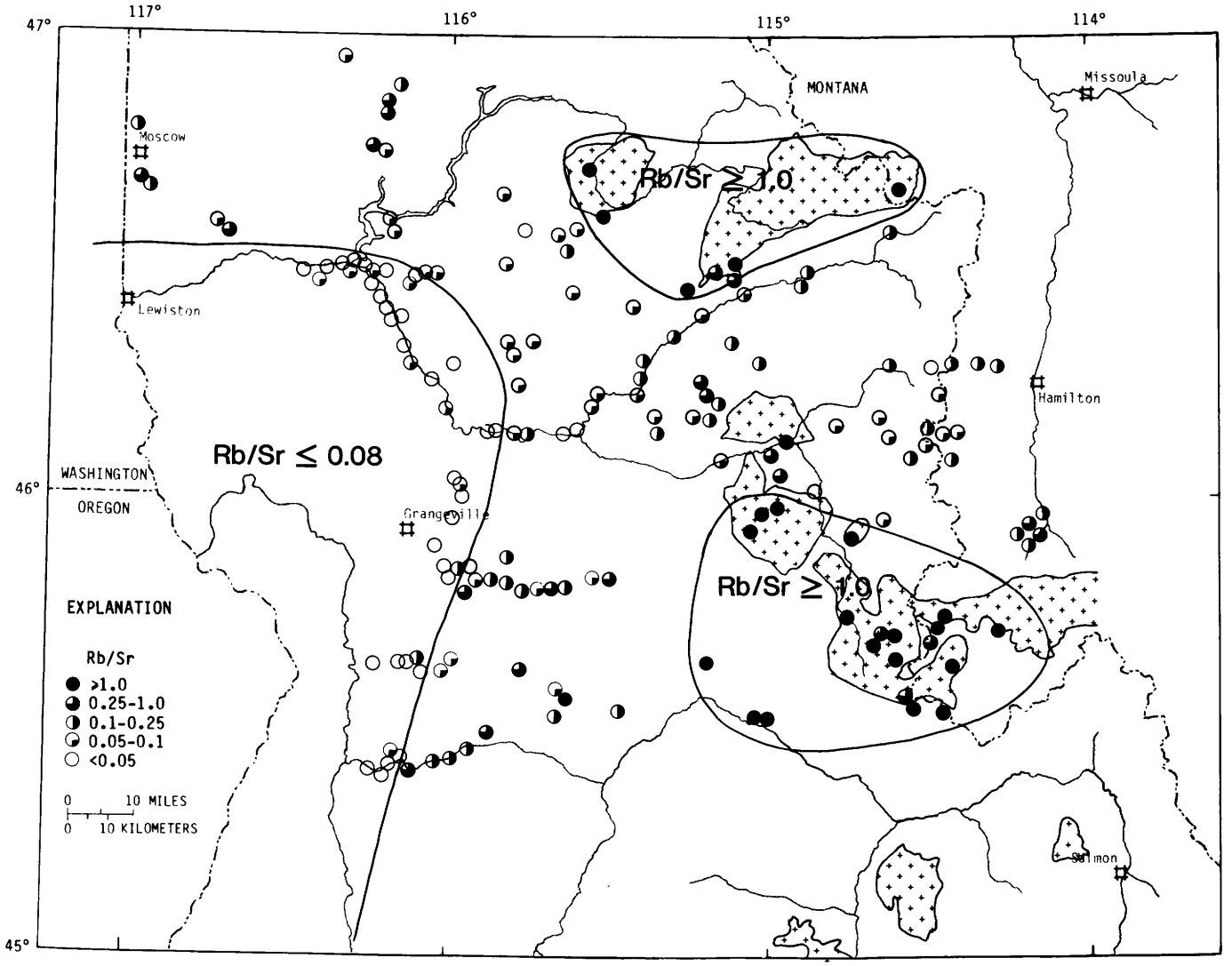

FIGURE 6.3.—Contour map showing the distribution of Rb/Sr concentration (weight) ratios for the plutons of north-central Idaho. The Jurassic and Cretaceous plutons in the Wallowa-Seven Devils terrane typically have Rb/Sr ratios $\leq$0.05, with most values being <0.08, whereas those for the Eocene epizonal plutons (+ pattern) are typically >1. Ratios for the main-phase plutons of the Bitterroot and Atlanta lobes are intermediate, ranging from 0.06 to 0.24 in most samples.

TABLE 6.2.—*Chemical analyses of granitic plutons from the northern Idaho batholith*

[Rapid rock analyses by Z.A. Hamlin and Nancy Skinner, U.S. Geological Survey]

Sample--	787-18A	787-18B	787-18C	787-18D	787-18E	787-18F	787-18G	787-18H	787-18I	787-18J
SiO_2----	71.1	71.0	72.3	73.3	71.3	71.4	71.4	69.1	67.4	75.2
Al_2O_3---	15.0	15.4	14.9	14.4	15.1	15.2	15.0	15.2	16.6	12.7
Fe_2O_3---	.96	.81	.97	.52	.64	.67	.58	.80	1.0	.76
FeO-----	.96	.84	.68	.64	.64	.76	.96	1.6	1.5	.72
MgO-----	.43	.39	.36	.30	.31	.36	.75	1.1	.62	.17
CaO-----	2.7	2.2	2.1	2.3	2.3	2.4	2.8	3.3	3.8	1.1
Na_2O----	4.0	4.3	4.5	4.6	4.4	4.4	4.1	4.1	4.6	4.0
K_2O-----	3.6	4.2	3.9	3.6	4.1	3.7	3.0	2.5	2.6	4.8
H_2O^+----	.43	.48	.43	.34	.40	.51	.79	.88	.54	.41
H_2O^-----	.10	.08	.10	.09	.06	.02	.09	.10	.12	.10
TiO_2----	.27	.22	.13	.12	.18	.22	.27	.38	.29	.18
P_2O_5----	.14	.09	.11	.08	.15	.09	.11	.15	.18	.06
MnO-----	.03	.03	.02	.02	.01	.02	.03	.03	.05	.04
CO_2-----	.03	.01	.01	.02	.02	.03	.01	.01	.02	.01
Total-	100	100	100	100	100	100	100	99	99	100

Sample--	787-19C	787-19E	787-19G	787-20A	787-20B*	787-20C	787-20D	787-20E	787-21A	787-21B
SiO_2----	62.1	57.6	72.7	63.7	73.0	70.9	65.8	64.8	68.7	76.3
Al_2O_3---	16.2	17.3	13.7	16.1	11.0	15.1	17.1	17.0	15.2	12.5
Fe_2O_3---	1.6	2.5	.97	2.8	.49	.42	1.1	1.6	.85	.64
FeO-----	3.4	5.0	.56	3.5	.88	1.3	2.2	2.6	1.7	.40
MgO-----	2.6	3.1	.25	2.0	4.2	.65	1.5	1.7	.96	.01
CaO-----	5.4	6.2	1.5	4.4	4.8	1.3	4.1	4.3	2.5	.29
Na_2O----	3.6	3.7	3.1	4.0	3.7	2.8	4.2	4.0	3.8	3.6
K_2O-----	2.2	2.3	5.4	2.1	.52	5.4	2.0	2.0	4.0	5.1
H_2O^+----	1.1	1.1	.52	.94	.36	.87	.74	.87	.80	.64
H_2O^-----	.17	.08	.16	.12	.04	.10	.08	.05	.07	.18
TiO_2----	.70	.96	.16	.79	.50	.26	.54	.64	.55	.09
P_2O_5----	.23	.30	.16	.40	.17	.17	.29	.27	.24	.10
MnO-----	.08	.09	.01	.08	.02	.02	.05	.07	.04	.01
CO_2-----	.02	.00	.01	.00	.01	.01	.01	.04	.01	.01
Total-	99	100	99	101	100	99	100	100	99	100

Sample--	787-21C	787-21D	787-21E	787-21F	787-24A	787-24B	787-24C	787-24D	787-24E	787-24F
SiO_2----	75.5	73.8	68.2	69.3	70.9	70.1	69.7	72.1	71.9	71.5
Al_2O_3---	12.4	13.2	17.1	16.1	15.5	15.9	16.2	14.9	15.1	15.1
Fe_2O_3---	.78	0.45	.91	.98	.68	.71	.79	0.56	.56	.69
FeO-----	.64	1.1	.92	1.0	.84	.84	.96	0.84	.68	.68
MgO-----	.03	.27	.45	.47	.40	.43	.43	0.31	.28	.26
CaO-----	.59	1.2	2.9	2.7	2.4	2.9	2.6	2.4	2.5	2.5
Na_2O----	3.8	3.6	5.1	4.6	4.5	4.9	4.6	4.3	4.5	4.3
K_2O-----	4.9	4.7	3.0	3.8	3.8	3.1	4.0	3.8	3.8	4.3
H_2O^+----	.51	.55	.61	.52	.58	.62	.52	.52	.55	.45
H_2O^-----	.09	.09	.03	.07	.08	.14	.10	.11	.11	.11
TiO_2----	.19	.23	.29	.26	.23	.23	0.26	.21	.20	.22
P_2O_5----	.10	.14	.14	.18	.16	.20	0.18	.15	.12	.15
MnO-----	.02	.02	.02	.03	.01	.02	0.02	.01	.02	.01
CO_2-----	.02	.02	.02	.01	.01	.01	0.01	.01	.01	.00
Total-	100	99	100	100	100	100	100	100	100	100

Sample--	787-24G	787-24I	787-25A	787-25C	787-26A	787-26B	787-26C	787-26D	787-26E	787-26F
SiO_2----	54.9	70.8	72.1	66.5	67.0	67.6	70.9	66.1	66.9	64.0
Al_2O_3---	17.0	15.2	14.1	16.9	15.3	14.5	14.9	17.4	15.4	16.0
Fe_2O_3---	1.7	.74	1.6	.77	1.4	1.9	1.2	.68	1.5	1.6
FeO-----	6.7	1.3	.92	1.8	2.3	2.5	1.9	2.2	2.2	3.7
MgO-----	3.4	.92	.11	1.4	1.4	1.6	0.97	1.5	1.4	2.7
CaO-----	7.1	2.7	1.5	3.5	3.8	4.4	4.5	4.7	3.8	4.9
Na_2O----	3.7	4.3	4.0	4.8	4.1	4.2	4.0	4.8	4.0	3.5
K_2O-----	2.3	3.6	5.7	3.4	3.9	2.4	1.3	1.5	4.1	2.3
H_2O^+----	1.2	.51	.61	.68	.66	.77	.75	.66	.61	1.0
H_2O^-----	.14	.07	.14	.10	.09	.10	.10	.14	.09	.09
TiO_2----	2.4	.31	.27	.46	.53	.63	.44	.55	.45	.82
P_2O_5----	.45	.15	.12	.19	.26	.29	.23	.26	.22	.32
MnO-----	.09	.02	.05	.03	.06	.09	.02	.03	.06	.06
CO_2-----	.00	.01	.02	.01	.05	.02	.19	.04	.05	.05
Total-	101	101	101	100	101	101	101	100	101	101

*Precambrian (?) metasedimentary rock.

originated from melting of ancient continental basement. Available data also indicate a significant Precambrian component in the Eocene plutons (Armstrong, 1974; Chase and others, 1978; Fleck and Criss, 1985), but do not completely deny the existence of a mantle component.

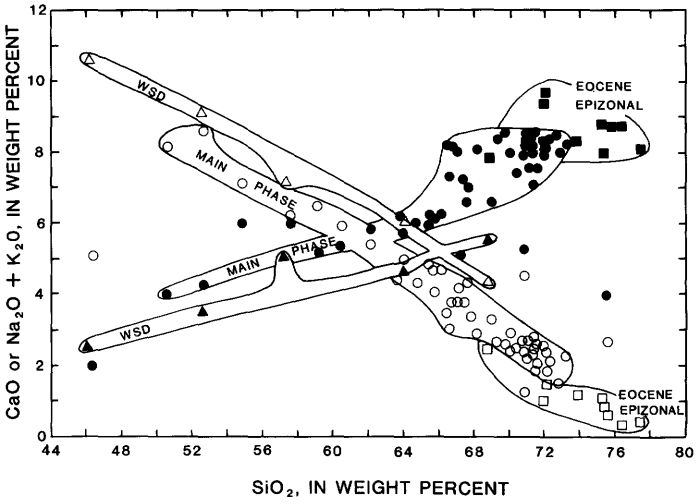

FIGURE 6.4.—Variation diagram of Mesozoic and Tertiary plutons of north-central Idaho showing total alkalis ($Na_2O + K_2O$, solid symbols) and CaO (open symbols) plotted against SiO_2. The calcic trend of the low-r_i WSD plutons (triangles) contrasts with the calcic to calc-alkaline trend of the Precambrian-hosted plutons in the Bitterroot lobe, including both the main-phase (circles) and Eocene epizonal plutons (squares). Analyses are from Lindgren (1904), Hietanen (1962, 1963), Larsen and Schmidt (1958), Ross (1934), and table 6.2.

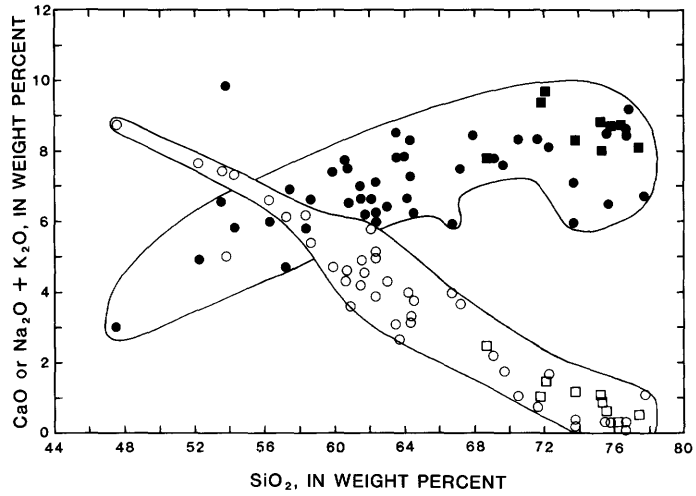

FIGURE 6.5.—Variation diagram showing that Eocene epizonal granitoids conform to the calc-alkaline trend defined by the Challis Volcanics. Volcanic-rock analyses (circles) are from Ross (1962) and McIntyre and others (1982); granitoid analyses (squares) are from the same references listed in figure 6.4. Solid symbols, $Na_2O + K_2O$; open symbols, CaO.

In fact, some values near 0.704 (table 6.1) suggest only minor contamination by either upper or lower sialic crust.

The r_i and $\delta^{18}O$ relations of the WSD samples are distinctly different from those of the Bitterroot lobe (fig. 6.8). The data points for these samples generally fall within the PRB band, but their flat trend is most similar to that of the Klamath Mountains granitoids. The relatively high $\delta^{18}O$ values of some samples (as high as +10.5 per mil; sample 807-27A) may reflect either incorporation of or exchange with high-^{18}O materials, or low-temperature alteration, but the uniformly low r_i values preclude significant participation of ancient sialic material. The isotopic relations strongly suggest that the WSD plutons were derived from island-arc or other mantle components.

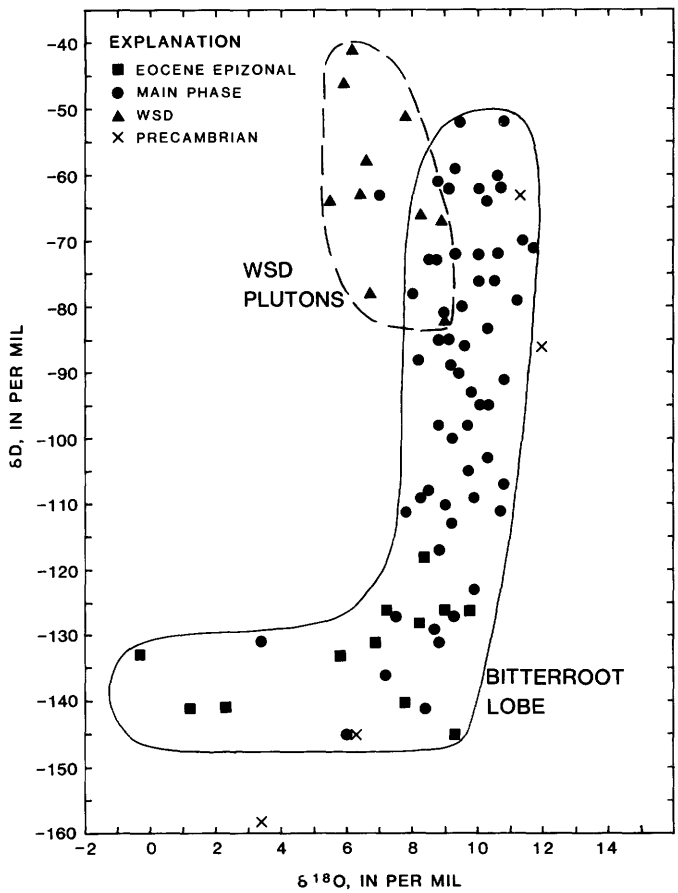

FIGURE 6.6.—Relation of $\delta^{18}O$ to δD for plutonic rocks of north-central Idaho. Rocks with the highest δD values are unaltered; these are low-r_i plutons in the Wallowa-Seven Devils terrane and main-phase plutons in the Bitterroot lobe that are remote from Eocene epizonal plutons. Because of interactions with meteoric-hydrothermal fluids, the epizonal plutons and their adjacent country rocks are significantly depleted in δD. Where δD is most depleted ($\delta D \leq -120$ per mil) the $\delta^{18}O$ values are lowered as well.

CRETACEOUS-EARLY TERTIARY AND EOCENE HYDROTHERMAL SYSTEMS

REGIONAL VARIATIONS OF δD AND $\delta^{18}O$ VALUES

Geographic variations of δD and $\delta^{18}O$ values provide important information on the location and geologic characteristics of hydrothermal systems (for example, Taylor, 1971, 1977; Taylor and Forester, 1979). Taylor and Magaritz (1978) made a reconnaissance map of δD values of the Idaho batholith and demonstrated the regional extent of Eocene meteoric-hydrothermal activity. Criss and Taylor (1983) used $\delta^{18}O$ data to map several meteoric-hydrothermal systems in the southern Idaho batholith, and Criss and others (1984, 1985) extended this method to the Challis volcanic field. As discussed below, shallow-level, Eocene meteoric-hydrothermal systems as well as deep-level, Cretaceous-early Tertiary metamorphic-hydrothermal systems operated in north-central Idaho.

A contour map of whole-rock δD values illustrates strong geographic variations (fig. 6.9). All WSD plutons, as well as the main-phase granitoids remote from Eocene epizonal plutons, have isotopically normal δD values of ≥ -82 per mil. The primary δD character of these plutons is further supported because the δD contours make the same right-angle bend as do the 0.704 and 0.708 initial-Sr contours of figure 6.2. Another zone of normal δD values occurs in the east-central Bitterroot lobe, immediately west of Hamilton (fig. 6.9). Included in this zone are several mylonized samples, indicating that deep-level penetration of meteoric-hydrothermal fluid was not essential to the development of the mylonite zone. In contrast, extremely low δD values (≤ -120) occur within several zones in the Bitterroot lobe, together constituting more than 7,000 km^2. All low values occur within or near the Eocene epizonal plutons and are indicative of meteoric-hydrothermal systems established during their emplacement, as originally pointed out by Taylor and Magaritz (1978). The most depleted samples (< -140 per mil) occur along the perimeter of these epizonal plutons, which is where the most intense fluid circulation would be expected.

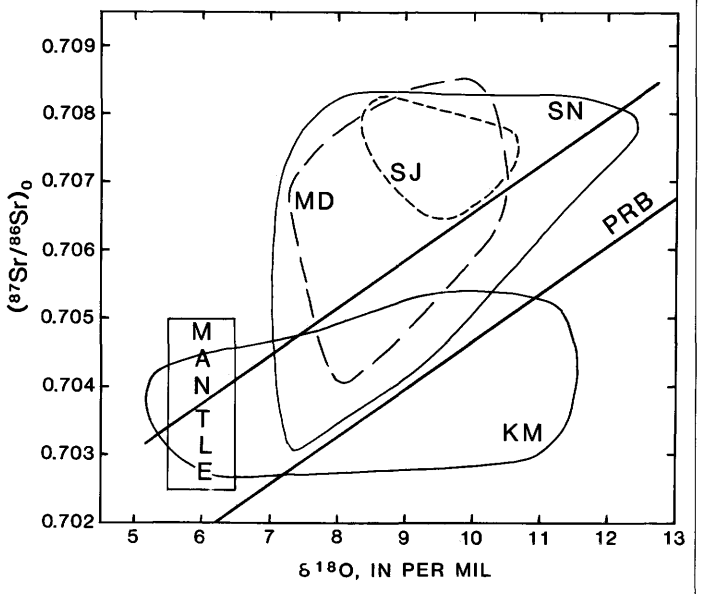

FIGURE 6.7.—Generalized graph of initial $^{87}Sr/^{86}Sr$ (r_i) versus $\delta^{18}O$ delineating granitoids of the Peninsular Ranges batholith (PRB), the San Jacinto block (SJ), the Klamath Mountains (KM), the Mojave Desert (MD), and the Sierra Nevada batholith (SN) from Taylor and Silver (1978) and Masi and others (1981). The San Jacinto, Mojave Desert, and many Sierra Nevada plutons occur in regions underlain by Precambrian wall rock and tend to have the highest r_i values at a given $\delta^{18}O$ content.

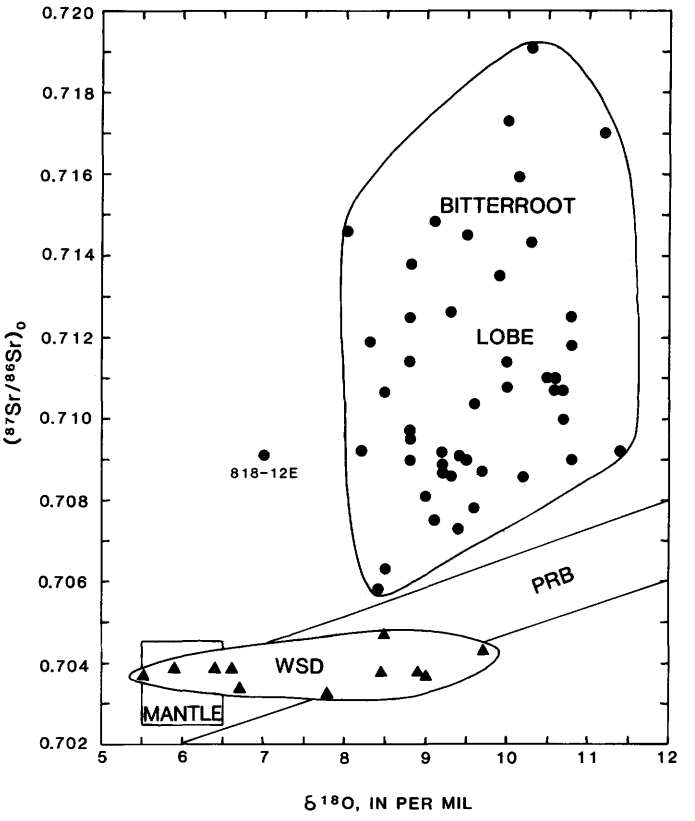

FIGURE 6.8.—Graph of r_i versus $\delta^{18}O$ for the plutons of north-central Idaho. Only essentially unaltered rocks with $\delta D \geq -120$ per mil are shown. Note the significant differences between the low-r_i plutons in the Wallowa-Seven Devils terrane (WSD), the high-r_i plutons in the Bitterroot lobe (including several samples from the northern Atlanta lobe), and the Peninsular Ranges batholith (PRB) trend from figure 6.7. These differences are explicable in terms of the source rocks from which the plutons were derived. Transition-zone samples collected along detailed traverses across the suture-zone boundary (0.704-0.708 line) have been discussed in detail by Fleck and Criss (1985) and are not included here.

Variations of $\delta^{18}O$ values in the plutons of north-central Idaho are illustrated in figure 6.10. With the exception of a few WSD plutons whose rather low $\delta^{18}O$ values are probably primary, all $\delta^{18}O$ values less than +8.0 per mil occur within the zones of extreme deuterium depletion in the Bitterroot lobe and are related to the meteoric-hydrothermal systems. High water/rock ratios of unity or greater are required to produce the most extreme $\delta^{18}O$ values (as low as −0.3 per mil). As discussed in the subsection "$\delta^{18}O$ and δD data," the high water-rock ratios that are required to produce significant $^{18}O/^{16}O$ changes in rocks demand complete reequilibration of D/H ratios, thus accounting for the observed spatial correspondence between low $\delta^{18}O$ and low δD values.

The zones of ^{18}O depletion in the plutons of the Bitterroot lobe are much smaller than the meteoric-hydrothermal systems mapped by Criss and Taylor (1983) in the southern Idaho batholith, many of which encompass several thousand square kilometers. Furthermore, the most extreme $\delta^{18}O$ values in the Bitterroot lobe are not as low as some of those observed farther south, several of which are −4.0 or less (Criss and Taylor, 1983). Petrographic examination of thin sections reveals that the propylitic alteration that generally attends moderate-temperature water-rock interactions is not as widespread or intense in the Bitterroot lobe as that observed in the southern Idaho batholith. These observations cannot simply be explained by a reduced volume of Eocene

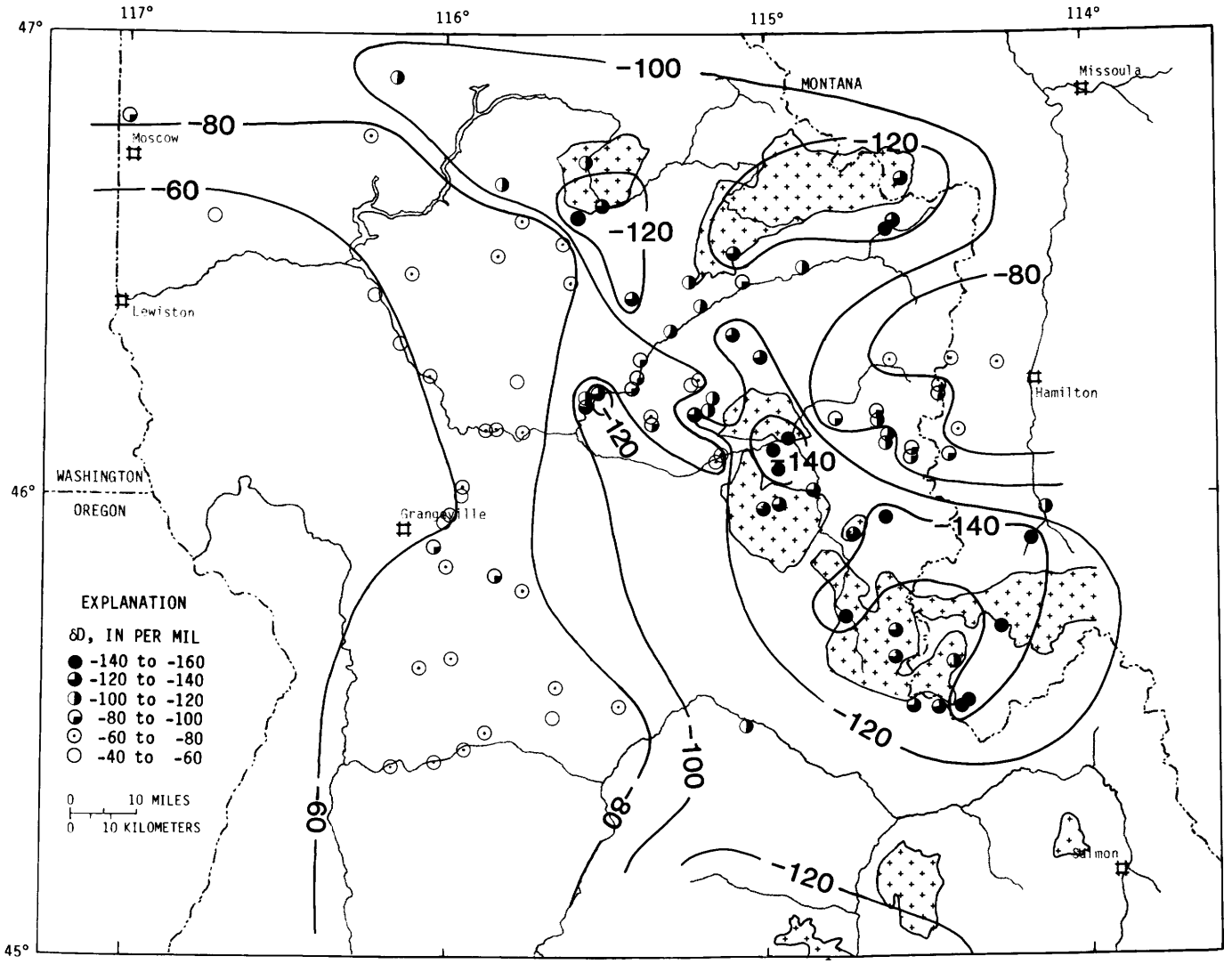

FIGURE 6.9.—Contour map of whole-rock δD values for the plutons of north-central Idaho. Relatively high (≥ -82 per mil) δD values of the plutons in the Wallowa-Seven Devils terrane are thought to be primary; note that the contours make a similar right-angle bend as do the 0.704 and 0.708 initial strontium contours shown in figure 6.2. High δD values also occur in the Bitterroot lobe at positions remote from the Eocene epizonal plutons (pattern). In contrast, marked δD depletions (≤ -120 per mil) caused by meteoric-hydrothermal alteration processes occur within and near the epizonal intrusions.

epizonal plutons in the north. In fact, recent mapping by Toth and others (1983) shows that the epizonal plutons are at least as areally abundant in the Bitterroot lobe as in the Atlanta lobe.

On the other hand, the age and temperature contrasts between host rocks and epizonal plutons in the Bitterroot lobe were almost certainly less than those of the Atlanta lobe. McDowell and Kulp (1969), Armstrong and others (1977), and Criss and others (1982) report biotite K-Ar ages of 70 to 60 Ma for most of the main-phase plutons of the Atlanta lobe, with some ages older than 80 Ma. These authors argue that much of the Atlanta lobe is Cretaceous. In contrast, K-Ar ages of main-phase plutons in the Bitterroot lobe where intruded by the belt of epizonal granites are only slightly older than or equal to those of the granites (62 to 45 Ma as compared to 51 to 44 Ma). Whereas temperature anomalies associated with the older plutonic rocks in the Atlanta lobe would have diminished to the geothermal gradient before emplacement of the Eocene plutons, host-rock temperatures for these epizonal plutons in the Bitterroot lobe would have been significantly higher. We suggest that smaller lateral temperature gradients and lower permeabilities in the Bitterroot lobe resulted in less intense fluid circulation than occurred in the Atlanta lobe.

Evidence for earlier, deep-level metamorphic-hydro-

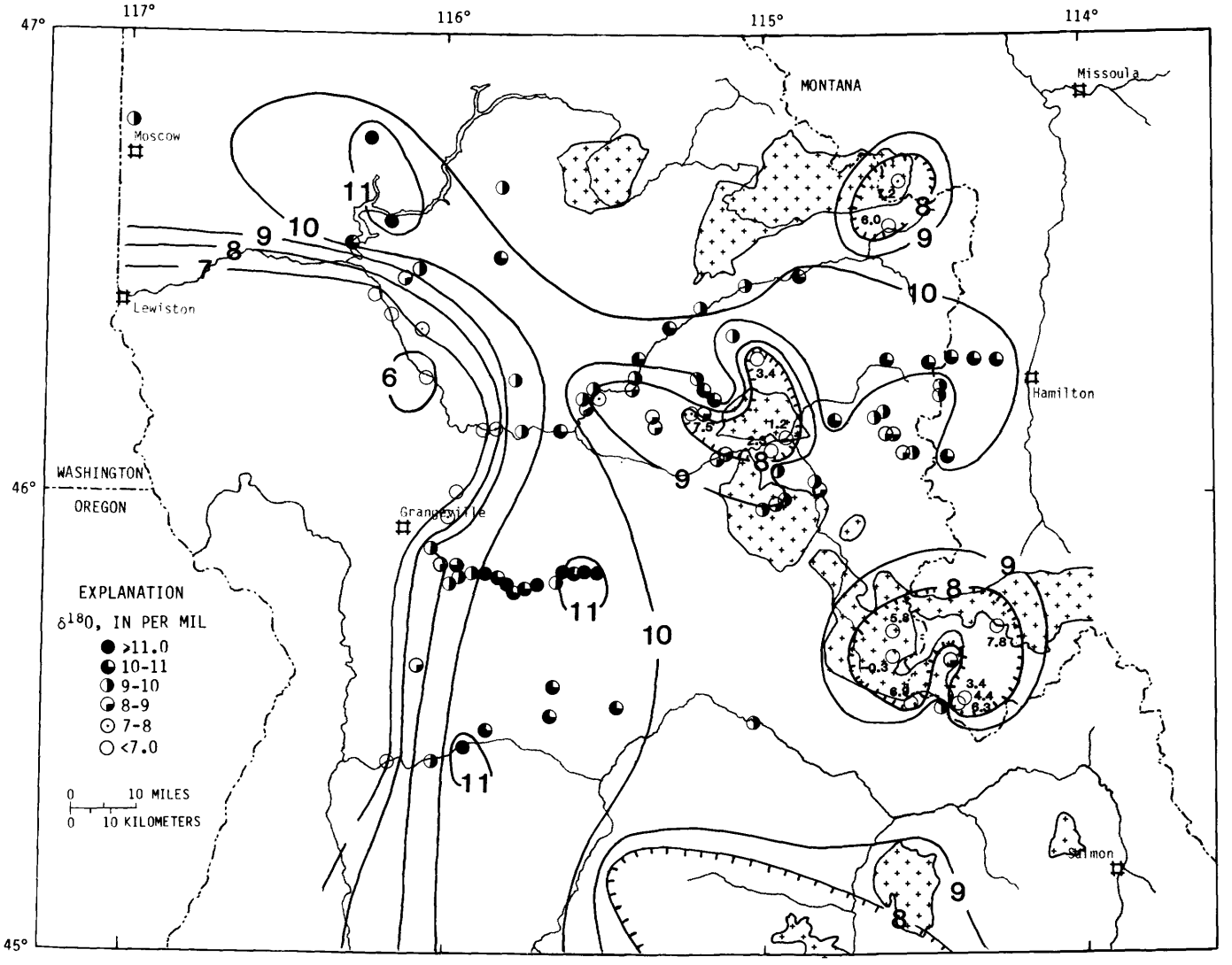

FIGURE 6.10.—Contour map of whole-rock $\delta^{18}O$ values for the plutons of north-central Idaho. Although the $\delta^{18}O$ values for some of the plutons in the Wallowa-Seven Devils terrane are rather low (as low as +5.5 per mil), these values are thought to be primary, partly because the δD values for the rocks are high. Note that the $\delta^{18}O$ contours in this zone make a similar right-angle bend as do the 0.704 and 0.708 initial strontium contours (fig. 6.2) and the −80 per mil δD contour (fig. 6.9). The $\delta^{18}O$ values from the Bitterroot lobe tend to be high ($\geq +8$ per mil) except in the zones of intense meteoric-hydrothermal alteration (hachured contours) within and adjacent to the Eocene epizonal plutons (pattern). Only representative samples are shown along a closely sampled traverse near 45°50′ N., 116° W. (see Fleck and Criss, 1985).

thermal activity is provided by $\delta^{18}O$ analyses of Belt Supergroup (Wallace Formation) pelitic metasedimentary rocks (table 6.3) collected around the north margin of the Bitterroot lobe. The $\delta^{18}O$ values progressively decrease toward the Idaho batholith (fig. 6.11), in the general direction of increasing metamorphic grade (Hietanen, 1962, 1984). Thus, the whole-rock $\delta^{18}O$ values decrease from about $+15 \pm 1$ per mil in the low-grade metamorphic zones at large distances from the batholith outcrop (>60 km) to generally $+11.5 \pm 1$ per mil in the highest grade, sillimanite $\pm$ kyanite zones adjacent to the batholith (fig. 6.11; table 6.3). The latter values are similar to those typical of the Idaho batholith ($+10 \pm 1.5$ per mil), with plutons near metasedimentary wall rock generally having the highest $\delta^{18}O$ values.

Hietanen (1984) and Lang and Rice (1985) recognize both synkinematic and postkinematic metamorphism in the region north of the Bitterroot lobe, with the later, higher temperature metamorphism and associated metasomatic effects being related to batholith intrusion. It is probable that the ^{18}O reductions in the metasedimentary rocks were principally produced during this later metamorphism, apparently in Cretaceous-early Tertiary time. Note that Fleck and Criss (1985) observed a similar approach to ^{18}O homogenization between plutons and adjacent wall rock along the west side of the Idaho batholith and argued that most of the indicated ^{18}O exchange occurred during emplacement of the Late Cretaceous plutons.

The large scale of ^{18}O exchange observed in the Wallace Formation metasedimentary rocks clearly indicates fluid migration rather than diffusion as the dominant transport process. The observations are consistent with convective circulation of high-^{18}O fluid, probably derived from metamorphic dehydration, connate sources, and magmatic water, mostly during batholith emplacement and associated postkinematic regional metamorphism. General correlations between $\delta^{18}O$ values and metamorphic grade have been observed in other areas by Garlick and Epstein (1967) and Dontsova (1970); ^{18}O exchange between igneous plutons and metasedimentary wall rock has been documented by Shieh and Taylor (1969) and Turi and Taylor (1971); and large-scale homogenization of oxygen isotopes among various rocks of high-grade metamorphic terranes has been reported by Taylor (1970), Shieh and Schwarcz (1974), and Hoernes and Friedrichsen (1980). The oxygen isotopic exchange was probably effected by high-temperature, high-^{18}O aqueous fluid in all of these cases.

COMPARISON OF δD AND AEROMAGNETIC MAPS

Several workers have pointed out that the Eocene epizonal plutons in the Idaho batholith region are commonly associated with positive magnetic anomalies (Kiilsgaard and others, 1970; Cater and others, 1973; Tschanz and others, 1974; Mabey and others, 1978). Criss and Champion (1984) showed that these Eocene plutons generally have much higher magnetic susceptibilities and remanent magnetic intensities than typical pre-Eocene rocks of the southern Idaho batholith interior, although they also outlined some areas that were exceptional. Thus, the aeromagnetic intensity maps of Zietz and others (1978, 1980) can greatly aid deduction of the distribution of the epizonal rocks, particularly in regions that have been mapped only in reconnaissance. Furthermore, in certain cases magnetic intensity maps provide unique interpretative data, such as when subsurface plutons are present. Criss and Taylor (1983) and Criss and Champion (1984) demonstrated a close correlation between the fossil hydrothermal systems (low $\delta^{18}O$ and δD zones) and positive magnetic anomalies in the southern Idaho batholith; this correlation was in some areas better than that between the isotopic data and geologic maps.

As regards the present investigations, however, a good correlation between aeromagnetic anomalies (Zietz and others, 1978, 1980) and δD values was found only in the southern part of the Bitterroot lobe (fig. 6.12). Most of the lowest δD values occur along and within the large, northwest-trending positive aeromagnetic anomaly (fig. 6.12, features A and B). Feature A clearly overlaps the outcrop of the epizonal Painted Rocks pluton. The Running Creek pluton lies along the same magnetic trend immediately to the northwest, between features A and B. Feature B is not clearly related to a mapped Eocene pluton, and a normal δD value of -73 per mil that occurs nearby is enigmatic. However, the only extremely low δD values in the western Bitterroot lobe lie on the northwest shoulder of feature B, on the Lochsa River near Lowell. It is possible that Eocene material, possibly present only in the subsurface, is at least partly responsible for feature B. The Whistling Pig and Paradise plutons (see map by Toth and others, 1983) occur along the north margin of the large aeromagnetic anomaly (A and B), but are not clearly related to it. Extremely low δD values occur within and near the Whistling Pig pluton. Pronounced hydrothermal effects are not associated with the Paradise pluton, but this Eocene intrusion was emplaced at a relatively deep level and probably is best referred to the main-phase group.

On the other hand, the correlation between positive magnetic anomalies and δD values is extremely poor in the main north-central mass of the Bitterroot lobe. Two large Eocene plutons, the Lolo Hot Springs and the Bungalow (see fig. 6.1), have been mapped in this region and both are associated with low δD values. Neither of these plutons is associated with a significant magnetic anomaly, and a rather intense positive anomaly nearby (feature C) is not clearly associated with a mapped Eocene

TABLE 6.3.—*Rb-Sr and $\delta^{18}O$ analyses of Wallace Formation metasedimentary rocks*

[Rb and Sr concentrations in parentheses are Kevex determinations; all others are by isotope dilution; †, diorite dike]

Sample	North latitude	West longitude	Rb (ppm)	Sr (ppm)	$^{87}Rb/^{86}Sr$	$^{87}Sr/^{86}Sr$	$\delta^{18}O$ (per mil)
68-9-10B	46°35.3'	115°47.8'	153.1	59.24	7.6016	0.88137	13.2
-10C	46°35.3'	115°47.8'	176.6	31.14	16.6532	.86190	12.1
-10D	46°35.3'	115°47.8'	159.6	27.15	17.2654	.86493	12.6
-11B	46°47.0'	115°49.3'	105.0	45.86	6.6694	.77983	11.8
-11C	46°47.0'	115°49.3'	(113.0)	32.74	10.0371	.75960	10.5
-11D	46°47.0'	115°49.6'	129.0	79.45	4.7066	.72518	10.8
-12A	46°49.8'	116°06.2'	153.5	58.68	4.6088	.76146	11.2
-12B	46°54.2'	116°06.9'	183.3	84.05	6.3750	.81509	12.0
-12C	46°54.3'	116°07.0'	213.5	68.91	9.0472	.80484	12.2
-12D	46°54.7'	116°09.6'	(164.8)	49.90	9.6844	.84696	11.3
-12E	47°00.3'	116°11.1'	179.8	(64.61)	--	--	12.7
-12F	47°00.5'	116°13.0'	178.2	(14.19)	--	--	12.7
-12G	47°05.2'	116°21.0'	200.0	48.57	12.1844	.93915	9.4
-12H	47°28.0'	116°34.6'	207.1	70.13	8.6346	.81470	12.7
-13A	47°28.4'	115°55.3'	(271.6)	14.43	56.5910	1.10938	15.0
-13B	47°25.8'	115°53.5'	(151.2)	29.93	14.8983	.90732	14.5
-13C	47°25.9'	115°53.7'	(154.6)	19.26	24.1304	1.10367	15.9
-13D	47°26.0'	115°54.3'	(190.1)	20.97	27.0060	1.01210	14.5
69-7-1A	47°00.7'	116°18.8'	98.8	23.16	12.4778	.81811	12.5
-1B	47°00.7'	116°19.1'	(75.4)	(66.55)	--	--	11.0
-1C	47°00.4'	116°20.8'	205.6	219.2	2.7356	.79272	12.0
-1D	47°00.2'	116°21.0'	187.6	51.84	10.6583	.88874	11.8
-1E	47°03.3'	116°19.4'	160.5	97.73	4.8018	.81628	11.7
-2A	47°12.1'	115°12.0'	171.0	(32.25)	15.34	.93207	13.0
-2B	47°11.9'	115°12.0'	146.7	31.59	13.8030	.98966	13.4
-2C†	47°11.7'	115°11.9'	(34.0)	(905.65)	.1108	.70689	8.6
-3A	47°04.1'	115°21.3'	165.5		--	--	12.8
-3B	47°04.9'	115°21.5'	181.1	46.40	11.5007	.89554	12.7
-3C	47°04.6'	115°21.8'	175.2	49.80	10.4310	.96188	12.6
-3D	47°04.4'	115°22.2'	105.0	110.20	2.7835	.80377	12.4
-3E	47°04.2'	115°22.5'	(179.4)	58.85	6.9685	.87788	12.1
-3F	47°04.2'	115°23.5'	(112.8)	45.31	7.2868	.82518	12.9
-3G	47°04.1'	115°24.0'	(167.0)	56.84	8.6070	.83663	12.5
-3H	47°04.0'	115°24.5'	(169.5)	73.25	6.7723	.82608	11.3
-3I	47°04.0'	115°25.3'	(164.3)	40.56	12.3187	.91093	12.4
-3J	47°03.9'	115°25.9'	(180.4)	64.05	8.2573	.84073	12.5
-3K	47°03.8'	115°26.5'	(166.4)	(113.91)	--	--	12.6
-3l	47°03.8'	115°26.9'	(204.7)	(71.69)	8.3664	.83696	12.0
-3M	47°03.5'	115°27.7'	(153.5)	99.61	4.4998	.80009	12.5
-4A	47°06.0'	115°30.9'	(149.8)	84.66	5.1640	.79654	12.5
-4B	47°06.5'	115°30.7'	151.5	73.56	6.0188	.81153	12.8
-4C	47°08.1'	115°29.2'	171.8	(71.41)	--	--	12.8
-4D	47°09.0'	115°27.9'	(193.5)	(102.09)	--	--	12.4
-4E	47°05.9'	115°30.8'	(207.2)	115.69	5.2369	.81582	12.0
-4F	47°05.5'	115°32.1'	(166.6)	61.24	7.9781	.84686	12.5
-5A	47°06.5'	115°35.9'	(156.4)	82.59	5.5264	.79407	13.3
-5B	47°17.4'	115°46.4'	(165.7)	(24.85)	--	--	15.5
-5C	47°16.3'	115°46.3'	(138.2)	76.31	5.2889	.80654	15.2
-5D	47°16.1'	115°46.4'	--	--	--	--	14.3

epizonal pluton or with low δD values. In addition, the large positive anomaly immediately west of the Bitterroot lobe (feature D) generally coincides with exposures of the Tertiary Columbia River Basalt Group; such rocks would be expected to have high magnetic susceptibilities and high remanent magnetizations. Several small anomalies south of feature D apparently reflect varying volcanic and plutonic lithologies of the WSD terrane and the transition zone.

Many of the above inconsistencies can be resolved by comparing the aeromagnetic anomalies to limited magnetic susceptibility data for the plutons (fig. 6.13). Although these data are preliminary, it is evident that extremely low magnetic susceptibilities are typical of the western and northern parts of the Bitterroot lobe. The absence of positive anomalies and the extremely low magnetic relief of such areas indicates that the low-susceptibility rocks extend to great depths. Most of these low-susceptibility samples represent main-phase plutons, but a surprising number come from Eocene plutons. Much higher susceptibilities occur in the east-central part of the Bitterroot lobe, within a zone partly associated with the

northwest-trending anomaly A-B (see fig. 6.12). An important and unexpected feature is that this high-susceptibility population is primarily composed of main-phase plutons, with the Eocene epizonal plutons generally having only moderate to low susceptibilities. Possibly, many of these main-phase rocks have enhanced susceptibilities due to Eocene alteration (see Criss and Champion, 1984), but further study is needed. In any case, no distinct susceptibility contrast exists between Eocene and older plutons in the Bitterroot lobe, in contrast to overall relations in the Atlanta lobe. Positive aeromagnetic anomalies and high magnetic susceptibilities are therefore not clearcut indicators of Eocene epizonal plutons in the northern Idaho batholith.

RELATION OF ORE DEPOSITS TO THE HYDROTHERMAL SYSTEMS

Following the discovery by Ross (1928, 1934) that Tertiary as well as Mesozoic plutonism was important in central Idaho, most workers have recognized that significant ore deposits were formed during both magmatic episodes (for example, Ross, 1931; Finch, 1932; Bergendahl, 1964; McIntyre and others, 1976). Ross (1931) believed that most central Idaho deposits are Mesozoic and related to the Idaho batholith; however, Anderson (1951) argued that most ores in the region are Tertiary and that the Idaho batholith was metallogenically insignificant. On the other hand, Finch (1932) concluded that most gold mineralization in north-central Idaho (for example, near Elk City and Warren) is related to the Idaho batholith, insofar as the deposits are mesothermal and generally occur near roof pendants, whereas most gold deposits in south-central Idaho are epithermal and related to younger magmas.

Stable-isotope data have considerable bearing on the genesis and probable ages of ore deposits in central Idaho. Criss and Taylor (1983) argued that most ore deposits in the southern half of the Idaho batholith are Tertiary because they are spatially associated with large zones of anomalous $\delta^{18}O$ values, generally related to shallow-level,

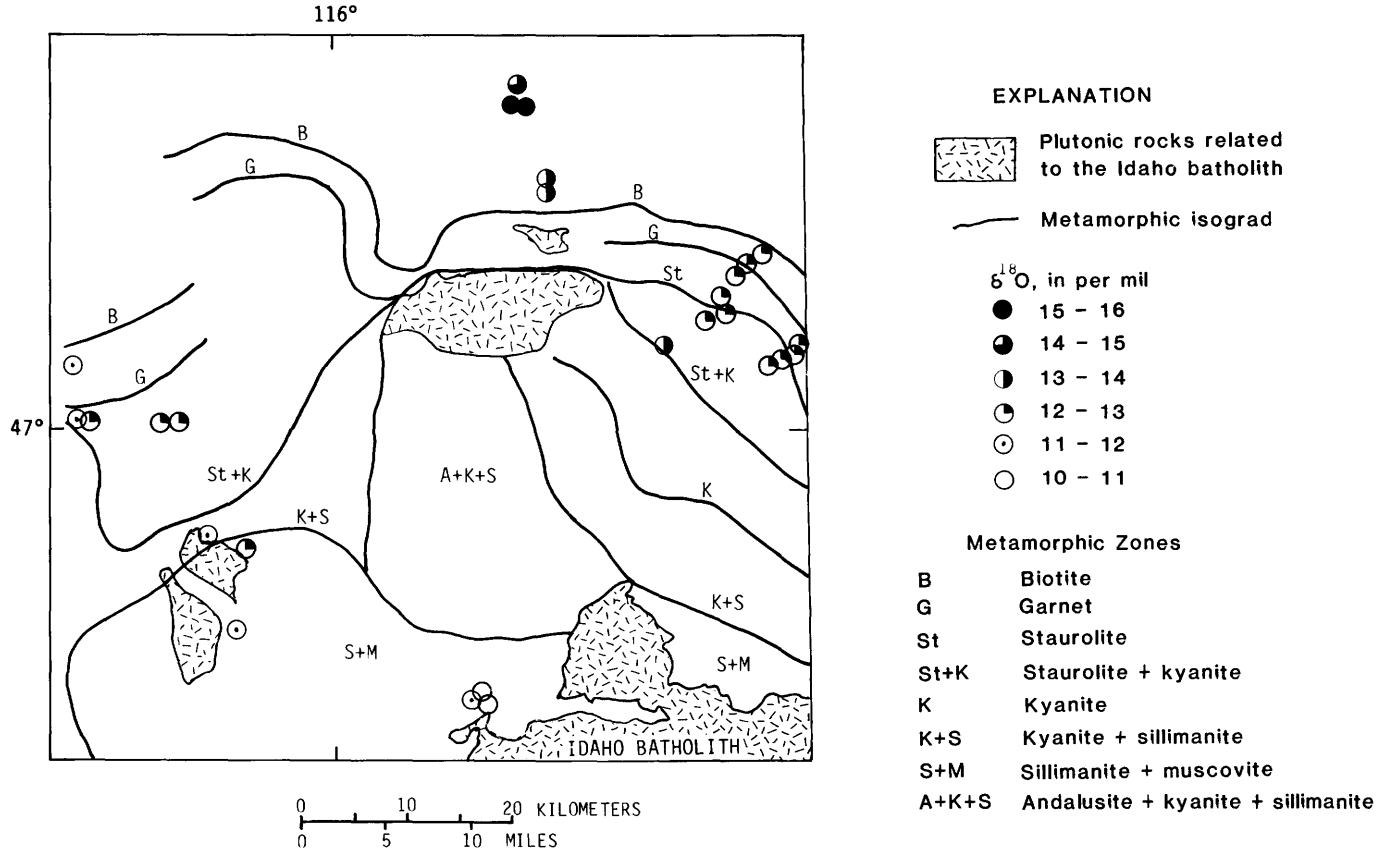

FIGURE 6.11.—Whole-rock $\delta^{18}O$ analyses of Belt Supergroup (Wallace Formation) pelitic metasedimentary rocks plotted on the metamorphic isograd map of Hietanen (1984). The $\delta^{18}O$ values decrease progressively toward the north margin of the Idaho batholith. These data indicate widespread and pervasive exchange of the metasedimentary rocks with the plutonic rocks and with high-^{18}O fluids during Cretaceous-early Tertiary time.

Tertiary meteoric-hydrothermal systems. In this regard, the deposits are similar to epithermal gold- and silver-bearing veins that occur in the Challis Volcanics (Criss and others 1984, 1985) as well as in even younger volcanic rocks at Silver City (Criss, unpub. data, 1983), all of which are irrefutably Tertiary in age. The following discussion, however, demonstrates that only minor mineralization is associated with the relatively weak Eocene meteoric-hydrothermal systems in the Bitterroot lobe, but that significant mineralization is more likely related to deep-level hydrothermal activity related to emplacement of the main-phase Cretaceous-early Tertiary plutons. The overall situation may therefore be similar to that envisaged by Finch (1932).

In order to evaluate mineral controls in the Idaho batholith, figure 6.14 was prepared to show the distribution of mines and prospects in the region, based on data compiled by Mitchell and others (1981a, b) in Idaho. In constructing this figure an attempt has been made to delete placer deposits, stone quarries, sedimentary deposits, and a few pegmatitic and metamorphic deposits, but the data are otherwise unedited. Very few of the deposits shown in figure 6.14 were productive and even fewer were significant, but no attempt is made here to evaluate the impor-

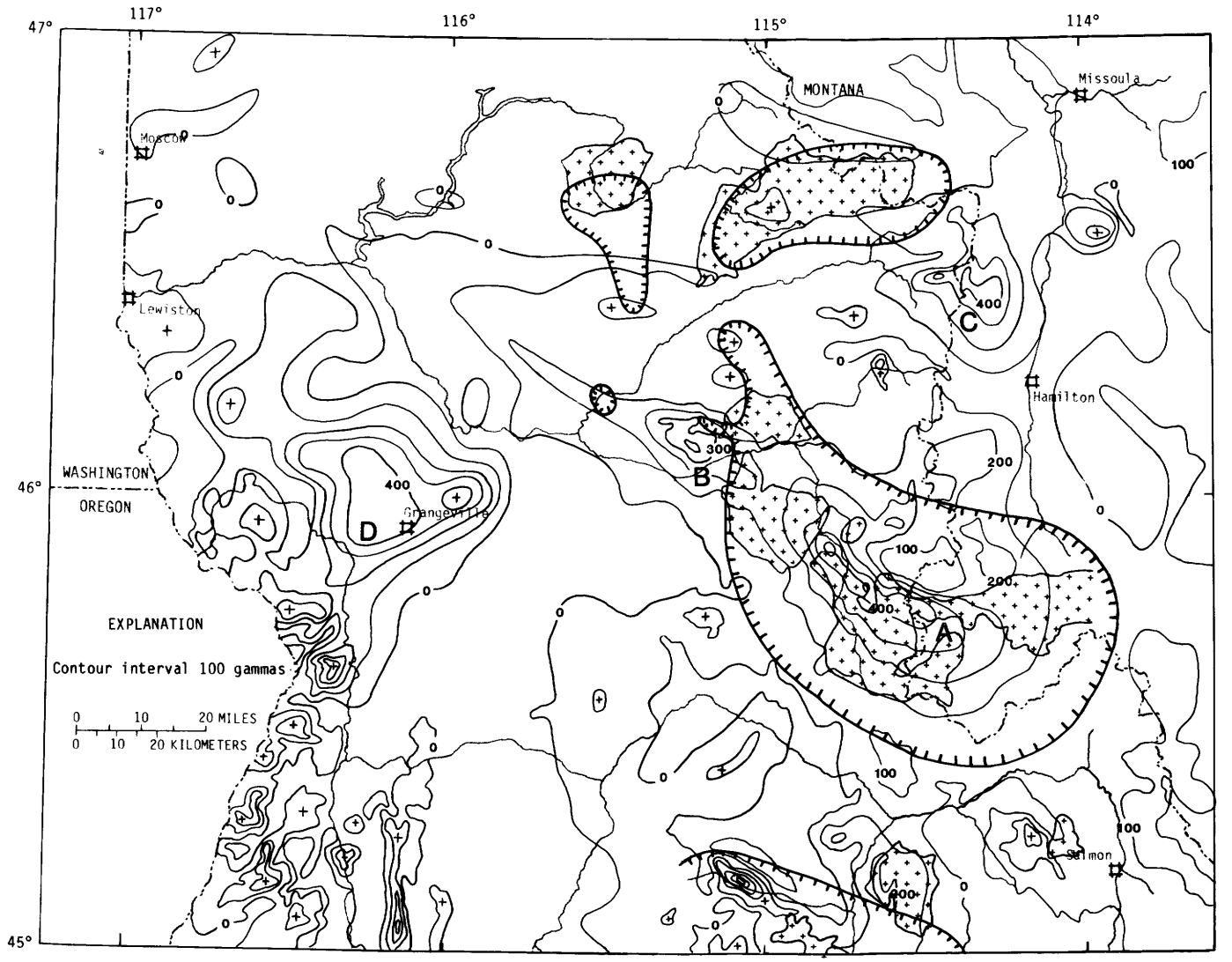

FIGURE 6.12.—Relation of positive aeromagnetic anomalies to the −120 per mil δD contour (hachured line, from fig. 6.9) in the northern Idaho batholith and adjacent areas. The 11,000-gamma contour of Zeitz and others (1978, 1980) is shown as the 0-gamma contour on this map. In places where the magnetic anomalies and the low-δD values are proximal (features A and B) the magnetic anomalies are probably related to Eocene granitoids with high magnetic susceptibilities. However, positive aeromagnetic anomalies are not associated with the low-δD Bungalow and Lolo Hot Springs plutons (see fig. 6.1). Other positive aeromagnetic anomalies in the region (C, D) are probably related to different sources (Columbia River basalt for D?).

tance of individual deposits. It can be assumed, however, that the areas around the most important mines were the most actively explored, so the density of points on figure 6.14 does give some indication of mineral potential.

Lindgren (1904) originally emphasized that the Bitterroot lobe is remarkably devoid of economic mineral deposits. Figure 6.14 clearly shows that most of the ore deposits are near the margins of the Bitterroot lobe, principally within highly metamorphosed Precambrian host rocks or within areas where screens and roof pendants of such rocks are closely interspersed with the batholith. This relation, combined with the nearly complete absence of correlation of the deposits to the low δD zones, suggests that most of the mineralization is related to emplacement of the main phase of the batholith rather than to the Eocene hydrothermal systems. This observation further suggests that most of the ore deposits in fact predate emplacement of the Eocene plutons; note that Snee and others (1985) have recently reported $^{40}Ar/^{39}Ar$ ages of 78 to 71 Ma for muscovites from gold-bearing quartz veins from several mining districts in north-central Idaho. As discussed above, the significant $\delta^{18}O$ depletions in the metasedimentary wall rock surrounding the batholith provide evidence that major deep-level metamorphic-hydrothermal systems existed in the region during Cretaceous-early Tertiary time.

On the other hand, Eocene meteoric-hydrothermal systems are probably responsible for at least a few of the

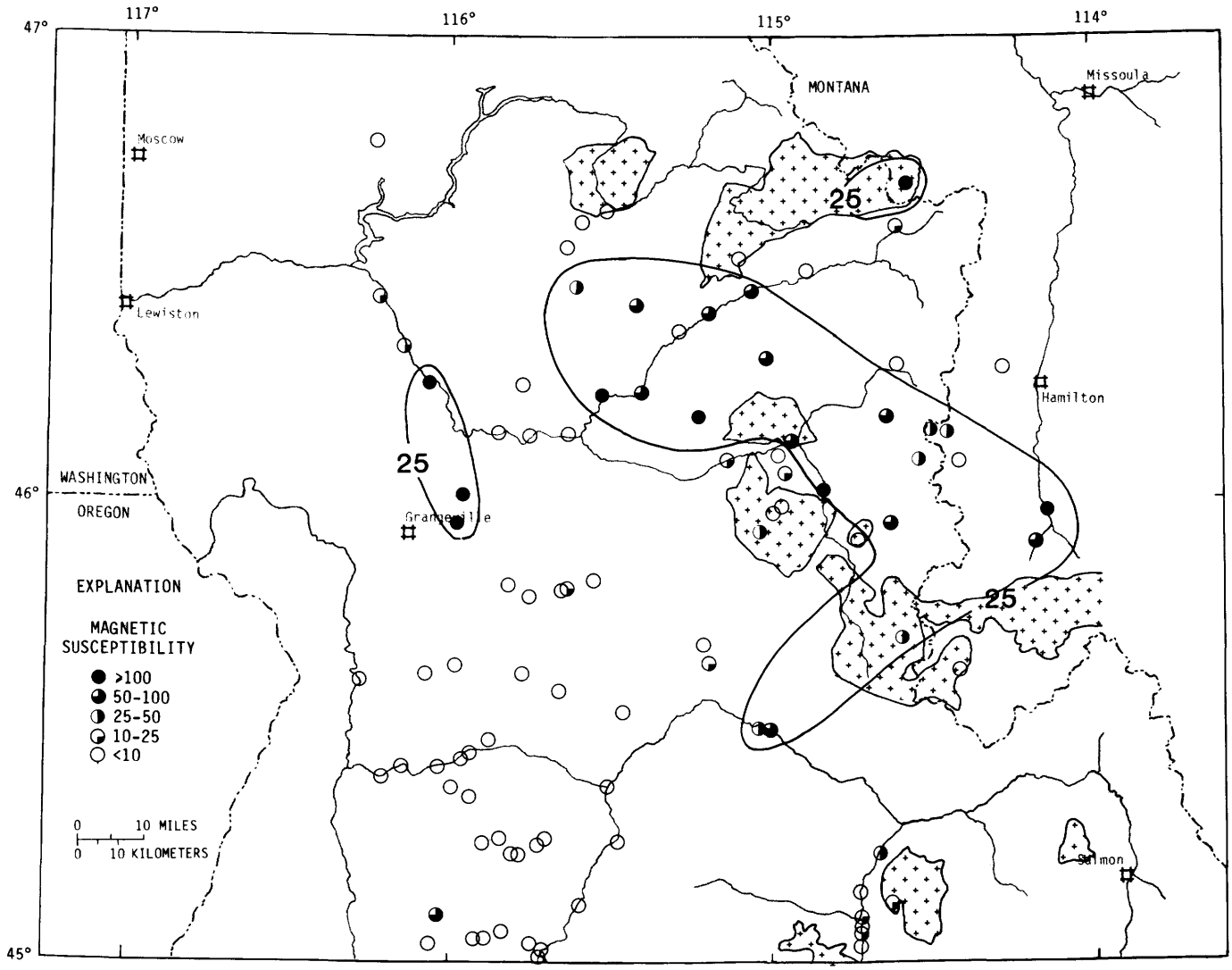

FIGURE 6.13.—Magnetic-susceptibility data for plutons of north-central Idaho. Low susceptibilities are typical of the west-central and northern parts of the Bitterroot lobe, but relatively high susceptibilities occur within a broad northwest-trending zone that contributes to high aeromagnetic intensities (see fig. 6.12). These rapid determinations were obtained on unmodified hand specimens using a hand-held magnetic susceptibility device and are reported as $\chi \times 10^{-5}$ cgs (see Criss and Champion, 1984). Patterned areas same as in figure 6.1.

ore deposits shown on figure 6.14; the commodities of interest are indicated for several of these. Obvious candidates are the Pb-Ag, Fe-Cu, and Mo deposits present within the Lolo Hot Springs pluton. Toth and others (1983) have additionally emphasized that many of the other Eocene epizonal plutons have Mo potential which could be of importance in the future. Furthermore, a few workings described by Toth and others (1983) in westernmost Montana occur in one of the low-δD zones and could very well be Eocene. Another possibility is a zone of Sb-Au-Ag mineralization near Lowell, which is near a small low-δD zone and near a positive aeromagnetic anomaly as well. Last, several significant deposits in the lowermost part of figure 6.14 (Edwardsburg and Profile districts) occur along the northwest side of the giant $\delta^{18}O$ anomaly mapped by Criss and others (1984) in the Challis volcanic field. However, prebatholithic rocks occur in the latter areas, so the origin of these deposits is unclear.

In summary, Eocene meteoric-hydrothermal activity was not as important to mineralization in north-central Idaho as in the Atlanta lobe; conversely, Cretaceous-early Tertiary metamorphic-hydrothermal activity was not as important in the Atlanta lobe as it was in the Bitterroot lobe. This difference between the Bitterroot and Atlanta lobes is almost certainly related to the rather low intensity of the Eocene hydrothermal systems in the north and to the scarcity of prebatholithic wall rock and inliers in the south. An important corollary is that future exploration for Eocene ore deposits in the Bitterroot lobe should be concentrated in the relatively small areas of intense meteoric-hydrothermal alteration which occur within and near areas having the lowest $\delta^{18}O$ values. Additional study of Cretaceous-early Tertiary hydrothermal activity and its relation to ore deposits is needed.

INFLUENCE OF HYDROTHERMAL SYSTEMS ON WHOLE-ROCK Rb-Sr ISOCHRONS

Hydrothermal transport processes have the potential of disturbing the whole-rock Rb-Sr isochron systematics of rocks by introducing subsolidus changes in either the $^{87}Sr/^{86}Sr$ ratio or the Rb/Sr ratio, or both. For example, any nonuniform modification of the $^{87}Sr/^{86}Sr$ ratios of rocks in a suite would contradict the necessary conditions of the isochron method, regardless of when the modification occurred. Additionally, hydrothermal alteration that significantly postdates crystallization of a rock suite could produce Rb/Sr ratios that are either much too low or too high to be consistent with observed $^{87}Sr/^{86}Sr$ ratios and the probable ages of the rocks.

An important aspect of the Bitterroot lobe data are that the hydrothermal alteration systems do not seem to have profoundly influenced r_i, even in cases where major ^{18}O depletions were produced. Thus, the altered ($\delta D \leq -120$ per mil) rocks have r_i and $\delta^{18}O$ values either similar to those of unaltered Bitterroot lobe rocks or simply display lower $\delta^{18}O$ values. More importantly, some suites of Eocene rocks define good Rb-Sr isochrons (fig. 6.15) in spite of the fact that many of the samples underwent major ^{18}O depletions. In any case, we submit that varying source characteristics, and not hydrothermal processes, were primarily responsible for the confused Rb-Sr isochrons observed by Armstrong and others (1977) and by Fleck and Criss (1985) in the main-phase granitoids.

Note that the above results differ from those observed in submarine hydrothermal systems, where pervasive seawater interactions can produce significant changes in the $^{87}Sr/^{86}Sr$ ratios of the rocks (for example, McCulloch and others, 1980). This difference between the Eocene hydrothermal systems in Idaho and submarine systems can partly be attributed to the low Sr concentration of typical meteoric-hydrothermal fluids compared to sea water. Furthermore, the Sr that existed in the Bitterroot lobe systems would have been largely derived from the Cretaceous and Tertiary rocks undergoing alteration, and not from some external reservoir having a markedly different $^{87}Sr/^{86}Sr$ ratio. The Precambrian rocks provide an exception to the last statement, but their high $^{87}Sr/^{86}Sr$ ratios are moderated by their low Sr concentrations.

As regards any possible hydrothermal alteration of Rb-Sr ratios, it is important in the case at hand that the Bitterroot lobe plutons are not drastically older than the hydrothermal systems responsible for the alteration. Even if Eocene hydrothermal transport processes changed the Rb-Sr ratios from the values at emplacement, such changes would introduce only moderate complications into the isochron systematics of Late Cretaceous and early Tertiary plutons, and the whole-rock Rb-Sr isochrons of the Eocene plutons would be essentially unaffected.

On the other hand, major complications in Precambrian isochrons would result from such nonclosed system behavior. An example is provided by Belt Supergroup (Wallace Formation) metasedimentary rocks collected peripheral to the northern margin of the Bitterroot lobe (fig. 6.16). Although a Precambrian age is still suggested by the data, the absence of conformity to a simple isochron is notable, especially when these data are compared to the good to excellent isochrons obtained on Belt sedimentary rocks elsewhere (Obradovich and Peterman, 1968). The effects shown in figure 6.16 probably reflect the high-grade regional metamorphism of the Belt rocks in the vicinity of the Bitterroot lobe, as well as the pervasive interactions with metamorphic-hydrothermal fluid which apparently occurred in Cretaceous-early Tertiary time. It is alternatively possible that the results indicate large spatial variations in the initial $^{87}Sr/^{86}Sr$ ratios of the sedimentary rocks in the region of study, but this is considered to be less likely.

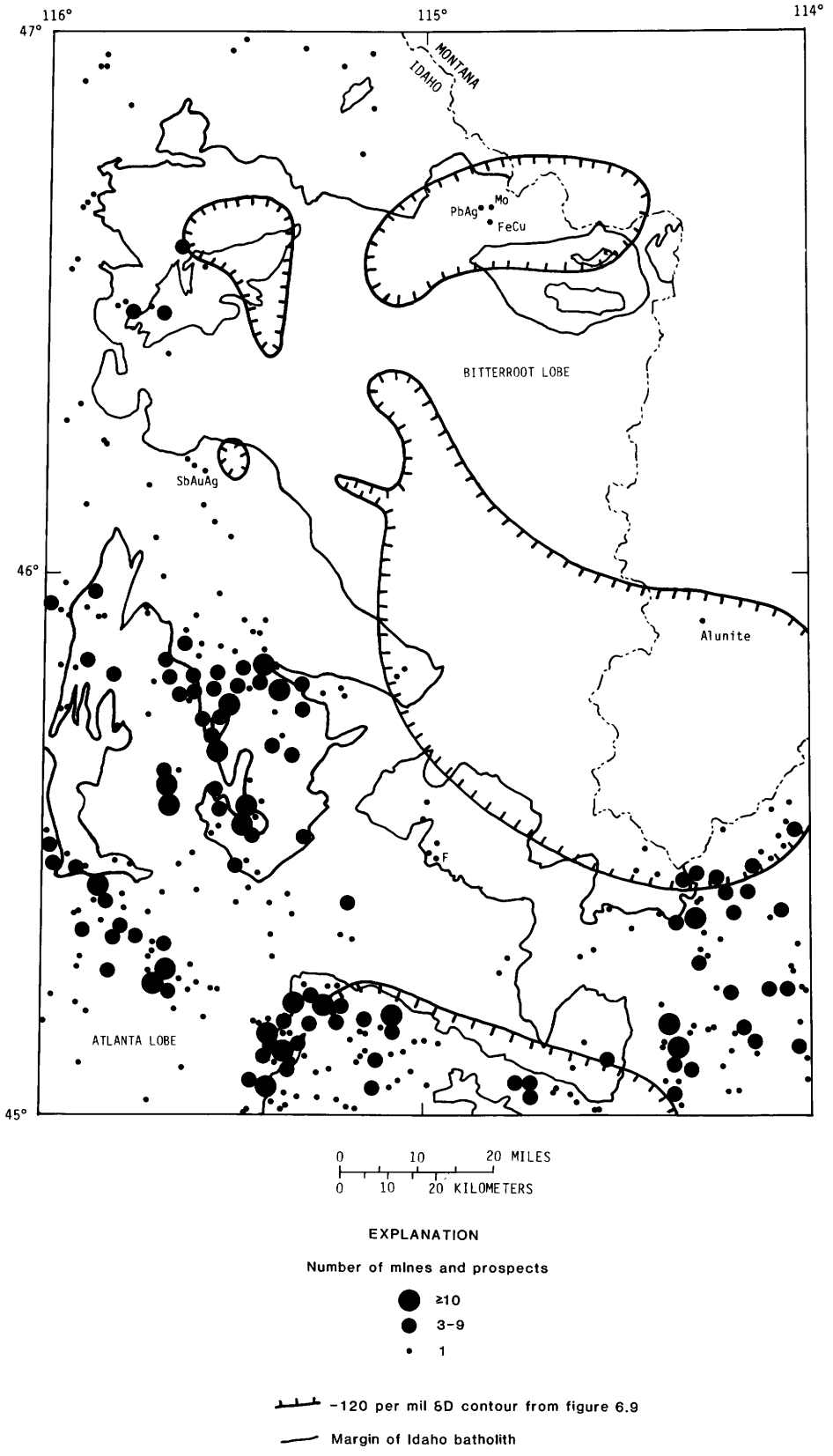
116°
115°
114°
47°
46°
45°
MONTANA
IDAHO
PbAg
Mo
FeCu
BITTERROOT LOBE
SbAuAg
Alunite
F
ATLANTA LOBE
0 10 20 MILES
0 10 20 KILOMETERS
EXPLANATION
Number of mines and prospects
≥10
3-9
1
-120 per mil δD contour from figure 6.9
Margin of Idaho batholith

K-Ar RELATIONS IN PLUTONS OF NORTH-CENTRAL IDAHO

REGIONAL VARIATIONS IN K-Ar AND $^{40}Ar/^{39}Ar$ APPARENT AGES OF BIOTITE

Excluding Precambrian rocks, the K-Ar apparent ages of biotite from plutons of north-central Idaho range from 136 to 39 Ma (fig. 6.17). These apparent ages are a function of both rock type and geographic position, and in many cases are significantly younger than the true emplacement ages of the rocks. The oldest K-Ar ages from biotites (136 to 78 Ma) are obtained from plutons in the Wallowa-Seven Devils terrane, west of the 0.704 line for $^{87}Sr/^{86}Sr$ initial ratios (compare figs. 6.17 and 6.2). Apparent ages of biotite in transition zone plutons that intrude the eastern and northern margins of the WSD terrane range from 82 to 76 Ma, similar to the youngest apparent ages of biotite of the WSD plutons (table 6.4; fig. 6.17). Such values occur only near the terrane boundary with Precambrian sialic crust.

Biotite K-Ar apparent ages of plutons of the Bitterroot lobe of the Idaho batholith are in most cases younger than 80 Ma. These apparent ages decrease systematically from about 80 Ma near the suture with the WSD terrane to less than 50 Ma in the broad central part of the Bitterroot lobe (fig. 6.17). The region of low (<51 Ma) K-Ar apparent ages is more than 10,000 km^2 in extent, as originally pointed out by Armstrong (1974). This unusual region completely encompasses the Bitterroot dome of Hyndman and others (1975). The youngest K-Ar apparent ages (45 to 39 Ma) occur either within and immediately adjacent to the Eocene plutons or within the extensive mylonite zone near the Idaho-Montana state line (see section "Geochronology and Structural Development of the Idaho Batholith").

As discussed by Armstrong (1974), the K-Ar apparent ages (51 to 44 Ma) of the Eocene plutons are essentially the same as those typical of the Challis Volcanics (also see Axelrod, 1966; McIntyre and others, 1982). This volcanic sequence contains an Eocene paleoflora (Axelrod, 1966) and is in places crosscut by the Eocene plutons (Ross, 1934; Cater and others, 1973). In the area of the Painted Rocks pluton (fig. 6.1), tuffs of the volcanic sequence yield biotite and sanidine K-Ar and $^{40}Ar/^{39}Ar$ ages ranging from 49 to 45 Ma (table 6.4, 6.5, sample 797-19C) and rest nonconformably on the epizonal plutonic rocks. Initial $^{87}Sr/^{86}Sr$ ratios of the volcanic rocks are indistinguishable from those of the Painted Rocks pluton (797-20E).

REGIONAL VARIATIONS IN K-Ar AND $^{40}Ar/^{39}Ar$ APPARENT AGES OF HORNBLENDE

The K-Ar and $^{40}Ar/^{39}Ar$ apparent ages of plutonic hornblende exhibit a range from 192 to 46 Ma within the central Idaho-westernmost Montana area (figs. 6.18, 6.19; tables 6.4, 6.5). Where zircon U-Pb ages are available for plutons of central Idaho, discordance with K-Ar ages on hornblende is generally small (Armstrong and others, 1977; J.S. Stacey, personal commun., 1983). Ages of plutonic hornblendes drop abruptly across the boundary between the WSD and Belt-Yellowjacket terranes and continue to decrease in steps eastward across the Idaho batholith (figs. 6.18, 6.19). The two terranes are sutured by transition zone plutons that intrude both crustal types and yield biotite, hornblende, and muscovite K-Ar ages of 87 to 75 Ma, many of which are concordant.

Excluding plutons of the transition zone, the youngest plutons intruding the WSD terrane are Early Cretaceous in age, commonly greater than 125 Ma. Sample 827-28G has concordant biotite and hornblende K-Ar ages at 135 Ma, and sample 818-10B is nearly concordant, with hornblende at 135 Ma and biotite at 129 Ma (table 6.4). Jurassic bodies, yielding K-Ar ages of 170 to 140 Ma on hornblende, are also common in the WSD terrane (Armstrong and others, 1977). Although Lower Jurassic to Upper Permian intrusive rocks are reported in eastern Oregon and south of 45° N. latitude in western Idaho (Armstrong and others, 1977; Avé Lallemant and others, 1980; Walker, 1983), only one of our samples yields K-Ar ages on hornblende greater than 170 Ma, and that sample is poorly reproducible, ranging from 199 to 170 Ma (tables 6.4, 6.5). These Jurassic and Early Cretaceous plutons are notably absent in the Belt-Yellowjacket terrane, north and east of the suture zone.

Hornblende K-Ar apparent ages in the Bitterroot lobe are oldest along the western margin and generally decrease to a minimum along the Bitterroot front. The hornblende ages define three groups of rather uniform ages—87 to 75 Ma, 66 to 62 Ma, and 51 to 46 Ma (fig. 6.19). These age groupings are based on too few data to be regarded as clearly discrete events and additional data must be obtained. However, the geographic pattern is consistent with eastward migration of plutonism across central Idaho during Late Cretaceous and early Tertiary time.

FIGURE 6.14.—Distribution of mines and prospects (dots; predominantly representing hydrothermal ore bodies) in north-central Idaho (modified from Mitchell and others, 1981a, b). Mineral deposits are scarce in the Bitterroot lobe, except along its margins and near inliers of Precambrian rocks, where metamorphic-hydrothermal activity related to the main-phase plutons occurred. Only a few deposits appear to be related to the Eocene meteoric-hydrothermal systems, whose positions are indicated by the −120 per mil δD contour (hachured lines). The commodities of interest are indicated for these Eocene deposits. Mineral deposits in Montana are not shown, except one alunite deposit (Eocene?) described by Toth and others (1983) is illustrated.

GEOCHRONOLOGY AND STRUCTURAL DEVELOPMENT OF THE IDAHO BATHOLITH REGION

GENERAL GEOCHRONOLOGIC RELATIONS

Potassium-argon ages of biotite, hornblende, and muscovite provide a pattern of decreasing apparent age from west to east across central Idaho, including plutons in the Wallowa-Seven Devils terrane, plutons on the western margins of both the Bitterroot and Atlanta lobes of the Idaho batholith, the main-phase plutons of the Bitterroot lobe, and the late-phase epizonal plutons. Jurassic-Early Cretaceous plutons were emplaced into older units of the WSD magmatic-sedimentary arc at a time when it was spatially remote from its present juxtaposition with Precambrian sialic crust. Plutons of this group are confined to the WSD terrane and yield ages from 192 Ma to 135 Ma (fig. 6.19). Late Cretaceous transition zone plutons yield K-Ar mineral ages of 87 to 75 Ma and define a belt of strongly deformed bodies centered along the terrane boundary (Armstrong and others, 1977; Fleck and Criss, 1985). Whereas some of the apparent ages may represent resetting during recrystallization, zircon U-Pb ages (J.S. Stacey, written commun., 1983) of some plutons are also concordant with the K-Ar determinations, and most intrusive rocks within the suture zone are probably syntectonic. As discussed by Hyndman (1983) and Zen and Hammarstrom (1984), depths of crystallization of these plutons were probably greater than 10 to 15 km. The near concordance of mineral ages virtually requires a tectonic emplacement, because slow uplift from these depths would yield extremely discordant ages in the order: zircon U-Pb > hornblende K-Ar > muscovite K-Ar ≥ biotite K-Ar. This mode of emplacement is consistent with the strongly deformed fabrics of the plutons and with high-grade metamorphism of Precambrian wall rocks.

A younger zone of nearly concordant ages occurs within the Bitterroot mylonite (figs. 6.1, 6.19 at about 100 km), a shallow-dipping zone of deformation in the youngest plutons of the main phase of the Bitterroot lobe. Zircon U-Pb ages (Chase and others, 1978, 1983; Bickford and others, 1981) and K-Ar ages on hornblende and biotite (table 6.4) are nearly concordant (52 to 45 Ma) for the youngest deformed plutons. Concordant biotite and hornblende K-Ar ages of mylonite sample 787-25C (table 6.4; Fleck and Criss, 1985) indicate an age of mylonization of 45.7 Ma, consistent with Garmezy and Sutter's (1983) determination of 45.5 to 43.5 Ma. As with the suture zone,

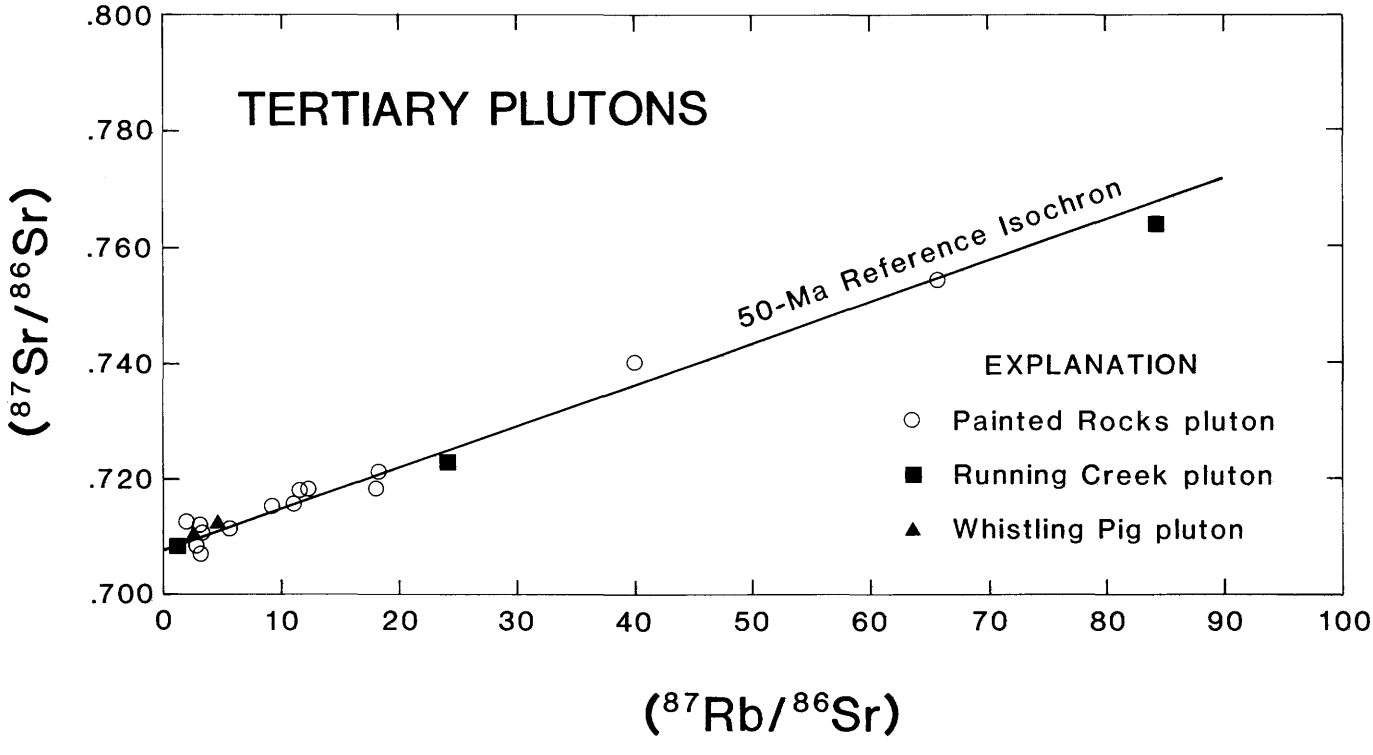

FIGURE 6.15.—Whole-rock Rb-Sr isochron diagram for epizonal granites from the most highly altered part of the Bitterroot lobe, namely, the Painted Rocks, Running Creek, and Whistling Pig plutons. These rocks define reasonable isochrons in spite of the high degree of alteration of several samples. Sample 797-20B is off scale, having an $^{87}Rb/^{86}Sr$ ratio of 145.9 and a present-day $^{87}Sr/^{86}Sr$ ratio of 0.8090, but this highly altered sample ($\delta^{18}O$ = 5.8 per mil; δD = −133 per mil) would also plot close to the 50-Ma reference isochron.

the plutons with mylonitic fabrics clearly crystallized at least in part at great depth, but rose abruptly (see subsection on "Bitterroot Lobe Uplift") to levels sufficiently shallow that biotite could retain argon (<250 to 300 °C).

Except for the two elongate zones discussed above and less common, undeformed, Early Cretaceous plutons in the accreted terrane (table 6.4), plutonic rocks of north-central Idaho generally yield discordant K-Ar apparent ages (fig. 6.19). The patterns of these age variations appear to be regular (figs. 6.17, 6.18), but ages tend to fall into several groups rather than being evenly distributed in time. Discordant ages of Late Cretaceous and early Tertiary plutons suggest uplift and cooling of an episodically emplaced batholith after about 75 Ma and before 45 Ma, with biotite apparent ages generally being 4 to 14 m.y. younger than hornblende. The youngest plutonic event in the region was represented by widespread volcanism, caldera formation, hydrothermal activity, and intrusion of the highly differentiated epizonal Eocene plutons at 51 to 44 Ma.

TIMING OF ACCRETION

Age patterns in and adjacent to the suture zone of the WSD terrane with the sialic crust of the North American continent restrict the time of accretion to the period between 135 and 75 Ma. West and south of the narrow zone of highly deformed transition zone plutons having nearly concordant mineral ages of 87 to 75 Ma, K-Ar apparent ages on biotite and hornblende from some tonalite and quartz diorite plutons are concordant at 135 Ma. These Early Cretaceous plutons have flat $^{40}Ar/^{39}Ar$ age spectra (hornblende) and have initial $^{87}Sr/^{86}Sr$ ratios of 0.7033 to 0.7035 that show no indication of proximity to a sialic craton of Precambrian age (fig. 6.20). Less than 7 km from these ensimatic plutons, Late Cretaceous syntectonic tonalite and trondhjemite bodies of the transition zone intrude the WSD terrane and yield flat hornblende age spectra and the nearly concordant mineral ages discussed above. Zircon fractions studied by J.S. Stacey (written commun., 1983) from one of these low-r_i trondhjemites yield a lower intercept U-Pb age concordant with muscovite K-Ar ages of 87 Ma (table 6.4; sample 797-26D), but contain a significant component of inherited Precambrian zircon. The initial $^{87}Sr/^{86}Sr$ ratio from this body is low (0.7037) but significantly above values from the Early Cretaceous plutons. Some transition zone plutons also intrude Precambrian crust, and their high r_i values (0.705 to 0.709) demonstrate a significant Precambrian component in these magmas (Fleck and Criss, 1985; table 6.1). All lines of evidence indicate at least some involvement of Precambrian sialic crust in the magmatic history of the transition zone plutons.

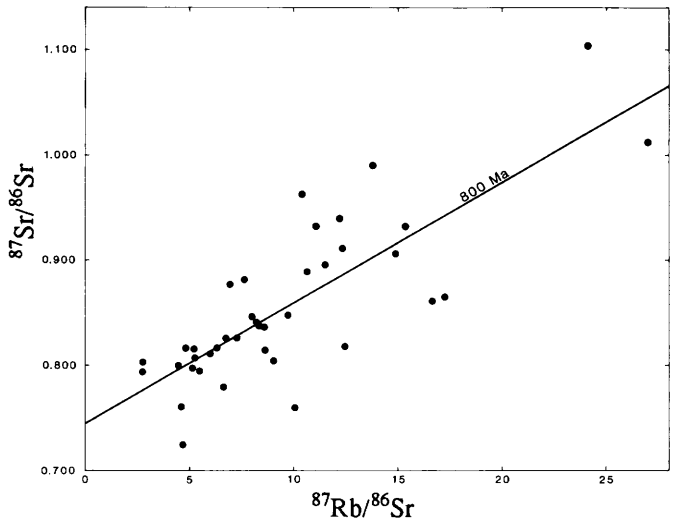

FIGURE 6.16.—Whole-rock Rb-Sr isochron diagram for Belt Supergroup (Wallace Formation) metasedimentary rocks collected north of the Bitterroot lobe. In contrast to a 1,100-Ma isochron (Obradovich and Peterman, 1968), data scatter widely about an 800-Ma reference isochron, perhaps reflecting hydrothermal metamorphism in Cretaceous-early Tertiary time.

Early Cretaceous tonalite (sample 797-25F) 1 to 2 km west of the suture zone near Kooskia, Idaho, has an initial $^{87}Sr/^{86}Sr$ ratio of 0.7034 (table 6.1) and a $^{40}Ar/^{39}Ar$ plateau age on hornblende of 130.4 ± 5.3 Ma (table 6.5), but biotite K-Ar apparent ages are about 78 Ma. Biotite may have been reset by deformation and intrusion within the suture zone during the Late Cretaceous event. On the other hand, hornblende in this sample, which yields a partially disturbed $^{40}Ar/^{39}Ar$ age spectrum (table 6.5) and conventional K-Ar ages of 118 Ma, still retains evidence of its Early Cretaceous age. The absence of Early Cretaceous intrusive bodies within the Precambrian terrane east of the suture zone and the evidence of a major magmatic and tectonic event at 87 to 75 Ma argue persuasively for a Late Cretaceous age for final accretion (fig. 6.20).

BITTERROOT LOBE UPLIFT

In addition to indicating the timing of the regional igneous events, K-Ar data provide important information on the uplift of the Bitterroot lobe. In the discussion below, we elaborate on Ferguson's (1975) suggestion that the K-Ar apparent ages of Bitterroot lobe plutons reflect early Tertiary uplift and cooling of the terrane. Uplift models have been advanced to explain apparent age patterns in several orogenic terranes, including the Alps (Jager, 1962), the Ruby Mountains of Nevada (Kistler and O'Neil, 1975), the Peninsular Ranges batholith (Krummenacher and others, 1975), the Sandpoint quadrangle of Washington and Idaho (Harms and Price, 1983; com-

pare with Miller and Engels, 1975), and the southern Idaho batholith (Criss and others, 1982).

Several independent lines of evidence are in accord with marked Late Cretaceous and early Tertiary uplift of the Idaho batholith, and these have been summarized earlier in this report. Structural evidence is also generally consistent with such an uplift history, although certain disagreements exist at present and many details remain to be elucidated. Chase and Talbot (1973) originally proposed that the Bitterroot lobe has a domelike structure that formed by an uplift mechanism. Hyndman and others (1975) and Hyndman (1980) suggested that the Bitterroot dome formed by isostatic rebound, following detachment of the Sapphire tectonic block along the major mylonite zone and the removal of this formerly superincumbent block by gravitational gliding. Hyndman proposed that the mylonite zone is therefore genetically connected to 78-Ma thrust faults more than 100 km to the east. However, Chase and others (1983) obtained U-Pb ages of 52 to 48 Ma for three sheared plutons and pointed out the age discrepancy between this result and the genetic implications of the early model. The timing of mylonite formation has been confirmed by Garmezy and Sutter (1983), who indicate an age range of 45.5 to 43.5 Ma for the mylonization event, significantly younger than the age of crystallization of the youngest mylonized plutons.

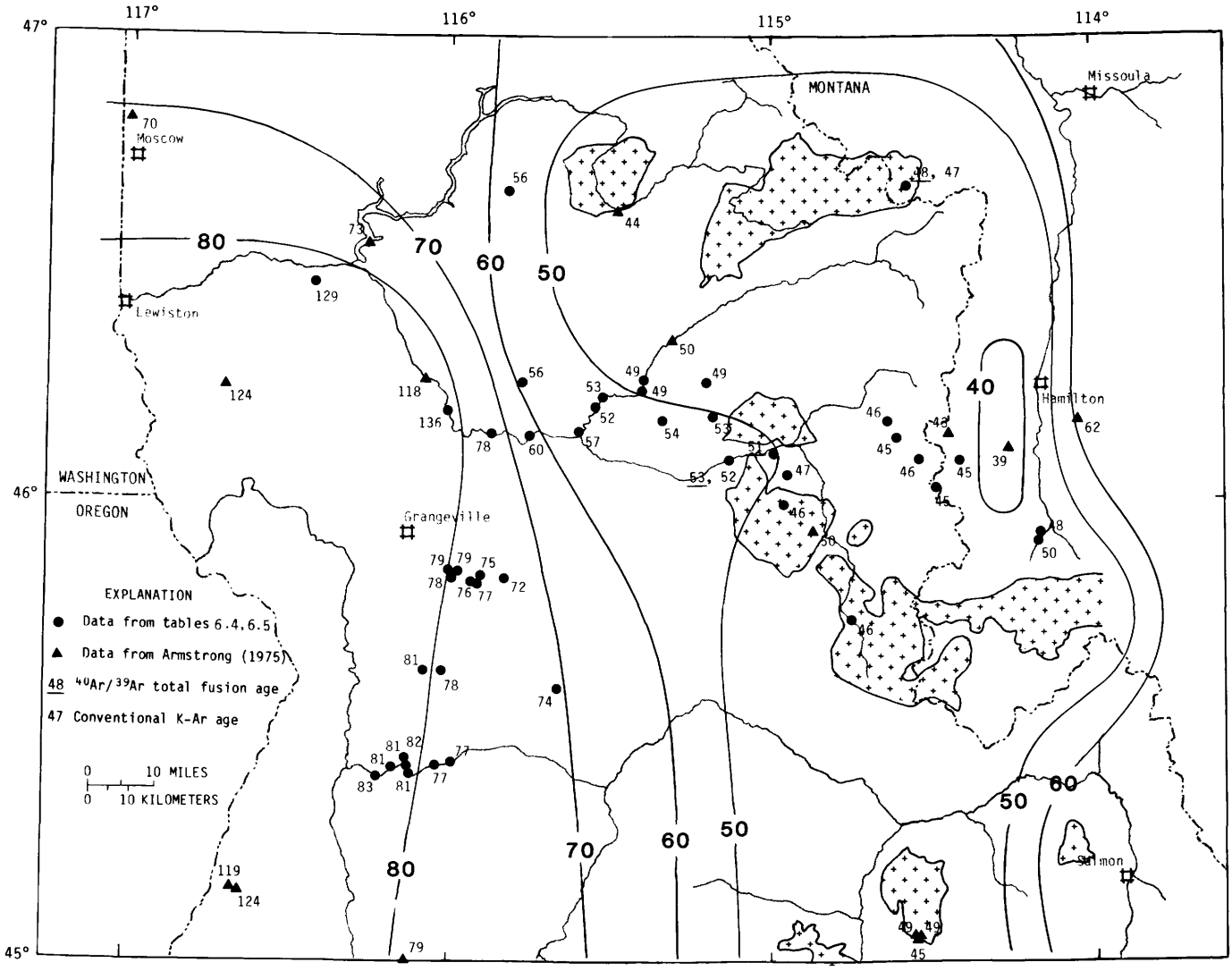

FIGURE 6.17.—Contour map of K-Ar and $^{40}Ar/^{39}Ar$ apparent ages of biotites from plutons of north-central Idaho. Note the large area of apparent age of 50 to 45 Ma that reflects Eocene intrusives as well as rapid uplift and cooling of the east-central Bitterroot lobe.

TABLE 6.4.—*K-Ar apparent ages of rocks of central Idaho and western Montana*

[Age uncertainties represent larger of (1) standard deviation of replicates, or (2) pooled estimates of standard deviations, using formula of Cox and Dalrymple (1967). Sample locations are given in table 6.1. ^{40}Ar refers to radiogenic argon. †, see table 6.5 for $^{40}Ar/^{39}Ar$ analyses. E, exponential to the negative value given]

Sample	Mineral	K_2O (weight percent)	mol $^{40}Ar/g$	Percent ^{40}Ar	Age (Ma)
		Plutonic rocks of the Wallowa-Seven Devils terrane			
797-25F†	Biotite	9.21, 9.23	1.058 E-9	73.1	77.9±0.5
	do.		1.056 E-9	77.7	
	Hornblende	.799, .818	1.424 E-10	77.7	118.6±0.8
	do.		1.429 E-10	70.3	
797-25I†	Hornblende	.319, .320	8.906 E-11	79.5	191.7±11.0
	do.		9.700 E-11	65.9	
807-28D (metavolcanic)	Biotite	8.76, 8.76	1.005 E-9	82.1	78.0±0.5
	Hornblende	.858, .863	1.000 E-10	55.9	78.2±1.1
	do.		9.796 E-11	53.5	
818-10B†	Biotite	9.68, 9.64	1.810 E-9	82.3	129.2±4.8
	do.		1.914 E-9	84.1	
	Hornblende	.805, .816	1.625 E-10	74.1	134.6±0.8
	do.		1.638 E-10	70.3	
818-16C	Biotite	9.88, 9.88	1.205 E-9	62.7	82.8±0.7
	Muscovite	10.27, 10.30	1.217 E-9	78.5	80.4±0.6
827-28G†	Biotite	9.51, 9.54	1.887 E-9	88.0	135.6±4.3
	do.		1.976 E-9	85.7	
	Hornblende	1.021, 1.021	2.049 E-10	86.9	135.4±1.6
	do.		2.085 E-10	67.9	
		Plutonic rocks of the transition zone			
797-25D	Biotite	9.34, 9.37	8.169 E-10	87.4	59.8±0.3
	do.		8.210 E-10	77.8	
	Hornblende	1.750, 1.777	1.919 E-10	69.7	74.4±0.5
	do.		1.935 E-10	83.9	
797-26D†	Muscovite	10.75, 10.76	1.382 E-9	67.1	87.2±0.5
	do.		1.385 E-9	85.1	
797-26E	Biotite	9.60, 9.65	1.117 E-9	70.8	79.2±0.6
	do.		1.128 E-9	83.2	
797-26H	Biotite	9.62, 9.64	1.020 E-9	89.5	72.1±0.4
	Muscovite	10.74, 10.76	1.159 E-9	86.4	73.4±0.4
797-26I†	Biotite	9.62, 9.63	1.078 E-9	51.7	75.1±1.6
	do.		1.046 E-9	89.2	
	Hornblende	1.594, 1.598	1.900 E-10	61.3	79.8±1.5
	do.		1.851 E-10	59.4	
807-27A	Biotite	9.28, 9.28	1.063 E-9	88.2	77.6±0.4
	do.		1.057 E-9	79.3	
807-28A	Biotite	9.17, 9.23	1.067 E-9	87.6	78.6±0.4
	do.		1.061 E-9	83.8	
	Muscovite	9.91, 9.93	1.134 E-9	72.6	78.1±0.9
	do.		1.147 E-9	18.1	
807-28H	Biotite	9.34, 9.42	1.059 E-9	93.8	76.6±0.4
	do.		1.054 E-9	73.0	
	Muscovite	9.95, 9.97	1.133 E-9	82.9	76.7±0.9
	do.		1.113 E-9	80.9	
807-28I†	Biotite	9.43, 9.45	1.057 E-9	76.8	75.8±0.5
	do.		1.046 E-9	71.5	
	Hornblende	1.165, 1.168	1.355 E-10	72.8	78.5±0.6
	do.		1.341 E-10	49.8	

TABLE 6.4.—*K-Ar apparent ages of rocks of central Idaho and western Montana*—Continued

[Age uncertainties represent larger of (1) standard deviation of replicates, or (2) pooled estimates of standard deviations, using formula of Cox and Dalrymple (1967). Sample locations are given in table 6.1. ^{40}Ar refers to radiogenic argon. †, see table 6.5 for $^{40}Ar/^{39}Ar$ analyses. E, exponential to the negative value given]

Sample	Mineral	K_2O (weight percent)	mol $^{40}Ar/g$	Percent ^{40}Ar	Age (Ma)
		Plutonic rocks of the transition zone--Continued			
818-11C	Hornblende	.385, .388	4.091 E-11	21.1	74.2±2.9
	do.		4.332 E-11	28.4	
818-15D	Biotite	8.67, 8.70	1.027 E-9	75.5	81.1±1.1
	do.		1.048 E-9	89.4	
	Hornblende	.898, .901	1.045 E-10	78.8	79.6±0.9
	do.		1.063 E-10	69.3	
818-16D	Biotite	9.01, 9.03	1.078 E-9	91.5	81.3±0.4
	do.		1.081 E-9	78.9	
	Hornblende	.830, .839	9.293 E-11	70.8	77.1±1.9
	do.		9.628 E-11	65.0	
818-16E	Biotite	9.16, 9.16	1.104 E-9	79.5	80.5±1.9
	do.		1.068 E-9	89.9	
818-16F†	Biotite	9.22, 9.24	1.080 E-9	73.2	81.0±2.1
	do.		1.122 E-9	92.8	
	Hornblende	.982, .985	1.178 E-10	70.3	87.5±8.7
	do.		1.360 E-10	85.6	
818-16I	Biotite	9.55, 9.68	1.086 E-9	82.7	76.6±0.5
	do.		1.081 E-9	89.1	
	Hornblende	1.312, 1.316	1.547 E-10	80.5	80.0±0.6
818-16J	Biotite	9.56, 9.56	1.066 E-9	78.4	76.8±1.4
	do.		1.094 E-9	92.9	
	Hornblende	1.411, 1.413	1.700 E-10	82.9	81.7±0.6
827-29F	Biotite	9.70, 9.65	1.117 E-9	82.6	78.4±0.6
827-29J	Biotite	9.33, 9.31	1.133 E-9	83.6	82.2±0.5
	do.		1.123 E-9	79.2	
	Hornblende	1.455, 1.446	1.834 E-10	67.2	82.9±4.2
	do.		1.705 E-10	68.1	
		Plutonic rocks of the Bitterroot lobe, undivided			
787-18A	Biotite	8.98, 9.04	6.392 E-10	71.5	48.7±0.3
	do.		6.410 E-10	78.2	
787-18B	Biotite	9.62, 9.64	6.943 E-10	81.7	49.0±0.6
	do.		6.820 E-10	84.4	
	Muscovite	10.74, 10.74	8.078 E-10	87.2	51.3±0.3
	do.		8.026 E-10	72.0	
787-19A†	Biotite	9.33, 9.34	7.226 E-10	83.9	53.8±1.1
	do.		7.441 E-10	78.4	
	Hornblende	1.463, 1.465	1.399 E-10	72.2	62.4±4.0
	do.		1.275 E-10	72.9	
787-19G	Biotite	9.23, 9.25	6.581 E-10	83.3	49.2±0.6
	do.		6.690 E-10	69.9	
	Muscovite	10.48, 10.50	7.840 E-10	81.4	51.5±0.4
	do.		7.927 E-10	73.7	
787-20A†	Biotite	9.32, 9.32	7.201 E-10	78.9	53.1±0.3
	do.		7.268 E-10	73.3	
	Hornblende	1.611, 1.642	1.482 E-10	72.5	62.2±0.4
787-20E†	Biotite	9.69, 9.71	7.331 E-10	76.1	52.0±0.3
	do.		7.397 E-10	75.6	
787-24A	Biotite	9.43, 9.45	6.263 E-10	72.1	45.5±0.2
	do.		6.263 E-10	77.8	
787-24G	Biotite	8.90, 8.95	5.850 E-10	66.6	45.0±0.2
	do.		5.864 E-10	86.6	

TABLE 6.4.—*K-Ar apparent ages of rocks of central Idaho and western Montana*—Continued

[Age uncertainties represent larger of (1) standard deviation of replicates, or (2) pooled estimates of standard deviations, using formula of Cox and Dalrymple (1967). Sample locations are given in table 6.1. ^{40}Ar refers to radiogenic argon. †, see table 6.5 for $^{40}Ar/^{39}Ar$ analyses. E, exponential to the negative value given]

Sample	Mineral	K_2O (weight percent)	mol $^{40}Ar/g$	Percent ^{40}Ar	Age (Ma)
		Plutonic rocks of the Bitterroot lobe, undivided--Continued			
	Hornblende	1.238, 1.240	8.933 E-11	74.6	49.6±0.3
	do.		9.007 E-11	78.1	
787-24H†	Biotite	9.21, 9.23	6.181 E-10	62.3	45.9±0.2
	do.		6.151 E-10	90.9	
	Hornblende		9.414 E-11	73.3	47.7±0.4
787-25C	Biotite	8.57, 8.59	5.703 E-10	73.7	45.3±0.4
	do.		5.630 E-10	74.4	
	Hornblende	1.211, 1.215	8.183 E-11	63.7	45.7±0.8
	do.		7.986 E-11	44.8	
787-26A†	Biotite	9.09, 9.10	7.042 E-10	79.4	53.0±0.3
	Hornblende	1.373, 1.376	1.277 E-10	80.3	64.9±2.0
	do.		1.335 E-10	68.1	
787-26F†	Biotite	9.34, 9.35	7.302 E-10	86.1	52.4±1.4
	do.		7.018 E-10	83.4	
	Hornblende	1.256, 1.260	1.138 E-10	79.8	61.7±0.3
	do.		1.136 E-10	63.6	
797-23A	Biotite	9.27, 9.28	7.735 E-10	18.9	57.3±0.6
	Muscovite	10.15, 10.16	8.148 E-10	77.5	55.0±0.2
	do.		8.190 E-10	79.5	
808-04E	Biotite	9.24, 9.25	6.722 E-10	70.0	49.9±0.3
	do.		6.743 E-10	67.7	
	Muscovite	10.31, 10.45	7.883 E-10	69.5	52.3±0.4
	do.		7.973 E-10	78.1	
808-04F	Biotite	9.54, 9.59	6.733 E-10	67.2	48.2±0.3
	Muscovite	10.43, 10.37	8.347 E-10	74.9	53.8±1.6
	do.		7.993 E-10	80.9	
818-12D	Biotite	9.56, 9.55	7.859 E-10	83.3	56.2±0.3
818-13A	Biotite	9.82, 9.86	1.083 E-9	82.2	74.0±1.2
	do.		1.058 E-9	86.4	
68-9-11A	Biotite	9.06, 9.08	7.489 E-10	81.6	56.1±0.5
	do.		7.398 E-10	82.1	
	Hornblende	1.413, 1.414	1.302 E-10	77.2	62.7±0.3
	do.	1.424, 1.434	1.308 E-10	53.6	
80-MT-246†	Biotite	9.12, 9.12	5.917 E-10	56.6	44.5±0.3
	Hornblende	1.160, 1.173	7.441 E-11	27.0	46.6±4.0
	do.		8.425 E-11	40.0	
		Eocene epizonal plutonic and associated volcanic rocks			
787-18J†	Biotite	8.71, 8.73	5.956 E-10	90.7	47.0±0.2
	do.		5.989 E-10	79.7	
787-21A	Biotite	8.89, 8.90	6.063 E-10	82.3	46.9±0.3
	do.		6.096 E-10	82.0	
787-21C	Biotite	7.18, 7.19	4.816 E-10	76.8	45.9±0.2
	do.		4.800 E-10	79.8	
797-19B	Biotite	8.60, 8.61	5.670 E-10	59.1	44.8±0.6
	do.		5.563 E-10	77.8	
	Sanidine	11.15, 11.15	7.665 E-10	89.8	46.3±1.2
	do.		7.376 E-10	78.8	
797-19C†	Biotite	8.65 8.66	5.914 E-10	72.3	46.6±0.3
(tuff)	do.		5.850 E-10	78.5	
	Sanidine	11.51, 11.53	7.788 E-10	82.3	44.6±2.5
	do.		7.189 E-10	94.5	

TABLE 6.4.—*K-Ar apparent ages of rocks of central Idaho and western Montana*—Continued

[Age uncertainties represent larger of (1) standard deviation of replicates, or (2) pooled estimates of standard deviations, using formula of Cox and Dalrymple (1967). Sample locations are given in table 6.1. ^{40}Ar refers to radiogenic argon. †, see table 6.5 for $^{40}Ar/^{39}Ar$ analyses. E, exponential to the negative value given]

Sample	Mineral	K_2O (weight percent)	mol $^{40}Ar/g$	Percent ^{40}Ar	Age (Ma)
Eocene epizonal plutonic and associated volcanic rocks--Continued					
797-20E	Biotite	5.50, 5.53	3.604 E-10	47.8	46.0±1.6
	do.		3.794 E-10	64.5	
	Hornblende	1.121, 1.128	7.635 E-11	73.0	46.6±0.4
Metamorphosed Precambrian rocks					
797-25C	Biotite	8.72, 8.81	7.196 E-10	28.9	58.2±2.9
	do.		7.723 E-10	72.0	
	Muscovite	9.35, 9.44	8.412 E-10	37.5	61.3±0.4
	do.		8.456 E-10	81.8	
807-31J	Biotite	9.19, 9.30	8.624 E-10	75.0	64.1±0.6
	do.		8.736 E-10	86.8	
807-31K†	Biotite	8.20, 8.23	7.910 E-10	82.0	65.0±1.0
	do.		7.734 E-10	78.0	
	Hornblende	0.964	1.082 E-10	57.2	74.6±2.4
	do.		1.033 E-10	59.6	
808-01D	Biotite	9.55, 9.57	9.121 E-10	81.5	65.0±0.4
	do.		9.091 E-10	77.3	
	Muscovite	10.69, 10.72	1.015 E-9	88.4	65.7±1.4
	do.		1.047 E-9	83.5	
808-01G†	Biotite	9.47, 9.54	9.510 E-10	79.9	72.4±6.0
	do.		1.071 E-9	91.9	
808-01I	Hornblende	1.521, 1.535	1.765 E-10	74.2	79.1±0.9
	do.		1.793 E-10	84.8	

Several unusual features of the K-Ar data in the Bitterroot lobe are consistent with the tectonic explanation. Principal among these is the large central zone of low (51 to 44 Ma) K-Ar mineral ages (figs. 6.17 and 6.18). This 10,000 km^2 area and the surrounding belt of high apparent-age gradients and high age discordance is much too large to be solely attributed to the thermal aureoles of the crosscutting Eocene plutons and is also much larger than the zones of intense meteoric-hydrothermal alteration (compare figs. 6.9 and 6.10). However, the observed age pattern could have been produced by relatively rapid uplift and cooling of the rocks in this broad area, in which case the terrane could constitute an infrastructure. This uplift and cooling was apparently sufficiently rapid that vertical gradients in the K-Ar apparent ages are not discernible given the topographic relief of the area. Garmezy and Sutter (1983) used $^{40}Ar/^{39}Ar$ data from hornblende, muscovite, biotite, and orthoclase to calculate that the uplift rate was about 20 ± 10 mm/yr from 45.5 to 43.5 Ma, approaching that observed in the Himalaya mountains. Chase and Talbot (1973) suggested that the Bitterroot dome plutons were emplaced during the uplift event in a semiconsolidated condition, and Garmezy and Greenwood (1981) proposed that the mylonite zone formed by injection and flowage of crystal mush. In any case, the high temperature conditions implied by these workers and the subsequent rapid cooling after uplift can explain the 51- to 44-Ma K-Ar mineral ages of these rocks.

CONCLUSIONS

North-central Idaho is composed of two essentially different terranes, each having distinct geologic and geochemical characteristics that are reflected by igneous intrusions. The western or Wallowa-Seven Devils terrane

TABLE 6.5.—*$^{40}Ar/^{39}Ar$ ages of rocks of the Bitterroot lobe of the Idaho batholith*

[Sample locations are given in table 6.1. ^{40}Ar refers to radiogenic argon. TF, total fusion of separate aliquant of sample; +, indicates temperature step omitted from plateau; J, measure of the integrated fast neutron flux determined using a monitor biotite, SB-3]

Sample	Temperature step (°C)	Mineral	Percent of total ^{39}Ar	Percent ^{40}Ar	Percent $^{36}Ar_{Ca}$	$^{40}Ar/^{39}Ar$	$^{37}Ar/^{39}Ar$	$^{36}Ar/^{39}Ar$	J	Age (Ma)
			Plutonic rocks of the Wallowa-Seven Devils terrane							
797-25F------	TF	Hornblende	100	71.0	10.11	15.42	6.259	0.0168	0.0066059	126.3±1.5
797-25F(IH)--	750+	do.	6.53	22.0	.36	52.00	1.845	.1378	.0066059	131.4±3
	850+d	do.	11.43	36.1	3.52	21.88	6.335	.0490	.0066059	92.1±1.8
	900+	do.	19.48	83.3	21.68	12.02	6.895	.0087	.0066059	116.0±1.5
	930	do.	15.89	87.4	24.29	12.88	6.470	.0072	.0066059	129.9±1.7
	960	do.	5.78	89.2	26.82	12.69	6.230	.0063	.0066059	130.6±3.3
	1000	do.	6.73	82.6	19.50	13.35	6.989	.0097	.0066059	127.4±3.0
	1040	do.	29.25	95.7	51.68	11.86	6.668	.0035	.0066059	130.9±1.4
	1100	do.	4.33	93.5	40.05	12.46	6.637	.0045	.0066059	134.3±4.3
	Fusion	do.	.588	46.4	4.29	23.13	6.910	.0438	.0066059	124.2±31.1
								Recalculated total-----		123.4
								Plateau age----------		130.4±5.3
797-25I------	TF	Hornblende	100	52.4	7.04	28.42	12.74	0.0492	0.0066059	170.6±2.2
797-25I(IH)--	750+	do.	.63	22.7	.17	690.8	11.55	1.810	.0066059	1289.7±131.1
	850+	do.	4.33	35.7	2.35	87.92	16.96	.1960	.0066059	343.2±11.6
	900	do.	43.78	81.8	23.30	17.39	12.59	.0141	.0066059	163.4±2.0
	930	do.	14.12	84.8	27.01	17.71	12.37	.0124	.0066059	171.9±3.9
	960	do.	3.38	56.7	9.02	23.96	12.78	.0385	.0066059	156.3±15.1
	1000	do.	5.53	74.3	16.37	21.18	13.25	.0220	.0066059	179.8±9.3
	1040	do.	7.89	69.6	13.64	21.85	13.04	.0260	.0066059	174.1±6.7
	1100	do.	13.97	81.3	23.34	17.78	12.59	.0147	.0066059	165.8±4.0
	Fusion	do.	6.37	70.8	14.47	20.20	12.465	.0234	.0066059	164.7±8.3
								Recalculated total-----		184.4
								Plateau age----------		169.9±3.6
797-26A------	TF	Hornblende	100	63.7	12.48	24.01	15.45	0.0337	0.005898	157.3±2.7
797-26A(IH)--	750+	do.	5.17	.01	.13	800.4	12.72	2.712	.005898	0.9±108
	900	do.	57.01	42.3	5.78	35.09	15.47	.0728	.005898	152.7±3.4
	940	do.	9.22	47.9	7.28	31.46	15.98	.0598	.005898	155.2±5.9
	960	do.	6.26	41.1	4.90	42.54	16.06	.0891	.005898	178.8±8.8
	1000	do.	12.25	52.3	8.08	30.46	15.90	.05351	.005898	163.4±5.4
	1050	do.	8.44	44.8	6.26	34.86	15.99	.06947	.005898	160.5±6.7
	1100+	do.	1.24	20.7	1.37	119.9	16.46	.3260	.005898	249.2±30.9
	Fusion+	do.	.40	9.1	.24	606.3	16.75	1.869	.005898	514.9±238.3
								Recalculated total-----		151.9
								Plateau age----------		157.9±2.8
818-10B(IH)--	750+	Hornblende	3.76	8.0	.4	90.24	4.593	.2821	0.007852	100.0±2.5
	850+	do.	8.59	53.3	6.3	17.87	7.009	.0301	.007852	130.6±1.4
	900	do.	19.56	62.0	8.2	15.82	6.729	.0222	.007852	134.3±1.3
	925	do.	34.75	88.7	29.7	11.06	6.565	.0060	.007852	134.4±1.3
	950	do.	9.85	92.9	42.4	10.52	6.733	.0043	.007852	133.9±1.4
	975	do.	3.93	91.5	37.8	10.74	6.853	.0049	.007852	134.6±1.6
	1000	do.	5.60	93.6	45.0	10.53	6.774	.0041	.007852	135.0±1.4
	1025	do.	7.66	89.6	32.1	11.00	6.698	.0057	.007852	134.4±1.4
	Fusion	do.	6.32	90.3	34.1	10.88	6.762	.0054	.007852	134.6±1.4
								Recalculated total-----		132.8
								Plateau age----------		134.4±0.5
827-28G------	TF	Hornblende	100	75.4	10.32	14.05	4.946	0.0130	0.007851	144.6±2.1
827-28G------	750+	do.	3.71	20.7	.34	59.82	2.008	.01610	.007851	167.7±2.3
	850+	do.	4.62	13.3	.47	97.59	4.997	.2883	.007851	173.0±2.9
	900	do.	57.64	58.8	5.38	17.79	5.172	.0262	.007851	143.0±1.4
	925	do.	13.53	95.6	46.37	10.75	4.987	.0029	.007851	140.5±1.4
	950	do.	2.46	70.7	9.01	14.88	5.366	.0162	.007851	143.7±2.2
	975	do.	5.59	91.7	32.24	11.29	5.537	.0047	.007851	141.5±1.6
	1000	do.	6.30	93.3	37.17	11.18	5.503	.0040	.007851	142.4±1.5
	1025	do.	5.47	92.6	38.65	11.15	6.398	.00465	.007851	141.1±1.6
	Fusion	do.	.67	46.0	5.39	21.66	8.143	.0411	.007851	139.2±6.1
								Recalculated total-----		144.7
								Plateau age----------		141.9±1.0

TABLE 6.5.—*$^{40}Ar/^{39}Ar$ ages of rocks of the Bitterroot lobe of the Idaho batholith*—Continued

[Sample locations are given in table 6.1. ^{40}Ar refers to radiogenic argon. TF, total fusion of separate aliquant of sample; +, indicates temperature step omitted from plateau; J, measure of the integrated fast neutron flux determined using a monitor biotite, SB-3]

Sample	Temperature step (°C)	Mineral	Percent of total ^{39}Ar	Percent ^{40}Ar	Percent $^{36}Ar_{Ca}$	$^{40}Ar/^{39}Ar$	$^{37}Ar/^{39}Ar$	$^{36}Ar/^{39}Ar$	J	Age (Ma)
Plutonic rocks of the transition zone										
797-26D------	TF	Muscovite	100	94.7	.03	7.892	0.0013	.0014	0.0066059	86.9±0.9
797-26I(IH)--	750+	Hornblende	.59	.4	.04	789.2	3.523	2.661	.005898	35.7±114.2
	900	do.	35.92	34.3	1.78	21.80	3.232	.0493	.005898	78.0±2.0
	940	do.	38.59	44.0	2.55	17.59	3.204	.0342	.005898	80.7±1.8
	960	do.	7.24	38.7	2.19	19.88	3.393	.0421	.005898	80.2±2.4
	1000	do.	16.55	49.4	3.16	15.96	3.272	.0282	.005898	82.2±1.7
	1050+	do.	.80	5.6	.17	164.8	3.248	.5272	.005898	96.2±24.7
	1100+	do.	.26	5.4	.20	142.8	3.293	.4582	.005898	80.2±46.5
	Fusion+	do.	.04	4.7	.03	1696	6.036	5.468	.005898	703.5±914.6
								Recalculated total-----		80.1
								Plateau age----------		80.5±1.0
807-28I------	TF	Hornblende	100	64.6	7.93	11.53	4.369	0.0150	0.006233	82.1±1.1
	TF	do.	100	65.0	9.9	9.110	4.350	.0120	.007852	82.1±1.4
807-28I(IH)--	750+	do.	5.26	24.6	1.6	26.31	4.083	.0682	.007852	89.8±1.1
	850	do.	29.88	70.9	13.4	8.125	4.553	.0092	.007852	80.0±0.8
	900	do.	28.61	90.2	36.9	6.448	4.531	.0033	.007852	80.8±0.8
	925	do.	10.28	70.2	12.7	8.252	4.439	.0095	.007852	80.4±0.8
	950	do.	17.00	95.7	57.8	6.126	4.418	.0021	.007852	81.4±0.8
	975	do.	7.61	91.0	37.7	6.448	4.345	.0031	.007852	81.4±0.9
	1000+	do.	.42	41.8	4.4	13.40	4.454	.0276	.007852	77.8±5.8
	1025+	do.	.57	35.6	3.4	15.86	4.506	.0358	.007852	78.4±4.3
	Fusion+	do.	.36	16.6	.98	44.06	4.519	.0156	.007852	100.7±6.9
								Recalculated total-----		81.2
								Plateau age----------		80.8±0.4
Plutonic rocks of the Bitterroot lobe, undivided										
818-16F------	TF	Hornblende	100	39.6	2.73	24.27	5.120	.0510	0.0050695	86.6±1.1
818-16F(IH)--	750+	Hornblende	.61	1.6	.01	653.1	1.031	2.174	.0050695	95.1±81.1
	840+	do.	.43	3.0	.02	749.4	2.202	2.461	.0050695	194.0±125.0
	890+	do.	.20	2.5	.02	1241	3.106	4.098	.0050695	261.8±414.9
	930+	do.	.32	.4	.02	1779	3.632	6.043	.0050695	-59.2±448.3
	960+	do.	.64	3.3	.22	162.8	4.371	.5342	.0050695	47.9±31.2
	1000	do.	15.85	59.7	6.31	15.17	5.119	.0220	.0050695	81.2±1.3
	1040	do.	61.43	83.7	19.23	1.87	5.243	.0074	.0050695	81.5±0.9
	1100	do.	20.33	74.1	11.53	12.75	5.352	.0126	.0050695	84.6±1.2
	Fusion+	do.	.19	7.6	.09	475.5	5.145	1.1488	.0050695	305.6±176.0
								Recalculated total-----		82.9
								Plateau age----------		82.3±0.6
787-19A------	TF	Hornblende	100	70.9	11.41	7.572	3.521	0.0084	0.006930	66.0±1.0
787-19A(IH)--	750+	do.	2.74	19.8	.30	68.74	2.044	.1872	.00693	162.6±8.1
	890+	do.	12.40	21.3	2.17	15.73	3.418	.0428	.00693	41.5±2.4
	925	do.	14.41	55.7	5.97	9.988	3.489	.0159	.00693	68.4±1.3
	960	do.	16.45	55.6	6.21	9.717	3.547	.0156	.00693	66.5±1.2
	1000	do.	15.73	50.5	5.48	10.03	3.575	.0177	.00693	62.4±1.3
	1075	do.	28.64	70.3	11.41	7.450	3.538	.0084	.00693	64.5±1.0
	Fusion	do.	9.63	48.4	4.83	11.12	3.169	.0204	.00693	66.2±1.6
								Recalculated total-----		65.1
								Plateau age----------		65.4±0.6
787-20A------	TF	Hornblende	100	55.7	4.76	10.97	3.020	.0173	0.005723	62.1±1.2
787-20E------	TF	Biotite	100	79.1	.02	5.360	.0029	.0038	.006979	52.6±0.8
787-24H(IH)--	750+	Hornblende	3.55	7.8	.03	127.9	.4398	.3992	.0062025	107.9±14.8
	755+	do.	.37	7.0	.01	565.7	.4838	1.782	.0062025	394.±149
	835+	do.	1.12	4.6	.11	154.7	2.053	.5002	.0062025	77.6±24.8
	900	do.	3.52	22.3	1.29	26.52	3.346	.0706	.0062025	65.3±7.2
	960	do.	14.24	48.1	5.96	9.777	3.995	.0183	.0062025	52.0±2.0
	1029	do.	36.74	71.3	14.81	6.174	3.816	.0070	.0062025	48.7±1.0
	1100	do.	38.09	80.3	22.16	5.496	3.812	.0047	.0062025	48.8±0.8
	Fusion+	do.	2.36	20.8	1.02	38.43	3.915	.1041	.0062025	87.5±10.8
								Recalculated total-----		54.6
								Plateau age----------		49.2±1.9

TABLE 6.5.—*$^{40}Ar/^{39}Ar$ ages of rocks of the Bitterroot lobe of the Idaho batholith*—Continued

[Sample locations are given in table 6.1. ^{40}Ar refers to radiogenic argon. TF, total fusion of separate aliquant of sample; +, indicates temperature step omitted from plateau; J, measure of the integrated fast neutron flux determined using a monitor biotite, SB-3]

Sample	Temperature step (°C)	Mineral	Percent of total ^{39}Ar	Percent ^{40}Ar	Percent $^{36}Ar_{Ca}$	$^{40}Ar/^{39}Ar$	$^{37}Ar/^{39}Ar$	$^{36}Ar/^{39}Ar$	J	Age (Ma)
Plutonic rocks of the Bitterroot lobe, undivided--Continued										
787-26A------	TF	Hornblende	100	17.0	.96	36.34	3.617	0.0103	0.005723	62.8±3.8
787-26F------	TF	do.	100	77.6	15.25	8.120	4.060	.0072	.005723	64.1±1.0
787-26F(IH)--	750+	do.	2.73	33.1	.75	40.01	2.501	.0913	.005723	131.9±8.4
	890+	do.	1.34	23.5	.94	28.64	2.576	.0749	.005723	68.2±7.5
	925+	do.	2.43	43.9	3.59	15.60	4.048	.0307	.005723	69.6±4.8
	960	do.	12.66	85.3	23.30	7.396	4.088	.0048	.005723	64.1±1.1
	1000	do.	18.90	90.6	34.09	6.678	4.019	.0032	.005723	61.5±0.9
	1050	do.	32.27	92.6	41.25	6.425	4.078	.0027	.005723	60.6±0.8
	Fusion	do.	28.67	88.4	28.82	7.163	4.160	.0039	.005723	64.4±0.9
								Recalculated total-----		64.6
								Plateau age----------		62.4±0.5
80MT246------	TF	Hornblende	100	31.0	3.72	12.95	4.292	.0314	0.006287	47.4±0.6
	TF	do.	100	52.1	8.16	8.086	4.271	.0142	.0066124	47.3±0.6
80MT246(IH)--	750+	Hornblende	1.52	3.9	.08	143.3	1.448	.4664	.0066124	65.2±11.4
	820+	do.	4.21	3.4	.35	85.72	3.648	.2813	.0066124	34.2±3.9
	875	do.	12.10	18.2	1.85	22.52	4.320	.0635	.0066124	42.5±1.4
	950	do.	26.64	54.0	9.57	7.278	4.404	.0125	.0066124	46.4±0.7
	1050	do.	53.86	61.8	12.73	6.464	4.470	.00956	.0066124	47.2±0.6
	Fusion+	do.	1.67	11.2	1.02	40.54	4.613	.1231	.0066124	53.4±8.9
								Recalculated total-----		46.9
								Plateau age----------		47.0±0.5
Eocene epizonal plutons and associated volcanic rocks										
787-18J------	TF	Biotite	100	74.7	.10	5.179	0.0164	0.0044	0.006979	48.1±0.7
787-25A------	TF	Hornblende	100	72.4	13.85	6.792	3.736	.0073	.006930	50.2±0.7
	TF	do.	100	56.0	8.50	7.423	3.767	.0121	.005723	51.3±1.0
787-25B------	TF	Biotite	100	36.4	4.03	11.35	3.767	.0254	.006930	51.1±1.4
797-19C------	TF	Sanidine	100	95.2	.35	4.89	.0100	.0078	.005898	48.9±0.6
807-29E------	TF	Sanidine	100	42.3	1.60	8.794	1.023	.0174	.0050695	34.0±0.7
(dike)	TF	do.	100	9.1	.21	44.12	1.042	.1360	.004771	34.2±1.1
Metamorphosed Precambrian rocks										
807-31K------	TF	Hornblende	100	18.2	1.27	41.32	5.391	.1159	0.006233	82.7±1.3
808-01G------	TF	Muscovite	100	87.2	.06	9.412	.0090	.0039	.004771	69.8±0.7

is devoid of Precambrian rocks and probably represents an accreted island-arc complex. Jurassic and Cretaceous granitic intrusions reflect the character of this zone in their low r_i values (≤ 0.7042), low Rb/Sr ratios (≤ 0.08), $\delta^{18}O$ values of +5.5 to +10.5 per mil, δD values of −41 to −82 per mil, and in their calcic and metaluminous major-element chemistry. The eastern or Belt-Yellowjacket terrane contains abundant Precambrian rocks and is intruded by both Cretaceous-early Tertiary main-phase granitoids and by Eocene epizonal plutons. The main-phase plutons reflect their Precambrian source region in their high r_i values (≥ 0.708), Rb/Sr ratios (0.04 to 0.24), high primary $\delta^{18}O$ values (+8.0 to +12.4 per mil), and in their calcic to calc-alkaline, metaluminous to peraluminous chemistry. The Eocene epizonal plutons all have r_i values of ≥ 0.704, suggesting the presence of an ancient component, but several values between 0.704 and 0.708 indicate limited wall-rock involvement. Rb/Sr ratios of these epizonal plutons are very large (as much as 49.0), probably due to differentiation. These calc-alkaline plutons are chemically similar to the Challis Volcanics.

Extensive hydrothermal circulation systems developed in the region during both Cretaceous-early Tertiary and Eocene times. The Cretaceous-early Tertiary hydrothermal activity was most pronounced near the perimeter of the Bitterroot lobe, where most of the ore deposits in the region are located. This deep hydrothermal system was probably contemporaneous with regional metamorphism

of the Precambrian wall rock. Major shallow hydrothermal systems involving fluids derived from low-^{18}O meteoric waters developed during the emplacement of the Eocene epizonal plutons. Water-rock interactions produced large reductions in the δD values (as low as -148 per mil) and $\delta^{18}O$ values (as low as -0.3 per mil) of the granitic rocks in the affected areas. Only a few ore deposits in the Bitterroot lobe appear to be related to these Eocene hydrothermal systems, however. The hydrothermal systems did not greatly disturb the Rb-Sr systematics of Bitterroot lobe plutons, partly because large intervals do not separate the times of emplacement and alteration, but the isochrons of Precambrian rocks appear to have been profoundly modified by later hydrothermal metamorphism.

The K-Ar apparent ages of hornblende range from ≥160 Ma for some Jurassic plutons in the Wallowa-Seven Devils terrane to as low as 44 Ma for Eocene granitic rocks. Some low-r_i plutons of the Wallowa-Seven Devils terrane have concordant biotite and hornblende ages of 135 Ma and show no geochemical indication of proximity to the Precambrian craton. Transition zone plutons having K-Ar mineral ages of 87 to 75 Ma intrude both the Wallowa-Seven Devils terrane and the Precambrian sialic rocks. These results indicate that the tectonic suture between these terranes formed between approximately 135 and 75 Ma, probably between 95 and 80 Ma. Most of the Bitterroot lobe was emplaced after this probable accretionary event. However, the hornblende and biotite K-Ar

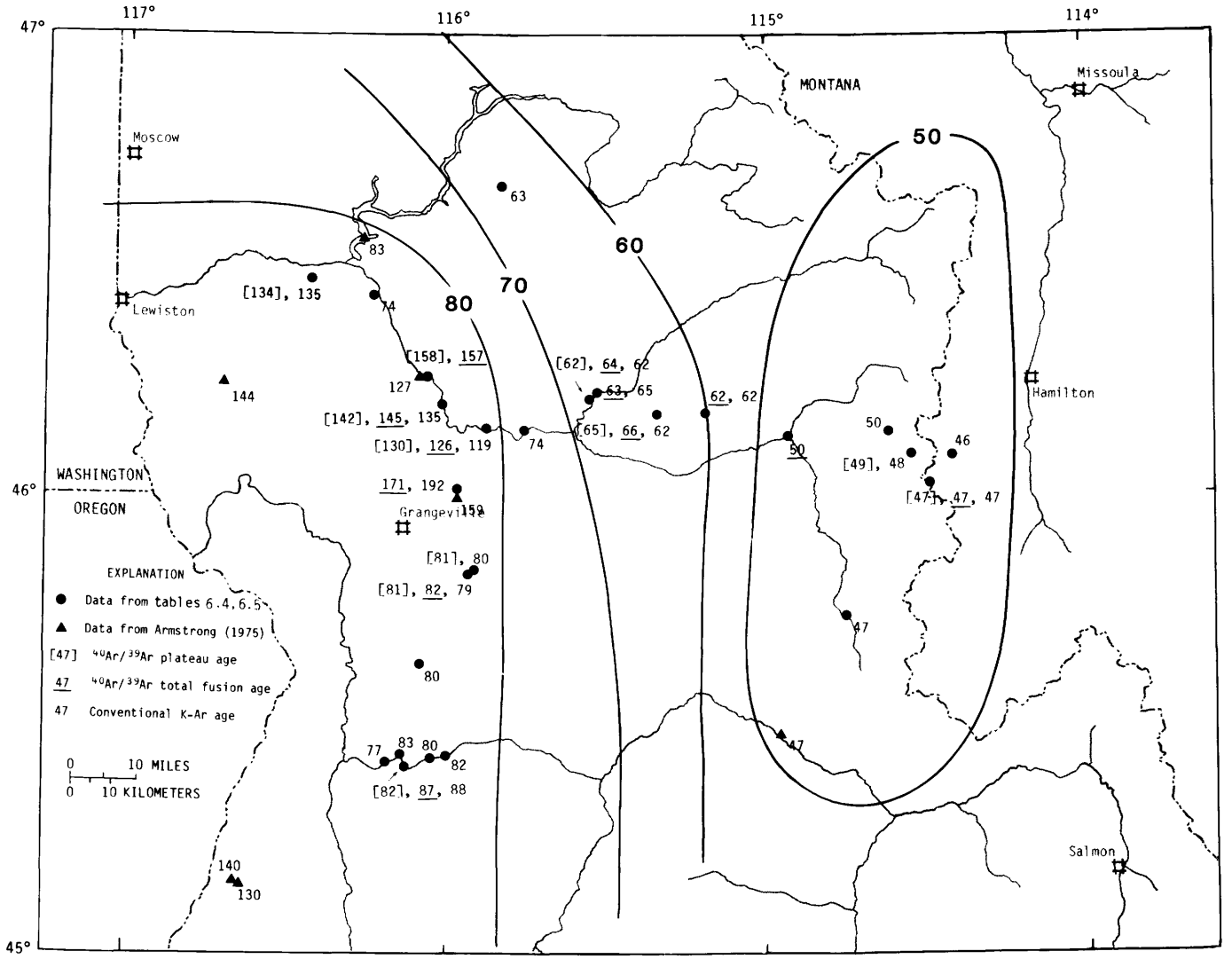

FIGURE 6.18.—Contour map of K-Ar and $^{40}Ar/^{39}Ar$ apparent ages of hornblende. Most of these apparent ages are thought to be within 10 m.y. of the emplacement ages and indicate that magmatism migrated progressively toward the east-central part of the Bitterroot lobe. The ages of the transition-zone plutons, which intrude the suture zone between the Precambrian craton and the accreted terrane, provide an absolute lower limit of 75 Ma for the accretionary event.

apparent ages become systematically younger toward the mylonitic front of the Bitterroot lobe, with biotite data defining a 10,000-km^2 area of apparent ages of 51 to 44 Ma. The detailed relations of hornblende and biotite K-Ar apparent ages in the Bitterroot lobe are thought to reflect temporal migration of magmatism as well as rapid uplift and cooling of the region.

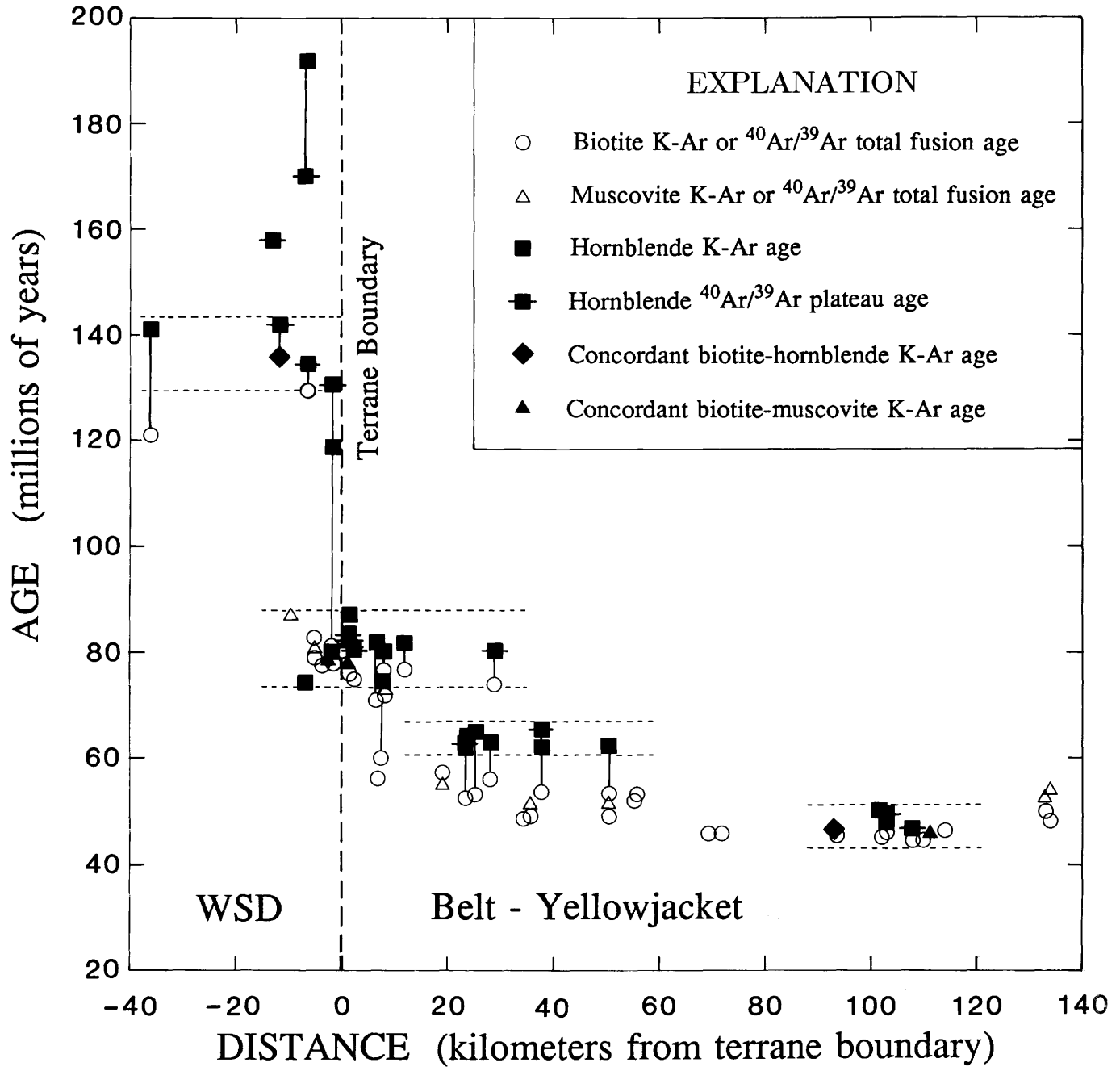

FIGURE 6.19.—K-Ar and $^{40}Ar/^{39}Ar$ ages of plutonic rocks plotted against their distance from the WSD/Belt-Yellowjacket terrane boundary. Vertical tielines connect ages determined from the same sample. Plutons yielding Jurassic and Early Cretaceous ages are confined to the WSD terrane. This abrupt termination at the terrane boundary suggests that the Jurassic-Early Cretaceous magmatic arc was truncated tectonically and juxtaposed with Precambrian sialic crust subsequent to 135 Ma. Ages determined on hornblende and muscovite from transition-zone plutons, which intrude both terranes in the 5- to 25-km zone on either side of the suture, range from 87 to 75 Ma. Within the Belt-Yellowjacket terrane, two early Tertiary plutonic episodes are defined by rather abrupt steps in hornblende ages: 62 to 66 Ma and 46 to 51 Ma. Note that no hornblende-bearing samples were found in the central part of the Bitterroot lobe (55 to 90 km from the terrane boundary). Biotite ages exhibit a smooth decrease in age normal to the terrane boundary, reflecting uplift and (or) argon loss due to younger intrusive events.

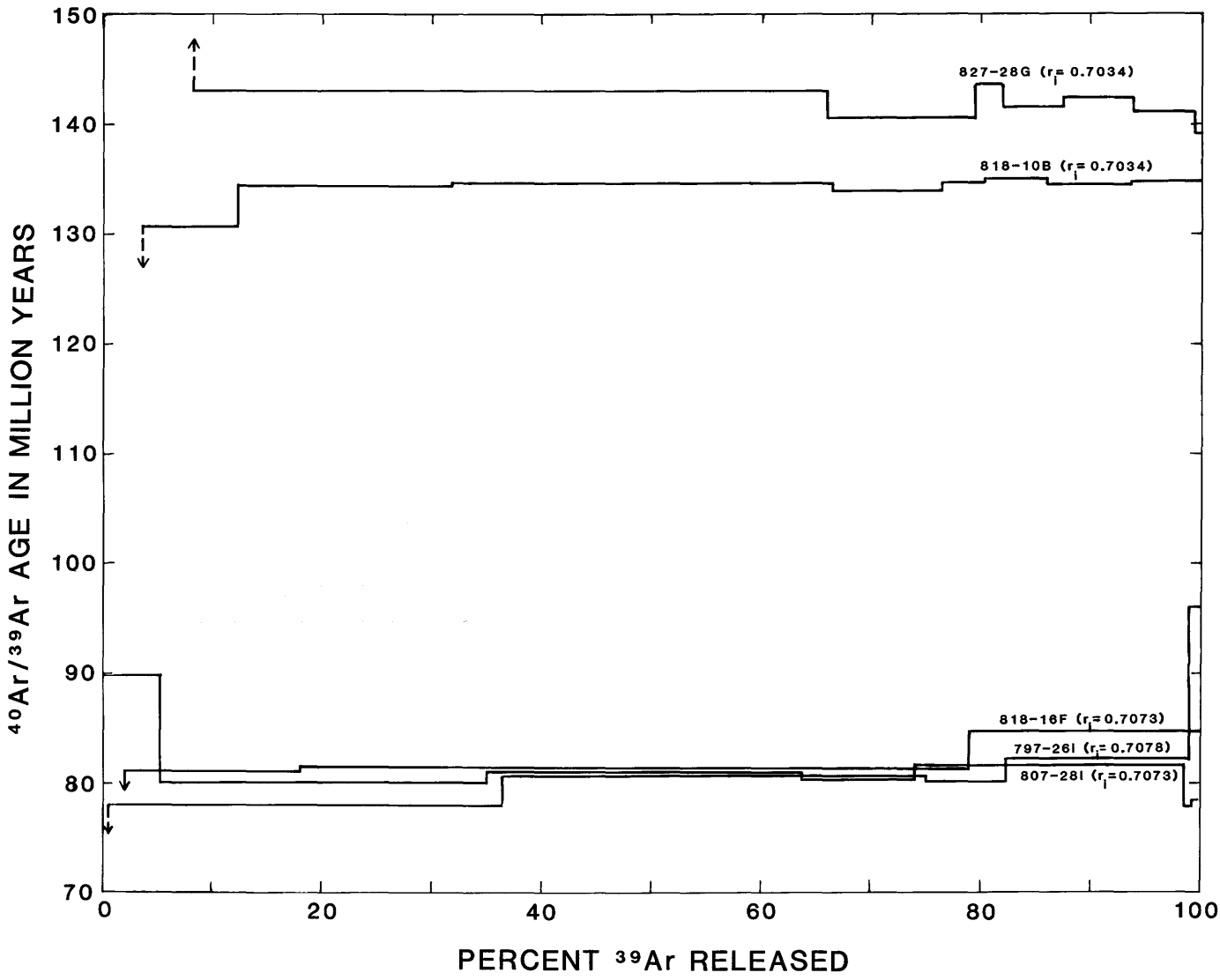

FIGURE 6.20.—$^{40}Ar/^{39}Ar$ age spectra of hornblende from granitic rocks within and near the tectonic suture between the Wallowa-Seven Devils terrane and the Precambrian craton. Samples 827-28G and 818-10B have flat Early Cretaceous age spectra, concordant or nearly concordant biotite and hornblende K-Ar ages, and low initial strontium (r_i) ratios that give no indication of assimilation of Precambrian rocks. Samples 818-16F, 807-28I, and 797-26I have flat Late Cretaceous age spectra, nearly concordant biotite and hornblende K-Ar ages, and higher initial strontium ratios that indicate involvement of both Precambrian and arc-derived materials in the magmas. Taken together, these data establish that the arc-continent suture zone formed between 135 and 80 Ma.

REFERENCES CITED

Anderson, A.L., 1951, Metallogenic epochs in Idaho: Economic Geology, v. 46, p. 592-607.

Armstrong, R.L., 1974, Geochronometry of the Eocene volcanic-plutonic episode in Idaho: Northwest Geology, v. 3, p. 1-15.

_____ 1975, The geochronometry of Idaho: Isochron/West, v. 14, p. 1-50.

Armstrong, R.L., Taubeneck, W.H., and Hales, P.O., 1977, Rb-Sr and K-Ar geochronometry of Mesozoic granitic rocks and their Sr isotopic composition, Oregon, Washington, and Idaho: Geological Society of America Bulletin, v. 88, 397-411.

Avé Lallemant, H.G., Phelps, D.W., and Sutter, J.F., 1980, ^{40}Ar-^{39}Ar ages of some pre-Tertiary plutonic and metamorphic rocks of eastern Oregon and their geologic relationships: Geology, v. 8, p. 371-374.

Axelrod, D.I., 1966, Potassium-argon ages of some western Tertiary floras: American Journal of Science, v. 264, p. 497-506.

Bateman, P.C., and Dodge, F.C.W., 1970, Variations of major chemical constituents across the central Sierra Nevada batholith: Geological Society of America Bulletin, v. 81, p. 409-420.

Bennett, E.H., 1980, Granitic rocks of Tertiary age in the Idaho batholith and their relation to mineralization: Economic Geology, v. 75, 278-288.

Bergendahl, M.H., 1964, Gold, *in* Mineral and water resources of Idaho: U.S. Geological Survey Special Report No. 1, p. 93-101.

Bickford, M.E., Chase, R.B., Nelson, B.K., Shuster, R.D., and Arruda, E.C., 1981, U-Pb studies of zircon cores and overgrowths, and monazite: Implications for age and petrogenesis of the northeastern Idaho batholith: Journal of Geology, v. 89, p. 433-457.

Bond, J.G., 1978, Geologic map of Idaho: Idaho Bureau of Mines and Geology.

Borthwick, J., and Harmon, R.S., 1982, A note regarding ClF_3 as an alternative to BrF_5 for oxygen isotope analysis: Geochimica et Cosmochimica Acta, v. 46, p. 1665-1668.

Cater, F.W., Pinckney, D.M., Hamilton, W.B., Parker, R.L., Weldin, R.D., Close, T.J., Zilca, N.T., Leonard, B.F., and Davis, W.E., 1973, Mineral resources of the Idaho primitive area and vicinity, Idaho: U.S. Geological Survey Bulletin 1304, 431 pp.

Chase, R.B., 1973, Petrology of the northeastern border zone of the Idaho batholith, Bitterroot Range, Montana: Montana Bureau of Mines and Geology Memoir 43, 28 p.

Chase, R.B., Bickford, M.E., and Arruda, E.C., 1983, Tectonic implications of Tertiary intrusion and shearing within the Bitterroot dome, northeastern Idaho batholith: Journal of Geology, v. 91, p. 462-470.

Chase, R.B., Bickford, M.E., and Tripp, S.E., 1978, Rb-Sr and U-Pb isotopic studies of the northeastern Idaho batholith and border zone: Geological Society of America Bulletin, v. 89, p. 1325-1334.

Chase, R.B., and Johnson, B.R., 1977, Border-zone relationships of the northern Idaho batholith: Northwest Geology, v. 6, no. 1, p. 38-50.

Chase, R.B., and Talbot, J.L., 1973, Structural evolution of the northeastern border zone of the Idaho batholith, western Montana [abs.]: Geological Society of America Abstracts with Programs, v. 5, p. 470-471.

Clayton, R.N., and Mayeda, T.K., 1963, The use of bromine pentafluoride in the extraction of oxygen from oxide and silicates for isotopic analysis: Geochimica et Cosmochimica Acta, v. 27, p. 43-52.

Cox, A., and Dalrymple, G.B., 1967, Statistical analysis of geomagnetic reversal data and the precision of potassium-argon dating: Journal of Geophysical Research, v. 72, p. 2603-2614.

Craig, H., 1961, Standard for reporting concentrations of deuterium and oxygen-18 in natural waters: Science, v. 133, 1833-1834.

Criss, R.E., 1981, An $^{18}O/^{16}O$, D/H and K-Ar study of the southern half of the Idaho batholith: Pasadena, California Institute of Technology, Ph.D. dissertation, 401 pp.

Criss, R.E., and Champion, D.E., 1984, Magnetic properties of granitic rocks from the southern half of the Idaho batholith: influences of hydrothermal alteration and implications for aeromagnetic interpretation: Journal of Geophysical Research, v. 89, p. 7061-7076.

Criss, R.E., Champion, D.E., and McIntyre, D.H., 1985, $\delta^{18}O$, aeromagnetic and gravity anomalies associated with hydrothermally altered zones in the Yankee Fork mining district, Custer County, Idaho: Economic Geology, v. 80, p. 1277-1296.

Criss, R.E., Ekren, E.B., and Hardyman, R.F., 1984, Casto ring zone: a 4,500-km^2 fossil hydrothermal system in the Challis volcanic field, central Idaho: Geology, v. 12, p. 331-334.

Criss, R.E., Lanphere, M.A., and Taylor, H.P., Jr., 1982, Effects of regional uplift, deformation, and meteoric-hydrothermal metamorphism on K-Ar ages of biotites in the southern half of the Idaho batholith: Journal of Geophysical Research, v. 87, p. 7029-7046.

Criss, R.E., and Taylor, H.P., Jr., 1983, An $^{18}O/^{16}O$ and D/H study of Tertiary hydrothermal systems in the southern half of the Idaho batholith: Geological Society of America Bulletin, v. 94, p. 640-663.

Dalrymple, G.B., and Lanphere, M.A., 1969, Potassium-argon dating, principles, techniques, and applications to geochronology: San Francisco, California, W.H. Freeman, 258p.

_____ 1971, $^{40}Ar/^{39}Ar$ technique of K-Ar dating: a comparison with the conventional technique: Earth and Planetary Science Letters, v. 12, p. 300-308.

Dontsova, Ye I., 1970, Oxygen isotope exchange in rock-forming processes: Geochemistry International, v. 7, p. 624-636.

Ferguson, J.A., 1975, Tectonic implications of some geochronometric data from the northeastern border zone of the Idaho batholith: Northwest Geology, v. 4, p. 53-58.

Finch, J.W., 1932, Prospecting for gold ores: Idaho Bureau of Mines and Geology Pamphlet, v. 36, p. 1-33.

Fleck, R.J. and Criss, R.E., 1985, Strontium and oxygen isotopic variations in Mesozoic and Tertiary plutons of central Idaho: Contributions to Mineralogy and Petrology, v, 90, p. 291-308.

Friedman, I., 1953, Deuterium content of natural waters and other substances: Geochimica et Cosmochimica Acta, v. 4, p. 89-103.

Garlick, G.D., and Epstein, S., 1967, Oxygen isotope ratios in coexisting minerals of regionally metamorphosed rocks: Geochimica et Cosmochimica Acta, v. 31, p. 181-214.

Garmezy, L., and Greenwood, W.R., 1981, Mylonitization coincident with batholith emplacement: Bitterroot lobe, Idaho batholith [abs]: Geological Society of America Abstracts with Programs, v. 13, p. 197.

Garmezy, L., and Sutter, J.F., 1983, Mylonization coincident with uplift in an extensional setting, Bitterroot Range, Montana-Idaho [abs.]: Geological Society of America Abstracts with Programs, v. 15, p. 578.

Godfrey, J.D., 1962, The deuterium content of hydrous minerals from the east-central Sierra Nevada and Yosemite National Park: Geochimica et Cosmochimica Acta, v. 26, p. 1215-1245.

Grauert, B., and Hofmann, A., 1973, Old radiogenic lead components in zircons from the Idaho batholith and its metasedimentary aureole: Carnegie Institution of Washington Year Book, v. 72, p. 297-299.

Greenwood, W.R., and Morrison, D.A., 1973, Reconnaissance geology of the Selway-Bitterroot Wilderness Area: Idaho Bureau of Mines and Geology Pamphlet, v. 154, 30 p.

Hamilton, W.B., 1963, Metamorphism in the Riggins region, western Idaho: U.S. Geological Survey Professional Paper 436, 95p.

Hamilton, W., 1976, Tectonic history of west-central Idaho [abs.]: Geological Society of America Abstracts with Programs, v. 8, p. 378.

Harms, T.A., and Price, R.A., 1983, The Newport fault: Eocene crustal stretching, necking and listric normal faulting in NE Washington and NW Idaho [abs.]: Geological Society of America Abstracts with Programs, v. 15, p. 309.

Hietanen, Anna, 1962, Metasomatic metamorphism in western Clearwater County, Idaho: U.S. Geological Survey Professional Paper 344-A, 116 p.

_____ 1963, Idaho batholith near Pierce and Bungalow, Clearwater County, Idhao: U.S. Geological Survey Professional Paper 344-D, p. 1-42.

_____ 1984, Geology along the northwest border zone of the Idaho batholith, northern Idaho: U.S. Geological Survey Bulletin 1608, 17 p.

Hoernes, S., and Friedrichsen, H., 1980, Oxygen and hydrogen isotope composition of Alpine and pre-Alpine minerals of the Swiss central Alps: Contributions to Mineralogy and Petrology, v. 72, p. 19-32.

Hyndman, D.W., 1980, Bitterroot dome-Sapphire tectonic block, an example of a plutonic gneiss-dome complex with its detached suprastructure, *in* Coney, P.J., Crittenden, Max, Jr., and Davis, G.H., eds., Cordilleran metamorphic core complexes: Geological Society of America Memoir 153, p. 427-443.

Hyndman, D.W., 1981, Controls on source and depth of emplacement of granitic magma: Geology, v. 9, p. 244-249.

_____ 1983, The Idaho batholith and associated plutons, Idaho and western Montana: Geological Society of America Memoir 159, p. 213-240.

_____ 1984, A petrographic and chemical section through the northern Idaho batholith: Journal of Geology, v. 92, p. 83-102.

Hyndman, D.W., Talbot, J.L., and Chase, R.B., 1975, Boulder batholith: a result of emplacement of a block detached from the Idaho batholith infrastructure?: Geology, v. 3, p. 401-404.

Hyndman, D.W., and Williams, L.D., 1977, The Bitterroot lobe of the Idaho batholith: Northwest Geology, v. 6., no. 1, p. 1-16.

Jager, E., 1962, Rb-Sr age determination on micas and total rocks from the Alps: Journal of Geophysical Research, v. 67, p. 5293-5306.

Jones, D.L., Silberling, N.J., and Hillhouse, J., 1977, Wrangellia—a displaced terrane in northwestern North America: Canadian Journal of Earth Sciences, v. 14, p. 2565-2577.

Kiilsgaard, T.H., Freeman, V.L., and Coffman, J.S., 1970, Mineral resources of the Sawtooth Primitive Area, Idaho: U.S. Geological Survey Bulletin 1319D, 174 pp.

Kistler, R.W., and O'Neil, J.R., 1975, Fossil geothermal gradients in crystalline rocks of the Ruby Mountains, Nevada as indicated by radiogenic and stable isotopes [abs.]: Geological Society of America Abstracts with Programs, v. 7, p. 334-335.

Kistler, R.W., and Peterman, Z.E., 1973, Variations in Sr, Rb, K, Na, and initial $^{87}Sr/^{86}Sr$ in Mesozoic granitic rocks and intruded wall rocks in central California: Geological Society of America Bulletin, v. 84, p. 3489-3512.

Krummenacher, Daniel, Gastil, R.G., Bushee, J., and Doupont, J., 1975, K-Ar apparent ages, Peninsular Ranges batholith, southern California and Baja California: Geological Society of America Bulletin, v. 86, p. 760-768.

Lang, H.M., and Rice, J.M., 1985, Metamorphism of pelitic rocks in the Snow Peak area, northern Idaho: sequence of events and regional implications: Geological Society of America Bulletin, v. 96, p. 731-736.

Langton, C.M., 1935, Geology of the northeastern part of the Idaho batholith and adjacent region in Montana: Journal of Geology, v. 43, p. 27-60.

Larsen, E.S., Jr., and Schmidt, R.G., 1958, A reconnaissance of the Idaho batholith and comparison with the southern California batholith: U.S. Geological Survey Bulletin 1070-A, p. 1-33.

Lindgren, Waldemar, 1904, A geologic reconnaissance across the Bitterroot Range and Clearwater Mountains in Montana and Idaho: U.S. Geological Survey Professional Paper 27, 123 p.

Mabey, D.R., Zietz, I. Eaton, G.P., and Kleinkopf, M.D., 1978, Regional magnetic patterns in part of the cordillera in the Western United States, *in* Smith, R.B. and Eaton, G.P., eds., Cenozoic tectonics and regional geophysics of the Western Cordillera: Geological Society of America Memoir 152, p. 93-106.

Magaritz, M., Whitford, D.J., and James, D.E., 1978, Oxygen isotopes and the origin of high $^{87}Sr/^{86}Sr$ andesites: Earth and Planetary Science Letters, v. 40, p. 220-230.

Masi, U., O'Neil, J.R., and Kistler, R.W., 1981, Stable isotope systematics in Mesozoic granites of central and northern California and southwestern Oregon: Contributions to Mineralogy and Petrology, v. 67, p. 116-126.

McCulloch, M.T., Gregory, R.T., Wasserburg, G.J., and Taylor, H.P., Jr., 1980, A neodymium, strontium, and oxygen isotopic study of the Cretaceous Samail ophiolite and implications for the petrogenesis and seawater-hydrothermal alteration of oceanic crust: Earth and Planetary Science Letters, v. 46, p. 201-211.

McDowell, F.W., and Kulp, J.L., 1969, Potassium-argon dating of the Idaho batholith: Geological Society of America Bulletin, v. 80, p. 2379-2382.

McGookey, D.P., Haun, J.D., Hale, L.A., Goodell, H.G., McCubbin, D.G., Weimer, J.R., and Wulf, G.R., 1972, Cretaceous System, *in* Mallory, W.M., ed., Geologic Atlas of the Rocky Mountain region: Rocky Mountain Association of Geologists, A.B. Hirschfeld Press, p. 190-228.

McIntyre, D.H., Ekren, E.B., and Hardyman, R.F., 1982, Stratigraphic and structural framework of the Challis Volcanics in the east half of the Challis 1° by 2° quadrangle, *in* Bonnichsen, B., and Breckenridge, R., eds., Cenozoic geology of Idaho: Idaho Bureau of Mines and Geology Bulletin 26, p. 3-33.

McIntyre, D.H., Hobbs, S.W., Marvin, R.F., and Mehnert, H.H., 1976, Late Cretaceous and Eocene ages for hydrothermal alteration and mineralization, Bayhorse district and vicinity, Custer County, Idaho: Isochron/West, v. 16, p. 11-12.

Miller, F.K., and Engels, J.C., 1975, Distribution and trends of discordant ages of the plutonic rocks of northeastern Washington and northern Idaho: Geological Society of America Bulletin, v. 86, p. 517-528.

Mitchell, V.E., Strowd, W.B., Hustedde, G.S., and Bennett, E.H., 1981a, Mines and prospects of the Elk City quadrangle, Idaho: Idaho Bureau of Mines and Geology, Mines and Prospects Map Series.

_____1981b, Mines and prospects of the Hamilton quadrangle, Idaho: Idaho Bureau of Mines and Geology, Mines and Prospects Map Series.

Motzer, W.E., 1985, Anorogenic granite plutons of the Selway-Bitterroot Wilderness (SBW), Idaho [abs.]: Geological Society of America Abstracts with Programs, v. 17, p. 257.

Obradovich, J.D., and Peterman, Z.E., 1968, Geochronology of the Belt Series, Montana: Canadian Journal of Earth Sciences, v. 5, p. 737-747.

Reid, R.R., Greenwood, W.R., and Morrison, D.A., 1970, Precambrian metamorphism of the Belt Supergroup in Idaho: Geological Society of America Bulletin, v. 81, p. 915-918.

Reid, R.R., Morrison, D.A., and Greenwood, W.R., 1973, The Clearwater orogenic zone: a relic of Proterozoic orogeny in central and northern Idaho: Belt Symposium, Moscow, University of Idaho, Department of Geology, p. 10-56.

Ross, C.P., 1928, Mesozoic and Tertiary granitic rocks in Idaho: Journal of Geology, v. 36, p. 673-693.

_____ 1931, A classification of the lode deposits of south-central Idaho: Economic Geology, v. 26, p. 169-185.

_____ 1934, Geology and ore deposits of the Casto quadrangle, Idaho: U.S. Geological Survey Bulletin 854, 135 pp.

_____ 1962, Stratified rocks in south-central Idaho: Idaho Bureau of Mines and Geology Pamphlet 125, 126 p.

Ross, C.P., Andrews, D.A., and Witkind, I.J., 1955, Geologic map of Montana, scale 1:500,000: U.S. Geological Survey.

Ryder, R.T., and Ames, H.T., 1970, Palynology and age of Beaverhead Formation and their paleotectonic implications in Lima region, Montana-Idaho: American Association of Petroleum Geologists Bulletin, v. 54, p. 1155-1171.

Ryder, R.T., and Scholten, R., 1973, Syntectonic conglomerates in southwestern Montana: their nature, origin, and tectonic significance: Geological Society of America Bulletin, v. 84, p. 773-796.

Scholten, R., and Onash, C.M., 1977, Genetic relations between the Idaho batholith and its deformed eastern and western margins: Northwest Geology, v. 6, no. 1, p. 25-37.

Shieh, Y.N., and Schwarcz, H.P., 1974, Oxygen isotope studies of granite and migmatite, Grenville province of Ontario, Canada: Geochimica et Cosmochimica Acta, v. 38, p. 21-45.

Shieh, Y.N., and Taylor, H.P., 1969, Oxygen and hydrogen isotope studies of contact metamorphism in the Santa Rosa Range, Nevada and other areas: Contributions to Mineralogy and Petrology, v. 20, p. 306-356.

Snee, L.W., Lund, K., and Gammons, C.H., 1985, Mineralization history of the central Idaho batholith: importance of fracture-controlled Cretaceous activity [abs.]: Geological Society of America Abstracts with Programs, v. 17, p. 265.

Sutter, J.F., Snee, L.W ., and Lund, K., 1984, Metamorphic, plutonic, and uplift history of a continent-island arc suture zone, west-central Idaho [abs.]: Geological Society of America Abstracts with Programs, v. 16, p. 670.

Swanberg, C.A., and Blackwell, D.D., 1973, Areal distribution and geophysical significance of heat generation in the Idaho batholith and adjacent intrusions in eastern Oregon and western Montana: Geological Society of America Bulletin, v. 84, 1261-1282.

Taylor, H.P., 1970, Oxygen isotope studies of anorthosites, with particular reference to the origin of bodies in the Adirondack Mountains, New York, *in* Origin of anorthosites: New York State Museum

and Science Service Memoir, v. 18, p. 111-134.

_____ 1971, Oxygen isotope evidence for large-scale interaction between meteoric ground waters and Tertiary granodiorite intrusions, western Cascade Range, Oregon: Journal of Geophysical Research, v. 76, p. 7855-7874.

_____ 1977, Water-rock interactions and the origin of H_2O in granitic batholiths: Geological Society of London Journal, v. 133, p. 509-558.

_____ 1981, The effects of assimilation of country rocks by magmas on $^{18}O/^{16}O$ and $^{87}Sr/^{86}Sr$ systematics in igneous rocks: Earth and Planetary Science Letters, v. 47, p. 243-254.

Taylor, H.P., Jr., and Forester, R.W., 1979, An oxygen and hydrogen isotope study of the Skaergaard intrusion and its country rocks: a description of a 55-m.y.-old fossil hydrothermal system: Journal of Petrology, v. 20, p. 355-419.

Taylor, H.P., Jr., and Magaritz, M., 1978, Oxygen and hydrogen isotope studies of the cordilleran batholiths of western North America, *in* Robinson, B.W., ed., Stable isotopes in the earth sciences: Wellington, New Zealand, New Zealand Department of Scientific and Industrial Research Bulletin, v. 220, p. 151-173.

Taylor, H.P., Jr., and Silver, L.T., 1978, Oxygen isotope relationships in plutonic igneous rocks of the Peninsular Ranges batholith, southern and Baja California, *in* Short papers of the Fourth International Conference on Geochronology, Cosmochronology, and Isotope Geology: U.S. Geological Survey Open-File Report 78-701, p. 423-426.

Tilling, R.I., 1973, The Boulder batholith, Montana: A product of two contemporaneous but chemically distinct magma series: Geological Society of America Bulletin, v. 84, p. 3879-3900.

Toth, M.I., Coxe, B.W., Zilka, N.T., and Hamilton, M.M., 1983, Mineral resource potential of the Selway-Bitterroot Wilderness, Idaho County, Idaho, and Missoula and Ravalli Counties, Montana: U.S. Geological Survey Miscellaneous Field Investigations Map MF 1495-A, scale 1:125,000.

Turi, B., and Taylor, H.P., 1971, An oxygen and hydrogen isotope study of a granodiorite pluton from the southern California batholith: Geochimica et Cosmochimica Acta, v. 35, p. 383-406.

Tschanz, C.M., and others, 1974, Mineral resources of the eastern part of the Sawtooth National Recreation Area, Custer and Blaine Counties, Idaho: U.S. Geological Survey Open-File Report, 648 p.

Vallier, T.L., 1977, The Permian and Triassic Seven Devils Group, western Idaho and northeastern Oregon: U.S. Geological Survey Bulletin 1437, 58 p.

Walker, N. W., 1983, Pre-Tertiary tectonic evolution of northeastern Oregon and west-central Idaho: constraints based on U/Pb ages of zircons [abs.]: Geological Society of America Abstracts with Programs, v. 15, p. 371.

Williams, L.D., 1979, General geology of a section across the Bitterroot lobe of the Idaho batholith: Northwest Geology, v. 8, p. 29-39.

Zen, E-an, and Hammarstrom, J.J., 1984, Magmatic epidote and its petrologic significance: Geology, v. 12, p. 515-518.

Zietz, I., Gilbert, F.P., and Kirby, J.R., Jr., 1978, Aeromagnetic map of Idaho: Color coded intensities: U.S. Geological Survey Geophysical Investigations Map GP-920, scale, 1:1,000,000.

Zietz, I., Gilbert, F.P., and Snyder, S.L., 1980, Aeromagnetic map of Montana: in color: U.S. Geological Survey Geophysical Investigations Map GP-934, scale, 1:1,000,000.

7. TEMPORAL AND SPATIAL RELATIONS BETWEEN FOLDING, INTRUSION, METAMORPHISM, AND THRUST FAULTING IN THE RIGGINS AREA, WEST-CENTRAL IDAHO

By CHARLES M. ONASCH[1]

ABSTRACT

Two pre-Cenozoic, largely volcanogenic rock sequences are exposed along the western margin of the Idaho batholith in the Riggins area, west-central Idaho. The eastern, upper sequence, the Riggins Group, is in contact with the Idaho batholith. It is separated from the unnamed, lower sequence to the west by an east-dipping imbricate thrust fault system, the Rapid River thrust.

The temporal and spatial relations between folding, intrusive activity, metamorphism, and thrust faulting in the two sequences were determined from textural data and crosscutting relations. In the Riggins Group, emplacement of associated peridotite and intrusion of quartz diorite and quartz monzonite predate all folding in the southern and central parts of the area. Metamorphism and intrusion of trondhjemite associated with the main phase of the batholith occurred with the first fold phase in the south, between the third and fourth fold phases in the central part, and followed the fifth fold phase in the north. In the lower sequence, intrusion of quartz diorite preceded the first phase of folding and associated metamorphism. Juxtaposition of the two sequences along the Rapid River thrust occurred just prior to or synchronous with the last phase of folding in each sequence, which is the only fold phase common to both. Following thrust faulting, both sequences were metamorphosed to the same grade and intruded by trondhjemite in the northern part of the area.

INTRODUCTION

The Riggins area in west-central Idaho contains the best exposures of pre-orogenic (pre-Late Cretaceous) rocks along the western margin of the Idaho batholith. This area has long been recognized as important to understanding the evolution of the western margin of North America during the Mesozoic. The western edge of the continental basement, defined on the basis of strontium isotopic data (Armstrong and others, 1977; Kistler, 1978), contains a deep embayment in the Riggins area (Davis and others, 1978). Eugeosynclinal additions to the craton were accreted during the Mesozoic construction of the cordilleran "collage" (Davis and others, 1978). Rocks in the Riggins area belong to distinctly different petrotectonic divisions that owe their present positions to structural juxtaposition (Brooks and Vallier, 1978). Lithologic similarities with the Seven Devils Group may support correlation of some Riggins area rocks with the far-traveled Wrangellia terrane (Jones and others, 1977; Hillhouse and others, 1982). Many authors have suggested that the tectonic development of the area was dominated by island-arc processes including subduction, which occurred either in the Riggins area or immediately to the west (Talbot and Hyndman, 1975; Hamilton, 1976; Onasch, 1976; Scholten and Onasch, 1976).

Various aspects of the geology in the Riggins area have been studied for many years. Folding in the area was discussed by Onasch (1977, 1979); thrust faulting was described by Hamilton (1963a, b) and Onasch (1977, 1980); and the metamorphism and intrusive history were studied by Hamilton (1963a, c). The purpose of this paper is to summarize the data on folding, thrust faulting, metamorphism, and the intrusive history and to examine the temporal and spatial relations between these events in order to establish a framework in which broader scale tectonic models may be constructed. Only the pre-Cenozoic history will be considered here. For an account of the Cenozoic block faulting, crustal warping, and eruption of the voluminous Columbia River Basalt Group, the reader is referred to Hamilton (1962, 1963d).

ACKNOWLEDGMENTS

Versions of this manuscript were reviewed by Robert Scholten, Karl Evans, Ferrell McCollough, Tracy Vallier, and Howard Brooks; their comments are greatly appreciated. Discussions in the field with Paul Myers and Edward Price proved helpful. Support for the field work was provided by the Geological Society of America, Sigma Xi, and the Paul D. Krynine Fund of The Pennsylvania State University.

[1]Department of Geology, Bowling Green State University, Bowling Green, OH 43403.

GEOLOGIC SETTING

The Riggins area lies along the western margin of the Idaho batholith (fig. 7.1). The traditional view of the batholith as a massive igneous body surrounded by a gneissic shell has proved too simple. The batholith is now known to consist of two lobes: the Atlanta lobe in the south and the Bitterroot lobe in the north. Both lobes are a composite of numerous smaller plutons rather than a single body. In general, the age of the batholith is Late Cretaceous. The Atlanta lobe is slightly older (43 to 100 Ma) than the Bitterroot lobe (38 to 80 Ma) (McDowell and Kulp, 1969; Armstrong, 1975; Armstrong and others, 1977). Numerous Eocene granitic plutons have resulted in widespread resetting of isotopic ages to 50 Ma or less (Armstrong, 1974).

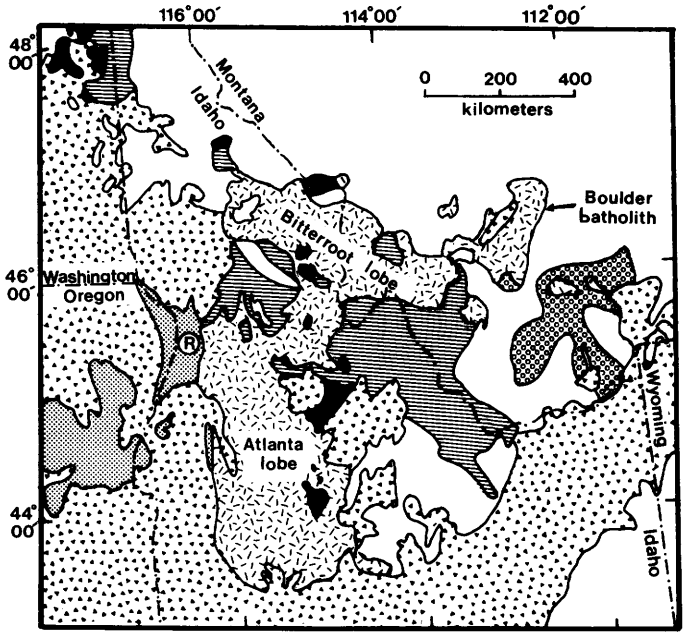

EXPLANATION

- Volcanic and sedimentary rocks (Cenozoic)
- Granite intrusions (early Cenozoic)
- Granitic rocks (Mesozoic)
- Eugeosynclinal rocks (Mesozoic and Paleozoic)
- Miogeosynclinal rocks (Mesozoic and Paleozoic) and Belt Supergroup (Middle Proterozoic), undivided
- Crystalline basement rocks of platform (pre-Belt Supergroup)
- Gneisses and intrusive rocks of Salmon River arch (pre-Belt Supergroup) and other gneisses (age uncertain), undivided

FIGURE 7.1.—Regional geologic map of Idaho batholith and vicinity modified from Armstrong (1975). Riggins area is indicated with circled R.

Armstrong (1975) ascribed the separation of the batholith into lobes to the presence of the Salmon River arch (fig. 7.1). This arch of older gneisses and intrusive rocks, some of which may predate the Belt Supergroup (pre-1,500 Ma) is postulated to have influenced the tectonics and paleotopography of central Idaho throughout its existence. However, Evans and Lund (1981) found that the area occupied by the Salmon River arch in east-central Idaho was a depositional basin that received thick accumulations of sediment during the Middle Proterozoic. In light of this work, the concept of the Salmon River arch, at least in east-central Idaho, may need to be re-evaluated.

Because the Columbia River Basalt Group forms an extensive cover in this region, prebatholithic eugeosynclinal rocks are only exposed in several isolated areas along the western margin of the Atlanta lobe. Where exposed, the nature of the border zone rocks changes markedly from north to south. Along the northwest corner of the Atlanta lobe, strongly deformed Belt and pre-Belt(?) to Late Triassic rocks are intruded by the batholith (Myers, 1968, 1972, 1976). The older rocks represent continental basement and presumably mark the northwest end of the Salmon River arch. Intrusive rocks of the batholith were injected along east-dipping thrust faults and high-angle reverse faults. Many of the country rocks were assimilated in the contact zone, leaving only schlieren and xenoliths of calc-silicate gneiss and quartzite.

Southward along the western margin, younger rocks are in contact with the batholith. The Belt and pre-Belt rocks found in the north appear to be absent in the Riggins area. Here, the batholith is in direct contact with volcanic rocks of Paleozoic and (or) Mesozoic age.

South of the Riggins area, the border zone consists of varied granitic gneisses with minor calc-silicate gneiss and quartzite of unknown age (Hamilton, 1969). These rocks are lithologically unlike those in the Riggins area and may mark the reappearance of Belt or older rocks in the marginal zone. The Riggins area may then be anomalous in that it is the only place along the western margin of the batholith where eugeosynclinal rocks are in direct contact with the batholith and not separated from it by older continental crust (Onasch, 1977).

ROCK UNITS

The pre-Cenozoic rock units in the Riggins area consist of two largely volcanogenic rock sequences of eugeo-

synclinal affinity separated by faults of the Rapid River thrust. The Riggins Group and the lower sequence have been variably metamorphosed and intruded by rocks related to the batholith. The metamorphic grade and amount of intrusive material in both sequences increases to the east, and to a lesser extent, to the south and north.

RIGGINS GROUP

Hamilton (1963a) named the thick sequence of metamorphosed volcanic and sedimentary rocks lying above and to the east of the Rapid River thrust the Riggins Group. He defined four formally named units that he assigned to the group. In addition, he recognized an informal ultramafic rock unit (mainly metaperidotite) which he noted as associated (fault emplaced) with the group. From lowest to highest, the formal units are: the Fiddle Creek Schist, the Lightning Creek Schist, the Berg Creek Amphibolite, and the Squaw Creek Schist (Hamilton, 1963a, p. 16-17). This succession, he pointed out, may be partly or wholly structural rather than stratigraphic.

During the present investigation, several members were defined in the units of the Riggins Group which aided in expanding the mapped extent of the group, especially to the east (Onasch, 1977). The other modification to Hamilton's original stratigraphy was the reduction of the Berg Creek Amphibolite to a member of the Lightning Creek Schist (Onasch, 1977, 1979, 1980). The amphibolite grades along strike into other lithologies and is believed to be a stratigraphic or metamorphic facies of the Lightning Creek Schist.

Abundant lithologic variations, due to the strong regional metamorphic gradient, occur in the area, not only between units of the Riggins Group but within each unit. Within any unit, the texture and mineralogy vary considerably in response to the changes in metamorphic grade (see Hamilton, 1963a, for a detailed description of the petrography and metamorphism).

To the east, the Riggins Group is in contact with intrusive rocks related to the batholith. The contact zone is not sharp; rather, it consists of an 8- to 10-km-wide border zone dominated by intrusive rocks that increase in abundance to the east. Subunits of the Riggins Group were traced well into this transition zone, and it appears that they persist until the rocks are entirely plutonic.

The exposed thickness of the Riggins Group, no doubt thickened structurally, is approximately 8 km. The age is unknown other than it must be older than the middle to Late Cretaceous rocks of the batholith. Brooks and Vallier (1978) have tentatively correlated the lower part of the Riggins Group with rocks ranging in age from Devonian to Middle Triassic, and the upper part with Jurassic rocks.

LOWER SEQUENCE

For convenience, the three units exposed below and to the west of the Rapid River thrust have been informally designated the lower sequence by Onasch (1977, 1979, 1980). They consist, from oldest to youngest, of the Early Permian (?) to Late Triassic Seven Devils Group, the Upper Triassic Martin Bridge Formation, and the Triassic (?) Lucile Formation. Restrictive lithologic names for the Martin Bridge and Lucile Formations were dropped in favor of "formation" because both units contain numerous lithologies. At low metamorphic grades, typical lithologies for the three lower sequence units are greenstone, marble, and phyllite, respectively. In the northern part of the area, where rocks of the lower sequence are intruded by trondhjemite related to the batholith, schist and marble predominate. For more lithologic detail, see Hamilton (1963a) and Vallier (1974, 1977).

CORRELATIONS BETWEEN THE RIGGINS GROUP AND THE LOWER SEQUENCE

The Riggins Group and the lower sequence display many lithologic similarities yet also differ in some important ways. This situation has led to a wide range of opinion regarding the original stratigraphic relations between the two rock sequences. Both sequences consist largely of volcanic and volcaniclastic rocks of similar bulk compositions, and both include admixtures of terrigenous and carbonate rocks. They differ in their gross stratigraphy and in the absence of peridotite in the lower sequence. Vallier (1974, 1977) and Onasch (1976) suggested that the two sequences may be partly correlative. Hamilton (1963a, 1978) believes that the two are unrelated other than many of the rock types in both are the product of intraoceanic arc volcanism. Any possible correlations will be important in some of the structural interpretations developed later.

FOLDING

Folding in both rock sequences is polyphase. In either sequence, the style of folding and type of associated foliation or lineation are strongly influenced by lithology and metamorphic grade. The folding in each rock sequence will be discussed separately. An additional subscript will be added to the standard structural shorthand notation to differentiate between the two sequences: R corresponds to the Riggins Group and B to the lower sequence. For example, F_{2R} corresponds to the folds of the second phase in the Riggins Group.

RIGGINS GROUP

Five phases of mesoscopic folding were identified in the Riggins Group. Although the style and degree of develop-

ment for any phase varies widely over the area, the orientations vary considerably less due to the relative simplicity of the macroscopic geometry (fig. 7.2).

The F_{1R} folds are isoclinal and are the only folds that deform compositional layering, S_{0R}, but not the regional foliation, S_{1R}. S_{1R} is generally parallel to S_{0R} except in the hinges of F_{1R} folds. F_{2R} folds are strongly asymmetric and indicate a rotation sense of east over west. F_{3R} and F_{4R} folds are upright, symmetrical, and the most widespread. F_{5R} folds are very open folds, or more rarely, kink-band folds. The average orientations of the fold axes and associated S-surfaces for all phases except the first are shown in figure 7.3*A*. First-phase structures have highly variable orientations.

The type of associated foliation and the style of most fold phases are strongly dependent on the metamorphic grade. Pressure solution and crenulation cleavages are typical at low metamorphic grades, whereas schistosity and gneissic layering predominate at higher grades. Correspondingly, open, concentric folds become tight and flattened and approach a similar style. The main exception to these generalizations are fifth-phase structures. This phase postdates metamorphism in most of the area and remains relatively constant in style and type of associated foliation and lineation.

As previously mentioned, the complexity seen on a mesoscopic scale is not evident on a macroscopic scale. The areal distribution of units in the Riggins Group is controlled mainly by two southeast-plunging folds (fig. 7.2), the Riggins synform and the Lake Creek antiform (Onasch, 1977, 1979). A second synform in the extreme eastern part of the area is defined by S_{1R} attitudes, but the homogeneous nature of the stratigraphy in this area precludes the tracing of individual units with any degree of certainty. All these folds correlate with F_{4R}. Macroscopic examples of F_{3R} and F_{5R} folds can be identified from S_{1R} attitudes in the southeast part of the area, but the absence of mappable units in this area prevents their recognition by map pattern.

Tectonic transport directions were determined for all fold phases, except F_{1R}, using separation angles (Hansen, 1971) and folded lineations (Ramsay, 1960). For F_{3R}, F_{4R}, and F_{5R} they are subvertical across the area. If the effects of subsequent deformations are removed, F_{2R} transport directions plunge to the east at progressively steeper angles.

LOWER SEQUENCE

Three phases of mesoscopic folding were identified in the lower sequence. The style of folding in the lower sequence is much more uniform than in the Riggins Group, owing to a smaller variation in metamorphic grade. Variations in style are due almost entirely to lithologic differences.

The F_{1B} folds are tight to isoclinal and deform compositional layering, S_{0B}. S_{1B} is parallel to the axial surfaces of these folds and is a poorly developed foliation in the marble defined by flattened calcite grains. In the phyllite, S_{1B} is a well developed schistosity. In the greenstone, S_{1B} consists of anastomosing surfaces defined by the preferred orientation of layer silicates. F_{2B} folds are strongly asymmetric with a west over east rotation sense. F_{3B} folds are open folds in all lithologies, or more rarely, kink-band folds in phyllite. The orientation of second- and third-phase structures is shown in figure 7.3*B*. First-phase structures are omitted due to their variable orientations.

The macroscopic geometry of the lower sequence is even less complex than that of the Riggins Group. S_{1B} and S_{0B} dip consistently at low angles to the east or southeast. The dominant control on the areal distribution of units in the lower sequence is the faults of the Rapid River thrust (fig. 7.2). Movement directions determined from separation angles for F_{2B} plunge gently to the east; for F_{3B} they are vertical.

Just north of the Riggins area, five phases of folding were recognized in the lower sequence (McCollough, 1984). The two additional phases occurred between F_{2B} and F_{3B} as defined in the Riggins area. Thus, the higher grade of metamorphism that affected the lower sequence north of the Riggins area is apparently accompanied by an increase in the structural complexity.

INTRUSIVE HISTORY

The intrusive history of both sequences is long and complex. Intrusion occurred prior to, synchronous with, and after folding in both sequences.

RIGGINS GROUP

The oldest intrusive rocks that are found within the mapped extent of the Riggins Group are lensoid bodies of metaperidotite. At low metamorphic grade, schists with varying proportions of talc, magnesite, antigorite, and chlorite are most common. At higher grades, these low-grade schists are replaced by anthophyllite-garnet schists. On the basis of their chemical composition, Hamilton (1963a) believes the parent rock to be an enstatite-bearing peridotite.

The metaperidotite bodies are typical of alpine-type ultramafic bodies. Their contacts with the enclosing schists are conformable and show no effects of contact metamorphism. The bodies are highly sheared and lack any internal stratigraphy. The origin of alpine-type ultramafic bodies is debatable, but most workers agree that their present position is a result of tectonic emplacement, commonly along faults. Because S_{1R} can be identified in most of the bodies, emplacement, presumably by

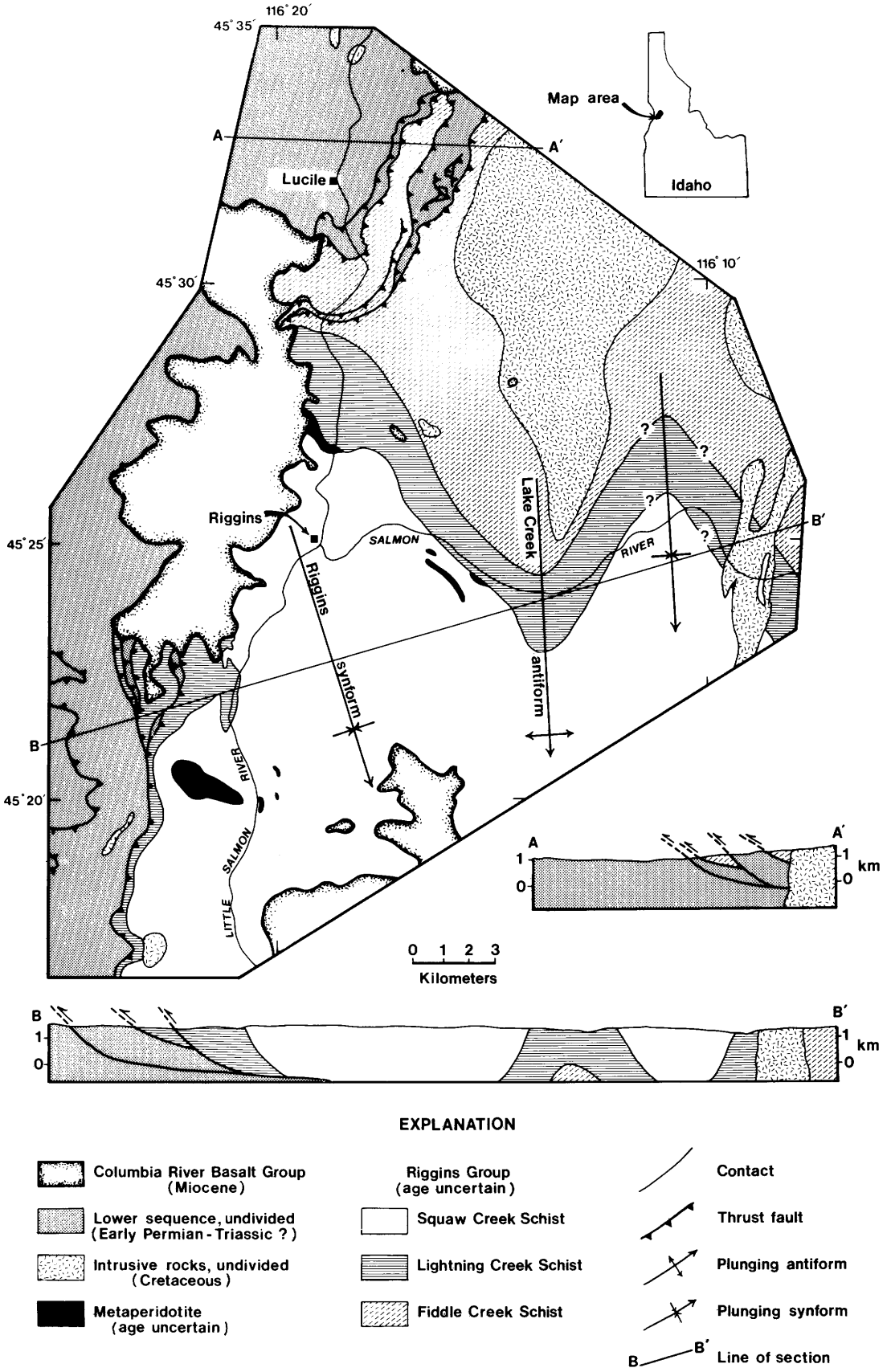

FIGURE 7.2.—Generalized geologic map and cross sections of the Riggins area.

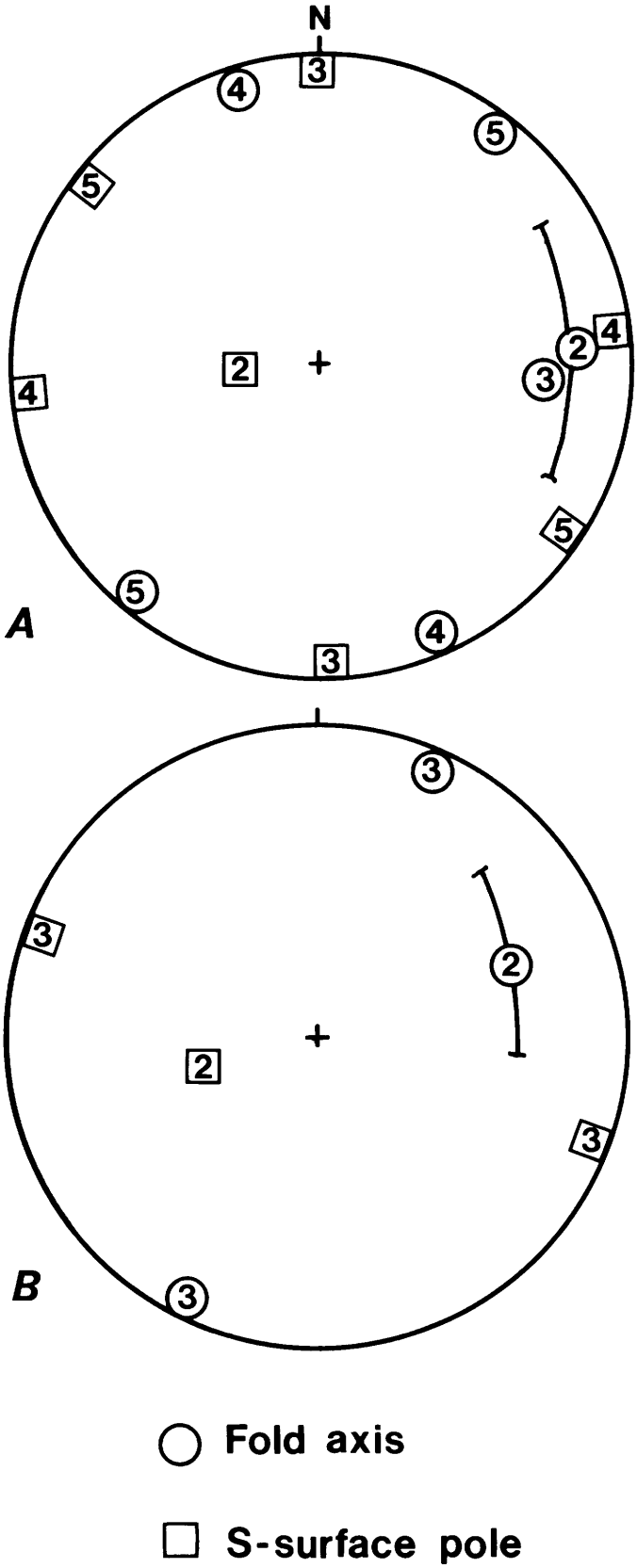

faulting, must have occurred prior to D_{1R}, the first phase of deformation in the Riggins Group.

The oldest intrusive rocks related to the Idaho batholith are quartz diorite and quartz monzonite. Both occur as semiconcordant stocks in the eastern part of the area (fig. 7.2). They are younger than the metaperidotite because they have not been everywhere metamorphosed to the same grade as the country rocks, as is the case with the metaperidotite. South of the Riggins area, the quartz diorite is intruded by the quartz monzonite (Hamilton, 1963c). The quartz diorite is an early mafic border phase of the batholith, whereas the quartz monzonite is nearly contemporaneous with the main phase of the batholith (Hyndman and Talbot, 1976). Both were intruded prior to D_{1R}, as deformed S_{1R} surfaces can be seen in each.

Trondhjemite associated with the main phase of the batholith is the most abundant granitic rock in the Riggins area. It was intruded at different times with respect to folding at different places. In the southern part of the area, trondhjemite dikes predate S_{1R}. In the central part of the area, a large composite pluton of variably foliated trondhjemite is confined to the axial region of the Lake Creek antiform (fig. 7.2), an F_{4R} fold, implying coeval formation. Ten kilometers north of the Riggins area, in the Slate Creek area, trondhjemite intrudes across the Rapid River thrust and into the lower sequence. The foliation parallels the fault, and it appears that intrusion was synchronous with faulting (Hamilton, 1963c). The foliation presumably is related to movements during faulting.

Although local exceptions are numerous, the intrusion of trondhjemite was apparently earlier than D_{1R} in the south, approximately synchronous with D_{4R} in the middle of the area, and possibly later in the north. The only intrusive rocks younger than trondhjemites are pegmatites and aplite dikes, most of which are unfoliated.

LOWER SEQUENCE

The intrusive history of the lower sequence is considerably less complex than that of the Riggins Group. The oldest intrusive rocks are small stocks of sheared and altered quartz diorite (Hamilton, 1963a, b). The shear surfaces are parallel to S_{1B}; therefore, intrusion occurred prior to D_{1B}. These quartz diorite bodies and others of similar composition are common throughout the Seven Devils Mountains, Snake River canyon, and eastern

FIGURE 7.3.—Summary plot of fold axis and S-surface orientations for all deformational phases except the first. Great circle segments show separation angles determined from fold asymmetry. *A*, Riggins Group. *B*, Lower sequence. Numbers refer to phases discussed in text.

Oregon. They range in age from Permian to Early Cretaceous, all predating the Idaho batholith (White, 1973; Vallier, 1974, 1977).

In the Slate Creek area, trondhjemite related to the batholith intrudes the lower sequence. This trondhjemite appears to crosscut all fold structures; hence, it is post-D_{3B}.

METAMORPHISM

With the exception of the younger intrusive rocks, all rocks in the Riggins area have been metamorphosed. The grade of metamorphism varies from lower greenschist to upper amphibolite facies in the Riggins Group and from lower to upper greenschist facies in the lower sequence. The metamorphic grade in both sequences increases from west to east, most markedly so in the Riggins Group. A noticeable northward increase in grade is also evident in the lower sequence just north of the Riggins area (McCollough, 1984).

The metamorphism in the Riggins Group and most of it in the lower sequence is related both spatially and temporally to intrusion of the Idaho batholith. This relation is expressed well in Hamilton's (1963a) reference to the metamorphism as contact metamorphism on a regional scale. An older, low-grade metamorphism was identified in the lower sequence by Hamilton and is believed to be part of a Late Jurassic event recognized over much of eastern Oregon and western Idaho (Armstrong and others, 1977). Any possible effects on the Riggins Group have been obliterated by the more intense Cretaceous event. The polymetamorphic history indicated by textures in some samples of both rock sequences is interpreted in most cases to be the result of multiple stages of metamorphism during a single event, because the textures are developed irregularly across the area. Where a polymetamorphic history is indicated, reference to the metamorphism will correspond to the thermal peak of metamorphism.

Metamorphic isograds in the Riggins area (fig. 7.4) have been defined by Hamilton (1963a) and Onasch (1977). The relation between the isograds and the faults of the Rapid River thrust changes progressively from south to north. In the southern part of the Riggins area, the isograds are truncated by the faults and metamorphism predates faulting. In the north, near Lucile, the isograds cross the faults undeflected, and both sequences were metamorphosed to the same grade after faulting. Somewhere in the central part of the area, beneath the Columbia River Basalt Group, thrust faulting must have been synchronous with metamorphism.

Metamorphism is also related intimately with folding. Rock textures show that the temporal relations between

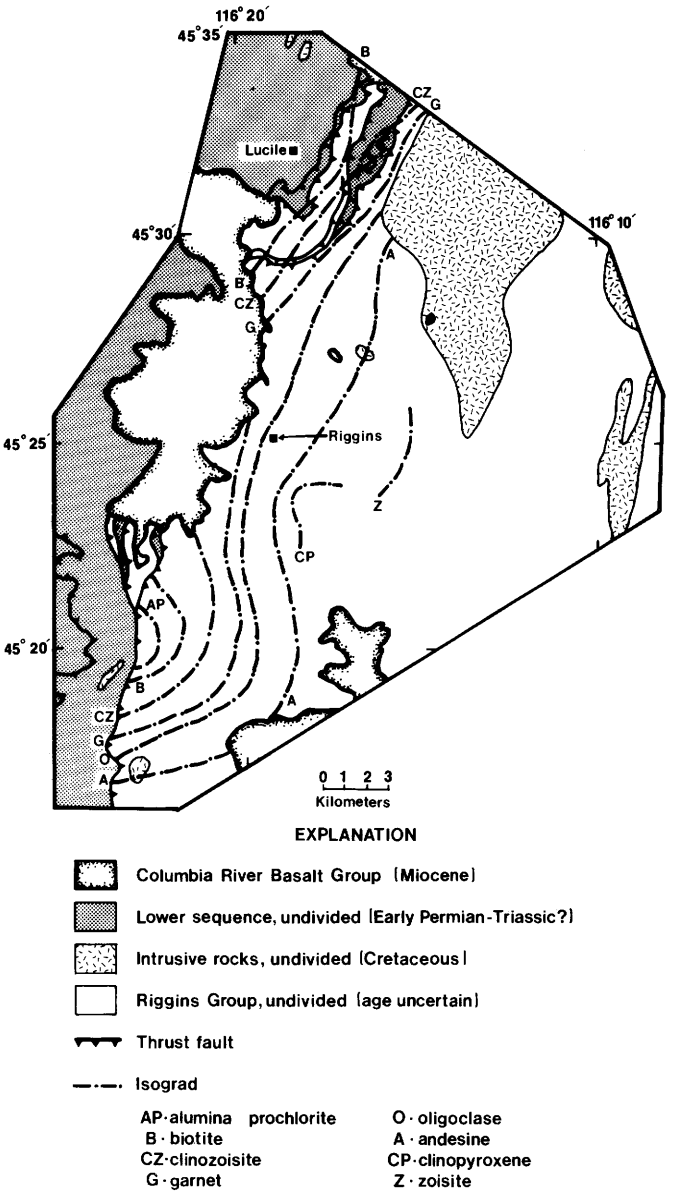

FIGURE 7.4.—Metamorphic isograds in the Riggins area defined by Hamilton (1963a) in the area around Riggins and near Lucile by Onasch (1977)

folding and metamorphism vary with latitude but are more constant with changes in longitude.

RIGGINS GROUP

In the extreme southern part of the Riggins area, the highest grade minerals in the Riggins Group define the S_{1R} surface, suggesting that the peak of metamorphism was synchronous with D_{1R}. Approximately 10 to 15 km to the north, clinozoisite porphyroblasts, the highest grade

mineral, grow across S_{1R} and S_{3R}, indicating that the metamorphic peak followed D_{3R}. Farther west, at the same approximate latitude, S_{4R} is defined by chlorite, indicative of a lower metamorphic grade than the oligoclase, garnet, and biotite assemblage that makes up the rest of the rock. From these two observations, it can be seen that the metamorphic peak in the central part of the area occurred between D_{3R} and D_{4R}. In the extreme northern part of the area, metamorphism followed D_{4R}, as garnet porphyroblasts grow across S_{4R} surfaces.

LOWER SEQUENCE

Shear surfaces and associated alteration in the quartz diorite bodies are believed to be the product of the Late Jurassic event (Hamilton, 1963b). As the S_{1B} surfaces in adjacent rocks are parallel to these shear surfaces, D_{1B} is interpreted to have been synchronous with this metamorphic event. In the northern part of the area, the lower sequence is metamorphosed to the same grade as the Riggins Group. Here, chloritoid in the Lucile Formation grows across F_{3B} kink bands, indicating that metamorphism followed D_{3B}.

RAPID RIVER THRUST

The Rapid River thrust extends the entire length of the Riggins area, making it the most obvious structural feature. It separates the two major rock sequences, and in some places, juxtaposes rocks displaying different grades of metamorphism. For these reasons, Hamilton (1963b) considered it to be a major westward-directed overthrust with as much as 24 km of displacement. The Rapid River thrust takes on added significance if the lower sequence is stratigraphically unrelated to the Riggins Group. Brooks and Vallier (1978) suggested that the thrust marks the suture between the Seven Devils volcanic arc and the lower part of the Riggins Group, which they included in their dismembered oceanic crust terrane. Correlation of the Seven Devils terrane by Jones and others (1977) to Wrangellia implies that the thrusting is a middle to Late Cretaceous event that coincides with the accretion of Wrangellia (Coney and others, 1981) and may represent many hundreds of kilometers of closure.

The character of the fault changes several times along its length (fig. 7.2). In the extreme southwest corner of the area, it is a single surface separating the two sequences. In the central part of the area, just before it disappears beneath the Columbia River Basalt Group, the fault splays into several surfaces that produce intercalation of the two sequences. Where it emerges from beneath the basalt farther north it is marked by at least two surfaces which split and reconnect, creating lens-shaped bodies.

In addition to the main belt of faults just described, at least one additional thrust fault was mapped approximately 3 km to the west of the main belt of thrusts in the central part of the area (fig. 7.2). Hamilton (1963a) recognized the possibility of additional faults in this area in his mention of intercalations of marble (Martin Bridge Limestone) in the Seven Devils Group. Other low-angle faults could be drawn in the lower sequence based on anomalous formation thicknesses and local stratigraphic inconsistencies.

The complex distribution of units along the fault is puzzling, and no single model can explain all the data. Hamilton (1963a, 1969) interpreted the fault to be imbricated southwest of Riggins. Based on reconnaissance mapping father north, near Lucile, he ascribed the distribution of units there to be the result of recumbent folding of the thrust. Detailed mapping along the entire length of the fault by this author has shown the geology to be more complex than indicated by Hamilton's reconnaissance map. This complexity is especially apparent in the Lucile area, where numerous intercalations of the lower sequence with itself and with the Riggins Group were found (Onasch, 1977, 1980). Recent work by McCollough (1984) just north of the Lucile area argues persuasively that intercalations of the lower sequence units are stratigraphic in nature. Intercalations of the lower sequence and the Riggins Group are, however, interpreted by McCollough and this author to everywhere be the result of imbricate thrust faulting.

Several lines of evidence suggest that the Rapid River thrust near Lucile is imbricated rather than recumbently folded. Graded bedding in the Lucile Formation indicates that the rocks are nowhere overturned. Compositional layering and schistosity in this area dip consistently to the east and southeast. No mesoscopic or macroscopic folding with an attitude or style compatible with recumbent folding was identified in either the lower sequence or the Riggins Group.

Just to the north of the Riggins area, McCollough (1984) identified open folds in a thrust within the Seven Devils Group which he believes is related to the Rapid River thrust. Approximately 5 km farther north, along Slate Creek, where both sequences are metamorphosed to the same grade, recumbent folds occur in both sequences and possibly the thrust itself (E. Price, oral commun., 1980). The metamorphic grade here is much higher, and the structural setting appears to be different. It is possible that thrusting is gradually replaced by folding and that, along Slate Creek, the two sequences are juxtaposed not by thrusting but by nappelike folding.

Interpreting the Riggins area in terms of an imbricate thrust fault model rather than recumbently folded thrust faults has important implications with regard to the structural history of the area. If recumbent folding were the

norm, a major post-thrust episode of folding would have had to occur. The imbrication model not only fits the data better but simplifies the structural history considerably.

TIMING OF THRUST FAULTING

The time of thrust faulting relative to folding can be determined by examining possible correlations between fold phases in the Riggins Group and those in the lower sequence. Using the criteria of style, asymmetry, orientation, and relative age as tools for correlation, only one fold phase appears to be common to both sequences. Both F_{5R} and F_{3B} are northwest- or southeast-plunging, open, upright folds with poorly developed axial plane foliations that developed late in their respective deformational sequences. All other fold phases show differences in style, asymmetry, orientation, or a combination thereof with respect to one another.

Correlation of only the youngest phase of folding in both sequences indicates that movement of the Rapid River thrust occurred after D_{4R} and D_{2B} and prior to D_{5R} and D_{3B}. The F_{5R} and F_{3B} folds are possibly a product of the same stresses responsible for the thrusting, in which case folding would be synchronous with faulting. Relative to metamorphism and intrusive activity, thrust faulting postdates both in the south and predates both in the north.

DISPLACEMENT ON THE RAPID RIVER THRUST

The direction of relative motion on the thrusts, based on slickenside striae, is west or northwest, approximately perpendicular to the trace of the fault. The sense of relative motion, based on the asymmetry of folds in fault-related shear zones, is reverse, as the east block has moved relatively westward.

An accurate estimate of the lateral shortening associated with the Rapid River thrust requires that the original stratigraphic relations between the two sequences be known. Based entirely on the discordance in metamorphic grade at the southern end of the fault and assuming a metamorphic gradient similar to that in the hanging wall, a minimum of 5 to 6 km of displacement is required. Detailed versions of the cross sections in figure 7.2 require a minimum of 6 to 8 km of displacement (Onasch, 1980). These estimates would approach the true displacement if the two sequences were stratigraphically equivalent and originally separated by a rapid facies change. If the two sequences are entirely unrelated, the actual amount of movement would most likely be much higher. The possibility of additional faults in the lower sequence increases the estimates in either case.

The structural histories of the two sequences differ in that only the youngest folding in each is correlative. Prior to this common fold phase, the two sequences must have been separated by a distance great enough to allow separate structural evolutions. This distance need not be extremely great but would undoubtedly be more than the 6 to 8 km minimum estimates determined from the cross sections.

SUMMARY

The structural, igneous, and metamorphic evolution of the Riggins area is complex, because the temporal relations between different events change from south to north. The relative ages of folding, igneous activity, metamorphism, and thrust faulting for southern, central, and northern parts of the area are summarized in figure 7.5. Changes in the relative age of events from one place to another are presumed to be gradual and continuous.

In the southern part of the area, the earliest events after deposition and eruption of the rocks of the Riggins Group were the intrusion of quartz diorite, quartz monzonite, and trondhjemite of the Idaho batholith. The onset of folding and the metamorphic peak followed the igneous activity. Movement on the Rapid River thrust preceded or accompanied the last stage of folding. In the lower sequence, intrusion of quartz diorite occurred prior to D_{1B} and associated low-grade metamorphism. The relative ages of the first two fold phases in the lower sequence and the first four fold phases in the Riggins Group are unknown; they may overlap, or early folding in the lower sequence may predate all folding and even the intrusive activity and metamorphism in the Riggins Group.

In the central part of the area, intrusion of quartz diorite and quartz monzonite and emplacement of peridotite all predate folding and the thermal peak in the Riggins Group. Intrusion of large volumes of trondhjemite and the metamorphic peak occurred between D_{3R} and D_{4R}. These events were followed by thrust faulting and D_{5R} and D_{3B}.

Just to the north of the Riggins area, along Slate Creek, intrusion of trondhjemite and metamorphic peak followed thrust faulting and most folding in both sequences. Thrusting was synchronous with or slightly older than the phase of folding common to both sequences (F_{5R} and F_{3B}).

Some temporal relations remain constant throughout the area, whereas others vary from north to south. Thrust faulting occurred at the same time relative to folding in both sequences everywhere in the Riggins area as did the intrusion of trondhjemite relative to the metamorphic peak. Relative to folding and thrust faulting, the locus of trondhjemite activity and metamorphism shifted progressively northward through the succession of fold phases. The changes in the relative age relations could result from folding and thrust faulting having affected the entire area at one time, while the intrusion of trondhjemite and the metamorphism became progressively younger toward the north. These changes could also result from intrusion and

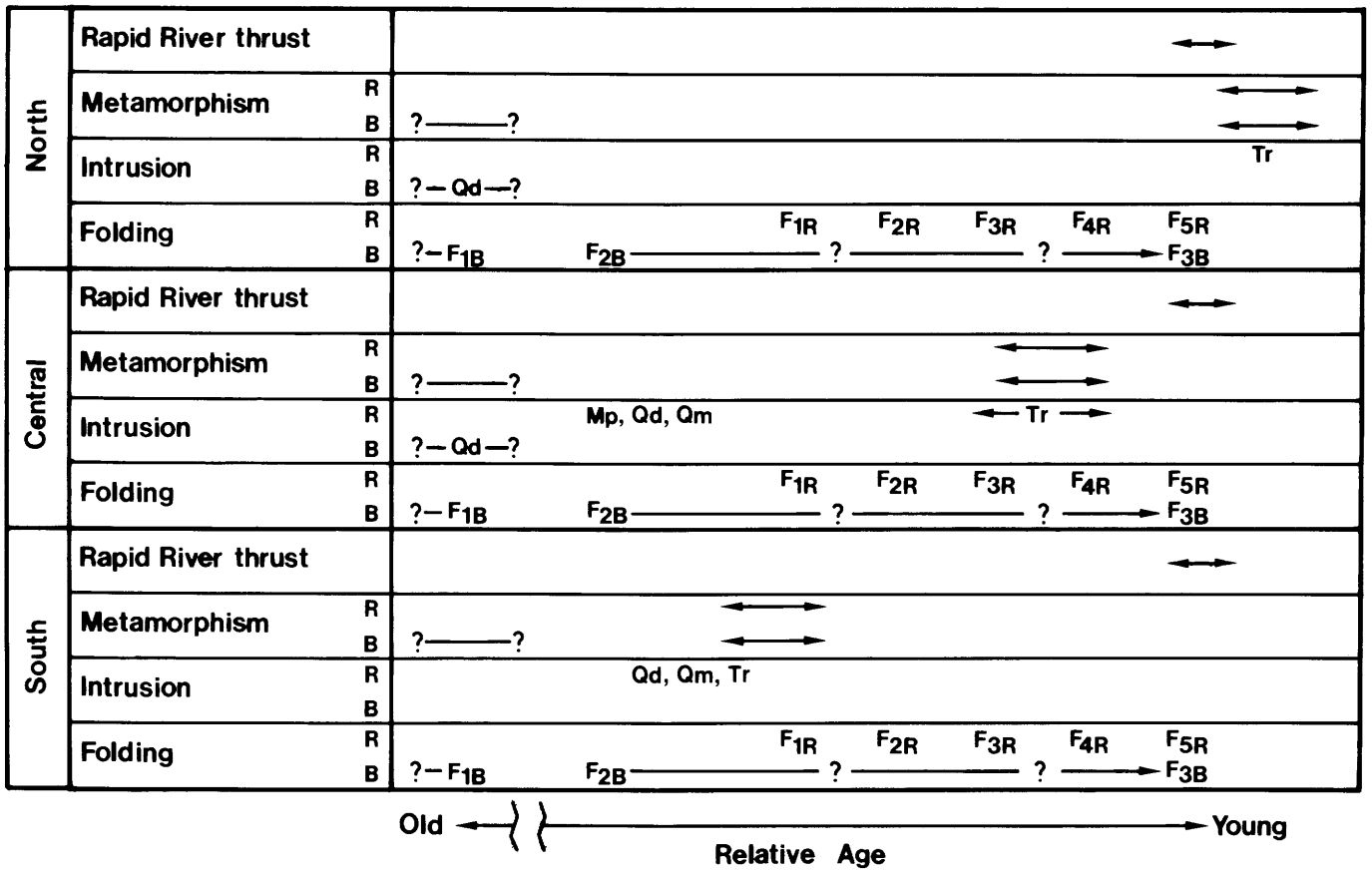

FIGURE 7.5.—Time-space diagram showing relative ages of various events in southern, central, and northern parts of the Riggins area. R, Riggins Group; B, lower sequence; Qd, quartz diorite; Mp, metaperidotite; Qm, quartz monzonite; Tr, trondhjemite; F, fold phase. Arrows show range of age, question marks show where age extent is uncertain. Significant hiatus may exist between F_{1B} and F_{2B}. Relative age of trondhjemite in north determined from outcrops in Slate Creek, north of the Riggins area.

metamorphism occurring everywhere at one time and folding and thrust faulting becoming progressively younger toward the south. Crosscutting relations in trondhjemite in the central part of the area suggest that the former is the case and that intrusion and metamorphism are the dynamic elements. The various generations of trondhjemite show a general trend of becoming younger toward the north.

The temporal relations between events in the Riggins Group and those in the lower sequence older than thrust faulting cannot be determined with certainty. In the lower sequence, the intrusion of quartz diorite, the low-grade metamorphism, D_{1B}, and possibly D_{2B} are all apparently related to a Late Jurassic event for which there is no record in the Riggins Group. The absence of this Jurassic event in the Riggins Group could have resulted from the lower sequence being unrelated stratigraphically to the Riggins Group or from the lower sequence being in a different location at that time, or both. As Hamilton (1963b) pointed out, the Rapid River thrust may mark the overlap of two orogens: a Late Jurassic one to the west and a Late Cretaceous one to the east. Following the juxtaposition of the two sequences during the Late Cretaceous event, they were both affected by the waning stages of this event. Polyphase folding in the lower sequence would then be the result of two distinctly different orogenic events rather than phases of a single event, as was the case in the Riggins Group.

REFERENCES CITED

Armstrong, R.L., 1974, Geochronology of the Eocene volcanic-plutonic episode in Idaho: Northwest Geology, v. 3, p. 1-15.

_____ 1975, Precambrian (1500 m.y. old) rocks of central Idaho—The Salmon River arch and its role in cordilleran tectonics and sedimentation: American Journal of Science, v. 275-A, p. 437-467.

Armstrong, R.L., Taubeneck, W.H, and Hales, P., 1977, Rb-Sr and K-Ar geochronometry of Mesozoic granitic rocks and their Sr isotopic composition, Oregon, Washington, and Idaho: Geological Society of America Bulletin, v. 88, p. 397-411.

Brooks, H.C., and Vallier, T.L., 1978, Mesozoic rocks and tectonic evolu-

tion of eastern Oregon and western Idaho, *in* Howell, D.G., and McDougall, K.A., eds., Mesozoic paleogeography of the Western United States: Society of Economic Paleontologists and Mineralogists, Pacific Coast Paleogeography Symposium, 2d, p. 133-146.

Coney, P.J., Jones, D.L., and Monger, J.W.H., 1981, Cordillera suspect terranes: Nature, v. 288, p. 329-333.

Davis, G.A., Monger, J.W.H., and Burchfiel, B.C., 1978, Mesozoic construction of the cordilleran "collage", central British Columbia to central California, *in* Howell, D.G., and McDougall, K.A., eds., Mesozoic paleogeography of the Western United States: Society of Economic Paleontologists and Mineralogists, Pacific Coast Paleogeography Symposium, 2d, p. 1-32.

Evans, K.V., and Lund, K., 1981, The Salmon River "arch"? [abs.]: Geological Society of America Abstracts with Programs, v. 13, p. 448.

Hamilton, W., 1962, Late Cenozoic structure of west-central Idaho: Geological Society of America Bulletin, v. 73, p. 511-516.

_____ 1963a, Metamorphism in the Riggins region, western Idaho: U.S. Geological Survey Professional Paper 436, 95 p.

_____ 1963b, Overlapping of Late Mesozoic orogens in western Idaho: Geological Society of America Bulletin, v. 74, p. 779.

_____ 1963c, Trondhjemite in the Riggins quadrangle, western Idaho: U.S. Geological Survey Professional Paper 450-E, p. E98-E101.

_____ 1963d, Columbia River basalt in the Riggins quadrangle, western Idaho: U.S. Geological Survey Bulletin 1141-L, 37 p.

_____ 1969, Reconnaissance geologic map of the Riggins quadrangle, west-central Idaho: U.S. Geological Survey Miscellaneous Geologic Investigations Map I-579, 1:125,000.

_____ 1976, Tectonic history of west-central Idaho [abs.]: Geological Society of America Abstracts with Programs, v. 8, p. 378-379.

_____ 1978, Mesozoic tectonics of the Western United States, *in* Howell, D.G., and McDougall, K.A., eds., Mesozoic paleogeography of the Western United States: Society of Economic Paleontologists and Mineralogists, Pacific Coast Paleogeography Symposium, 2d, p. 33-70.

Hansen, E., 1971, Strain facies: New York, Springer-Verlag, 207 p.

Hillhouse, J.W., Grommé, C.S., and Vallier, T.L., 1982, Paleomagnetism and Mesozoic tectonics of the Seven Devils volcanic arc in northeastern Oregon: Journal of Geophysical Research, v. 87, p. 3777-3794.

Hyndman, D.H., and Talbot, J.L., 1976, The Idaho batholith and related subduction complex: Geological Society of America Annual Meeting, Cordilleran Section, 72d, Field Guide No. 4, Pullman, Washington, 14 p.

Jones, D.L., Siberling, N.J., and Hillhouse, J.W., 1977, Wrangellia—a displaced terrane in northwestern North America: Canadian Journal of Earth Sciences, v. 14, p. 2565-2577.

Kistler, R.W., 1978, Mesozoic paleogeography of California: A viewpoint from isotope geology, *in* Howell, D.G., and McDougall, K.A., eds., Mesozoic paleogeography of the Western United States: Society of Economic Paleontologists and Mineralogists, Pacific Coast Paleogeography Symposium, 2d, p. 75-84.

McCollough, W.F., 1984, Stratigraphy, structure, and metamorphism of Permo-Triassic rocks along the western margin of the Idaho batholith, John Day Creek, Idaho: University Park, Pennsylvania State University, M.S. thesis, 140 p.

McDowell, F.W., and Kulp, J.L., 1969, Potassium-argon dating of the Idaho batholith: Geological Society of America Bulletin, v. 80, p. 2379-2382.

Myers, P.E., 1968, The geology of the Harpster quadrangle and vicinity, Idaho: Ann Arbor, University of Michigan, Ph.D. dissertation, 130 p.

_____ 1972, Batholithic emplacement in the Harpster region, Idaho [abs.]: Geological Society of America Abstracts with Programs, v. 4, p. 206.

_____ 1976, Batholithic emplacement in the Harpster region, Idaho County, Idaho: Idaho Bureau of Mines and Geology Pamphlet 80, 25 p.

Onasch, C.M., 1976, Infrastructure-suprastructure relations and structural mechanics along the western margin of the Idaho batholith [abs.]: Geological Society of America Abstracts with Programs, v. 8, p. 407-408.

_____ 1977, Structural evolution of the western margin of the Idaho batholith in the Riggins, Idaho, area: University Park, Pennsylvania State University, Ph.D. dissertation, 196 p.

_____ 1979, Multiple folding along the western margin of the Idaho batholith in the Riggins, Idaho, area: Northwest Geology, v. 8, p. 94-100.

_____ 1980, A model for evolution of the Rapid River thrust in the Riggins area, Idaho: Northwest Geology, v. 9, p. 19-25.

Ramsay, J.G., 1960, The deformation of early linear structures in areas of repeated folding: Journal of Geology, v. 68, p. 79-93.

Scholten, R., and Onasch, C.M., 1976, Genetic relations between the Idaho batholith and its deformed eastern and western margins [abs.]: Geological Society of America Abstracts with Programs, v. 8, p. 407-408.

Talbot, J.L., and Hyndman, D.W., 1975, Consequence of subduction along the Mesozoic continental margin of the Idaho batholith [abs.]: Geological Society of America Abstracts with Programs, v. 7, p. 1290.

Vallier, T.L., 1967, Geology of part of the Snake River canyon and adjacent areas in northwestern Oregon and western Idaho: Corvallis, Oregon State University, Ph.D. dissertation, 267 p.

_____ 1974, A preliminary report on the geology of part of the Snake River canyon, Oregon and Idaho: Oregon Department of Geology and Mineral Industries Geologic Map Series GM-6, 15 p.

_____ 1977, The Permian and Triassic Seven Devils Group, western Idaho and northeastern Oregon: U.S. Geological Survey Bulletin 1437, 58 p.

White, W.H., 1973, Flow structure and form of the Deep Creek stock, southern Seven Devils Mountains, Idaho: Geological Society of America Bulletin, v. 84, p. 199-210.

8. PRE-CENOZOIC GEOLOGY OF THE WEST MOUNTAIN-COUNCIL MOUNTAIN-NEW MEADOWS AREA, WEST-CENTRAL IDAHO

By Bill Bonnichsen[1]

ABSTRACT

Pre-Tertiary rocks are exposed in two areas west of McCall and Donnelly and south of New Meadows in west-central Idaho. The southern area, called the West Mountain-Council Mountain block, contains the West Mountain, Council Mountain, and Deserette dioritic to tonalitic plutons and the No Business Mountain monzodioritic to syenitic pluton. Five provisional metamorphic rock units are recognized in that block: (1) metavolcanic rocks northeast of No Business Mountain, (2) a plagioclase-quartz-biotite gneiss unit, (3) metavolcanic rocks on Council Mountain, (4) a unit containing abundant metasedimentary rocks, and (5) a small marble-calc-silicate rock-hornfelsed amphibolite unit adjacent to the No Business Mountain pluton. Both the plutons and the metamorphic units are elongate north to south and both show moderately to steeply eastward-dipping north-south foliations.

The northern area, called the New Meadows block, contains pre-Tertiary rocks that are mostly peridotite accompanied by metachert and metagraywacke with local manganese-enriched beds and layers of possible volcaniclastic derivation. The peridotite is mainly unaltered dunite that locally is severely deformed. The dunite masses contain harzburgite and local chromitite segregations, and serpentinite and chlorite-amphibole schist zones at their margins. The deformed olivine and pyroxene grains in the peridotite commonly are cut by undeformed acicular anthophyllite crystals that have largely been replaced by talc. The growth of these hydrous minerals clearly occurred after the deformation of the olivine and pyroxene. Their presence implies that a thermal metamorphic and hydration event affected the peridotite masses after they were emplaced into their present tectonic setting. The associated metachert and other metasedimentary rocks in the New Meadows block show a similar history. Locally their layering is strongly deformed, yet these rocks have hornfelsic textures indicative of reheating and annealing after emplacement into their present tectonic setting.

The lithologies, structures, and metamorphic grades of the rocks in the New Meadows block differ so much from those in the nearby West Mountain-Council Mountain block that the two areas must have had quite different geologic histories and probably are separated by a zone (or zones) of major tectonic displacement. The metavolcanic and associated metasedimentary rocks in the West Mountain-Council Mountain block may be correlative with the Lightning Creek and Fiddle Creek Schists of the Riggins Group to the north. The peridotite and associated metasedimentary rocks of the New Meadows block are postulated to be a melange assemblage that was mixed together and deformed in an oceanic trench environment. The rocks in the New Meadows block probably are part of the dismembered oceanic crust terrane that is exposed in northeastern Oregon.

[1]Idaho Geological Survey, Moscow, Idaho 83843.

INTRODUCTION

Pre-Cenozoic rocks west of the Idaho batholith are exposed in the West Mountain-Council Mountain area and in the New Meadows area, both of west-central Idaho. In this paper these two areas are referred to as the West Mountain-Council Mountain block and the New Meadows block. The pre-Cenozoic rocks in the West Mountain-Council Mountain block consist of metamorphosed plutons of probable Cretaceous age. Previous authors generally have included these metamorphic rocks as part of the western border zone of the Cretaceous Idaho batholith. The pre-Cenozoic rocks in the New Meadows block, approximately 20 kilometers north-northwest of the West Mountain-Council Mountain area, include dunite and peridotite of unknown age and associated strongly deformed quartz-rich rocks, interpreted as metachert, and intercalated metagraywacke. A strongly sheared tectonic boundary exposed along the east side of the New Meadows block separates this small block from a terrane to the east that contains metamorphic rocks generally resembling those in the West Mountain-Council Mountain block. The purpose of this paper is to briefly describe the pre-Cenozoic rock units in the West Mountain-Council Mountain block and in the New Meadows block. At the end of the paper, brief comments regarding how these rock units may be related to other geologic units in the region are included.

The West Mountain-Council Mountain-New Meadows area consists of north- to north-northwest-trending ridges and intervening valleys displaced along late Cenozoic faults. The pre-Cenozoic metamorphic rocks comprising these blocks are exposed primarily along the east sides of the fault-block ridges. The relief in this area is about 1,300 meters from the low point at New Meadows to the top of Council Mountain, which is at an elevation of 2,477 meters. Exposures are poor due to trees and heavy brush at lower elevations. Extensive fresh bedrock exposures are present only above about 2,100 meters elevation, where Pleistocene glaciation has occurred. Such areas are

along parts of the West Mountain and Council Mountain ridges. Sufficient exposures along streams and roads allowed preparation of the preliminary geologic map included in this report. To date, my mapping has been of a reconnaissance nature designed to identify the major rock units, to gain an understanding of their gross lithologic and general structural relations, and to identify more clearly the geologic problems that need to be resolved in order to better elucidate the geologic history. The information used for this report was obtained from 29 days of field work during 1978, 1979, and 1983 and from the examination of about 100 thin sections.

The IUGS classification and nomenclature for plutonic rocks (Streckeisen and others, 1973) and volcanic rocks (Streckeisen, 1979) are used in this paper. For the names of most metamorphic rocks, all abundant minerals (greater than 5 or 10 percent) are listed in decreasing order of abundance.

ACKNOWLEDGMENTS

I am pleased to thank Cathy Allen, Earl Bennett, Howard Brooks, and Tracy Vallier for reviewing this paper and providing many useful suggestions for improving it. In addition, I would like to acknowledge the assistance of Ruth Barrett, Charles Knowles, Robert Jones, and James Zarubica for help with my research. Finally, I would like to thank Serena Smith and Melinda Nichols for typing various versions of my manuscript, Roger Stewart for his valuable editorial comments, and Margaret Jenks for drafting the figures.

GEOLOGIC SETTING AND PREVIOUS WORK

The West Mountain-Council Mountain-New Meadows area lies between the Cretaceous Idaho batholith (Schmidt, 1964; Fisher and others, 1983), which was intruded into a crystalline Precambrian basement and Paleozoic marine strata to the east, and the collage of Paleozoic and Mesozoic volcanic arc and dismembered oceanic crust terranes to the west (Brooks and others, 1976; Brooks and Vallier, 1978; Hamilton, 1978; Brooks, 1979a, b), which was accreted onto the North American craton during the Mesozoic. The West Mountain-Council Mountain-New Meadows area lies astride the postulated western limit of Precambrian rocks in North America, as deduced from the change in initial $^{87}Sr/^{86}Sr$ ratios from greater than 0.706 to the east to less than 0.704 to the west (Armstrong and others, 1977; see fig. 8.1). This isotopic boundary may denote the paleomargin of the North American plate after it was truncated but before the accretion of the volcanic-arc and dismembered oceanic-crust terranes to the west (see Armstrong and others, 1977; Hamilton, 1978; Davis and others, 1978).

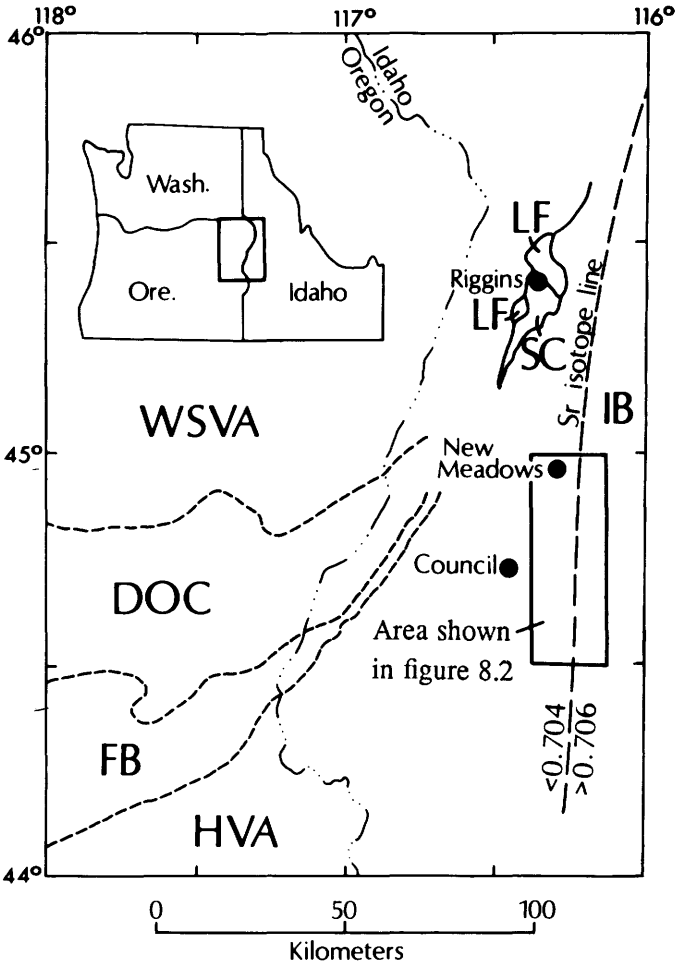

FIGURE 8.1.—Index map showing the geologic setting of the West Mountain-Council Mountain-New Meadows area in west-central Idaho. The terrane boundaries are adapted from Brooks (1979a); the Riggins area geology is simplified from Hamilton (1969); and the 0.704–0.706 initial strontium isotope line is from Armstrong and others (1977). WSVA, Wallowa Mountains-Seven Devils volcanic arc terrane; DOC, dismembered oceanic-crust terrane; FB, forearc basin terrane; HVA, Huntington volcanic arc terrane; SC, Squaw Creek Schist, Riggins Group; LF, Lightning Creek and Fiddle Creek Schists, undivided, Riggins Group; IB, Idaho batholith.

Immediately north of the West Mountain-Council Mountain-New Meadows area, the Riggins Group is present within the tectonic boundary zone between the Permian and Triassic volcanic-arc rocks to the west and the Cretaceous Idaho batholith and remnants of Precambrian rocks to the east (fig. 8.1). The Riggins Group consists of metamorphosed sedimentary and volcanic rocks; associated with the Riggins Group are enclosed blocks of serpentinized ultramafic rocks (Hamilton, 1963, 1969, 1978). Myers (1982) mapped the Riggins Group north of

the Riggins area but still within this tectonic boundary zone. Previous workers have not identified the Riggins Group in the West Mountain-Council Mountain-New Meadows area. Brooks and Vallier (1978) and Brooks (1979a) have suggested that the Riggins Group is the northeastward extension of late Paleozoic to middle Mesozoic dismembered oceanic-crust and forearc-basin terranes that lie between the Wallowa Mountains-Seven Devils volcanic arc terrane and the Huntington volcanic arc terrane in northeastern Oregon (fig. 8.1).

Palmer (1963) subdivided the southern part of the pre-Cenozoic crystalline rock area at Council Mountain into a migmatite unit and an undifferentiated metamorphic suite. Schmidt (1964) subdivided the pre-Cenozoic rocks in the West Mountain-Council Mountain area, from west to east, into the following three units: (1) the gneiss of Council Mountain, (2) the migmatite of McCall, and (3) the quartz dioritic gneiss of Donnelly. Taubeneck (1971) prepared a reconnaissance geologic map of the West Mountain-Council Mountain area in which he subdivided the pre-Cenozoic rocks, from west to east, into five units: (1) the quartz diorite of Deserette, (2) the quartz diorite of Council Mountain, (3) a zone of schist, gneiss, and minor pegmatite, (4) a zone of gneiss, migmatite, pegmatite, and granitic rocks, and (5) the quartz diorite of Donnelly. Both Schmidt (1964) and Taubeneck (1971) published modal analyses of the units that they recognized. Armstrong and others (1977) determined the initial strontium isotope ratios for the quartz diorites of Deserette, Council Mountain, and Donnelly, and for the nearby units to the north and east.

Very little descriptive information, previous to this study, exists for the pre-Cenozoic units in the New Meadows area. In a study of the Columbia River Basalt Group, Breeser (1972) included the pre-Cenozoic rocks south of New Meadows as part of a map unit consisting of metasedimentary schist and gneiss injected by quartz diorite and trondhjemite. She did not comment on the extensive occurrence of ultramafic rocks in that area, although she did report that chromite is present south of New Meadows. Thayer and Brown (1964) first mentioned that ultramafic rocks and associated chromitite deposits are present south of New Meadows, but they did not describe the rocks.

The Columbia River Basalt Group is present throughout the West Mountain-Council Mountain-New Meadows area and essentially covers the pre-Cenozoic rocks for many kilometers to the southwest and west, so the relation between the rocks discussed in this report and those in the Huntington volcanic arc terrane to the west (fig. 8.1) are nowhere exposed. The Columbia River Basalt Group has been described in the Council Mountain area by Palmer (1963), near New Meadows by Breeser (1972), and throughout the region by Fitzgerald (1982).

THE WEST MOUNTAIN-COUNCIL MOUNTAIN BLOCK

The West Mountain-Council Mountain block, in the southern part of the study area (fig. 8.2), contains the larger of the two exposures of pre-Cenozoic rocks. This block contains several metamorphosed plutons, which are outlined on figure 8.2, and metamorphosed volcanic and sedimentary rocks that I have subdivided into several provisional map units on the basis of differences in lithologic assemblages. Foliation and lineation attitudes throughout the area are essentially the same in the metamorphosed volcanic and sedimentary rocks as in the metamorphosed plutons (fig. 8.3). Foliations generally trend north-south and dip moderately to steeply east (fig. 8.2). Where present, the lineations plunge moderately to steeply eastward in the plane of foliation. The lineations commonly consist of mineral streaking or elongation (fig. 8.4). Where compositional layering is present in the metavolcanic and metasedimentary rocks and in the plutons, it is parallel to the foliation in most instances. Small-scale isoclinal folds, which are a common feature in many metamorphic terranes, were not observed in the metamorphosed plutons and were rarely seen in the metavolcanic and metasedimentary rocks in the West Mountain-Council Mountain block. Ptygmatic injections of thin aplite dikes are present locally, however, as are boudinage structures (figs. 8.5, 8.6) in some parts of the metavolcanic and metasedimentary sequences.

Obvious major late Cenozoic faults that offset the Columbia River Basalt Group and that have had an important influence on the physiographic development are shown in figure 8.2. Undoubtedly, significant faults of pre-Cenozoic age, as well as numerous additional faults of Cenozoic age, are present in the area, but careful mapping will be required to find them.

PLUTONIC ROCKS

Several felsic to intermediate plutons are present in the West Mountain-Council Mountain block. The characteristics of four of the largest plutons are noted in table 8.1. Other plutonic bodies appear to have been injected into the area, but due to their poor exposures, smaller sizes, and structural dismemberment they have not been outlined on figure 8.2. All the plutons were metamorphosed to a greater or lesser degree, depending on their location, so they have been modified by recrystallization and the development of foliation (fig. 8.3). Where deformation was intense, a lineation developed and compositional banding formed.

The West Mountain pluton has been called the quartz dioritic gneiss of Donnelly (Schmidt, 1964) and the quartz diorite of Donnelly (Taubeneck, 1971). Schmidt's (1964) map shows that this unit extends more than 30 kilometers

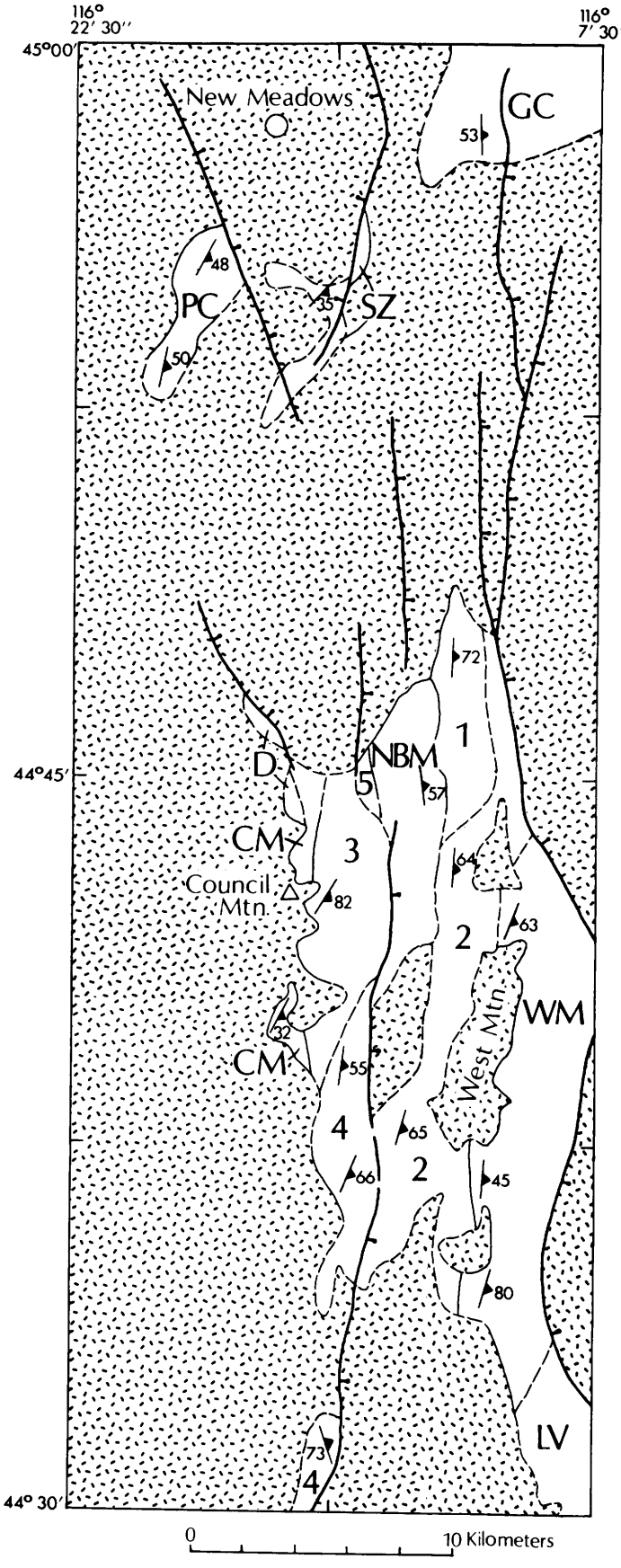

north-northeast of West Mountain. The Council Mountain and Deserette plutons were referred to as the quartz diorites of Council Mountain and Deserette by Taubeneck (1971), and they form an undifferentiated part of Schmidt's (1964) gneiss of Council Mountain. Palmer (1963) recognized that the Council Mountain pluton probably had an igneous origin and outlined the southern part of it as a migmatite complex. No previous workers recognized the relatively deformed No Business Mountain pluton as an igneous body. Inasmuch as most of the rock exposed in these plutonic bodies is something other than quartz diorite, according to the widely accepted IUGS classification system (Streckeisen and other, 1973), and because the bodies vary somewhat in composition, I have dropped the rock-type designation from the names of the plutons.

COUNCIL MOUNTAIN AND DESERETTE PLUTONS

The least metamorphosed and least deformed plutons in the West Mountain-Council Mountain block are the Council Mountain and Deserette plutons on the west side of the area. The Council Mountain pluton is exposed in two areas adjacent to the region covered by later basalt flows to the west (fig. 8.2). Although it is uncertain if both exposures are part of the same pluton, their great similarities in composition and appearance, as well as in their north-south alignments, suggest they are.

The Deserette pluton, which adjoins and extends northwestward from the Council Mountain pluton, is much

FIGURE 8.2.—Preliminary geologic map of the West Mountain-Council Mountain-New Meadows area. Compiled principally from the reconnaissance geologic mapping of the writer, with minor additions from Palmer (1963), Schmidt (1964), Schmidt and Mackin (1970), Taubeneck (1971), Breeser (1972), Mitchell and Bennett (1979), and Fitzgerald (1982). The New Meadows block consists of the peridotite and metachert (PC) and the intensely sheared schistose rock (SZ) zones in the northern part of the area. The West Mountain-Council Mountain block includes the various plutonic and metamorphic rock units in the central and southern parts of the area. Plutonic rock units: CM, Council Mountain pluton; D, Deserette pluton; WM, West Mountain pluton; NBM, No Business Mountain pluton; LV, quartz diorite of Little Valley. Metamorphic rock units: 1, metavolcanic rocks northeast of No Business Mountain; 2, plagioclase-quartz-biotite gneiss; 3, metavolcanic rocks on Council Mountain; 4, zone with abundant metasedimentary rocks; 5, zone of marble, calc-silicate rocks, and hornfelsed amphibolite. Other units: PC, peridotite and metachert along west side of New Meadows block; SZ, zone consisting mainly of intensely sheared schistose rocks; GC, Goose Creek mylonitic gneiss (C. Allen and M. Kuntz, oral commun., 1984). Symbols: heavy lines, faults, bar and ball on downthrown side; light lines, geologic contacts, dashed where approximately located; foliation symbols, strikes and dips of representative foliations; patterned area, Cenozoic materials: consist mainly of the Columbia River Basalt Group and unconsolidated sediments.

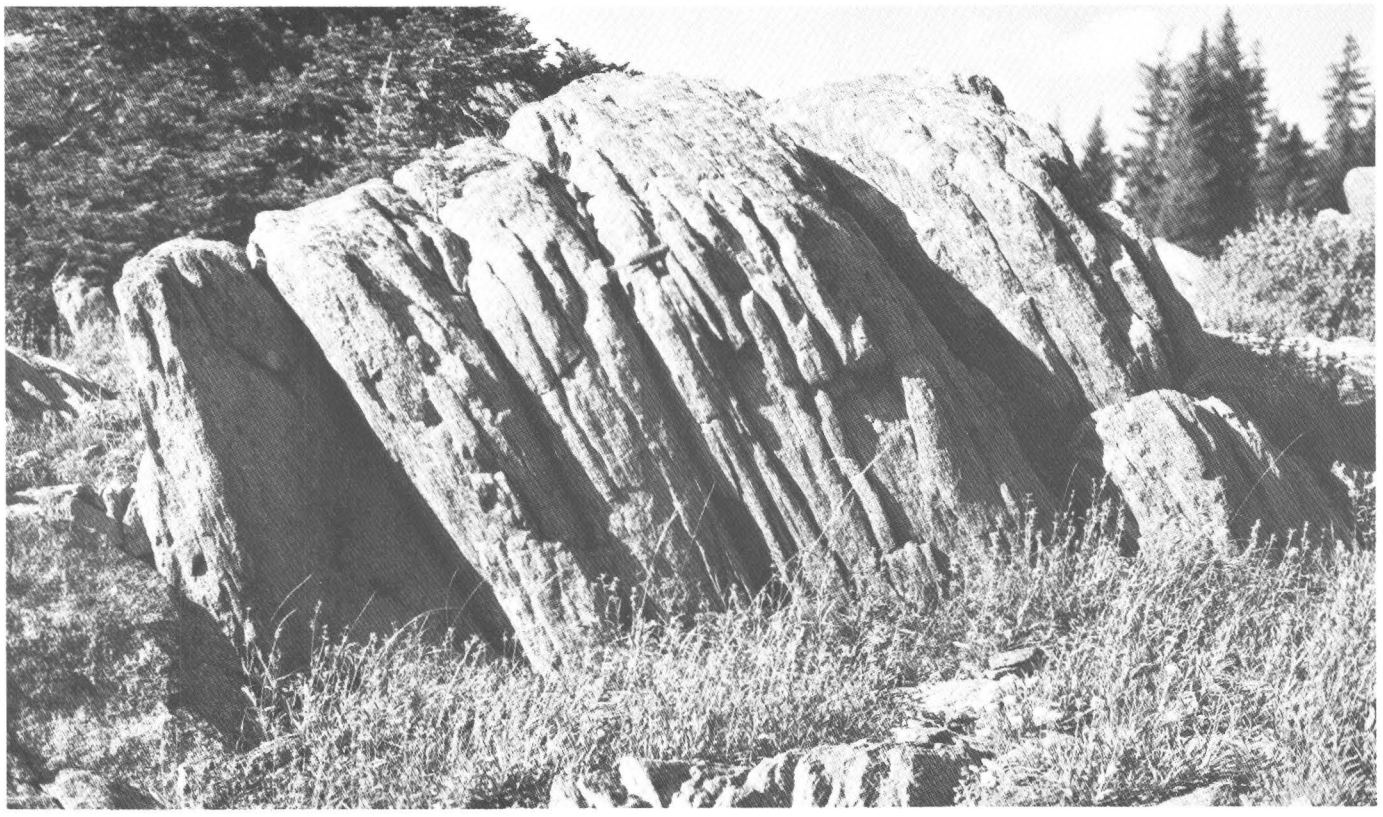

FIGURE 8.3.—View of eastward-dipping foliation and shearing within the West Mountain pluton. Note hammer for scale.

more leucocratic than the Council Mountain pluton. It generally contains less than 10 percent mafic minerals, whereas the Council Mountain pluton typically has nearly 30 percent (table 8.1). Although these two plutons adjoin, their contact is not exposed (Taubeneck, 1971). Their proximity and nearly identical initial $^{87}Sr/^{86}Sr$ ratios and K-Ar biotite ages (table 8.1) suggest that they are genetically related. Such a relation is also suggested by the occurrences of fairly leucocratic zones and leucocratic tonalite dikes in the Council Mountain pluton. These two plutons may have formed from the same parent magma, with the more leucocratic Deserette pluton crystallizing later and intruding parts of the earlier crystallized, more mafic Council Mountain pluton.

WEST MOUNTAIN PLUTON

The West Mountain pluton, commonly having slightly more than 30 percent mafic minerals (table 8.1), generally is similar in appearance and composition to the Council Mountain pluton. It differs by containing augite, which the Council Mountain pluton evidently lacks, and by having much less epidote than can be found in the Council Mountain pluton (table 8.1). The West Mountain pluton also has a considerably higher initial $^{87}Sr/^{86}Sr$ ratio and a younger K-Ar biotite age than the Council Mountain pluton and shows a greater degree of gneissic structure and foliation disrupting its original plutonic fabric (fig. 8.3).

NO BUSINESS MOUNTAIN PLUTON

The No Business Mountain pluton covers 10 square kilometers or more at the top and on the south and west slopes of No Business Mountain. It lies between the Council Mountain and Deserette plutons to the west and the West Mountain pluton to the east (fig. 8.2). Due to the paucity of exposures and its deformed character, the southern extent of this body is poorly known. Its contact with metavolcanic and metasedimentary rocks is exposed at elevation point 7,340 feet on the top of No Business Mountain (sec. 34, T. 17 N., R. 2 E.).

The No Business Mountain pluton varies greatly in composition from one location to another; overall, it ranges from diorite to syenite (table 8.1). Most samples are enriched in potassium feldspar, in contrast to the West

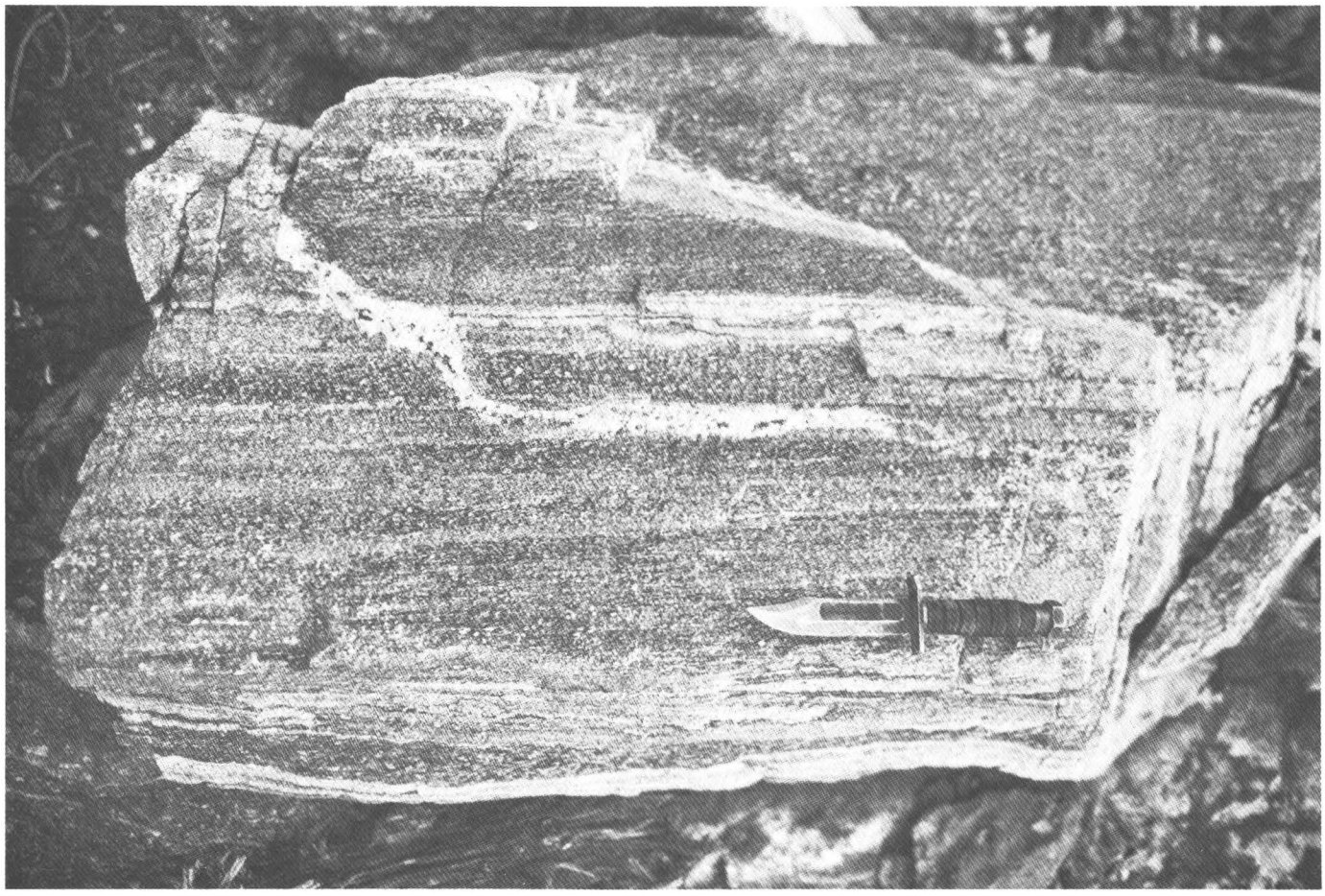

FIGURE 8.4.—Well-developed lineation in the form of mineral streaking developed on a foliation plane in the Council Mountain pluton.

Mountain and Council Mountain plutons. The No Business Mountain pluton apparently has much less quartz than the others. Furthermore, parts of the No Business Mountain pluton contain relatively high quantities of augite, sphene (indicating titanium enrichment), and zeolites, whereas none of the samples has more than a trace of biotite. In contrast, the tonalitic rocks of the nearby plutons are rich in biotite.

The potassium feldspar in the No Business Mountain pluton typically is perthitic, with small to abundant quantities of exsolved plagioclase. Where strongly deformed, the potassium feldspars show well-developed microcline-grid twinning. Aplitic dikes which cut the calc-silicate rocks on the west side of the No Business Mountain pluton (fig. 8.2) and which very likely are apophyses of the pluton consist mainly of a single alkali feldspar. These habits of potassium feldspar are generally quite different from those in the other plutonic rocks or in the nearby metamorphosed volcanic and sedimentary rocks.

The petrographic features outlined above suggest that the No Business Mountain pluton may be petrogenetically different from the other plutons in the area, even though samples from all of them are superficially similar. The range of rock types, from quartz monzodiorite to syenite (table 8.1), indicates that the No Business Mountain pluton is more alkalic than the nearby tonalites and quartz diorites. Thus, it may be one of the group of early Mesozoic alkalic intrusions that occur near the Mesozoic continental margin, from southern California to the middle of British Columbia (Miller, 1978). These plutons typically have high strontium contents compared to the calc-alkaline plutons with which they are associated. X-ray fluorescence analyses of one sample from the No Business Mountain pluton and one from the West Mountain pluton indicate that the No Business Mountain pluton sample contains 3 to 4 times more strontium than the sample from the West Mountain pluton (C. Knowles, oral commun., 1984). This contrast, along with the high abundance of

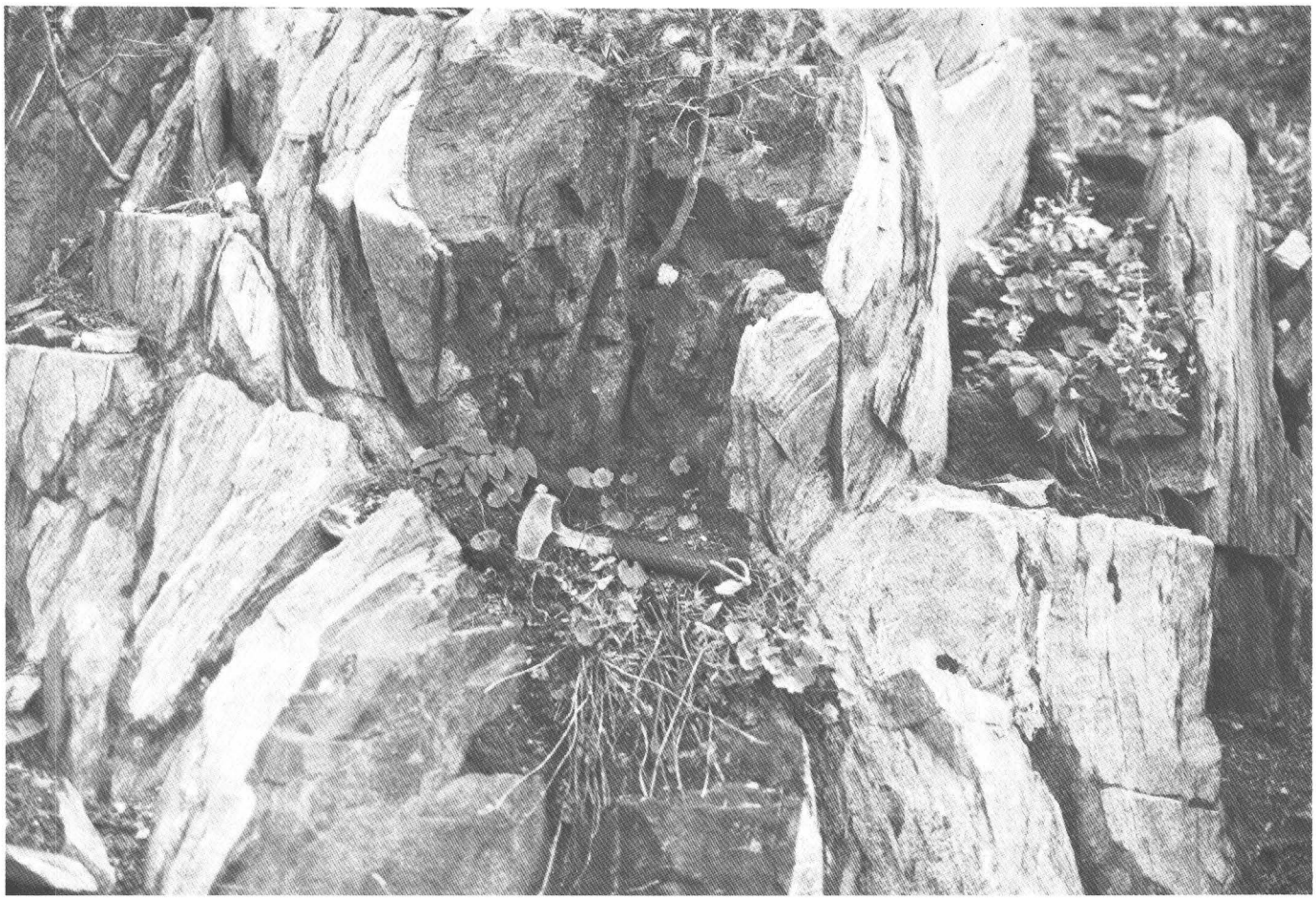

FIGURE 8.5.—Boudinage of an amphibolitic layer within a more ductile matrix of quartzofeldspathic gneiss, within the unit of metavolcanic rocks on Council Mountain.

sphene within the No Business Mountain pluton, again suggests that the No Business Mountain pluton may be part of the continental margin group of early Mesozoic (Triassic?) alkalic plutons. In this regard, it is interesting to note that the No Business Mountain pluton actually lies exactly on the old continental margin, as inferred from the initial strontium isotope boundary determined by Armstrong and others (1977).

OTHER PLUTONIC ROCKS

Additional plutonic rocks are present in the West Mountain-Council Mountain area but are not yet well enough understood to show as map units. These include scattered occurrences of metamorphosed hornblende-bearing quartz diorite or tonalite within the two metavolcanic rock units and within the plagioclase-quartz-biotite gneiss map unit on the west side of the West Mountain pluton (fig. 8.2). These metaplutonic rocks are similar to the metamorphosed tonalites in the Council Mountain and West Mountain plutons. Taubeneck (1971) suggested that part of this belt of plagioclase-quartz-biotite gneiss includes mafic-poor plutonic rocks of tonalitic composition. He referred to these rocks as the quartz diorite west of the Donnelly (West Mountain) pluton but did not indicate their distribution on his map, although he included several modal analyses.

Additional plutonic rocks are present immediately south of the area shown in figure 8.2 and are believed to extend into the southeast corner of the map area. Rocks collected on reconnaissance traverses in secs. 7 and 8, T. 13 S., R. 3 E., near the crest of West Mountain ridge, about 2 kilometers south of the south edge of the area shown in figure 8.2, are largely foliated quartz diorites or tonalites that contain biotite, muscovite, and garnet, but no hornblende. Additional two-mica plutonic rocks were observed locally farther west, about 2 kilometers south of the south edge of the area shown in figure 8.2,

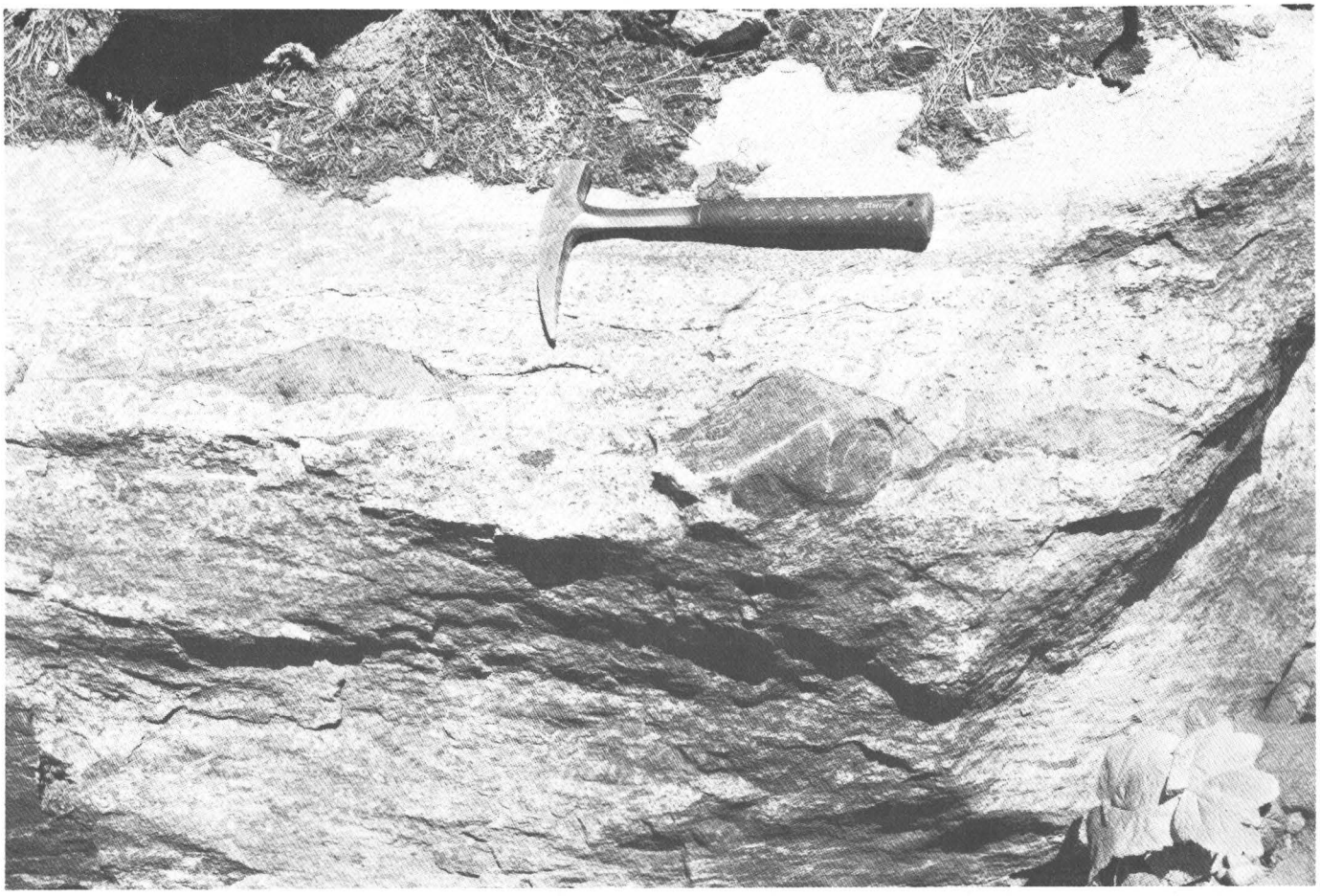

FIGURE 8.6.—Pods or boudins of amphibolite, interpreted as a dismembered, originally continuous, amphibolite layer in the metavolcanic rock unit northeast of No Business Mountain.

in sec. 7, T. 13 S., R. 2 E. These two-mica plutonic rocks have only about half the mafic minerals as the tonalitic plutons on Council and West Mountains. Their general compositions and their locations on the map compiled by Mitchell and Bennett (1979) suggest that they are part of the leucocratic quartz diorite of Little Valley (Schmidt, 1964), which was mapped by Fisher and others (1983) as the sphene-enriched variety (Kgds) of biotite granodiorite, a widespread interior unit of the Idaho batholith. Fisher and others (1983) considered this unit to be younger than the tonalitic rocks in the West Mountain-Council Mountain block.

METAVOLCANIC AND METASEDIMENTARY ROCKS

Five provisional map units within the area of metavolcanic and metasedimentary rocks that surrounds the metamorphosed plutons have been outlined within the West Mountain-Council Mountain block (fig. 8.2). These units are: (1) a zone interpreted as mostly metavolcanic rocks northeast of No Business Mountain, (2) a zone of mostly plagioclase-quartz-biotite gneiss west and north of the West Mountain pluton, (3) a second zone of probable metavolcanic rocks along the western part of the area and best exposed on Council Mountain, (4) a zone having abundant metasedimentary rocks in the southern part of the area, and (5) a small area of marble, skarnlike calc-silicate rocks, and hornfelsed amphibolite next to the No Business Mountain pluton.

The respective ages of these metamorphic rock units are unknown, and it is not yet known if their boundaries are depositional or tectonic. The first two units noted above generally correspond to Schmidt's (1964) migmatite of McCall and to the unit that Taubeneck (1971) designated as gneiss, migmatite, pegmatite, and granitic rocks. The other three generally correspond to Schmidt's (1964) gneiss of Council Mountain and to the unit that Taubeneck (1971) referred to as schist, gneiss, and minor pegmatite.

TABLE 8.1.—*Characteristics of plutons in the West Mountain-Council Mountain area*

[Rock type nomenclature from Streckeisen and others (1973). K-Ar ages were recalculated for revised decay constants using the method of Dalrymple (1979). Table includes data from Palmer (1963); Schmidt (1964); Taubeneck (1971); Armstrong (1975); Armstrong and others (1977). tr, trace]

	Council Mountain pluton	Deserette pluton	West Mountain (Donnelly) pluton	No Business Mountain pluton
		Modal composition		
Number of modes averaged	6	7	8	range noted
Quartz	16.2	29.7	21.0	0-10
K-feldspar	.4	2.6	1.3	15-50
Plagioclase	54.5	59.5	48.4	5-50
Augite	--	--	.4	0-15
Hornblende	13.9	--	13.0	10-40
Biotite	10.5	5.9	15.5	tr.
Epidote	3.4	1.1	tr.	tr.-5
Muscovite	--	.7	--	--
Black opaques	tr.	tr.	tr.	tr.
Apatite	tr.	tr.	tr.	tr.
Zircon	tr.	--	tr.	--
Sphene	--	tr.	tr.	tr.-3
Zeolites	--	tr.	--	tr.
Pyrite	--	--	--	tr.
An content of plagioclase	30 (?)	--	34-39	--
		Rock types		
	tonalite quartz diorite diorite	tonalite quartz diorite granodiorite	tonalite quartz diorite	syenite monzonite quartz monzonite quartz monzo-diorite diorite
		Average initial $^{87}Sr/^{86}Sr$ ratio		
Number of locations averaged	5	4	4	--
	.7039	.0739	.7086	--
		K-Ar ages (Ma)		
Biotite	84.1±2	86.1±3	77.9±2	--
Hornblende	119.9±4	--	92.3±3	--

METAVOLCANIC ROCKS NORTHEAST OF NO BUSINESS MOUNTAIN

The zone of probable metavolcanic rocks northeast of No Business Mountain (fig. 8.2) consists predominantly of strongly foliated, mostly homogeneous to weakly layered schist typically containing 50 to 80 percent plagioclase, as much as 20 percent quartz, and from 5 to 15 percent biotite plus hornblende. Biotite commonly is more abundant than hornblende. Potassium feldspar generally accounts for less than 10 percent of the schist but locally is as abundant as 30 percent. Minor minerals include muscovite, apatite, zircon, sphene, opaque oxides, clinozoisite, traces of chlorite replacing biotite, and local garnet adjacent to the No Business Mountain pluton.

The rocks in this zone have mineral compositions that suggest they originally might have been felsic andesites or dacites. Locally the schist contains uniformly distributed feldspar porphyroblasts in a textural arrangement similar to that in metamorphosed volcanic rocks of many other regions. The rocks in this map unit may have originated as a combination of lava flows, welded or nonwelded pyroclastic rocks or sedimentary tuffs, and immature sediments derived from a volcanic terrane.

Foliated fine-grained layers of amphibolite and plagioclase-hornblende-augite-potassium feldspar gneiss are intercalated with the felsic metavolcanic rocks and generally show sharp contacts. These rocks consist of about equal parts of felsic and mafic constituents. Plagioclase is the principal felsic mineral. It is accompanied by 0 to 5 percent quartz and minor to locally as much as 15 percent potassium feldspar. Hornblende is the predominant mafic mineral, but augite locally may account for as much as 20 percent of the rock. Minor constituents include biotite, chlorite, epidote, opaque oxides, apatite, sphene, and calcic scapolite as a local vein-filling mineral. The mineralogy of these amphibolitic rocks suggests that the parent rocks were lava flows or tuffs of basalt to basaltic andesite compositions, carbonate-bearing volcanogenic sedimentary rocks, or perhaps spillitized basalt or tuff. Rocks having compositions intermediate between the felsic and mafic varieties are rare in this unit.

The amphibolite layers commonly are only a few meters in maximum thickness and some are less than a meter thick. During deformation, many of the mafic layers were broken into boudins (fig. 8.6) that are partially to completely surrounded by the more ductile feldspar- and quartz-rich schist matrix. The thin nature of many of the amphibolite layers suggests that they originated as sedimentary or tuffaceous layers rather than as lava flows, and the local presence of augite and scapolite suggests that these were carbonate bearing.

Locally, along the west side of this map unit, the schist is medium to coarse grained and gneissic and resembles some of the more strongly deformed gneissic parts of the metamorphosed plutons on West Mountain and Council Mountain. This relation indicates that some metamorphosed intrusive rocks are present within this metavolcanic unit.

At many localities the rocks in this unit are cut by thin alkali feldspar- and quartz-rich pegmatitic dikes. Many of the dikes have sharp contacts and are generally concordant with the layering and foliation of the enclosing schists. These dikes are probably the result of incipient partial melting of their enclosing host rocks during metamorphism.

PLAGIOCLASE-QUARTZ-BIOTITE GNEISS

The plagioclase-quartz-biotite gneiss north of and immediately west of the West Mountain pluton (fig. 8.2) is largely felsic and fine to medium grained, and typically contains 65 to 75 percent plagioclase, 10 to 25 percent quartz, as much as 10 percent potassium feldspar, and generally only 5 to 15 percent mafic minerals, mostly biotite. As much as 10 percent hornblende locally is present but more commonly is absent. Trace amounts of apatite, zircon, and opaque oxide minerals generally are present, and minor amounts of augite, sphene, epidote, muscovite, tourmaline, and graphite have been noted locally. The premetamorphic textural features have generally been obliterated by deformation and recrystallization.

The rock compositions in this unit typically consist of diorites, quartz diorites, and tonalites, or their volcanic equivalents. The augite-, hornblende-, and sphene-bearing rocks may largely be plutonic in origin, whereas at least part of the finer grained gneiss with biotite as the main mafic mineral may be volcanic in origin. The local homogeneity of most exposures also suggests an igneous origin for most of this unit.

Rocks suspected of having a volcanic origin are present principally in the northern part of this unit near the metavolcanic rocks northeast of No Business Mountain (fig. 8.2), whereas most of the rocks in the southern part of this unit are probably of plutonic origin. Alkali feldspar- and quartz-rich aplitic to pegmatitic dikes as much as one meter thick are present in many exposures in the southern part of this unit. The unit which Taubeneck (1971) designated as the quartz diorite west of the Donnelly (West Mountain) pluton probably corresponds to the metaplutonic southern part of this unit.

Rocks that are compositionally heterogeneous locally or rocks that contain minerals whose presence would infer a probable sedimentary origin, such as garnet, muscovite, diopsidic pyroxene, calcite, or scapolite are notably sparse. To date, the only area identified in this unit that might contain significant quantities of metasedimentary rocks is in the east half of secs. 15 and 22, T. 16 N., R. 2 E.,

where traces of graphite occur in a medium-grained, compositionally layered plagioclase-quartz-biotite mixture of gneiss and schist.

Sparse to abundant potassium feldspar megacrysts are present to conspicuous in the northern part of the plagioclase-quartz-biotite gneiss and perhaps elsewhere. Where these megacrysts occur the gneiss is very similar in appearance to the Goose Creek mylonitic gneiss (C. Allen and M. Kuntz, oral commun., 1984) located in the northeastern corner of the area shown in figure 8.2. The Goose Creek mylonitic gneiss sits astride the initial strontium isotope line in its occurrence east of New Meadows in the same fashion as can be inferred for the plagioclase-quartz-biotite gneiss in the West Mountain-Council Mountain block.

METAVOLCANIC ROCKS ON COUNCIL MOUNTAIN

The zone of predominantly metavolcanic rocks on Council Mountain, along the west side of the pre-Cenozoic exposure belt (fig. 8.2), contains gneisses and schistose rocks very similar to those in the metavolcanic rock unit northeast of No Business Mountain. As in the No Business Mountain area, two rock types, felsic and mafic, dominate in the metavolcanic rock unit on Council Mountain. The more felsic rocks consist mostly of plagioclase and quartz, commonly having 5 to 15 percent biotite plus hornblende, with biotite generally predominating. These rocks typically are strongly foliated and fine grained, and locally display textures resembling those of metavolcanic rocks of other regions around the world. These felsic rocks probably were initially dacites to felsic andesites.

Most of the more mafic rocks are moderately to strongly lineated amphibolites having about equal amounts of plagioclase and hornblende. The abundance and thickness of the amphibolite layers in the Council Mountain area typically are much greater than in the No Business Mountain area; this relation implies that many of the mafic layers of the Council Mountain area may initially have been mafic andesite or basaltic flows or tuffs. Also supporting a metavolcanic rather than metasedimentary origin for most of the Council Mountain amphibolites is the apparent absence of diopsidic pyroxene segregations within most amphibolite masses, in contrast to the behavior described below for some of the hornblende-rich rocks within the map unit of abundant metasedimentary rocks.

Locally within the Council Mountain area, thin amphibolite layers display boudinage structure within the more ductile felsic matrix (fig. 8.5). Aplitic and pegmatitic dikes cutting the metavolcanic rocks are quite common throughout the Council Mountain area. Most pegmatites contain either albite or potassium feldspar and quartz, and minor biotite or muscovite. Rarely, small garnets are present in the pegmatites and aplites. Most dikes appear to have been metamorphosed, as they commonly display foliation concordant to the regional foliation. Quartz veins are present locally in the metavolcanic rocks around Council Mountain. Most were recrystallized and segmented during the deformation of their host rocks.

Felsic rocks that may originally have been plutonic are present locally in the metavolcanic rocks on Council Mountain. Such rocks are less abundant than the rocks of probable volcanic origin. A few metasedimentary rocks that locally contain garnets and thin quartz- and muscovite-rich layers are also present in this area. These layers may have formed from thin felsic-tuff layers.

MAP UNIT WITH ABUNDANT METASEDIMENTARY ROCKS

A zone having abundant metasedimentary rocks is present southwest of the plagioclase-quartz-biotite gneiss in the southern part of the area shown in figure 8.2. Two main rock types are in this unit: (1) Ca- and Mg-rich rocks composed largely of clinopyroxene and hornblende which appear to have originated as carbonate-rich sediments, and (2) quartzofeldspathic gneisses and schists that commonly contain garnets and two micas, but which vary in minor mineral content. This second group predominates within the map unit and encloses the Ca- and Mg-rich rocks. The quartzofeldspathic gneisses and schists include rocks that were probably deposited as sediments and others that may have been intermediate to silicic volcanic rocks. Metaplutonic rocks are scarce or absent from this unit, as are rocks with quartz-rich or pelitic compositions.

The Ca- and Mg-rich rocks include compositionally layered types consisting mostly of diopsidic clinopyroxene, tremolitic amphibole, plagioclase, and quartz or calcic scapolite and calcite, accompanied by minor potassium felspar, apatite, sphene, and opaque minerals. Palmer (1963) also noted the occurrence of similar interlayered marble, amphibolite, and quartz-orthoclase-diopside-scapolite gneiss within this unit, in either sec. 6, T. 14 N., R. 2 E. or sec. 31, T. 15 N., R. 2 E.

Other Ca- and Mg-rich rocks are present as groups of irregular to streamlined pods similar to the boudin shown in figure 8.6. These pods are as much as a few meters long and are present within some of the quartzofeldspathic gneisses. The cores of the larger pods commonly consist of augite or diopside that is partly replaced by hornblende and that is accompanied by small percentages of calcite, epidote, opaque minerals, apatite, and sphene. The clinopyroxene-rich cores commonly are surrounded by hornblende-rich coronas as much as several centimeters thick. These pods are believed to be boudins which initially were thin layers rich in carbonate minerals of the dolomite-ankerite series.

The appearance, overall compositions, and absence of muscovite, garnet, graphite, or other minerals that infer a sedimentary origin suggest that the gneisses enclosing the clinopyroxene-rich pods probably were andesitic to dacitic flows or tuffs. Closely associated with the local metavolcanic rocks that enclose the clinopyroxene-rich pods are sparse occurrences of leucocratic schistose to gneissic rocks that are rich in plagioclase, potassium feldspar, and quartz. These rocks have compositions and textures that suggest a rhyolitic tuff origin.

The quartzofeldspathic gneisses and schists of this map unit are predominantly medium grained and foliated, and contain 40 to 80 percent plagioclase, 10 to 40 percent quartz, and 0 to 15 percent mafic minerals. Potassium feldspar generally is absent or is present in trace amounts. Biotite is the principal mafic mineral. Some of the gneisses are leucocratic but contain little or no potassium feldspar. These rocks contain traces to a few percent muscovite or garnet (almandine?), or both. Traces of apatite, zircon, opaque minerals, and chlorite (replacing biotite) commonly are present, but clinopyroxene, hornblende, epidote, sphene, and carbonate minerals have not been noted. The presence of muscovite and garnet, coupled with the absence or paucity of potassium feldspar, suggests that these gneisses are metamorphosed sediments rather than volcanic rocks. The common appearance of thin biotite-rich layers and streaks within the gneiss also suggests a metasedimentary origin.

MARBLE, CALC-SILICATE ROCKS, AND HORNFELSED AMPHIBOLITE

A small area of Ca- and Mg-rich rocks, including marble and gneissic- to hornfelsic-textured rocks with varying amounts of hornblende, clinopyroxene, and plagioclase, is present near the corner of secs. 4, 5, 8, and 9, T. 16 N., R. 2 E., between the No Business Mountain pluton and the metavolcanic rocks on Council Mountain (fig. 8.2). A marble body that may be as much as several tens of meters thick is present in that area. It varies from approximately 50 percent quartz to nearly pure calcite. Accessory minerals include tremolite, phlogopite(?), graphite, and magnetite or pyrite. As noted above, Palmer (1963) reported an additional marble occurrence at a location about 18 kilometers to the south in the map unit having abundant metasedimentary rocks (fig. 8.2). Leucocratic dikes and irregular masses of aplite locally cut the marble and the associated calc-silicate rocks.

The hornfelsic- to gneissic-textured rocks vary widely in their mineral proportions. Overall, these rocks resemble the amphibolites in the region but locally include calc-silicate skarn. The textures in some of these rocks suggest that reheating partially annealed a preexisting gneissic fabric to a hornfelsic arrangement. Less abundant minerals include grossularite to andradite garnet, quartz, potassium feldspar, calcite, epidote, scapolite, opaque minerals, chalcopyrite, apatite, sphene, and idocrase. The minor-mineral assemblage suggests that these rocks were derived from carbonate-bearing to carbonate-rich (dolomitic to ankeritic) sedimentary material, rather than mafic volcanic rocks.

The composition of the aplitic dikes and masses and their proximity to the No Business Mountain pluton, suggest they are apophyses of the No Business Mountain pluton that were injected into and thermally metamorphosed the sedimentary rocks in this small area. All the rocks in this unit, including the skarnlike mass, were deformed and metamorphosed again, along with the rest of the rocks in the West Mountain-Council Mountain block. Although this small area of metasedimentary rocks is approximately on line with the map unit containing abundant metasedimentary rocks to the south (fig. 8.2), it is not yet clear if this area represents a northward extension of that unit.

THE NEW MEADOWS BLOCK

The New Meadows block is in the northern part of the West Mountain-Council Mountain-New Meadows area (fig. 8.2). The western part of the block consists of a north-northeast-trending, 7-kilometer-long zone of mainly peridotite and impure quartzite. Both rock types are cut by aplitic to pegmatitic dikes and masses having granitic to trondhjemitic compositions. Scattered outcrops in the eastern part of the block are a mixture of amphibolite, quartzofeldspathic schist, and local metapyroxenite and serpentinite, all cut by aplites and pegmatites.

The foliation in the New Meadows block trends north to north-northeast and dips moderately to steeply eastward, as in the West Mountain-Council Mountain block. Lineations in the western part of the block, however, are subhorizontal within the foliation plane. They are commonly in the form of elongate mineral streaks and shallow elongate grooves that kink the wispy to thin layers in the quartz-rich rocks. Their attitude is in marked contrast to the eastward-plunging, down-dip lineations in the West Mountain-Council Mountain block.

The strong deformation and juxtapositioning of various rock types in this area, along with many straight stream courses, escarpments, and other topographic features, indicate a complex history of pre- and post-Columbia River basalt faulting. Aside from noting on figure 8.2 the obvious major postbasalt faults that control topographic features and the distribution of pre-Cenozoic rock exposures no attempt has been made to decipher the faulting history of the New Meadows block.

ULTRAMAFIC ROCKS

Ultramafic rocks are abundant in a 4-kilometer-long zone along the west side of the New Meadows block in secs. 2, 3, 10, and 15, T. 18 N., R. 1 E. Reconnaissance traverses indicate the presence of several different ultramafic rock bodies separated by quartzose, and locally schistose quartzofeldspathic to amphibolitic, rocks. The ultramafic rocks vary from nearly unaltered peridotite to schists composed of various proportions of anthophyllite, tremolite, talc, serpentine (mainly antigorite and lizardite), and chlorite (probably corundophilite). These schistose rocks generally occupy the peripheral parts of the ultramafic masses and occur as zones that crosscut fresh peridotite.

Forsteritic olivine, enstatitic orthopyroxene, and chromite are the principal minerals in the unaltered peridotite. Clinopyroxene has not been seen, but small quantities were likely present judging from locally abundant tremolite in hydrated zones. Olivine is much more abundant than orthopyroxene, so most of the ultramafic rock is dunite. None of the peridotite examined to date contains plagioclase. Float samples of chromitite have been found near prospect pits in the SW¼ NW¼ sec. 2, T. 18 N., R. 1 E. The chromitite probably originated as a magmatic segregation when the peridotite crystallized.

The peridotites vary from cumulates with equant olivine grains packed loosely in an interstitial orthopyroxene matrix (fig. 8.7) to severely tectonized rocks in which large (about 1 cm or more) olivine grains have been strained into sets of subparallel, curved lamellae (fig. 8.8). The small percentage of chromite consists mainly of equant grains that are enclosed by orthopyroxene but not by olivine, suggesting that chromite is also a cumulus mineral. The overall petrologic, mineralogic, and structural characteristics of the peridotite bodies resemble those of alpine peridotites or fragments of ophiolite complexes, including the Canyon Mountain Complex (Thayer, 1977; Avé Lallemant, 1976) in northeastern Oregon within the dismembered oceanic crust terrane (fig. 8.1) described by Brooks and Vallier (1978) and Brooks (1979a).

Peridotite that has been partially converted to hydrous minerals shows evidence of having undergone at least two hydration episodes, both postdating the straining of the olivine. During the first episode, numerous thin veins and local patches of very fine grained serpentine developed throughout the rocks, cutting across olivine and pyroxene (fig. 8.7). Locally forming with this early serpentine were veins and patches of chlorite and traces of fine-grained magnetite. No amphiboles and little, if any, talc appeared during this early serpentinization episode.

During the second hydrous alteration episode, anthophyllite and talc formed and were accompanied locally by tremolite and additional serpentine, chlorite, and magnetite. The anthophyllite developed throughout the peridotite masses, both within olivine and pyroxene and cutting the earlier serpentine veins (fig. 8.9). Tremolite developed concurrently with anthophyllite and very likely consumed calcium released by the alteration of clinopyroxene. Following the formation of anthophyllite and tremolite, abundant talc formed, both in veins and as masses replacing anthophyllite (fig. 8.9). Talc formation was an early retrograde stage of the second hydration episode. Accompanying and following the talc, additional serpentine, chlorite, and magnetite formed as a late retrograde stage.

Although anthophyllite and talc are present throughout the peridotite masses, they are much more conspicuous in some areas. Their maximum development is on the northwest side of Vick Creek in NE¼ sec. 15, T. 18 N., R. 1 E., where the anthophyllite occurs as sheaves and rosettes of acicular crystals (fig. 8.10), some longer than 20 centimeters. After they formed, the anthophyllite sheaves and rosettes were largely replaced by talc (fig. 8.9).

There is a marked contrast between the nondeformed anthophyllite and talc and the strongly deformed olivine grains in the peridotite (compare figs. 8.8 and 8.10). The nondeformed character of the anthophyllite and talc suggests that the peridotite bodies were near their present structural positions when they were reheated, allowing the anthophyllite and talc to grow statically. The strong olivine deformation probably occurred during the emplacement of the peridotite masses into their present tectonic settings, or it might be inherited from an earlier stage.

Locally cutting the peridotite are trondhjemitic to granitic dikes of aplitic to pegmatitic texture. Their injection probably was contemporaneous with the heating event that formed the anthophyllite, tremolite, and talc.

The thoroughly hydrated ultramafic rocks that are marginal to or that cut the peridotite masses range from almost pure anthophyllite, tremolite, talc, chlorite, or serpentine to mixtures of these minerals. Their textures vary from schistose to decussate. Inasmuch as these rocks are entirely hydrated, their evolution is not as easily deciphered as that of rocks containing olivine and pyroxene. Nevertheless, assuming the amphiboles and talc formed in response to heating after the ultramafic rocks were in place, it is probable that the peripheral concentrations of these minerals developed concurrently, probably as water migrated from adjacent rocks into the peridotite. Whether the serpentinite and chlorite schist adjacent to the peridotite bodies formed at this time, or earlier, is not known.

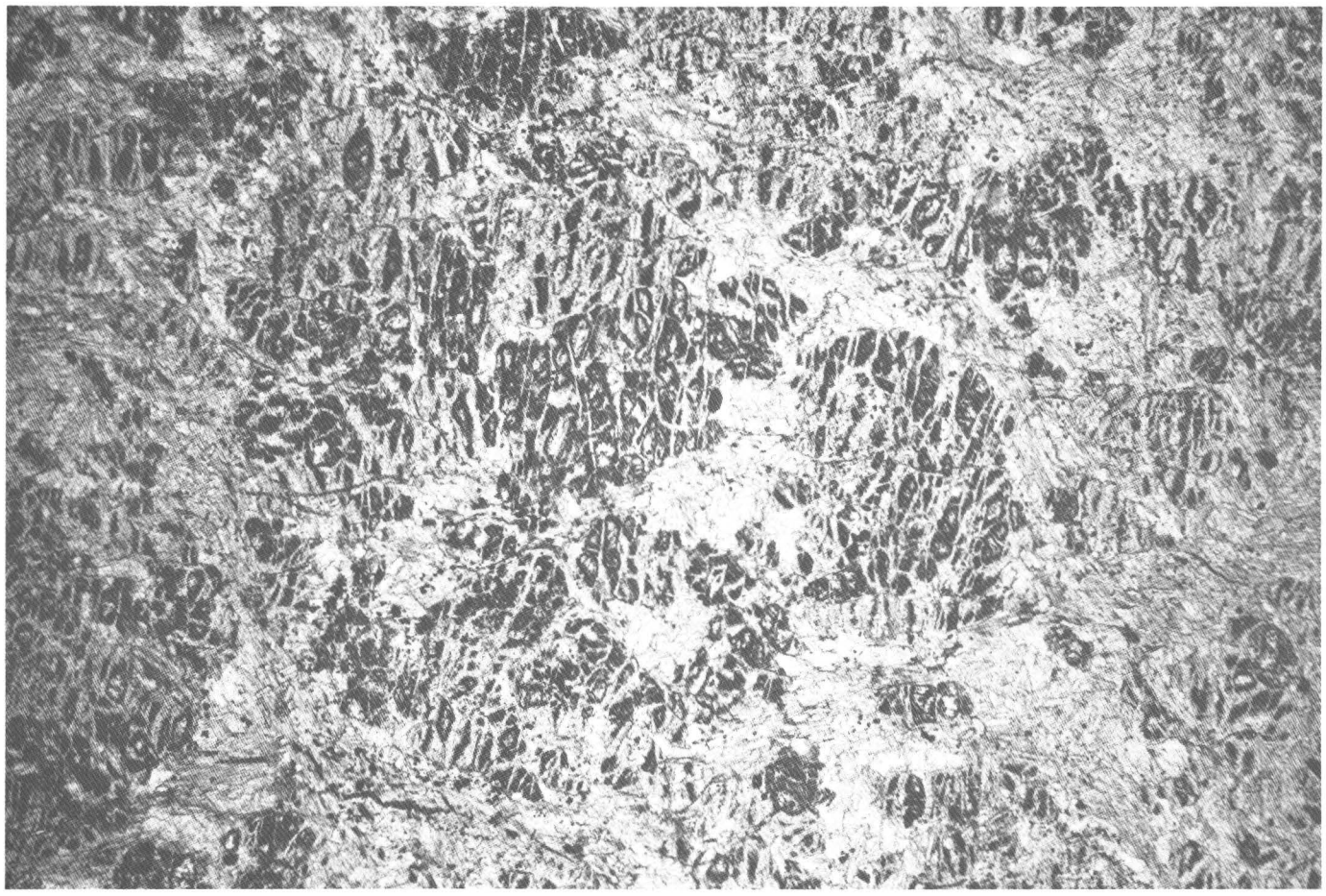

FIGURE 8.7.—Photomicrograph of remnants of equant olivine grains, about a millimeter across, set in a talc-rich matrix developed mostly from orthopyroxene that was interstitial to the olivine. This texture is interpreted as a relict cumulate texture. Note the abundant thin veins of serpentine cutting the olivine grains. Thin section in plane light; width of view is about 7 millimeters.

METAMORPHIC ROCKS

Mixed with the peridotite is an assortment of thinly layered quartz-rich metasedimentary rocks that range from gneissic to hornfelsic in texture. Present with these quartz-rich rocks, mainly to the south, are layered rocks having quartzofeldspathic to amphibolitic compositions that originally may have been graywackes or similar clastic sedimentary rocks. Also associated with the quartz-rich rocks are bedded manganese-oxide occurrences (SE¼ sec. 3, T. 18 N., R. 1 E., and vicinity). Only the quartz-rich rocks have been studied in thin section.

The quartz-rich rocks in the western part of the New Meadows block consist of alternating quartz-rich layers and thinner, strongly deformed layers and pods of Ca- and Mg-rich to Fe- or Al-bearing rocks that are less abundant. The quartz-rich layers commonly are 90 percent or more quartz and have a few percent hornblende, biotite, or magnetite, and minor amounts of garnet (almandine?), epidote, and apatite. Local traces of sphene, calcite, muscovite, tourmaline, chlorite, and rutile(?) have been noted. The layers with little or no quartz (typically less than 20 percent) consist largely of hornblende (20–70 percent), epidote (as much as 50 percent), clinopyroxene (0–20 percent), plagioclase (0–20 percent), and zoisite (as much as 15 percent), accompanied by sparse magnetite, sphene, and hematite(?) or rutile(?). Minerals occurring locally include as much as a few percent scapolite, minor amounts of xanthophyllite(?) or clintonite(?), and traces of apatite. No potassium feldspar has been found in either the quartz-rich or quartz-poor layers. These quartz-rich metasedimentary rocks may have originated as pelagic marine

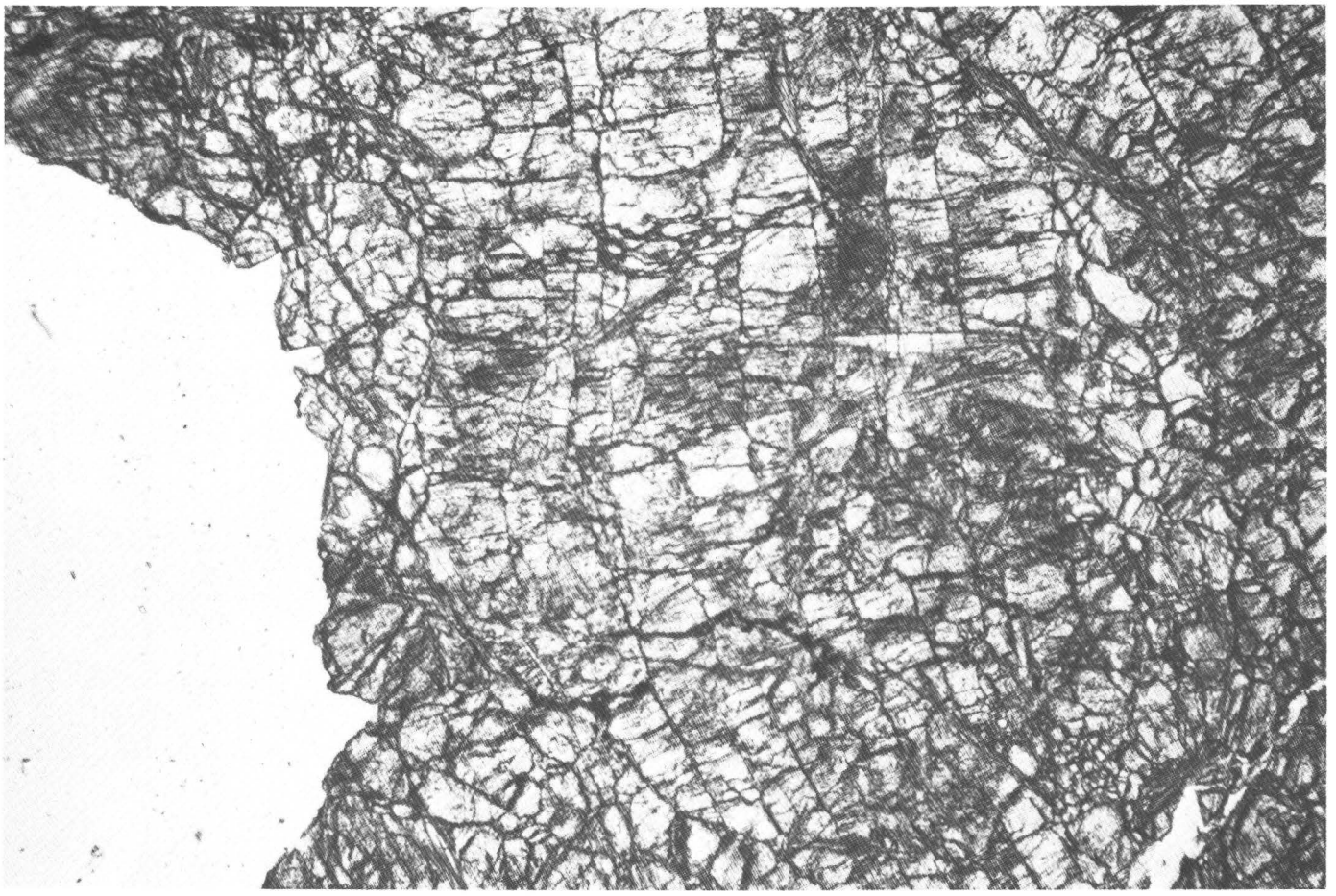

FIGURE 8.8.—Photomicrograph of an olivine crystal that initially was about 5 millimeters across that has been reorganized into parallel, but bent, lamellae. Note the acicular anthophyllite crystals cutting the olivine in the middle of the view. Thin section in plane light; width of view is about 6 millimeters.

cherts, in which the intercalated quartz-poor layers were marl or other carbonate-rich and clay-bearing material having local concentrations of ferruginous material.

Structural features in these quartzose rocks are complex. Tight folds and fragmented layers are common in hand samples and small outcrops. Although poorly exposed, part of the interlayered quartz-rich and quartz-poor material was apparently so strongly deformed as to locally rupture and scramble the layering. At other places, however, the layering is much less deformed, or even planar.

Well after the disruption of their layering, the quartz-rich and other metasedimentary rocks were hornfelsed. This sequence of deformation and recrystallization is similar to that noted for the peridotite. The deformation of the layering may have occurred during or before the emplacement of these metasedimentary rocks into their present tectonic position, whereas the development of the hornfelsic texture, similar to the growth of the undeformed anthophyllite crystals in the peridotite, probably occurred during reheating. Aplitic to pegmatitic dikes, generally having granitic to trondhjemitic compositions, cut the metasedimentary rocks as they cut the periodotite.

Metamorphic rocks, mostly of quartzofeldspathic and amphibolitic compositions, are present to the east of the metasedimentary rocks and peridotite in secs. 5 and 18, T. 18 N., R. 2 E. (fig. 8.2). Most of these rocks are strongly sheared but appear to have been mostly plutonic, ranging from gabbro to tonalite. They are thought to be within a major zone of faulting. Locally present in the zone are detached pyroxene- and hornblende-rich boudins of gabbroic and pyroxenitic compositions and tectonic slivers as

FIGURE 8.9.—Texture of acicular crystals of anthophyllite, now almost entirely replaced by talc (light colored), developed at the expense of olivine. Note the fine-grained magnetite (black grains) within the talc and the numerous thin serpentine veins cutting the olivine but truncated by the talc masses. Thin section in plane light; width of view is about 9.5 millimeters.

much as a few meters across composed of chlorite, serpentine, and talc, similar in composition to the peridotite to the west. The shear zone is cut by many pegmatitic dikes, consisting of albite, quartz, white mica, and traces of red-brown garnet. The pegmatites are foliated locally but are essentially intact. Evidently their injection largely postdated the shearing and dismemberment of their host rocks. These sheared rocks on the eastern side of the New Meadows block are probably either part of a tectonic zone between accreted terranes or within the major tectonic zone between the North American craton and the accreted terranes to the west.

DISCUSSION

As is common in geology, the presence of the thoroughly deformed and metamorphosed sedimentary, volcanic, ultramafic, and plutonic rocks in the West Mountain-Council Mountain-New Meadows area raises more questions than answers about the evolution of this part of Idaho and of the Pacific Northwest. By taking into account the regional geology as deciphered by various geologists in the papers cited and by attempting to interpret the premetamorphic nature of the rock units, it seems that the rocks may have originated somewhere in the Pacific Ocean basin during the Paleozoic and Mesozoic. No available evidence suggests that any of the metasedimentary or metavolcanic rocks in the West Mountain-Council Mountain-New Meadows area were part of the early or middle Precambrian North American craton, or part of the supracrustal cover of Middle Proterozoic (Belt Supergroup or its lateral equivalents) and Paleozoic miogeosynclinal sedimentary rocks.

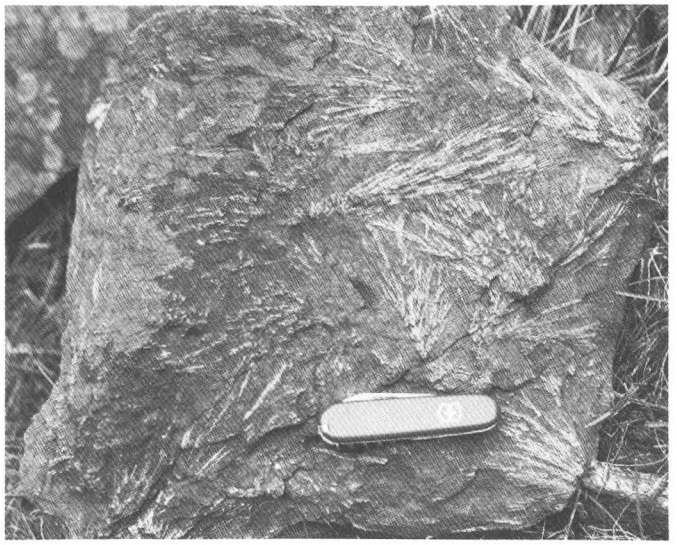

FIGURE 8.10.—Radiating sheaves of talc that replaced earlier formed anthophyllite in a matrix consisting mostly of olivine. Note the nondeformed habit of the hydrous minerals. Pocket knife is 8.5 centimeters long.

My interpretation that these rocks are not part of the Precambrian craton agrees with the observation of Armstrong and others (1977) that the 0.704–0.706 initial strontium isotope ratio line, which demarks the western margin of the Precambrian North American craton, passes through the area. This boundary, which separates rocks having initial $^{87}Sr/^{86}Sr$ ratios of greater than 0.706 to the east from those having less than 0.704 to the west, passes between the West Mountain pluton and the Deserette and Council Mountain plutons on Council Mountain (table 8.1). The West Mountain pluton, as part of the Idaho batholith, probably was intruded after the continental accretion process was completed. By the reasoning of Armstrong and others (1977), its higher strontium isotope ratio is due to contamination by old crustal material. The plutons on Council Mountain, however, do not contain excess radiogenic strontium and thus were not contaminated by assimilating older crustal rocks.

Lithologic similarities suggest that the metavolcanic and metasedimentary rocks in the West Mountain-Council Mountain block might be the southern extension of the Lightning Creek and Fiddle Creek Schists. These dominantly volcanic units form the structurally lower part of the Paleozoic or Mesozoic Riggins Group (Hamilton, 1963). Brooks and Vallier (1978) and Brooks (1979a) have suggested that the Fiddle Creek and Lightning Creek Schists are part of their dismembered oceanic crust terrane (fig. 8.1), and, at least in part, are correlative with the Burnt River Schist and the Elkhorn Ridge Argillite in northeastern Oregon. If this correlation is correct, then the metavolcanic and associated metasedimentary rocks in the West Mountain-Council Mountain block also should be considered as part of the dismembered oceanic crust between the two volcanic arc terranes.

As an alternative, the metavolcanic and metasedimentary rocks in the West Mountain-Council Mountain block may be unrelated to the Riggins Group or to the other terranes to the west noted in figure 8.1. If so, the rocks in the West Mountain-Council Mountain block could be either substantially younger or older than the rocks in either the Riggins Group or the Huntington volcanic arc terrane.

The peridotite bodies in the New Meadows block probably are related to other ultramafic occurrences in northeastern Oregon and western Idaho. In Oregon these ultramafic rocks include the Canyon Mountain Complex (Avé Lallemant, 1976; Thayer, 1977) and small ultramafic rock outcrops near Sparta, in the Virtue Hills, along the Connor Creek fault (Brooks, 1979a), and in the Greenhorn Mountains (T. Vallier, oral commun., 1984). In western Idaho there are several serpentinized peridotite bodies near Riggins along the contact between the Squaw Creek Schist and the Lightning Creek Schist (Hamilton, 1963, 1969, 1978; Onasch, 1977; Sarewitz, 1982), some occurrences at Asbestos Peak about 20 kilometers east of Whitebird (in secs. 26, 35, and vicinity, T. 28 N., R. 3 E.), an occurrence near West Fork Grouse Creek (sec. 31, T. 29 N., R. 4 E.) (A. Hoover, oral commun., 1984), metagabbro and metaperidotite at Blacktail Butte near Harpster (Anderson, 1930; Myers, 1982), several occurrences of dunite extensively replaced by anthophyllite in the Glenwood area and near the mouth of Pete King Creek east of Kamiah (Anderson, 1930, 1931), and additional occurrences mentioned by Anderson (1930) near Ahsahka and Teakean in western Clearwater County. Among this western Idaho group, the occurrences that Anderson (1930, 1931) described in the Glenwood area most resemble the peridotite in the New Meadows block. He shows photographs of anthophyllite rosettes similar to those in figure 8.10. Furthermore, his description of the sequence in which the hydrous minerals formed at the expense of original olivine, first involving serpentinization and then the formation of anthophyllite, is identical to that which is described above for the New Meadows peridotite bodies.

The writer knows of no other occurrences in western Idaho of quartz-rich rocks having accompanying quartz-poor layers quite like those mixed with the peridotite masses that have been interpreted as metacherts and associated pelagic metasedimentary rocks. However, chert is a common lithology in the dismembered oceanic crust terrane in northeastern Oregon (Brooks and Vallier, 1978; Brooks, 1979a). These cherts probably formed in an oceanic environment far removed from a source of clastic sediments. The metacherts in the New Meadows

block might be equivalent to part of the Squaw Creek Schist, although neither Hamilton (1963) nor Myers (1982) indicates quartz-rich rocks to be an important part of that formation. Around Riggins, the Squaw Creek Schist is dominated by volcanic rocks and sedimentary rocks derived from volcanic rocks, although Hamilton (1963, p. 32) briefly mentions a local type of schist typically having 75 to 95 percent quartz within the formation.

The structural disruption of the metacherts in the New Meadows block suggests that, after deposition, they may have been tectonically incorporated, along with the peridotite, into a melange wedge that accumulated between an active trench and an island arc or continental margin. I believe this explanation is the most plausible for the association of metachert and peridotite, and I suggest that the rocks in the western part of the New Meadows block are dismembered oceanic crust—probably an eastward extension of the oceanic crust terrane of Brooks and Vallier (1978) and Brooks (1979a) (fig. 8.1).

The plutons in the West Mountain-Council Mountain block resemble other tonalite and quartz diorite plutons along the western margin of the Atlanta lobe of the Idaho batholith and those plutonic outliers west of the batholith (Schmidt, 1964; Taubeneck, 1971; Myers, 1982; Fisher and others, 1983; and E.H. Bennett, oral commun., 1984), and thus are assumed to be related to the early development phase of the composite Atlanta lobe. The Council Mountain, Deserette, and West Mountain plutons clearly are part of this group. However, because the No Business Mountain pluton has a somewhat alkalic character, a relative abundance of clinopyroxene (table 8.1), and an apparent enrichment in Sr and Ti in comparison to nearby, more typical, quartz diorite and tonalite plutons, it is not yet clear whether the No Business Mountain pluton is a normal pluton of the group along the western margin of the Idaho batholith that has assimilated considerable calcareous material or a part of the group of early Mesozoic plutons that constitutes the alkalic magmatic belt in western North America (Miller, 1978).

After intrusion, the plutons in the West Mountain-Council Mountain block were metamorphosed to the amphibolite facies, and a fairly pervasive foliation and lineation, along with abundant but somewhat localized shears, were formed within the plutons. Foliation, lineation, and shear zones that developed concurrently in the enclosing metavolcanic and metasedimentary rocks generally obliterated whatever earlier metamorphic features they may have contained. The complex tectonic history of the area and the composite nature of the nearby Idaho batholith imply that the metamorphism may have lasted for several million years or more and may have involved more than one intense pulse of thermal or structural activity. A better understanding of the metamorphic history will require more detailed mapping, radiometric ages and chemical characterization of the rocks and minerals.

The latter, most obvious part of the metamorphism may have partly been in response to the intrusion of plutons, including the West Mountain pluton, within the Atlanta lobe of the Idaho batholith. Forces accompanying this event could have helped form the moderately to steeply eastward-dipping foliaton and shear zones and the eastward-plunging lineation in the West Mountain-Council Mountain block. Such attitudes could have occurred in response to a diapiric rise and westward spreading of parts of the Idaho batholith, in the same fashion envisioned by Myers (1982, fig. 28) for the northern tip of the Atlanta lobe.

Emplacement of the Atlanta lobe may have been accompanied by east-west-directed compressive stress that resulted from east-directed subduction of oceanic crust in an active trench somewhere to the west or by tectonic pushing or crumpling of a forearc basin or island arc against the North American plate. Vallier and Engebretson (1983) have suggested that such large-scale structural events may have occurred in western Idaho during about 95 to 100 Ma, when the Blue Mountains island arc completed its accretion to the North American craton and when the first plutons of the Atlanta lobe were emplaced. Accordingly, the east-dipping structural and metamorphic features may have resulted from a shear couple operating around a north-south locus of horizontal axes, as the continental margin was compressed and the Idaho batholith was emplaced (looking northward parallel to this axial direction, the rotation sense during the shearing would have been counterclockwise).

The deformation and metamorphism of the New Meadows block differ from that in the West Mountain-Council Mountain block. Although the foliations are similar in attitude for the two blocks (fig. 8.2), the lineations in the New Meadows block dip shallowly rather than steeply and are approximately at right angles to those in the West Mountain-Council Mountain block. These differences indicate that the structural histories of the two blocks were quite different, even though the reasons are not entirely clear. The metamorphism in the West Mountain-Council Mountain block appears to have culminated with recrystallization under amphibolite-facies conditions, accompanied by strong shearing but little thermal readjustment of the textures after deformation. In the New Meadows block, however, the metamorphic grade was probably within the epidote-amphibolite facies. Additionally, the static growth habit of undeformed anthophyllite rosettes in the peridotite and the hornfelsed nature of the previously strongly deformed metacherts are convincing evidence that the latter part of the metamorphism in that block was primarily thermal. The presence of pegmatitic to aplitic dikes cutting the

ultramafic and quartz-rich rocks (these cannot be interpreted as due to partial melting of their host rocks) suggests that the thermal metamorphism in the western part of the New Meadows block may be due to a hidden granitic pluton rather than to a regional heating event.

Cooling to subamphibolite-facies temperatures probably occurred in the metamorphosed volcanic and sedimentary rocks and plutons after about 84 to 86 Ma, in the western part of the West Mountain-Council Mountain block, as these are the K-Ar ages of biotite from the Council Mountain and Deserette plutons (table 8.1). Cooling of the West Mountain pluton, to the east, to similar temperatures may have been more prolonged, as suggested by the biotite K-Ar age there of about 78 million years (table 8.1). The K-Ar age of approximately 120 Ma (table 8.1) on hornblende from the Council Mountain pluton indicates that the pluton is at least this old, according to Armstrong and others (1977). Similarly, the approximate 92-Ma K-Ar age on hornblende from the West Mountain pluton (table 8.1) should also be considered as a minimum age, because of the possible loss of radiogenic argon from hornblende between the time of its original crystallization in the pluton and the cooling near the end of the metamorphism. Because of the metamorphism, U-Pb ages on zircons will probably be required to obtain the true igneous ages of the metamorphosed quartz diorites and tonalites in the West Mountain-Council Mountain block.

REFERENCES CITED

Anderson, A.L., 1930, The geology and mineral resources of the region about Orofino, Idaho: Idaho Bureau of Mines and Geology Pamphlet 34, 63 p.

_____ 1931, Genesis of the anthophyllite deposits near Kamiah, Idaho: Journal of Geology, v. XXXIX, no. 1, p. 68-81.

Armstrong, R.L., 1975, The geochronometry of Idaho: Isochron/West, no. 14, p. 1-50.

Armstrong, R.L., Taubeneck, W.H. and Hales, P.O., 1977, Rb-Sr and K-Ar geochronomtry of Mesozoic granitic rocks and their Sr isotopic composition, Oregon, Washington, and Idaho: Geological Society of America Bulletin, v. 88, p. 397-411.

Avé Lallemant, H.G., 1976, Structure of the Canyon Mountain (Oregon) ophiolite complex and its implication for sea-floor spreading: Geological Society of America Special Paper 173, 49 p.

Breeser, P.J., 1972, General geology and highway realignment considerations in the Pinehurst-New Meadows-Tamarack area, west-central Idaho: Moscow, Idaho, University of Idaho, M.S. thesis, 103 p.

Brooks, H.C., 1979a, Plate tectonics and the geologic history of the Blue Mountains: Oregon Geology, v. 41, no. 5, p. 71-80.

_____ 1979b, Geologic map of Huntington and part of Olds Ferry quadrangles, Oregon: Oregon Department of Geology and Mineral Industries Geologic Map Series GMS-13, scale 1:62,500.

Brooks, H.C., McIntyre, J.R., and Walker, G.W., 1976, Geology of the Oregon part of the Baker 1° by 2° quadrangle: Oregon Department of Geology and Mineral Industries Geologic Map Series GMS-7, scale 1:250,000, 25 p.

Brooks, H.C., and Vallier, T.L., 1978, Mesozoic rocks and tectonic evolution of eastern Oregon and western Idaho, *in* Howell, D.G., and McDougall, K.A., eds., Mesozoic paleogeography of the Western United States: Society of Economic Paleontologists and Mineralogists, Pacific Section, Pacific Coast Paleogeography Symposium, 2d, p. 133-145.

Dalrymple, G.B., 1979, Critical tables for conversion of K-Ar ages from old to new constants: Geology, v. 7, p. 558-560.

Davis, G.A., Monger, J.W.H., and Burchfiel, B.C., 1978, Mesozoic construction of the cordilleran "collage," central British Columbia to central California, *in* Howell, D.G. and McDougall, K.A., eds., Mesozoic paleogeography of the Western United States: Society of Economic Paleontologists and Mineralogists, Pacific Section, Pacific Coast Paleogeography Symposium, 2d, p. 1-32.

Fisher, F.S., McIntyre, D.H., and Johnson, K.M., compilers, 1983, Geologic map of the Challis 1° × 2° quadrangle, Idaho: U.S. Geological Survey Open-File Report 83-523, scale 1:250,000, 60 p.

Fitzgerald, J.F., 1982, Geology and basalt stratigraphy of the Weiser embayment, west-central Idaho, *in* Bonnichsen, Bill, and Breckenridge, R.M., eds., Cenozoic Geology of Idaho: Idaho Bureau of Mines and Geology Bulletin 26, p. 103-128.

Hamilton, Warren, 1963, Metamorphism in the Riggins region, western Idaho: U.S. Geological Survey Professional Paper 436, 95 p.

_____ 1969, Reconnaissance geologic map of the Riggins quadrangle, west-central Idaho: U.S. Geological Survey Miscellaneous Geologic Investigations Map I-579, scale 1:125,000.

_____ 1978, Mesozoic tectonics of the Western United States, *in* Howell, D.G., and McDougall, K.A., eds., Mesozoic paleogeography of the Western United States: Society of Economic Paleontologists and Mineralogists, Pacific Section, Pacific Coast Paleogeography Symposium, 2d, p. 33-70.

Miller, C.F., 1978, An early Mesozoic alkalic magmatic belt in western North America, *in* Howell, D.G., and McDougall, K.A., eds., Mesozoic paleogeography of the Western United States: Society of Economic Paleontologists and Mineralogists, Pacific Section, Pacific Coast Paleogeography Symposium, 2d, p. 163-173.

Mitchell, V.E., and Bennett, E.H., compilers, 1979, Geologic map of the Baker quadrangle, Idaho: Idaho Bureau of Mines and Geology Geologic Map Series, Baker 1° × 2° quadrangle, scale 1:250,000.

Myers, P.E., 1982, Geology of the Harpster area, Idaho County, Idaho: Idaho Bureau of Mines and Geology Bulletin 25, 46 p.

Onasch, C.M., 1977, Structural evolution of the western margin of the Idaho batholith in the Riggins, Idaho area: University Park, Pennsylvania, Pennsylvania State University, Ph.D. dissertation, 296 p.

Palmer, I.F., Jr., 1963, Geology of the Council Mountain area, Adams County, Idaho: Moscow, Idaho, University of Idaho, M.S. thesis, 54 p.

Sarewitz, D.R., 1982, Geology of a part of the Heavens Gate quadrangle, Seven Devils Mountains, western Idaho: Corvallis, Oregon, Oregon State University, M.S. thesis, 144 p.

Schmidt, D.L., 1964, Reconnaissance petrographic cross section of the Idaho batholith in Adams and Valley Counties, Idaho: U.S. Geological Survey Bulletin 1181-G, 50 p.

Schmidt, D.L., and Mackin, J.H., 1970, Quaternary geology of Long and Bear Valleys, west-central Idaho: U.S. Geological Survey Bulletin 1311-A, 22 p.

Streckeisen, Albert, 1979, Classification and nomenclature of volcanic rocks, lamprophyres, carbonatites, and melilitic rocks: Recommendations and suggestions of the IUGS Subcommission on the Systematics of Igneous Rocks: Geology, v. 7, p. 331-335.

Streckeisen, Albert (chairman), and others, 1973, Plutonic rocks, classification and nomenclature recommended by the IUGS Subcommission on the Systematics of Igneous Rocks: Geotimes, v. 18, no. 10, p. 26-30.

Taubeneck, W.H., 1971, Idaho batholith and its southern extension: Geological Society of America Bulletin, v. 82, p. 1899-1928.

Thayer, T.P., 1977, The Canyon Mountain Complex, Oregon, and some

problems of ophiolites, *in* Coleman, R.G., and Irwin, W.P., eds., North American ophiolites: Oregon Department of Geology and Mineral Industries Bulletin 95, p. 93-105.

Thayer, T.P., and Brown, C.E., 1964, Pre-Tertiary orogenic and plutonic intrusive activity in central and northeastern Oregon: Geological Society of America Bulletin, v. 75, p. 1255-1262.

Vallier, T.L., and Engebretson, D.C., 1983, The Blue Mountains island arc of Oregon, Idaho, and Washington: an allochthonous coherent terrane from the ancestral western Pacific Ocean?, *in* Howell, D.G., Jones, D.L., Cox, Allen, and Nur, Amos, eds., Proceedings of the Circum-Pacific Terrane Conference: Stanford University Publications in Geological Sciences, v. 18, p. 197-199.

9. LITHOLOGIC AND CHEMICAL CHARACTERISTICS OF THE CENTRAL AND SOUTHEASTERN PART OF THE SOUTHERN LOBE OF THE IDAHO BATHOLITH

By REED S. LEWIS, THOR H. KIILSGAARD, EARL H. BENNETT, and WAYNE E. HALL

ABSTRACT

The Late Cretaceous Idaho batholith consists of the Bitterroot and Atlanta lobes, which are separated by Precambrian metamorphic rocks. Mapping in the southern (Atlanta) lobe indicates the presence of several plutonic phases. The oldest unit is tonalite, intruded by biotite granodiorite, which is transitional into a core of muscovite-biotite granite. The youngest phase is fine-grained leucocratic granite. Locally, potassium metasomatism resulted in the formation of porphyritic (K-feldspar megacryst-bearing) granodiorite. Seven outlying stocks intrude Paleozoic metasedimentary rocks east of the Atlanta lobe and, with the exception of the pyroxene-bearing quartz monzodiorite of the Croesus stock, they are lithologically similar to the main batholithic mass to the west.

Major-element data from 105 samples document the remarkable homogeneity of the Atlanta lobe; a tonalitic west margin gives way eastward to biotite granodiorite and muscovite-biotite granite that show minimal variation along a 90-km transect. Tonalite along the westernmost margin of the batholith is low in radiogenic strontium and was probably formed from magma generated in or above a subducting slab of oceanic lithosphere. Rocks to the east have high initial $^{87}Sr/^{86}Sr$ ratios and probably formed by partial melting of pre-Belt Supergroup basement in the lower crust, with only a minor mantle contribution.

Rocks in the Bitterroot and Atlanta lobes of the Idaho batholith are similar both chemically and mineralogically. The Idaho batholith has a lower mafic mineral content and is higher in SiO_2 content than the Sierra Nevada batholith, and it lacks zoned plutons in sharp contact with one another that characterize the Sierra Nevada batholith. These differences result from the Sierra Nevada batholith being largely underlain by oceanic material, whereas the Idaho batholith is largely underlain by continental crust. In addition, the Idaho batholith may have had a higher water content during emplacement, which inhibited the rise of magma and resulted in slow cooling and diffuse contacts.

INTRODUCTION

The Idaho batholith, a large granitoid body that is widely exposed in central Idaho, was emplaced during the Late Cretaceous. It is composed of several plutonic phases, most being of great areal extent, that range in composition from granite to tonalite. A northwest-trending belt of Precambrian metamorphic rocks, part of the Salmon River arch as defined by Armstrong (1975a), separates the northern (Bitterroot) and southern (Atlanta) lobes of the batholith (fig. 9.1). Both lobes were intruded by Eocene plutons having ages of 49 to 44 Ma (Bennett, 1980).

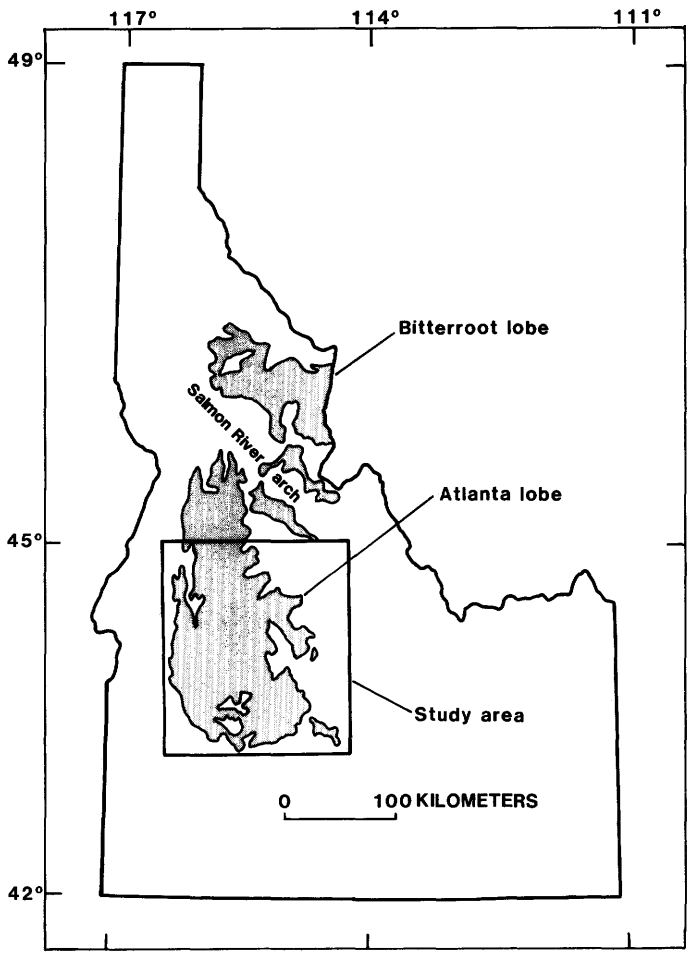

FIGURE 9.1.—Index map of the northern (Bitterroot) and southern (Atlanta) lobes of the Idaho batholith and the area of study.

This paper outlines the lithologic and chemical characteristics of Late Cretaceous plutonic rocks in an area south of the 45th parallel (fig. 9.1). Chemical emphasis is on major-element data from 105 samples collected in the central and southeastern parts of the Atlanta lobe. The samples were collected during geologic mapping of the Challis 1° by 2° quadrangle by the U.S. Geological Survey and the Idaho Geological Survey (Fisher and others, 1983), the Ten Mile West Roadless area (Kiilsgaard, 1983), and part of the Hailey 1° by 2° quadrangle (Hall and others, 1978; unpublished mapping by the authors). Eocene plutonic rocks have not been included in this study, so the reader is referred to Bennett (1980) and Bennett and Knowles (1985) for discussion of those rocks.

Early work on the Atlanta lobe of the batholith was done chiefly by Ross (1928, 1934) and Anderson (1947, 1952), who recognized several phases of Mesozoic rocks as well as Tertiary plutonism. Subsequent mapping by Schmidt (1964) in the western part of the Atlanta lobe near Cascade delineated four Late Cretaceous rock units, and Reid (1963) and Kiilsgaard and others (1970) separated Late Cretaceous from Tertiary rocks in the Sawtooth Range southwest of Stanley. Swanberg and Blackwell (1973), using gamma-ray spectrometry to subdivide rocks of the Atlanta lobe, recognized the extensive nature of the rock units that form the core of the batholith. Reconnaissance geology of the southwest corner of the batholith was performed by Taubeneck (1971). Mapping in the southeast part of the batholith was done by Schmidt (1962) and by Hall and others (1978). A comparison of the Idaho batholith with the southern California batholith was made by Larsen and Schmidt (1958); their study included a compilation of available chemical analyses.

Numerous radiometric ages of the Idaho batholith, using mostly K-Ar dating techniques, have been published, including those by McDowell and Kulp (1969) and Armstrong (1975b). Criss and others (1982) outlined the complex nature of K-Ar systematics in the Idaho batholith, and Criss and Taylor (1983) used oxygen-isotope data to document the effect of Eocene hydrothermal systems on rocks of the Late Cretaceous batholith. Criss and Fleck (chapter 6) review their earlier work and interpret new data. An extensive review of research on the batholith was made by Hyndman (1983).

GEOLOGIC SETTING

Along its eastern margin (fig. 9.2) the Idaho batholith intruded Paleozoic sedimentary rocks that were metamorphosed to hornfels and calc-hornfels (Ross, 1934; Hall and others, 1978; Hall, 1985); some of the eastern contact is now covered by the Eocene Challis Volcanics (Ross, 1937; McIntyre and others, 1982).

The northern part of the Atlanta lobe intrudes various types of metasedimentary and metaigneous rocks, the majority of which have yet to be adequately mapped. These rocks are in a structural setting referred to as the Salmon River arch by Armstrong (1975a), who postulated an approximate age of 1,500 Ma, based on Rb-Sr systematics, for granitic and gneissic rocks near Shoup. Granitic rocks of the Salmon River arch intrude argillaceous quartzite of the Yellowjacket Formation (Ross, 1934; Ruppel, 1975; Lopez, 1982). Armstrong (1975a) suggested that the Yellowjacket Formation is pre-Belt Supergroup in age, though most workers consider it time-correlative with the Prichard Formation of the lower part of the Belt Supergroup (Evans and Zartman, 1981; Lopez, 1982; Hahn and Hughes, 1984). Although the base of the Yellowjacket is not exposed, high-grade gneiss and schist found west of Shoup at the mouth of the Middle Fork of the Salmon River may represent Precambrian basement rocks older than the Yellowjacket Formation (Cater and others, 1973). Paragneiss and orthogneiss immediately north of the main Salmon River were tentatively assigned a pre-Belt Supergroup age (Weis and others, 1972) and may be part of the same basement complex.

A northwest-trending belt of isolated metasedimentary roof pendants extends across the northeastern part of the study area (Fisher and others, 1983). These rocks are exposed chiefly on high ridge tops and are probably near or at the intrusive roof of the batholith. Most of these roof pendants are probably Paleozoic in age, but correlation with known formations has not been established.

Rocks adjacent to the western margin of the batholith are part of an allochthonous Permian and Triassic volcanic-arc complex with oceanic affinities (Hamilton, 1963; Brooks and Vallier, 1978; Myers, 1982; Lund, 1984). This volcanic-arc complex includes the Wallowa-Seven Devils terrane, composed of metavolcanic and metasedimentary rocks, and the structurally overlying, higher grade metavolcaniclastic rocks of the Riggins Group. This complex was believed to have been accreted to the old continental margin during the Triassic or Jurassic (Hamilton, 1976; Jones and others, 1977; Brooks and Vallier, 1978). This assumption was based primarily on the presence of Triassic and Jurassic plutons intrusive into the volcanic-arc complex. However, recent mapping in the suture area, coupled with $^{40}Ar/^{39}Ar$ age-spectrum dating of a 118-Ma metamorphic event in the Riggins Group, has shown that juxtaposition of the arc terrane with continental rocks, at least in this part of Idaho, may have begun as late as 118 Ma along a right-lateral transcurrent fault (Lund, 1984; Sutter and others, 1984). Thus, the Triassic and Jurassic plutons were accreted along with the volcanic and sedimentary arc rocks.

The western margin of the Idaho batholith is at the edge of the old continental margin, as shown by Armstrong and

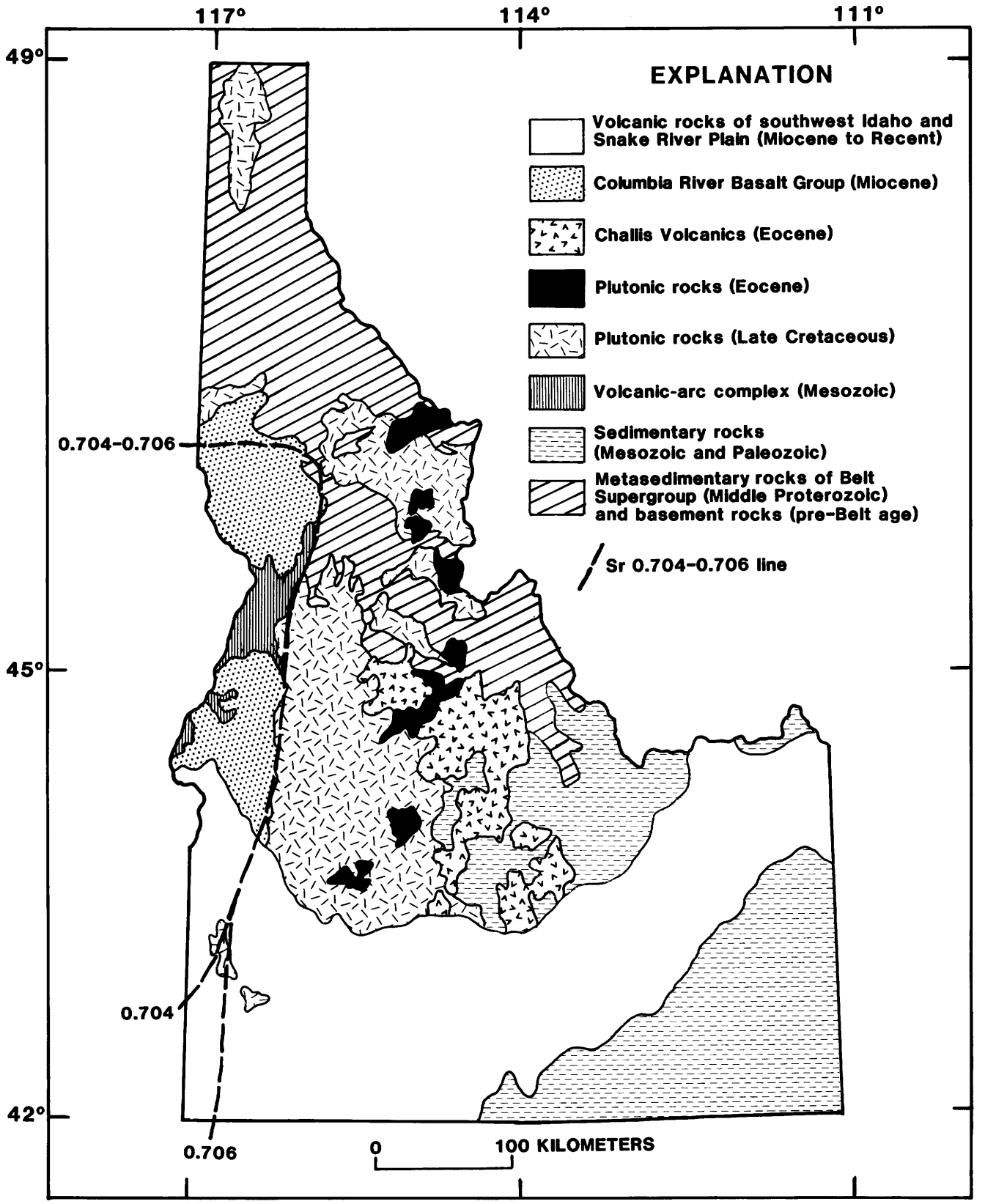

FIGURE 9.2.—Generalized geologic map of Idaho showing the geologic setting of the Idaho batholith. Compiled from Armstrong and others (1977), Bond (1978), Bennett (1980), Fisher and others (1983), and Kiilsgaard (1983).

others (1977), who delineated a sharp break in initial $^{87}Sr/^{86}Sr$ ratios of igneous rocks in this area. A north-south-trending line extends along the westernmost edge of the batholith, with initial Sr ratios of greater than 0.7055 to the east and ratios less than 0.7043 to the west (0.704-0.706 line, fig. 9.2). More detailed work by Fleck and Criss (1985) shows a continuum of initial $^{87}Sr/^{86}Sr$ ratios across this line, but the transition zone is nevertheless narrow, typically no more than several hundred meters wide.

Intrusive relations in the vicinity of the western margin of the Idaho batholith are in large part obscured by extensive flows of the Miocene Columbia River Basalt Group. Miocene and younger volcanic and sedimentary rocks of the Snake River Plain overlap the entire southern margin of the Atlanta lobe, masking intrusive features in this area.

LITHOLOGY OF THE CENTRAL ATLANTA LOBE

A peculiarity of the Atlanta lobe of the Idaho batholith is the absence of numerous small, separate granitic plutons that typify other batholiths. Instead, the plutons are very large, approximately 1,000 to 10,000 km^2 in area, and generally display gradational contacts between each other. Even where exposures are good, sharp contacts are rare.

Mapping in the central part of the Atlanta lobe (Fisher and others, 1983) indicates that the batholith can be subdivided into six major rock types of Late Cretaceous age. The rock types are tonalite, hornblende-biotite granodiorite, porphyritic granodiorite, biotite granodiorite, muscovite-biotite granite, and leucocratic granite. A brief summary of the field relations and lithologies of these units is given in the following subsections, and a discussion of the geochronology is presented in the section "Geochronology of the Central Atlanta Lobe." More detailed rock descriptions can be found in Kiilsgaard and Lewis (1985). Granitic rocks are classified in this report according to recommendations of Streckeisen and others (1973).

TONALITE

Tonalite grading to granodiorite has been mapped along the northwestern margin of the Atlanta lobe and, to a lesser extent, in the eastern part of the lobe (fig. 9.3). A large mass of unmapped tonalitic rock is present west of long 116° W. and is well exposed near Banks. Tonalitic and gneissic rocks in the McCall area have been studied by Kuntz and Allen (1984) and are presently under investigation by them (oral commun., 1985).

Field evidence and radiometric age determinations indicate that tonalite is the oldest of the batholithic rocks. Northeast of Banks tonalite xenoliths are enclosed by younger biotite granodiorite. The tonalite is typically dark gray, medium grained, and equigranular, with a varying foliation defined by biotite. Hornblende content is generally 2 to 8 percent, and biotite, 5 to 15 percent. Sphene is a conspicuous accessory mineral and magnetite is common. Modally the rock plots as tonalite grading to granodiorite (fig. 9.4), with a mean composition, excluding mafic and opaque constituents, of 29 percent quartz, 8 percent potassium feldspar, and 63 percent plagioclase.

HORNBLENDE-BIOTITE GRANODIORITE

Small exposures of hornblende-biotite granodiorite are found on the high ridges in the central part of the Atlanta lobe (fig. 9.3). This granodiorite is typically gray, medium grained, and slightly foliated. It has more potassium feldspar and less hornblende than the tonalite, but in general appearance the rocks are similar. Modally it is a granodiorite (fig. 9.4), with a mean composition, excluding mafic and opaque minerals, of 28 percent quartz, 14 percent K-feldspar, and 58 percent plagioclase. Hornblende content is generally 1 to 4 percent, and biotite, 8 to 15 percent. Intrusive relations are ambiguous, but this unit probably represents a discontinuous roof phase that is slightly older than the biotite granodiorite that lies beneath it. No radiometric ages have been obtained for the hornblende-biotite granodiorite.

PORPHYRITIC GRANODIORITE

A discontinuous, northwest-trending belt of porphyritic (K-feldspar megacryst-bearing) granodiorite 125 km long extends across the northeastern part of the study area (fig. 9.3). This unit crops out primarily on ridge tops, similar to the hornblende-biotite granodiorite. The porphyritic granodiorite is gray, medium to coarse grained, and characterized by pink or light-pinkish-gray microcline megacrysts as long as 10 cm. Locally biotite defines a foliation. Modally the rocks plot as granodiorite grading to granite (fig. 9.4), with a mean composition, excluding mafic and opaque constituents, of 30 percent quartz, 22 percent potassium feldspar, and 48 percent plagioclase. Biotite is the primary mafic constituent, but as much as 5 percent hornblende is present in many places, particularly north and east of Stanley. The porphyritic granodiorite that contains hornblende is similar to the tonalite described earlier, differing mainly in that it contains megacrysts. Where hornblende is absent the rock more closely resembles biotite granodiorite. Ross (1963) postulated formation of the megacrysts late in the origin of the rock, probably as a result of fluid circulating through the rock after it had consolidated but while it remained hot. Olson (1968) and Criss (1981) thought the megacrysts may have resulted from similar subsolidus

deuteric porphyroblastic growth. Lewis (1984) and Kiilsgaard and Lewis (1985) described the megacrysts as resulting from potassium metasomatism. Numerous potassium feldspar-rich veinlets cut the rock and appear to have been a source of potassium-rich fluid for the metasomatism. This metasomatism affected both the tonalite and the biotite granodiorite and was most pronounced near the roof of the batholith.

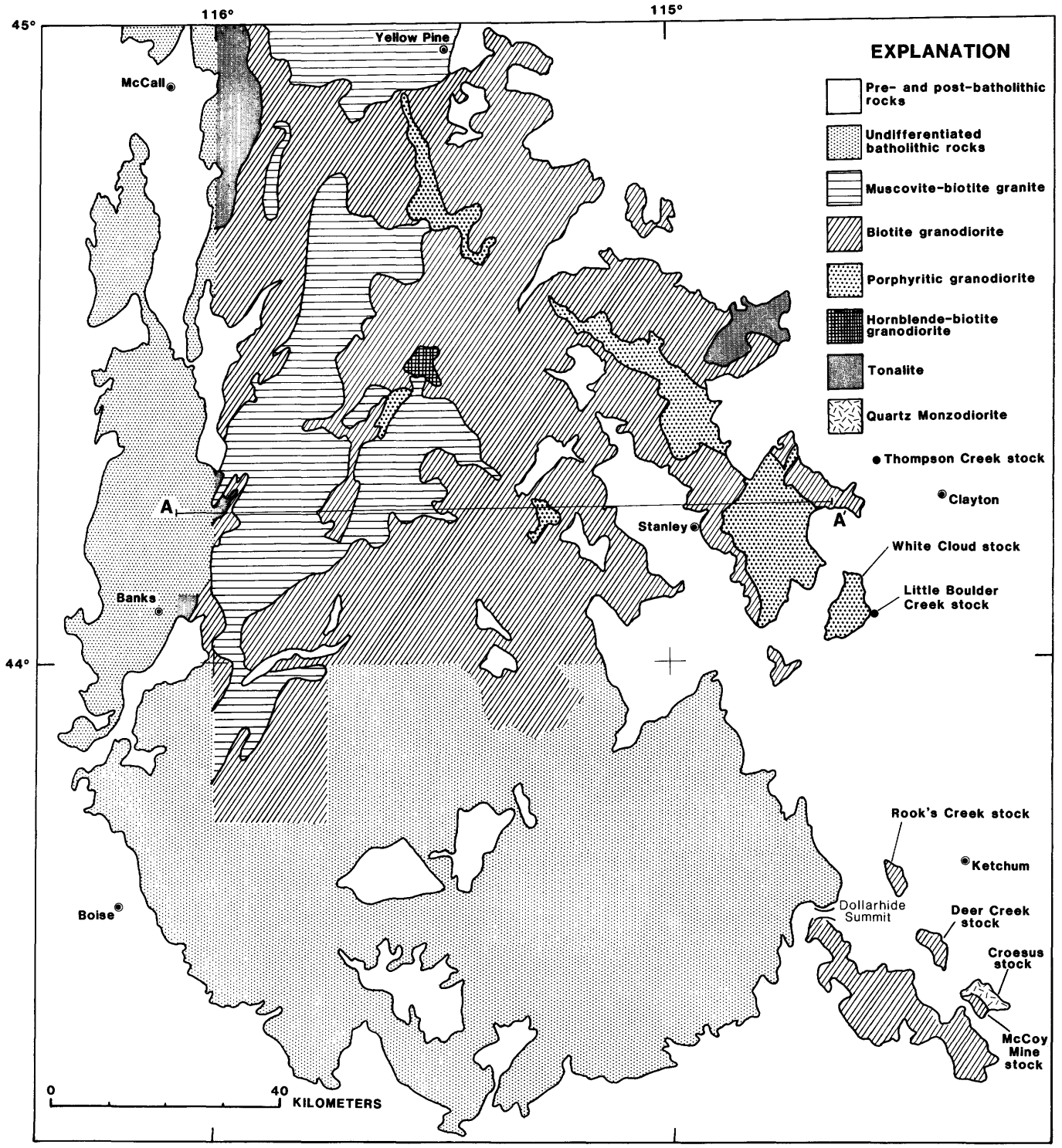

FIGURE 9.3.—Simplified geologic map of Cretaceous rocks in the Atlanta lobe of the Idaho batholith. Also shown is the location of transect A-A′. Compiled from Bond (1978), Fisher and others (1983), Kiilsgaard (1983), and unpublished mapping by the authors.

BIOTITE GRANODIORITE

Biotite granodiorite is the most extensive rock unit in the Atlanta lobe (fig. 9.3). It is light gray, medium to coarse grained, and locally porphyritic, containing K-feldspar phenocrysts 2 cm or less in length. Foliation is rarely present within this unit, and where seen may have resulted from the movement of one mass of granodiorite magma into another. Modally the unit consists of granodiorite grading to granite (fig. 9.4), with a mean composition, excluding mafic and opaque constituents, of 30 percent quartz, 22 percent potassium feldspar, and 48 percent plagioclase. The biotite content is generally 2 to 8 percent, and hornblende and primary muscovite are rarely present. Field relations indicate that the biotite granodiorite is younger than the tonalite and the hornblende-biotite granodiorite. The biotite granodiorite is gradational into muscovite-biotite granite, and together these units comprise what is considered the main phase of the Atlanta lobe.

MUSCOVITE-BIOTITE GRANITE

A discontinuous, north-south-trending body of muscovite-biotite (2-mica) granite is present in the core of the southern lobe of the batholith (fig. 9.3). It grades into biotite granodiorite over a zone as wide as 2 km or more. The 2-mica granite is massive, light gray, medium to coarse grained, and equigranular to slightly porphyritic. The presence of books of primary muscovite was the principal field criterion used in mapping this unit. Muscovite comprises as much as 5 percent of the rock, but generally averages about 2 percent, as does biotite. Garnet is present locally. Modally the unit consists of granite and granodiorite (fig. 9.4), with a mean composition, excluding mafic minerals, of 32 percent quartz, 23 percent K-feldspar, and 45 percent plagioclase. The radiometric ages and transitional contact with biotite granodiorite suggest that this unit is slightly younger than the biotite granodiorite.

LEUCOCRATIC GRANITE

Leucocratic granite (not indicated on fig. 9.3, for locations refer to Fisher and others, 1983) is present as dikes, sills, and irregular small stocks that cut sharply across all earlier phases of the batholith. The granite is light gray, fine grained, and equigranular and is generally considered to be a late differentiate of the batholith (Anderson, 1947; Reid, 1963; Luthy, 1981). The leucocratic granite was mapped as alaskite by Cater and others (1973). Modally the rock plots as granite (fig. 9.4), with a mean composition of 31 percent quartz, 33 percent K-feldspar, and 36 percent plagioclase. The leucocratic granite generally contains 2 percent or less biotite, and trace amounts of primary muscovite. Locally, on the east side of the batholith, the granite contains as much as 10 percent biotite. This biotite is very fine grained, however, so the rock retains its light color. Garnet grains as large as 2 mm in diameter are present locally.

GEOCHRONOLOGY OF THE CENTRAL ATLANTA LOBE

Application of radiometric dating techniques in the central Atlanta lobe has met with only limited success. Most of the radiometric ages available were done by the K-Ar method, and they give only a minimum age of emplacement. Some of the K-Ar ages are too young due to argon loss during Eocene reheating (Armstrong, 1974), and all of them record only the time since the rock cooled past the argon-blocking temperature of the mineral dated. Criss and others (1982) studied the effects of both Eocene plutonism and regional uplift on K-Ar ages of biotite and found that argon loss was primarily confined to areas close to Tertiary plutons, and that the rest of the "ages" could be accounted for by slow (about 0.1–0.14 mm/yr) uplift of the batholith. Uplift rates of much higher magnitude have been postulated by Snee and others (1985) for Late Cretaceous batholithic rocks in the Elk City area in the northern part of the Atlanta lobe.

The K-Ar biotite ages that have been determined for tonalitic rocks on the west side of the Atlanta lobe range from 82 to 67 Ma (table 9.1; Armstrong, 1975b; Criss and others, 1982). Tonalite on the east side of the lobe southeast of Stanley yielded an age of 81.2 ± 2.9 Ma on biotite (table 9.1). This wide age spread is typical in the Idaho batholith, and it illustrates the difficulty encountered with using the K-Ar method to date these rocks. Even the age of 82 Ma represents cooling below the blocking temperature of biotite (about 280 ± 40 °C, Harrison and McDougall, 1980; Snee, 1982), so true emplacement ages are older, probably in the range of 85 to 95 Ma. Available geochronologic data for the tonalite and the other five rock units in the central Atlanta lobe are summarized in figure 9.5.

A sample of porphyritic (K-feldspar megacryst-bearing) granodiorite from the east side of the Atlanta lobe east of Stanley yielded a U-Pb zircon age of 88 ± 6 Ma (Lynn Fischer, written commun., 1983). Another sample from the same outcrop gave a K-Ar hornblende age of 84.7 ± 2.9 Ma and a K-Ar biotite age of 79.8 ± 2.7 Ma (table 9.1). This granodiorite, sampled 13 km east of Stanley at milepost 201, U.S. Highway 75, is a metasomatically altered tonalite. A sample of the same unit south of Yellow Pine yielded a K-Ar biotite age of 77.9 ± 2.8 Ma (table 9.1). The 88 ± 6 Ma U-Pb zircon age approximates the age of emplacement of the porphyritic granodiorite (fig. 9.5).

K-Ar ages on biotite from the biotite granodiorite unit span a wide range (table 9.1; Armstrong, 1975b; Criss and

others, 1982). Samples from the central and western part of the Atlanta lobe give apparent ages ranging from 79 to 54 Ma. Many of these rocks have probably undergone partial Ar loss. An area of intense Ar loss (greater than 75 percent) surrounds the Eocene plutons, and K-Ar ages there range from 46 to 37 Ma (Criss and others, 1982). The actual age of the biotite granodiorite is probably between 85 and 75 Ma (fig. 9.5), but the present data do not adequately constrain the age of this unit. Intrusion of the biotite granodiorite may have directly followed the tonalite magmatism, or several million years may have passed between intrusive events.

K-Ar ages on biotite and muscovite in the 2-mica granite are generally concordant, with muscovite giving apparent ages as much as 4 m.y. older than biotite in the same rocks (table 9.1). Dated samples in this study have muscovite ages of 76 to 69 Ma. $^{40}Ar/^{39}Ar$ determinations on 2-mica granite west of Landmark and west of Yellow Pine gave ages of 72 and 70 Ma, respectively, but geologic relations in these areas are not known well enough to interpret these as emplacement or cooling ages (L.W. Snee, oral commun., 1985). In addition, muscovite-bearing biotite granite 14 km east of Yellow Pine at Stibnite is cut by mineralized veins dated by Snee at 78 Ma. Excluding the rocks at Stibnite, the actual emplacement age of the muscovite-biotite granite is probably between 78 and 72 Ma, though it may be slightly older (fig. 9.5).

K-Ar ages on biotite in the leucocratic granite range from 76 to 64 Ma, and most are from 73 to 70 Ma (table 9.1; Criss, 1981). The young (65 to 64 Ma) ages are from samples collected near Eocene plutons. Emplacement age is probably 75 to 70 Ma (fig. 9.5).

LITHOLOGY OF THE SOUTHEASTERN PART OF THE ATLANTA LOBE

The batholith immediately north and west of Dollarhide Summit (fig. 9.3) contains biotite granodiorite and subordinate hornblende-biotite granodiorite, but more mapping is necessary to differentiate these units. Both appear similar to previously described granodiorites in the central part of the study area. A sample of the biotite granodiorite (H22, table 9.1) yielded a K-Ar age on biotite of 60.7 ± 1.8 Ma. This rock almost certainly underwent Ar

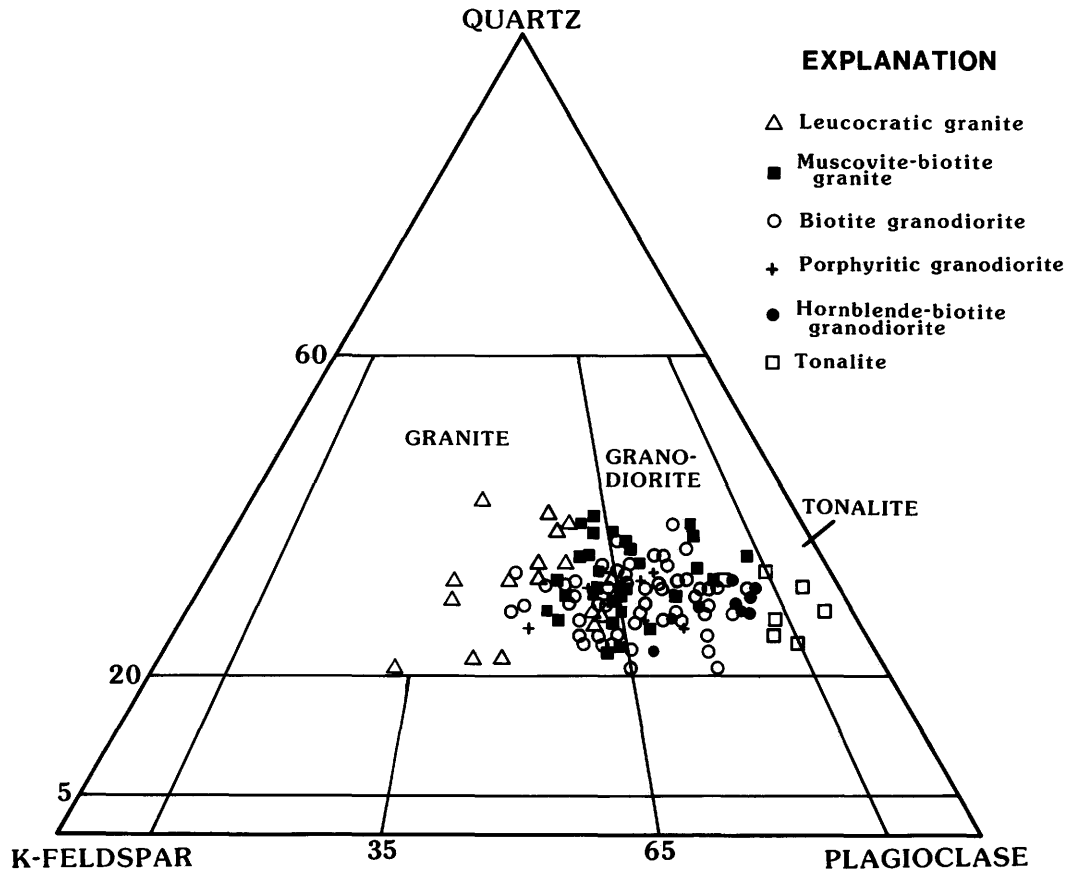

FIGURE 9.4.—Modal plot of rock samples from the central part of the Atlanta lobe of the Idaho batholith. Classification is that of Streckeisen and others (1973).

TABLE 9.1.—*K-Ar ages of Cretaceous rocks of the Idaho batholith*

[All samples were collected by the authors except BL1-BL4, which were collected by B.F. Leonard, U.S. Geological Survey, Denver, Colo. Rock unit symbols: Kt, tonalite; Kgdp, porphyritic (K-feldspar megacryst-bearing) granodiorite; Kgdh, hornblende-biotite granodiorite; Kgd, biotite granodiorite; Kg, muscovite-biotite granite; Klg, leucocratic granite; Peg, pegmatite. Minerals analyzed: B, biotite; M, muscovite; H, hornblende. Analysts: RM, R.F. Marvin; HM, H.H. Mehnert; VM, V.M. Merritt; KF, K. Futa; JK, J.J. Kenny; JG, J. Graves; EB, E.L. Brandt; RF, R.J. Fleck; JVE, J.C. Von Essen]

Sample	Rock unit	Age, Ma	Mineral	K_2O, Weight percent	$^{40}Ar_{rad}$, 10^{-10}mol/g	$^{40}Ar_{rad}$, percent	Analysts	Latitude (North)	Longitude (West)	Location
B01	Kt	81.6 ± 2.9	B	7.635	9.175	84	RM,HM,EB	44°40'55"	115°59'27"	NE. of Cascade.
B19	Kt	81.2 ± 2.9	B	8.41	10.06	86	RM	44°10'21"	114°48'26"	SE. of Stanley.
BL1	Kt	78.9 ± 2.6	B	8.635	10.03	80	RM,HM,VM	44°55'25"	116°01'00"	E. of McCall.
BL2	Kt	71.9 ± 2.5	B	7.555	7.977	77	RM,HM,VM	44°56'00"	115°56'40"	E. of McCall.
K08	Kt	73.6 ± 3.0	B	9.445	10.516	73	RF	44°05.6'	116°06.5'	E. of Banks.
					9.9004	84	RF			
K09	Kt	72.1 ± 1.6	B	9.510	9.9205	67	RF	44°05.7'	116°02.3'	E. of Banks.
					10.233	22				
B20	Kgdp	79.8 ± 2.7	B	9.46	11.12	83	RM,HM,VM,JK	44°15'50"	114°45'50"	E. of Stanley
		84.7 ± 2.9	H	1.075	1.342	88				(Milepost 201).
B21	Kgdp	77.9 ± 2.8	B	7.39	8.471	88	RM	44°47'18"	115°31'23"	S. of Yellow Pine.
H09	Kgdh	76.7 ± 1.5	B	8.57	9.641	79	JVE	43°31.8'	114°31.8'	W. of Ketchum.
		114 ± 2	H	0.941	1.600	77				
H03	Kgdh	84.0 ± 2.5	B	7.71	9.547	81	JVE	43°32.5'	114°38.5'	W. of Ketchum.
B03	Kgd	73.0 ± 2.5	B	8.35	8.959	82	RM,HM,VM,KF	44°42'17"	115°49'30"	E. of Cascade.
B04	Kgd	72.7 ± 2.6	B	8.35	8.914	78	RM,HM,JG	44°43'36"	115°38'21"	NW. of Landmark.
B05	Kgd	78.9 ± 2.8	B	8.32	9.667	91	RM,HM,EB	44°35'41"	115°57'10"	SW. of Landmark.
B22	Kgd	76.3 ± 2.6	B	7.035	7.899	92	RM,HM,VM,KF	44°34'19"	115°01'30"	NW. of Stanley.
B23	Kgd	74.9 ± 2.5	B	8.745	9.635	87	RM,HM,JK,VM	44°36'49"	115°23'46"	E. of Landmark.
H22	Kgd	60.7 ± 1.8	B	8.26	7.339	74	JVE	43°38.5'	114°51.0'	W. of Ketchum.
R04	Kgd	81.3 ± 2.9	B	8.215	9.832	89	RM	44°17'13"	114°43'24"	E. of Stanley.
B24	Kg	72.1 ± 2.6	B	7.495	7.933	86	RM,HM,EB	44°57'25"	115°38'00"	W. of Yellow Pine.
		72.2 ± 1.7	M	10.05	10.67	85				
B25	Kg	73.1 ± 2.6	B	8.60	9.243	81	RM,HM,EB	44°54'23"	115°52'21"	NE. of Cascade.
		74.7 ± 2.7	M	8.555	9.398	81				
B26	Kg	73.9 ± 2.7	B	5.585	6.066	86	RM,HM,EB	44°38'44"	115°36'33"	W. of Landmark.
		75.8 ± 2.7	M	8.495	9.472	80				
BL3	Kg	69.8 ± 2.3	B	8.13	8.333	87	RM,HM,VM	44°57'42"	115°38'50"	W. of Yellow Pine.
		74.1 ± 1.7	M	10.38	11.30	83				
BL4	Kg	69.5 ± 2.3	B	7.69	7.847	75	RM,HM,VM	44°57'10'	115°34'00"	W. of Yellow Pine.
		70.7 ± 2.3	M	8.27	8.585	86				
K52	Kg	66.2 ± 0.9	B	8.945	8.6049	78	RF	44°24'31"	115°33'15"	S. of Landmark.
					8.7764	80				
		68.8 ± 0.2	M	10.59	10.0715	95				
					10.0655	90				
B29	Klg	70.3 ± 2.5	B	6.385	6.591	83	RM,HM,JG	44°50'15"	115°53'24"	NE. of Cascade.
B30	Klg	72.6 ± 2.5	B	8.32	8.876	89	RM,HM,VM,JK	44°41'00"	115°30'07"	NW. of Landmark.
B31	Klg	63.6 ± 1.4	B	7.019	6.546	84	RM,HM,JK,KF,VM	44°11'02"	115°05'57"	SW. of Stanley.
B32	Klg	72.1 ± 1.7	B	5.046	5.343	49	RM,HM,JK,KF,VM	44°36'52"	115°23'42"	E. of Landmark.
K53	Klg	65.1 ± 0.8	B	6.500	6.1478	74	RF	44°08'10"	115°18'20"	E. of Lowman.
					6.2575	32				
B35	Klg	75.0 ± 2.7	M	9.43	10.40	84	RM	44°35'54"	114°52'49"	Lost Packer Mine.
B33	Klg	86.6 ± 3.1	B	7.955	10.16	91	RM,HM,EB	44°19'05"	114°32'47"	Thompson Creek stock.
B16	Kgdp	84.7 ± 1.9	B	7.445	9.290	88	RM,HM,VM,KF	44°05'45"	114°35'26"	White Cloud stock.
B34	Klg	83.2 ± 2.8	B	7.575	9.285	85	RM,HM,VM,KM	44°06'26"	114°36'23"	White Cloud stock.
H23	Peg	76.4 ± 1.5	M	10.62	11.91	90	JVE	43°36.6'	114°38.1'	W. of Ketchum.

loss during Eocene reheating. Biotite granodiorite and hornblende-biotite granodiorite southeast of Dollarhide Summit, termed the Hailey granodiorite unit by Schmidt (1962), are separated from the main batholith mass by the Challis Volcanics. These rocks are light gray, medium to coarse grained, equigranular to porphyritic, and probably continuous with the rest of the batholith.

K-Ar ages of 76.7 ± 1.5 Ma (biotite) and 114 ± 2 Ma (hornblende), as well as 84.0 ± 2.5 Ma (biotite), were obtained from two samples southeast of Dollarhide Summit (H09 and H03, table 9.1). The 114-Ma age on hornblende is unusually high and may be the result of incorporation of additional argon into the hornblende. If correct, it represents the oldest (by 17 m.y.) K-Ar age yet determined for the main batholith. Additional geologic mapping is needed to determine the exact relation between these southeastern batholithic rocks and those in the central and western part of the Atlanta lobe.

SATELLITE PLUTONS

Seven outlying stocks intrude Paleozoic metasedimentary rocks east of the main Atlanta lobe (fig. 9.3). Modes of most of these stocks are given in figure 9.6. The descriptions that follow are of the stocks, from north to south.

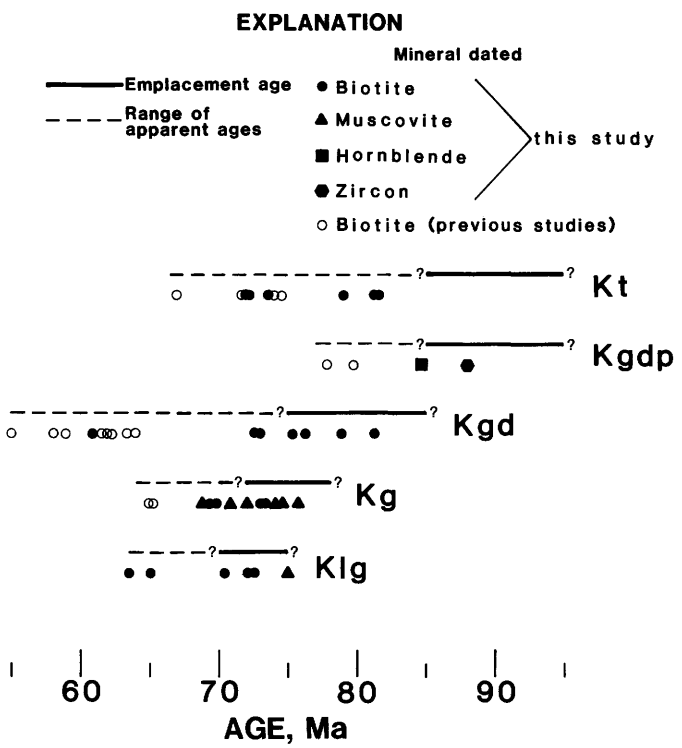

FIGURE 9.5.—Radiometric ages for tonalite (Kt), porphyritic granodiorite (Kgdp), biotite granodiorite (Kgd), 2-mica granite (Kg), and leucocratic granite (Klg) in the central part of the Atlanta lobe of the Idaho batholith. Data from this study and Criss and others (1982, tables 1 and 2). Biotite, muscovite, and hornblende were dated by the K-Ar method. Zircon age was determined by U-Pb systematics.

THOMPSON CREEK STOCK

The Thompson Creek stock consists of medium-grained equigranular biotite granodiorite that is intruded by equigranular to porphyritic biotite granite (Hall and others, 1984). Both of these units are cut by leucocratic granite. Potassic alteration is imprinted on all rock types. The Thompson Creek stock contains ore-grade molybdenite mineralization and is the site of the open-pit Thompson Creek mine. A K-Ar age of 86.6 ± 3.1 Ma (biotite) was obtained as part of this study from a sample of the leucocratic granite (table 9.1). D.L. Schmidt (oral commun., 1980) reported an age of 88.4 ± 3 Ma on the biotite granodiorite. Muscovite in the ore body yielded $^{40}Ar/^{39}Ar$ ages of 87.35 ± 0.43 Ma and 87.58 ± 0.31 Ma (L. Snee, written commun., 1985).

WHITE CLOUD STOCK

The White Cloud stock is a zoned intrusion with a porphyritic (K-feldspar megacryst-bearing) granodiorite core and an outer rim of equigranular biotite granodiorite. The megacrysts are similar to, though not as large as, those found in the porphyritic granodiorite unit of the main batholith. Locally the stock is cut by dikes of leucocratic granite. K-Ar (biotite) ages of 83.2 ± 2.8 Ma and 84.7 ± 1.9 Ma were obtained on two samples of the White Cloud stock collected during this study (table 9.1).

LITTLE BOULDER CREEK STOCK

The Little Boulder Creek stock is a small, poorly exposed granitoid body that lies near the head of Little Boulder Creek 300 m east of the White Cloud stock. The stock is exposed for 600 m in a north-south direction and about 240 m in an east-west direction. The stock is sheared and intensely silicified and has undergone potassic alteration. The least altered rock is a medium-grained, equigranular leucocratic granitoid that contains 40 to 50 percent plagioclase, 40 to 45 percent quartz, minor potassium feldspar, and about 5 percent amphibole. Locally the plagioclase has been replaced nearly entirely by potassium feldspar. The stock is associated with disseminated molybdenite (Little Boulder Creek deposit) in adjacent hornfelsed Paleozoic quartzite. The Little Boulder Creek stock is probably a satellitic body of the equigranular border facies of the White Cloud stock, but it has been so sheared, silicified, and altered that its original composition is uncertain.

ROOK'S CREEK STOCK

The Rook's Creek stock ranges in composition from biotite granodiorite at the margins to biotite granite in the interior. The stock is light gray, medium to fine grained, and generally equigranular; locally it is porphyritic. Marvin and Dobson (1979) obtained a K-Ar age of 92.2 ± 2.2 Ma on biotite from this stock. The western and central parts of the Rook's Creek stock have undergone intense argillic and potassic alteration associated with the intrusion of dikes and the intrusion of a fine-grained, medium-gray, hornblende-biotite granodiorite stock of probable Eocene age.

DEER CREEK STOCK

The Deer Creek stock was first delineated by Lindgren (1900). The stock ranges in composition from fine-grained, equigranular biotite-hornblende tonalite at the margin to coarse-grained, porphyritic biotite granite in the interior. Equal amounts of biotite and hornblende, and very minor augite, are present in the marginal rocks. Euhedral K-feldspar phenocrysts in the interior of the pluton are 6 to 8 mm long.

CROESUS STOCK

Originally described by Lindgren (1900) and later by Anderson and others (1950), the rocks of the Croesus stock do not resemble any other plutonic rocks in this part of Idaho. The Croesus stock consists of medium- to dark-gray quartz monzodiorite that contains hypersthene, augite, hornblende, and biotite. It is intruded by the McCoy Mine stock. The Croesus stock may actually be older than, and unrelated to, the Late Cretaceous Idaho batholith.

McCOY MINE STOCK

The McCoy Mine stock, consisting of light-gray, medium- to coarse-grained, equigranular to porphyritic biotite granodiorite, intrudes the Croesus stock. The McCoy Mine stock is part of what Schmidt (1962) termed the Hailey granodiorite unit. Described by Lindgren (1900) and Anderson and others (1950) as a quartz monzonite, this stock is very similar to biotite granodiorite found in the main batholith to the west. A K-Ar age on biotite of 83.8 ± 2.5 Ma (recalculated from Berry and others, 1976) was obtained from a sample collected at the McCoy mine.

EMPLACEMENT DEPTH

The depth of emplacement of the Idaho batholith has been discussed by Hyndman (1981, 1983), who suggested a depth of 17 to 20 km for the base of the Bitterroot lobe. He based this estimate on: (1) the presence of muscovite-bearing granite that had to form at pressures greater than the intersection of the muscovite breakdown curve and the granite solidus ($\sim$5 kbar), (2) an estimated 17- to 21-km-thick cover of Belt metasedimentary rocks, and (3) emplacement shortly after culmination of regional high-grade metamorphism. The composition of the muscovite in the Idaho batholith has not been well established, but samples from the Bitterroot lobe have a high celadonite component (M. Toth, oral commun., 1985). Experimental work by Centanni (1985) has shown that muscovite with a high celadonite component has an extended stability field when compared to ideal muscovite. The presence of the celadonite component reduces the minimum pressure restriction on the equilibrium between muscovite and a granitic melt and requires a re-evaluation of depth estimates of the Idaho batholith. Although sillimanite-grade metasedimentary rocks are present as roof pendants in the Atlanta lobe, Smitherman (1985) found only contact metamorphism associated with the batholith in the Yellow Pine area, and he attributed higher grade mineral assemblages to a prebatholithic event. A depth of emplacement of 12 ± 3 km was estimated for most of the Atlanta lobe, using heat-generation values (Swanberg and Blackwell, 1973), but a recent $^{40}Ar/^{39}Ar$ age-spectrum analysis indicates a depth of emplacement of between 4 and 9 km for 2-mica granite north of the study area in the Buffalo Hump region (Lund and others, 1986). Resolution of the emplacement depth problem requires more study.

The Idaho batholith may at least locally be thinner along the east side than along the west. Tonalitic gneiss, migmatite, and other rocks interpreted to lie beneath the batholith have been described in the deep canyon of the Middle Fork of the Salmon River (Hamilton, 1978), in the south-central part of the Bitteroot lobe (Wiswall, 1979), and along the northeastern margin of the Bitteroot lobe (Chase, 1973).

GEOCHEMISTRY

Over 140 rock samples were analyzed for ten major elements, and limited trace-element determinations were made on 25 of these samples. Of the original analyses, 105 are reported in table 9.2. The remaining samples had unusually low or high total oxides, had undergone moderate to extreme alteration, or had large errors in replicate samples. The latter case involved many samples of porphyritic (megacryst-bearing) rock, where the size and varied distribution of 5- to 10-cm-long microcline megacrysts made representative sampling extremely difficult. Also listed in table 9.2 are CIPW normative calculations; sample locations are shown in figure 9.7.

Major-element oxides were determined mostly by X-ray fluorescence spectroscopy (XRF) at the U.S. Geological Survey laboratory in Denver, Colorado. Twenty samples were analyzed by the XRF method at the Washington State University laboratory in Pullman, Washington. Samples H02 to H22 were analyzed in the U.S. Geological Survey laboratory in Reston, Virginia, using spectrophotometry and atomic-absorption spectrometry as described by Shapiro (1975). Trace elements were determined in the U.S. Geological Survey laboratory in Denver, Colorado, using inductively coupled plasma spectroscopy (for Ba, Sr, Y, Zr) and atomic-absorption spectrometry (for Rb), except for samples H02, H04, H09, H21, and H22, which were analysed by XRF methods in the U.S. Geological Survey laboratory in Reston, Virginia. Samples with trace-element data are limited in number and widely distributed. Thus, attempts at interpreting the results will have to await further sampling and analysis.

The chemical analyses show that rocks of the tonalite unit vary the most in SiO_2 content, ranging from 60.6 to 68.7 percent with a standard deviation (σ) of 2.4 percent. The muscovite-biotite granite and biotite granodiorite units exhibit minimal variation between samples as shown by the low standard deviations among the various oxides. This homogeneity is a significant feature of the main phase of the southern lobe of the batholith, and it reflects the unusually large and chemically monotonous units. The limited chemical variation is compatible with geophysical data, which also indicate that the main phase of the southern lobe of the batholith is a remarkably uniform rock (Mabey, 1982). Large parts of the northern lobe of the batholith also are homogeneous, both chemically and mineralogically (Hyndman, 1984).

To illustrate the variation of major-element oxides in rocks of the Atlanta lobe a chemical transect was made across the central part of the study area (A to A′, fig. 9.7) from west to east. Oxide contents from samples 10 km north and south of line A-A′ (fig. 9.7) were plotted against distance, as shown in figure 9.8. Sample locality elevations range from a high of 2,910 m (9,550 ft) to a low of 975 m (3,200 ft) along this transect. Leucocratic granite was omitted from the projection because the samples of

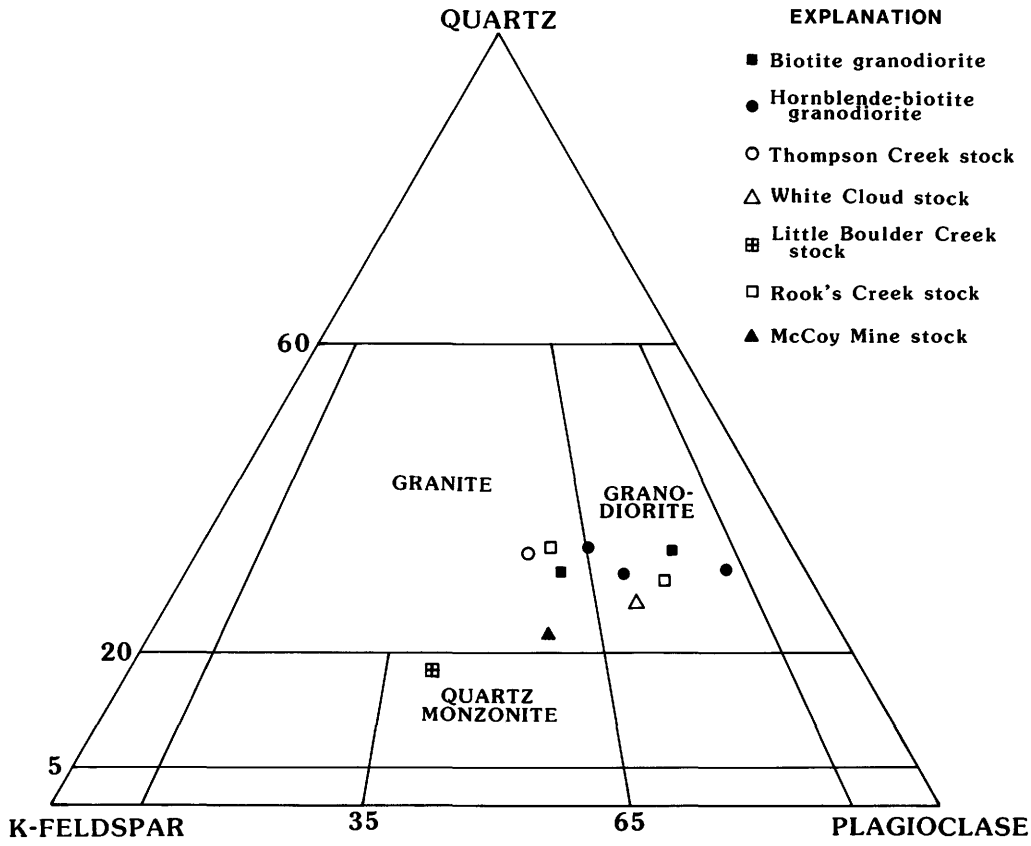

FIGURE 9.6.—Modal plot of rock samples from the southeastern part of the Atlanta lobe of the Idaho batholith and satellite plutons along its eastern margin. Plot is only of those rocks analyzed for major elements in this study. Classification is that of Streckeisen and others (1973).

TABLE 9.2.—*Major- and trace-element analyses and CIPW norms of selected samples from study area*

[Analysts: J.S. Walhberg, J.E. Taggart, J.D. Baker, A.J. Bartel, K. Stewart, L.L. Jackson, G.R. Mason, H.G. Neiman, E. Engleman, and D.B. Hatfield, U.S. Geological Survey, Denver, Colo.; H. Smith, G. Holmes, Z.A. Hamlin, N. Skinner, K. Coates, H.J. Rose, J. Lindsay, B. McCall, G. Sellers, and R. Johnson, U.S. Geological Survey, Reston, Va.; J. Amistoso, F.J. Moye, S.T. Luthy, W.B. Strowd, and D. Johnson, Washington State University, Pullman, Wash. Leaders (---), not determined]

	Tonalite																Hornblende-biotite granodiorite			
Sample number	K01	K02	K03	K04	K05	K06	K07	K08	K09	R01	K10	S01	B01	B02	Mean N=14	σ	R02	R03	E01	H03
Major-element oxides in weight percent																				
SiO_2	63.2	62.6	63.9	66.7	62.6	63.5	65.4	63.6	68.7	60.6	63.0	66.56	68.49	65.1	64.6	2.4	66.5	66.9	66.0	64.0
Al_2O_3	16.7	18.0	17.4	16.5	16.5	17.3	16.9	17.4	16.5	15.9	17.3	16.76	17.41	16.3	16.9	.6	15.7	15.5	15.2	15.3
$FeTO_3$[1]	--	--	--	--	--	--	--	--	--	--	--	4.26	3.73	--	4.29	1.02	3.76	--	3.88	--
Fe_2O_3	1.31	1.14	1.51	1.00	2.28	2.02	.94	1.16	.92	1.55	1.07	--	--	1.19	--	--	--	1.18	--	1.3
FeO	3.83	2.38	1.96	1.74	3.34	2.54	2.15	3.33	1.89	3.90	3.05	--	--	2.22	--	--	--	2.30	--	3.2
MgO	1.75	1.51	1.44	1.03	1.76	1.24	1.18	1.9	1.0	3.23	1.99	1.37	1.02	1.49	1.6	.6	1.53	1.61	1.95	2.4
CaO	4.38	5.14	4.96	3.79	4.88	4.54	3.64	4.56	4.07	5.58	5.48	4.40	3.99	5.07	4.61	.61	4.20	3.85	3.90	4.2
Na_2O	3.57	3.65	3.82	3.41	3.48	3.84	3.72	3.9	3.9	3.05	3.92	3.57	3.70	3.48	3.6	.2	3.41	3.55	3.01	3.7
K_2O	1.89	2.70	2.41	3.10	2.27	2.33	2.95	2.44	2.06	2.28	1.53	2.45	2.85	2.04	2.38	.43	2.84	2.58	3.50	2.3
TiO_2	1.19	.73	.57	.68	.91	.64	.62	.87	.50	1.02	.76	.80	.60	.64	.75	.19	.66	.53	.69	.73
P_2O_5	.41	.22	.22	.17	.26	.23	.20	.3	.2	.31	.32	.25	.21	.25	.25	.06	.22	.19	.21	.23
MnO	.1	.07	.07	.04	.08	.05	.05	.06	.03	.1	.07	.05	.04	.06	.06	.02	.06	.08	.08	.09
H_2O+	--	--	--	--	--	--	--	.51	.38	1.14	.59	--	--	.69	--	--	--	.85	--	1.1
H_2O-	--	--	--	--	--	--	--	.07	.08	.15	.10	--	--	.08	--	--	--	.10	--	.22
CO_2	--	--	--	--	--	--	--	.03	.07	<.01	.01	--	--	.17	--	--	--	.01	--	.03
LOI[2]	.34	.41	.59	.37	.30	.44	.69	--	--	--	--	--	--	--	--	--	.48	--	.76	--
Total	98.7	98.6	98.9	98.5	98.7	98.7	98.4	100.1	100.3	98.8	99.2	100.47	102.04	98.8	--	--	99.4	99.2	99.2	98.8
Trace elements in parts per million																				
Ba	--	--	--	--	--	--	--	1340	1500	--	--	--	--	--	--	--	--	--	--	--
Rb	--	--	--	--	--	--	--	80	46	--	--	--	--	--	--	--	--	--	--	--
Sr	--	--	--	--	--	--	--	751	910	--	--	--	--	--	--	--	--	--	--	--
Y	--	--	--	--	--	--	--	21	12	--	--	--	--	--	--	--	--	--	--	--
Zr	--	--	--	--	--	--	--	205	190	--	--	--	--	--	--	--	--	--	--	--
CIPW norms in weight percent																				
Q	22.8	17.6	19.9	25.7	20.3	20.8	23.0	18.2	25.5	17.3	19.2	24.9	25.4	24.4	--	--	24.9	25.6	24.2	20.8
Or	11.4	16.3	14.5	18.7	13.6	14.0	17.8	14.5	15.3	13.8	9.2	14.4	16.5	12.3	--	--	17.0	15.5	21.1	13.9
Ab	30.7	31.5	32.9	29.4	29.9	33.1	32.2	33.2	32.9	26.5	33.7	30.1	30.8	30.1	--	--	29.2	30.6	25.9	32.1
An	19.4	24.5	23.6	18.0	22.9	21.4	17.1	20.8	18.8	23.5	25.5	20.2	18.1	23.3	--	--	19.4	18.2	18.0	18.8
C	1.8	.3	--	1.1	.1	.8	1.5	.8	.3	--	--	.8	1.5	--	--	--	--	.3	--	--
Di	--	--	--	--	--	--	--	--	--	2.2	--	--	--	.6	--	--	.2	--	.3	.8
Hy	8.7	6.2	5.2	4.0	7.4	5.2	5.3	8.6	4.4	11.7	8.7	5.0	4.0	5.7	--	--	5.3	6.6	6.4	9.6
Mt	1.9	1.7	2.2	1.5	3.4	3.0	1.4	1.7	1.3	2.3	1.6	2.5	2.1	1.8	--	--	2.2	1.7	2.3	1.9
Il	2.3	1.4	1.1	1.3	1.8	1.2	1.2	1.7	.9	2.0	1.5	1.5	1.1	1.2	--	--	1.3	1.0	1.3	1.4
Ap	1.0	.5	.5	.4	.6	.6	.5	.7	.5	.8	.8	.6	.5	.6	--	--	.5	.5	.5	.6

Sample number	Hornblende-biotite granodiorite				Mean[3] N=8	σ	Biotite granodiorite													
	HO6	HO7	HO9	H13			K11	K12	K13	K14	K15	K16	K17	K18	K19	K20	K21	K22	K23	K24
Major-element oxides in weight percent																				
SiO_2	68.3	68.4	69.1	70.4	67.5	2.0	69.2	72.8	71.4	70.74	72.7	71.4	74.6	72.3	73.5	70.4	72.2	72.4	72.9	71.0
Al_2O_3	15.1	15.1	15.1	15.3	15.3	.2	16.0	15.1	16.2	15.15	15.1	15.6	14.5	15.2	14.8	15.9	14.5	15.3	14.6	15.7
$FeTO_3$[1]	--	--	--	--	3.61	.62	--	--	--	1.74	--	1.28	--	.97	.98	1.90	1.67	1.11	1.58	1.50
Fe_2O_3	1.4	1.5	.79	1.8	--	--	.92	.49	.63	--	.57	--	.42	--	--	--	--	--	--	--
FeO	1.6	1.8	2.0	1.0	--	--	1.50	1.01	.65	--	.73	--	.91	--	--	--	--	--	--	--
MgO	1.3	1.6	1.3	1.0	1.6	.4	.81	.52	.5	.29	.4	.41	.3	.29	.26	.59	.54	.33	.31	.34
CaO	3.6	3.6	3.5	2.9	3.7	.4	3.26	2.16	1.36	2.08	1.66	1.79	1.49	1.52	1.59	2.40	1.94	1.72	1.29	1.76
Na_2O	2.8	3.4	3.5	3.2	3.3	.3	4.0	3.5	4.9	3.44	4.5	4.46	4.2	3.98	3.84	4.25	3.43	4.73	4.09	4.48
K_2O	3.6	3.3	3.6	3.2	3.1	.5	2.71	4.27	3.04	4.13	2.89	3.26	3.40	3.96	3.04	2.45	3.76	2.61	3.62	3.37
TiO_2	.49	.60	.45	.58	.59	.10	.43	.26	.20	.28	.16	.14	.15	.10	.13	.36	.29	.15	.17	.18
P_2O_5	.23	.17	.22	.16	.20	.03	.2	<.1	<.1	.09	<.1	<.05	<.1	<.05	<.05	.09	.09	<.05	<.05	.06
MnO	.06	.03	.12	.06	.07	.03	.03	<.02	<.02	.03	<.02	.03	.04	.03	.02	<.02	.04	.04	.04	.04
H_2O+	.85	.57	.72	1.2	--	--	.49	.28	.72	--	.60	--	.33	--	--	--	--	--	--	--
H_2O-	.04	.14	.03	.22	--	--	.05	.04	.12	--	.02	--	.04	--	--	--	--	--	--	--
CO_2	.01	.02	.01	.02	--	--	<.01	<.01	.04	--	.34	--	<.01	--	--	--	--	--	--	--
LOI[2]	--	--	--	--	--	--	--	--	--	--	--	.63	--	.48	.65	.44	.35	.47	.49	.49
Total	99.4	100.2	100.4	101.0	--	--	99.6	100.4	99.8	97.97	99.7	99.0	100.4	98.8	98.8	98.8	98.8	98.8	99.1	98.9
Trace elements in parts per million																				
Ba	--	--	733	--	--	--	1300	1300	1800	--	1300	--	1360	--	--	--	--	--	--	--
Rb	--	--	147	--	--	--	85	94	51	--	57	--	68	--	--	--	--	--	--	--
Sr	--	--	427	--	--	--	455	697	736	--	588	--	477	--	--	--	--	--	--	--
Y	--	--	13	--	--	--	4	13	8	--	6	--	5	--	--	--	--	--	--	--
Zr	--	--	108	--	--	--	50	97	79	--	62	--	53	--	--	--	--	--	--	--
CIPW norms in weight percent																				
Q	29.2	26.1	25.3	32.4	--	--	27.6	30.4	28.0	30.6	31.7	28.9	33.2	30.7	36.3	30.8	33.4	31.1	32.3	28.1
Or	21.6	19.6	21.3	19.0	--	--	16.2	25.2	18.1	24.9	17.3	19.6	20.1	23.8	18.3	14.7	22.6	15.7	21.7	20.3
Ab	24.1	28.9	29.7	27.2	--	--	34.2	29.5	41.9	29.7	38.5	38.4	35.5	34.2	33.1	36.6	29.5	40.7	35.1	38.5
An	16.6	16.3	14.9	13.4	--	--	15.0	10.0	6.2	9.9	7.7	8.7	6.7	7.3	7.7	11.5	9.2	8.3	6.2	8.5
C	.6	--	--	1.7	--	--	1.0	1.0	2.6	1.5	1.8	1.6	1.4	1.8	2.5	2.1	1.5	1.7	1.8	1.7
Di	--	.4	.9	--	--	--	--	--	--	--	--	--	--	--	--	--	--	--	--	--
Hy	4.4	4.9	5.3	2.5	--	--	3.4	2.3	1.6	1.5	1.7	1.7	1.9	1.3	1.1	2.2	2.1	1.4	1.6	1.6
Mt	2.1	2.2	1.1	1.7	--	--	1.3	.7	.9	1.0	.8	.8	.6	.6	.6	1.1	1.0	0.7	.9	.9
Il	.9	1.1	.9	1.1	--	--	.8	.5	.4	.5	.3	.3	.3	.2	.3	.7	.6	.3	.3	.3
Ap	.6	.4	.5	.4	--	--	.5	.2	.2	.2	.2	.1	.2	.1	.1	.2	.2	.1	.1	.1

TABLE 9.2.—*Major- and trace-element analyses and CIPW norms of selected samples from study area*—Continued

[Analysts: J.S. Walhberg, J.E. Taggart, J.D. Baker, A.J. Bartel, K. Stewart, L.L. Jackson, G.R. Mason, H.G. Neiman, E. Engleman, and D.B. Hatfield, U.S. Geological Survey, Denver, Colo.; H. Smith, G. Holmes, Z.A. Hamlin, N. Skinner, K. Coates, H.J. Rose, J. Lindsay, B. McCall, G. Sellers, and R. Johnson, U.S. Geological Survey, Reston, Va.; J. Amistoso, F.J. Moye, S.T. Luthy, W.B. Strowd, and D. Johnson, Washington State University, Pullman, Wash. Leaders (---), not determined]

Sample number	Biotite granodiorite																			
	K25	K26	K27	K28	R03	RO4	R05	R06	WO1	K29	LO1[4]	LO2[4]	BO3	BO4	BO5	BO6	BO7	BO8	H11	H12
Major-element oxides in weight percent																				
SiO_2	73.1	71.0	72.1	73.5	72.1	70.4	71.22	72.0	70.9	71.4	73.84	73.06	72.32	72.68	69.48	71.85	71.63	73.4	69.6	70.3
Al_2O_3	14.8	15.2	15.1	14.4	14.6	15.1	14.98	15.2	15.3	16.0	14.91	15.18	14.82	15.16	17.04	16.41	15.01	14.6	14.4	15.3
$FeTO_3$[1]	--	--	--	--	--	--	1.88	1.63	1.90	--	1.30	.85	1.33	2.08	2.07	2.50	1.63	--	--	--
Fe_2O_3	.43	.92	.78	.43	.64	.86	--	--	--	.39	--	--	--	--	--	--	--	.49	1.3	1.4
FeO	.82	1.08	.76	.62	.87	1.11	--	--	--	.90	--	--	--	--	--	--	--	.29	1.2	1.0
MgO	.31	.46	.40	.14	.48	.66	.38	.45	.56	.4	.48	.31	.49	.63	.56	1.07	.63	.16	1.1	.92
CaO	1.97	2.19	1.73	.78	2.14	2.05	2.12	2.17	2.57	2.29	1.60	1.20	1.83	2.54	2.95	3.19	2.49	1.04	2.4	2.1
Na_2O	4.19	3.74	4.02	3.93	3.85	3.96	3.44	3.75	3.58	4.7	3.79	3.76	3.09	3.47	3.39	4.22	3.61	4.09	3.2	3.6
K_2O	2.74	3.35	3.30	4.56	3.20	3.63	3.59	3.25	3.21	2.99	2.82	4.03	3.18	2.56	4.54	2.32	3.63	4.16	4.6	4.0
TiO_2	.14	.27	.22	.09	.26	.31	.35	.22	.26	.18	.16	.13	.21	.29	.41	.38	.34	.08	.39	.39
P_2O_5	<.05	.07	.08	<.05	.09	.11	.11	.11	.08	<.1	.04	.03	.05	.05	.13	.09	.10	<.05	.13	.13
MnO	.03	.04	.03	.03	.02	.04	.03	<.02	.03	<.02	.03	.03	.03	.03	.02	.03	.10	<.02	.03	.06
H_2O+	--	--	--	--	.33	.33	--	--	--	.17	--	--	--	--	--	--	--	.32	.50	.88
H_2O-	--	--	--	--	.11	.10	--	--	--	.06	--	--	--	--	--	--	--	.10	.21	.17
CO_2	--	--	--	--	.10	.20	--	--	--	.01	--	--	--	--	--	--	--	<.01	.04	.02
LOI[2]	.25	.44	.49	.34	--	--	--	.41	.48	--	--	--	--	--	--	--	--	--	--	--
Total	98.8	98.8	99.0	98.8	98.8	98.9	98.10	99.2	98.9	99.5	98.97	98.58	97.35	99.49	100.59	102.6	99.17	98.7	99.1	100.3
Trace elements in parts per million																				
Ba	--	--	--	--	--	--	--	--	--	2260	--	--	--	--	--	--	--	--	--	--
Rb	--	--	--	--	--	--	--	--	--	38	--	--	--	--	--	--	--	--	--	--
Sr	--	--	--	--	--	--	--	--	--	834	--	--	--	--	--	--	--	--	--	--
Y	--	--	--	--	--	--	--	--	--	3	--	--	--	--	--	--	--	--	--	--
Zr	--	--	--	--	--	--	--	--	--	69	--	--	--	--	--	--	--	--	--	--
CIPW norms in weight percent																				
Q	33.7	31.4	32.3	31.6	32.7	28.5	32.4	32.8	31.8	27.1	33.1	37.1	38.5	36.3	25.2	29.2	30.7	31.9	27.2	29.3
Or	16.4	20.1	19.8	27.3	19.2	21.8	21.2	19.5	19.3	17.8	16.9	24.2	19.3	15.2	16.7	13.5	21.7	25.0	27.6	23.8
Ab	36.0	32.2	34.5	33.8	33.2	34.1	29.1	32.1	30.8	40.0	32.4	32.3	26.9	29.5	28.6	35.0	30.8	35.2	27.5	30.7
An	9.6	10.6	8.2	3.6	10.2	9.6	9.8	10.2	12.4	10.8	7.8	5.8	9.0	12.4	13.7	15.0	11.8	4.9	11.2	7.9
C	1.5	1.6	2.0	1.7	1.1	1.2	1.8	1.9	1.5	1.1	2.8	2.6	3.2	2.2	1.5	1.3	.9	1.6	.1	2.2
Di	--	--	--	--	--	--	--	--	--	--	--	--	--	--	--	--	--	--	--	--
Hy	1.8	2.0	1.5	1.1	1.9	2.6	1.7	1.9	2.3	2.1	1.9	1.2	1.8	2.5	2.1	3.7	2.3	.4	3.3	2.9
Mt	.6	1.4	1.1	.6	.9	1.3	1.1	1.0	1.1	.6	.8	.5	.8	1.2	1.2	1.4	1.0	.7	1.9	2.0
Il	.3	.5	.4	.2	.5	.6	.7	.4	.5	.3	.3	.3	.4	.6	.8	.7	.7	.2	.8	.2
Ap	.1	.2	.2	.1	.2	.3	.3	.3	.2	.2	.1	.1	.1	.1	.3	.2	.2	.1	.3	.9

Sample number	Biotite granodiorite				Muscovite-biotite granite															
	H16	H22	Mean[3] N=36	σ	K30	K31	K32	K33	K34	K35	K36	K37	K38	K39	K40	WO2	B09	B10	Mean[3] N=14	σ
Major-element oxides in weight percent																				
SiO_2	71.1	68.5	71.8	1.4	73.5	74.6	73.3	71.3	74.6	73.5	74.7	74.9	73.6	74.3	72.9	74.5	73.7	75.03	73.9	1.0
Al_2O_3	14.9	15.6	15.2	.6	14.8	14.1	14.9	16.1	14.2	14.7	14.1	14.0	14.7	14.4	14.7	14.6	15.0	14.37	14.6	.5
$FeTO_3$[1]	--	--	1.69	.58	1.04	.72	1.04	1.20	--	--	--	--	--	-	1.16	--	--	.90	.95	.20
Fe_2O_3	.82	2.1	--	--	--	--	--	--	.33	.24	.34	.29	.23	.33	--	.40	.58	--	--	--
FeO	.62	1.4	--	--	--	--	--	--	.47	.66	.22	.38	.65	.42	--	.54	.67	--	--	--
MgO	.23	1.0	.5	.2	.27	.16	.28	.43	.19	.24	.13	.17	.25	.24	.31	.3	.30	.55	.3	.1
CaO	1.5	3.2	2.0	.6	1.63	.53	1.42	2.57	.54	1.48	.88	1.21	1.64	1.79	1.62	1.66	1.59	1.39	1.43	.53
Na_2O	5.0	4.0	4.0	.5	3.85	3.78	3.83	4.35	3.47	4.01	3.75	3.87	3.76	3.71	3.89	3.7	3.63	3.28	3.8	.2
K_2O	3.4	3.2	3.4	.6	3.24	4.41	3.50	2.23	4.15	3.44	4.06	3.41	3.50	2.87	3.23	3.62	2.74	4.17	3.47	.60
TiO_2	.11	.51	.24	.11	.12	.05	.10	.18	.06	.11	.04	.1	.13	.09	.11	.1	.14	.12	.10	.04
P_2O_5	.06	.17	.07	.04	<.05	<.05	.07	.07	<.05	<.05	<.05	<.05	<.05	<.05	<.05	<.1	<.05	.02	.04	.02
MnO	.09	.05	.03	.02	<.02	.02	.04	.02	.1	.04	.02	.04	.02	<.02	.04	<.02	<.02	.03	.03	.02
H_2O+	.55	.76	--	--	--	--	--	--	--	--	--	--	--	--	--	.30	.74	--	--	--
H_2O-	.17	.36	--	--	--	--	--	--	--	--	--	--	--	--	--	.17	.24	--	--	--
CO_2	.03	--	--	--	--	--	--	--	--	--	--	--	--	--	--	<.01	.04	--	--	--
LOI[2]	--	--	--	--	.49	.64	.62	.49	.80	.33	.53	.39	.34	.36	1.02	--	--	--	--	--
Total	98.6	100.9	--	--	98.9	99.0	99.1	98.9	98.9	98.8	98.8	98.8	98.8	98.5	99.0	99.9	99.4	99.86	--	--
Trace elements in parts per million																				
Ba	--	1564	--	--	--	--	--	--	--	--	--	--	--	--	--	1400	--	--	--	--
Rb	--	80	--	--	--	--	--	--	--	--	--	--	--	--	--	100	--	--	--	--
Sr	--	800	--	--	--	--	--	--	--	--	--	--	--	--	--	886	--	--	--	--
Y	--	12	--	--	--	--	--	--	--	--	--	--	--	--	--	20	--	--	--	--
Zr	--	220	--	--	--	--	--	--	--	--	--	--	--	--	--	228	--	--	--	--
CIPW norms in weight percent																				
Q	26.0	25.1	--	--	35.3	34.9	34.6	31.8	37.6	33.7	36.0	37.1	34.7	38.2	34.5	35.3	38.7	36.1	--	--
Or	20.5	19.0	--	--	19.4	26.5	21.0	13.4	25.0	20.6	24.4	20.5	21.0	17.3	19.5	21.5	16.5	24.7	--	--
Ab	43.2	33.9	--	--	33.1	32.5	32.9	37.4	29.9	34.5	32.3	33.3	32.3	32.0	33.6	31.5	31.2	27.8	--	--
An	7.2	14.8	--	--	7.9	2.3	6.7	12.5	2.4	7.1	4.1	5.8	7.9	8.7	7.9	7.6	7.7	6.8	--	--
C	.4	.1	--	--	2.1	2.3	2.4	2.1	3.2	1.8	2.1	1.9	1.9	2.1	2.0	1.8	3.3	2.0	--	--
Di	--	--	--	--	--	--	--	--	--	--	--	--	--	--	--	--	--	--	--	--
Hy	1.0	2.6	--	--	1.2	.8	1.3	1.6	1.2	1.5	.4	.8	1.5	1.0	1.4	1.3	1.3	1.8	--	--
Mt	1.2	3.1	--	--	.6	.4	.6	.7	.5	.4	.5	.4	.3	.5	.7	.6	.9	.5	--	--
Il	.2	1.0	--	--	.2	.1	.2	.3	.1	.2	.1	.2	.3	.2	.2	.2	.3	.2	--	--
Ap	.1	.4	--	--	.1	.1	.2	.2	.1	.1	.1	.1	.1	.1	.1	.2	.1	.1	--	--

TABLE 9.2.—*Major- and trace-element analyses and CIPW norms of selected samples from study area*—Continued

[Analysts: J.S. Walhberg, J.E. Taggart, J.D. Baker, A.J. Bartel, K. Stewart, L.L. Jackson, G.R. Mason, H.G. Neiman, E. Engleman, and D.B. Hatfield, U.S. Geological Survey, Denver, Colo.; H. Smith, G. Holmes, Z.A. Hamlin, N. Skinner, K. Coates, H.J. Rose, J. Lindsay, B. McCall, G. Sellers, and R. Johnson, U.S. Geological Survey, Reston, Va.; J. Amistoso, F.J. Moye, S.T. Luthy, W.B. Strowd, and D. Johnson, Washington State University, Pullman, Wash. Leaders (---), not determined]

Sample Number	Leucocratic granite																			
	K41	K42	K43	K44	K45	K46	K47	K48	K49	K50	K51	LO3[4]	LO4[4]	B11	B12	B13	B14	B15	Mean[3] N=18	σ
Major-element oxides in weight percent																				
SiO_2	74.9	76.8	73.9	75.1	75.6	74.1	76.7	71.9	77.5	75.3	76.7	75.51	76.06	73.30	74.77	73.45	74.93	71.9	74.9	1.6
Al_2O_3	13.8	13.3	14.8	13.8	14.0	14.7	13.8	16.0	12.0	14.0	13.9	14.59	15.07	14.72	14.53	14.47	14.82	15.5	14.3	.9
$FeTO_3$[1]	--	--	--	.87	--	--	--	--	--	--	--	.12	.12	.02	.59	.87	.34	--	.59	.32
Fe_2O_3	.23	.22	.15	--	.32	.31	.28	.71	.40	.47	.03	--	--	--	--	--	--	.70	--	--
FeO	.65	.23	.68	--	.36	.43	.27	.20	.23	.38	.18	--	--	--	--	--	--	.23	--	--
MgO	.12	.1	.2	<.10	.2	.07	.1	.2	<.10	.2	.1	.30	.35	.29	.45	.27	.33	.16	.2	.1
CaO	.65	.90	1.12	.57	.62	1.12	.72	.84	.68	.77	.58	.64	1.03	1.35	1.08	1.32	1.10	.78	.88	.25
Na_2O	4.09	3.6	4.4	4.77	4.5	4.78	4.9	5.2	3.41	4.1	4.0	3.38	3.58	3.76	2.51	3.68	4.31	5.08	4.1	.7
K_2O	4.44	4.31	3.82	3.71	3.98	4.10	3.39	4.10	3.96	4.74	4.65	4.10	3.95	4.75	4.53	4.34	3.97	3.49	4.13	.40
TiO_2	.08	<.02	.07	<.02	.05	.09	<.02	.09	.04	.09	<.02	.05	.04	.05	.03	.11	.06	.11	.06	.03
P_2O_5	.03	<.1	<.1	<.05	<.1	.03	<.1	.1	<.05	<.1	<.1	.01	.02	.05	.02	.02	.01	<.05	.04	.02
MnO	.04	<.02	.04	<.02	<.02	.01	<.02	<.02	<.02	.03	<.02	.01	.00	.01	.03	.03	.01	<.02	.02	.01
H_2O+	.37	.25	.30	--	.24	.42	.06	.28	--	.17	.30	--	--	--	--	--	--	.44	--	--
H_2O-	.13	.06	.07	--	.09	.13	.04	.14	--	.04	.07	--	--	--	--	--	--	.12	--	--
CO_2	--	.01	<.01	--	.02	--	<.01	<.01	--	<.01	.01	--	--	--	--	--	--	.03	--	--
LOI[2]	--	--	--	.31	--	--	--	--	.20	--	--	--	--	--	--	--	--	--	--	--
Total	99.5	99.8	99.6	99.1	100.0	100.3	100.3	99.8	98.4	100.3	100.5	98.71	100.22	98.30	98.54	98.56	99.88	98.5	--	--
Trace elements in parts per million																				
Ba	--	1420	1520	--	880	--	150	2080	--	740	680	--	--	--	--	--	--	--	--	--
Rb	--	92	70	--	84	--	79	83	--	71	126	--	--	--	--	--	--	--	--	--
Sr	--	440	393	--	252	--	75	700	--	221	168	--	--	--	--	--	--	--	--	--
Y	--	5	3	--	7	--	5	10	--	6	16	--	--	--	--	--	--	--	--	--
Zr	--	21	46	--	15	--	45	52	--	8	1	--	--	--	--	--	--	--	--	--
CIPW norms in weight percent																				
Q	32.5	37.6	31.0	32.0	32.8	28.1	33.6	24.3	41.7	31.5	34.3	38.9	37.4	30.6	40.3	32.5	31.8	27.8	--	--
Or	26.5	25.6	22.7	22.2	23.6	24.3	20.0	24.4	23.8	28.0	27.4	24.5	23.3	28.6	27.2	26.0	23.5	21.0	--	--
Ab	34.9	30.6	37.5	40.8	38.2	40.6	41.3	44.3	29.3	34.6	33.8	29.0	30.2	32.4	21.6	31.6	36.5	43.9	--	--
An	3.1	3.8	4.9	2.5	2.4	5.4	2.9	3.5	3.1	3.1	2.2	3.2	5.0	6.5	5.3	6.5	5.4	3.6	--	--
C	1.2	1.3	1.6	1.0	1.4	.4	1.0	1.7	1.0	1.0	1.5	3.5	3.1	1.1	3.6	1.4	1.5	2.1	--	--
Di	--	--	--	--	--	--	--	--	--	--	--	--	--	--	--	--	--	--	--	--
Hy	1.3	.5	1.6	.8	.9	.6	.5	.5	.3	.7	.6	.8	.9	.7	1.5	1.1	1.0	.4	--	--
Mt	.3	.3	.2	.5	.5	.5	.4	.5	.6	.7	.0	.1	.1	.0	.4	.5	.2	.5	--	--
Il	.2	.0	.1	.0	.1	.2	.0	.2	.1	.2	.0	.1	.1	.0	.1	.2	.1	.2	--	--
Ap	.1	.2	.2	.1	.2	.1	.2	.2	.1	.2	.2	.0	.0	.1	.0	.0	.0	.1	--	--

Sample number	Thompson Creek stock H19	Thompson Creek stock H21[5]	Thompson Creek stock B17	Thompson Creek stock B18	White Cloud stock R08	White Cloud stock H17	White Cloud stock B16	Little Boulder Creek stock H15[6]	Rook's Creek stock H05	Rook's Creek stock H18	McCoy Mine stock H04	Croesus stock H02
Major-element oxides in weight percent												
SiO_2	72.9	77.8	73.28	72.45	70.5	71.2	71.49	70.8	68.0	72.1	67.3	57.8
Al_2O_3	14.3	12.8	15.45	15.29	15.3	15.7	14.90	15.3	16.5	14.7	14.7	18.0
$FeTO_3$[1]	--	--	1.73	1.04	--	--	1.74	--	--	--	--	--
Fe_2O_3	.53	.27	--	--	.93	.65	--	.56	.72	.53	.56	2.1
FeO	.76	.84	--	--	.86	1.1	--	.60	2.6	1.6	2.7	4.6
MgO	.33	.28	.73	.69	.58	.46	.68	.38	.95	.66	2.0	2.8
CaO	1.1	.94	2.29	1.74	2.07	2.2	1.77	2.2	3.1	2.0	3.1	7.7
Na_2O	3.0	2.4	2.95	2.85	4.15	4.1	4.16	3.1	3.4	2.9	3.1	3.8
K_2O	4.5	4.8	3.07	4.27	3.59	3.2	3.60	6.5	3.1	4.2	3.6	1.3
TiO_2	.24	.15	.30	.28	.26	.35	.27	.35	.56	.45	.65	1.2
P_2O_5	.07	.08	.10	.10	.11	.11	.09	.11	.18	.14	.09	.52
MnO	.03	.02	.03	.03	.03	.03	.04	.02	.06	.03	.02	.08
H_2O+	.84	.76	--	--	.30	.43	--	.43	.65	.62	.90	.95
H_2O-	.12	.28	--	--	.07	.08	--	.28	.65	.19	.16	.17
CO_2	.03	.01	--	--	<.01	.02	--	.10	.30	.08	.10	.10
LOI	--	--	--	--	--	--	--	--	--	--	--	--
Total	98.8	101.4	99.93	99.74	98.75	99.6	98.74	100.7	100.8	100.2	99.0	101.1
Trace elements in parts per million												
Ba	--	1034	--	--	--	776	--	939	--	1092	702	720
Nb	--	14	--	--	--	18	--	17	--	21	25	11
Rb	--	117	--	--	--	80	--	200	--	171	168	35
Sr	--	633	--	--	--	800	--	735	--	557	550	938
Y	--	15	--	--	--	11	--	17	--	14	30	24
Zr	--	148	--	--	--	190	--	198	--	171	314	214
CIPW norms in weight percent												
Q	36.1	42.6	38.9	34.8	27.9	29.8	29.0	23.2	27.5	33.7	25.1	10.7
Or	27.2	28.3	17.5	25.3	21.6	19.1	21.6	38.4	18.5	25.0	21.7	7.7
Ab	26.0	20.2	25.0	24.2	35.7	35.0	35.7	26.3	29.0	24.7	26.8	32.2
An	5.1	4.1	10.7	8.0	9.7	10.3	8.3	8.6	14.3	9.1	15.1	28.2
C	2.7	2.1	3.5	3.1	1.1	1.8	1.2	--	2.4	2.1	.3	--
Di	--	--	--	--	--	--	--	1.2	--	--	--	5.4
Hy	1.5	1.8	2.5	2.7	1.9	2.1	2.5	.5	5.8	3.5	8.6	9.2
Mt	.8	.4	1.0	1.2	1.4	1.0	1.0	.8	1.1	.8	.8	3.0
Il	.5	.3	.6	.5	.5	.7	.5	.7	1.1	.9	1.3	2.3
Ap	.2	.2	.2	.2	.3	.3	.2	.3	.4	.3	.2	1.2

[1]Total iron reported as Fe_2O_3. Fe_2O_3/FeO ratio of .75 assigned for CIPW norm calculation.
[2]Loss on ignition at 900° C.
[3]Assigned values for calculation of mean and standard deviation are as follows: <.1=.05; <.05-.03; <.02=.01.
[4]Data from Luthy (1981).
[5]Sample has undergone silicification.
[6]Sample has undergone K-feldspar alteration.

leucocratic granite along the transect were taken from dikes. A sharp increase in SiO_2 content and a corresponding decrease in total Fe and CaO contents are evident over a distance of 10 km from the western edge of the transect, where the east margin of the tonalite gives way to the core of biotite granodiorite and 2-mica granite. Variation in concentrations of SiO_2, CaO, and total Fe is minimal eastward across the next 90 km of the batholith; CaO and

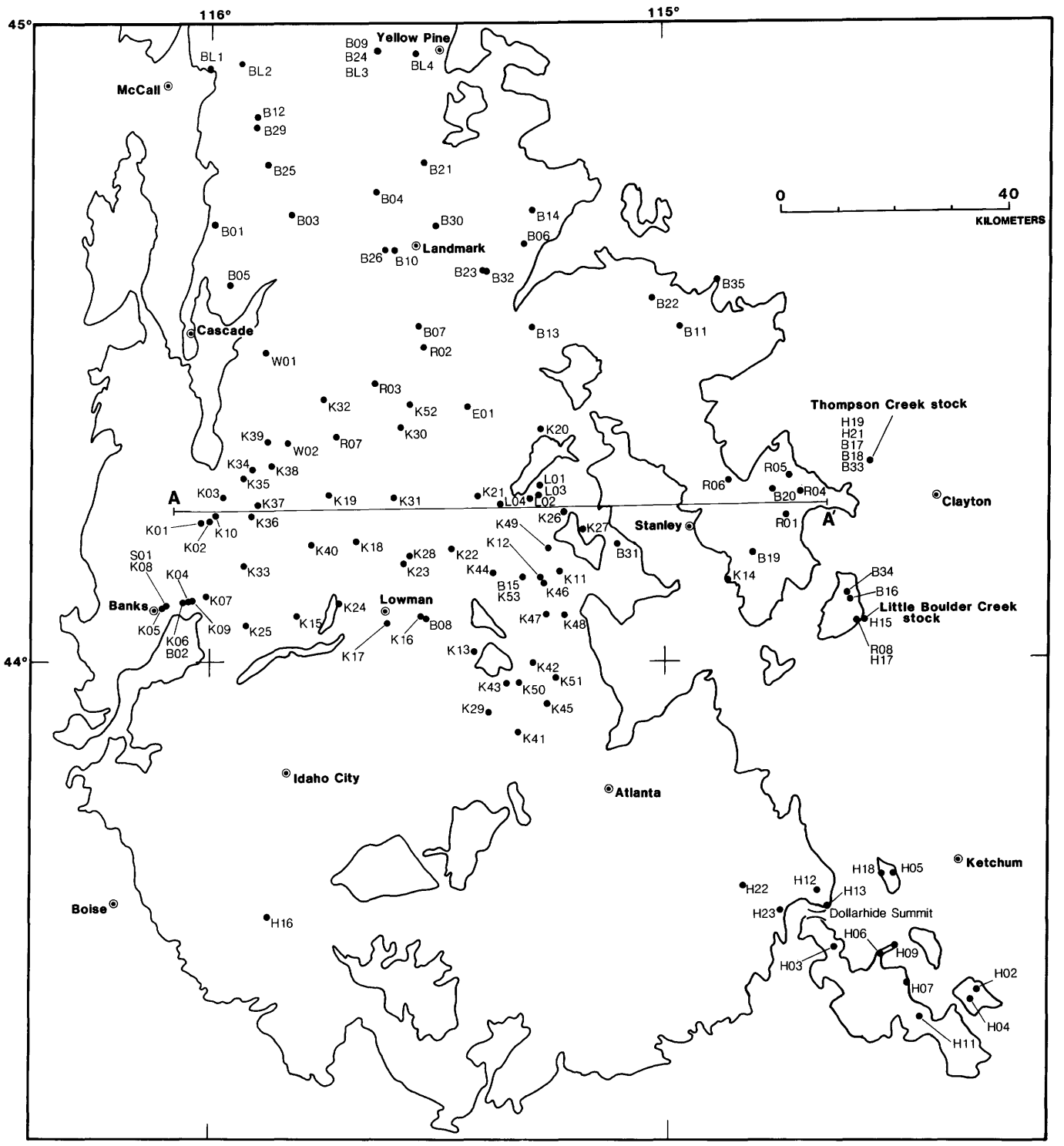

FIGURE 9.7.—Locations of samples collected for this study, and location of transect A-A'.

total Fe contents then increase and SiO_2 content decreases. At the extreme eastern edge SiO_2 content again rises and concentrations of total Fe and CaO decrease. Relations along the eastern margin are complex, owing to the discontinuous nature of the tonalitic rocks in this area. The K_2O and Na_2O contents display very little systematic variation along the transect, though there is an increase in K_2O in the nontonalitic phases of the batholith. The minimal chemical variation across the central 90-km part of the batholith suggests that little or no differentiation took place as these rocks were emplaced. A similar conclusion was reached by Hyndman (1983) for the Bitterroot lobe of the batholith. Fleck and Criss (1985) have shown that assimilation-fractional crystallization models permit only insignificant amounts of crystal fractionation during anatexis and mixing for the majority of the plutons in the Bitterroot lobe.

The break between the western tonalite and more felsic rocks to the east corresponds to the quartz diorite line of Moore (1959). The initial $^{87}Sr/^{86}Sr$ 0.704-0.706 line is not coincident with the quartz diorite line, but lies in the tonalitic rocks to the west (Armstrong and others, 1977; Fleck and Criss, 1985).

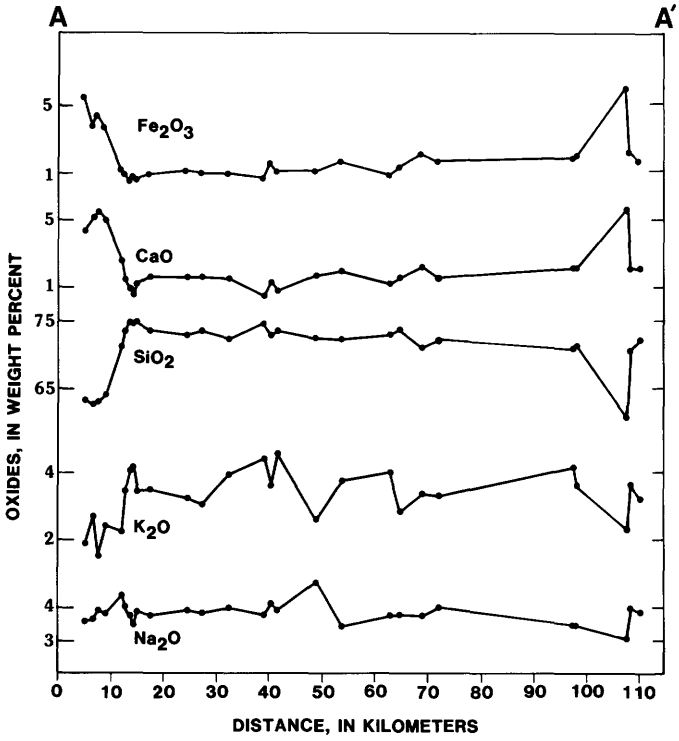

FIGURE 9.8.—Chemical variation of selected oxides from samples across the central part of the Atlanta lobe of the Idaho batholith. Fe_2O_3 is total Fe as Fe_2O_3. Locations of sample sites and transect A-A′ are given in figure 9.7.

An AFM plot of the Atlanta lobe rocks (fig. 9.9) shows a calc-alkaline alkali-enrichment trend. Harker diagrams with Al_2O_3, total Fe, CaO, and K_2O concentrations plotted against SiO_2 concentrations (fig. 9.10) also show typical trends for a granitic suite of rocks. Both CaO and total Fe contents have excellent inverse correlations with SiO_2 content, a relation also seen in figure 9.8. Considerable scatter, however, occurs in the Al_2O_3 and K_2O concentration plots. Although rock suites that show smooth variation on such diagrams are interpreted by some authors as being comagmatic (for example, Hyndman, 1972), the distribution of data in figure 9.10 is probably not a good indicator of, or evidence against, a comagmatic suite in the Idaho batholith because of the size of the study area and the scatter seen for some of the major-element oxides.

A K_2O-CaO-Na_2O plot (fig. 9.11) shows the range and average value of rocks in the study area compared with the range and average values of some other granitoids in the Western United States. The Tuolumne Intrusive Suite (Bateman and Chappell, 1979) of the Sierra Nevada batholith and the quartz monzonite and granodiorite plutons in the southern California batholith (Baird and others, 1974) have virtually identical average K_2O-CaO-Na_2O values. Both are more calcic than the average value of Idaho batholith rocks in this study, though there is considerable overlap among individual samples. Hyndman (1983) has shown that rocks of the Idaho batholith are similar chemically to Tilling's (1973) "sodic series" in the Boulder batholith of Montana; the "main series" of the Boulder batholith is appreciably richer in K_2O. Data from this study supports Hyndman's correlation, as seen in figure 9.11.

Rocks of the Atlanta lobe of the Idaho batholith are predominantly peraluminous according to the definition of Shand (1949), with molecular $Al_2O_3/(CaO + Na_2O + K_2O)$ ratios (A/CNK) greater than 1.0 (fig. 9.12). Some of the tonalite and hornblende-biotite granodiorite is metaluminous by this classification.

SOURCE REGION

Chappell and White (1974) recognized two major orogenic granite types (I and S) in the Lachlan fold belt of Australia, which they separated on the basis of mineralogy and chemistry. The I-type granite was thought to have formed from partial melting of gabbroic to granitic igneous rocks and the S-type granite, from partial melting of sedimentary rocks. A late-formed group of felsic anorogenic granitoids (A-type) has since been recognized (Collins and others, 1982; White and Chappell, 1983). Application of this classification system in the Idaho batholith meets with only limited success. The tonalite has I-type characteristics, such as the presence of biotite and horn-

blende, high CaO content, and low A/CNK ratios; the muscovite-biotite granite has many S-type features, such as high A/CNK ratios, the presence of muscovite, and low CaO content. However, the biotite granodiorite, which is the most extensive unit in the southern lobe, has both I- and S-type characteristics. The A/CNK ratios (fig. 9.12) of the biotite granodiorite best illustrate the transitional nature of this unit. The ratios range from 1.0 to 1.25; Chappell and White (1974) indicate that S-type granites have ratios of greater than 1.1. Hyndman (1984) has found that the central part of the northern lobe of the Idaho batholith is neither clearly I- nor S-type, and he concluded that such a distinction may not be appropriate for these rocks.

The I-type granitoids of Australia are high in sodium, whereas the S-type granitoids are low in sodium. Chappell and White (1974) proposed that the low sodium content in the S-type rocks reflected a sedimentary source region that had been through a chemical weathering cycle. During this cycle potassium was incorporated into clays, and sodium was removed into sea water, resulting in sodium-depleted sediment. The S-type (2-mica) granite of the Idaho batholith does not show a sodium depletion, however, and is indistinguishable from the other batholith rock types on a Na_2O versus K_2O plot (fig. 9.13). The peraluminous nature of the Idaho two-mica granite suggests that these rocks may have had a sedimentary source region, hence a Na_2O versus K_2O plot is not adequate for distinguishing granitoid source regions in the Idaho batholith. A similar conclusion has been reached by Armstrong and Boudette (oral commun., 1985), who found no overlap between the western European 2-mica granitoids and the Australian S-type granitoids on a Na_2O versus K_2O diagram, even though these European rocks are thought to have been derived from a sedimentary source region.

Because large bodies of biotite granodiorite in the Atlanta lobe cannot be categorized as either I- or S-type granite, this classification scheme is of limited use in the Idaho batholith. The usefulness of the I and S classification

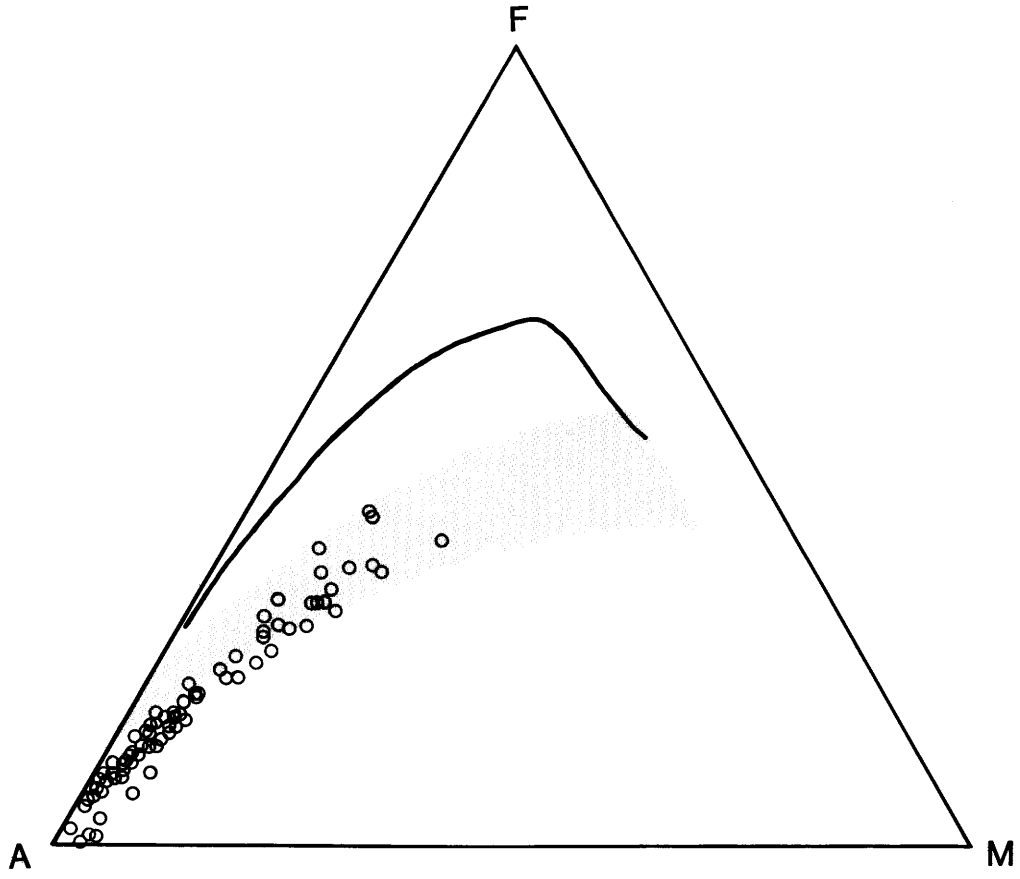

FIGURE 9.9.—AFM plot of nonsatellitic granitic rocks of the Atlanta lobe of the Idaho batholith showing alkali-enrichment trend. Solid line is an iron-enrichment (tholeiitic) trend and shaded area is a composite of several calc-alkaline trends. A = $Na_2O + K_2O$; F = total Fe as FeO; M = MgO.

system has been questioned by Czamanske and others (1981), and Barker (1981) has pointed out that although the S-type designation of Chappell and White (1974) is often applicable, the I-type category has not met with similar widespread application.

The tonalitic rocks along the westernmost margin of the batholith are low in radiogenic strontium (initial Sr-isotope ratios of less than 0.704, fig. 9.2). Armstrong and others (1977) have suggested that these tonalites formed from mantle-derived magmas that assimilated young crustal rocks not greatly enriched in radiogenic Sr. They postulate that the remainder of the batholith, with initial ratios greater than 0.706, was formed by similar magma that encountered and assimilated large quantities of Precambrian (largely pre-Belt Supergroup) rocks rich in radiogenic Sr. Hyndman (1983) has pointed out that the low

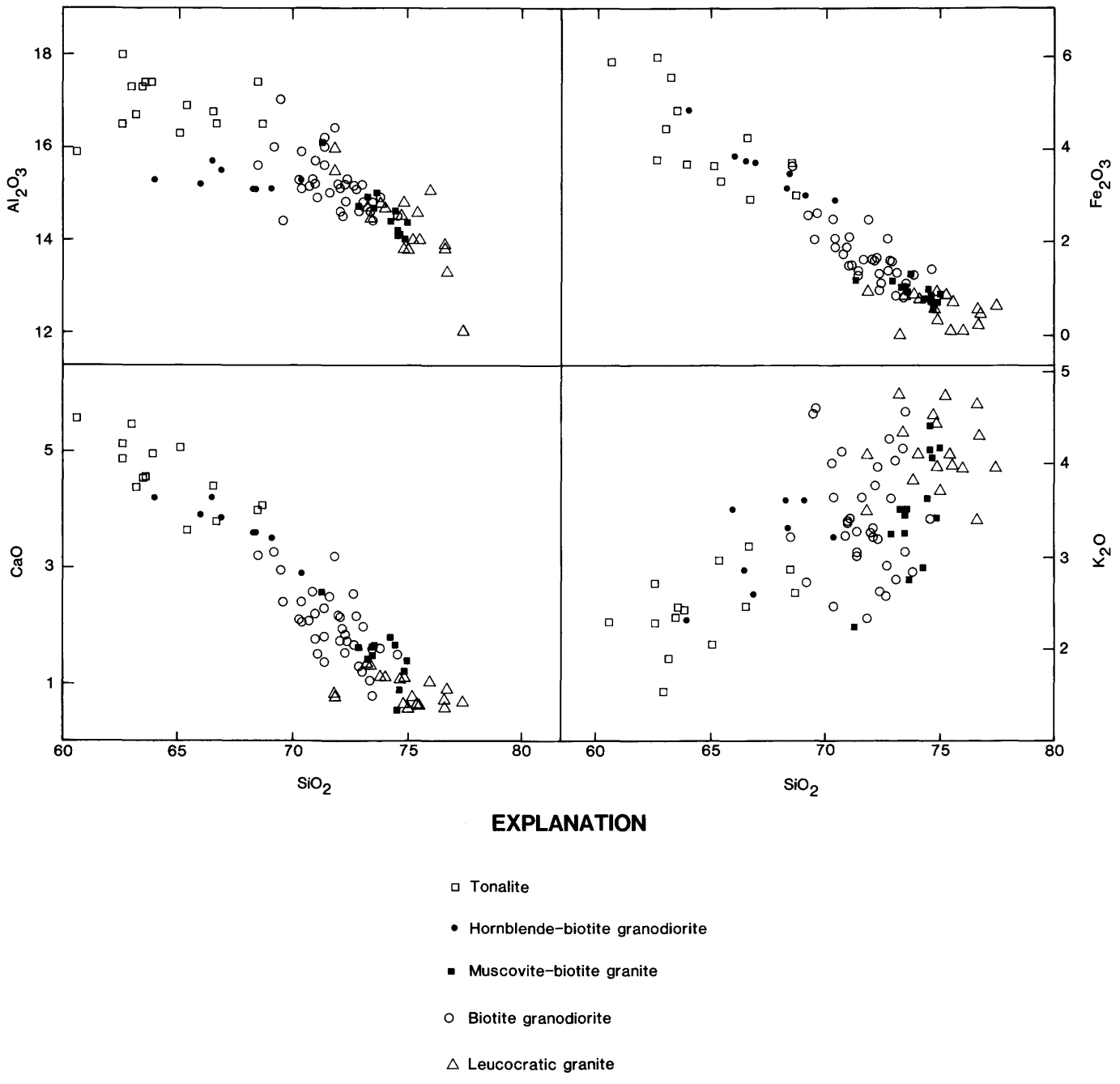

FIGURE 9.10.—Harker diagrams showing SiO_2 plotted against Al_2O_3, Fe_2O_3 (total Fe as Fe_2O_3), CaO, and K_2O (all in weight percent) for nonsatellitic granitic rocks in the Atlanta lobe of the Idaho batholith.

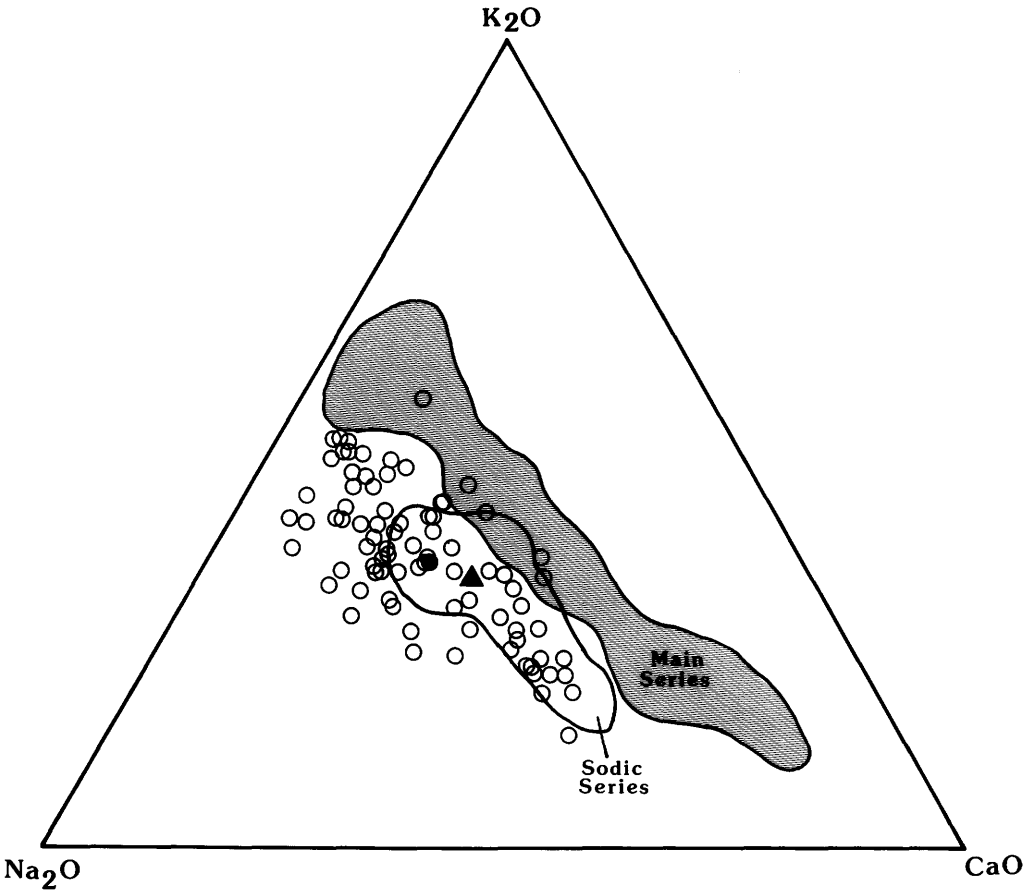

FIGURE 9.11.—K_2O-CaO-Na_2O plot for nonsatellitic granitic rocks of the Atlanta lobe (shown as open circles with the average value given by the solid circle) of the Idaho batholith. Also shown are average values for the Tuolumne Intrusive Suite of the Sierra Nevada batholith (Bateman and Chappell, 1979) and the quartz monzonite and granodiorite plutons in the southern California batholith (Baird and others, 1974), which are coincident and indicated by the solid triangle. The "Main Series" and "Sodic Series" fields of the Boulder batholith of Montana (Tilling, 1973) are also shown for comparison.

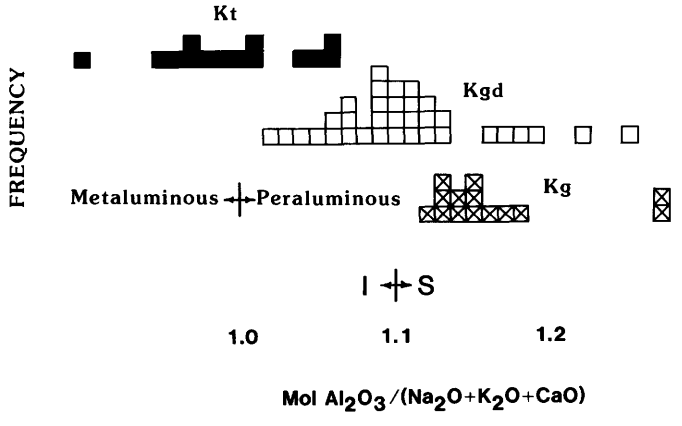

FIGURE 9.12.—Ratios of molecular $Al_2O_3/(Na_2O+K_2O+CaO)$ for tonalite (Kt), biotite granodiorite (Kgd), and 2-mica granite (Kg) in the Atlanta lobe of the Idaho batholith.

initial $^{87}Sr/^{86}Sr$ rocks along the west side of the batholith could have formed by melting of the volcanic rocks of the Seven Devils Group, subducted oceanic crust, or upper mantle. He considers the main body of the batholith to be from crustal-derived magma and not the product of extensive assimilation by mantle-derived magmas. This idea is supported by Fleck and Criss (1985), whose oxygen- and strontium-isotopic study of the Bitterroot lobe documents plutons that are mixtures of Precambrian wall rock and melts dominated by continental lower crust (initial $^{87}Sr/^{86}Sr$ greater than 0.708) rather than mantle components. The immense volume of the batholith and the peraluminous nature of the central and eastern part suggest, at the very least, a high crustal component. Initial Sr ratios are not high enough, however, to permit a simple anatectic, intracrustal genesis (Armstrong and others,

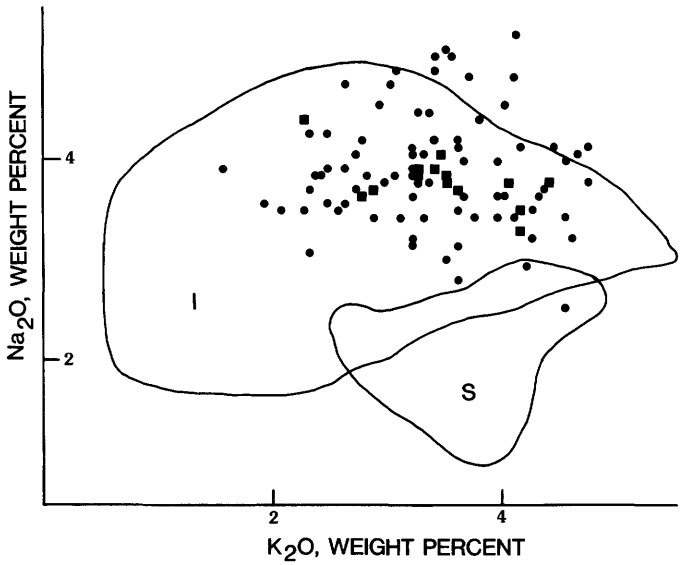

FIGURE 9.13.—Na_2O versus K_2O plot of nonsatellitic granitic rocks of the Atlanta lobe of the Idaho batholith. Muscovite-biotite (2-mica) granite shown as squares, all other units shown as circles. I and S fields of White and Chappell (1983) shown for comparison.

1977). Whether the crustal component was from metasedimentary rocks such as those of the Belt Supergroup and (or) the Yellowjacket Formation, or from pre-Belt Supergroup basement rocks is unknown. However, owing to the low metamorphic grade of the bulk of the Belt Supergroup and Yellowjacket lithologies, the pre-Belt Supergroup basement is a more likely source. The sodic nature of the batholith indicates that it originated in rocks enriched in sodium relative to calcium and potassium.

COMPARISON OF THE ATLANTA LOBE WITH THE BITTERROOT LOBE

Rocks of the Atlanta lobe of the Idaho batholith are more massive and contain less schlieren than those of the Bitterroot lobe. Particularly lacking in the Atlanta lobe is the penetrative foliation and lineation that is present in a 0.5-km-wide mylonitic shear zone on the east flank of the Bitterroot lobe (Chase, 1977; Hyndman, 1979; Bittner, chapter 5). K-Ar ages are younger in the Bitterroot lobe than in the Atlanta lobe, and some authors (for example, Toth, 1985) consider the main mass of the Bitterroot lobe to be Paleocene in age. The Atlanta lobe also differs in that it lacks metamorphosed mafic dikes, which are found in the Bitterroot lobe and which were apparently emplaced into fractures in the granite just before crystallization of the last pegmatite fluids. Hyndman (1984) has interpreted these dikes as the later stages of rising basalts that supplied heat for melting of the crust, producing the batholith magmas.

Biotite granodiorite and muscovite-biotite granite are the most abundant rock types in both lobes of the batholith and together can be considered to be the main phase of the batholith. A comparison of averaged major-element oxides from samples of the main phase of each lobe (table 9.3) shows remarkable similarities. The Atlanta lobe is slightly higher in SiO_2 content and lower in Al_2O_3 and K_2O contents, but otherwise the average concentration values are virtually identical. This relation suggests that both lobes of the batholith formed under similar conditions from a source material of nearly the same composition. The main phase of the Bitterroot lobe shows minimal chemical variation, as does the main phase in the Atlanta lobe. Both are relatively sodic compared to the main series of the Boulder batholith. Although K_2O varies more in the Atlanta lobe, there is no eastward increase in either lobe.

COMPARISON OF THE IDAHO BATHOLITH WITH THE SIERRA NEVADA BATHOLITH

As already noted, one characteristic of the Idaho batholith is its lack of numerous separate granitic plutons in sharp contact with one another. This distinction is in contrast to the Sierra Nevada batholith (Bateman, 1983), as well as other large batholiths (Pitcher, 1978), where a wide variety of plutons are present, many of which are texturally and compositionally zoned in a concentric fashion (Bateman and Chappell, 1979). The unusual homogeneity of the Idaho batholith compared to the Sierra Nevada batholith suggests generation by partial melting of broadly similar rocks, coupled with only minimal amounts of differentiation. Hyndman (1981) proposed that the Idaho batholith was formed by relatively "wet" magma that was unable to rise far above its source region in the crust before reaching the solidus. If so, the differences between the Idaho and Sierra Nevada batholiths may in part be due to a higher water content and thus deeper emplacement level of the Idaho batholith. The deep emplacement level and resultant slow cooling would produce diffuse contacts such as those present in most of the Idaho batholith. Hamilton (1983) pointed out the possible water content differences between the two batholiths and further suggested that a batholith similar to the one in Idaho may underlie the Sierra Nevada batholith. He also suggested that a Sierra-type batholith once existed above the Idaho batholith, a proposal that seems unlikely, as metasedimentary roof pendants are present across the top of the Atlanta lobe. An exception to the "wet" magma proposal for the Idaho batholith is found with the Croesus stock, which lies southeast of the main batholith 20 km south of Ketchum (fig. 9.3). In this pluton pyroxene and biotite are major mafic constituents, whereas amphibole is a secondary mineral. Thus, the magma that formed the

TABLE 9.3.—*Major-element oxide averages of the Atlanta and Bitterroot lobes of the Idaho batholith and of the Tuolumne Intrusive Suite of the Sierra Nevada batholith*

[Idaho batholith averages are only for the main-phase (biotite granodiorite and 2-mica granite) rocks; values given are in weight percent. Atlanta lobe values from this study; Bitterroot lobe values from Coxe and Toth (1983) and Hyndman (1984); Tuolumne Intrusive Suite values from Bateman and Chappell (1979). n, number of samples. Total Fe as Fe_2O_3]

	Atlanta lobe n=50	Bitterroot lobe n=81	Tuolumne Intrusive Suite n=22
SiO_2------	72.4	71.9	68.2
Al_2O_3-----	15.0	15.4	15.7
K_2O-------	3.4	3.8	3.6
Na_2O------	3.9	4.1	4.0
Total Fe--	1.48	1.37	3.0
MgO-------	.4	.4	1.1
CaO-------	1.84	1.80	3.2
TiO_2------	.20	.18	.5

quartz monzodiorite of the Croesus stock was relatively dry.

The principle difference between the Idaho and Sierra Nevada batholiths is composition. The Idaho batholith has a lower mafic-mineral content and is dominated by granite and granodiorite. Granodiorite and tonalite are the dominant rock types in the Sierra Nevada batholith. The Idaho batholith is predominantly muscovite and biotite bearing with subordinate hornblende, whereas biotite and hornblende predominate in the Sierra Nevada rocks. Chemically, the Idaho batholith is higher in SiO_2 content and lower in CaO and total Fe contents than many of the Sierra Nevada rocks (table 9.3). The K_2O content does not increase at constant SiO_2 content eastward across the Idaho batholith as it does in the Sierra Nevada batholith.

The initial $^{87}Sr/^{86}Sr$ 0.704 line extends down the western side of both batholiths (Kistler, 1974; Armstrong and others, 1977). However, the 0.706 line extends through the central part of the Sierra Nevada, whereas it is nearly coincident with the 0.704 line in Idaho. This represents a fundamental difference in the nature of the lithosphere below each batholith. Much of the Sierra Nevada batholith is underlain by oceanic (island arc) crust, but the Idaho batholith is largely underlain by continental crust. These crustal differences greatly contributed to the contrasts between the two granitoid bodies.

SUMMARY

The Atlanta lobe of the Idaho batholith consists primarily of biotite granodiorite and muscovite-biotite granite, with subordinate amounts of tonalite, hornblende-biotite granodiorite, K-feldspar megacryst granodiorite, and leucocratic granite. The oldest rocks are tonalite, which have emplacement ages of approximately 95 to 85 Ma. The youngest rocks are fine-grained leucocratic granite, emplaced at about 75 to 70 Ma. Major-element chemistry documents the remarkable homogeneity of the batholith, with minimal east-west variation across 90 km of the central part of the Atlanta lobe. The bulk of the batholithic rocks are peraluminous, and they show a calc-alkaline alkali-enrichment trend.

Available Sr-isotope data show that tonalite along the extreme western margin of the Idaho batholith formed from magma depleted in radiogenic strontium. These rocks were probably generated by partial melting in or above a subducting slab of oceanic lithosphere. Tonalite, granodiorite, and granite to the east have high initial Sr ratios and probably formed by partial melting of pre-Belt Supergroup basement rocks in the lower crust. The mantle component in these rocks is minor.

Chemical and mineralogical comparisons show the Bitterroot and Atlanta lobes of the Idaho batholith to be similar in composition. Significant foliation and lineation, as well as metamorphosed basaltic dikes, are absent in the Atlanta lobe but are present in the Bitterroot lobe. The Idaho batholith differs from the Sierra Nevada batholith in two significant ways. First, the Idaho batholith has a lower mafic-mineral content than the Sierra Nevada batholith, and second, it lacks the numerous zoned plutons in sharp contact with one another that is characteristic of the Sierra Nevada batholith. Biotite and muscovite predominate in the Idaho batholith, whereas hornblende and biotite are characteristic of the Sierra Nevada rocks. Chemically, the Idaho batholith tends to be higher in SiO_2 content and lower in CaO and total Fe contents. Higher water content in the magma during emplacement of the Idaho batholith may have inhibited the rise of magma there relative to the Sierra Nevada batholith. The nature of the lithosphere, as reflected in initial $^{87}Sr/^{86}Sr$ ratios, is different below the two batholiths. The Sierra Nevada batholith is largely underlain by oceanic material, and the Idaho batholith is underlain almost entirely by continental crust, thus resulting in numerous contrasts between the two batholiths.

REFERENCES CITED

Anderson, A.L., 1947, Geology and ore deposits of Boise Basin, Idaho: U.S. Geological Survey Bulletin 944-C, 319 p.

_____ 1952, Multiple emplacement of the Idaho batholith: Journal of Geology, v. 60, no. 3, p. 255-265.

Anderson, A.L., Kiilsgaard, T.H., and Fryklund, V.C., Jr., 1950, Detailed geology of certain areas in the Mineral Hill and Warm Springs mining districts, Blaine County, Idaho: Idaho Bureau of Mines and Geology Pamphlet 90, 73 p.

Armstrong, R.L., 1974, Geochronometry of the Eocene volcanic-plutonic episode in Idaho: Northwest Geology, v. 3, p. 1-15.

_____ 1975a, Precambrian (1500 m.y. old) rocks of central Idaho—the Salmon River arch and its role in cordilleran sedimentation and tectonics: American Journal of Science, v. 275-A, p. 437-467.

_____ 1975b, The geochronometry of Idaho: Isochron West, no. 14, 50 p.

Armstrong, R.L., Taubeneck, W.H., and Hales, P.O., 1977, Rb-Sr and K-Ar geochronometry of Mesozoic granitic rocks and their Sr isotopic composition, Oregon, Washington, and Idaho: Geological Society of America Bulletin, v. 88, p. 397-411.

Baird, A.K., Baird, K.W., and Welday, E.E., 1974, Chemical trends across Cretaceous batholithic rocks of southern California: Geology, v. 2, no. 10, p. 493-495.

Barker, F., 1981, Introduction to special issue on granites and rhyolites: a commentary for the nonspecialist: Journal of Geophysical Research, v. 86, no. B11, p. 10131-10135.

Bateman, P.C., 1983, A summary of critical relations in the central part of the Sierra Nevada batholith, California, U.S.A.: Geological Society of America Memoir 159, p. 241-254.

Bateman, P.C., and Chappell, B.W., 1979, Crystallization, fractionation, and solidification of the Tuolumne intrusive series, Yosemite National Park, California: Geological Society of America Bulletin, Part I, v. 90, p. 465-482.

Bennett, E.H., 1980, Granitic rocks of Tertiary age in the Idaho batholith and their relation to mineralization: Economic Geology, v. 75, p. 278-288.

Bennett, E.H., and Knowles, C.R., 1985, Tertiary plutons and related rocks in central Idaho, *in* McIntyre, D.H., ed., Symposium on the geology and mineral deposits of the Challis 1° × 2° quadrangle, Idaho: U.S. Geological Survey Bulletin 1658 A-S.

Berry, A.L., Dalrymple, G.B., Lanphere, M.A., and Von Essen, J.C., compilers, 1976, Summary of miscellaneous potassium-argon age measurements, U.S. Geological Survey, Menlo Park, California, for the years 1972–1974: U.S. Geological Survey Circular 727, 13 p.

Bond, J.G., compiler, 1978, Geologic map of Idaho: Idaho Bureau of Mines and Geology, scale 1:500,000.

Brooks, H.C., and Vallier, T.C., 1978, Mesozoic rocks and tectonic evolution of eastern Oregon and western Idaho, *in* Howell, D.G., and McDougall, K.A., eds., Mesozoic paleogeography of the Western United States: Society of Economic Paleontologists and Mineralogists, Pacific Coast Paleogeography Symposium II, Pacific Section, p. 133-145.

Cater, F.W., Pinckney, D.M., Hamilton, W.B., Parker, R.L., Weldin, R.D., Close, T.J., and Zilka, N.T., 1973, Mineral resources of the Idaho Primitive Area and vicinity, Idaho: U.S. Geological Survey Bulletin 1304, 431 p.

Centanni, J.P., 1985, Composition, synthesis and thermal stability of celadonitic white mica: implications for plutonic muscovite [abs.]: Geological Society of America Abstracts with Programs, v. 17, no. 6, p. 347.

Chappell, B.W., and White, A.J.R., 1974, Two contrasting granite types: Pacific Geology, v. 8, p. 173-174.

Chase, R.B., 1973, Petrology of the northeastern border zone of the Idaho batholith, Bitterroot Range, Montana: Montana Bureau of Mines and Geology Memoir 43, 28 p.

_____ 1977, Structural evolution of the Bitterroot dome and zone of cataclasis: Geological Society of America, Annual Meeting, Rocky Mountain Section, Missoula, Montana, Guidebook, no. 1.

Collins, W.J., Beams, S.D., White, A.J.R., and Chappel, B.W., 1982, Nature and origin of A-type granites with particular reference to southeastern Australia: Contributions to Mineralogy and Petrology, v. 80, p. 189-200.

Coxe, B.W., and Toth, M.I., 1983, Geochemical maps of the Selway-Bitterroot Wilderness, Idaho County, Idaho, Missoula and Ravalli Counties, Montana: U.S. Geological Survey Miscellaneous Field Studies Map MF-1495-C, scale 1:125,000 (2 sheets).

Criss, R.E., 1981, An $^{18}O/^{16}O$, D/H and K-Ar study of the southern half of the Idaho batholith: Pasadena, California Institute of Technology, Ph.D. dissertation, 401 p.

Criss, R.E., Lanphere, M.A., and Taylor, H.P., Jr., 1982, Effects of regional uplift, deformation, and meteoric-hydrothermal metamorphism on K-Ar ages of biotites in the southern half of the Idaho batholith: Journal of Geophysical Research, v. 87, no. B8, p. 7029-7046.

Criss, R.E., and Taylor, H.P., Jr., 1983, An $^{18}O/^{16}O$ and D/H study of Tertiary hydrothermal systems in the southern half of the Idaho batholith: Geological Society of America Bulletin, v. 94, p. 640-663.

Czamanske, G.K., Ishihara, S., and Atkin, S.A., 1981, Chemistry of rock-forming minerals of the Cretaceous-Paleocene batholith in southwestern Japan and implications for magma genesis: Journal of Geophysical Research, v. 86, no. B11, p. 10431-10469.

Evans, K.V., and Zartman, R.E., 1981, U-Th-Pb zircon geochronology of Proterozoic Y granite intrusions in the Salmon area, east-central Idaho [abs.]: Geological Society of America Abstracts with Programs, v. 13, no. 4, p. 195.

Fisher, F.S., McIntyre, D.H., and Johnson, K.M., 1983, Geologic map of the Challis 1° × 2° quadrangle, Idaho: U.S. Geological Survey Open-File Report 83-523, 41 p., 2 maps, scale 1:250,000.

Fleck, R.J., and Criss, R.E., 1985, Strontium and oxygen isotopic variations in Mesozoic and Tertiary plutons of central Idaho: Contributions to Mineralogy and Petrology, v. 90, p. 291-308.

Hahn, G.A., and Hughes, G.J., Jr., 1984, Sedimentation, tectonism, and associated magmatism of the Yellowjacket Formation in the Idaho cobalt belt, Lemhi County, Idaho, *in* Hobbs, S.W., ed., Abstracts and summaries, Belt Symposium II: Montana Bureau of Mines and Geology Special Publication 90, p. 65-67.

Hall, W.E., 1985, Stratigraphy and mineral deposits in Middle and Upper Paleozoic rocks of the black-shale mineral belt, central Idaho, *in* McIntyre, D.H., ed., Symposium on the geology and mineral deposits of the Challis 1° × 2° quadrangle, Idaho: U.S. Geological Survey Bulletin 1658 A-S.

Hall, W.E., Rye, R.O., and Doe, B.R., 1978, Wood River mining district, Idaho—intrusion-related lead-silver deposits derived from country rock source: U.S. Geological Survey Journal of Research, v. 6, no. 5, p. 579-592.

Hall, W.E., Schmidt, E.A., Howe, S.S., and Broch, M.J., 1984, The Thompson Creek, Idaho, porphyry molybdenum deposit—an example of a fluorine-deficient molybdenum granodiorite system: Proceedings of the Sixth Quadrennial International Association on the Genesis of Ore Deposits Symposium, Stuttgart, Germany, p. 349-357.

Hamilton, Warren, 1963, Metamorphism in the Riggins region, western Idaho: U.S. Geological Survey Professional Paper 436, 95 p.

_____ 1976, Tectonic history of west-central Idaho [abs.]: Geological Society of America Abstracts with Programs, v. 8, no. 3, p. 378-379.

_____ 1978, Mesozoic tectonics of the Western United States, *in* Howell, D.G., and McDougall, K.A., eds., Mesozoic paleogeography of the Western United States: Society of Economic Paleontologists and Mineralogists, Pacific Coast, Paleogeography Symposium II, Pacific Section, p. 33-70.

_____ 1983, Depth-related contrasts between Idaho and Sierra Nevada batholiths [abs.]: Geological Society of America Abstracts with Programs, v. 15, no. 5., p. 334.

Harrison, T.M., and McDougall, I., 1980, Investigations of an intrusive contact, northwest Nelson, New Zealand—I. Thermal, chronological, and isotopic constraints: Geochimica et Cosmochimica Acta, v. 44, p. 1985-2003.

Hyndman, D.W., 1972, Petrology of igneous and metamorphic rocks: New York, McGraw-Hill Book Co., p. 86.

_____ 1979, Major tectonic elements and tectonic problems along the line of section from northeastern Oregon to west-central Montana: Geological Society of America Map and Chart Series MC-28C, 11 p., scale 1:250,000.

_____ 1981, Controls on source and depth of emplacement of granitic

magma: Geology, v. 9, p. 244-249.
_____ 1983, The Idaho batholith and associated plutons, Idaho and western Montana: Geological Society of America Memoir 159, p. 213-240.
_____ 1984, A petrographic and chemical section through the northern Idaho batholith: Journal of Geology, v. 92, p. 83-102.
Jones, D.L., Silberling, N.J., and Hillhouse, J., 1977, Wrangellia—a displaced terrane in northwestern North America: Canadian Journal of Earth Sciences, v. 14, p. 2565-2577.
Kiilsgaard, T.H., 1983, Geologic map of the Ten Mile West Roadless area, Boise and Elmore Counties, Idaho: U.S. Geological Survey Miscellaneous Field Studies Map MF-1500-A, scale 1:62,500.
Kiilsgaard, T.H., Freeman, V.L., and Coffman, J.S., 1970, Mineral resources of the Sawtooth Primitive Area, Idaho: U.S. Geological Survey Bulletin 1319-D, 174 p.
Kiilsgaard, T.H., and Lewis, R.S., 1985, Plutonic rocks of Cretaceous age and faults in the Atlanta lobe of the Idaho batholith, Challis quadrangle, *in* McIntyre, D.H., ed., Symposium on the geology and mineral deposits of the Challis 1° × 2° quadrangle, Idaho: U.S. Geological Survey Bulletin 1658 A-S.
Kistler, R.W., 1974, Phanerozoic batholiths in western North America: Annual Reviews, Earth and Planetary Science Letters, v. 2, p. 403-418.
Kuntz, M.A., and Allen, C.C., 1984, Rock units and deformation on the western margin of the Idaho batholith near McCall, Idaho [abs.]: Geological Society of America Abstracts with Programs, v. 16, no. 4, p. 227.
Larsen, E.S., Jr., and Schmidt, R.G., 1958, A reconnaissance of the Idaho batholith and comparison with the southern California batholith: U.S. Geological Survey Bulletin 1070-A, 33 p.
Lewis, R.S., 1984, Geology of the Cape Horn Lakes quadrangle, south-central Idaho: University of Washington, Seattle, M.S. thesis, 91 p.
Lindgren, W., 1900, The gold and silver veins of Silver City, De Lamar, and other mining districts in Idaho: U.S. Geological Survey 20th Annual Report, part 3, p. 65-256.
Lopez, D.A., 1982, Constraints on the shape and position of the Yellowjacket (Proterozoic Y) depositional basin [abs.]: Geological Society of America Abstracts with Programs, v. 14, no. 6, p. 320.
Lund, K., 1984, The continent-island arc juncture in west-central Idaho—a missing link in cordilleran tectonics [abs.]: Geological Society of America Abstracts with Programs, v. 16, no. 6, p. 580.
Lund, K., Snee, L.W., and Evans, K.V., 1986, Age and genesis of precious metals deposits, Buffalo Hump district, central Idaho: Implications for depth of emplacement of quartz veins: Economic Geology, v. 81, no. 4, p. 990-996.
Luthy, S.T., 1981, Petrology of Cretaceous and Tertiary intrusive rocks, Red Mountain-Bull Trout Point area, Boise, Valley, and Custer Counties, Idaho: Missoula, University of Montana, M.S. thesis, 109 p.
Mabey, D.R., 1982, Gravity and magnetic features along the eastern margin of the Idaho batholith in central Idaho [abs.]: Geological Society of America Abstracts with Programs, v. 14, no. 6, p. 320.
Marvin, R.F., and Dobson, S.W., 1979, Radiometric ages: Compilation B, U.S. Geological Survey: Isochron/West, no. 26, p. 17.
McDowell, F.W., and Kulp, J.L., 1969, Potassium-argon dating of the Idaho batholith: Geological Society of America Bulletin, v. 80, p. 2379-2382.
McIntyre, D.H., Ekren, E.B., and Hardyman, R.F., 1982, Stratigraphic and structural framework of the Challis Volcanics in the eastern half of the Challis 1° × 2° quadrangle, Idaho, *in* Bonnichsen, B., and Breckenridge, R.M., eds., Cenozoic geology of Idaho: Idaho Bureau of Mines and Geology Bulletin 26, p. 3-22.
Moore, J.G., 1959, The quartz diorite boundary line in the Western United States: Journal of Geology, v. 67, no. 2, p. 198-210.
Myers, P.E., 1982, Geology of the Harpster area, Idaho County, Idaho: Idaho Bureau of Mines and Geology Bulletin 25, 46 p.
Olson, H.J., 1968, The geology and tectonics of the Idaho porphyry belt from the Boise Basin to the Casto quadrangle: Tucson, University of Arizona, Ph.D. dissertation, 154 p.
Pitcher, W.S., 1978, The anatomy of a batholith: Journal of the Geological Society of London, v. 135, p. 157-182.
Reid, R.R., 1963, Reconnaissance geology of the Sawtooth Range: Idaho Bureau of Mines and Geology Pamphlet 129, 37 p.
Ross, C.P., 1928, Mesozoic and Tertiary granitic rocks in Idaho: Journal of Geology, v. 36, no. 8, p. 673-693.
_____ 1934, Geology and ore deposits of the Casto quadrangle, Idaho: U.S. Geological Survey Bulletin 854, 135 p.
_____ 1937, Geology and ore deposits of the Bayhorse region, Custer County, Idaho: U.S. Geological Survey Bulletin 877, 161 p.
_____ 1963, Geology along U.S. Highway 93 in Idaho: Idaho Bureau of Mines and Geology Pamphlet 130, 98 p.
Ruppel, E.T., 1975, Precambrian and Lower Ordovician rocks in east-central Idaho: U.S. Geological Survey Professional Paper 889, 34 p.
Schmidt, D.L., 1962, Quaternary geology of the Bellevue area in Blaine and Camas Counties, Idaho: U.S. Geological Survey Open-File Report 62-120, 92 p.
_____ 1964, Reconnaissance petrographic cross section of the Idaho batholith in Adams and Valley Counties, Idaho: U.S. Geological Survey Bulletin 1181-G, 50 p.
Shand, S.J., 1949, Eruptive rocks: New York, John Wiley and Sons, Inc., 3d ed., 488 p.
Shapiro, L., 1975, Rapid analysis of silicate, carbonate, and phosphate rocks—revised edition: U.S. Geological Survey Bulletin 1401, 76 p.
Smitherman, J.R., 1985, Geology of the Stibnite roof pendant, Valley County, Idaho: Moscow, University of Idaho, M.S. thesis.
Snee, L.W., 1982, Emplacement and cooling of Pioneer batholith, southwestern Montana: Columbus, Ohio State University, Ph.D. dissertation, 320 p.
Snee, L.W., Lund, K., and Hoover, A.L., 1985, Discrimination of Idaho batholith plutons by structure and age [abs.]: Geological Society of America Abstracts with Programs, v. 17, no. 6, p. 409.
Streckeisen, A.L., and others, 1973, Plutonic rocks—classification and nomenclature recommended by the IUGS Subcommission on the systematics of igneous rocks: Geotimes, v. 18, no. 10, p. 26-30.
Sutter, J.F., Snee, L.W., and Lund, K., 1984, Metamorphic, plutonic, and uplift history of a continent-island arc suture zone, west-central Idaho [abs.]: Geological Society of America Abstracts with Programs, v. 16, no. 6, p. 670-671.
Swanberg, C.A., and Blackwell, D.D., 1973, Areal distribution and geophysical significance of heat generation in the Idaho batholith and adjacent intrusions in eastern Oregon and western Montana: Geological Society of America Bulletin, v. 84, p. 1261-1282.
Taubeneck, W.H., 1971, Idaho batholith and its southern extension: Geological Society of America Bulletin, v. 82, p. 1899-1928.
Tilling, R. I., 1973, Boulder batholith, Montana: a product of two contemporaneous but chemically distinct magma series: Geological Society of America Bulltein, v. 84, p. 3879-3900.
Toth, M.I., 1985, Petrology and evolution of the Bitterroot lobe of the Idaho batholith [abs.]: Geological Society of America Abstracts with Programs, v. 17, no. 4, p. 269.
Weis, P.L., Schmitt, L.J., Tuchek, E.T., and Davis, W.E., 1972, Mineral resources of the Salmon River Breaks Primitive Area, Idaho: U.S. Geological Survey Bulletin 1353-C, 91 p.
White, A.J.R., and Chappell, B.W., 1983, Granitoid types and their distribution in the Lachlan fold belt, southeastern Australia: Geological Society of America Memoir 159, p. 21-34.
Wiswall, C.G., 1979, Structure and petrology below the Bitterroot lobe of the Idaho batholith: Northwest Geology, v. 8, p. 18-28.

GPO 785-048/48039


U.S. DEPARTMENT OF THE INTERIOR
March 3, 1849